IMPORTANCE OF ROOT SYMBIOMES FOR PLANT NUTRITION: NEW INSIGHTS, PERSPECTIVES, AND FUTURE CHALLENGES

EDITED BY: Kevin Garcia, Heike Bücking and Sabine Dagmar Zimmermann

PUBLISHED IN: Frontiers in Plant Science and Frontiers in Microbiology

frontiers Research Topics

frontiers

ISSN 1664-8714
ISBN 978-2-88963-814-7
DOI 10.3389/978-2-88963-814-7

About Frontiers

Frontiers is more than just an open-access publisher of scholarly articles: it is a pioneering approach to the world of academia, radically improving the way scholarly research is managed. The grand vision of Frontiers is a world where all people have an equal opportunity to seek, share and generate knowledge. Frontiers provides immediate and permanent online open access to all its publications, but this alone is not enough to realize our grand goals.

Frontiers Journal Series

The Frontiers Journal Series is a multi-tier and interdisciplinary set of open-access, online journals, promising a paradigm shift from the current review, selection and dissemination processes in academic publishing. All Frontiers journals are driven by researchers for researchers; therefore, they constitute a service to the scholarly community. At the same time, the Frontiers Journal Series operates on a revolutionary invention, the tiered publishing system, initially addressing specific communities of scholars, and gradually climbing up to broader public understanding, thus serving the interests of the lay society, too.

Dedication to Quality

Each Frontiers article is a landmark of the highest quality, thanks to genuinely collaborative interactions between authors and review editors, who include some of the world's best academicians. Research must be certified by peers before entering a stream of knowledge that may eventually reach the public - and shape society; therefore, Frontiers only applies the most rigorous and unbiased reviews.
Frontiers revolutionizes research publishing by freely delivering the most outstanding research, evaluated with no bias from both the academic and social point of view. By applying the most advanced information technologies, Frontiers is catapulting scholarly publishing into a new generation.

What are Frontiers Research Topics?

Frontiers Research Topics are very popular trademarks of the Frontiers Journals Series: they are collections of at least ten articles, all centered on a particular subject. With their unique mix of varied contributions from Original Research to Review Articles, Frontiers Research Topics unify the most influential researchers, the latest key findings and historical advances in a hot research area! Find out more on how to host your own Frontiers Research Topic or contribute to one as an author by contacting the Frontiers Editorial Office: researchtopics@frontiersin.org

IMPORTANCE OF ROOT SYMBIOMES FOR PLANT NUTRITION: NEW INSIGHTS, PERSPECTIVES, AND FUTURE CHALLENGES

Topic Editors:
Kevin Garcia, North Carolina State University, United States
Heike Bücking, South Dakota State University, United States
Sabine Dagmar Zimmermann, Délégation Languedoc Roussillon (CNRS), France

Citation: Garcia, K., Bücking, H., Zimmermann, S. D., eds. (2020). Importance of Root Symbiomes for Plant Nutrition: New Insights, Perspectives, and Future Challenges. Lausanne: Frontiers Media SA. doi: 10.3389/978-2-88963-814-7

Table of Contents

frontiers in Plant Science

EDITORIAL
published: 13 May 2020
doi: 10.3389/fpls.2020.00594

Editorial: Importance of Root Symbiomes for Plant Nutrition: New Insights, Perspectives and Future Challenges

Kevin Garcia[1]*, *Heike Bücking*[2] and *Sabine D. Zimmermann*[3]

[1] Department of Crop and Soil Sciences, North Carolina State University, Raleigh, NC, United States, [2] Department of Biology and Microbiology, South Dakota State University, Brookings, SD, United States, [3] BPMP, Univ Montpellier, CNRS, INRAE, Institut Agro, Montpellier, France

Keywords: biological nitrogen fixation, mycorrhizal symbiosis, plant growth promoting rhizobacteria, plant nutrition, root microbiome

The Editorial on the Research Topic

Importance of Root Symbiomes for Plant Nutrition: New Insights, Perspectives and Future Challenges

Plants interact with a plethora of soil microbes that help them to acquire nutritional resources, to be protected against pathogens, and to face challenging and fluctuating external conditions. Understanding how the microbiota of roots and rhizospheres is shaped and conserved by host plants, and how it changes in response to genetic and environmental pressures, is crucial for the preservation of natural ecosystems and to harness its potential for the development of novel strategies in agroecosystems. This Research Topic presents a series of articles that summarizes the latest research updates on the impact of the plant microbiota and its specific symbionts [i.e., arbuscular mycorrhizal (AM) and ectomycorrhizal (ECM) fungi, nitrogen-fixing rhizobia, and plant growth-promoting rhizobacteria (PGPR)] on plant performance and resilience, and the external factors that influence plant microbiota assembly.

Novel next generation sequencing technologies and analytical platforms provide us with more insights into the plant microbiome. In this Research Topic, Ma et al. discussed the development and potential use of single-cell RNA-sequencing technology in the area of plant microbiomes. Although still challenging to apply routinely, it opens the way toward the discovery of very specific and localized functions of bacterial communities in plant microbiota. Multiple studies have shown that the microbiome composition differs among cultivars of a given plant species, such as corn (Walters et al., 2018), cotton (Wei et al., 2019), or grape (Mezzasalma et al., 2018). Using three switchgrass cultivars grown under various conditions (i.e., monoculture, intraspecific, or interspecific mixtures), Revillini et al. showed that plant diversity influences the structure of AM fungal and bacterial communities in the root rhizosphere, but that nitrogen fertilization only affects the composition of the AM community but not of the rhizobacterial community. These findings highlight the importance of adapted cultivar and management practices in agricultural settings to maintain optimal microbiomes. Although it is described that herbivores can also influence the leaf microbiota composition (Humphrey and Whiteman, 2020), their impact on root microbiota assembly, and particularly on AM fungi, is still unclear. In this Research Topic, Wilkinson et al. demonstrated that the inoculation with aphids does not alter the AM colonization and community composition in barley, but that the formation of fungal vesicles and the relative abundance of some fungal species in these communities is affected.

Edited by:
Andrea Genre, University of Turin, Italy

Reviewed by:
Philipp Franken, Friedrich Schiller University Jena, Germany

***Correspondence:**
Kevin Garcia
kgarcia2@ncsu.edu

Specialty section:
This article was submitted to Plant Microbe Interactions, a section of the journal Frontiers in Plant Science

Received: *03 April 2020*
Accepted: *20 April 2020*
Published: *13 May 2020*

Citation:
Garcia K, Bücking H and Zimmermann SD (2020) Editorial: Importance of Root Symbiomes for Plant Nutrition: New Insights, Perspectives and Future Challenges. Front. Plant Sci. 11:594. doi: 10.3389/fpls.2020.00594

The root microbiome also has a tremendous influence on forest diversity, evolution, and dynamic, defining a complex "ecosystem microbiome" (Baldrian, 2016). ECM fungi play a significant role in Northern hemisphere forest ecosystems (Becquer et al., 2019). Nagati et al. investigated the community assembly of ECM fungi on balsam fir seedlings in two biotically different environments and their potential role in the spread of the species. Using path analysis, they identified significant correlations between stand type, sapling growth, foliar nitrogen content and understory vegetation on community composition, and presented an exciting effort toward a better understanding of the microbial mechanisms underlying forest succession. Although significant progress has been made in the identification and characterization of plant and fungal transport proteins (Garcia et al., 2016; Plassard et al., 2019) in the ECM symbiosis, there are many key players that are still missing, particularly for micronutrients such as zinc. In this Research Topic, Coninx et al. revealed the dual function of the transporter SlZRT2 from the ECM fungus *Suillus luteus* in zinc acquisition from the external medium and its redistribution in fungal hyphae in response to zinc availability (Ruytinx et al., 2020).

Biological nitrogen fixation within root nodules is a tremendous advantage conferred by specific soil rhizobia bacteria to certain plant families, allowing the acquisition of atmospheric nitrogen (Griesmann et al., 2018). Purple acid phosphatase is a class of proteins involved in phosphorus acquisition and utilization, particularly under limiting conditions. Using transcriptomic and reverse genetics approaches, Wang et al. described a novel purple acid phosphatase of soybean (GmPAP12) required for nodule formation and nitrogen fixation, reinforcing the importance of plant phosphorus nutrition in biological nitrogen fixation. The impact of an inoculation with nitrogen fixing bacteria on agroecosystems and forest ecosystems for restoration purposes highly depends on various soil amendments. Egamberdieva et al. studied the effect of two maize biochars on biological nitrogen fixation in chickpea under drought and irrigated conditions, and observed an improved growth, nitrogen uptake, and symbiotic performance under both conditions. Zhang et al. investigated the effect of different nitrogen sources on the colonization with rhizobia in two major forest restoration species (*Robinia pseudoacacia* and *Lupinus latifolius*), and found a synergistic response between nitrogen supply and bacterial inoculation. *Parasponia* (Cannabaceae) is the only non-legume lineage that has evolved the ability to develop symbiotic nodules with nitrogen-fixing rhizobia (Op den Camp et al., 2011). In legumes and actinorhizal plants, soil nitrate acts as a negative regulator of nodule development (Ferguson et al., 2019). Using *Parasponia andersonii* as a model plant, Dupin et al. investigated the impact of increasing ammonium nitrate concentrations on tissue weight, nodule formation, and nodule number. The authors observed that *P. andersonii* displayed a reduction of symbiotic nodules after external nitrogen application, or even an elimination at high concentrations, indicating the presence of a similar autoregulation mechanism than has been described for legume and actinorhizal plants.

PGPR are soil bacteria that infect roots and confer various benefits to the colonized plants, such as improved growth, resistance to biotic and abiotic stress, or nutrient acquisition (Backer et al., 2018). Gupta and Pandey isolated two new bacterial strains from the rhizosphere of *Allium sativum* exhibiting ACC deaminase activity, as well as the production of indole acetic acid, siderophore, ammonia, and hydrogen cyanide. These bacteria, identified by 16S rRNA sequencing as *Aneurinibacillus aneurinilyticus* and *Paenibacillus* sp., are also able to solubilize insoluble forms of phosphate and zinc. The combined application of these two strains on *Phaseolus vulgaris* was able to improve root length, shoot length, and root and shoot biomass under salt stress conditions. Another study from Mukherjee et al. described the isolation of a novel *Halomonas* species from the rhizosphere of true mangrove *Avicennia marina*. Inoculated with rice, this PGPR led to growth promotion under combined salt and arsenic stresses, through the direct involvement of bacterial exopolysaccharide. Both studies highlight the importance of natural diversity screenings to isolate novel plant beneficial microbes that can be used in agroecosystems. Finally, Chang et al. reviewed the current research on cycad-cyanobacteria symbioses. Due to the slow growth of cycads, these palmlike woody plants are under-researched, and the authors revealed important gaps in our knowledge about these interactions which should be addressed by the functional comparison with other cyanobacterial symbioses.

Overall, our knowledge on the diversity, composition, and impact of plant microbiota is still limited. It is crucial to continue investigating the molecular biology, physiology, and ecology of mutualistic interactions to isolate novel symbionts and microbial properties that improve plant performance and resilience. We hope that the work presented in this Research Topic will help to both consolidate the field of plant-microbe symbioses and bring light on the importance of understanding and preserving the plant microbiota in natural and agroecosystems.

AUTHOR CONTRIBUTIONS

KG wrote the editorial, which was revised, proofed, and accepted by all the authors.

ACKNOWLEDGMENTS

The Topic Editors are grateful to the authors who contributed to this Research Topic, to the reviewers for evaluating the work, and to the Frontiers editorial staff for their guidance and production assistance.

REFERENCES

Backer, R., Rokem, J. S., Ilangumaran, G., Lamont, J., Praslickova, D., Ricci, E., et al. (2018). Plant Growth-Promoting Rhizobacteria: context, mechanisms of action, and roadmap to commercialization of biostimulants for sustainable agriculture. *Front. Plant Sci.* 9:1473. doi: 10.3389/fpls.2018.01473

Baldrian, P. (2016). Forest microbiome: diversity, complexity and dynamics. *FEMS Microbiol. Rev.* 41, 109–130. doi: 10.1093/femsre/fuw040

Becquer, A., Guerrero-Galán, C., Eibensteiner, J. L., Houdinet, G., Bücking, H., Zimmermann, S. D., et al. (2019). The ectomycorrhizal contribution to tree nutrition. *Adv. Bot. Res.* 89, 77–126. doi: 10.1016/BS.ABR.2018.11.003

Ferguson, B. J., Mens, C., Hastwell, A. H., Zhang, M., Su, H., Jones, C. H., et al. (2019). Legume nodulation: the host controls the party. *Plant. Cell Environ.* 42, 41–51. doi: 10.1111/pce.13348

Garcia, K., Doidy, J., Zimmermann, S. D., Wipf, D., and Courty, P.-E. (2016). Take a trip through the plant and fungal transportome of mycorrhiza. *Trends Plant Sci.* 21, 937–950. doi: 10.1016/j.tplants.2016.07.010

Griesmann, M., Chang, Y., Liu, X., Song, Y., Haberer, G., Crook, M. B., et al. (2018). Phylogenomics reveals multiple losses of nitrogen-fixing root nodule symbiosis. *Science* 361:eaat1743. doi: 10.1126/science.aat1743

Humphrey, P. T., and Whiteman, N. K. (2020). Insect herbivory reshapes a native leaf microbiome. *Nat. Ecol. Evol.* 4, 221–229. doi: 10.1038/s41559-019-1085-x

Mezzasalma, V., Sandionigi, A., Guzzetti, L., Galimberti, A., Grando, M. S., Tardaguila, J., et al. (2018). Geographical and cultivar features differentiate grape microbiota in northern Italy and Spain vineyards. *Front. Microbiol.* 9:946. doi: 10.3389/fmicb.2018.00946

Op den Camp, R., Streng, A., De Mita, S., Cao, Q., Polone, E., Liu, W., et al. (2011). LysM-type mycorrhizal receptor recruited for rhizobium symbiosis in nonlegume *Parasponia*. *Science* 331, 909–912. doi: 10.1126/science.1198181

Plassard, C., Becquer, A., and Garcia, K. (2019). Phosphorus transport in mycorrhiza: how far are we? *Trends Plant Sci.* 24, 794–801 doi: 10.1016/j.tplants.2019.06.004

Ruytinx, J., Kafle, A., Usman, M., Coninx, L., Zimmermann, S. D., and Garcia, K. (2020). Micronutrient transport in mycorrhizal symbiosis; zinc steals the show. *Fungal Biol. Rev*. 34, 1–9. doi: 10.1016/j.fbr.2019.09.001

Walters, W. A., Jin, Z., Youngblut, N., Wallace, J. G., Sutter, J., Zhang, W., et al. (2018). Large-scale replicated field study of maize rhizosphere identifies heritable microbes. *Proc. Natl. Acad. Sci. U.S.A.* 115, 7368–7373. doi: 10.1073/pnas.1800918115

Wei, F., Zhao, L., Xu, X., Feng, H., Shi, Y., Deakin, G., et al. (2019). Cultivar-dependent variation of the cotton rhizosphere and endosphere microbiome under field conditions. *Front. Plant Sci.* 10:1659. doi: 10.3389/fpls.2019.01659

Conflict of Interest: The authors declare that the research was conducted in the absence of any commercial or financial relationships that could be construed as a potential conflict of interest.

frontiers in Plant Science

ORIGINAL RESEARCH
published: 14 May 2020
doi: 10.3389/fpls.2020.00450

GmPAP12 Is Required for Nodule Development and Nitrogen Fixation Under Phosphorus Starvation in Soybean

Yue Wang†, Zhanwu Yang†, Youbin Kong, Xihuan Li, Wenlong Li, Hui Du and Caiying Zhang**

State Key Laboratory of North China Crop Improvement and Regulation, Hebei Agricultural University, Baoding, China

OPEN ACCESS

Edited by:
Heike Bücking, South Dakota State University, United States

Reviewed by:
Pierre Frendo, University of Nice Sophia Antipolis, France
Maurizio Chiurazzi, Italian National Research Council, Italy

***Correspondence:**
Hui Du
duhui668@126.com
Caiying Zhang
zhangcaiying@hebau.edu.cn

† These authors have contributed equally to this work

Specialty section:
This article was submitted to Plant Nutrition, a section of the journal Frontiers in Plant Science

Received: *16 September 2019*
Accepted: *26 March 2020*
Published: *14 May 2020*

Citation:
Wang Y, Yang Z, Kong Y, Li X, Li W, Du H and Zhang C (2020) GmPAP12 Is Required for Nodule Development and Nitrogen Fixation Under Phosphorus Starvation in Soybean. Front. Plant Sci. 11:450. doi: 10.3389/fpls.2020.00450

Nodulation process in legume plants is essential for biological nitrogen fixation during which process a large amount of phosphorus (P) is required. Under P deficiency, nodule formation is greatly affected, and induction of purple acid phosphatases (PAPs) is an adaptive strategy for nodules to acquire more P. However, regulation roles of PAPs in nodules remain largely understood. In this study, by transcriptome sequencing technology, five *PAP* genes were found to be differentially expressed, which led to the greatly increased acid phosphatase (APase) and phytase activities in soybean mature nodules under P starvation conditions; and among the five *PAP* genes, *GmPAP12* had the highest transcript level, and RT-PCR indicated expression of *GmPAP12* was gradually increasing during nodule development. GUS activity driven by *GmPAP12* promoter was also significantly induced in low phosphorus conditions. Further functional analysis showed that under low phosphorus stress, overexpression of *GmPAP12* resulted in higher nodule number, fresh weight, and nitrogenase activity as well as the APase activity than those of control plant nodules, whereas the growth performance and APase activity of nodules on hairy roots were greatly lower when *GmPAP12* was suppressed, indicating that *GmPAP12* may promote P utilization in soybean nodules under low P stress, which thus played an important role in nodulation and biological nitrogen fixation. Moreover, P1BS elements were found in the promoter of *GmPAP12*, and yeast one-hybrid experiment further proved the binding of P1BS by transcription factor GmPHR1 in the promoter of *GmPAP12*. At last, overexpression and suppression of *GmPHR1* in nodules indeed caused highly increased and decreased expression of *GmPAP12*, respectively, indicating that *GmPAP12* is regulated by GmPHR1 in soybean nodules. Taken together, these data suggested that *GmPAP12* was a novel soybean PAP involved in the P utilization and metabolism in soybean root nodules and played an important role in the growth and development of root nodules and biological nitrogen fixation.

Keywords: nodulation, nitrogen fixation, P deficiency, acid phosphatase, APase activity

INTRODUCTION

Legumes, such as soybean (*Glycine max*), pea (*Pisum sativum*), common bean (*Phaseolus vulgaris*), alfalfa (*Medicago sativa*), and chickpea (*Cicer arietinum* L.), interact with specific soil nitrogen (N)-fixing rhizobia to develop symbiotic relationships that result in the formation of a new organ called root nodules (Oldroyd and Downie, 2008; Ferguson et al., 2010). Soybean, one of the most widely grown legume crops in the world with more than 1,734 million acres of harvest area in 2015, is a very important oil crops that can also provide food, feed, and protein materials (Yuan et al., 2017). Soybean nodules can fix atmospheric N_2 via rhizobia that provide plants with nitrogen source for growth in rotation systems, which is an efficient way to sustain agricultural system due to symbiotic nitrogen fixation (SNF). Nitrogen is an essential nutrient for plant growth, being one of the important components of amino acid and nucleic acids in the cells. However, the availability of N for plants is very limited in soils that restrict the production of crops. To deal with this situation, agriculture has been largely reliant on nitrogen fertilizers to maximize the crop productivity with about 50% of the nitrogen fertilizers leaching into aquatic system, resulting in environmental pollution. To produce more nitrogen fertilizers, more fossil fuel is used, which costs a heavy price. Thus, it is urgent to find an alternative and effective way to provide nitrogen available for soybean growth; at the moment, biological nitrogen fixation in legume nodules arises as being one of the most hot issues in the world (Oldroyd, 2007; Marx et al., 2016).

SNF of legume nodules is a high-energy-demand process, which requires a large amount of P in energy transfer for optimal nodule functioning than do non-nodulating plants (Makoudi et al., 2018; Ferguson et al., 2019). P is also an essential macronutrient required for optimal plant growth and development. In soil, the low P availability is a critical constriction for plants, especially legume crops in agricultural and natural ecosystems, and is becoming a global problem. Legume nodules are particularly P-rich sinks owing to intensive carbon and energy turnover in which the P content is up to three times that of other plant organs (Schulze et al., 2006; Cabeza et al., 2014). For nodules in particular, the role of P is vital for SNF (Liang et al., 2014; Valentine et al., 2017; Makoudi et al., 2018). Pi deficiency not only affects legume nodule formation and development, nodule number and mass, N_2 and CO_2 fixation, and photosynthesis but also N acquisition and metabolism. Great efforts have been made to understand how legumes nodules are responding to P deficiency while symbiotically interacting with rhizobia (Cabeza et al., 2014; Nasr Esfahani et al., 2017). Physiological studies on different legumes plants such as chickpea, common bean, *Medicago truncatula* have shown that legume nodules have developed a series of adaptive strategies that could help conserve P supply to maintain symbiotic activity under Pi starvation conditions (Cabeza et al., 2014; Nasr Esfahani et al., 2017; Isidra-Arellano et al., 2018). These strategies include low P conditions but are not limited to the following: P is preferentially relocated from other organs to nodules to maintain high P content (Tang et al., 2001; Hogh-Jensen et al., 2002); more efficient use of internal phosphate sources to increase P acquisition (Hernandez et al., 2009; Isidra-Arellano et al., 2018), increasing N_2 fixation of per unit nodule mass while reducing nodule number; and higher oxygen (O_2) consumption for one unit reduced N_2 that is related with higher nodule permeability. For nodules, especially in limited P availability conditions, maintenance of P homeostasis is extremely critical for legume growth, development, and symbiosis. Despite that a significant series of studies have done on nodule development and molecular response underlying the adaption of nodules to Pi starvation, it remains a great challenge to explore the molecular and physiological mechanisms that could enable the development of more efficient symbiotic crops for sustainable farming practices (Vance et al., 2003; Schulze, 2004; Sulieman and Tran, 2015).

To cope with P deficiency and stress tolerance for growth, plants have evolved a diverse set of biochemical, physiological, and developmental adaptive strategies that could help their acquisition and utilization of P (Vance et al., 2003). These strategies include alteration of root morphology and architecture, increased activity of high affinity of Pi transporters and acid phosphatases (APases), and accumulation of anthocyanins (Franco-Zorrilla et al., 2004; Jain et al., 2012; Liang et al., 2014). At the molecular level, in order to elucidate the mechanism of plant response to P deficiency, several transcription factors were identified, including MYB, bHLH, GRAS, ERF, and WRKY families (Zhang et al., 2016; Diedhiou and Diouf, 2018; Xue et al., 2018). MYB is one of the largest transcription factor families in the plant kingdom, among which PHR1 (phosphate starvation response regulator (1) functions as a central regular in P starvation signaling, first identified in *Arabidopsis thaliana*. PHR1 binds to the P1BS *cis*-element (5'-GNATATNC-3'), which was prevalently present in the promoters of Pi starvation-induced (PSI) genes (Rubio et al., 2001; Wu et al., 2013; Sun et al., 2016). However, data suggested that expression of *PHR1* was detected in Pi-sufficient conditions and not induced in Pi starvation conditions, indicating that *PHR1* was not or only slightly responsive to Pi starvation (Rubio et al., 2001; Lv et al., 2014; Sun et al., 2016).

Also, it has been reported that under P-deficient conditions, purple acid phosphatases (PAPs) are greatly induced and secreted to improve the acquisition and utilization of Pi. PAPs are a family of metal-containing enzymes found in a wide range of plant species, which exhibit a variety of biological function including P foraging and recycling. In soybean, 23 out of 35 *GmPAP*s were induced by P starvation in different tissues, and nine of them were highly expressed in nodules, indicating that these PAPs may have roles in soybean symbiosis with rhizobia (Li et al., 2012). Recently, soybean *GmPAP21* is found to be induced by P starvation and enhances internal P utilization in nodules, suggesting a role in soybean symbiosis with rhizobia (Yuan and Liu, 2008; Li et al., 2017). Although members of PAPs have been studied in soybean, little is known about the function of PAPs in nodule development and nitrogen fixation under P starvation conditions except *GmPAP21*. Here, we exhibited a low P stress-induced PAP gene, *GmPAP12*, in soybean nodules. Functional analysis by overexpression or suppression

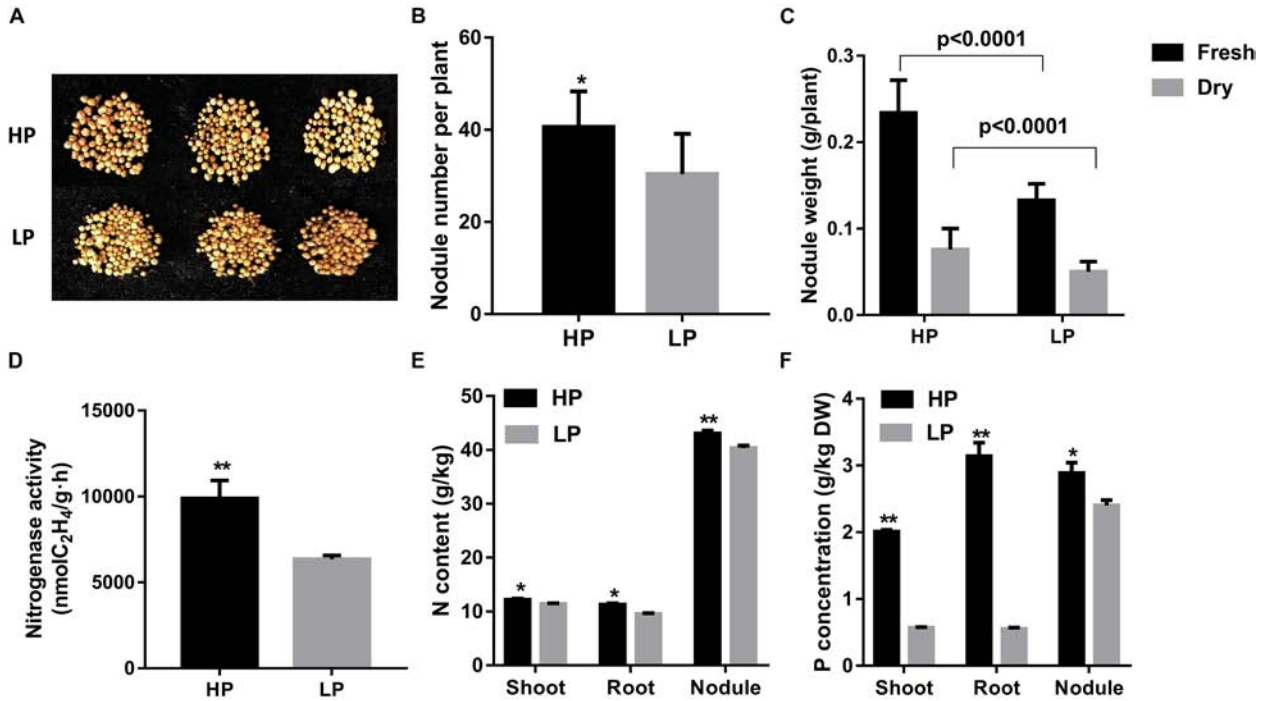

FIGURE 1 | Nodulation parameter analysis of soybean plant nodules treated by different P levels. **(A)** Photographs of plant nodule growth performance. **(B)** Nodule number. **(C)** Nodule total weight per plant. **(D)** Nitrogenase activities of nodules measured by acetylene reduction assay. **(E)** Nodule N content. **(F)** Nodule P content. Soybean plant samples were harvested 28 days after inoculation with rhizobium watered with nitrogen-free nutrient solution. Data are presented as the average of three different biological replicates and 20 plants for each replicate. Bars show the means ± SD values. Asterisks indicate significant difference within a P level in *t*-tests. $^{*}p < 0.05$, $^{**}p < 0.01$.

of *GmPAP12* in hairy root nodules showed that *GmPAP12* is involved in P homeostasis and nitrogen fixation under P starvation conditions.

MATERIALS AND METHODS

Plant Growth Conditions

Seeds of [*Glycine max* (L.) Merr.] cultivar Williams 82 were surface sterilized and germinated in Petri dishes with wet and sterile filter papers for 3 days under dark conditions in a growth chamber (28°C, 16/8 h light/dark photoperiod). After a 3 days germination, seedlings were transplanted in pots with vermiculite after being inoculated with *Bradyrhizobium diazoefficiens* USDA 110 (*Bradyrhizobium japonicum* USDA 110). Until the first trifoliate leaves were fully developed, soybean plants were watered with nitrogen-free nutrient solution containing 5 μM (low P:LP) and 500 μM (high P:HP) of KH_2PO_4, respectively. At 10, 17 days after inoculation with *B. diazoefficiens* USDA 110, only nodules were harvested. At 28 days, soybean leaves, roots, and nodules were separately harvested for measuring fresh weight, dry weight, height of shoot and root, total P and N content, nodule number and nodule size, phytase and phosphatase activities, and acetylene reduction assay; nodule size was calculated as the average fresh weight of a single nodule. For dry weight and total P and N content, samples were oven-dried, and other fresh samples were stored at −80°C for RNA extraction and quantitative real-time PCR (qRT-PCR) analysis.

RNA Isolation and RNA-Seq

Twenty-eight-day nodules collected with three independent biological replicates for each Pi treatment were ground in liquid nitrogen, and total RNA was extracted using TRIzol reagent (Invitrogen, United States). RNA purity was checked using the NanoPhotometer® spectrophotometer (IMPLEN, CA, United States), and RNA concentration was measured using Qubit® RNA Assay Kit in Qubit® 2.0 Flurometer (Life Technologies, CA, United States). RNA samples were treated with RNase-free DNase I (TaKaRa, Tokyo, Japan) to avoid genomic DNA contamination. cDNA was transcribed using a Prime Script™ RT reagent Kit (Perfect Real Time) with gDNA Eraser (TaKaRa Bio, Inc.). Six cDNA libraries were generated and sequenced on an Illumina NovaSeq 6000 platform. After quality control, a total of 25,155,773 clean reads were analyzed for differential expression of two conditions, which was performed using the DESeq R package (1.18.0). FPKM method was used to estimate gene expression levels. The resulting *p*-values were adjusted using the Benjamini and Hochberg approach for controlling the false discovery rate. Genes with an adjusted $p < 0.05$ found by DESeq were assigned as differentially expressed genes (DEGs).

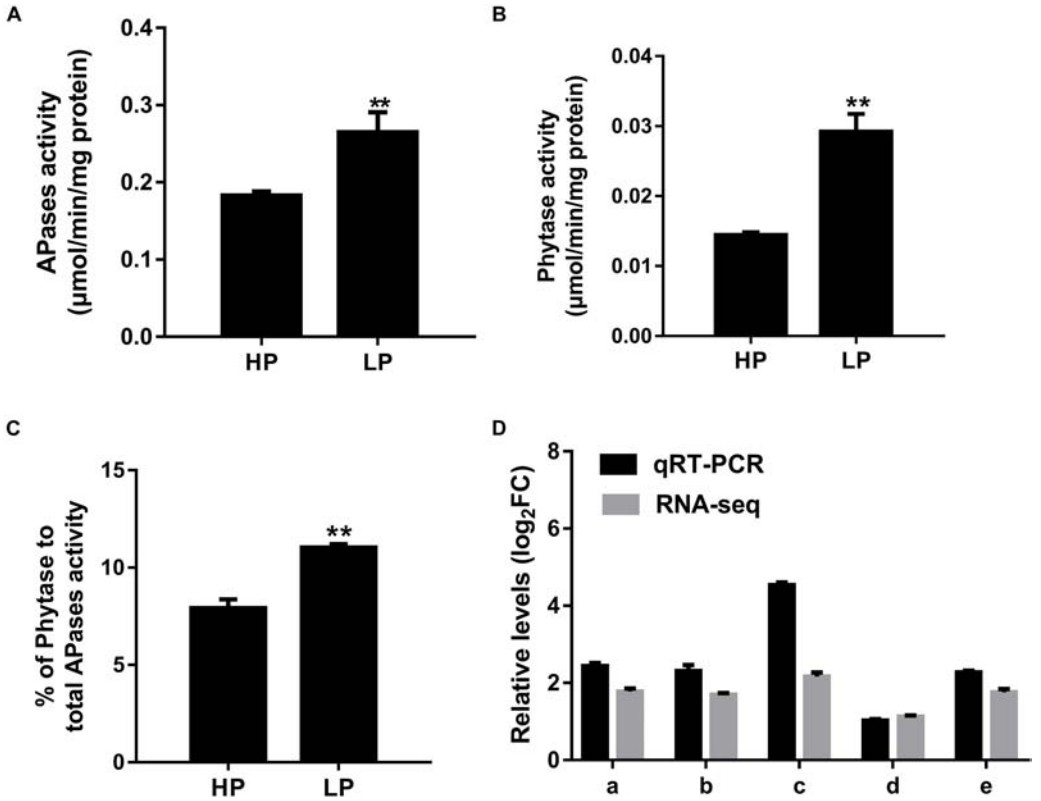

FIGURE 2 | Relative transcript levels and phytase and APase activities of *GmPAP*s in nodules obtained in low P (LP) and high P (HP) conditions. **(A)** Nodule APase activity. **(B)** Nodule phytase activity. **(C)** Percentage of phytase activity to total APases of nodules grown under different P conditions. Asterisks indicate significant difference within a P level in *t*-tests. $^{**}p < 0.01$. **(D)** A heatmap presentation of fold changes of *PAP*s identified from RNA-seq and qRT-PCR in LP conditions compared with HP conditions. qRT-PCR was performed using three different biological samples with three repeats for each sample. Phytase and APase activities were analyzed from four independent experiments, and average results were shown. For each repeat, five plants were used. (a) *Glyma.06G170300*-LP/*Glyma.06G170300*-HP, expression of *Glyma.06G170300* in nodules under P-deficient condition vs. P-sufficient conditions; (b) *Glyma.08G093500*-LP/*08G093500-HP*, expression of *Glyma.08G093500* in nodules under P-deficient condition vs. P-sufficient conditions; (c) *Glyma.06G028200*-LP/*06G028200*-HP, expression of *Glyma.06G028200* in nodules under P-deficient conditions vs. P-sufficient conditions; (d) *Glyma.05G247800*-LP/*Glyma.05G247800*-HP, expression of *Glyma.05G247800* in nodules under P-deficient condition vs. P-sufficient conditions; (e) *Glyma.07G191500*-LP/*Glyma.07G191500*-HP expression of *Glyma.07G191500* in nodules under P-deficient condition vs. P-sufficient conditions.

Quantitative Real-Time PCR

qRT-PCR was performed using SYBR Premix EX Tag^{TM} (TaKaRa) on a CFX96^{TM} real-time system (Bio-Rad). The soybean *Actin11* gene was used as an endogenous control to normalize the other samples. The specific primers used are shown in **Supplementary Table S2**. The qRT-PCR conditions were as follows: 30 s at 95°C followed by 40 cycles of 5 s at 95°C, 15 s at 60°C and 12 s at 72°C, and a final 5 s at 72°C. The cycle threshold (CT) values of each sample were standardized using *Actin11* gene, and the relative changes of gene expression were analyzed using the $2^{-\Delta\Delta CT}$ method (Livak and Schmittgen, 2001).

Construction of *GmPAP12* Promoter, Overexpression, and RNAi Constructs and Soybean Hairy Root Transformation

For the analysis of the *GmPAP12* promoter, 2,000-bp fragment upstream of *GmPAP12* transcription start codon was generated by PCR and cloned into the pBI121 vector between *Hin*dIII and *Bam*HI restriction enzyme site in-frame with *GUS* reporter gene to make *pGmPAPA12-GUS* construct. To generate overexpression construct, full-length open reading frame (ORF) of *GmPAP12* or *GmPHR1* was amplified using PCR from soybean root nodule cDNA and then cloned into pCAMBIA1390 under *CaMV 35S* promoter. For *RNAi* constructs, about 220 bp of sense and antisense fragments targeting *GmPAP12* or *GmPHR1* was cloned into pTCK-303 vector under *CaMV 35S* promoter (Du et al., 2016). Also, the corresponding constructs were transformed into *Agrobacterium rhizogenes* strain K599 for hairy root transformation. Transgenic hairy roots emerging from K599 infection site were examined for GUS expression. Only one GUS positive root was left, and all the other roots were cut in the plant root system. Then the plants were inoculated with *B. diazoefficiens* USDA 110 and grown in two different P conditions. At 28 days after rhizobium inoculation, nodules were harvested and analyzed for nodule number, nodule weight, nitrogenase activity, RNA isolation, N and P contents, and APase activity measurement (Kim et al., 2013; Li et al., 2017).

Acetylene Reduction Assay

Nitrogenase activity was measured by acetylene reduction assay; the method was used as described previously (Oh et al., 2001).

Measurement of N and P Contents

First, samples were dried, weighed, ground into fine powder, and then digested with HNO_3 in a microwave oven; the resulting samples were used for determination of N and P contents. P content was measured by the color reaction of P-molybdate blue at absorbance of 700 nm (Grunwald et al., 2009). N content was measured using semimicro-Kjeldahl determination method in a nitrogen analyzer.

TABLE 1 | Differentially expressed *GmPAP*s induced by low P stress in nodules.

	Gene_id	log_2 fold change	*p*-value	*p*-adj
GmPAPs	Glyma.06G170300	1.7044	3.59E–20	2.67E–16
	Glyma.08G093500	1.6811	2.67E–09	1.15E–06
	Glyma.05G247800	1.1965	6.40E–09	2.35E–06
	Glyma.07G191500	1.1877	1.90E–05	0.0016919
	Glyma.06G028200	1.9881	0.00010032	0.016771

E = 10, E–20 = 10^{-20}; pval = p-value; padj = p adjust = q-value.

Acid Phosphatase and Phytase Activity Measurements

APase activity of nodules was determined by measuring the amount of nitrophenol from *p*-nitrophenyl phosphate (*p*-NPP). Total nodule protein extracts were mixed with Na-acetate buffer containing 1 mM of *p*-NPP and incubated at 37°C for 30 min; the reaction was stopped by adding 1 M of NaOH. The absorbance was measured at 405 nm. APase activity was expressed as micromoles of *p*-NPP per minute per milligram of protein.

For phytase activities, total nodule proteins were added to a mixture containing 1 mmol/L of phytate and then incubated with malachite green reagent; the optical density (OD) values were measured at 650 nm. Phytase activity was calculated as micromoles of Pi released per minute per milligram of protein (Kong et al., 2019). All experiments were triplicate with five independent samples per replicate.

Yeast One-Hybrid Assay

Yeast one-hybrid (Y1H) experiment was performed using Matchmaker Gold Systems (Clontech). *GmPHR1* was cloned into PGADT7-AD vector (TaKaRa), and the resulting construct was named PGADT7-AD-*GmPHR1*. Three P1BS sequences were found in the promoter of *GmPAP12*: 5'-GTATATTC-3', 5'-GCATATTC-3', and 5'-GAATATTC-3'. Three tandem repeats of each P1BS element were synthesized and cloned into

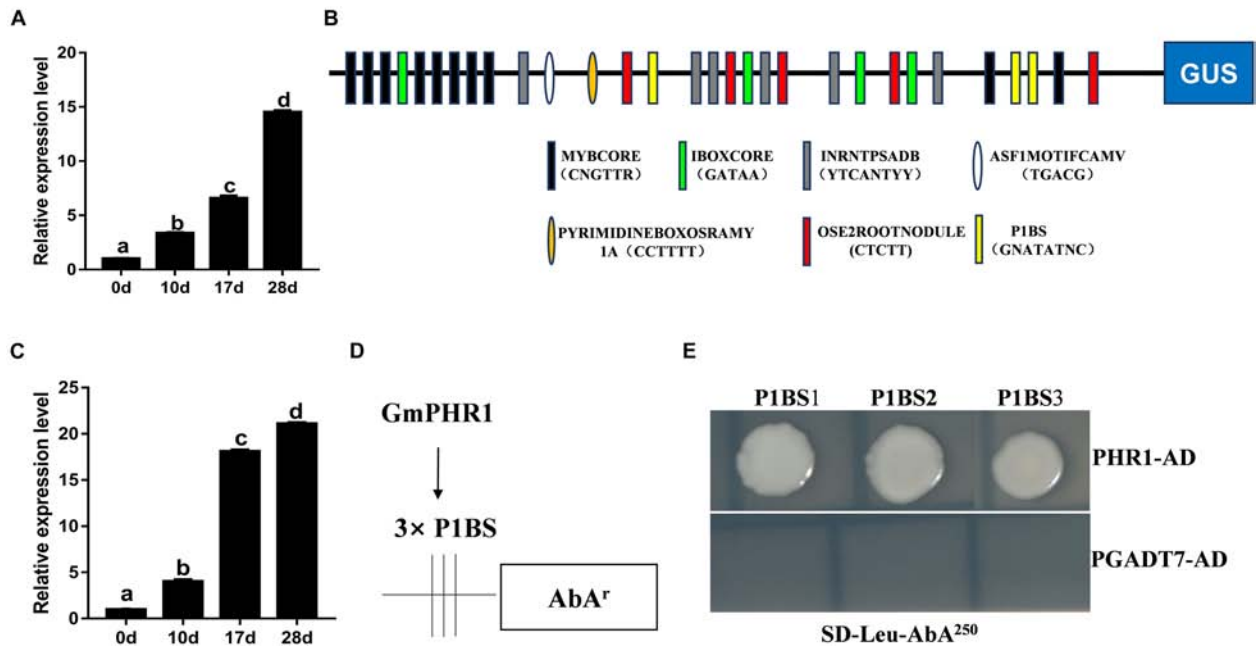

FIGURE 3 | Promoter analysis of *GmPAP12* in transgenic soybean nodules. **(A)** Expression of *GmPAP12* in nodules determined by qRT-PCR. **(B)** *cis*-Elements of *GmPAP12* promoter analyzed by PlantCARE. **(C)** Expression of *GmPHR1* in nodules determined by qRT-PCR. Nodules were harvested at 0, 10, 17, and 28 days post rhizobium inoculation in normal growth condition. **(D)** The diagram shows the construct of *GmPAP12* promoter for yeast one-hybrid (Y1H). **(E)** Y1H results. Three tandem repeats of each P1BS element were used as baits and cloned into pAbAi vector. The resulting pAbAi-3xP1BS vectors were transformed into Y1H cells expressing PGADT7-AD (negative control) or PGADT7-AD-GmPHR1, respectively. The transformants were grown on selective medium SD-Leu containing antibiotic AbA (250 μg/ml), and pictures were taken after 4 days of incubation at 30°C. The Y1H assays were repeated three times. Letters in **(A,C)** indicate significant differences (one-way ANOVA, $p < 0.05$).

pAbAi vector (TaKaRa) used as baits. The consequent pAbAi-3xP1BS vectors were digested with *Bst*BI (NEB, New England Biolabs) restriction enzyme and then transformed into Y1H cells containing PGADT7-AD (negative control) or PGADT7-AD-GmPHR1, respectively. The transformants were grown on selective medium SD-Leu containing antibiotic aureobasidin A (AbA) (250 μg/ml) for 4 days at 30°C. AbA is used as a stringent, highly selective reporter.

Histochemical GUS Staining Assay

To detect GUS activity in transgenic soybean root nodules, fresh root tissues were incubated at 37°C for 12 h in 5-bromo-4-chloro-3-indolyl-β-D-glucuronic acid (X-Gluc) containing solution (Zhong et al., 2013). After X-Gluc incubation, the root tissues were washed with ethanol (70% v/v), and then photographs were taken.

GUS Activity Assay

Total proteins of transgenic soybean root nodules were extracted and quantified as previously described (Freitas et al., 2019). GUS assay was performed in a mixture containing 10 mM of 4-methylumbelliferyl-β-D-glucuronide (MUG; Sigma, United States), and the mixture was incubated for 1 h at 37°C. The fluorescence product of 4-methylumbelliferone (4-MU) was monitored using a VersaFluor Fluorometer (Bio-Rad) with excitation at 365 nm and emission at 455 nm. GUS activity was calculated in picomoles of MU produced per minute per microgram of soluble protein. The assay was repeated at least three times. The results were shown as the mean of independent experiments with the respective standard deviation. Asterisks (**) above the bars indicate significant differences at $p < 0.01$.

Statistical Methods

Statistical analyses were performed using SPSS 17.0 software (IBM, United States).

RESULTS

Soybean Performance Was Significantly Reduced Under P-Deficient Conditions

The performance of soybean plants was assessed at 28 days post inoculation with rhizobium *Bradyrhizobium diazoefficiens* USDA 110 when the nodules of soybean are mature and are responsible for nitrogen fixation (Cheng et al., 2011; Ferguson et al., 2010; Zhang et al., 2014). In low P treatment, soybean growth was significantly affected with reduced plant height and yellow leaves in the base of the soybean plant (**Supplementary Figure S1A**). The root-to-shoot ratio of soybean plants was increased in the P-deficient supply, which was consistent with previously data in other plant species in low P conditions (**Supplementary Figure S1B**) (Lopez-Bucio et al., 2003; Gruber et al., 2013; Sun et al., 2014). Consequently, plant shoot and root growth were decreased in low P stress leading to reduced total (shoot, and root plus nodule) fresh weight and dry weight production by 29.2 and 26.2%, respectively, when compared with those in high P conditions (**Supplementary Figures S1C,D**). All these data suggested that P deficiency greatly affects soybean plant growth and biomass production in decreased P supply.

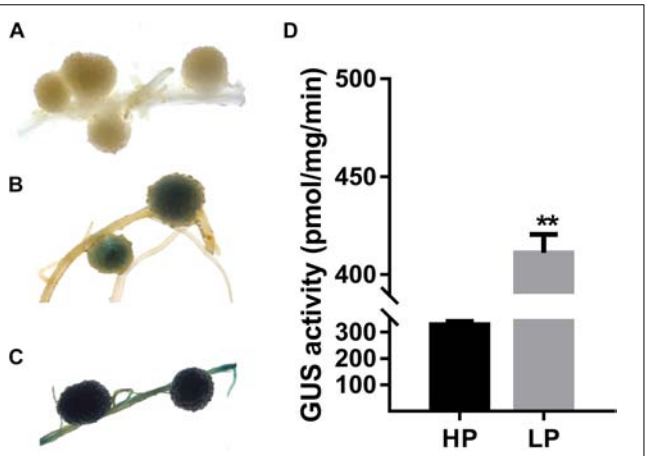

FIGURE 4 | Promoter analysis of *GmPAP12* gene in transgenic soybean nodules. **(A)** Histochemical GUS staining of wild-type (WT) nodules growing in low P (LP) conditions. **(B)** Histochemical GUS staining of *GmPAP12* promoter transgenic nodules growing in high P (HP) conditions. **(C)** Histochemical GUS staining of *GmPAP12* promoter in transgenic nodules growing in LP conditions. Promoter of *GmPAP12-GUS* transgenic composite soybean plants was treated with different P levels, and nodules were harvested 28 days after inoculation with rhizobia for GUS staining. **(D)** GUS activity of *GmPAP12* promoter in transgenic nodules. Values are means of 10 independent lines for each P treatment. Bars show the means ± SD values. Asterisks indicate significant difference within a P level in *t*-tests. $^{**}p < 0.01$.

Next, nodulation parameters were investigated here to know the effect of low P supply on nodule organogenesis. Significantly reduced soybean nodulation was observed in soybean plants under low P conditions (**Figure 1A**). Nodule number and nodule fresh and dry weight accumulation were greatly decreased by 25.0, 41.6, and 33.3%, respectively, in P-deficient conditions compared with high P conditions (**Figures 1B,C**). Moreover, nitrogenase activity of nodules was dramatically affected and reduced by 58% in low P stress conditions (**Figure 1D**). These results further illustrated that low P supply affected nodule growth and development as well as N_2 fixation in soybean. Next, N assimilation was evaluated in different organs (shoot, root, and nodules) and was found to be decreased under P depletion stress (**Figure 1E**). P content in shoot and root was dramatically reduced by 72.5 and 82.2% respectively, although in nodules, it was decreased by only 20.8%, which was less strong in low P stress than in high P conditions (**Figure 1F**). These data suggested that low P supply affected soybean nodulation and that P homeostasis was very important for soybean growth and symbiotic N_2 fixation.

Purple Acid Phosphatase Genes Were Highly Induced in Low P Stress in Soybean Nodules

Under low P stress, APases and phytase are always induced and secreted. Here, with regard to APase and phytase activities of

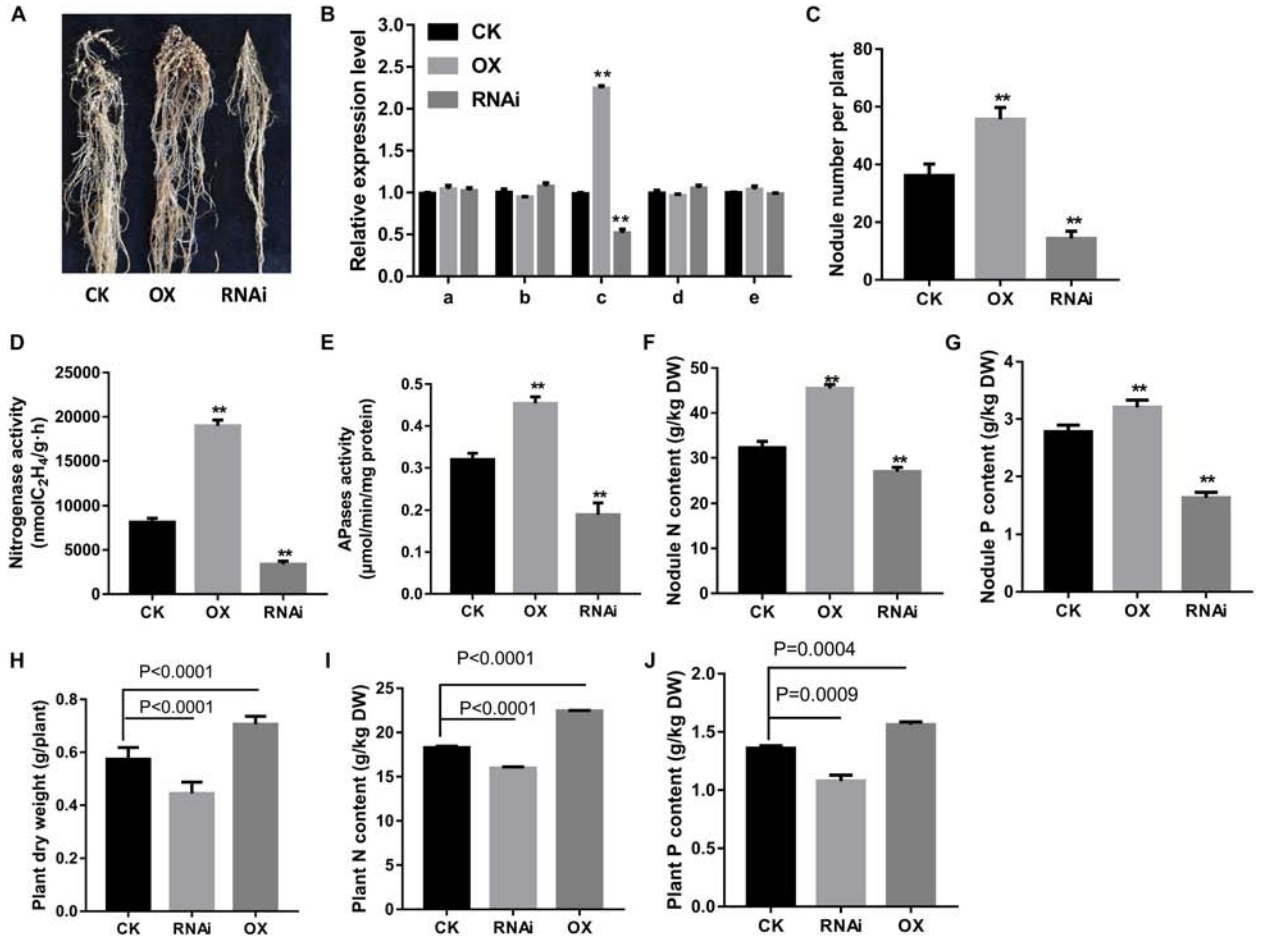

FIGURE 5 | Effects of *GmPAP12* on nodulation in *GmPAP12* overexpressing (OX) or suppressing (*RNAi*) transgenic composite lines. **(A)** Nodule performance. **(B)** Relative transcript levels of PAPs in nodules. **(C)** Nodule number. **(D)** Nitrogenase activity. **(E)** APase activity. **(F)** Nodule N content. **(G)** Nodule P content. **(H)** Plant shoot dry weight. **(I)** Plant N content. **(J)** Plant P content. *GmPAP12* OX or RNAi transgenic composite plants were examined 28 days after inoculation with rhizobia in low P conditions watered with N-free nutrient solution. Data are presented as the average of three different biological replicates and 20 plants for each replicate. Bars show the means ± SD values. Asterisks indicate significant difference within a P level in *t*-tests. $^{**}p < 0.01$. CK means control.

soybean nodules under low P conditions, we found that APase and phytase activities were greatly increased by about 50.0 and 100%, respectively, than in high P conditions (**Figures 2A,B**). Further, the percentage of phytase activity to total APase activity was also raised by 36.6%, which indicates increased PAP activities under phosphorus deficiency (**Figure 2C**).

In order to investigate the mechanisms at molecular level for the enhanced APase and phytase activities in soybean nodules under low P conditions, RNA sequencing was conducted to elucidate the transcriptome of soybean mature nodules. As expected, five PAP genes were greatly up-regulated, which could explain the increased phytase and APase activities indicating importance of Pi remobilization and recycling activities in soybean nodules under low P conditions (**Table 1**). Transcripts of these PAPs in nodules were verified via qRT-PCR, and all the PAPs here were largely induced under P starvation conditions compared with high P conditions, which was consistent with RNA-seq results (**Figure 2D**).

GmPAP12 Plays Essential Roles in Nodule Development Under P Deficiency

In order to explore the effects of PAPs on soybean nodulation further, *Glyma.06G028200*, which was named *GmPAP12* according to the genome of soybean (the Phytozome website)[1], was chosen for further study owing to its highest expression level among these five PAPs in nodules induced by low P stress. First, the expression pattern of *GmPAP12* was checked and increasingly expressed during nodule development in normal growth conditions, which suggested that *GmPAP12* might be involved in soybean nodulation and nitrogen fixation (**Figure 3A**). Next, promoter of *GmPAP12* was analyzed using a promoter analysis program PlantCARE, and several *cis*-elements within 2-kb sequence upstream of start codon were found to respond to stress, gibberellin, photosynthesis, light, and so on (**Supplementary Table S1** and **Figure 3B**). Three P1BS

[1]https://phytozome.jgi.doe.gov/pz/portal.html

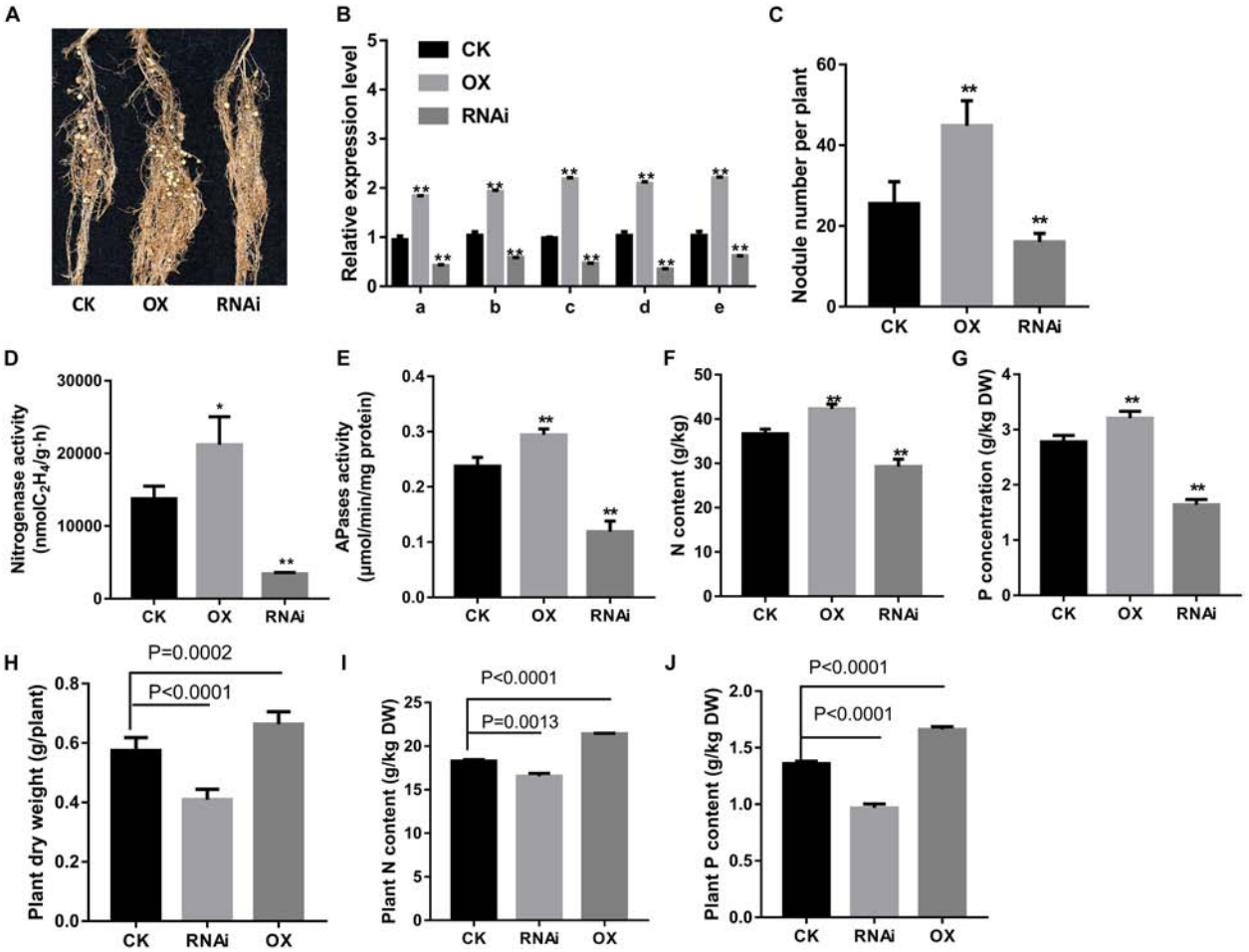

FIGURE 6 | Effects of *GmPHR1* on nodulation in *GmPHR1* overexpressing (OX) or suppressing (*RNAi*) transgenic composite lines. **(A)** Nodule performance. **(B)** Relative transcript levels of PAPs in nodules. **(C)** Nodule number. **(D)** Nitrogenase activity. **(E)** APase activity. **(F)** Nodule N content. **(G)** Nodule P content. **(H)** Plant shoot dry weight. **(I)** Plant N content. **(J)** Plant P content. *GmPAP12* OX or RNAi transgenic composite plants were examined 28 days after inoculation with rhizobia in low P conditions watered with N-free nutrient solution. Data are presented as the average of three different biological replicates and 20 plants for each replicate. Bars show the means ± SD values. Asterisks indicate significant difference in LP conditions in *t*-tests. $^{*}p < 0.05$, $^{**}p < 0.01$. CK means control.

cis-elements present in the promoter of *GmPAP12* suggested that GmPHR1 may directly bind to and regulate *GmPAP12*. To test this hypothesis, *Glyma.19G122700* (Accession No. HQ007311) named *GmPHR1* in our previous study was used for further research (Li et al., 2014). qRT-PCR showed that the transcript pattern of *GmPHR1* was similar with that of *GmPAP12* during the process of nodule growth (**Figure 3C**). A Y1H assay was performed against all the three P1BS sequences from *GmPAP12* promoter, and results showed that GmPHR1 can directly bind to all the three P1BS elements, indicating the regulation of *GmPAP12* by GmPHR1 in the transcript level during nodule development (**Figures 3D,E**).

Next, expression of *GmPAP12* was confirmed by *GmPAP12* promoter:*GUS* construct in transgenic composite root nodules under P starvation conditions. Visual GUS staining was observed in transgenic mature nodules with about 36.5% higher GUS activity in low P stress than in P-sufficient conditions (**Figure 4**). Furthermore, the functional analysis of transgenic composite root nodules either overexpressing (OX) or suppressing (RNAi) *GmPAP12* was generated, and the related phenotypes were evaluated in low P conditions only (**Figure 5A**). First, qRT-PCR demonstrated that the transcript level of *GmPAP12* in OX transgenic root nodules was about 120% higher, whereas in *GmPAP12*, RNAi transgenic nodules showed only 50% lower expression than those of control (CK) lines under P-deficient conditions, while the expression of the other four PAP genes was unchanged (**Figure 5B**). The total nodule number, and nodule nitrogenase and APase activities of *GmPAP12* OX composite lines were increased by 44.8, 100, and 38.7%, respectively, resulting in increased N content by 17.0% and P content by 19.0%, whereas in *GmPAP12*, RNAi composite lines, the total nodule number, and nitrogenase and APase activities decreased by 51.2, 50.0, and 40.1%, respectively, when compared with those of control lines in low P stress, resulting in decreased N and P contents by 33.6 and 37.0%, respectively (**Figures 5C–G**). These data indicated that *GmPAP12* can enhance P utilization efficiency and nodule

nitrogen fixation. Next, the effect of low P stress on *GmPAP12* OX or RNAi whole transgenic composite plants was analyzed. The plant shoot dry weight and N and P contents in *GmPAP12* OX transgenic composite plants were increased by 22.9, 22.8, and 14.8%, respectively, whereas *GmPAP12* RNAi transgenic composite plant shoot dry weight and N and P contents were decreased by 22.5, 12.6, and 14.8% compared with those of control plants in low P stress. All these data indicated that altering *GmPAP12* gene expression could significantly influence soybean nodulation and nitrogen fixation capacity as well as plant growth performance in low P stress (**Figures 5H–J**).

GmPAP12 Is Mainly Regulated by GmPHR1 Under P Starvation Conditions

Next, in order to elucidate the regulation of *GmPAP12* by GmPHR1 underlying transcript response to low P stress in nodules, a function of GmPHR1 was further analyzed in transgenic composite soybean plants. It showed significantly increased and decreased expression of *GmPAP12* as well as the other four PAPs in *GmPHR1* OX and RNAi transgenic composite nodules, respectively, compared with control nodules in low P stress. The *GmPHR1* OX lines showed significantly improved nitrogen fixation capacity proved by increased nodule performance, nodule number, and nitrogenase and APase activities, which led to the significantly increased N and P contents, whereas *GmPHR1* RNAi lines had much lower nitrogen fixation than had control nodules in low P conditions (**Figures 6A–G**). These data indicated that *GmPHR1* can also enhance P utilization efficiency and nodule development and regulate the expression of these five PAPs. Next, the effect of low P stress on *GmPHR1* OX or RNAi whole transgenic composite plants was analyzed. The plant shoot dry weight and N and P contents in *GmPHR1* OX transgenic composite plants were increased by 15.7, 17.1, and 22.2%, respectively, whereas *GmPHR1* RNAi transgenic composite plants showed decreased plant shoot dry weight and N and P contents by 28.7, 9.6, and 24.6% than did control plants in low P stress. All these data indicated that altering *GmPHR1* gene expression could significantly influence soybean nodulation and nitrogen fixation capacity as well as plant growth performance by regulating PAPs in low P stress. Also these data further illustrated that *GmPAP12* facilitates nodule development as well as nitrogen fixation mainly regulated by GmPHR1 under low P conditions.

DISCUSSION

Nitrogen is a component of biological molecules in plants, which are critical for sustained plant development. In agriculture, nitrogen available is becoming a constraint on crop yield and reproduction. Although there is plenty of nitrogen in the atmosphere, it is not directly available for plants. Legume plants such as soybean can have a symbiotic association with nitrogen-fixing bacteria called rhizobia, resulting in the formation of nodule, which is responsible for biological nitrogen fixation. P deficiency significantly affected N_2 fixation documented in nodules of chickpea, *Medicago truncatula*, soybean, and common bean. Additionally, the secretion of PAPs in plants is a widely known as an adaptation strategy in response to P deficiency. Under low P conditions, in nodules of *M. truncatula*, chickpea, and soybean, they were found to be differentially upregulated by RNA-seq transcriptome analysis, which indicates that nodules acclimated to P deficiency by increasing P turnover (Cabeza et al., 2014; Nasr Esfahani et al., 2017; Xue et al., 2018).

In this work, consistent with the significantly increased APase activity in soybean nodules under P deficiency, five PAP genes were found among the DEG in RNA-seq data, indicating that PAPs play vital role in P metabolism and mobilization in soybean nodules (**Table 1** and **Figure 2D**). Although functions of PAPs in soybean have been studied, including *GmPAP3* and *GmPAP4*, roles of P starvation-induced PAPs in nodules need to be more explored. Recently, *GmPAP21* was proved to be highly induced in nodules by P limitation, which indicated that the involvement of *GmPAP21* in internal P metabolism and overexpression of *GmPAP21* significantly decreased plant dry weight and N and P contents, thus inhibiting nodule growth (Li et al., 2017). Here, expression of *GmPAP12* was notably increased during nodule development, and GUS activity driven by the promoter of *GmPAP12* was also more induced in nodules as well as roots under P starvation compared with P-sufficient conditions (**Figures 3A**, **4**). Furthermore, the functional analysis of transgenic hairy root nodules in *GmPAP12* OX lines showed increased plant shoot dry weight and N and P contents, which indicated that *GmPAP12* promoted nodule development and nitrogen fixation under low P conditions (**Figure 5**). These data indicate that *GmPAP12* is involved in P utilization and integrates the SNF and P metabolism signaling in nodules under P starvation situation.

Nodules require much more P for legume nodulation and SNF, so the P content in nodules is relatively high. Under low P conditions, P is preferentially relocated from other organs to nodules to maintain nitrogen fixation, indicating that P homeostasis is very important in the nodule. In soybean, in low P stress growing in hydroponic conditions, P content in both leaves and roots are 10 times higher in high P than in low P treatment, whereas in nodules, only 1.75 times are increased (Sulieman et al., 2010; Qin et al., 2012). In this study, with regard to P content, it was much less affected in nodules than in shoot and root in P deficiency, suggesting that nodules represent a P sink to maintain Pi homeostasis and the ability of N_2 fixation during nodule development; it is hypothesized that nodules try to regulate N_2 fixation process to adaptation to low P stress by allocating P from other organs to nodules (Cabeza et al., 2014; Xue et al., 2018).

Previous research also showed that increase in the exudation and APase activity of PAPs is one of the strategies for plants to increase P recycling in nodules (Li et al., 2012). Also, in nodules of common bean at limited P conditions, activities of APase increased, indicating that nitrogen fixation can enhance P utilization in nodules in response to P deficiency (Araújo et al., 2008; Mandri et al., 2012; Makoudi et al., 2018). In this study, APase activities of nodules in low P conditions were also greatly increased in *GmPAP12* OX transgenic composite nodules, indicating that *GmPAP12* is responsible for P homoeostasis

in nodules (**Figure 5A**). In high P conditions, *GmPAP12* showed increasing expression during nodule development, which suggested that *GmPAP12* might be involved in nodulation and nitrogen fixation beyond P recycling (**Figure 3A**). All these data suggest that GmPAP12 plays a role in nodulation and sustains nitrogen fixation in low P conditions.

PHR1, a transcription factor mainly studied well in *Arabidopsis* and rice, is playing a key role in P starvation signaling by binding to the P1BS element in the promoters of PSI genes (Rubio et al., 2001; Zhou et al., 2008). Under P-deficient conditions, overexpression of PHR1 results in induction of PSI genes and cellular P accumulation, whereas loss of function of PHR1 reduces expression of PSI genes and accumulation of anthocyanins, which are typical symptoms in plants under P starvation (Nilsson et al., 2007). Recently, in *Arabidopsis*, evidence indicates that P starvation-induced APase *AtPAP10* was regulated by AtPHR1, which binds to the only P1BS element of *AtPAP10* promoter. In this study, the promoter analysis indicates that *GmPAP12* contains three P1BS elements, and Y1H confirmed that GmPHR1 can bind to all the three P1BS elements (**Figures 3D,E** and **Supplementary Table S1**). In *GmPHR1* OX or RNAi transgenic nodules, expression of *GmPAP12* was also greatly affected under P starvation conditions. These data indicate under P starvation conditions that *GmPAP12* functions in nodulation and that nitrogen fixation is transcriptionally regulated by *GmPHR1* (**Figure 3E**). Also, expression of *GmPHR1* was gradually increasing in nodules in normal growth conditions, indicating that *GmPHR1* functions in nodule development also beyond P utilization. In *GmPHR1* OX or RNAi transgenic composite plants, plant shoot dry weight and N and P contents were increased or decreased, respectively, which suggested that *GmPHR1* is involved in nitrogen fixation process dealing with low P stress (**Figures 3C**, **6**).

Previous evidence indicates that PHR1 was expressed in normal conditions and not responsive to P starvation (Rubio et al., 2001; Zhou et al., 2008). Also, their function in P signaling is modulated by SPX4 protein regulating the targeting of PHR1 from cytoplasm to nucleus (Lv et al., 2014). In our mRNA-seq data, several *Arabidopsis PHR1* homolog *PHR1* genes were identified in soybean nodules, and none of them showed response to Pi starvation. Expression of five *GmPHR1* genes was confirmed by RT-PCR, and also no significant expression changes were detected between P-sufficient and P-deficient conditions (**Supplementary Figure S2**). This suggested in nodules that it also has SPX-containing proteins or others to interact with PHR1 to regulate downstream PSI genes such as *GmPAP12*, so our further study is going to identify interacting partners of PHR1 in nodules and explore more about the molecular mechanism underlying the relationship between nitrogen fixation capacity and P availability, which will help the development of more efficient soybean plants.

DATA AVAILABILITY STATEMENT

The datasets generated for this study can be found in the NCBI BioProject, https://www.ncbi.nlm.nih.gov/bioproject/PRJNA605671.

AUTHOR CONTRIBUTIONS

CZ, HD, YW, and ZY conceived of and designed the research. YW, ZY, and HD performed the entirety of the experiment and analyzed the data. HD wrote the manuscript. XL and WL provided suggestions during all the processes of the experiments. All authors participated in the revision of the manuscript.

FUNDING

This research was funded by the Project of Hebei Province Science and Technology Support Program (17927670H and 16227516D-1) and Hebei Agricultural University special support program for the introduction of oversea doctor (ZD201602).

ACKNOWLEDGMENTS

We are very thankful to Professor Zhiying Ma for the critical advice on this manuscript.

SUPPLEMENTARY MATERIAL

The Supplementary Material for this article can be found online at: https://www.frontiersin.org/articles/10.3389/fpls.2020.00450/full#supplementary-material

REFERENCES

Araújo, A. P., Plassard, C., and Drevon, J. J. (2008). Phosphatase and phytase activities in nodules of common bean genotypes at different levels of phosphorus supply. *Plant Soil* 312, 129–138.

Cabeza, R. A., Liese, R., Lingner, A., von Stieglitz, I., Neumann, J., Salinas-Riester, G., et al. (2014). RNA-seq transcriptome profiling reveals that Medicago truncatula nodules acclimate N-2 fixation before emerging P deficiency reaches the nodules. *J. Exp. Bot.* 65, 6035–6048.

Cheng, X. G., Wang, L., Wang, H., Yu, G. H., Ba, Y. L., and Liu, M. M. (2011). Specific expression of a novel nodulin GmN479 gene in the infected cells of soybean (Glycine max) nodules. *Agr. Sci. China* 10, 1512–1524.

Diedhiou, I., and Diouf, D. (2018). Transcription factors network in root endosymbiosis establishment and development. *World J. Microb. Biot.* 4:37.

Du, Y., He, W., Deng, C., Chen, X., Gou, L., Zhu, F., et al. (2016). Flowering-related RING Protein 1 (FRRP1) regulates flowering time and yield potential by Affecting Histone H2B monoubiquitination in rice (Oryza Sativa). *PloS One* 11:e0150458. doi: 10.1371/journal.pone.0150458

Ferguson, B. J., Indrasumunar, A., Hayashi, S., Lin, M. H., Lin, Y. H., Reid, D. E., et al. (2010). Molecular analysis of legume nodule development and autoregulation. *J. Integrat Plant Biol.* 52, 61–76. doi: 10.1111/j.1744-7909.2010.00899.x

Ferguson, B. J., Mens, C., Hastwell, A. H., Zhang, M., Su, H., Jones, C. H., et al. (2019). Legume nodulation: the host controls the party. *Plant Cell Environ.* 42, 41–51. doi: 10.1111/pce.13348

Franco-Zorrilla, J. M., Gonzalez, E., Bustos, R., Linhares, F., Leyva, A., and Paz-Ares, J. (2004). The transcriptional control of plant responses to phosphate limitation. *J. Exp. Bot.* 55, 285–293.

Freitas, E. O., Melo, B. P., Lourenco-Tessutti, I. T., Arraes, F. B. M., Amorim, R. M., Lisei-de-Sa, M. E., et al. (2019). Identification and characterization of the GmRD26 soybean promoter in response to abiotic stresses: potential tool for biotechnological application. *BMC Biotechnol.* 19:79. doi: 10.1186/s12896-019-0561-3

Gruber, B. D., Giehl, R. F., Friedel, S., and von Wiren, N. (2013). Plasticity of the *Arabidopsis* root system under nutrient deficiencies. *Plant Physiol.* 163, 161–179. doi: 10.1104/pp.113.218453

Grunwald, U., Guo, W., Fischer, K., Isayenkov, S., Ludwig-Muller, J., Hause, B., et al. (2009). Overlapping expression patterns and differential transcript levels of phosphate transporter genes in arbuscular mycorrhizal. Pi-fertilised and phytohormone-treated Medicago truncatula roots. *Planta* 229, 1023–1034. doi: 10.1007/s00425-008-0877-z

Hernandez, G., Valdes-Lopez, O., Ramirez, M., Goffard, N., Weiller, G., Aparicio-Fabre, R., et al. (2009). Global changes in the transcript and metabolic profiles during symbiotic nitrogen fixation in phosphorus-stressed common bean plants. *Plant Physiol.* 151, 1221–1238. doi: 10.1104/pp.109.143842

Hogh-Jensen, H., Schjoerring, J. K., and Soussana, J. F. (2002). The influence of phosphorus deficiency on growth and nitrogen fixation of white clover plants. *Ann. Bot. Lond.* 90, 745–753.

Isidra-Arellano, M. C., Reyero-Saavedra, M. D. R., Sanchez-Correa, M. D. S., Pingault, L., Sen, S., Joshi, T., et al. (2018). Phosphate deficiency negatively affects early steps of the symbiosis between common bean and rhizobia. *Genes* 9:498. doi: 10.3390/genes9100498

Jain, A., Nagarajan, V. K., and Raghothama, K. G. (2012). Transcriptional regulation of phosphate acquisition by higher plants. *Cell Mol. Life Sci.* 69, 3207–3224. doi: 10.1007/s00018-012-1090-6

Kim, Y. K., Kim, S., Um, J. H., Kim, K., Choi, S. K., Um, B. H., et al. (2013). Functional implication of beta-carotene hydroxylases in soybean nodulation. *Plant Physiol.* 162, 1420–1433. doi: 10.1104/pp.113.215020

Kong, Y., Wang, B., Du, H., Li, W., Li, X., and Zhang, C. (2019).). GmEXLB1, a soybean expansin-like b gene, alters root architecture to improve phosphorus acquisition in *Arabidopsis*. *Front. Plant Sci.* 10:808. doi: 10.3389/fpls.2019.00808

Li, C., Li, C., Zhang, H., Liao, H., and Wang, X. (2017). The purple acid phosphatase GmPAP21 enhances internal phosphorus utilization and possibly plays a role in symbiosis with rhizobia in soybean. *Physiol. Plant.* 159, 215–227. doi: 10.1111/ppl.12524

Li, C. C., Gui, S. H., Yang, T., Walk, T., Wang, X. R., and Liao, H. (2012). Identification of soybean purple acid phosphatase genes and their expression responses to phosphorus availability and symbiosis. *Ann. Bot. Lond.* 109, 275–285. doi: 10.1093/aob/mcr246

Li, X. H., Wang, Y. J., Wu, B., Kong, Y. B., Li, W. L., Chang, W. S., et al. (2014). GmPHR1, a novel homolog of the AtPHR1 transcription factor, plays a role in plant tolerance to phosphate starvation. *J. Integr. Agr.* 13, 2584–2593.

Liang, C. Y., Wang, J. X., Zhao, J., Tian, J., and Liao, H. (2014). Control of phosphate homeostasis through gene regulation in crops. *Curr. Opin. Plant Biol.* 21, 59–66. doi: 10.1016/j.pbi.2014.06.009

Livak, K. J., and Schmittgen, T. D. (2001). Analysis of relative gene expression data using real-time quantitative PCR and the 2(-Delta Delta C(T)) Method. *Methods* 25, 402–408.

Lopez-Bucio, J., Cruz-Ramirez, A., and Herrera-Estrella, L. (2003). The role of nutrient availability in regulating root architecture. *Curr. Opin. Plant Biol.* 6, 280–287.

Lv, Q., Zhong, Y., Wang, Y., Wang, Z., Zhang, L., Shi, J., et al. (2014). SPX4 negatively regulates phosphate signaling and homeostasis through its interaction with PHR2 in rice. *Plant Cell* 26, 1586–1597.

Makoudi, B., Kabbadj, A., Mouradi, M., Amenc, L., Domergue, O., Blair, M., et al. (2018). Phosphorus deficiency increases nodule phytase activity of faba bean-rhizobia symbiosis. *Acta Physiol. Plant* 40:63.

Mandri, B., Drevon, J. J., Bargaz, A., Oufdou, K., Faghire, M., Plassard, C., et al. (2012). Interactions between common bean genotypes and rhizobia strains isolated from moroccan soils for growth, phosphatase and phytase activities under phosphorus deficiency conditions. *J. Plant Nutr.* 35,1477–1490.

Marx, H., Minogue, C. E., Jayaraman, D., Richards, A. L., Kwiecien, N. W., Siahpirani, A. F., et al. (2016). A proteomic atlas of the legume Medicago truncatula and its nitrogen-fixing endosymbiont Sinorhizobium meliloti. *Nat. Biotechnol.* 34, 1198–1205. doi: 10.1038/nbt.3681

Nasr Esfahani, M., Inoue, K., Chu, H. D., Nguyen, K. H., Van Ha, C., Watanabe, Y., et al. (2017). Comparative transcriptome analysis of nodules of two Mesorhizobium-chickpea associations with differential symbiotic efficiency under phosphate deficiency. *Plant J Cell Mo. Biol.* 91, 911–926. doi: 10.1111/tpj.13616

Nilsson, L., Muller, R., and Nielsen, T. H. (2007). Increased expression of the MYB-related transcription factor, PHR1, leads to enhanced phosphate uptake in *Arabidopsis thaliana*. *Plant Cell Env.* 30, 1499–1512.

Oh, H. S., Son, O., Chun, J. Y., Stacey, G., Lee, M. S., Min, K. H., et al. (2001). The *Bradyrhizobium japonicum hsfA* gene exhibits a unique developmental expression pattern in cowpea nodules. *Mol. Plant Microbe Interact.* 14, 1286–1292. doi: 10.1094/MPMI.2001.14.11.1286

Oldroyd, G. E. (2007). Plant science. Nodules and hormones. *Science* 315, 52–53.

Oldroyd, G. E., and Downie, J. A. (2008). Coordinating nodule morphogenesis with rhizobial infection in legumes. *Annu. Rev. Plant Biol.* 59, 519–546. doi: 10.1146/annurev.arplant.59.032607.092839

Qin, L., Zhao, J., Tian, J., Chen, L. Y., Sun, Z. A., Guo, Y. X., et al. (2012). The high-affinity phosphate transporter GmPT5 regulates phosphate transport to nodules and nodulation in soybean. *Plant Physiol.* 159, 1634–1643. doi: 10.1104/pp.112.199786

Rubio, V., Linhares, F., Solano, R., Martin, A. C., Iglesias, J., Leyva, A., et al. (2001). A conserved MYB transcription factor involved in phosphate starvation signaling both in vascular plants and in unicellular algae. *Genes Dev.* 15, 2122–2133.

Schulze, J. (2004). How are nitrogen fixation rates regulated in legumes? *J. Plant Nutr. Soil Sc.* 167, 125–137.

Schulze, J., Temple, G., Temple, S. J., Beschow, H., and Vance, C. P. (2006). Nitrogen fixation by white lupin under phosphorus deficiency. *Ann. Bot. Lond.* 98, 731–740.

Sulieman, S., Fischinger, S. A., Gresshoff, P. M., and Schulze, J. (2010). Asparagine as a major factor in the N-feedback regulation of N2 fixation in Medicago truncatula. *Physiol. Plant* 140, 21–31. doi: 10.1111/j.1399-3054.2010.01380.x

Sulieman, S., and Tran, L. S. (2015). Phosphorus homeostasis in legume nodules as an adaptive strategy to phosphorus deficiency. *Plant Sci.* 239, 36–43. doi: 10.1016/j.plantsci.2015.06.018

Sun, H., Tao, J., Liu, S., Huang, S., Chen, S., Xie, X., et al. (2014). Strigolactones are involved in phosphate- and nitrate-deficiency-induced root development and auxin transport in rice. *J. Exp. Bot.* 65, 6735–6746. doi: 10.1093/jxb/eru029

Sun, L., Song, L., Zhang, Y., Zheng, Z., and Liu, D. (2016). *Arabidopsis* PHL2 and PHR1 Act redundantly as the key components of the central regulatory system controlling transcriptional responses to phosphate starvation. *Plant Physiol.* 170, 499–514. doi: 10.1104/pp.15.01336

Tang, C., Hinsinger, P., Drevon, J. J., and Jaillard, B. (2001). Phosphorus deficiency impairs early nodule functioning and enhances proton release in roots of Medicago truncatula L. *Ann. Bot. Lond.* 88, 131–138.

Valentine, A. J., Kleinert, A., and Benedito, V. A. (2017). Adaptive strategies for nitrogen metabolism in phosphate deficient legume nodules. *Plant Sci.Int. J. Exp. Plant Biol.* 256, 46–52. doi: 10.1016/j.plantsci.2016.12.010

Vance, C. P., Uhde-Stone, C., and Allan, D. L. (2003). Phosphorus acquisition and use: critical adaptations by plants for securing a nonrenewable resource. *New Phytol.* 157, 423–447.

Wu, P., Shou, H. X., Xu, G. H., and Lian, X. M. (2013). Improvement of phosphorus efficiency in rice on the basis of understanding phosphate signaling and homeostasis. *Curr. Opin. Plant Biol.* 16, 205–212. doi: 10.1016/j.pbi.2013.03.002

Xue, Y., Zhuang, Q., Zhu, S., Xiao, B., Liang, C., Liao, H., et al. (2018). Genome wide transcriptome analysis reveals complex regulatory mechanisms underlying phosphate homeostasis in soybean nodules. *Int. J. Mol. Sci.* 19:2924. doi: 10.3390/ijms19102924

Yuan, H., and Liu, D. (2008). Signaling components involved in plant responses to phosphate starvation. *J. Integrat. Plant Biol.* 50, 849–859. doi: 10.1111/j.1744-7909.2008.00709.x

Yuan, S. L., Li, R., Chen, H. F., Zhang, C. J., Chen, L. M., Hao, Q. N., et al. (2017). RNA-Seq analysis of nodule development at five different developmental stages of soybean (Glycine max) inoculated with Bradyrhizobium japonicum strain 113-2. *Sci. Rep.* 7:42248. doi: 10.1038/srep42248

Zhang, J., Zhou, X., Xu, Y., Yao, M., Xie, F., Gai, J., et al. (2016). Soybean SPX1 is an important component of the response to phosphate deficiency for phosphorus homeostasis. *Plant Sci.Int. J. Exp. Plant Biol.* 248, 82–91. doi: 10.1016/j.plantsci.2016.04.010

Zhang, S., Wang, Y., Li, K., Zou, Y., Chen, L., and Li, X. (2014). Identification of Cold-Responsive miRNAs and their target genes in nitrogen-fixing nodules of soybean. *Int. J. Mol. Sci.* 15, 13596–13614. doi: 10.3390/ijms150813596

Zhong, L., Zhou, W., Wang, H., Ding, S., Lu, Q., Wen, X., et al. (2013). Chloroplast small heat shock protein HSP21 interacts with plastid nucleoid protein pTAC5 and is essential for chloroplast development in *Arabidopsis* under heat stress. *Plant cell* 25, 2925–2943. doi: 10.1105/tpc.113.111229

Zhou, J., Jiao, F., Wu, Z., Li, Y., Wang, X., He, X., et al. (2008). OsPHR2 is involved in phosphate-starvation signaling and excessive phosphate accumulation in shoots of plants. *Plant Physiol.* 146, 1673–1686. doi: 10.1104/pp.107.111443

Conflict of Interest: The authors declare that the research was conducted in the absence of any commercial or financial relationships that could be construed as a potential conflict of interest.

frontiers in Plant Science

ORIGINAL RESEARCH
published: 14 August 2019
doi: 10.3389/fpls.2019.01018

Plant Diversity and Fertilizer Management Shape the Belowground Microbiome of Native Grass Bioenergy Feedstocks

Daniel Revillini[1,2], Gail W. T. Wilson[3], R. Michael Miller[4], Ryan Lancione[1] and Nancy Collins Johnson[1,5]*

[1] Department of Biological Sciences, Northern Arizona University, Flagstaff, AZ, United States [2] Department of Biology, University of Miami, Coral Gables, FL, United States, [3] Department of Natural Resource Ecology, Management, Oklahoma State University, Stillwater, OK, United States [4] Environmental Science Division, Argonne National Laboratory, Lemont, IL, United States, [5] School of Earth, Sustainability, Northern Arizona University, Flagstaff, AZ, United States

OPEN ACCESS

Edited by:
Heike Bücking, South Dakota State University, United States

Reviewed by:
Rodica Pena, University of Göttingen, Germany
Raffaella Balestrini, Italian National Research Council (IPSP-CNR), Italy

***Correspondence:**
Daniel Revillini
dan.revillini@miami.edu

Specialty section:
This article was submitted to Plant Microbe Interactions, a section of the journal Frontiers in Plant Science

Received: *12 April 2019*
Accepted: *22 July 2019*
Published: *14 August 2019*

Citation:
Revillini D, Wilson GWT, Miller RM, Lancione R and Johnson NC (2019) Plant Diversity and Fertilizer Management Shape the Belowground Microbiome of Native Grass Bioenergy Feedstocks. Front. Plant Sci. 10:1018. doi: 10.3389/fpls.2019.01018

Plants may actively cultivate microorganisms in their roots and rhizosphere that enhance their nutrition. To develop cropping strategies that substitute mineral fertilizers for beneficial root symbioses, we must first understand how microbial communities associated with plant roots differ among plant taxa and how they respond to fertilization. Arbuscular mycorrhizal (AM) fungi and rhizobacteria are of particular interest because they enhance nutrient availability to plants and perform a suite of nutrient cycling functions. The purpose of this experiment is to examine the root and soil microbiome in a long-term switchgrass (*Panicum virgatum*) biofuel feedstock experiment and determine how AM fungi and rhizobacteria respond to plant diversity and soil fertility. We hypothesize that intra- and interspecific plant diversity, nitrogen fertilization (+N), and their interaction will influence the biomass and community composition of AM fungi and rhizobacteria. We further hypothesize that +N will reduce the abundance of nitrogenase-encoding nifH genes on the rhizoplane. Roots and soils were sampled from three switchgrass cultivars (Cave-in-Rock, Kanlow, Southlow) grown in monoculture, intraspecific mixture, and interspecific planting mixtures with either *Andropogon gerardii* or diverse native tallgrass prairie species. Molecular sequencing was performed on root and soil samples, fatty acid extractions were assessed to determine microbial biomass, and quantitative polymerase chain reaction (qPCR) was performed on nifH genes from the rhizoplane. Sequence data determined core AM fungal and bacterial microbiomes and indicator taxa for plant diversity and +N treatments. We found that plant diversity and +N influenced AM fungal biomass and community structure. Across all plant diversity treatments, +N reduced the biomass of AM fungi and nifH gene abundance by more than 40%. The AM fungal genus *Scutellospora* was an indicator for +N, with relative abundance significantly greater under +N and in monoculture treatments. Community composition of rhizobacteria was influenced by plant diversity but not by +N. *Verrucomicrobia* and *Proteobacteria* were the dominant bacterial phyla in both roots and soils. Our findings provide evidence that

soil fertility and plant diversity structure the root and soil microbiome. Optimization of soil communities for switchgrass production must take into account differences among cultivars and their unique responses to shifts in soil fertility.

Keywords: soil microbiome, switchgrass, rhizobacteria, arbuscular mycorrhizal fungi, resource availability, plant–microbial interaction

INTRODUCTION

National initiatives to increase energy independence spurred interest in biofuel cropping systems and native feedstock options (Perlack et al., 2011). The use of tallgrass prairie plants, including switchgrass (*Panicum virgatum* L.) and big bluestem (*Andropogon gerardii* Vitman) as biofuel feedstocks can be both economical and ecologically beneficial (Parrish and Fike, 2005; Tilman et al., 2006; Yang et al., 2018). Native, perennial warm-season grasses are broadly adapted to North America, are well-suited to grow on marginal soils, and can maintain high levels of productivity with minimal fertilization. They also provide additional ecosystem services including erosion control, increased C sequestration (Adkins et al., 2016; Hungate et al., 2017), reduction of nutrient leaching, and wildlife habitat (Parrish and Fike, 2005).

Studies have determined the importance of plant diversity on productivity in native feedstock cropping systems (Tilman et al., 2006; Mangan et al., 2011; Morris et al., 2016), but considerably less is understood about the interactions between plants and their microbial partners in roots and soil. Switchgrass and big bluestem are highly responsive to arbuscular mycorrhizal (AM) fungi (Chagnon and Bradley, 2013; Johnson et al., 2010) and rhizobacteria, though substantially less is known about their interactions with rhizobacteria (Brejda et al., 1998; Mao et al., 2014). Microbial symbionts likely provide the nutritional support needed for these native grasses to thrive in low-fertility soils and under drought. These beneficial plant–microbial relationships are locally adapted (Johnson et al., 2010; Revillini et al., 2016) and can be actively promoted in a plant taxa-specific manner (Berg et al., 2014; Agler et al., 2016). An understanding of the belowground microbiome on roots and in soils is necessary to begin to understand how microbial symbioses can facilitate and maintain high plant yields in any cropping system (Johansson et al., 2004; Schlaeppi and Bulgarelli, 2015; Alori et al., 2017). This will be particularly useful for native biofuel feedstocks, as they are promoted for cultivation on marginal lands no longer suitable for row cropping and where soil microbes will have likely been altered by conventional agricultural practices (Hart and Trevors, 2005; Verbruggen et al., 2015). Furthermore, given the relatively recent breeding history of native grasses for biofuel production, it is important to begin to understand the roles of plant cultivar, plant diversity, and fertilization regime on the microbial communities that nutritionally support their productivity on marginal soils (Busby et al., 2017).

Much like the human microbiome (Gilbert et al., 2018) and the plant surface microbiome (Vacher et al., 2016), root and soil-borne microbial communities play significant roles in host productivity and nutrient cycling from a variety of mechanisms (Bakker et al., 2018), but they also influence host-plant community dynamics (Bardgett and van der Putten, 2014; Vandenkoornhuyse et al., 2015; van der Heijden et al., 2016). The functioning of AM fungi and rhizobacteria can be influenced by both the relative availability of resources [e.g. soil nitrogen (N) and phosphorus (P)], functional traits within plant communities, and the feedbacks between plant and microbial communities (Larimer et al., 2010). Feedbacks between plants and soil microbial communities over seasons and generations are common (van der Putten et al., 2013) and can influence plant diversity, disease resistance, and resource-use efficiency (Bever, 2015; Mariotte et al., 2017). Plants can preferentially allocate photosynthate to microbial symbionts that provide the most resources (Bever et al., 2009; Kiers et al., 2003; Ji and Bever, 2016), and in turn, AM fungi and rhizobial bacteria may reciprocate by provisioning the most P or N to the most generous host plants (Kiers et al., 2011). Theory predicts that these resource allocation relationships, which are recognized most strongly in nutrient-limited systems (Semchenko et al., 2018), can influence the composition and functionality of microbial symbiont communities found in soil through preferential selection of the most beneficial partners (Kiers and Denison, 2008; Bever, 2015). The realized abundance and composition of microbial communities under different environmental contexts and management regimes are influenced by the interplay of preferential selection for more beneficial nutritional partners versus the accumulation of commensalistic or parasitic organisms (Adesemoye et al., 2009; Wei et al., 2013; Rubin et al., 2017).

Switchgrass cultivars may differ in the degree to which they form symbiotic associations to acquire essential resources (Brejda et al., 1998; Bouton, 2007; Bauer et al., 2012). Consequently, the diversity of feedstock planting mixtures, including intraspecific diversity among switchgrass cultivars, may be expected to influence the abundance and community composition of bacteria and AM fungi. This would be a likely consequence of the extended plant phenotype, which incorporates plant-associated microbiota critical to plant productivity and survival into the observed "plant" phenotype. This concept integrates the direct and often reciprocal effects among plant and microbial communities that can be structured by resource transfer mechanisms including optimal resource allocation (Berg et al., 2014; Vandenkoornhuyse et al., 2015). In a recent study, switchgrass genotypes and ecotypes were found to strongly drive differences in bacterial and fungal community composition, documenting the ability of switchgrass to maintain host-selected microbiomes (Singer et al., 2019). Optimal resource allocation between plants and microbial symbionts occurs when the investment of resources is targeted to specific structures, taxa, or functions that most strongly alleviate

the limitations to productivity. This has been experimentally shown in AM fungal and legume–rhizobia mutualisms (Johnson, 2010; Kiers et al., 2011; Zheng et al., 2014). Optimal allocation to microbial structures or taxa may be directed by functional requirements specific to switchgrass cultivars that exhibit a range of phenotypes. Switchgrass cultivars have different root architectures and respond differently to fertilization (Oates et al., 2016; Sprunger et al., 2017). Morris et al. (2016) showed that the most diverse planting mixtures provided consistently high yields of high-quality feedstock. Consequently, we hypothesized that microbial community composition and biomass may be influenced by the interplay of intra- and interspecific plant diversity and soil fertility.

Nitrogen fertilization (+N) is a standard but costly management practice for switchgrass plantings (Yang et al., 2018), and there is interest in developing management strategies to harness naturally occurring bacteria and fungi that promote plant health so that fertilizer inputs may be minimized (Bender et al., 2016; Busby et al., 2017; Toju et al., 2018). Mutualistic legume–rhizobia interactions play an important role in N acquisition and cycling, but the vast majority of archaea and bacteria that promote plant growth in soils are "free-living" and not under the strict controls found in symbiotic relationships (Lugtenberg and Kamilova, 2009; Reed et al., 2011; Moore et al., 2015). Although it is well documented that AM fungi often contribute to plant uptake of N from soils (Govindarajulu et al., 2005; Hodge and Storer, 2015), they may also compete for N (Püschel et al., 2016) and not ameliorate N limitation of their host plants (Reynolds et al., 2005). The availabilities of P and N interact to determine AM fungal responses to +N (Johnson et al., 2003b; Johnson et al., 2015). When P is not in limited supply, +N likely decreases the abundance of both AM fungi and N-fixing bacteria as plants allocate more photosynthate to aboveground production rather than to nutritional mutualisms. In arable soils that often have sufficient levels of P, the biomass of AM fungi and the abundance of nifH genes (a proxy for N_2-fixation) may be expected to decrease with +N as plants rely less on microbial N-cycling functions (Wei et al., 2013; Jach-Smith and Jackson, 2018). The fungal/bacterial (F/B) biomass ratio, a broad functional measure of microbial composition, may respond strongly to changes in nutrient availability and also change as a result of shifting plant allocation patterns (de Vries et al., 2006; Hannula et al., 2017). In many grassland studies, F/B ratio decreases with fertilization as fungal biomass declines significantly (Strickland and Rousk, 2010), and this response may be useful to understand the mechanisms of microbially mediated plant responses to N fertilization.

Baseline studies of communities of fungi and bacteria may reveal potentially important responses to plant diversity, N fertilization, and their interactions. For example, bacteria in the phylum *Verrucomicrobia* are very common in grassland soil (Bergmann et al., 2012; Fierer et al., 2013) and have been reported to be negatively correlated with soil N availability (Ramirez et al., 2012), but little is known about their functional role in soil ecology. Discovery of microbial indicator species or changes in relative abundance of particular taxa could indicate plant optimization of microbial communities with beneficial traits (Hart and Trevors, 2005; Azcón-Aguilar and Barea, 2015). Switchgrass cultivars can differ in the degree to which they respond to +N and to microbial mutualisms (Mao et al., 2014; Morris et al., 2016), so the diversity of feedstock planting mixtures and their responses to +N are likely to provide useful insights. The purpose of our study is to assess the effects of intra- and interspecific plant diversity and +N on the biomass and composition of communities of bacteria and AM fungi associated with both switchgrass roots and rhizosphere soils. We specifically tested the hypotheses that:

1) Switchgrass cultivars vary in the degree to which they support AM fungi and N-fixing bacteria and archaea.
2) Species richness of AM fungi should be greater with higher plant diversity (interspecific diversity > intraspecific diversity > monocultures).
3) Bacterial N-fixing activity should vary with intraspecific switchgrass diversity.

Additionally, we tested the hypotheses that N fertilization should:

4) Result in greater biomass allocation to aboveground production.
5) Reduce the biomass of AM fungi, N-fixing activity of bacteria, and decrease the F/B ratio.
6) Influence the community composition of AM fungi and bacteria, particularly in ways specific to switchgrass cultivar.

A robust evaluation of microbiome composition and the key members in plant–microbial interactions will provide a starting point for tests of specific functional relationships between soil microbial taxa and target crops (Bender et al., 2016). In this study, we analyzed microbial community composition to identify both indicator taxa and core bacterial and fungal communities that associate with different levels of plant diversity and fertilization to establish a baseline understanding of the extended plant phenotypes of switchgrass that are commonly used in biofuel feedstock experiments and production trials (Wright and Turhollow, 2010).

MATERIALS AND METHODS

Study Site and Experimental Design

Experimental plots 36 m x 20 m were established in June 2008 at the Fermilab National Environmental Research Park in Batavia, IL, to compare the performance of switchgrass cultivars grown in monocultures, intraspecific mixture, and interspecific mixtures with big bluestem grass or with 10 other native prairie plants. The experiment includes three randomized complete blocks with split-plot treated with or without N fertilizer (+67 kg N ha^{-1} $year^{-1}$ of 46-0-0 granular urea). Three switchgrass cultivars were planted in monoculture: Cave-in-Rock, a commercial upland cultivar; Kanlow, a commercial lowland cultivar; and Southlow, a regional upland cultivar in early breeding development. Southlow had slow initial establishment in monoculture at this experiment (Morris et al., 2016). In the switchgrass mixture treatment, the

three cultivars were planted in equal proportions (33%) and were estimated to each be well-represented in switchgrass mixture. In the big bluestem mixture treatment, three switchgrass cultivars were planted in equal proportion with three cultivars of big bluestem. Finally, the prairie mixture treatment included equal proportions of the switchgrass and big bluestem cultivars (7% each) and ten additional common, native prairie grasses and forbs (**Supplemental Table 1**, and see Morris et al. (2016) for additional design details). Root samples were collected from three monocultures with two fertilization treatments, replicated six times for a total of 36 root samples. Soil samples were collected from all six planting treatments with two fertilization treatments, replicated six times for a total of 72 soil samples.

Plant Biomass and Soil Nutrients

After the first killing frost (~mid-November), aboveground biomass was harvested ~15 cm above ground level, baled, and weighed using a hanging scale. Mean aboveground biomass from production years 2013–2015 was used to account for inter-annual variability. Mean percent change from unfertilized plots was calculated for fertilization responses as ($Fertilized_{mean}$ – $Unfertilized_{mean}$/$Unfertilized_{mean}$)*100 and presented in figures, though statistical analyses were performed on raw data (**Table 1**). Root biomass was sampled from monoculture plots using soil root cores (5 cm diameter) to a depth of 15 cm. Three cores per plot were collected, the 0–5 and 5–15 cm portions from cores were separated, and respective portions were homogenized. Roots were separated from soil by rinsing with water over a 500 μm sieve, dried, and weighed. Root biomass was converted to g m^{-2} using soil bulk density, and root mass fraction was calculated as root biomass/root + shoot biomass (Wilsey and Wayne Polley, 2006). In 2013, three soil cores (2 cm × 15 cm) were collected from each plot, roots were removed, soils were homogenized, and extractable P was analyzed using the Mehlich-3 method (Mehlich, 1984). Inorganic N was analyzed following extraction using 1M KCl extraction and isotope ratio mass spectrometry to measure NO_3^- and NH_4^+ (Burger and Jackson, 2003), which were combined for total N measures. Inorganic N was not measured in the soils collected from diverse prairie plots; therefore, statistical analyses do not include these data.

Microbial Biomass

Biomass of AM fungi and bacteria was measured using signature fatty acids (Olsson et al., 1995). Phospholipid fatty acids (PLFAs) are constituents of biological membranes that can be used to estimate active biomass of bacteria and fungi, as biovolume and cell surface area are well correlated (Frostegård et al., 2011). Neutral lipid fatty acids (NLFAs) are basic storage products of many fungi and serve as the primary energy reserve in AM fungi (Sharma and Buyer, 2015). PLFAs and NLFAs were extracted from soils (n = 72) using an extraction outlined in Zogg et al. (1997). Soils cores were homogenized, freeze-dried, and then sent to Oklahoma State University (OSU) for lipid extractions. Briefly, total lipid extracts were separated into PLFAs and NLFAs using silicic acid chromatography, the fatty acids were cleaved from the glycerol backbone using KOH saponification, and the harvested fatty acids were methylated to form fatty acid methyl esters (FAMEs). The FAMEs were then analyzed by gas chromatography and mass selection detection using a gas chromatography mass spectrometry (GCMS) unit Agilent MS 5975C/GC 7890A. We utilized c:19 as an internal standard. For extraradical AM fungal biomass, we utilized the 16:1ω5c FAME biomarker for both PLFA and NFLA determination (Sakamoto et al., 2004). Biomarkers 18:2ω6,9c and 18:1ω9c were used to determine saprotrophic fungal biomass (Gray et al., 2011). Bacterial biomarkers were used to determine both Gram-negative and Gram-positive bacterial biomass following Frostegård and Bååth (1996). F/B ratio was calculated using the sums of all measured bacterial PLFA and fungal NLFA biomarkers.

TABLE 1 | Mean aboveground biomass (g m^{-2}), root biomass (g m^{-2}), available soil phosphorus (Mehlich P), and total available soil nitrogen (N; NO_3^- + NH_4^+) from all applicable planting treatments under unfertilized or N-fertilized plots (+67 kg N ha^{-1} $year^{-1}$).

Planting treatment	Fertilization	Aboveground biomass (± SD)	Root biomass (± SD)	Soil P (± SD); ppm	Soil N (± SD); ppm
Monocultures					
Cave-in-Rock	Unfertilized	621 (37)^{a}	336.6 (77)^{d}	6.65 (3.18)^{ab}	9.05 (1.33)^{b}
	Fertilized	**837 (9.4)^{c}**	283.8 (53)^{cd}	5.67 (0.33)^{a}	**14.52 (2.86)^{cd}**
Kanlow	Unfertilized	338 (8.7)^{e}	249.4 (44)^{bc}	5.28 (1.67)^{a}	10.54 (0.84)^{ab}
	Fertilized	**629 (16)^{ab}**	**148.2 (12)^{a}**	5.30 (1.24)^{a}	12.79 (1.81)^{ac}
Southlow	Unfertilized	588 (20)^{a}	218.6 (30)^{abc}	9.65 (3.34)^{b}	9.42 (1.53)^{ab}
	Fertilized	**697 (8.1)^{b}**	193.9 (72)^{ab}	6.15 (2.52)^{ab}	**16.49 (3.61)^{d}**
Mixtures					
Switchgrass	Unfertilized	613 (56)^{a}	242.3 (16)^{abcd}	5.36 (1.57)^{ab}	9.09 (0.91)^{ab}
	Fertilized	**836 (22)^{c}**	184.1 (48)^{abc}	5.40 (1.54)^{ab}	**13.5 (1.35)^{acd}**
Big bluestem	Unfertilized	795 (5.8)^{c}	–	–	–
	Fertilized	**929 (27)^{d}**	–	–	–
Prairie	Unfertilized	649 (79)^{ab}	–	–	–
	Fertilized	**815 (43)^{c}**	–	–	–

Mean values in bold indicate significant ($p < 0.05$) differences between fertilization treatments determined by ANOVA, and letters indicate differences from Tukey's HSD post hoc of N-fertilization by planting treatment. Switchgrass = intraspecific mixture of the three switchgrass genotypes; big bluestem = interspecifc mixture of three switchgrass genotypes + three big bluestem genotypes; prairie = big bluestem mixture + 10 native grasses and forbs.

Sampling and Molecular Analysis of Roots and Soils

Root and soil samples were collected from the experimental plots in June 2015. Root samples were collected by "tracing" primary and lateral roots (<3mm diameter) below six switchgrass plants from each monoculture plot (n = 3). Six soil cores (2 cm x 15 cm) were taken randomly from within each sub-plot (16 m x 8 m) of all planting treatments. Root and soil samples were transported from the field to the laboratory in a cooler and frozen within four hours of collection. Samples were stored at -20°C until further processing for molecular analyses.

Next-generation sequencing was performed on DNA extracted from roots (n = 36) collected from monocultures of Cave-in-Rock, Kanlow, and Southlow switchgrass cultivars. The roots were not surface-sterilized, in order to retain an intact rhizoplane community along with endophytic bacteria. DNA was also extracted from homogenized soil cores (n = 72) from every plot for sequencing. DNA was extracted from roots and soils using the PureLink Microbiome DNA Purification Kit (Invitrogen, Carlsbad, CA, USA) following protocol from the "soil samples user guide." Genomic DNA was observed by NanoDrop and then purified using magnetic beads in 18% Polyethylene glycol (PEG) to remove potential polymerase chain reaction (PCR) inhibitors. PCR was carried out utilizing the 515F-806R primers to amplify the V4 region of the 16S rRNA (Gilbert et al., 2014) to characterize bacterial/archaeal communities, and WANDA-AML2 primers to amplify the small subunit (SSU) region to characterize AM fungal communities (Lee et al., 2008; Dumbrell et al., 2011). This region was targeted for AM fungal communities as the taxonomy of this region is well-supported by the MaarjAM database (Öpik et al., 2010). DNA quantitation was performed using standard dsDNA quantitation for PicoGreen (Thermo Fisher Scientific, Inc., Waltham, MA, USA), and all samples were normalized to 2ng DNA/μL prior to pooling into 16S or SSU libraries. The libraries were purified, concentrated, and quantified using qPCR against Illumina DNA standards (Kapa Biosystems, Wilmington, MA). Samples were paired-end sequenced (2 x 250 mode for 16S and 2 x 300 mode for SSU) using the Illumina MiSeq desktop platform (Illumina, Inc., San Diego, CA, USA) in the Environmental Genetics and Genomics Laboratory at Northern Arizona University (NAU) (https://in.nau.edu/enggen/).

NifH Gene Abundance

Abundance of the nifH gene was used as a proxy measure for N-fixation potential (Levy-Booth et al., 2014). Absolute nifH gene abundance was measured using qPCR with the targeted nifH amplicon primers IGK3/DVV. DNA from root samples (n = 36) free of PCR inhibitors (see above) was used for nifH qPCR, which was performed following a slightly modified method from Gaby and Buckley (2012). Briefly, reaction volumes were 20 μl, and 0.35 μM of each primer was used in each reaction. 40 cycles at annealing temperature of 56°C was used for initial PCR with IGK3/DVV. qPCR standards were created by first normalizing initial nifH PCR to 0.5 ng μl^{-1}, nifH tailing with a 15x cycle PCR, and 18% PEG bead cleaning, and quantified using standard dsDNA quantitation with PicoGreen (Thermo Fisher Scientific, Inc., Waltham, MA, USA) prior to qPCR with QuantStudio 5 (Applied Biosystems, Waltham, MA, USA).

Data Processing

All data processing methods were performed on both SSU and 16S data, unless specifically noted. Contaminating PhiX sequence was removed using the akutils *phix_filtering* command in akutils v1.2 (Krohn, 2016; https://github.com/alk224/akutils-v1.2). For bacterial data, read pairs were merged in akutils using the *join_paired_reads* command. Merged bacterial/archaeal data had an average length of 253 nt. Reads were not joined for AM fungal data and had an average length of 501 nt. Demultiplexing and quality filtering were carried out with the split_libraries_fastq.py command in QIIME 1.9.1 (Caporaso et al., 2010b) using a minimum quality threshold of q20, 0 bad characters allowed, and retaining only reads that satisfied these requirements for at least 95% of their length (-q 19 -r 0 -p 0.95). Chimeras were removed using the –uchime_ref option in vsearch 1.1.1 (Rognes et al., 2016) and the Gold reference database (http://drive5.com/uchime/gold.fa). One root sample was removed from downstream analyses due to low sequence count. Sequences were de-replicated on the first 100 bases using the prefix/suffix Operational taxanomic unit (OTU) picker in QIIME. OTU picking was performed *de novo* with Swarm (Mahé et al., 2014) at d4 resolution (~98.4% similarity). Taxonomic identities were assigned with BLAST using default settings in QIIME 1.9.1 against the 97% Greengenes database (McDonald et al., 2012) for bacterial data and at 90% similarity against the MaarjAM database (Öpik et al., 2010) for AM fungal data. AM fungal taxa in the MaarjAM database are classified as virtual taxa (VT) but are referred to as OTUs in methods for brevity. outsequences were aligned using PyNAST (Caporaso et al., 2010a), and the resulting alignment was used to construct a phylogenetic tree with FastTree (Price et al., 2009). OTUs constituting less than 0.005% of the total data set were removed (Bokulich et al., 2012). OTU tables were rarefied to the lowest sample depth (3,449 for 16S; 3,484 for SSU) for α-diversity analyses. Relative abundance of taxa by treatments was analyzed for planting and fertilization treatments using the *group_significance.py* command in QIIME. Tests of ß-diversity and differential abundance were performed on OTU tables transformed by cumulative sum scaling (CSS) normalization (Paulson et al., 2013). Diversity analyses were conducted with the *core_diversity* command in akutils unless specified.

Statistical Analyses

Analyses were only performed on plots with paired sequencing and physical plant or soil measurements, leaving n = 35 for root samples and n = 72 for soil samples. Blocking did not have effects on any measures across all statistical analyses in this study and therefore was not presented. Plant biomass, AM fungal biomass (PLFA/NLFA), and nifH gene abundance were tested using nonparametric Kruskal–Wallis, or parametric analysis of variance (ANOVA) and Tukey's honestly significant difference (HSD) *post hoc* (*aov* and *TukeyHSD* in R, respectively) to determine +N, plant

treatment, and +N * plant treatment interactions. All data were log-transformed when necessary to meet normality assumptions. Bacterial and fungal community α-diversities were compared by nonparametric Student's T-test using rarefied OTU tables. Log_2 fold change from control after +N of rarefied fungal and bacterial taxonomic relative abundance was calculated using DESeq2 (Love et al., 2014). Briefly, log_2 fold change data presented are taxa with relative abundance that was significantly different after +N using the likelihood ratio test (LRT) where $p < 0.05$. Indicator species analyses were performed with rarefied OTU tables for each treatment, or treatment interaction using both the indicator value (IndVal = fidelity and relative abundance) and point-biserial correlation (r_{pb}) coefficient with 9,999 permutations with multipatt function from the *indicspecies* package in R (De Cáceres and Legendre, 2009), and results are only presented when Benjamini–Hochberg false discovery rate (fdr)–corrected $p < 0.05$ (De Cáceres et al., 2010). The compute_core_microbiome.py command to was used to identify the core microbiome communities, defined here as OTUs that are present in 50% of samples for a treatment or treatment combination. Differences in bacterial and fungal ß-diversity were assessed by Permutational ANOVA (PERMANOVA) (Anderson, 2001) using weighted and unweighted UniFrac (Lozupone and Knight, 2005) for bacterial data and Bray–Curtis dissimilarity for AM fungal data. PERMANOVA was initially performed across all samples (n = 107) to determine differences in root and soil microbial communities with the respective diversity metrics. A pairwise PERMANOVA function (https://github.com/pmartinezarbizu/pairwiseAdonis) was used to determine microbial community dissimilarities within planting treatments under unfertilized or +N plots. Statistical significance from pairwise PERMANOVA was indicated when Bonferroni-corrected $p < 0.05$. All analyses were performed in R and with the use of the NAU High Performance Computing cluster (https://nau.edu/high-performance-computing/overview/).

RESULTS

Plant Biomass and Soil Nutrients

Aboveground biomass from all planting mixtures was significantly greater in +N plots compared to unfertilized plots, with increases in monocultures of 35% for Cave-in-Rock, 85% for Kanlow, 18.5% for Southlow, 16.9% in big bluestem, and 25.5% in prairie mixtures (**Table 1**, **Figures 1A–B**). The big bluestem planting mixture produced higher biomass yields than all other planting treatments in both the unfertilized and +N plots (**Table 1**, **Figure 1A**). Root biomass was greater in unfertilized plots than fertilized plots ($F_{1,12} = 5.62$, $p < 0.05$) and different between switchgrass monocultures ($F_{2,12} = 8.1$, $p = 0.005$; **Supplemental Figure 1**). Root biomass was greater in Cave-in-Rock than Kanlow or Southlow ($p < 0.01$ and $p < 0.05$, respectively; **Supplemental Figure 1A**) and decreased with +N in Kanlow ($p = 0.039$). Root mass fraction was lower in +N plots ($F_{1,32} = 19.2$, $p < 0.005$; **Supplemental Figure 1B**) and higher under Kanlow than Southlow ($F_{3,18} = 5.5$, $p = 0.02$; **Supplemental Figure 1B**). In Kanlow, root mass fraction decreased in +N plots ($p < 0.01$; **Supplemental Figure 1B**). Soil available P was lower under +N ($F_{1,34} = 4.1$, $p = 0.0508$; **Table 1**) and higher under Southlow than Kanlow ($F_{3,34} = 3.8$, $p = 0.018$; **Table 1**). There was no fertilization–by–planting treatment interaction for soil P. Soil N ($NH_4^+ + NO_3^-$; ppm) increased with +N overall ($F_{1,34} = 67.6$, $p < 0.001$; **Table 1**) and within Cave-in-Rock and Southlow monocultures and switchgrass mixture plots (**Table 1**).

AM Fungal and Bacterial Biomass

Soil concentration of the PLFA AM fungal biomarker (16:1ω5c) did not vary with +N or planting mixtures; however, NLFA decreased with +N ($F_{1,72} = 19.37$, $p < 0.001$; **Supplemental Figure 2**). There was a fertilization–by–planting mixture interaction ($F_{5,72} = 3.413$, $p = 0.017$;

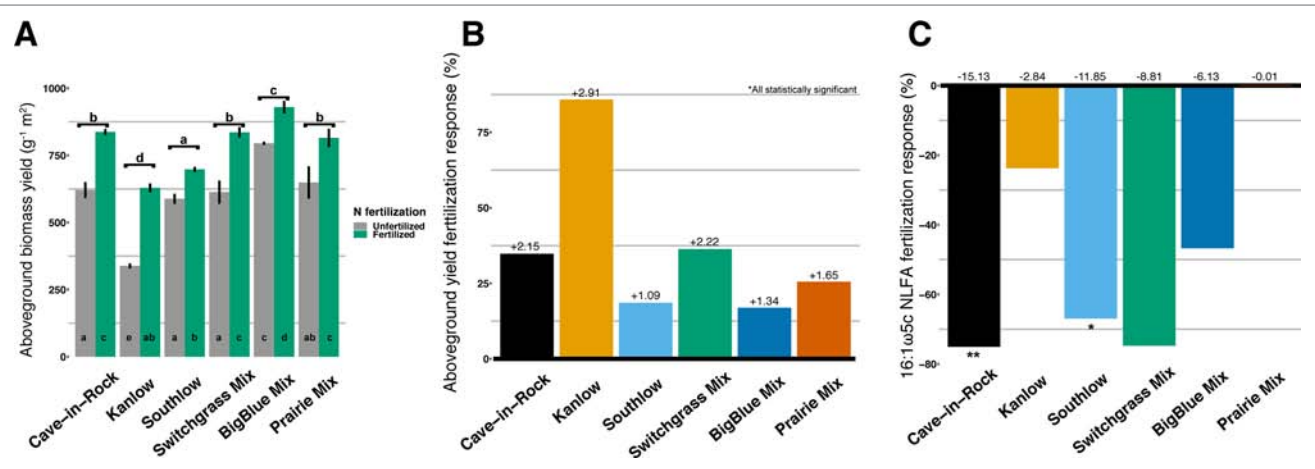

FIGURE 1 | Total aboveground plant biomass (g m^2) from each planting mixture under unfertilized or N-fertilized conditions **(A)** and aboveground biomass response to N fertilization (percent change) for all planting mixtures **(B)**. Arbuscular mycorrhizal (AM) fungal neutral lipid fatty acid (NLFA) response (percent change) to N fertilization for all planting mixtures **(C)**. Zero bar **(B**, **C)** represents unfertilized means per planting treatment. Values above bars in B are mean increases in plant biomass (Mg ha^{-1}), and those in C are mean decreases in AM fungal biomass (nmol g^{-1} soil) per planting mixture. Letters indicate significant differences from Tukey's HSD *post hoc* testing. Asterisks indicate significant differences from ANOVA (**$p < 0.01$, *$p < 0.05$).

Supplemental Figure 2), with lower fungal biomass in +N Cave-in-Rock and Southlow moncultures ($p < 0.005$ and $p = 0.02$, respectively; **Supplemental Figure 2**). There were negative linear relationships between aboveground plant biomass yields (Mg ha^{-1}) and fungal biomass for Cave-in-Rock ($r^2 = -0.91$, $p < 0.001$; **Figure 2A**), Southlow ($r^2 = -0.76$, $p = 0.006$), and the switchgrass mixture ($r^2 = -0.81$, $p = 0.001$; **Figure 2A**). Root mass fraction was positively correlated with fungal biomass ($r^2 = 0.16$, $p = 0.05$; **Figure 2B**). There was a fertilization–by–planting mixture interaction on total PLFA bacterial biomass ($F_{5,72} = 3.56$, $p < 0.01$); **Supplemental Figure 3**), and Tukey's HSD revealed an increase in total bacterial PLFA biomass under the prairie mixture after +N ($p < 0.05$; **Supplemental Figure 3**). The F/B ratio was lower

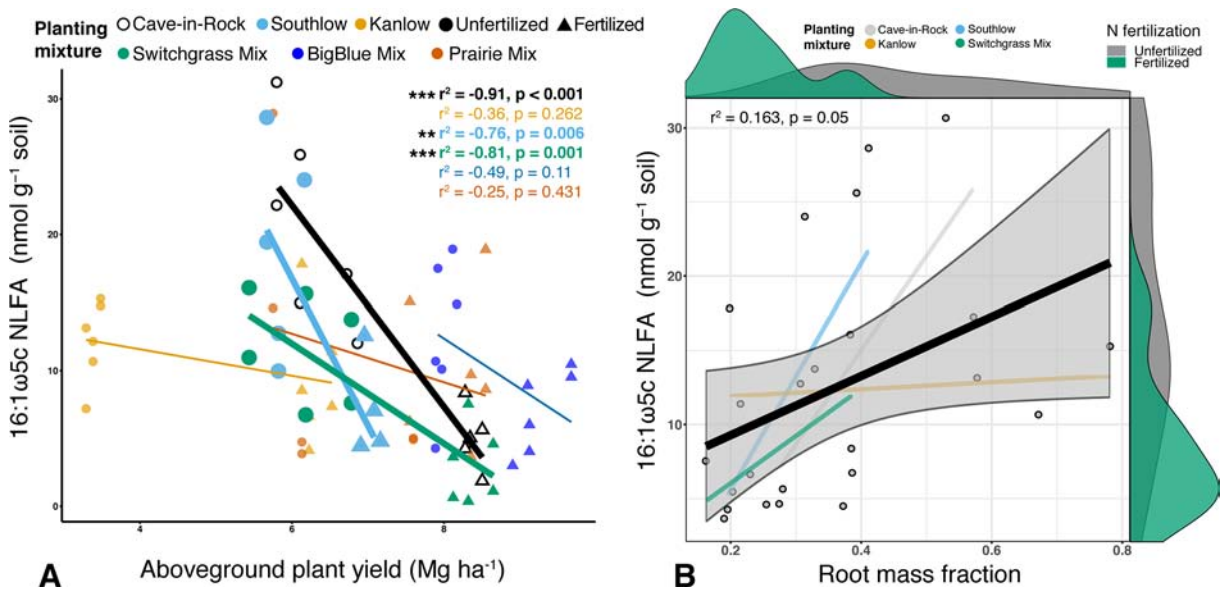

FIGURE 2 | Relationship between AM fungal biomass in soil and aboveground plant biomass **(A)**, colored by planting mixture and either unfertilized (circles) or N-fertilized (triangles) plots. Cave-in-Rock (black/white), Southlow (light blue), and the switchgrass mixture plot (green) have significant negative correlations between aboveground plant biomass and the abundance of AM fungi in soils. Correlation statistics are provided in the upper right corner for all planting treatments. The relationship between AM fungal biomass in soil and root mass fraction **(B)** for all monocultures and the switchgrass mixture is represented by the black bar. 95% confidence limit is shaded, value densities for root mass fraction and NLFA abundance are on opposing x- and y-axes, and statistics are provided in the top left corner $^{**}p < 0.01$, $^{***}p \leq 0.001$.

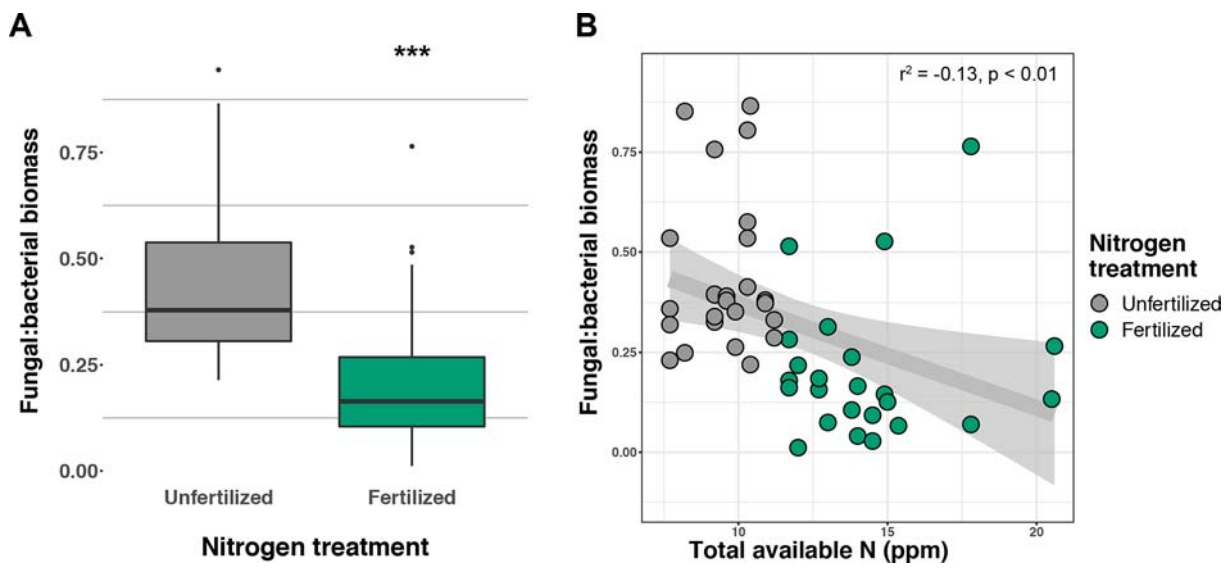

FIGURE 3 | Response of fungal:bacterial biomass ratio to nitrogen (N) fertilization **(A)** and relationship of fungal:bacterial ratio to available soil inorganic N (NH^{4+} + NO^{3-}) **(B)** $^{***}p \leq 0.001$.

under +N than in unfertilized plots ($F_{1,72}$ = 32.44, p < 0.001; **Figure 3A**), and there was a negative linear relationship with total available soil N (r^2 = -0.16, p < 0.005; **Figure 3B**).

Arbuscular Mycorrhizal Fungal Communities

The species richness of AM fungal communities in soil was higher for the combination of all interspecific diversity mixture plots than combined switchgrass monoculture plots ($F_{1,36}$ = 3.77, p < 0.05; **Figure 4A**). Nitrogen fertilization reduced fungal richness in the soil of switchgrass mixture plots (adj-p < 0.01) and increased Shannon diversity (*H*) in roots and soils under Kanlow monocultures (p < 0.05 and p < 0.05, respectively; **Figure 4B**). The compositions of AM fungal communities in roots and soil were different (PERMANOVA Bray–Curtis; pseudo-$F_{1,108}$ = 3.48, p < 0.001; **Supplemental Figure 4A**). The ß-diversity of AM fungal communities in roots was not altered by +N. Pairwise PERMANOVA indicated that the AM fungal community in roots of Cave-in-Rock was different from that in roots of Southlow (pseudo-$F_{2,31}$ = 1.93, adj-p = 0.013; **Table 2**, **Figure 5A**), and +N influenced the Bray–Curtis dissimilarity of AM fungal communities in roots of the Kanlow cultivar (pseudo-$F_{1,11}$ = 2.88, p < 0.05; **Table 2**, **Figure 5B**). The ß-diversity of AM fungal communities from soils was altered by planting mixture (PERMANOVA; pseudo-$F_{5,72}$ = 2.84, p < 0.001; **Figure 5C**) and +N (PERMANOVA; pseudo-$F_{1,72}$ = 2.24, p < 0.005; **Figure 5D**). The ß-diversity of the AM community in soil was influenced by planting mixture (**Table 2**) but not +N within planting mixtures (**Supplemental Figure 5**).

TABLE 2 | Significant Bray–Curtis dissimilarities of AM fungal communities between planting mixtures or N fertilization within planting mixture from roots and soils calculated using pairwise PERMANOVA.

	pseudo-F	r^2	adj-p-value
Roots			
Between planting mixtures			
Cave-in-Rock vs. Southlow	1.87	0.083	0.013
Within Kanlow			
Unfertilized vs. fertilized	1.88	0.130	0.024
Soil			
Between planting mixtures			
Cave-in-Rock vs. switchgrass mix	2.84	0.110	0.012
Cave-in-Rock vs. big blue mix	3.06	0.122	0.001
Kanlow vs. switchgrass mix	1.69	0.072	0.006
Kanlow vs. big blue mix	1.66	0.069	0.015
Southlow vs. switchgrass mix	1.56	0.066	0.039
Southlow vs. big blue mix	3.11	0.130	0.001
Southlow vs. prairie mix	2.61	0.105	0.002

Relative abundance of core AM fungal taxa are presented as heat maps, and indicator species analyses revealed multiple indicator taxa for +N or certain planting mixture treatments

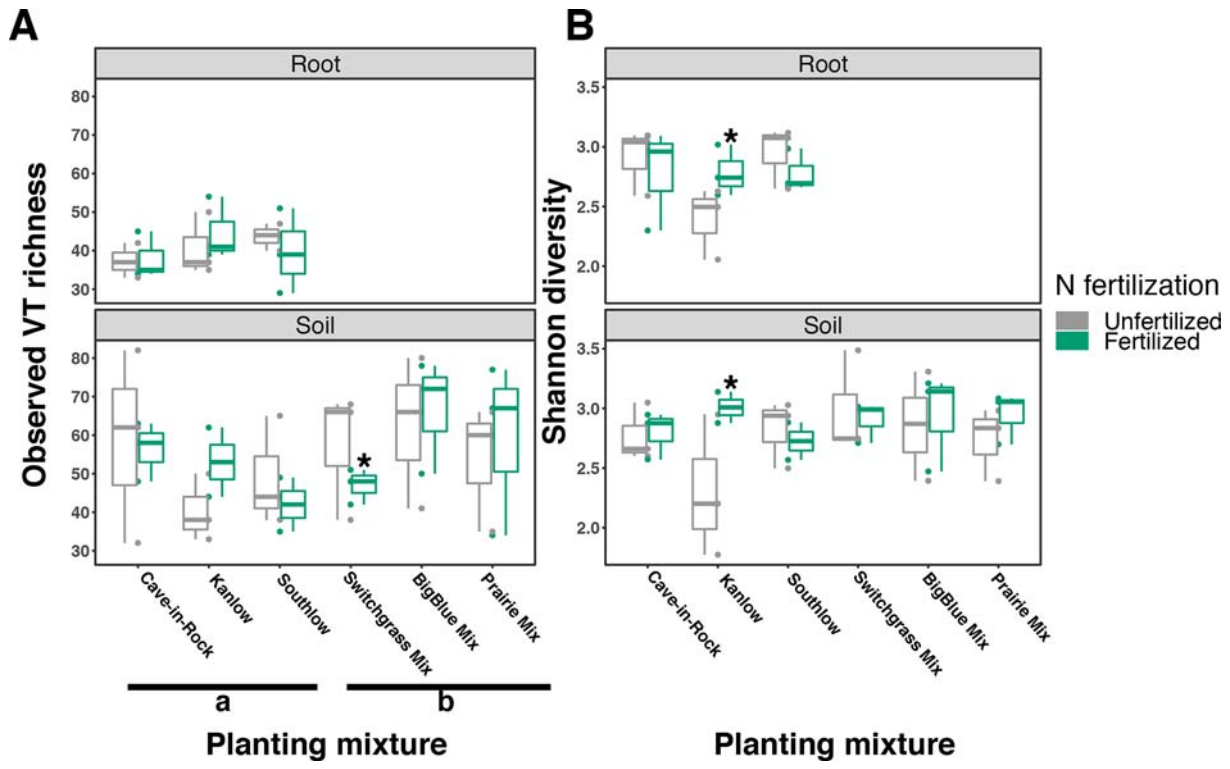

FIGURE 4 | Arbuscular mycorrhizal (AM) fungal diversity observed in roots and soils measured as virtual taxa (VT) **(A)** and Shannon diversity **(B)** for all planting mixtures. Gray indicates unfertilized and green indicates N-fertilized treatments. Letters indicate significant differences between groups (adj-p < 0.05), and asterisks indicate significant ANOVA differences from fertilization within groups (p < 0.05).

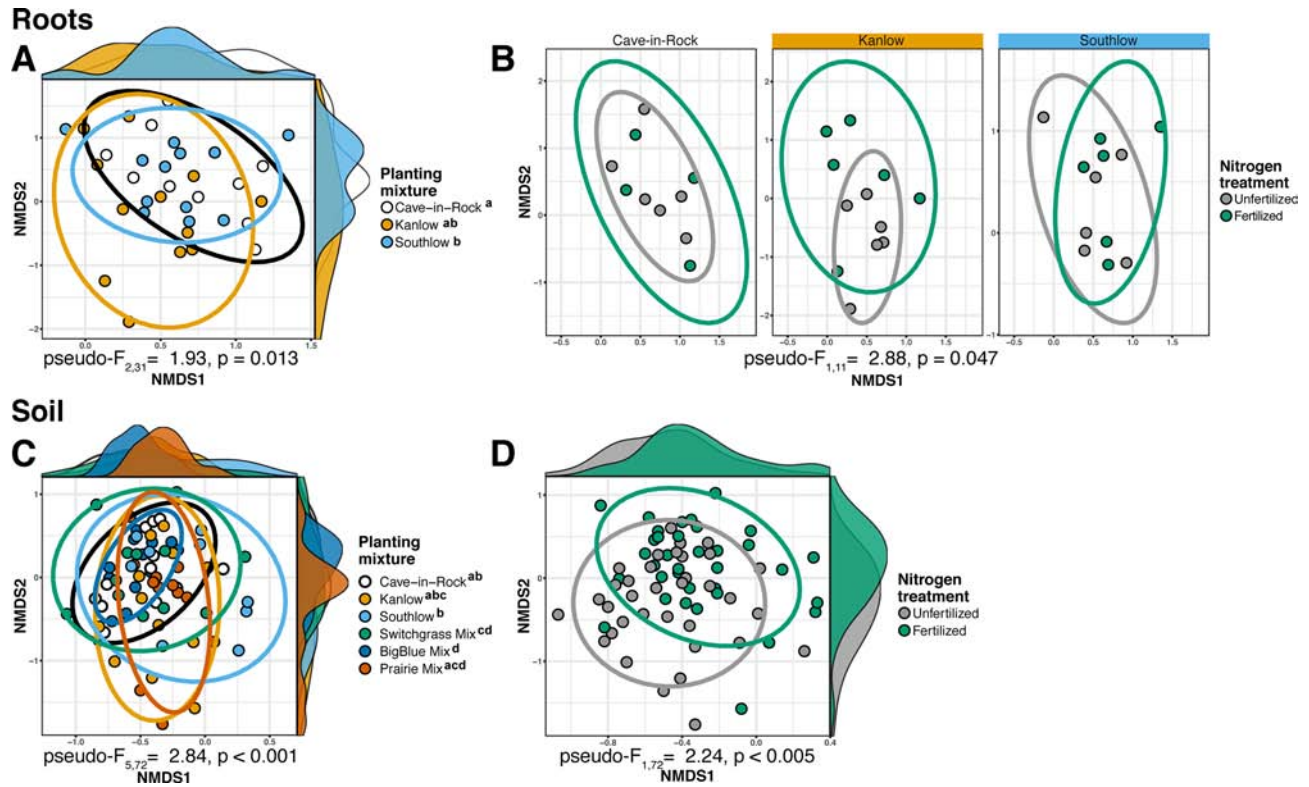

FIGURE 5 | NMDS of AM fungal community Bray–Curtis dissimilarity from roots (top) and soils (bottom) colored by planting mixture **(A**, **C)** and colored by N fertilization treatment **(B**, **D)**. Ellipses represent 95% confidence areas around respective treatments. Letters indicate significant differences between groups (adj-p < 0.05).

(**Figures 6A–B**). The genus *Scutellospora* was an indicator under +N both in roots (IndVal = 0.81, fdr-p = 0.02; r_{pb} = 0.42, fdr-p = 0.02; **Figure 6A**) and in soils (IndVal = 0.65, fdr-p = 0.02; r_{pb} = 0.27, fdr-p = 0.058; **Figure 6B**). The genus *Gigaspora* was an indicator in soils under the switchgrass mixture (IndVal = 0.46, fdr-p = 0.036; r_{pb} = 0.39, fdr-p = 0.017), but it was not included in the heat map, because it was not observed in more than 50% of the samples. In soils under all three monocultures (Cave-in-Rock, Kanlow, Southlow), *Paraglomus* was determined to be an indicator genus (r_{pb} = 0.41, fdr-p = 0.01; **Figure 6B**). The relative abundance of *Scutellospora* was higher in +N plots (Kruskal–Wallis H = 11.72, FDR-p = 0.012; **Figures 6A–D**), and specifically in roots of Cave-in-Rock (H = 9.11, FDR-p < 0.01; **Figure 6A**), and in soil from prairie mixture plots (H = 14.25, FDR-p < 0.005; **Figure 6B**). *Glomus* was the most abundant genus across all treatments (**Supplemental Figure 6**), and the relative abundance of *Glomus* decreased in soil from prairie mixture +N plots (H = 13.6, FDR-p < 0.005; **Figure 6B**). Five AM fungal genera in roots and six genera in soils had significant $\log_2$ fold changes in relative abundance in +N plots (LRT; p < 0.05; **Figures 6C–D**). In roots, AM fungal taxa in the genera *Claroideoglomus* and *Glomus* had species that both increased and decreased with +N, while *Paraglomus* and *Scutellospora* increased with +N (**Figure 6C**). In soils, we found a similar pattern for *Glomus* and *Scutellospora* species, while *Arachaeospora* relative abundance increased and *Claroideoglomus* relative abundance declined with +N (**Figure 6D**).

Bacterial Communities

Compared to other treatments, the richness of bacterial OTUs was lower on roots of Southlow in the +N plots ($F_{3,18}$ = 2.8, p < 0.01; **Figure 7A**) and higher in soil under the prairie mixture ($F_{6,36}$ = 3.8, p < 0.5; **Figure 7A**). Shannon diversity (*H*) of soil bacteria was higher in the combination of all monoculture plots compared to the combination of all diverse mixture plots ($F_{1,36}$ = 2.1, p = 0.04; **Figure 7B**). Shannon diversity of soil bacteria in Kanlow plots was higher than in Southlow plots ($F_{2,18}$ = 2.07, p < 0.01; **Figure 7B**). In +N plots, Shannon diversity of bacteria was higher on Kanlow roots and in soil in Cave-in-Rock plots (p < 0.05 and p < 0.05, respectively; **Figure 7B**). Bacterial communities were different in roots and soils (pseudo-$F_{1,108}$ = 9.48, p < 0.001; **Supplemental Figure 4B**). Bacterial community weighted UniFrac ß-diversity from roots was altered by planting mixture (pseudo-$F_{2,35}$ = 1.6, p = 0.012; **Figure 8A**). The bacterial community on roots of Southlow was different from Kanlow (pairwise PERMANOVA pseudo-$F_{1,12}$ = 1.7, adj-p = 0.03; **Figure 8A**). Bacterial community unweighted and weighted UniFrac ß-diversity from soils were altered by planting mixture (pseudo-$F_{5,72}$ = 1.34, p < 0.01, and pseudo-$F_{5,72}$ = 1.54,

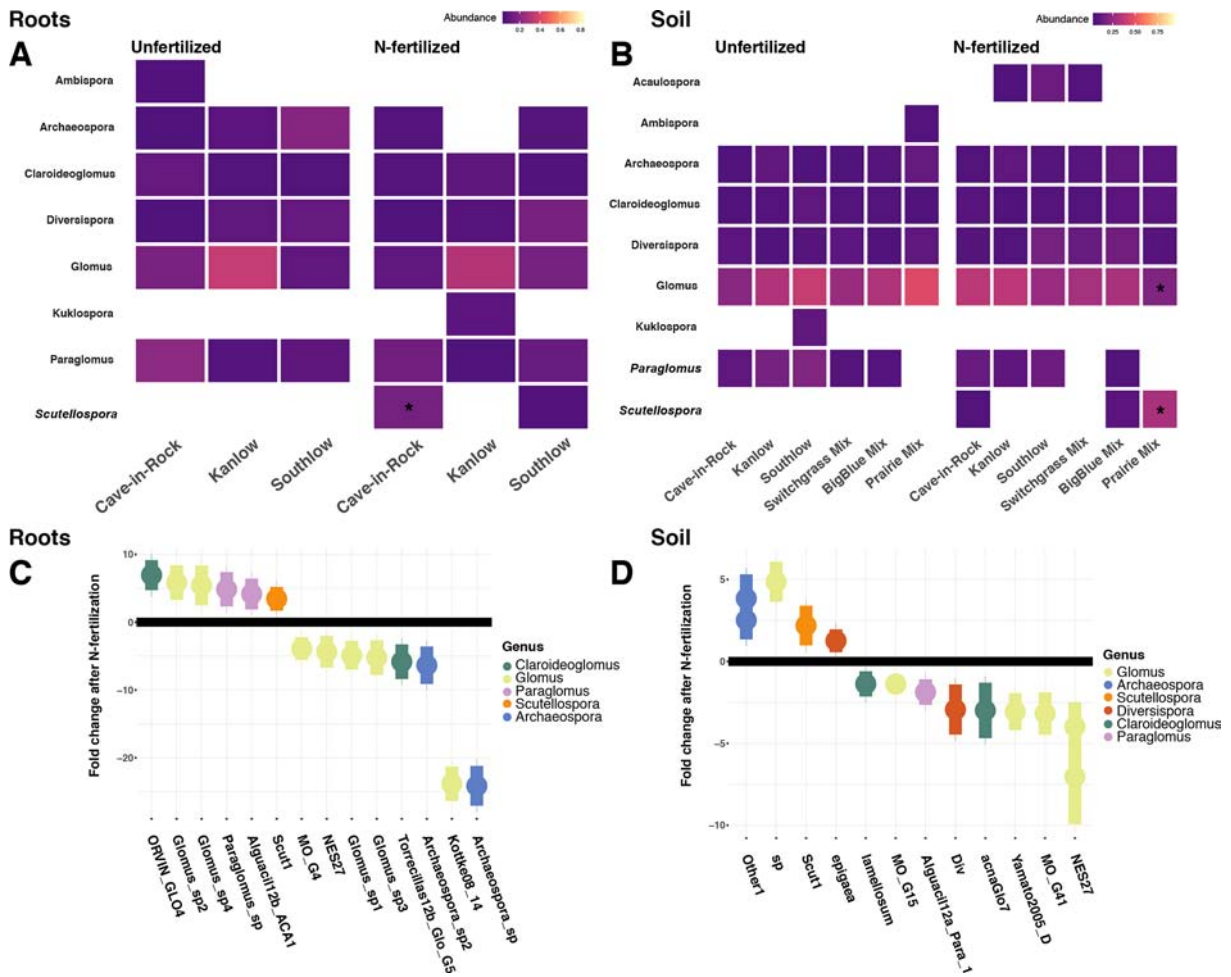

FIGURE 6 | Heat maps of relative abundance of AM fungal genera for all planting treatments that are either unfertilized or N-fertilized, from roots **(A)** and soil **(B)**. The taxa presented here are core taxa, which represent only those genera present in more than 50% of all samples. Italicized taxa represent significant indicator taxa determined using either IndVal or r_{pb} ($p < 0.05$). Darker tiles in the heat map indicate lower relative abundance, and asterisks indicate a significant increase or decrease in relative abundance determined using Kruskal–Wallis H tests for each planting treatment after fertilization (FDR-$p < 0.05$). Empty tiles indicate that the taxa were not present in that treatment combination. The bottom **(C–D)** shows $\log_2$ fold change of AM fungal relative abundance that significantly differs after N fertilization (LRT; $p < 0.05$) for roots **(C)** and soils **(D)**. AM fungal "species" are on the x-axis, and points are colored by genus.

$p < 0.01$, respectively; **Figure 8B**). The soil bacterial community under Southlow was different from all planting mixtures except for the switchgrass mixture (see **Table 3** for details, **Figure 8B**). Nitrogen fertilization had no effects on bacterial community ß-diversity from roots or soils; however, indicator species analyses of bacterial taxa revealed some differences. *Verrucomicrobia* and *Proteobacteria* were the most abundant phyla across all treatments (**Supplemental Figure 7**). The order N1423WL in the phylum *Gemmatimonadetes* was an indicator of +N in roots (IndVal = 0.44, fdr-p = 0.023), while in soils, RCP1-48 in the phylum *Gammaproteobacteria* was an indicator taxon of +N (IndVal = 0.58, fdr-p = 0.037). Bacterial order Mariprofundales (class *Zetaproteobacteria*) was an indicator taxa for unfertilized plots (IndVal = 0.5, fdr-p = 0.039). Bacteria in the phylum FCPU426 were indicator taxa associated with soils under Southlow monocultures (r_{pb} = 0.51, fdr-p = 0.026). *Acidobacteria* abundance increased on roots of Kanlow with +N (H = 9.7, $p < 0.05$; **Figure 9A**). The relative abundance of bacteria in the class *Alphaproteobacteria* was higher in soils under Southlow with +N (H = 7.04, FDR-p = 0.048; **Figure 9B**). *Nitrospirae* relative abundance was higher in soils under prairie mixtures with +N (H = 22.6, $p < 0.01$; **Figure 9B**). Verrucomicrobial relative abundance was lower on roots of Southlow with +N (H = 14.8, FDR-$p < 0.01$; **Figure 9A**) and lower in soils under Cave-in-Rock with +N (H = 9.4, FDR-p = 0.048; **Figure 9B**).

Six bacterial phyla in roots and eight phyla in soils had significant $\log_2$ fold changes in relative abundance with +N (LRT; $p < 0.05$; **Figures 9C–D**). Relative abundance of *Verrucomicrobia* declined with +N under roots and soils (**Figures 9C–D**), as did *Actinobacteria* in roots (**Figure 9C**). *Nitrospirae* and *Crenarchaeota* consistently increased with +N, while taxa in the *Proteobacteria* and *Planctomycetes* exhibited both increases and decreases in relative abundance with +N (**Figures 9C–D**).

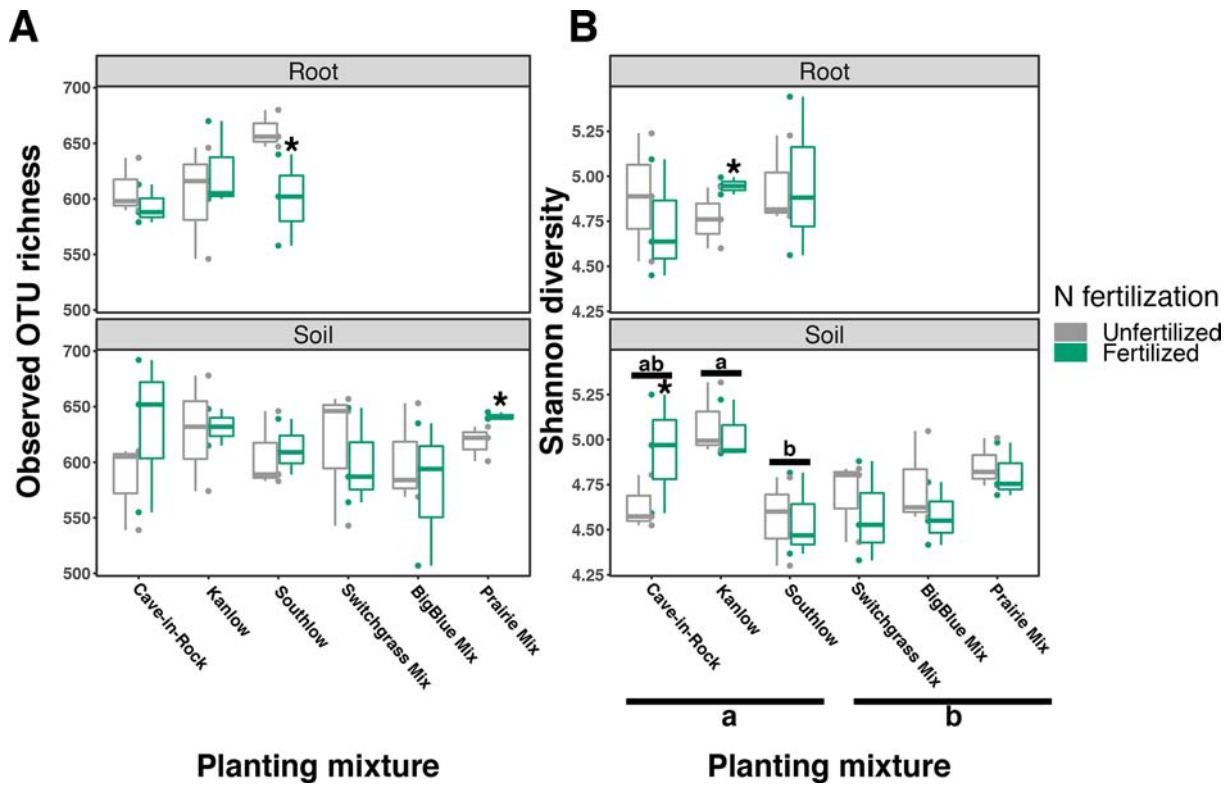

FIGURE 7 | Bacterial diversity observed in roots and soils measured as OTU richness **(A)** and Shannon diversity **(B)** for all planting mixtures. Gray indicates unfertilized and green indicates N-fertilized treatments. Letters indicate significant differences between groups (adj-p < 0.05), and asterisks indicate significant ANOVA differences from fertilization within groups (p < 0.05).

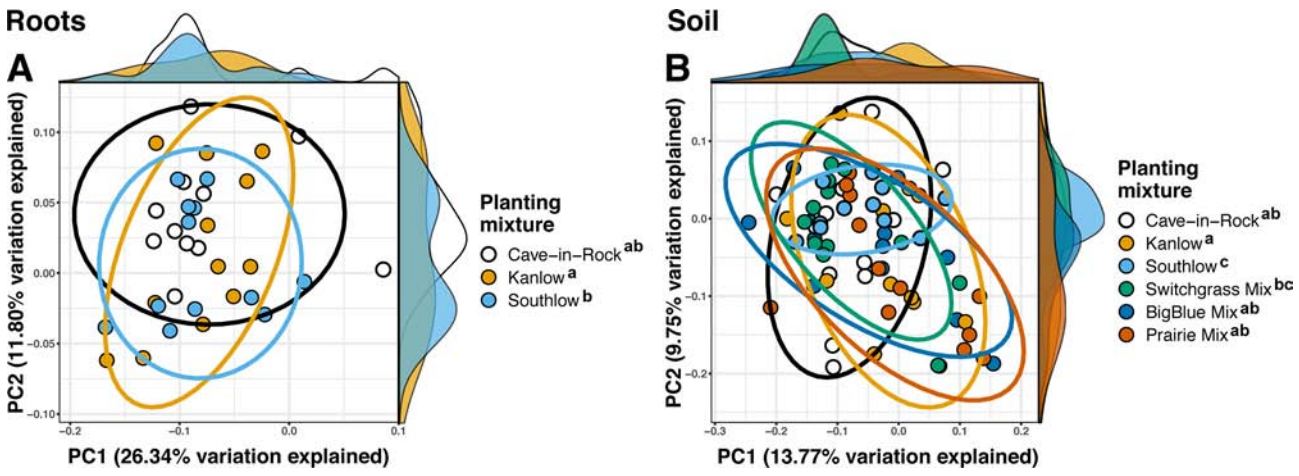

FIGURE 8 | Principal coordinate analyses of bacterial community ß-diversity from roots **(A)**; weighted UniFrac or soils **(B)**; unweighted UniFrac, colored by planting treatment. Ellipses represent 95% confidence areas around respective treatments. Letters indicate significant differences between groups (adj-p < 0.05).

NifH Gene Abundance

Abundance of the nifH gene declined with +N (ANOVA; $F_{1,32} = 5.16$, $p = 0.029$; **Supplemental Figure 8**) and differed among switchgrass cultivars (ANOVA; $F_{2,32} = 14.327$, $p < 0.001$). Cave-in-Rock had the lowest total nifH gene abundance ($p < 0.01$; **Supplemental Figure 8**), and N fertilization decreased nifH abundance for Kanlow ($F_{1,10} = 6.1$, $p < 0.05$; **Figure 10A**). NifH gene abundance was positively correlated with root biomass under Kanlow ($r^2 = 034$, $p < 0.01$; **Figure 10B**) and with root mass fraction across all monocultures ($F_{1,16} = 8.25$, adj-$r^2 = 0.306$, $p = 0.01$; **Figure 10C**). There was no

TABLE 3 | Significant unweighted UniFrac differences of bacterial communities between planting mixtures from roots and soils calculated using pairwise PERMANOVA.

	pseudo-F	r^2	adj-p-value
Roots			
Between planting mixtures			
Kanlow vs. Southlow	2.40	0.057	0.045
Soil			
Between planting mixtures			
Cave-in-Rock vs. Southlow	2.16	0.061	0.038
Kanlow vs. Southlow	2.72	0.074	0.015
Kanlow vs. switchgrass mix	3.30	0.089	0.011
Southlow vs. big blue mix	2.61	0.072	0.009
Southlow vs. prairie mix	2.29	0.063	0.027

correlation between the relative abundance of *Verrucomicrobia* and nifH gene abundance from roots (**Supplemental Figure 9**).

DISCUSSION

Our results support the hypotheses that intra- and interspecific plant diversity influences soil microbial communities and that N fertilization (+N) shifts plant allocation of photosynthate towards aboveground production and away from root-associated microorganisms. The reduction in AM fungal biomass, nifH gene abundance, and F/B ratios after +N may reveal important functional trade-offs in particular planting treatments. Predictably, +N reduced the value of bacterial

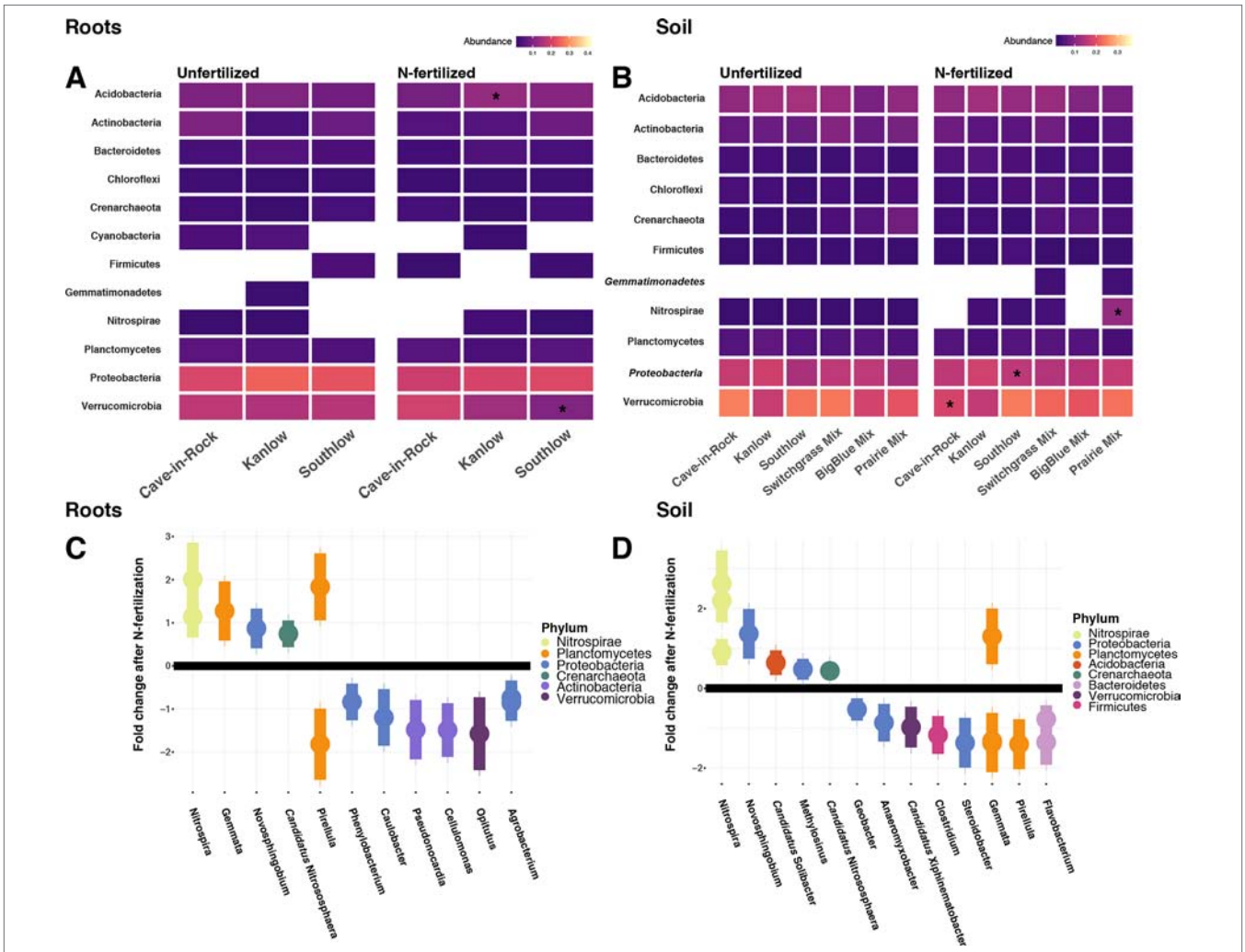

FIGURE 9 | Heat maps of relative abundance of bacterial phyla for all planting treatments that are either unfertilized or N-fertilized, from roots **(A**, **C)** and soil **(B**, **D)**. The taxa presented here are core taxa, which represent only those phyla present in more than 50% of all samples. Italicized taxa represent significant indicator taxa determined using either IndVal or r_{pb} ($p < 0.05$). *Gemmatimonadetes* were indicator taxa for N-fertilized plots in soil **(B)**, while *Zetaproteobacteria* were indicator taxa for unfertilized plots in soil **(B)**. Darker-color tiles in the heat map indicate lower relative abundance, asterisks indicate a significant increase or decrease in relative abundance determined using Kruskal–Wallis H tests for each planting treatment (FDR-$p < 0.05$). Empty tiles indicate that the taxa were not present in that treatment combination. Log_2 fold change of bacterial relative abundance that significantly differs after N fertilization (LRT; $p < 0.05$) for roots **(C)** and soils **(D)**. Bacterial families are on the x-axis, and points are colored by bacterial phylum.

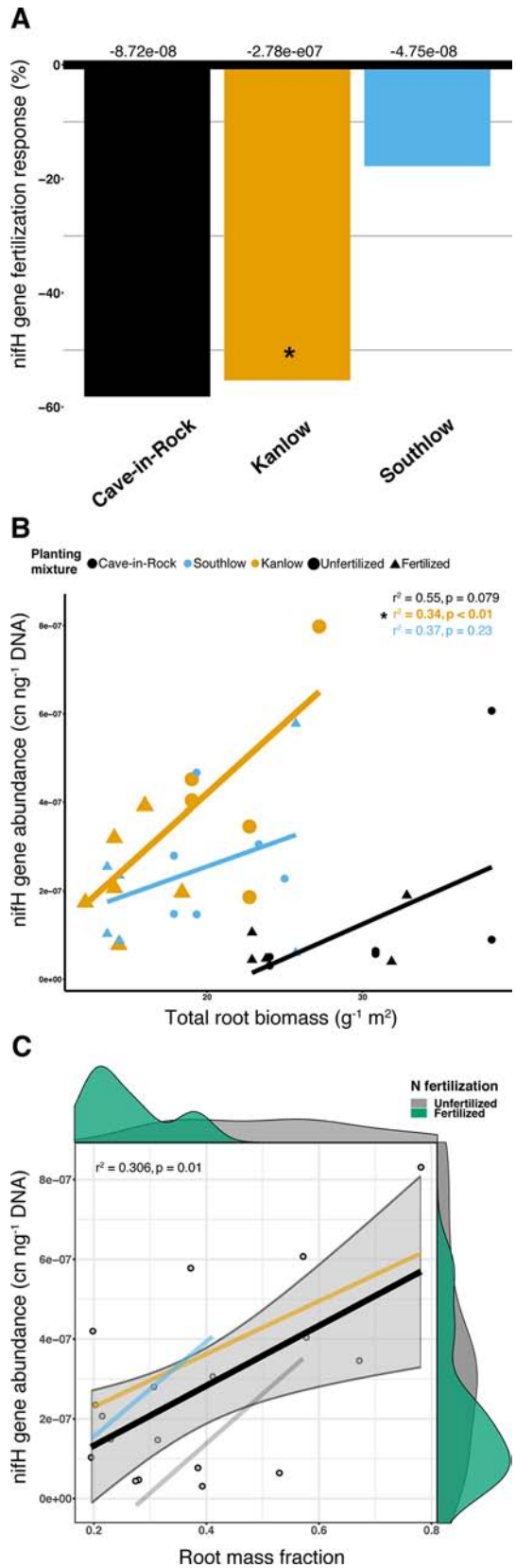

FIGURE 10 | Continued

FIGURE 10 | The abundance of nifH gene response (percent change) to N fertilization for three switchgrass monocultures **(A)**, where zero bar represents means from unfertilized plots. Values above the bars are mean decreases in total nifH gene abundance (copy number ng^{-1} DNA) per planting mixture. Relationship between nifH gene abundance and plant root biomass **(B)**, colored by planting mixture and either unfertilized (circles) or N-fertilized (triangles). Correlation statistics are provided in the upper right corner for each monoculture. The relationship between nifH gene abundance and root mass fraction **(C)** for all monocultures combined is represented by the black bar. 95% confidence limit is shaded, value densities for root mass fraction and nifH gene abundance colored by N fertilization treatment are on opposing x- and y-axes, and correlation statistic is provided in the top left corner.

N-fixation (Kiers et al., 2003) as reflected in lower nifH gene abundance. Furthermore, the decrease in F/B ratio with +N might indicate a shift from nutrient conservation within mycorrhizal networks to a "leakier" system with more substrate available for opportunistic bacteria (de Vries et al., 2006; Fierer et al., 2009). The shift in allocation from belowground nutritional symbioses to aboveground plant structures provides support for optimal resource allocation strategies in the extended plant phenotype, particularly when adopting the collective view of functions and interactions among plants and microbial consortia (Johnson et al., 2003a; Vandenkoornhuyse et al., 2015).

Plant Biomass, Nutritional Symbioses, and Plant Diversity

Aboveground plant growth increased after +N for all planting treatments, but the strength of these responses was dependent on planting mixture (**Figure 1**). For example, the big bluestem mixture produced the greatest aboveground biomass of all the planting treatments (**Figure 1A**), but +N only increased biomass by ~17%. Kanlow monocultures, on the other hand, had the lowest total yields, and +N increased aboveground biomass by ~85% (**Figure 1**). Further, Kanlow allocated significantly more biomass aboveground to shoots after +N but did not significantly decrease allocation to AM fungal biomass in soil (**Figures 1C**, **2A**), despite it being the only switchgrass cultivar to exhibit significant changes in AM fungal communities in response to +N (**Figure 5B**). Compared to the other cultivars, unfertilized Kanlow monocultures had higher total abundance of nifH in the rhizosphere that was positively correlated with root biomass (**Supplemental Figure 7**; **Figure 10**). Furthermore, Kanlow was the only cultivar in which +N caused a significant decrease in root mass fraction (**Supplemental Figure 1B**). The "case study" of Kanlow might suggest that this switchgrass cultivar reduces its reliance on bacterial N-fixing activity and selectively utilizes particular AM fungal taxa to acquire co-limiting resources in soil (e.g., P), although this was not specifically tested and warrants further study.

In contrast to the monoculture treatments, the big bluestem and prairie mixtures maintained high aboveground productivity and responded less strongly to +N. In the prairie mixture, there was no reduction in AM fungal biomass in soil with +N (**Supplemental Figure 2**). NifH gene abundance was not

measured in roots collected from the diverse planting mixtures, but given the lower growth response to +N, high aboveground productivity, and maintenance of C allocation to AM fungal biomass, it would be interesting to determine if N-fixation under the more diverse big bluestem mixture is maintained or even increased with +N, as was observed in a long-term field experiment in Minnesota (Revillini, 2018). Overall, our study indicates that functional responses to +N depended on plant intra- or interspecific diversity. These cultivar-dependent shifts can be explained by a variety of mechanisms, but our data may indicate selective shifts in microbial associations.

The AM fungal Microbiome

Our findings do not support the hypothesis that species richness of AM fungi should be higher with diverse plant communities compared to monocultures. Responses of AM fungal richness and diversity to plant diversity and +N were subtle and highly variable across the treatments (**Figure 4**). The ß-diversity of AM fungal communities also responded variably to planting mixture whether in roots or soils (**Table 2**) and to +N across plant diversity treatments (**Figure 5B**). Indicator analyses and significant changes in relative abundances of particular AM fungal taxa suggest that AM fungal taxa are individualistic in their responses to plant diversity and N availability (**Figures 6**). For example, *Scutellospora* increased in relative abundance with +N, in roots of Cave-in-Rock monocultures, and in +N prairie mixture plots (**Figure 6**). Fungi within the genus *Scutellospora* have been shown to both increase and decrease in response to N enrichment depending on the study (Johnson et al., 1992; Johnson, 1993; Egerton-Warburton et al., 2007). Environmental context, especially the relative availability of limiting resources, influences the structure and function of AM symbioses (Hoeksema et al., 2010; Johnson, 2010). We observed that plant diversity and +N influenced the structure of AM fungal communities, and additional research is necessary to determine specific functional relationships between switchgrass cultivars and AM fungal taxa. Previous studies have measured the performance of *individual* plant–AM fungal taxa combinations (Ji and Bever, 2016), as well as the *cumulative effects of entire suites* of AM fungi in soils (Bennett and Klironomos, 2018; Kulmatiski, 2018). Substantially more research must be performed in field-based studies to sufficiently elucidate the dynamic interactions among plants, AM fungi, and other soil communities before the mechanisms by which plants engage and select for soil biota to enhance nutrient availability can be understood.

The Bacterial Microbiome

As with AM fungi, plant diversity was not a good predictor of bacterial α-diversity. This supports the conclusion that plant and bacterial diversity are often uncoupled (Wardle, 2006; Prober et al., 2015). However, the ß-diversity of bacterial communities in roots and soils was influenced by the diversity and composition of plants (**Table 3**, **Figure 8**). Bacterial indicator taxa and shifts in relative abundance under +N were observed under the different planting combinations (**Figure 9**). Relative abundance of *Verrucomicrobia* declined significantly with +N (**Figures 9C–D**), on roots of Southlow (**Figure 9A**), and in soils under Cave-in-Rock (**Figure 9B**). This finding corroborates previous studies that show that verrucomicrobial abundance is influenced by N availability in soils (Ramirez et al., 2012; Shen et al., 2017). *Gemmatimonadetes* were indicators of +N in our study, which supports results from Nemergut et al. (2008). It has been proposed that bacterial taxa dominant and active in the rhizosphere, including *Gemmatimonadetes*, may be superior competitors for plant-derived C exudates (Gkarmiri et al., 2017), which can increase under +N despite reduced root biomass allocation (Badri and Vivanco, 2009).

Increasing resource availability can influence the abundance and functioning of bacterial taxa involved with nutrient cycling (Dai et al., 2018). Relative abundance of bacterial taxa related to N-cycling declined predictably after +N in our experiment. Putative N_2-fixing taxa determined previously from switchgrass roots (Bahulikar et al., 2014) such as *Rhizobium*, *Methylobacterium*, *Burkholderia*, and *Azoarcus* were present in roots and soil in our experiment. As predicted, the relative abundance of the putative N_2-fixing families *Agrobacterium*, *Caulobacter*, and *Clostridium* (Zehr et al., 2003; Bahulikar et al., 2014) declined significantly after +N (**Figures 9C–D**). Known nitrifying taxa, *Nitrospira* and *Crenarchaeota* consistently increased in relative abundance after +N (**Figures 9C–D**), which supports conclusions of many previous studies that these taxa should become more abundant with N enrichment (Treusch et al., 2005; Zhou et al., 2015). Interestingly, a previous study showed a potential competitive shift between bacterial *Nitrospira* and archaeal *Crenarchaeota* at high N fertilization rates, but this was not observed in our experiment (Bates et al., 2011). Additional research is necessary to examine how shifts in the structure of bacterial communities may influence their function on roots and in the soil.

CONCLUSIONS

Our results provide a baseline for switchgrass microbiome research. Functional diversity of soil microbial symbionts, though sometimes ecologically coherent and exhibiting phylogenetic trait conservatism (Martiny et al., 2013; Philippot et al., 2010), is influenced by taxa-specific interactions with the environment and other organisms (Martiny et al., 2015). We focused on the important *nutritional* relationships between plants and their AM fungal or bacterial microbiomes in the context of resource trade theories but are aware of other valuable functional roles played by both AM fungal and rhizobacterial communities such as biological control of pathogens and pests, drought tolerance, or induced systemic resistance. Research and methods that can further tease apart the multifunctionality of microbiomes in field studies will be critical to the developing field of plant and soil microbiome management in grasslands (Bender et al., 2016; Toju et al., 2018). This work can help generate hypotheses for future targeted studies that link microbiome assembly with microbial function and facilitation of plant nutrition and health. For example, what relationships can be identified between plant nutrition, plant productivity, or bioenergy production and the shifts in microbial nutrient cycling functions? How are quantities and types of soil organic carbon under different planting mixtures affecting bacterial community structure and function in perennial feedstock

cropping systems over time? Across broad geographic ranges, are there consistent plant–microbial responses to fertilization regimes? Future research of plant growth–promoting microorganisms should identify specific P- and N-cycling microbial functions in field-based studies along nutrient availability gradients to determine thresholds where microbial benefits to plants can be maximized.

DATA AVAILABILITY

The raw data supporting the conclusions of this manuscript will be made available by the authors, without undue reservation, to any qualified researcher.

AUTHOR CONTRIBUTION

DR, NJ, GW, and MM conceived of the experiment. DR performed the majority of the sampling, analyses, and writing. RL performed qPCR of the nifH gene, and all authors contributed equally to manuscript preparation.

FUNDING

Funding was provided by the USDA-AFRI (2010-03894) to GW, MM, and NJ, an NAU Genes to Environment Fellowship to DR, and also science-supporting friends and family of DR on the crowdsourcing site experiment.com (doi:10.18258/7891).

ACKNOWLEDGMENTS

We would like to thank Timothy Vugteveen, Morgan Noland, and Dr. Mitch Greer for help at Fermilab and OSU. Many thanks to Parker Coppick at OSU for measuring NLFA and PLFA from soil samples. Special thanks to Dr. Lela Andrews for support in the lab and molecular sequencing at EnGGen at NAU. Thanks to the Bowker–Johnson soil ecology group at NAU for theoretical development and mental health sessions, and specifically to Bo Stevens for bioinformatics support.

SUPPLEMENTARY MATERIAL

The Supplementary Material for this article can be found online at: https://www.frontiersin.org/articles/10.3389/fpls.2019.01018/full#supplementary-material

REFERENCES

Adesemoye, A. O., Torbert, H. A., and Kloepper, J. W. (2009). Plant growth–promoting rhizobacteria allow reduced application rates of chemical fertilizers. *Microb. Ecol.* 58, 921–929. doi: 10.1007/s00248-009-9531-y

Adkins, J., Jastrow, J. D., Morris, G. P., Six, J., and de Graaff, M.-A. (2016). Effects of switchgrass cultivars and intraspecific differences in root structure on soil carbon inputs and accumulation. *Geoderma* 262, 147–154. doi: 10.1016/j.geoderma.2015.08.019

Agler, M. T., Ruhe, J., Kroll, S., Morhenn, C., Kim, S., Weigel, D., et al. (2016). Microbial hub taxa link host and abiotic factors to plant microbiome variation. *PLoS Biol.* 14, e1002352. doi: 10.1371/journal.pbio.1002352

Alori, E. T., Glick, B. R., and Babalola, O. O. (2017). Microbial phosphorus solubilization and its potential for use in sustainable agriculture. *Front. Microbiol.* 8, 1–8. doi: 10.3389/fmicb.2017.00971

Anderson, M. J. (2001). A new method for non-parametric multivariate analysis of variance. *Austral. Ecol.* 26, 32–46. doi: 10.1111/j.1442-9993.2001.tb00081.x

Azcón-Aguilar, C., and Barea, J. M. (2015). Nutrient cycling in the mycorrhizosphere. *J. Soil Sci. Plant Nutr.* 25, 372–396. doi: 10.4067/S0718-95162015005000035

Badri, D. V., and Vivanco, J. M. (2009). Regulation and function of root exudates. *Plant. Cell Environ.* 32, 666–681. doi: 10.1111/j.1365-3040.2009.01926.x

Bahulikar, R. A., Torres-Jerez, I., Worley, E., Craven, K., and Udvardi, M. K. (2014). Diversity of nitrogen-fixing bacteria associated with switchgrass in the native tallgrass prairie of Northern Oklahoma. *Appl. Environ. Microbiol.* 80, 5636–5643. doi: 10.1128/AEM.02091-14

Bakker, P. A. H. M., Pieterse, C. M. J., de Jonge, R., and Berendsen, R. L. (2018). The soil-borne legacy. *Cell* 172, 1178–1180. doi: 10.1016/j.cell.2018.02.024

Bardgett, R. D., and van der Putten, W. H. (2014). Belowground biodiversity and ecosystem functioning. *Nature* 515, 505–511. doi: 10.1038/nature13855

Bates, S. T., Berg-Lyons, D., Caporaso, J. G., Walters, W., Knight, R., and Fierer, N. (2011). Examining the global distribution of dominant archaeal populations in soil. *ISME J.* 5, 908–917. doi: 10.1038/ismej.2010.171

Bauer, J. T., Kleczewski, N. M., Reynolds, H. L., Bever, J. D., and Clay, K. (2012). Nitrogen-fixing bacteria, arbuscular mycorrhizal fungi, and the productivity and structure of prairie grassland communities. *Oecologia* 170, 1089–1098. doi: 10.1007/s00442-012-2363-3

Bender, S. F., Wagg, C., and van der Heijden, M. G. A. (2016). An underground revolution: biodiversity and soil ecological engineering for agricultural sustainability. *Trends Ecol. Evol.* 31, 440–452. doi: 10.1016/j.tree.2016.02.016

Bennett, J. A., and Klironomos, J. (2018). Mechanisms of plant–soil feedback: interactions among biotic and abiotic drivers. *New Phytol.* 91–96. doi: 10.1002/ecs2.2132

Berg, G., Grube, M., Schloter, M., and Smalla, K. (2014). Unraveling the plant microbiome: Looking back and future perspectives. *Front. Microbiol.* 5, 1–7. doi: 10.3389/fmicb.2014.00148

Bergmann, G. T., Bates, S. T., Eilers, K. G., Lauber, C. L., Caporaso, J. G., Walters, W. A., et al. (2012). The under-recognized dominance of Verrucomicrobia in soil bacterial communities. *Soil Biol. Biochem.* 43, 1450–1455. doi: 10.1016/j.soilbio.2011.03.012

Bever, J. D. (2015). Preferential allocation, physio-evolutionary feedbacks, and the stability and environmental patterns of mutualism between plants and their root symbionts. *New Phytol.* 205, 1503–1514. doi: 10.1111/nph.13239

Bever, J. D., Richardson, S. C., Lawrence, B. M., Holmes, J., and Watson, M. (2009). Preferential allocation to beneficial symbiont with spatial structure maintains mycorrhizal mutualism. *Ecol. Lett.* 12, 13–21. doi: 10.1111/j.1461-0248.2008.01254.x

Bokulich, N., Subramanian, S., Faith, J. J., Gevers, D., Gordon, J. I., Knight, R., et al. (2012). Quality-filtering vastly improves diversity estimates from Illumina amplicon sequencing. *Nat. Methods* 10, 57–59. doi: 10.1038/nmeth.2276

Bouton, J. H. (2007). Molecular breeding of switchgrass for use as a biofuel crop. *Curr. Opin. Genet. Dev.* 17, 553–558. doi: 10.1016/j.gde.2007.08.012

Brejda, J. J., Moser, L. E., and Vogel, K. P. (1998). Evaluation of switchgrass rhizosphere microflora for enhancing seedling yield and nutrient uptake. *Agron. J.* 90, 753–758. doi: 10.2134/agronj1998.00021962009000060006x

Burger, M., and Jackson, L. E. (2003). Microbial immobilization of ammonium and nitrate in relation to ammonification and nitrification rates in organic and conventional cropping systems. *Soil Biol. Biochem.* 35, 29–36. doi: 10.1016/S0038-0717(02)00233-X

Busby, P. E., Soman, C., Wagner, M. R., Friesen, M. L., Kremer, J., Bennett, A., et al. (2017). Research priorities for harnessing plant microbiomes in sustainable agriculture. *PLoS Biol.* 15, 1–14. doi: 10.1371/journal.pbio.2001793

Caporaso, J. G., Bittinger, K., Bushman, F. D., Desantis, T. Z., Andersen, G. L., and Knight, R. (2010a). PyNAST: a flexible tool for aligning sequences to a template alignment. *Bioinformatics* 26, 266–267. doi: 10.1093/bioinformatics/btp636

Caporaso, J. G., Kuczynski, J., Stombaugh, J., Bittinger, K., Bushman, F. D., Costello, E. K., et al. (2010b). QIIME allows analysis of high-throughput community sequencing data. *Nat. Methods* 7, 335–336. doi: 10.1038/nmeth.f.303

Chagnon, P. L., and Bradley, R. L. (2013). Evidence that soil nutrient stoichiometry controls the competitive abilities of arbuscular mycorrhizal vs. root-borne non-mycorrhizal fungi. *Fungal Ecol.* 6, 557–560. doi: 10.1016/j.funeco.2013.09.005

Dai, Z., Su, W., Chen, H., Barberán, A., Zhao, H., Yu, M., et al. (2018). Long-term nitrogen fertilization decreases bacterial diversity and favors the growth of Actinobacteria and Proteobacteria in agro-ecosystems across the globe. *Glob. Chang. Biol.* 24, 3452–3461. doi: 10.1111/gcb.14163

De Cáceres, M., and Legendre, P. (2009). Associations between species and groups of sites: indices and statistical inference. *Ecology* 90, 3566–3574. doi: 10.1890/08-1823.1

De Cáceres, M., Legendre, P., and Moretti, M. (2010). Improving indicator species analysis by combining groups of sites. *Oikos* 119, 1674–1684. doi: 10.1111/j.1600-0706.2010.18334.x

de Vries, F. T., Hoffland, E., van Eekeren, N., Brussaard, L., and Bloem, J. (2006). Fungal/bacterial ratios in grasslands with contrasting nitrogen management. *Soil Biol. Biochem.* 38, 2092–2103. doi: 10.1016/j.soilbio.2006.01.008

Dumbrell, A. J., Ashton, P. D., Aziz, N., Feng, G., Nelson, M., Dytham, C., et al. (2011). Distinct seasonal assemblages of arbuscular mycorrhizal fungi revealed by massively parallel pyrosequencing. *New Phytol.* 190, 794–804. doi: 10.1111/j.1469-8137.2010.03636.x

Egerton-Warburton, L. M., Johnson, N. C., and Allen, E. B. (2007). Mycorrhizal community dynamics following nitrogen fertilization: a cross-site test in five grasslands. *Ecol. Monogr.* 77, 527–544. doi: 10.1890/06-1772.1

Fierer, N., Ladau, J., Clemente, J. C., Leff, J. W., Owens, S. M., Pollard, K. S., et al. (2013). Reconstructing the microbial diversity and function of pre-agricultural tallgrass prairie soils in the United States. *Science* 342, 621–624. doi: 10.1126/science.1243768

Fierer, N., Strickland, M. S., Liptzin, D., Bradford, M. A., and Cleveland, C. C. (2009). Global patterns in belowground communities. *Ecol. Lett.* 12, 1238–1249. doi: 10.1111/j.1461-0248.2009.01360.x

Frostegård, A., and Bååth, E. (1996). The use of phospholipid fatty acid analysis to estimate bacterial and fungal biomass in soil. *Biol. Fertil. Soils* 22, 59–65. doi: 10.1007/s003740050076

Frostegård, Å., Tunlid, A., and Bååth, E. (2011). Use and misuse of PLFA measurements in soils. *Soil Biol. Biochem.* 43, 1621–1625. doi: 10.1016/j.soilbio.2010.11.021

Gaby, J. C., and Buckley, D. H. (2012). A comprehensive evaluation of PCR primers to amplify the nifH gene of nitrogenase. *PLoS ONE.* 7, e42149.

Gilbert, J. A., Blaser, M. J., Caporaso, J. G., Jansson, J. K., Lynch, S. V., and Knight, R. (2018). Current understanding of the human microbiome. *Nat. Med.* 24, 392. doi: 10.1038/nm.4517

Gilbert, J. A., Jansson, J. K., and Knight, R. (2014). The Earth Microbiome Project: successes and aspirations. *BMC Biol.* 12, 69. doi: 10.1186/s12915-014-0069-1

Gkarmiri, K., Mahmood, S., Ekblad, A., and Finlay, R. (2017). Identifying the active microbiome associated with roots and rhizosphere soil of oilseed rape. *Appl. Environ. Microbiol.* 83, 1–14. doi: 10.1128/AEM.01938-17

Govindarajulu, M., Pfeffer, P. E., Jin, H., Abubaker, J., Douds, D. D., Allen, J. W., et al. (2005). Nitrogen transfer in the arbuscular mycorrhizal symbiosis. *Nature* 435, 819–823. doi: 10.1038/nature03610

Gray, S. B., Classen, A. T., Kardol, P., Yermakov, Z., and Michael Miller, R. (2011). Multiple climate change factors interact to alter soil microbial community structure in an old-field ecosystem. *Soil Sci. Soc. Am. J.* 75, 2217. doi: 10.2136/sssaj2011.0135

Hannula, S. E., Morriën, E., De Hollander, M., Van Der Putten, W. H., Van Veen, J. A., and De Boer, W., (2017). Shifts in rhizosphere fungal community during secondary succession following abandonment from agriculture. *ISME J.* 11 (10), 2294–2304. doi: 10.1038/ismej.2017.90

Hart, M. M., and Trevors, J. T. (2005). Microbe management: application of mycorrhizal fungi in sustainable agriculture. *Front. Ecol. Environ.* 3, 533–539. doi: 10.1890/1540-9295(2005)003[0533:MMAOMF]2.0.CO;2

Hodge, A., and Storer, K. (2015). Arbuscular mycorrhiza and nitrogen: implications for individual plants through to ecosystems. *Plant Soil.* 386 (1–2), 1–19.doi: 10.1007/s11104-014-2162-1

Hoeksema, J. D., Chaudhary, V. B., Gehring, C. A., Johnson, N. C., Karst, J., Koide, R. T., et al. (2010). A meta-analysis of context-dependency in plant response to inoculation with mycorrhizal fungi. *Ecol. Lett.* 13, 394–407. doi: 10.1111/j.1461-0248.2009.01430.x

Hungate, B. A., Barbier, E. B., Ando, A. W., Marks, S. P., Reich, P. B., Gestel, N., et al. (2017). The economic value of grassland species for carbon storage. *Sci. Adv.* 3 (4), e1601880. doi: 10.1126/sciadv.1601880

Jach-Smith, L. C., and Jackson, R. D. (2018). N addition undermines N supplied by arbuscular mycorrhizal fungi to native perennial grasses. *Soil Biol. Biochem.* 116, 148–157. doi: 10.1016/j.soilbio.2017.10.009

Ji, B., and Bever, J. D. (2016). Plant preferential allocation and fungal reward decline with soil phosphorus: implications for mycorrhizal mutualism. *Ecosphere* 7, 1–11. doi: 10.1002/ecs2.1256

Johansson, J. F., Paul, L. R., and Finlay, R. D. (2004). Microbial interactions in the mycorrhizosphere and their significance for sustainable agriculture. *FEMS Microbiol. Ecol.* 48, 1–13. doi: 10.1016/j.femsec.2003.11.012

Johnson, N. C. (1993). Can fertilization of soil select less mutualistic mycorrhizae? *Ecol. Appl.* 3, 749–757. doi: 10.2307/1942106

Johnson, N. C. (2010). Resource stoichiometry elucidates the structure and function of arbuscular mycorrhizas across scales. *New Phytol.* 185, 631–647. doi: 10.1111/j.1469-8137.2009.03110.x

Johnson, N. C., Rowland, D. L., Corkidi, L., Egerton-Warburton, L. M., and Allen, E. B. (2003a). Nitrogen enrichment alters mycorrhizal allocation at five mesic to semiarid grasslands. *Ecology* 84, 1895–1908. doi: 10.1890/0012-9658(2003)084[1895:NEAMAA]2.0.CO;2

Johnson, N. C., Wilson, G. W. T., Bowker, M. A., Wilson, J. A., and Miller, R. M. (2010). Resource limitation is a driver of local adaptation in mycorrhizal symbioses. *Proc. Natl. Acad. Sci. U. S. A.* 107, 2093–2098. doi: 10.1073/pnas.0906710107

Johnson, N. C., Wilson, G. W. T., Wilson, J. A., Miller, R. M., and Bowker, M. A. (2015). Mycorrhizal phenotypes and the Law of the Minimum. *New Phytol.* 205, 1473–1484. doi: 10.1111/nph.13172

Johnson, N. C., Wolf, J., and Koch, G. W. (2003b). Interactions among mycorrhizae, atmospheric CO2 and soil N impact plant community composition. *Ecol. Lett.* 6, 532–540. doi: 10.1046/j.1461-0248.2003.00460.x

Johnson, N., Copeland, P., Crookston, R., and Pfleger, F. (1992). Mycorrhizae: possible explanation for yield decline with continuous corn and soybean. *Agron* 84, 387–390. doi: 10.2134/agronj1992.00021962008400030007x

Kiers, E. T., and Denison, R. F. (2008). Sanctions, cooperation and the stability of plant–rhizosphere mutualisms. *Annu. Rev. Ecol. Evol. Syst.* 39, 215–236. doi: 10.1146/annurev.ecolsys.39.110707.173423

Kiers, E. T., Rousseau, R. A., West, S. A., and Denison, R. F. (2003). Host sanctions and the legume–rhizobium mutualism. *Nature* 425, 78–81. doi: 10.1038/nature01931

Kiers, T. E., Duhamel, M., Beesetty, Y., Mensah, J. A., Franken, O., Verbruggen, E., et al. (2011). Reciprocal rewards stabilize cooperation in the mycorrhizal symbiosis. *Science* 333, 880–882. doi: 10.1126/science.1208473

Krohn, A. (2016). akutils-v12: facilitating analyses of microbial communities through QIIME. *Zenodo.* 10, 5281.

Kulmatiski, A. (2018). Community-level plant–soil feedbacks explain landscape distribution of native and non-native plants. *Ecol. Evol.* 8, 2041–2049. doi: 10.1002/ece3.3649

Larimer, A. L., Bever, J. D., and Clay, K. (2010). The interactive effects of plant microbial symbionts: a review and meta-analysis. *Symbiosis* 51, 139–148. doi: 10.1007/s13199-010-0083-1

Lee, J., Lee, S., and Young, J. P. W. (2008). Improved PCR primers for the detection and identification of arbuscular mycorrhizal fungi. *FEMS Microbiol. Ecol.* 65, 339–349. doi: 10.1111/j.1574-6941.2008.00531.x

Levy-Booth, D. J., Prescott, C. E., and Grayston, S. J. (2014). Microbial functional genes involved in nitrogen fixation, nitrification and denitrification in forest ecosystems. *Soil Biol. Biochem.* 75, 11–25. doi: 10.1016/j.soilbio.2014.03.021

Love, M., Anders, S., and Huber, W. (2014). Differential analysis of count data–the DESeq2 package. *Genome Biol.* 15 (550), 10–1186. doi: 10.1186/s13059-014-0550-8

Lozupone, C., and Knight, R. (2005). UniFrac: a new phylogenetic method for comparing microbial communities. *Appl. Environ. Microbiol.* 71, 8228–8235. doi: 10.1128/AEM.71.12.8228-8235.2005

Lugtenberg, B., and Kamilova, F. (2009). Plant-growth-promoting rhizobacteria. *Annu. Rev. Microbiol.* 63, 541–556. doi: 10.1146/annurev.micro.62.081307.162918

Mahé, F., Rognes, T., Quince, C., de Vargas, C., and Dunthorn, M. (2014). Swarm: robust and fast clustering method for amplicon-based studies. *PeerJ* 2, e593. doi: 10.7717/peerj.593

Mangan, M. E., Sheaffer, C., Wyse, D. L., Ehlke, N. J., and Reich, P. B. (2011). Native perennial grassland species for bioenergy: establishment and biomass productivity. *Agron. J.* 103, 509–519. doi: 10.2134/agronj2010.0360

Mao, Y., Li, X., Smyth, E. M., Yannarell, A. C., and Mackie, R. I. (2014). Enrichment of specific bacterial and eukaryotic microbes in the rhizosphere of switchgrass (*Panicum virgatum* L.) through root exudates. *Environ. Microbiol. Rep.* 6, 293–306. doi: 10.1111/1758-2229.12152

Mariotte, P., Canarini, A., and Dijkstra, F. A. (2017). Stoichiometric N: P flexibility and mycorrhizal symbiosis favour plant resistance against drought. *J. Ecol.* 105(4), 958–967. doi: 10.1111/1365-2745.12731

Martiny, A. C., Treseder, K., and Pusch, G. (2013). Phylogenetic conservatism of functional traits in microorganisms. *ISME J.* 7 (4), 830–838. doi: 10.1038/ismej.2012.160

Martiny, J. B., Jones, S. E., Lennon, J. T., and Martiny, A. C. (2015). Microbiomes in light of traits: a phylogenetic perspective. *Science* 350 (6261), aac9323. doi: 10.1126/science.aac9323

McDonald, D., Price, M. N., Goodrich, J., Nawrocki, E. P., DeSantis, T. Z., Probst, A., et al. (2012). An improved Greengenes taxonomy with explicit ranks for ecological and evolutionary analyses of bacteria and archaea. *ISME J.* 6, 610–618. doi: 10.1038/ismej.2011.139

Mehlich, A. (1984). Mehlich 3 soil test extractant: a modification of Mehlich 2 extractant. *Commun. Soil Sci. Plant Anal.* 15, 1409–1416. doi: 10.1080/00103628409367568

Moore, J. A. M., Jiang, J., Patterson, C. M., and Mayes, M. A. (2015). Interactions among roots, mycorrhizas and free-living microbial communities differentially impact soil carbon processes. *J. Ecol.* 103, 1442–1453. doi: 10.1111/1365-2745.12484

Morris, G. P., Hu, Z., Grabowski, P. P., Borevitz, J. O., de Graaff, M. A., Miller, R. M., et al. (2016). Genotypic diversity effects on biomass production in native perennial bioenergy cropping systems. *GCB Bioenergy* 8, 1000–1014. doi: 10.1111/gcbb.12309

Nemergut, D. R., Townsend, A. R., Sattin, S. R., Freeman, K. R., Fierer, N., Neff, J. C., et al. (2008). The effects of chronic nitrogen fertilization on alpine tundra soil microbial communities: implications for carbon and nitrogen cycling. *Environ. Microbiol.* 10, 3093–3105. doi: 10.1111/j.1462-2920.2008.01735.x

Oates, L. G., Duncan, D. S., Sanford, G. R., Liang, C., and Jackson, R. D. (2016). Bioenergy cropping systems that incorporate native grasses stimulate growth of plant-associated soil microbes in the absence of nitrogen fertilization. *Agric. Ecosyst. Environ.* 233, 396–403. doi: 10.1016/j.agee.2016.09.008

Olsson, P. A., Bååth, E., Jakobsen, I., and Söderström, B. (1995). The use of phospholipid and neutral lipid fatty acids to estimate biomass of arbuscular mycorrhizal fungi in soil. *Mycol. Res.* 99, 623–629. doi: 10.1016/S0953-7562(09)80723-5

Öpik, M., Vanatoa, E., Moora, M., Davison, J., Kalwij, J. M., Reier, U., et al. (2010). The online database Maarj AM reveals global and ecosystemic distribution patterns in arbuscular mycorrhizal fungi (Glomeromycota). *New Phytol.* 188, 223–241. doi: 10.1111/j.1469-8137.2010.03334.x

Parrish, D. J., and Fike, J. H. (2005). The biology and agronomy of switchgrass for biofuels. *CRC. Crit. Rev. Plant Sci.* 24, 423–459. doi: 10.1080/07352680500316433

Paulson, J. N., Stine, O. C., Bravo, H. C., and Pop, M. (2013). Differential abundance analysis for microbial marker-gene surveys. *Nat. Methods* 10, 1200–1202. doi: 10.1038/nmeth.2658

Perlack, R. D., Stokes, B. J., Eaton, L. M., and Turnhollow, A. F. (2011). US billion-ton update. Biomass supply for a bioenergy and bioproducts industry. *Renew. Energy* 7, 1–229. doi: 10.1089/ind.2011.7.375

Philippot, L., Andersson, S. G., Battin, T. J., Prosser, J. I., Schimel, J. P., Whitman, W. B. et al. (2010). The ecological coherence of high bacterial taxonomic ranks. *Nat. Rev. Microbiol.* 8 (7), 523–529. doi: 10.1038/nrmicro2367

Price, M. N., Dehal, P. S., and Arkin, A. P. (2009). FastTree: computing large minimum evolution trees with profiles instead of a distance matrix. *Mol. Biol. Evol.* 26, 1641–1650. doi: 10.1093/molbev/msp077

Prober, S. M., Leff, J. W., Bates, S. T., Borer, E. T., Firn, J., Harpole, W. S., et al. (2015). Plant diversity predicts beta but not alpha diversity of soil microbes across grasslands worldwide. *Ecol. Lett.* 18, 85–95. doi: 10.1111/ele.12381

Püschel, D., Janoušková, M., Hujslová, M., Slavíková, R., Gryndlerová, H., and Jansa, J. (2016). Plant–fungus competition for nitrogen erases mycorrhizal growth benefits of *Andropogon gerardii* under limited nitrogen supply. *Ecol. Evol.* 6, 4332–4346. doi: 10.1002/ece3.2207

Ramirez, K. S., Craine, J. M., and Fierer, N. (2012). Consistent effects of nitrogen amendments on soil microbial communities and processes across biomes. *Glob. Chang. Biol.* 18, 1918–1927. doi: 10.1111/j.1365-2486.2012.02639.x

Reed, S. C., Cleveland, C. C., and Townsend, A. R. (2011). Functional ecology of free-living nitrogen fixation: a contemporary perspective. *Annu. Rev. Ecol. Evol. Syst.* 42, 489–512. doi: 10.1146/annurev-ecolsys-102710-145034

Revillini, D. (2018). The role of shifting resource availability in shaping grassland-soil microbial symbiont interactions.

Revillini, D., Gehring, C. A., and Johnson, N. C. (2016). The role of locally adapted mycorrhizas and rhizobacteria in plant–soil feedback systems. *Funct. Ecol.* 30, 1086–1098. doi: 10.1111/1365-2435.12668

Reynolds, H. L., Hartley, A. E., Vogelsang, K. M., Bever, J. D., and Schultz, P. A. (2005). Arbuscular mycorrhizal fungi do not enhance nitrogen acquisition and growth of old-field perennials under low nitrogen supply in glasshouse culture. *New Phytol.* 167, 869–880. doi: 10.1111/j.1469-8137.2005.01455.x

Rognes, T., Flouri, T., Nichols, B., Quince, C., and Mahé, F. (2016). VSEARCH: a versatile open source tool for metagenomics. *PeerJ* 4, e2584. doi: 10.7287/peerj.preprints.2409v1

Rubin, R. L., Groenigen, K. J., and Hungate, B. A. (2017). Plant growth promoting rhizobacteria are more effective under drought: a meta-analysis. *Plant Soil.* 416 (1–2), 309–323. doi: 10.1007/s11104-017-3199-8

Sakamoto, K., Iijima, T., and Higuchi, R. (2004). Use of specific phospholipid fatty acids for identifying and quantifying the external hyphae of the arbuscular mycorrhizal fungus *Gigaspora rosea*. *Soil Biol. Biochem.* 36, 1827–1834. doi: 10.1016/j.soilbio.2004.04.037

Schlaeppi, K., and Bulgarelli, D. (2015). The plant microbiome at work. *Mol. Plant–Microbe Interact.* 28, 212–217. doi: 10.1094/MPMI-10-14-0334-FI

Semchenko, M., Leff, J. W., Lozano, Y. M., Saar, S., Davison, J., Wilkinson, A., et al. (2018). Fungal diversity regulates plant–soil feedbacks in temperate grassland. *Sci. Adv.* 4, eaau4578. doi: 10.1126/sciadv.aau4578

Sharma, M. P., and Buyer, J. S. (2015). Comparison of biochemical and microscopic methods for quantification of arbuscular mycorrhizal fungi in soil and roots. *Appl. Soil Ecol.* 95, 86–89. doi: 10.1016/j.apsoil.2015.06.001

Shen, C., Ge, Y., Yang, T., and Chu, H. (2017). Verrucomicrobial elevational distribution was strongly influenced by soil pH and carbon/nitrogen ratio. *J. Soils Sediments* 17, 2449–2456. doi: 10.1007/s11368-017-1680-x

Singer, E., Bonnette, J., Kenaley, S. C., Woyke, T., and Juenger, T. E. (2019). Plant compartment and genetic variation drive microbiome composition in switchgrass roots. *Environ. Microbiol. Rep.* 11, 185–195. doi: 10.1111/1758-2229.12727

Sprunger, C. D., Oates, L. G., Jackson, R. D., and Robertson, G. P. (2017). Plant community composition influences fine root production and biomass allocation in perennial bioenergy cropping systems of the upper Midwest, USA. *Biomass Bioenergy* 105, 248–258. doi: 10.1016/j.biombioe.2017.07.007

Strickland, M. S., and Rousk, J. (2010). Considering fungal:bacterial dominance in soils—methods, controls, and ecosystem implications. *Soil Biol. Biochem.* 42, 1385–1395. doi: 10.1016/j.soilbio.2010.05.007

Tilman, D., Hill, J., and Lehman, C. (2006). Carbon-negative biofuels from low-input high-diversity grassland biomass. *Science* 314, 1598–1600. doi: 10.1126/science.1133306

Toju, H., Peay, K. G., Yamamichi, M., Narisawa, K., Hiruma, K., Naito, K., et al. (2018). Core microbiomes for sustainable agroecosystems. *Nat. Plants* 4, 247–257. doi: 10.1038/s41477-018-0139-4

Treusch, A. H., Leininger, S., Kietzin, A., Schuster, S. C., Klenk, H. P., and Schleper, C. (2005). Novel genes for nitrite reductase and Amo-related proteins indicate a role of uncultivated mesophilic crenarchaeota in nitrogen cycling. *Environ. Microbiol.* 7, 1985–1995. doi: 10.1111/j.1462-2920.2005.00906.x

Vacher, C., Hampe, A., Porté, A. J., Sauer, U., Compant, S., and Morris, C. E. (2016). The phyllosphere: microbial jungle at the plant–climate interface. *Annu. Rev. Ecol. Evol. Syst.* 47, 1–24. doi: 10.1146/annurev-ecolsys-121415-032238

van der Heijden, M. G., Bruin, S., Luckerhoff, L., van Logtestijn, R. S., and Schlaeppi, K. (2016). A widespread plant–fungal–bacterial symbiosis promotes plant biodiversity, plant nutrition and seedling recruitment. *ISME J.* 10, 389–399. doi: 10.1038/ismej.2015.120

van der Putten, W. H., Bardgett, R. D., Bever, J. D., Bezemer, T. M., Casper, B. B., Fukami, T., et al. (2013). Plant–soil feedbacks: the past, the present and future challenges. *J. Ecol.* 101, 265–276. doi: 10.1111/1365-2745.12054

Vandenkoornhuyse, P., Quaiser, A., Duhamel, M., Le Van, A., and Dufresne, A. (2015). The importance of the microbiome of the plant holobiont. *New Phytol.* 206, 1196–1206. doi: 10.1111/nph.13312

Verbruggen, E., Xiang, D., Chen, B., Xu, T., and Rillig, M. C. (2015) Mycorrhizal fungi associated with high soil N:P ratios are more likely to be lost upon conversion from grasslands to arable agriculture. *Soil Biol. Biochem*. 86, 1–4. doi: 10.1016/j.soilbio.2015.03.008

Wardle, D. A. (2006). The influence of biotic interactions on soil biodiversity. *Ecol. Lett*. 9, 870–886. doi: 10.1111/j.1461-0248.2006.00931.x

Wei, C., Yu, Q., Bai, E., Lü, X., Li, Q., Xia, J., et al. (2013). Nitrogen deposition weakens plant–microbe interactions in grassland ecosystems. *Glob. Chang. Biol.* 19, 3688–3697. doi: 10.1111/gcb.12348

Wilsey, B. J., and Wayne Polley, H. (2006). Aboveground productivity and root–shoot allocation differ between native and introduced grass species. *Oecologia* 150, 300–309. doi: 10.1007/s00442-006-0515-z

Wright, L., and Turhollow, A. (2010). Switchgrass selection as a "model" bioenergy crop: a history of the process. *Biomass Bioenergy* 34, 851–868. doi: 10.1016/j.biombioe.2010.01.030

Yang, Y., Tilman, D., Lehman, C., and Trost, J. J. (2018). Sustainable intensification of high-diversity biomass production for optimal biofuel benefits. *Nat. Sustain.* 11, 686. doi: 10.1038/s41893-018-0166-1

Zehr, J. P., Jenkins, B. D., Short, S. M., and Steward, G. F. (2003). Nitrogenase gene diversity and microbial community structure: a cross-system comparison. *Environ. Microbiol.* 5, 539–554. doi: 10.1046/j.1462-2920.2003.00451.x

Zheng, C., Ji, B., Zhang, J., Zhang, F., and Bever, J. D. (2014). Shading decreases plant carbon preferential allocation towards the most beneficial mycorrhizal mutualist. *New Phytol.* 205, 361–368. doi: 10.1111/nph.13025

Zhou, X., Fornara, D., Anne, E., Wang, D., Ren, G., Christie, P., et al. (2015). Effects of 44 years of chronic nitrogen fertilization on the soil nitrifying community of permanent grassland. *Soil Biol. Biochem.* 91, 76–83. doi: 10.1016/j.soilbio.2015.08.031

Zogg, G. P., Zak, D. R., Ringelberg, D. B., White, D. C., MacDonald, N. W., and Pregitzer, K. S. (1997). Compositional and functional shifts in microbial communities due to soil warming. *Soil Sci. Soc. Am. J.* 61, 475. doi: 10.2136/sssaj1997.03615995006100020015x

Conflict of Interest Statement: The authors declare that the research was conducted in the absence of any commercial or financial relationships that could be constructed as a potential conflict of interest.

frontiers in Microbiology

REVIEW
published: 29 October 2019
doi: 10.3389/fmicb.2019.02452

Single-Cell RNA Sequencing of Plant-Associated Bacterial Communities

Qin Ma[1†], Heike Bücking[2], Jose L. Gonzalez Hernandez[1,2] and Senthil Subramanian[1,2]*

[1] Department of Agronomy, Horticulture, and Plant Science, South Dakota State University, Brookings, SD, United States,
[2] Biology and Microbiology Department, South Dakota State University, Brookings, SD, United States

Plants in soil are not solitary, hence continually interact with and obtain benefits from a community of microbes ("microbiome"). The meta-functional output from the microbiome results from complex interactions among the different community members with distinct taxonomic identities and metabolic capacities. Particularly, the bacterial communities of the root surface are spatially organized structures composed of root-attached biofilms and planktonic cells arranged in complex layers. With the distinct but coordinated roles among the different member cells, bacterial communities resemble properties of a multicellular organism. High throughput sequencing technologies have allowed rapid and large-scale analysis of taxonomic composition and metabolic capacities of bacterial communities. However, these methods are generally unable to reconstruct the assembly of these communities, or how the gene expression patterns in individual cells/species are coordinated within these communities. Single-cell transcriptomes of community members can identify how gene expression patterns vary among members of the community, including differences among different cells of the same species. This information can be used to classify cells based on functional gene expression patterns, and predict the spatial organization of the community. Here we discuss strategies for the isolation of single bacterial cells, mRNA enrichment, library construction, and analysis and interpretation of the resulting single-cell RNA-Seq datasets. Unraveling regulatory and metabolic processes at the single cell level is expected to yield an unprecedented discovery of mechanisms involved in bacterial recruitment, attachment, assembly, organization of the community, or in the specific interactions among the different members of these communities.

Keywords: rhizosphere, microbiome, droplet-sequencing, split pool ligation-based transcriptome sequencing, fluorescence-activated cell sorting, rolling circle amplification, single primer isothermal amplification

OPEN ACCESS

Edited by:
Pierre-Emmanuel Courty, Institut National de la Recherche Agronomique (INRA), France

Reviewed by:
Samuel Mondy, INRA Centre Dijon Bourgogne Franche-Comté, France
Claudia Knief, University of Bonn, Germany

***Correspondence:**
Senthil Subramanian
Senthil.Subramanian@sdstate.edu

†Present address:
Qin Ma, Department of Biomedical Informatics, Ohio State University, Columbus, OH, United States

Specialty section:
This article was submitted to Plant Microbe Interactions, a section of the journal Frontiers in Microbiology

Received: *05 April 2019*
Accepted: *11 October 2019*
Published: *29 October 2019*

Citation:
Ma Q, Bücking H, Gonzalez Hernandez JL and Subramanian S (2019) Single-Cell RNA Sequencing of Plant-Associated Bacterial Communities. Front. Microbiol. 10:2452. doi: 10.3389/fmicb.2019.02452

INTRODUCTION

Plants are holobionts and are associated with complex and very diverse microbiomes (Simon et al., 2019). The long co-evolution of plants and their microbial communities has shaped the holobiont, and contributed to the development of microbial species that are specifically adapted to their respective plant host, and play a significant role in plant productivity and stress resistance. The microbiome or the second plant genome (Turner et al., 2013) represents a highly under-explored genetic resource with thousands of genes that can potentially be harnessed to increase crop yield and to alleviate stress responses. The advantages of using a microbiome-based solution include: (1) a typically shorter discovery to application pipeline due to a streamlined regulatory process,

(2) a higher specificity compared to currently available crop protection products, and (3) a better compatibility with emerging precision agriculture technologies (Parnell et al., 2016; Deshayes et al., 2017). Due to the important role that the microbiome plays in plant health, stress resistance and nutrition acquisition, there is an increasing interest to design microbial communities that can promote plant growth in diverse environments. Plant-associated microbial communities are not randomly assembled; structure and composition of these microbiomes change in response to different environmental parameters (Bogino et al., 2013). Primary determinants of plant-associated microbial community composition and function include soil type (Lundberg et al., 2012), plant compartment (Bai et al., 2015), plant genotype (Bouffaud et al., 2014), activity of the plant immune system, and plant developmental stage (reviewed by Hassani et al., 2018). However, our current understanding about how microbial community compositions are shaped, how these communities are assembled, and how the interactions among specific bacteria affect the function of these communities is very limited.

Most plant-associated microbial communities, for example root surface bacterial communities, are spatially organized structures composed of root-attached biofilms and planktonic cells arranged in complex layers (Castiblanco and Sundin, 2016). In addition, evidence for bacterial co-association, symbiosis, and habitat sharing suggest that interactions among members might dynamically shape the community composition and function (Sloan and Lebeis, 2015). In this context, a microbiome can be compared to a multi-cellular organism, in which different cells serve distinct, but coordinated roles that control organismal function (Stovicek et al., 2012). The development of high throughput sequencing technologies allowed rapid and large-scale analysis of microbial ribosomal amplicons, metagenomes, or metatranscriptomes, and have provided us with insights into the taxonomic composition, collective gene pool, and gene expression patterns of microbiomes (Knief, 2014; Zhou et al., 2015). However, these methods are unable to reconstruct how gene pools and gene expression patterns are organized in individual cells of microbiomes. Single-cell genomics of microbial cells offers a solution to this limitation and can define the metabolic features and potential of individual cells that shape microbiome function. Application of single-cell approaches in microbes including single-cell transcriptomics of individual species have been reviewed recently (Chen Z. et al., 2017; Hwang et al., 2018; Zhang et al., 2018). Here, we discuss strategies on how currently available methods in single-cell RNA-Seq (scRNA-seq) including the highly scalable split pool ligation-based transcriptome sequencing (SPLiT-seq; Rosenberg et al., 2017, 2018) can be adapted for the exploration of plant-associated bacterial communities.

METHODS FOR ISOLATION OF SINGLE BACTERIAL CELLS FOR GENOMICS ANALYSES

Methods for isolation of bacterial communities from plant root surfaces and apoplastic compartments without plant tissue contamination are available (White et al., 2015; McPherson et al., 2018; Gentzel et al., 2019). Isolation of bacterial cells from root surfaces typically involves sonication or vortexing in buffers containing mild detergents to dislodge cells from the root. Bacteria residing in plant apoplasts can be isolated by infiltrating the plant tissues with appropriate buffers followed by centrifugation to isolate the apoplastic wash fluids. Contamination with plant cells or other materials can be minimized by passing these fractions through a 20 μm sieve. These methods have been used to evaluate the composition of bacterial communities in a variety of plant species (Lundberg et al., 2012; Peiffer et al., 2013; Edwards et al., 2015; Wang et al., 2017; White et al., 2017). The same methods can be used to obtain source communities for single cell isolation and analysis. The compatibility of these methods with fixed cells negates any concerns on changes in microbial gene expression during the isolation process. Several approaches have been developed/adapted for genomics of single bacterial cells including serial dilution (Zhang et al., 2006), microfluidics (Chen et al., 2011), flow cytometry (Raghunathan et al., 2005), micromanipulation (Ishoy et al., 2006), or encapsulation in droplets (Tolonen and Xavier, 2017). The majority of these methods require the capability to isolate single cells and prepare individually labeled sequencing libraries from each of these cells. scRNA-Seq approaches of bacterial cells, however, are particularly challenging due to the lack of polyadenylated mRNAs and the lower number of template molecules per cell compared to those in plants and other eukaryotes. Strategies to adapt specialized methods to distinguish coding and non-coding RNAs and those for linear amplification of RNA/cDNA molecules for successful scRNA-Seq of bacterial cells are discussed in see section "Methods for construction of RNA-seq libraries from single bacterial cells".

Serial Dilution

A simple but effective method to isolate single cells from a bacterial population is serial dilution. After determining cell densities by direct counting via a Helber counting chamber or other reliable methods, cells are diluted to single cells into microtiter plate wells. These single cells can be enzymatically manipulated to lyse the cell wall and denature the membrane to release cellular contents for cDNA synthesis and library construction. Serial dilution has successfully been applied to single cells of *Escherichia coli* and *Procholorococcus* to develop a polymerase-based whole genome amplification method, polymerase cloning or "ploning" (Zhang et al., 2006). Serial dilution is an easy method that can be applied by most laboratories as it is simple and does not require any specialized instrumentation. One of the major limitations for this technique is, however, the risk of DNA contaminations from the environment or from reagents and labware that can lead to background amplifications. Strict sample handling and experimental protocols involving a clean air chamber and UV treatment of reagents and labware can lower these contamination risks. However, current assessments suggest that the precision of this methodology is insufficient, even if its

accuracy of 88% is comparable to traditional flow cytometry-based technologies for single cell isolation (Raghunathan et al., 2005; Zhang et al., 2006).

Micromanipulation

Many micromanipulation methods driven by the desire to culture single prokaryotic and eukaryotic cells were developed and improved throughout the last century (reviewed by Fröhlich and König, 2006). The low magnification of standard microscopical systems precluded their use for the isolation of single prokaryotic cells. Developments in resolution and magnification of modern microscopy has led to the adaptation of these methods for the investigation of larger prokaryotes such as filamentous bacteria (Kämpfer, 2006) and cyanobacteria (Šulčius et al., 2017). Micromanipulation has also been used to isolate individual bacterial cells from food samples (Hohnadel et al., 2018) and hot spring sediments (Ishoy et al., 2006). Two of the major approaches used in micromanipulation are (1) the use of a focused laser beam to capture and transfer the cell of interest from a population to a compartment (e.g., Keloth et al., 2018), and (2) the use of microinjectors in combination with the precision of a micromanipulator that can handle single prokaryotic cells (e.g., Ishoy et al., 2006). While the methodology is continuously improving and can be applied to address questions of organismal survival and success rate of recovery, it is laborious, very low throughput, and requires specialized equipment.

Laser Capture Microdissection (LCM)

Laser Capture Microdissection is a contact- and contamination-free method for isolating specific single cells or entire areas of tissue from a wide variety of samples. In this technique the desired cell, or group of cells, is cut off a tissue section or other source, and is transferred without contact to a microtube for further processing (Nakazono, 2003). The advantage of this method is that it allows selecting individual cells of interest; but since the technique is very laborious and time-consuming, it only supports low throughput approaches. While this method has been used to for example study cell development in plant tissues or gene expression in mutualistic and pathogenic interactions (Balestrini et al., 2009; Gomez and Harrison, 2009), the insufficient spatial resolution makes this technique undesirable to isolate small bacterial cells from a dense community. Unlike eukaryotic cells that are in complex tissues, individual cells in bacterial communities can be easily separated by vortexing or other methods to obtain single cells. Therefore, other methods such as serial dilution (see section "Serial dilution") or flow cytometry (see section "Fluorescence activated cell sorting") may be more practicable than LCM. However, the ability to observe bacterial cells by LCM before they are selected provides some advantages, and the technique has been applied to isolate single bacterial cells from environmental samples. When plant microbe interactions are examined, LCM can be effectively applied to evaluate gene expression patterns in plant endophytes that are associated with specific regions of the plant. For example, root cortex and vascular tissues that are isolated by LCM can be subsequently used to evaluate single-cell genomics of endophytic microbes that reside within these tissues (Jahiri, 2013).

Fluorescence Activated Cell Sorting

Fluorescence activated cell sorting (FACS) can be used to detect and sort cells from a population based on their different chemical or physical characteristics. Cells in suspension are transported, one cell at a time, and pass through a laser beam. Scattered light is characteristic of individual cells based on their composition and/or physical properties and is used to gate cells into collection chambers (Müller and Nebe-von-Caron, 2010). Typically, cells are labeled with one or more fluorescence markers to sort the cells into different chambers. This principle has been used to collect individual bacterial cells and determine their identities using multiple displacement amplification (Raghunathan et al., 2005).

One of the most common labels used for bacterial cell sorting is target-specific 16S rRNA fluorescence-*in situ*-hybridization (FISH). Limitations of the traditional 16S rRNA FISH technology, for example the limited and variable amounts of rRNA, have been addressed by the development of liquid phase tyramide signal amplification FISH (TSA-FISH), which is compatible with flow sorting. Similarly, custom made μFACS systems have been developed that support faster throughput and less expensive applications with lower contamination risks due to their use of closed systems, and their higher sorting efficiency (Chen et al., 2011). However, the sorting accuracy of these systems still needs to be significantly improved to be comparable to commercial cell sorters. However, single-cell genomics approaches do not rely on accurate sorting of different cell types, but rather accurate sorting of one cell per container (i.e., cell clumps must be avoided). Therefore, the combination of μFACS systems with viable cell deposition modules such as microwell arrays could make these technologies applicable despite their inaccuracies in sorting. The ability of μFACS systems to apply optical, electroosmotic, dielectrophoretic, and hydrodynamic switching methods for cell sorting offers advantages for their adaptability to a broad range of sample types (Müller and Nebe-von-Caron, 2010). Typical contamination risks from cell free DNA in liquid phase cell isolation systems particularly in environmental samples can be reduced in FACS/μFACS systems by multiple rounds of sorting (Chen et al., 2011).

Droplet-Based Systems

Recent developments in microfluidic technologies have led to the development of instrumentation capable of sorting individual cells by encapsulating each of them in individually barcoded gel beads followed by the library preparation of individually barcoded RNAseq libraries. The current commercially available microfluidic platforms are the 10 X Genomics Chromium platform (Pleasanton, CA, United States) with a cell size range of up to 50 μm, and the Fluidigm C1 platform (South San Franscisco, CA, United States) with a cell size range of 10–17 μm. Recently, single-cell printing methods were adapted for the encapsulation of single bacterial cells in droplets (Riba et al., 2016). These systems use a transparent microfluidic drop-on-demand dispenser chip coupled with a camera-assisted automatic cell detection system. Cell detection and classification helps to avoid the collection of empty droplets and thus enables a "one cell per droplet" printing mode (Gross et al., 2013). Dispenser chips

with smaller channel depth and nozzle to allow the detection and printing of cells down to 1 μm in size were developed for bacterial cells (Riba et al., 2016). However, in all these platforms, bacterial cell walls need first to be permeabilized in order to incorporate the barcoded beads. In recent studies, partial spheroplasts of yeast were generated by treating the cell suspensions with zymolyase to digest cell walls before the encapsulation (Gasch et al., 2017). A similar approach can be adapted for bacterial cells. The main advantage of microfluidics resides in the high throughput capabilities by which these systems can yield encapsulated cells; up to 100,000 or 800 cells in the 10 X and Fluidigm platforms, respectively.

Alternatively, it is possible to use custom-made drop-seq devices in combination with commercially available barcoded beads (Macosko et al., 2015). It is important to note that the approach also requires modifications in the cDNA synthesis phase due to the lack of polyadenylation of bacterial transcripts.

METHODS FOR CONSTRUCTION OF RNA-SEQ LIBRARIES FROM SINGLE BACTERIAL CELLS

Many of the cell isolation methods have successfully been used to obtain genome sequences of individual bacterial cells, and can be adapted to obtain epigenomes as well. However, their adaptability for scRNA-seq is limited. Lack of polyadenylation in bacterial mRNAs, for example, requires methodologies to selectively enrich these molecules from the ∼10 times more abundant tRNA and rRNA molecules (see section "Methods to enrich bacterial mRNAs"). The very low RNA content of bacterial cells is another challenge, and requires the amplification of RNA or cDNA molecules, while amplification biases are avoided (see section "Methods to amplify RNA or cDNA"). Finally, the highly complex bacterial cell wall poses a challenge since enzymatic and chemical approaches to disrupt the cell wall and membrane may not be compatible with the reagents for the subsequent steps in RNA-seq library construction.

Methods to Enrich Bacterial mRNAs

The need to prepare individually labeled sequencing libraries from individual cells precludes the use of typical affinity-based methods for enrichment of mRNAs or removal of rRNAs. In contrast, in-cell mRNA enrichment methods are suitable for this purpose.

Selective Exonuclease Based Enrichment of Messenger RNAs

Terminator^{TM} 5′-phosphate-dependent-5′- 3′exonuclease digests rRNAs and tRNAs, but not RNA molecules with a 5′-triphosphate, a 5′-cap, or a 5′-hydroxyl group. Consequently, Terminator^{TM} exonuclease can be used to selectively degrade rRNA and tRNA molecules with a 5′-phosphate structure, but not mRNA molecules. An exonuclease treatment at optimal concentrations enriched mRNA molecules from single cells of *Burkholderia thailandensis* and enables its potential use for next-generation sequencing (Kang et al., 2011, 2015). Measurements of different classes of RNA molecules by q-PCR indicated a significant reduction in the levels of tRNAs and rRNAs after exonuclease treatment. Comparison of gene expression profiles between enriched and unenriched samples using microarrays showed a negligible bias after the enrichment. While the use excess nuclease resulted in a better enrichment of mRNA molecules, a higher level of amplification bias was observed, possibly due to a non-specific digestion of mRNAs.

Reducing Non-desired Molecules in a Sequence-Specific Manner

There are two other methods with which rRNA or other non-target molecules can be reduced or eliminated. In the "not-so-random" (NSR) primer approach, random hexamers that match rRNA (or other non-target RNA) sequences are left out from the pool of random primers used for cDNA synthesis (Armour et al., 2009). This approach enriched non-rRNA derived cDNA molecules by four-fold (22% of the library to 87%). However, it is possible that a selected subset of hexamer primers can distort the resulting cDNA populations. In an alternate method, undesired sequences were eliminated after cDNA synthesis by random priming (Armour et al., 2018). Here, first strand synthesis was performed using random primers with an adapter containing a restriction enzyme recognition sequence. Subsequently, a second strand synthesis reaction was performed using primers specific to rRNAs or other undesired molecules resulting in double stranded cDNA molecules that contained these undesirable sequences. Next, restriction digestion was used to remove the adapters from these molecules and prevented their amplification during the next step of library preparation. In either case, prior knowledge about the undesirable sequences is required, what makes it difficult to use these methods for the evaluation of bacterial communities of unknown composition. A successful application of these methods for the enrichment of bacterial RNA has not yet been demonstrated.

Methods to Amplify RNA or cDNA

Rolling Circle Amplification of RNA

Rolling circle amplification has been used to evaluate global gene expression in single cells of *B. thailandensis* (Kang et al., 2011). After cDNA synthesis, bacterial chromosomal DNA or other contaminant DNA molecules were digested by methylation-dependent restriction enzymes (e.g., McrBC and *Dpn*I), and the newly synthesized single-stranded cDNA (ss-cDNA) was circularized via 5′-end phosphorylation and intramolecular ligation. The circularized ss-cDNA was then randomly primed with RNA hexamers and subjected to multiple displacement amplifications using ϕ29 DNA polymerase. Thiophosphate-linked RNA random hexamers were used to reduce primer dimers and non-specific priming (Takahashi et al., 2009). This method yielded 25–30 μg cDNA from 0.2 to 1 pg RNA. The method was efficient and successfully amplified approximately 94–96% of the total transcripts. While absolute gene expression levels were poorly correlated between amplified single-cell transcriptomes vs. non-amplified bulk cell transcriptomes, the fold-change values were highly correlated. Using the same protocol single cell transcriptomes of *Pseudomonas aeruginosa*

and *Burkholderia pseudomallei* were analyzed, and the authors suggested that the protocol might also be suitable for the analysis of mixed bacterial communities, and that identical amplification conditions for all samples should be used to avoid any interference from amplification bias (Kang et al., 2011, 2015).

Single Primer Isothermal Amplification

In single primer isothermal amplification (SPIA), a unique chimeric 5′-RNA/DNA-3′ primer is used for first strand cDNA synthesis. Second strand synthesis results in a double-stranded cDNA with a unique DNA/RNA heteroduplex at one end. RNase H–mediated degradation of RNA in this heteroduplex enables binding of another chimeric 5′-RNA/DNA-3′ primer which is then extended to displace the existing first strand. The process of chimeric DNA/RNA primer binding, DNA replication, strand displacement and repeated RNA cleavage leads to a rapid accumulation of amplified cDNA (Kurn et al., 2005). SPIA was successfully used to obtain ∼7–17 μg of cDNA from just 5 fg of RNA from single cells of *Synechocystis* sp. PCC 6803. RNA-seq was used to evaluate changes in gene expression in three single cells each after nitrogen starvation. The average gene numbers in single cells were comparable to the numbers of bulk cell populations at each individual time point. Up to 98.6% of the genes in bulk cell populations were also detected in single cells underscoring the efficiency of SPIA amplification (Wang et al., 2015).

A number of other methods typically used for the amplification of polyadenylated mRNA molecules from single cells of eukaryotic organisms (Ziegenhain et al., 2017) can also be modified to amplify single-cell bacterial mRNA, but examples for the successful adaptation of these techniques are not yet available. Some of these techniques, such as single-cell universal poly(A)-independent RNA sequencing (SUPeR-seq) (Fan et al., 2015) are compatible with drop-seq and microfluidics-based approaches reviewed by Chen Z. et al. (2017). However, these methods might need to be preceded by mRNA enrichment as they do not distinguish between bacterial mRNAs, rRNAs or tRNAs.

ADAPTING SPLIT POOL LIGATION-BASED TRANSCRIPTOME SEQUENCING FOR BACTERIAL SINGLE-CELL RNA-SEQ

Split pool ligation-based transcriptome sequencing, a recently developed alternative for scRNA-seq, labels the cellular origin of RNA through combinatorial indexing (Rosenberg et al., 2018). This method has two major advantages: (1) it does not require the physical separation of single cells, and thus there is no need for specialized equipment; and (2) it uses unencapsulated and fixed cells and therefore provides maximized reagent compatibility with downstream molecular biological reactions for library construction (Rosenberg et al., 2017, 2018). For combinatorial indexing, (1) fixed and permeabilized cells are split into different microtiter plate wells, (2) a well-specific barcode is appended to intracellular transcripts, and (3) the cells are pooled back together (**Figure 1**). By repeating this process several times, each cell travels through a unique combination of wells with very high likelihood. Consequently, all transcripts from the same cell will contain a unique combination of barcodes indicating their cellular origin (**Figure 1**).

This method was originally developed for single-cell transcriptomics of mammalian cells, but could be ideal for scRNA-seq of bacterial communities due to its robust scalability in addition to the above described benefits. However, the presence of the bacterial cell wall and transcripts without a polyA tail will require the optimization of steps that are involved in cellular fixation, permeabilization, and in-cell library construction (see below). The successful application of methods for the permeabilization of bacteria for *in situ* hybridization and PCR as well as the selective enrichment and amplification of bacterial mRNAs are very promising for the effective adaptation of SPLiT-seq for bacterial scRNA-seq (**Figure 1**).

Cell Permeabilization

Methods have already been established for the *in situ* localization of RNA through hybridization and PCR in a number of Gram-positive and Gram-negative bacteria (Tani et al., 1998; Russell and Keiler, 2009; Parsley et al., 2010). These methods can be used to effectively permeabilize bacterial cells for SPLiT-seq. Fixation of bacterial cells using para-formaldehyde and ethanol, followed by permeabilization using lysozyme and proteinase K treatment, for example, enabled the successful identification of specific transcripts in microbial communities through *in situ* reverse transcription (RT) and PCR with labeled nucleotides (Hodson et al., 1995; Tani et al., 1998). Since in-cell RNA-seq library construction essentially utilizes RT, adapter ligation, and PCR, we propose the use of these methods for the fixation and permeabilization of bacterial cells for SPLiT-seq.

mRNA Enrichment

Terminator^{TM} 5′-phosphate-dependent-5′ – 3′exonuclease treatment to selectively enrich prokaryotic mRNA will be ideal for bacterial SPLiT-seq. Following mRNA enrichment, multiple options exist for amplification and library construction. For example, the remaining RNA molecules (primarily mRNAs) can be polyadenylated at the 3′-end using a Poly(A) polymerase in the presence of ATP (**Figure 1**). These molecules will now be compatible with the cell scRNA-seq library construction method that has been developed for eukaryotic cells (Rosenberg et al., 2017). However, the relatively small amounts of RNA in single bacterial cells might make efficient library construction difficult. In that case, the SPLiT-seq protocol can be easily modified to incorporate one of the RNA/cDNA amplification methods that have successfully been applied in prokaryotic systems (e.g., rolling circle amplification or SPIA, see above).

In-Cell Library Construction

The SPLiT-seq method involves in-cell RT using barcoded oligo-dT and/or random hexamer primers, followed by ligation of subsequent barcodes. Briefly, the cells are split into 48 wells each

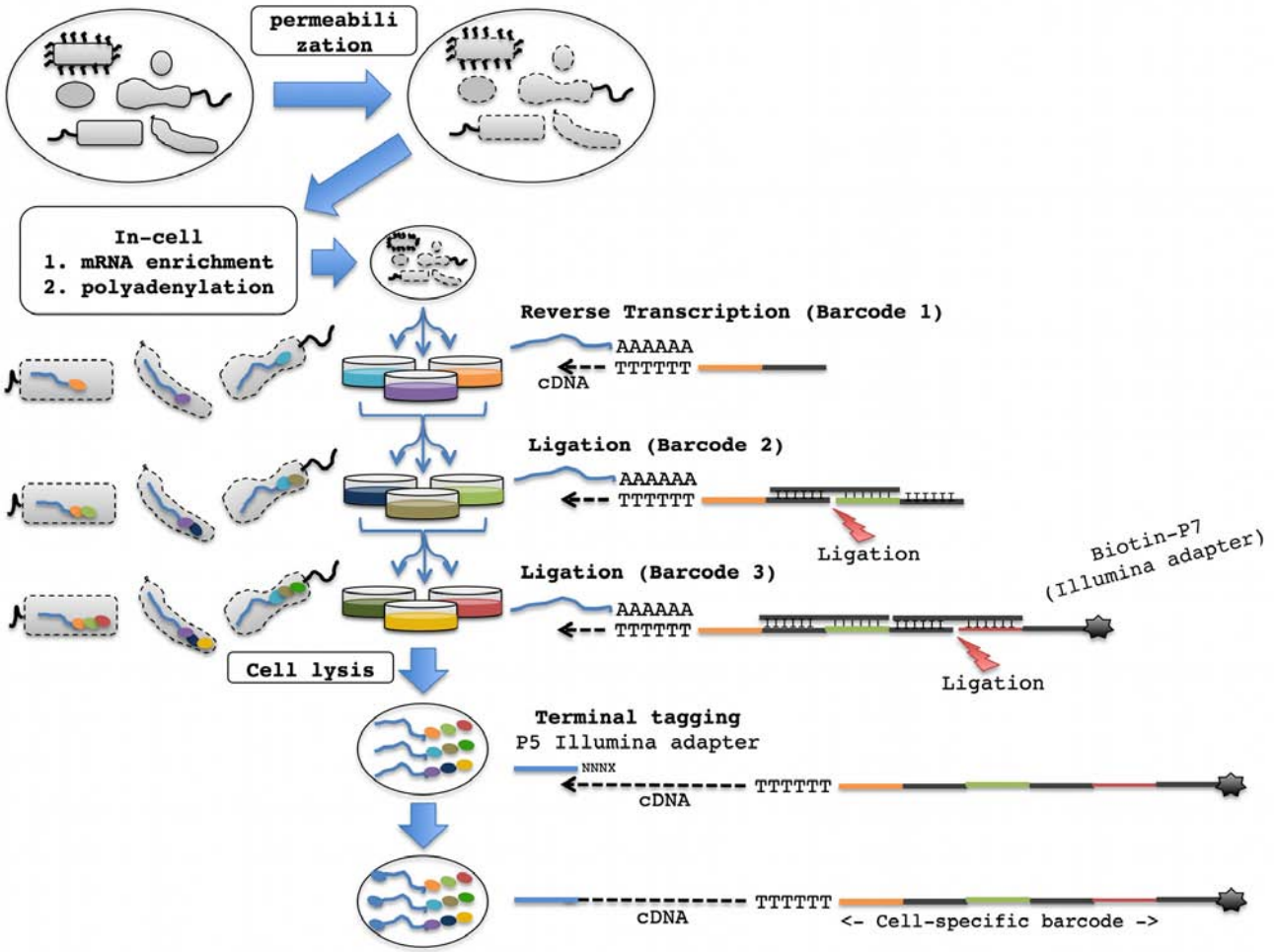

FIGURE 1 | Proposed SPLiT-Seq workflow for scRNA-seq of bacterial communities. Following cell permeabilization and in-cell mRNA enrichment and polyadenylation, the cells go through three rounds of splitting and pooling, first for RT, followed by two rounds for adapter ligation. Wells of different colors depict distinct barcode sequences. Sequential addition of 3′ barcodes to a single mRNA molecule followed by terminal tagging to add the 5′ adapter is depicted on the right. The sequential addition of barcodes to mRNA molecules in different bacterial cells at each split-pool round is depicted on the left.

containing barcoded well-specific RT primers, and subjected to in cell RT reactions. If amplification is desired, random hexamer primers can be used in the RT step followed by barcoded primers for rolling circle amplification. This will be followed by two rounds of pooling and random splitting into 48 wells for barcode ligation (**Figure 1**). A total of three rounds of barcoding (one via RT and two via ligation) can sufficiently distinguish 100,000 single-cell libraries (48^3 = 110,592 potential barcode combinations). The ligation plate wells would have dsDNA molecules with three distinct functional domains: a 5′-overhang that is complementary to the 5′-end on the cDNA molecule (originating from the RT primer), a unique well-specific barcode sequence, and the other 5′-overhang complementary to the 5′-overhang present on the DNA molecule that is ligated in the next ligation round (**Figure 1**). For the barcodes in the third round, the dsDNA molecules will have a 5′-overhang that is complementary to the 5′-end on the ligated cDNA molecule (originating from the previous round of ligation), a unique well-specific barcode sequence, and the other 5′-overhang with a universal PCR handle (suitable for Illumina Next-Gen sequencing and flow cell amplification), and a biotin molecule (**Figure 1**).

Terminal Tagging and Amplification

After in-cell cDNA synthesis and a third round of barcoding, the cells can be lysed, and first strand cDNAs can be isolated by biotin-streptavidin affinity purification. A second Illumina compatible sequencing adapter will be appended to the 3′-end of the first strand cDNAs through terminal tagging (Illumina Script Seq kit; **Figure 1**). The resulting molecules that are tagged on both ends with Illumina-compatible adapters can be amplified, size-selected for 300–400 bp amplicons using solid phase reversible immobilization (SPRI) beads, and will be ready for next-generation sequencing. Based on the already available examples, we believe that adaptation of SPLiT-Seq for

scRNA-Seq of bacterial communities will provide the entire plant-associated microbiome research community with a transformative technology to explore single-cell level changes in gene expression, and to spatially reconstruct microbiome processes.

BIOINFORMATICS OF BACTERIAL SCRNA-SEQ DATA

Read Mapping and Normalization

The major steps in the analytical pipelines for scRNA-seq typically mirror those used for bulk cell RNA-seq analysis. Reads from each cell after barcode splitting and quality control will be mapped separately to reference genomes. For a bacterial community RNA-seq, >13,500 complete bacterial genomes (NCBI as of 04/2019) is a good starting point, as a reference resource. Following regular read mapping (Langmead, 2010), normalization of read counts is a crucial step in RNA-seq analysis. It is generally agreed that compared to "within sample" normalization methods (e.g., FPKM - Fragments Per Kilobase per Million mapped reads), "between sample" normalization methods (e.g., TMM – Trimmed Mean of M values, DESeq) are more robust and accurate (Evans et al., 2018). However, the latter methods might perform poorly when zero counts are present due to a relatively large number of dropouts or cell-specific transcripts in scRNA-seq datasets. A recent method overcomes this by performing normalization based on summed expression values from pools of cells (Lun et al., 2016). While this improves normalization accuracy, it is obvious that the normalized expression values will only be applicable to the pools of cells, what makes this method undesirable for single-cell expression analysis. Therefore, the authors deconvolved the estimates for each pool into the estimates for its constituent cells, ensuring proper normalization of cell-specific biases. Therefore, pool-based normalized read counts can be effectively combined with differential expression analysis methods such as edgeR (McCarthy et al., 2012).

Due to the complex nature of microbiomes, one can expect a large number of unmapped reads. The use of single cell transcriptomes would allow generation and/or updating of reference resources. For example, *de novo* assembly of unmapped reads in each single cell to construct contigs using the assembly tool, Minia (Chikhi and Rizk, 2013) followed by scaffolding can be used to generate a new genome based on the Genome-organization-framework-assisted assembly pipeline and our previous knowledge of prokaryotic genome organization principles (Yin et al., 2010; Ma and Xu, 2013; Yuan et al., 2017).

Bacterial Transcription Unit Profiling

Based on the normalized read counts data, the basic transcript units (TU) and their expression values are determined by counting the number of reads that map to each TU. Machine learning algorithms such as SeqTU also enable accurate prediction and identification of TUs (Chou et al., 2015). A web server of this algorithm[1] was developed in 2017 and is available to automatically identify TUs with given RNA-seq data for any bacterium (Chen X. et al., 2017). In 2019, an R package was released to perform the TU identification locally (Niu et al., 2019). The predicted TUs are displayed intuitively using HTML format along with a graphic visualization of the prediction.

Species and Cell Clustering

In scRNA-seq of bacterial communities, clustering based on their expression profiles and the cluster can be evaluated in two different ways: (1) biological process-based, and (2) taxonomy-based. In the first approach, each cluster is evaluated for enriched biological processes compared to other clusters using Gene set enrichment analysis (Subramanian et al., 2005) and the Database for annotation, visualization and integrated discovery (Dennis et al., 2003). This approach can be expected to determine distinct groups of cells within the microbiome that are enriched in distinct biological processes, for example chemotaxis, cell attachment, N fixation and metabolism, and cell multiplication. In addition, it may be possible to identify groups of cells with a distinct spatial location within the plant-associated microbiome based on their expression profiles; for example, those bacterial cells expressing attachment proteins are likely to be attached to plant surfaces, those expressing extra cellular matrix-associated proteins and displaying reduced expression of flagellar proteins are likely to be embedded in biofilms, and those expressing flagellar proteins are likely to be planktonic cells. In the second approach, the distribution of cells of the same species in different functional clusters and spatial groups can be evaluated. The results can be used to determine if and how different cells of the same species are functionally organized within the microbiome community at each given time point. Reconstructing the predicted microbiomes at each time point based on their spatial and functional information can be a crucial outcome of these analyses. A number of additional single-cell analytical tools are also available for these steps (see **Table 1**).

DEVELOPMENT OF SCRNA-SEQ METHODS FOR PLANT-ASSOCIATED BACTERIAL COMMUNITIES

Establishment of Defined Microbial Communities for Method Development

We suggest selecting a defined microbial community with 8–10 distinct representative bacterial isolates. For example, to evaluate the assembly of a diazotroph community in cereal plant rhizospheres a mixture of *Herbaspirillum seropedicae (20%), Azospirillum brasiliense (5%), Bacillus thuringiensis (10%), Rhizobium leguminosarum (15%), Flavobacterium frigidarium (8%), Actinokineospora diospyrosa (12%), Bradyrhizobium* sp.

[1] http://bmbl.sdstate.edu/SeqTU_dev/

TABLE 1 | Summary of popular analytical tools for scRNA-Seq.

Tools	Year	Program	Tags
SAMtools (Li et al., 2009)	2009	C	(Not scRNA-Seq specific) post-alignment processing
STAR (Dobin et al., 2013)	2013	C	(Not scRNA-Seq specific) alignment
Monocle2 (Qiu et al., 2017)	2017	R	Clustering, differential expression, dimensionality reduction, visualization
BackSPIN (Zeisel et al., 2015)	2015	Python	Gene filtering, biclustering, cell type prediction
SINCERA (Guo et al., 2015)	2015	R	Quality control, normalization, gene filtering, clustering, differential expression, marker genes, cell type prediction
MAST (Finak et al., 2015)	2015	R	Quality control, normalization, differential expression, network construction
Kallisto (Bray et al., 2016)	2016	C	Quantification
BPSC (Vu et al., 2016)	2016	R	beta-Poisson mixture model
salmon (Patro et al., 2017)	2017	C++	UMI, quantification
UMI-tools (Smith et al., 2017)	2017	Python	UMI, quantification
SC3 (Kiselev et al., 2017)	2017	R	Gene filtering, clustering, cell type prediction
Scater (McCarthy et al., 2017)	2017	R	Quantification, quality control, normalization, dimensional reduction, visualization
SCENIC (Aibar et al., 2017)	2017	R/Python	Clustering, network construction, regulon prediction, visualization
Seurat (Butler et al., 2018)	2018	R	Normalization, gene filtering, clustering, differential expression, marker gene, dimensionality reduction, visualization
SAVER (Huang et al., 2018)	2018	R	Imputation
SCDE (Fan et al., 2016)	2016	R	Differential expression, pathway analysis, visualization
GeneQC (McDermaid et al., 2018)	2018	Server	Alignment, mapping uncertainty, realignment, quantification
IRIS-EDA (Monier et al., 2019)	2019	Server Database	Correlation analysis, clustering, differential expression, visualization, dimensionality reduction
KEGG (Kanehisa et al., 2017)	2017		Gene annotation
EnrichR (Kuleshov et al., 2016)	2016	Database	Enrichment analysis
Harmonizome (Rouillard et al., 2016)	2016		Gene/protein function
SwissRegulon (Pachkov et al., 2012)	2013		Regulon database
reactome (Joshi-Tope et al., 2005)	2005		Gene annotation, pathway construction

The tool names are hyperlinked to the relevant package, and the publication year is hyperlinked to the relevant reference.

(20%), and *Methylibium* sp. (10%) can be used (Mao et al., 2014; Soni et al., 2017). A subset of ∼5,000 cells of this defined microbiome can be used to develop and optimize bacterial single-cell sequencing technologies. Single-cell transcriptomes of mammalian cells at a depth of 50,000 paired end reads per cell were sufficient to distinguish different stages of developing human neuronal cortex cells (Pollen et al., 2014). This and other similar studies showed that merged single-cell transcriptomes accurately represent a majority of the ensembled transcriptomes with strongly correlated expression levels. Plant-associated microbial communities on the other hand, contain uncharacterized species with genomes that are not as well annotated as the human genome. However, bacterial genomes typically have <5000 ORFs. Therefore, we expect that a sequencing depth of ∼100,000 reads per cell will allow a meaningful gene annotation and data interpretation.

Evaluation of scRNA-Seq Results

Distinct benchmarks are essential to evaluate the results from scRNA-seq of the defined microbiomes and to validate the developed method for experimental samples. After reads are split according to barcode or assigned to individual microbial cells, they can be mapped to the known genomes of the 8 selected microbial species (see above) in a defined community. Ideally, all reads with the same barcode or those that came from a single cell should map to a single bacterial genome barring some highly conserved genes. Nevertheless, the results from these analyses can provide a benchmark to evaluate the accuracy with which scRNA-seq is able to distinguish transcripts from each individual bacterial species. Similar to the comparison of scRNA-seq data to bulk cell RNA-seq datasets from individual species (Kang et al., 2011; Wang et al., 2015), community scRNA-seq data need to be compared to metatranscriptomes of the same defined microbiome after mRNA enrichment and *in vitro* library construction. The results from this comparison can be used to evaluate the conformity of both data sets.

OPPORTUNITIES AND CHALLENGES IN SCRNA-SEQ OF PLANT-ASSOCIATED BACTERIAL COMMUNITIES

Evaluating the gene expression patterns in individual cells of plant-associated bacterial communities can provide transformative information not only about the gene expression levels and thereby function in individual members of different species but also about the spatial organization of bacterial communities in plant microbiomes. For example, cells with a higher expression of genes involved in exopolysaccharide synthesis are likely part of biofilms, while those expressing pili-encoding genes are likely attached to the plant surface. The

estimated sequencing depth of 500 million reads per sample of 5000 cells [100,000 reads per cell] can be obtained from two sequencing runs (e.g., one high output run with ∼350–400 Mio reads and one medium output run with 120–130 Mio reads on an Illumina NextSeq500) making this approach relatively inexpensive given the depth of information obtained. One of the major challenges is the complexity associated with multiple bacterial genomes present in the community, and the extent of genome sequence information available for each species. Nevertheless, since transcripts from each cell are tagged, general functional capacities expressed in individual bacterial cells can be determined. In fact, it becomes increasingly clear that the metabolic functions of bacterial communities are more important than their taxonomic composition (Louca et al., 2016; Wallace et al., 2018).

AUTHOR CONTRIBUTIONS

SS conceptualized the review topic. All authors wrote and edited the manuscript.

FUNDING

Research in the authors' laboratories are supported by funds from grant awards from the National Science Foundation/EPSCoR Cooperative Agreements #IIA-1355423 and 1849206, NSF-PGRP (IOS-1350189 to SS), NSF-MRI (#1532189 to JG), USDA-NIFA-AFRI (2016-67014-24589 to SS and 2017-67014-26530 to HB), and SD Agricultural Experiment Station (SD00H543-15 to SS and SD00H642-18 to HB).

REFERENCES

Aibar, S., Gonzalez-Blas, C. B., Moerman, T., Huynh-Thu, V. A., Imrichova, H., Hulselmans, G., et al. (2017). SCENIC: single-cell regulatory network inference and clustering. *Nat. Methods* 14, 1083–1086. doi: 10.1038/nmeth.4463

Armour, C. D., Amorese, D., Li, B., and Kurn, N. (2018). *Compositions and Methods for Negative Selection of Non-Desired Nucleic Acid Sequences*. Palo Alto, CA: USA patent application.

Armour, C. D., Castle, J. C., Chen, R., Babak, T., Loerch, P., Jackson, S., et al. (2009). Digital transcriptome profiling using selective hexamer priming for cDNA synthesis. *Nat. Methods* 6, 647–649. doi: 10.1038/nmeth.1360

Bai, Y., Muller, D. B., Srinivas, G., Garrido-Oter, R., Potthoff, E., Rott, M., et al. (2015). Functional overlap of the *Arabidopsis* leaf and root microbiota. *Nature* 528, 364–369. doi: 10.1038/nature16192

Balestrini, R., Gómez-Ariza, J., Klink, V. P., and Bonfante, P. (2009). Application of laser microdissection to plant pathogenic and symbiotic interactions. *J. Plant Interact.* 4, 81–92. doi: 10.1080/17429140902770396

Bogino, P., Abod, A., Nievas, F., and Giordano, W. (2013). Water-limiting conditions alter the structure and biofilm-forming ability of bacterial multispecies communities in the alfalfa rhizosphere. *PLoS One* 8:e79614. doi: 10.1371/journal.pone.0079614

Bouffaud, M. L., Poirier, M. A., Muller, D., and Moenne-Loccoz, Y. (2014). Root microbiome relates to plant host evolution in maize and other Poaceae. *Environ. Microbiol.* 16, 2804–2814. doi: 10.1111/1462-2920.12442

Bray, N. L., Pimentel, H., Melsted, P., and Pachter, L. (2016). Near-optimal probabilistic RNA-seq quantification. *Nat. Biotechnol.* 34, 525–527. doi: 10.1038/nbt.3519

Butler, A., Hoffman, P., Smibert, P., Papalexi, E., and Satija, R. (2018). Integrating single-cell transcriptomic data across different conditions, technologies, and species. *Nat. Biotechnol.* 36, 411–420. doi: 10.1038/nbt.4096

Castiblanco, L. F., and Sundin, G. W. (2016). New insights on molecular regulation of biofilm formation in plant-associated bacteria. *J. Integr. Plant Biol.* 58, 362–372. doi: 10.1111/jipb.12428

Chen, C. H., Cho, S. H., Chiang, H. I., Tsai, F., Zhang, K., and Lo, Y. H. (2011). Specific sorting of single bacterial cells with microfabricated fluorescence-activated cell sorting and tyramide signal amplification fluorescence in situ hybridization. *Anal. Chem.* 83, 7269–7275. doi: 10.1021/ac2013465

Chen, X., Chou, W.-C., Ma, Q., and Xu, Y. (2017). SeqTU: a web server for identification of bacterial transcription units. *Sci. Rep.* 7:43925. doi: 10.1038/srep43925

Chen, Z., Chen, L., and Zhang, W. (2017). Tools for genomic and transcriptomic analysis of microbes at single-cell level. *Front. Microbiol.* 8:1831. doi: 10.3389/fmicb.2017.01831

Chikhi, R., and Rizk, G. (2013). Space-efficient and exact de Bruijn graph representation based on a Bloom filter. *Algorithms Mol. Biol.* 8:22. doi: 10.1186/1748-7188-8-22

Chou, W.-C., Ma, Q., Yang, S., Cao, S., Klingeman, D. M., Brown, S. D., et al. (2015). Analysis of strand-specific RNA-seq data using machine learning reveals the structures of transcription units in *Clostridium thermocellum*. *Nucleic Acids Res.* 43:e67. doi: 10.1093/nar/gkv177

Dennis, G., Sherman, B. T., Hosack, D. A., Yang, J., Gao, W., Lane, H. C., et al. (2003). DAVID: database for annotation, visualization, and integrated discovery. *Genome Biol.* 4:R60.

Deshayes, C., Siegwart, M., Pauron, D., Froger, J. A., Lapied, B., and Apaire-Marchais, V. (2017). Microbial pest control agents: are they a specific and safe tool for insect pest management? *Curr. Med. Chem.* 24, 2959–2973. doi: 10.2174/0929867324666170314144311

Dobin, A., Davis, C. A., Schlesinger, F., Drenkow, J., Zaleski, C., Jha, S., et al. (2013). STAR: ultrafast universal RNA-seq aligner. *Bioinformatics* 29, 15–21. doi: 10.1093/bioinformatics/bts635

Edwards, J., Johnson, C., Santos-Medellin, C., Lurie, E., Podishetty, N. K., Bhatnagar, S., et al. (2015). Structure, variation, and assembly of the root-associated microbiomes of rice. *Proc. Natl. Acad. Sci. U.S.A.* 112, E911–E920. doi: 10.1073/pnas.1414592112

Evans, C., Hardin, J., and Stoebel, D. M. (2018). Selecting between-sample RNA-Seq normalization methods from the perspective of their assumptions. *Brief Bioinform.* 19, 776–792. doi: 10.1093/bib/bbx008

Fan, J., Salathia, N., Liu, R., Kaeser, G. E., Yung, Y. C., Herman, J. L., et al. (2016). Characterizing transcriptional heterogeneity through pathway and gene set overdispersion analysis. *Nat. Methods* 13, 241–244. doi: 10.1038/nmeth.3734

Fan, X., Zhang, X., Wu, X., Guo, H., Hu, Y., Tang, F., et al. (2015). Single-cell RNA-seq transcriptome analysis of linear and circular RNAs in mouse preimplantation embryos. *Genome Biol.* 16:148. doi: 10.1186/s13059-015-0706-1

Finak, G., Mcdavid, A., Yajima, M., Deng, J., Gersuk, V., Shalek, A. K., et al. (2015). MAST: a flexible statistical framework for assessing transcriptional changes and characterizing heterogeneity in single-cell RNA sequencing data. *Genome Biol.* 16:278. doi: 10.1186/s13059-015-0844-5

Fröhlich, J., and König, H. (2006). "Micromanipulation techniques for the isolation of single microorganisms," in *Intestinal Microorganisms of Termites and Other Invertebrates*., Vol. 6, eds H. König, and A. Varma, (Heidelberg: Springer), 425–437. doi: 10.1007/3-540-28185-1_18

Gasch, A. P., Yu, F. B., Hose, J., Escalante, L. E., Place, M., Bacher, R., et al. (2017). Single-cell RNA sequencing reveals intrinsic and extrinsic regulatory heterogeneity in yeast responding to stress. *PLoS Biol.* 15:e2004050. doi: 10.1371/journal.pbio.2004050

Gentzel, I., Giese, L., Zhao, W., Alonso, A. P., and Mackey, D. (2019). A simple method for measuring apoplast hydration and collecting apoplast contents. *Plant Physiol.* 179, 1265–1272. doi: 10.1104/pp.18.01076

Gomez, S. K., and Harrison, M. J. (2009). Laser microdissection and its application to analyze gene expression in arbuscular mycorrhizal symbiosis. *Pest. Manag. Sci.* 65, 504–511. doi: 10.1002/ps.1715

Gross, A., Schondube, J., Niekrawitz, S., Streule, W., Riegger, L., Zengerle, R., et al. (2013). Single-cell printer: automated, on demand, and label free. *J. Lab. Autom.* 18, 504–518. doi: 10.1177/2211068213497204

Guo, M., Wang, H., Potter, S. S., Whitsett, J. A., and Xu, Y. (2015). SINCERA: a pipeline for single-cell RNA-Seq profiling analysis. *PLoS Comput. Biol.* 11:e1004575. doi: 10.1371/journal.pcbi.1004575

Hassani, M. A., Durán, P., and Hacquard, S. (2018). Microbial interactions within the plant holobiont. *Microbiome* 6:58. doi: 10.1186/s40168-018-0445-0

Hodson, R. E., Dustman, W. A., Garg, R. P., and Moran, M. A. (1995). In situ PCR for visualization of microscale distribution of specific genes and gene products in prokaryotic communities. *Appl. Environ. Microbiol.* 61, 4074–4082.

Hohnadel, M., Maumy, M., and Chollet, R. (2018). Development of a micromanipulation method for single cell isolation of prokaryotes and its application in food safety. *PLoS One* 13:e0198208. doi: 10.1371/journal.pone.0198208

Huang, M., Wang, J., Torre, E., Dueck, H., Shaffer, S., Bonasio, R., et al. (2018). SAVER: gene expression recovery for single-cell RNA sequencing. *Nat. Methods* 15:539. doi: 10.1038/s41592-018-0033-z

Hwang, B., Lee, J. H., and Bang, D. (2018). Single-cell RNA sequencing technologies and bioinformatics pipelines. *Exp. Mol. Med.* 50:96. doi: 10.1038/s12276-018-0071-8

Ishoy, T., Kvist, T., Westermann, P., and Ahring, B. K. (2006). An improved method for single cell isolation of prokaryotes from meso-, thermo- and hyperthermophilic environments using micromanipulation. *Appl. Microbiol. Biotechnol.* 69, 510–514. doi: 10.1007/s00253-005-0014-x

Jahiri, X. (2013). *Isolation of Fungal Endophytes from Grasses by Laser Micro Dissection & Pressure Catapulting*. Harstad: The Arctic University of Norway.

Joshi-Tope, G., Gillespie, M., Vastrik, I., D'eustachio, P., Schmidt, E., De Bono, B., et al. (2005). Reactome: a knowledgebase of biological pathways. *Nucleic Acids Res.* 33, D428–D432.

Kämpfer, P. (2006). Detection and cultivation of filamentous bacteria from activated sludge. *FEMS Microbiol. Ecol.* 23, 169–181. doi: 10.1111/j.1574-6941.1997.tb00400.x

Kanehisa, M., Furumichi, M., Tanabe, M., Sato, Y., and Morishima, K. (2017). KEGG: new perspectives on genomes, pathways, diseases and drugs. *Nucleic Acids Res.* 45, D353–D361. doi: 10.1093/nar/gkw1092

Kang, Y., Mcmillan, I., Norris, M. H., and Hoang, T. T. (2015). Single prokaryotic cell isolation and total transcript amplification protocol for transcriptomic analysis. *Nat. Protoc.* 10, 974–984. doi: 10.1038/nprot.2015.058

Kang, Y., Norris, M. H., Zarzycki-Siek, J., Nierman, W. C., Donachie, S. P., and Hoang, T. T. (2011). Transcript amplification from single bacterium for transcriptome analysis. *Genome Res.* 21, 925–935. doi: 10.1101/gr.116103.110

Keloth, A., Anderson, O., Risbridger, D., and Paterson, L. (2018). Single cell isolation using optical tweezers. *Micromachines* 9:E434. doi: 10.3390/mi9090434

Kiselev, V. Y., Kirschner, K., Schaub, M. T., Andrews, T., Yiu, A., Chandra, T., et al. (2017). SC3: consensus clustering of single-cell RNA-seq data. *Nat. Methods* 14, 483–486. doi: 10.1038/nmeth.4236

Knief, C. (2014). Analysis of plant microbe interactions in the era of next generation sequencing technologies. *Front. Plant Sci.* 5:216. doi: 10.3389/fpls.2014.00216

Kuleshov, M. V., Jones, M. R., Rouillard, A. D., Fernandez, N. F., Duan, Q., Wang, Z., et al. (2016). Enrichr: a comprehensive gene set enrichment analysis web server 2016 update. *Nucleic Acids Res.* 44, W90–W97. doi: 10.1093/nar/gkw377

Kurn, N., Chen, P., Heath, J. D., Kopf-Sill, A., Stephens, K. M., and Wang, S. (2005). Novel isothermal, linear nucleic acid amplification systems for highly multiplexed applications. *Clin. Chem.* 51, 1973–1981. doi: 10.1373/clinchem.2005.053694

Langmead, B. (2010). Aligning short sequencing reads with bowtie. *Curr. Protoc. Bioinform.* Chapter 11:Unit11.7. doi: 10.1002/0471250953.bi1107s32

Li, H., Handsaker, B., Wysoker, A., Fennell, T., Ruan, J., Homer, N., et al. (2009). The sequence alignment/map format and SAMtools. *Bioinformatics* 25, 2078–2079. doi: 10.1093/bioinformatics/btp352

Louca, S., Jacques, S. M. S., Pires, A. P. F., Leal, J. S., Srivastava, D. S., Parfrey, L. W., et al. (2016). High taxonomic variability despite stable functional structure across microbial communities. *Nat. Ecol. Evol.* 1:15. doi: 10.1038/s41559-016-0015

Lun, A. T., Bach, K., and Marioni, J. C. (2016). Pooling across cells to normalize single-cell RNA sequencing data with many zero counts. *Genome Biol.* 17:75. doi: 10.1186/s13059-016-0947-7

Lundberg, D. S., Lebeis, S. L., Paredes, S. H., Yourstone, S., Gehring, J., Malfatti, S., et al. (2012). Defining the core *Arabidopsis thaliana* root microbiome. *Nature* 488, 86–90. doi: 10.1038/nature11237

Ma, Q., and Xu, Y. (2013). Global genomic arrangement of bacterial genes is closely tied with the total transcriptional efficiency. *Genom. Proteomics Bioinform.* 11, 66–71. doi: 10.1016/j.gpb.2013.01.004

Macosko, E. Z., Basu, A., Satija, R., Nemesh, J., Shekhar, K., Goldman, M., et al. (2015). Highly parallel genome-wide expression profiling of individual cells using nanoliter droplets. *Cell* 161, 1202–1214. doi: 10.1016/j.cell.2015.05.002

Mao, Y., Li, X., Smyth, E. M., Yannarell, A. C., and Mackie, R. I. (2014). Enrichment of specific bacterial and eukaryotic microbes in the rhizosphere of switchgrass (*Panicum virgatum* L.) through root exudates. *Environ. Microbiol. Rep.* 6, 293–306. doi: 10.1111/1758-2229.12152

McCarthy, D. J., Campbell, K. R., Lun, A. T., and Wills, Q. F. (2017). Scater: pre-processing, quality control, normalization and visualization of single-cell RNA-seq data in R. *Bioinformatics* 33, 1179–1186. doi: 10.1093/bioinformatics/btw777

McCarthy, D. J., Chen, Y., and Smyth, G. K. (2012). Differential expression analysis of multifactor RNA-Seq experiments with respect to biological variation. *Nucleic Acids Res.* 40, 4288–4297. doi: 10.1093/nar/gks042

McDermaid, A., Chen, X., Zhang, Y., Wang, C., Gu, S., Xie, J., et al. (2018). A new machine learning-based framework for mapping uncertainty analysis in rna-seq read alignment and gene expression estimation. *Front. Genet.* 9:313. doi: 10.3389/fgene.2018.00313

McPherson, M. R., Wang, P., Marsh, E. L., Mitchell, R. B., and Schachtman, D. P. (2018). Isolation and analysis of microbial communities in soil, rhizosphere, and roots in perennial grass experiments. *J. Vis. Exp.* 137:e57932. doi: 10.3791/57932

Monier, B., Mcdermaid, A., Wang, C., Zhao, J., Miller, A., Fennell, A., et al. (2019). IRIS-EDA: an integrated RNA-Seq interpretation system for gene expression data analysis. *PLoS Comput. Biol.* 15:e1006792. doi: 10.1371/journal.pcbi.1006792

Müller, S., and Nebe-von-Caron, G. (2010). Functional single-cell analyses: flow cytometry and cell sorting of microbial populations and communities. *FEMS Microbiol. Rev.* 34, 554–587. doi: 10.1111/j.1574-6976.2010.00214.x

Nakazono, M. (2003). Laser-capture microdissection, a tool for the global analysis of gene expression in specific plant cell types: identification of genes expressed differentially in epidermal cells or vascular tissues of maize. *Plant Cell* 15, 583–596. doi: 10.1105/tpc.008102

Niu, S.-Y., Liu, B., Ma, Q., and Chou, W.-C. (2019). rSeqTU—a machine-learning based R package for prediction of bacterial transcription units. *Front. Genet.* 10:374. doi: 10.3389/fgene.2019.00374

Pachkov, M., Balwierz, P. J., Arnold, P., Ozonov, E., and Van Nimwegen, E. (2012). SwissRegulon, a database of genome-wide annotations of regulatory sites: recent updates. *Nucleic Acids Res.* 41, D214–D220. doi: 10.1093/nar/gks1145

Parnell, J. J., Berka, R., Young, H. A., Sturino, J. M., Kang, Y., Barnhart, D. M., et al. (2016). From the lab to the farm: an industrial perspective of plant beneficial microorganisms. *Front. Plant Sci.* 7:1110. doi: 10.3389/fpls.2016.01110

Parsley, L. C., Newman, M. M., and Liles, M. R. (2010). Fluorescence in situ hybridization of bacterial cell suspensions. *Cold Spring Harb. Protoc.* 2010:pdb.prot5493. doi: 10.1101/pdb.prot5493

Patro, R., Duggal, G., Love, M. I., Irizarry, R. A., and Kingsford, C. (2017). Salmon provides fast and bias-aware quantification of transcript expression. *Nat. Methods* 14:417. doi: 10.1038/nmeth.4197

Peiffer, J. A., Spor, A., Koren, O., Jin, Z., Tringe, S. G., Dangl, J. L., et al. (2013). Diversity and heritability of the maize rhizosphere microbiome under field conditions. *Proc. Natl. Acad. Sci. U.S.A.* 110, 6548–6553. doi: 10.1073/pnas.1302837110

Pollen, A. A., Nowakowski, T. J., Shuga, J., Wang, X., Leyrat, A. A., Lui, J. H., et al. (2014). Low-coverage single-cell mRNA sequencing reveals cellular heterogeneity and activated signaling pathways in developing cerebral cortex. *Nat. Biotechnol.* 32, 1053–1058. doi: 10.1038/nbt.2967

Qiu, X., Mao, Q., Tang, Y., Wang, L., Chawla, R., Pliner, H. A., et al. (2017). Reversed graph embedding resolves complex single-cell trajectories. *Nat. Methods* 14, 979–982. doi: 10.1038/nmeth.4402

Raghunathan, A., Ferguson, H. R. Jr., Bornarth, C. J., Song, W., Driscoll, M., Lasken, R. S., et al. (2005). Genomic DNA amplification from a single

bacterium. *Appl. Environ. Microbiol.* 71, 3342–3347. doi: 10.1128/aem.71.6.3342-3347.2005

Riba, J., Gleichmann, T., Zimmermann, S., Zengerle, R., and Koltay, P. (2016). Label-free isolation and deposition of single bacterial cells from heterogeneous samples for clonal culturing. *Sci. Rep*. 6:32837. doi: 10.1038/srep32837

Rosenberg, A. B., Roco, C., Muscat, R. A., Kuchina, A., Mukherjee, S., Chen, W., et al. (2017). Scaling single cell transcriptomics through split pool barcoding. *bioRxiv* [preprint]. doi: 10.1101/105163

Rosenberg, A. B., Roco, C. M., Muscat, R. A., Kuchina, A., Sample, P., Yao, Z., et al. (2018). Single-cell profiling of the developing mouse brain and spinal cord with split-pool barcoding. *Science* 360, 176–182. doi: 10.1126/science.aam8999

Rouillard, A. D., Gundersen, G. W., Fernandez, N. F., Wang, Z., Monteiro, C. D., Mcdermott, M. G., et al. (2016). The harmonizome: a collection of processed datasets gathered to serve and mine knowledge about genes and proteins. *Database* 2016:baw100. doi: 10.1093/database/baw100

Russell, J. H., and Keiler, K. C. (2009). Subcellular localization of a bacterial regulatory RNA. *Proc. Natl. Acad. Sci. U.S.A.* 106, 16405–16409. doi: 10.1073/pnas.0904904106

Simon, J. C., Marchesi, J. R., Mougel, C., and Selosse, M. A. (2019). Host-microbiota interactions: from holobiont theory to analysis. *Microbiome* 7:5. doi: 10.1186/s40168-019-0619-4

Sloan, S. S., and Lebeis, S. L. (2015). Exercising influence: distinct biotic interactions shape root microbiomes. *Curr. Opin. Plant Biol.* 26, 32–36. doi: 10.1016/j.pbi.2015.05.026

Smith, T., Heger, A., and Sudbery, I. (2017). UMI-tools: modeling sequencing errors in unique molecular identifiers to improve quantification accuracy. *Genome Res.* 27, 491–499. doi: 10.1101/gr.209601.116

Soni, R., Kumar, V., Suyal, D. C., Jain, L., and Goel, R. (2017). "Metagenomics of plant rhizosphere microbiome," in *Understanding Host-Microbiome Interactions - An Omics Approach: Omics of Host-Microbiome Association*, eds R. P. Singh, R. Kothari, P. G. Koringa, and S. P. Singh, (Singapore: Springer Singapore), 193–205. doi: 10.1007/978-981-10-5050-3_12

Stovicek, V., Vachova, L., and Palkova, Z. (2012). Yeast biofilm colony as an orchestrated multicellular organism. *Commun. Integr. Biol.* 5, 203–205. doi: 10.4161/cib.18912

Subramanian, A., Tamayo, P., Mootha, V. K., Mukherjee, S., Ebert, B. L., Gillette, M. A., et al. (2005). Gene set enrichment analysis: a knowledge-based approach for interpreting genome-wide expression profiles. *Proc. Natl. Acad. Sci. U.S.A.* 102, 15545–15550. doi: 10.1073/pnas.0506580102

Šulčius, S., Slavuckytė, K., Januškaitė, M., and Paškauskas, R. (2017). Establishment of axenic cultures from cyanobacterium *Aphanizomenon* flos-aquae akinetes by micromanipulation and chemical treatment. *Algal Res.* 23, 43–50. doi: 10.1016/j.algal.2017.01.006

Takahashi, H., Yamamoto, K., Ohtani, T., and Sugiyama, S. (2009). Cell-free cloning using multiply-primed rolling circle amplification with modified RNA primers. *Biotechniques* 47, 609–615. doi: 10.2144/000113155

Tani, K., Kurokawa, K., and Nasu, M. (1998). Development of a direct in situ PCR method for detection of specific bacteria in natural environments. *Appl. Environ. Microbiol.* 64, 1536–1540.

Tolonen, A. C., and Xavier, R. J. (2017). Dissecting the human microbiome with single-cell genomics. *Genome Med.* 9:56. doi: 10.1186/s13073-017-0448-7

Turner, T. R., Ramakrishnan, K., Walshaw, J., Heavens, D., Alston, M., Swarbreck, D., et al. (2013). Comparative metatranscriptomics reveals kingdom level changes in the rhizosphere microbiome of plants. *ISME J.* 7, 2248–2258. doi: 10.1038/ismej.2013.119

Vu, T. N., Wills, Q. F., Kalari, K. R., Niu, N., Wang, L., Rantalainen, M., et al. (2016). Beta-Poisson model for single-cell RNA-seq data analyses. *Bioinformatics* 32, 2128–2135. doi: 10.1093/bioinformatics/btw202

Wallace, J. G., Kremling, K. A., Kovar, L. L., and Buckler, E. S. (2018). Quantitative genetics of the maize leaf microbiome. *Phytobiomes J.* 2, 208–224. doi: 10.1016/j.scitotenv.2018.07.260

Wang, J., Chen, L., Chen, Z., and Zhang, W. (2015). RNA-seq based transcriptomic analysis of single bacterial cells. *Integr. Biol.* 7, 1466–1476. doi: 10.1039/c5ib00191a

Wang, P., Marsh, E. L., Ainsworth, E. A., Leakey, A. D. B., Sheflin, A. M., and Schachtman, D. P. (2017). Shifts in microbial communities in soil, rhizosphere and roots of two major crop systems under elevated CO2 and O3. *Sci. Rep.* 7:15019. doi: 10.1038/s41598-017-14936-2

White, L. J., Brozel, V. S., and Subramanian, S. (2015). Isolation of rhizosphere bacterial communities from soil. *Bio Protoc.* 5:e1569.

White, L. J., Ge, X., Brozel, V. S., and Subramanian, S. (2017). Root isoflavonoids and hairy root transformation influence key bacterial taxa in the soybean rhizosphere. *Environ. Microbiol.* 19, 1391–1406. doi: 10.1111/1462-2920.13602

Yin, Y., Zhang, H., Olman, V., and Xu, Y. (2010). Genomic arrangement of bacterial operons is constrained by biological pathways encoded in the genome. *Proc. Natl. Acad. Sci. U.S.A.* 107, 6310–6315. doi: 10.1073/pnas.0911237107

Yuan, L., Yu, Y., Zhu, Y., Li, Y., Li, C., Li, R., et al. (2017). GAAP: genome-organization-framework-Assisted assembly pipeline for prokaryotic genomes. *BMC Genomics* 18:952. doi: 10.1186/s12864-016-3267-0

Zeisel, A., Muñoz-Manchado, A. B., Codeluppi, S., Lönnerberg, P., La Manno, G., Juréus, A., et al. (2015). Cell types in the mouse cortex and hippocampus revealed by single-cell RNA-seq. *Science* 347, 1138–1142. doi: 10.1126/science.aaa1934

Zhang, K., Martiny, A. C., Reppas, N. B., Barry, K. W., Malek, J., Chisholm, S. W., et al. (2006). Sequencing genomes from single cells by polymerase cloning. *Nat. Biotechnol.* 24, 680–686. doi: 10.1038/nbt1214

Zhang, Y., Gao, J., Huang, Y., and Wang, J. (2018). Recent developments in single-cell RNA-Seq of microorganisms. *Biophys. J.* 115, 173–180. doi: 10.1016/j.bpj.2018.06.008

Zhou, J., He, Z., Yang, Y., Deng, Y., Tringe, S. G., and Alvarez-Cohen, L. (2015). High-throughput metagenomic technologies for complex microbial community analysis: open and closed formats. *mBio* 6:e02288-14. doi: 10.1128/mBio.02288-14

Ziegenhain, C., Vieth, B., Parekh, S., Reinius, B., Guillaumet-Adkins, A., Smets, M., et al. (2017). Comparative analysis of single-cell RNA sequencing methods. *Mol. Cell* 65:e634.

Conflict of Interest: The authors declare that the research was conducted in the absence of any commercial or financial relationships that could be construed as a potential conflict of interest.

frontiers in Plant Science

ORIGINAL RESEARCH
published: 18 July 2019
doi: 10.3389/fpls.2019.00932

Facilitation of Balsam Fir by Trembling Aspen in the Boreal Forest: Do Ectomycorrhizal Communities Matter?

Mélissande Nagati[1,2], Mélanie Roy[2], Annie Desrochers[1], Sophie Manzi[2], Yves Bergeron[1] and Monique Gardes[2]*

[1] UQAT-UQAM Industrial Chair in Sustainable Forest Management, Forest Research Institute, University of Québec in Abitibi-Témiscamingue, Rouyn-Noranda, QC, Canada, [2] UMR5174, Laboratory Evolution and Biological Diversity, Centre National de la Recherche Scientifique – IRD, Université Paul Sabatier, Toulouse, France

Succession is generally well described above-ground in the boreal forest, and several studies have demonstrated the role of interspecific facilitation in tree species establishment. However, the role of mycorrhizal communities for tree establishment and interspecific facilitation, has been little explored. At the ecotone between the mixed boreal forest, dominated by balsam fir and hardwood species, and the boreal forest, dominated by black spruce, several stands of trembling aspen can be found, surrounded by black spruce forest. Regeneration of balsam fir seems to have increased in the recent decades within the boreal forest, and it seems better adapted to grow in trembling aspen stands than in black spruce stands, even when located in similar abiotic conditions. As black spruce stands are also covered by ericaceous shrubs, we investigated if differences in soil fungal communities and ericaceous shrubs abundance could explain the differences observed in balsam fir growth and nutrition. We conducted a study centered on individual saplings to link growth and foliar nutrient concentrations to local vegetation cover, mycorrhization rate, and mycorrhizal communities associated with balsam fir roots. We found that foliar nutrient concentrations and ramification indices (colonization by mycorrhiza per length of root) were greater in trembling aspen stands and were positively correlated to apical and lateral growth of balsam fir saplings. In black spruce stands, the presence of ericaceous shrubs near balsam fir saplings affected ectomycorrhizal communities associated with tree roots which in turn negatively correlated with N foliar concentrations. Our results reveal that fungal communities observed under aspen are drivers of balsam fir early growth and nutrition in boreal forest stands and may facilitate ecotone migration in a context of climate change.

Keywords: ***Abies balsamea*, boreal forest, ectomycorrhiza, ericaceous shrubs, facilitation, *Picea mariana*, *Populus tremuloides***

OPEN ACCESS

Edited by:
Kevin Garcia, North Carolina State University, United States

Reviewed by:
Jaqueline Hess, University of Vienna, Austria
Plassard Claude, Ecologie Fonctionnelle et Biogéochimie des Sols et des Agro-Écosystèmes (Eco&Sols) INRA, France

****Correspondence:***
Mélissande Nagati
melissande.nagati@uqat.ca

Specialty section:
This article was submitted to Plant Microbe Interactions, a section of the journal Frontiers in Plant Science

Received: *03 April 2019*
Accepted: *03 July 2019*
Published: *18 July 2019*

Citation:
Nagati M, Roy M, Desrochers A, Manzi S, Bergeron Y and Gardes M (2019) Facilitation of Balsam Fir by Trembling Aspen in the Boreal Forest: Do Ectomycorrhizal Communities Matter? Front. Plant Sci. 10:932. doi: 10.3389/fpls.2019.00932

INTRODUCTION

Tree establishment, growth and survival in a new area are primarily dependent upon seed availability and local environmental conditions. For a given tree species, its capacity to establish under new biotic conditions is predominantly driven by either facilitation or competitive processes (Callaway and Walker, 1997). Within a multi-species environment, species can compete for

resources such as light, nutrients or water. At the same time, survival of one species can be facilitated by another species providing protection against predators or extreme climate events (Stachowicz, 2001), or by the presence of their mycorrhizal symbionts which could result in mycorrhizal networks (Simard et al., 2015; Pickles and Simard, 2017), or exchanges of resources (Brooker et al., 2008; Teste et al., 2009). Among the consequences of climate change, changes in species distribution are already observed and could result in new or modified species interactions. Changes in distribution range of species are particularly visible at ecotones between forested ecosystems (Messaoud et al., 2007; Barbeta and Peñuelas, 2017) or at the northern tree line (Harsch et al., 2009; Ratcliffe et al., 2017).

In Québec (Canada), the 49th parallel represents the ecotone between the southern balsam fir-paper birch (mixedwood boreal forest) and the northern black spruce-feather moss (boreal forest) bioclimatic domains. It has been suggested that this ecotone is likely to migrate northward with climate change (Messaoud et al., 2007). South of this ecotone, forest stands are mixed and dominated by *Abies balsamea* [L.] Mill. (balsam fir-BF), *Picea glauca* [Moench] Voss (white spruce), *Populus tremuloides* Michx.(trembling aspen-TA), and *Betula papyrifera* Marsh. (paper birch), whereas *Picea mariana* [Mill.] BSP (black spruce-BS), and *Pinus banksiana* Lamb.(Jack pine) dominate north of the ecotone (Robitaille and Saucier, 1996). In the southern part of the black spruce-feather moss domain, small stands of trembling aspen occur, in which trembling aspen can be dominant (more than 75% of the canopy cover) or mixed with black spruce (between 25 and 75% of the canopy cover; Légaré et al., 2005; Cavard et al., 2011). Following classical forest dynamics in these forests, TA would eventually be replaced by BS in the absence of disturbance (Lecomte and Bergeron, 2005; Belleau et al., 2011), thereby maintaining BS dominance in the area. In areas where balsam fir establishes under BS- and TA-dominated stands, a greater abundance of more vigorous saplings has been observed under TA (Arbour and Bergeron, 2011). As those two types of stands are very close geographically and grow under similar climate, slope and substrates (Légaré et al., 2005; Cavard et al., 2011), the idea of an abiotic determinism could be rejected. On the contrary, aspen-dominated and spruce-dominated stands have different understorey plant and fungal communities, and soil organic contents (Légaré et al., 2005; Cavard et al., 2011; Nagati et al., 2018), suggesting that biotic factors could explain differences in balsam fir growth. Indeed several mechanisms resulting from microbe–mediated interactions could enhance or reduce BF nutrition and growth, and may be involved in plant–plant interactions in the boreal forest.

Among the fungi that interact with tree roots, including BF roots, ectomycorrhizal fungi (EMF) are particularly abundant in boreal soils (Taylor et al., 2013). These fungi improve tree growth and foliar nutrient status in ecosystems where nutrients are mainly found in organic forms, as in boreal forests (Smith and Read, 2008; Inselsbacher and Näsholm, 2012; Franklin et al., 2014). At a worldwide scale, closely related host species tend to share more similar EMF communities than more phylogenetically distant host species (Tedersoo et al., 2013), which may result in greater similarity between BF and BS fungal communities. However, at the local scale, cases of facilitation through mycorrhizal symbioses have rather been detected between phylogenetically distinct plants (Nara and Hogetsu, 2004; Dickie et al., 2006; van der Heijden and Horton, 2009). Mycorrhizal fungi could also shape plant–plant interactions through indirect interactions with plants (Bever et al., 2010). The understorey vegetation under TA is dominated by various ectomycorrhizal tree saplings, endomycorrhizal (AM) shrubs and herbaceous species (Légaré et al., 2005; Cavard et al., 2011) while BS stands understorey is covered by a thick layer of bryophytes and ericaceous shrubs. Limitations to tree establishment and growth for EMF tree species that are adjacent to ericaceous shrubs, which are associated with ericoid fungi, have been documented many times in various ecosystems (e.g., Peterson, 1965; Zackrisson et al., 1997; Yamasaki et al., 1998; Walker et al., 1999; Mallik, 2003). Although the mechanisms explaining such regeneration failures of EMF plant species near ericoid shrubs are not clearly understood (Peterson, 1965; Gallet, 1994; Collier and Bidartondo, 2009; Richard et al., 2009), potential alterations to BF mycorrhizal colonization and mycorrhizal networks cannot be excluded in our system that would explain BF growth differences between TA- and BS-dominated stands.

Our aim was to disentangle the processes controlling BF early growth and nutrition at this boreal ecotone. To achieve this goal, we monitored growth parameters of individual BF saplings for two consecutive years and investigated their EMF communities and their foliar nutrient concentrations under BS and TA stands. We hypothesized that (1) local conditions under TA would lead to greater mycorrhization rates and different EMF communities than under BS and (2) the presence of ericaceous shrubs near BF saplings would reduce growth and mineral nutrition through their effects on EMF symbioses.

MATERIALS AND METHODS

Site Description and Fir Sapling Selection

The study was located across a 36-km^2 area within the Clay Belt of northern Québec and Ontario (Canada). Four paired and unmanaged sites within the black spruce-feather moss domain were selected for study (**Table 1**). Each pair of stands contained one that was dominated by TA, while the other one was dominated by BS (for more information on sites, see Nagati et al., 2018). At each site, 15 BF saplings that were 25–75 cm tall and separated from one another by at least 5 m were selected: five in TA stands; five in BS stands at least 4m away from an ericaceous shrub; and five in BS stands at a maximum distance of 3 m from an ericaceous shrub [BSE, Labrador tea (*Rhododendron groenlandicum* [Oeder] Kron and Judd) or sheep-laurel (*Kalmia angustifolia* L.)]. Our sampling design permitted to sample 15 saplings per site (10 in BS stands and 5 in TA stands), resulting in 60 saplings.

TABLE 1 | GPS coordinates of sites.

Site	Stand	Latitude	Longitude
1	BS	49.19061	−78.82797
	TA	49.18942	−78.82817
2	BS	49.19367	−78.83556
	TA	49.19375	−78.8345
3	BS	49.196695	−78.842092
	TA	49.196422	−78.84237
4	BS	49.168972	−78.885194
	TA	49.180417	−78.883611

BS, black spruce – Picea Mariana; TA, trembling aspen – Populus Tremuloides.

Balsam Fir Measurements

Annual apical growth (cm) was measured in August 2015 and 2016 with calipers and the two measures were summed. Annual lateral growth was measured on two randomly selected branches per sapling in August 2015 and 2016 with calipers, averaged by year, and then summed. In 2016, the basal diameter of stems (cm) was measured with calipers. Fir needles were harvested in August 2016, forced air-dried at 30°C for 12 h, and sent to the Laurentian Forestry Centre, Canadian Forest Service (Quebec) for chemical analyses. Percentage foliar C and N were measured with a Leco TruMac CNS mass spectrometer (LECO Corporation, St. Joseph, MI, United States). Minor and major cation concentrations (g/kg of needles) were obtained by ICP-OES with a Perkin-Elmer Optima 7300 DV (Waltham, MA, United States), following the method proposed by Kalra (1998).

Characterization of Local Biotic Environment

Given that the main goal of our study was to determine whether biotic interactions affected BF growth and foliar nutritional status, we characterized their local biotic environment. Forest composition within a 3 m radius around each balsam fir sapling was evaluated by measuring the percentages of TA, BS and BF relative to their diameter at DBH (diameter at breast height, 1.3 m). Only trees >5 cm DBH were taken into account. These data allowed to calculate the percent of each tree species (TA, BS, and BF) in the canopy around each BF sapling.

Mycorrhizal Root Tip Counts, Mycorrhizal DNA Extraction, Amplification, and Sequencing

Mycorrhizal communities were assessed for each sapling to test their effect on individual BF growth and foliar nutrient status. The root system of each sapling was gently excavated in August 2016 and washed to preserve mycorrhizal root tips. Mycorrhizal root tip counts were performed the same day that the roots were extracted. For each sapling, we randomly selected three 10-cm root fragments for live mycorrhizal root tip counts under a magnifying glass to calculate mycorrhization rate (number of EMF root tips/total number of root tips) and ramification index (number of EMF root tips per 10 cm root). For each fir sapling, 50 mycorrhizal root tips were sampled and stored in CTAB 2X at −20°C until DNA extraction. Root tips were pooled by tree sapling and manually ground with a pestle before DNA extraction. DNA was extracted with a PowerSoil DNA extraction kit (MoBio, Carlsbad, CA, United States) following the manufacturer's instructions. A negative blank extraction (extraction without any material) was performed for every set of 23 extractions. In addition, a tool control was performed on tools that were used for field and laboratory work by extracting DNA from distilled water that was used to wash tools. DNA amplification was performed using the method described in Nagati et al. (2018). Briefly, the fungal ITS1 region (Forward: ITS5 GGAAGTAAAAGTCGTAACAAGG, White et al., 1990; and a modified version of Reverse: 5.8S_Fungi CAAGAGATCCGTTGTTGAAAGTK, Epp et al., 2012) was amplified for 35 PCR cycles. PCR samples were sent to GENETOUL GetPlaGe (Toulouse, France) for sequencing on an Illumina MiSeq platform with the TruSeq Nano PCR-free kit. Sequencing was conducted using the paired-end sequencing technology (2 × 250pb) with the chemistry V2.

Bioinformatics and Sequence Analysis

An abundance matrix was constructed with *OBITool* packages (Boyer et al., 2016) and R script (R Core Team, 2018, version 3.2.3, 2017) based upon the occurrence of sequences among samples. We performed read-pairing assembly, read attribution to samples, read dereplication, and removal of low-quality sequences (shorter than expected, containing ambiguous nucleotides, displaying low score paired-end alignments, or corresponding to singletons). *OBITool Sumaclust* was used to cluster sequences as OTUs (Operational Taxonomic Units) at a 97% identity threshold (Nilsson et al., 2008). Taxonomic assignment was performed with the *OBITool Ecotag* function against the GenBank extracted database[1]. As was the case for our previous dataset that was collected in the same geographic area (Nagati et al., 2018), taxonomic assignments were more accurate with Genbank than with the UNITE public database[2]. Trophic guild assignment was based upon FUNguild software outputs (Nguyen et al., 2016). Sequences belonging to the same OTU were then summed by sample. Lastly, we removed OTUs that were dominant (with the highest read count) in negative or tool extraction and amplification controls, OTUs not belonging to fungi, or OTUs with coarse-resolution taxonomic assignments (i.e., assigned to Eukaryota).

Statistical Analyses

Statistical analyses were performed in R (R Core Team, 2018). Data are available at Dryad repository (doi: 10.5061/dryad.

[1]ftp://ftp.ncbi.nih.gov/genbank/

[2]https://unite.ut.ee/

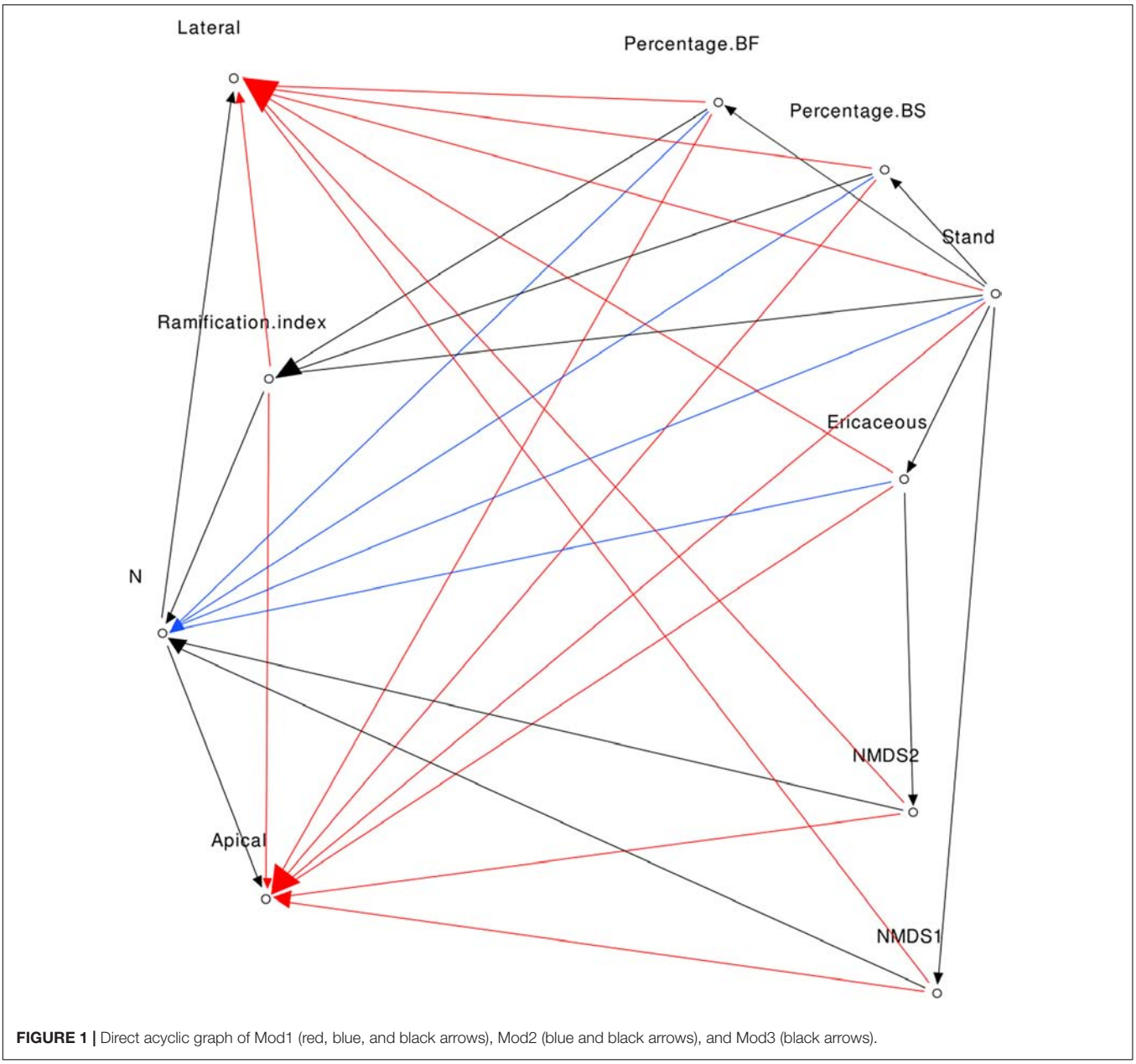

FIGURE 1 | Direct acyclic graph of Mod1 (red, blue, and black arrows), Mod2 (blue and black arrows), and Mod3 (black arrows).

914j5m0) Our main goal was to compare individual traits and fungal communities among sapling types (BS, BSE, and TA). Abundance of each OTU was used to avoid giving too much importance to rare OTUs, as recommended for fungal ITS (Unterseher et al., 2011; Lindahl et al., 2013). Ectomycorrhizal species richness, Shannon index (*H*'), ramification index and mycorrhization rate were each calculated and compared according to one-way ANOVA (three levels), followed by Tukey *post hoc* tests of the means. Foliar nutrient status among saplings growing under BS, BSE, and TA, were compared for each nutrient (N, P, K, Ca, and Mg) with non-parametric Kruskall–Wallis tests, given that the data were not normally distributed, followed by Dunn's *post hoc* tests with Bonferroni corrections. As well, sapling growth between the three modalities was compared with Kruskall-Wallis tests and Dunn's *post hoc* tests with Bonferonni corrections.

Differences in abundance of each ectomycorrhizal family represented in root tip samples were tested between sapling types with Kruskall–Wallis tests, followed by Dunn *post hoc* tests with Bonferroni corrections. We only tested differences in abundance at the family level, given that about 30% of OTUs could not be assigned to a genus. Differences in ectomycorrhizal community structure between the roots of the three sapling types were visually described with Non-Metric Multidimensional Scaling (NMDS, *vegan* package in R; Oksanen et al., 2017) and coordinates of scores on the first two axes of NMDS were extracted for further analyses. Correlation between the NMDS space and individual measures of fir saplings (nutrient

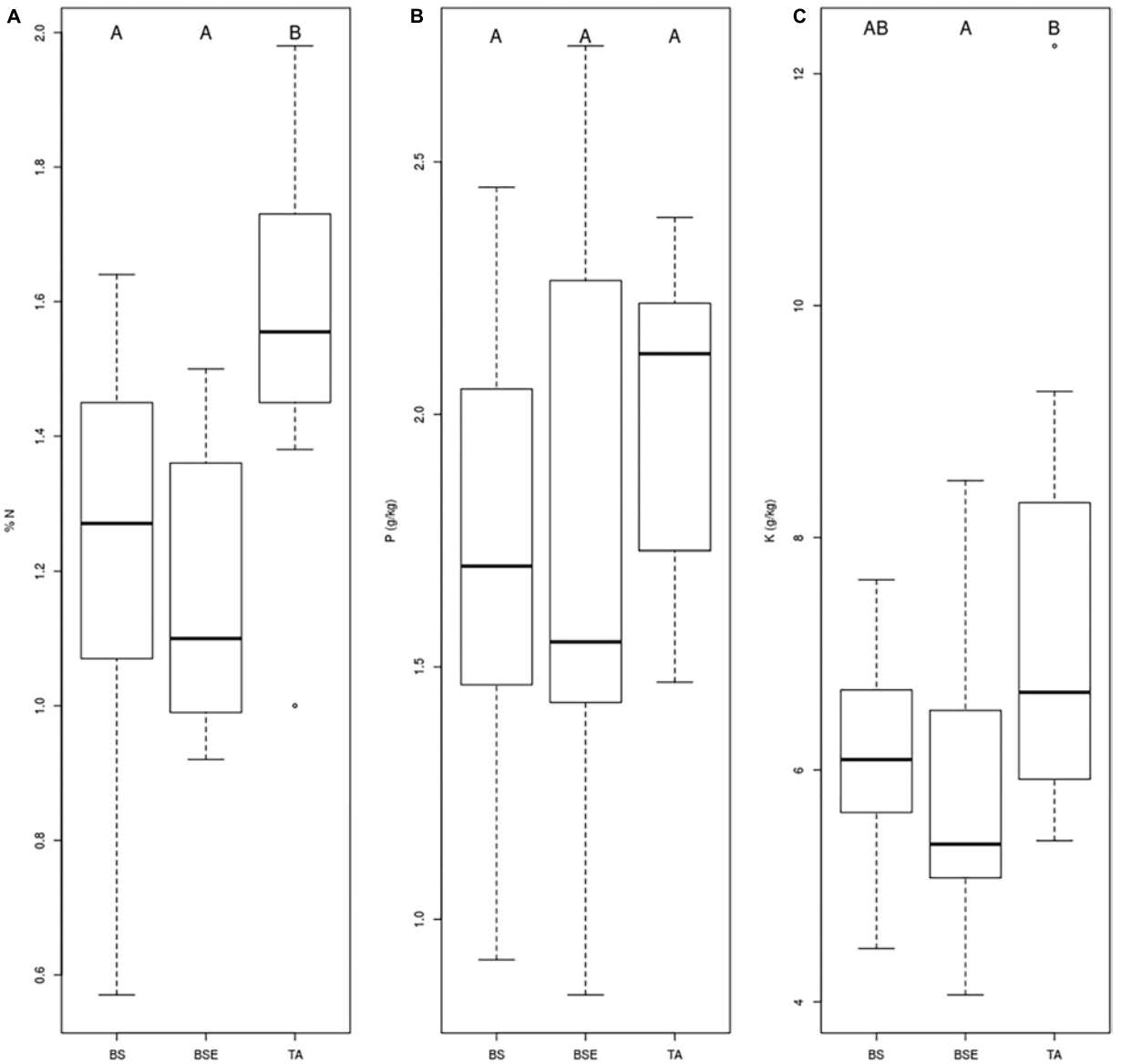

FIGURE 2 | Boxplot chart representing foliar **(A)** N, **(B)** P, and **(C)** K concentrations of BF needles sampled in different stands (BS, black spruce; BSE, black spruce plus ericaceous shrubs; TA, trembling aspen). Different letters indicate differences between modalities.

concentrations and growth) were tested with envfit (vegan package). Envfit vectors of individual measures were plotted on the NMDS space when *p*-Values where significant ($p < 0.05$). Differences in ectomycorrhizal community structure between sites, dominant plant communities (BS, BSE, and TA) were tested with PERMANOVA (*Adonis* function, *vegan* package; Oksanen et al., 2017) with nested factors (site/plant community).

Path Analysis

To test direct and indirect effects of the local biotic environment on growth (for this analysis, growth measures from 2015 to 2016 were summed) and foliar N concentrations, we compared three hypotheses by fitting structural equation models (SEM) to the data (with lavaan package; Rosseel et al., 2018). We included only foliar N concentrations in our model, as it was the only nutrient concentration available for all saplings. We constructed three SEMs to represent three *a priori* hypotheses. Each of the hypotheses is rooted in current knowledge regarding the processes that have been described in the literature, and which are described below. All models were fitted to centered and reduced data.

Complete Model Mod1

Considering direct links, we formulated five hypotheses. The first was that foliar N concentration was positively correlated with growth (Pallardy and Kozlowski, 2008). The second one

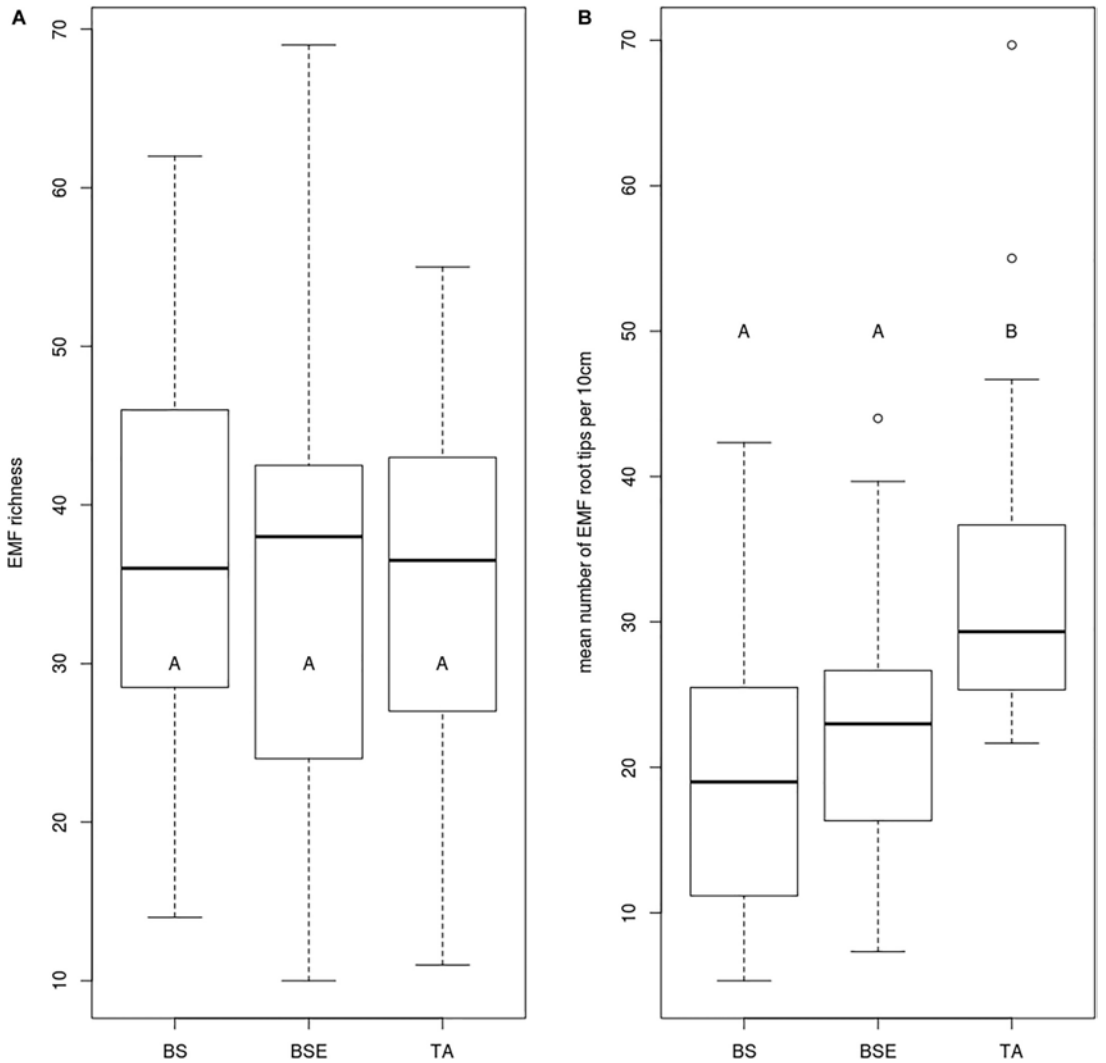

FIGURE 3 | Boxplot charts showing **(A)** EMF richness and **(B)** number of EMF root tips per 10 cm roots of BF saplings sampled in different stands. BS, black spruce; BSE, black spruce plus ericaceous shrubs; TA, trembling aspen. Different letters indicate differences between modalities.

was that EMF abundance and communities were positively correlated with growth and foliar N concentrations (Smith and Read, 2008). The third hypothesis was that BS stands and the percent of BS near fir saplings were negatively correlated with BF growth and foliar N concentrations (Arbour and Bergeron, 2011). The fourth hypothesis was that the presence of ericaceous shrubs near saplings was negatively correlated with BF growth and nutrition (Peterson, 1965; Yamasaki et al., 1998; Mallik, 2003). Finally, we hypothesized that the percentage of conspecific mature trees near BF saplings was positively correlated with their growth and foliar N, given that local conditions have permitted their growth and survival. Lateral and apical growth were added as co-variables in the model and together co-varied with basal diameter of BF saplings.

For this model, we also formulated indirect linkage hypotheses. The relative percentage of BF was correlated with stand type (Arbour and Bergeron, 2011). The relative percentage of BS was correlated with the stand (Cavard et al., 2011). The presence of ericaceous shrubs was correlated with the stand type (BF saplings in TA stands were never next to ericaceous shrubs). The ramification index was correlated with the stand (see **Figure 3**), and percent of BF (the presence of mature trees near BF saplings increased the probability of encountering EMF partners). The NMDS first axis was correlated with the stand and the second axis negatively with the presence of ericaceous shrubs (see **Figure 5** and PERMANOVA results). The complete model is presented in **Figure 1**.

Nutrient Model Mod2

The indirect links are the same as for Mod1 but in this model we assumed that foliar N concentration was the only variable that was correlated to growth.

TABLE 2 | Results of PERMANOVA conducted on EMF community of balsam fir saplings.

	df	F-model	R^2	*P*-value
Site	3	1.1749	0.06437	0.104
Site: plant community	8	1.1852	0.16855	0.035
Residuals	42	–	0.76708	–

Fungi Centered Model Mod3

The links are the same as for Mod2, but in this model we assumed that only variables linked to EMF were correlated with foliar N concentrations. In this model, NMDS first and second axes and ramification index were the only variables directly linked to N concentrations.

To ensure that our models respected independence between non-linked variables, we performed Fisher's C test (*ggm* package, Marchetti et al., 2015). Models with *p*-Values greater than 0.05 are considered to have respected claims of independence (Shipley, 2000). A model was considered to be representative of the population if the *p*-Value of the Chi-square test was greater than 0.05. For each model, we calculated the Comparative Fit Index (CFI) and the Tucker-Lewis Index (TLI) to evaluate how each model fits to the data. Values greater than 0.95 were considered to be good fits (Hu and Bentler, 1999). Each structural equation model with Fisher's C test and Chi-Square *p*-values > 0.05, CFI > 0.95, and TLI > 0.95 could describe the data well, we used these values as a primary filter to ensure that models fit well the data and are representative of the population. After applying this filter our aim was to select the best model based on AIC criterion, however, only Mod1 passed the primary filter and was de facto selected.

RESULTS

Fir Sapling Traits and Differences Between Stands

Given that 6 of the 60 BF saplings were missing after the first year of fieldwork, the results presented here are based on 18 saplings for each sapling type (i.e., 54 saplings). For 11 saplings, the quantity of needles was insufficient to measure minor and major cations, thereby further reducing the sample size.

Mean foliar N concentrations of BF saplings were highest in TA stands compared to BS and BSE stands ($p < 0.05$, **Figure 2A**). Mean foliar K concentration was higher in TA than in BSE stands ($p < 0.05$, **Figure 2C**). Foliar P (**Figure 2B**), Ca, and Mg did not vary between sapling types ($p > 0.05$). No significant differences were found in root tip EMF richness and Shannon index among sapling types (**Figure 3A**, $p > 0.05$). Mean lateral growth of fir saplings did not differ between stands in 2015 and 2016. Apical growth was greater in TA than in BSE stands in 2015, while no difference was detected for apical growth in 2016. Summed lateral and apical growth did not differ between stands. Ramification index of BF roots was higher in TA than in other stands (**Figure 3B**, $p < 0.05$).

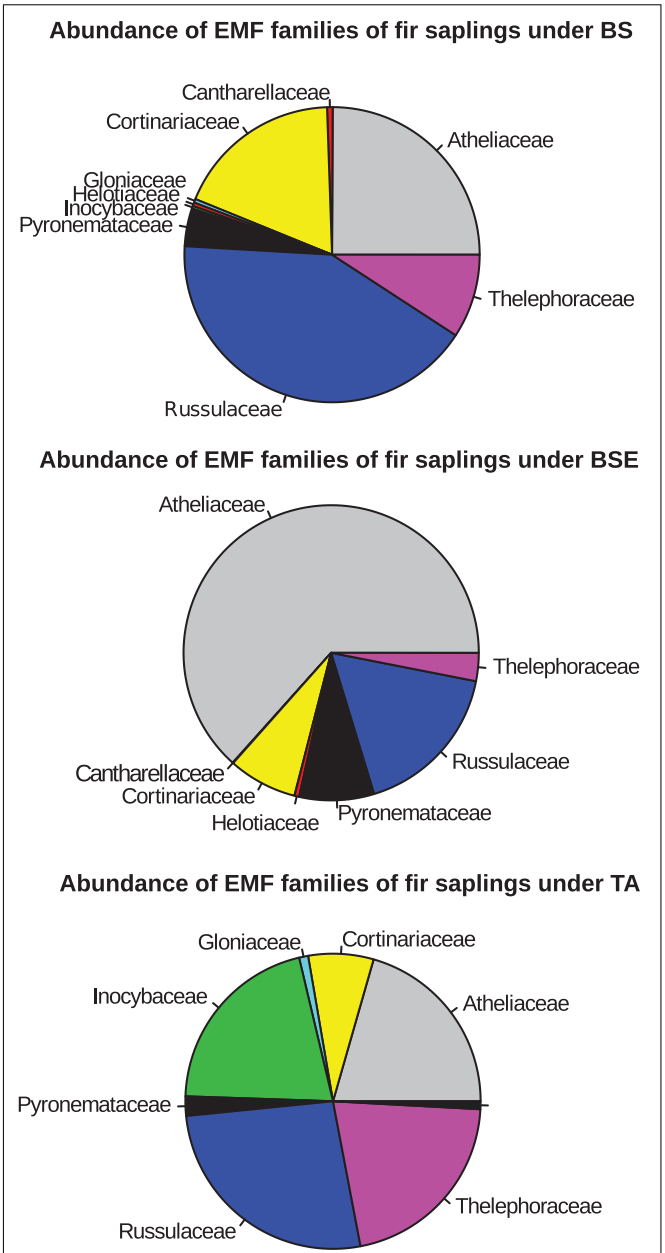

FIGURE 4 | Pie chart representing percent of EMF families per stand type for root tips samples of BF saplings (based on the abundance of reads). BS, black spruce; BSE, black spruce plus ericaceous shrub; TA, trembling aspen.

Ectomycorrhizal Community

A total of 400 EMF OTUs (655,495 reads) were found in EMF root tips from BF saplings, representing 19.5% of OTUs and 59.7% of reads, with an average of 35.4 OTUs and 12,056.8 reads per sample. Variation in EMF root tip communities was explained by plant community (*p*-Value = 0.035, $F = 1.1852$, $R^2 = 0.169$), but no effect of site was detected (**Table 2**). Clavulinaceae were only found under TA. Further, the abundance of Cortinariaceae was higher under BS compared to TA stands, that of Gloniaceae was higher under TA than under BSE, and

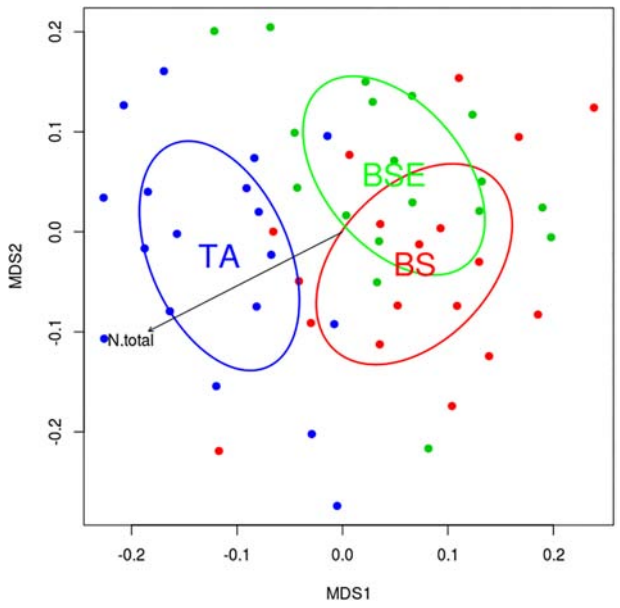

FIGURE 5 | Non-metric multidimensional scaling (NMDS) plots representing similarity between EMF communities of BF root tips in black spruce (BS, red), black spruce + ericaceous shrubs (BSE, green) and trembling aspen (TA, blue) stands. Arrow represents the correlation between N concentration in fir needle and NMDS space.

that of Helotiaceae was higher under BSE than under TA. Finally, abundance of Inocybaceae and Thelephoraceae were greater under TA than under BS and BSE (Kruskal-Wallis and Dunn *post hoc* tests, $p < 0.025$, **Figure 4**). According to the NMDS, EMF communities on root tips from the TA stands were distinct from those under BS and BSE, while communities in BS and BSE overlapped (**Figure 5**). *Envfit* test demonstrated that N concentration were significantly associated with NMDS structure ($p < 0.05$, **Figure 5**).

Path Analysis

The *p*-Values of the Fisher's *C*-tests were greater than 0.05 for the three models, indicating that all models could be accepted. The *p*-Values of the associated Chi-Square tests ranged between 0.019 and 0.401. CFI ranged between 0.930 and 0.997, while those for TLI ranged between 0.901 and 0.991 (**Table 3**). Given these results, the interactions model Mod1 was the only one passing the primary filter. Here, we present direct and indirect links for which *p*-Values were significant at $p < 0.05$ (for a summary of the parameter estimates, see **Supplementary Table 1**). Apical and lateral growth was directly correlated with foliar N concentrations (path coefficients were 0.547 and 0.609, respectively) and the ramification index (0.253 and 0.254). Of interest, foliar N concentrations were negatively correlated with NMDS second axis (−0.226) and the percentage of BS (−0.469). The ramification index was negatively correlated with BS stand (−1.573). NMDS first axis was positively correlated with BS stands (1.499), while the second axis was positively correlated with the presence of ericaceous shrubs (0.773). The presence of ericaceous shrubs, in turn, was positively correlated with BS stands (0.500). Percentage of BS was positively correlated with BS stands (1.708), while the percentage of BF was negatively correlated with BS stands (−1.306). Significant direct and indirect links between variables are presented in **Figure 6**. All significant and non-significant parameter estimates are presented in **Supplementary Table 1**.

DISCUSSION

The role of biotic interactions was investigated here to explain observed growth differences in balsam fir saplings growing at a northern ecotone of the boreal forest. We hypothesized that biotic interactions could explain the greater nutrition under aspen than under spruce. Our results suggest that facilitation through ectomycorrhizal fungi, together with competition with ericaceous shrubs under BS, are significant drivers of BF growth and nutrition.

As soil EMF communities were strongly divergent between TA and BS-dominated stands (Nagati et al., 2018), we hypothesized that young BF would associate with distinct EMF in the two stands, and that BF would have greater mycorrhization rates under TA stands. Contrary to our hypothesis, observation of BF root tips revealed EM root tips in all conditions, with similar mycorrhization rate. Sequencing of EM root tips confirmed our observation as species richness was not different between stands. We rather detected differences of root architecture and community composition. Indeed, we observed a higher ramification index under TA than under BS stands, probably leading to differences in abilities to explore soil for resources. Our path analyses suggested that soil conditions in TA stands led to a higher ramification index, which in turn improved BF early growth, likely by enhancing foliar nutrient concentrations. Moreover we detected that percent BS around saplings was negatively correlated to sapling N content, this is probably linked to the greater N availability in TA than in BS stands (Nagati et al., 2018). As demonstrated by path analysis, N availability (reflected by the stand and so on, by the percent of BS) was not the only factor affecting sapling needle N content and EMF community structure was also correlated to N nutrition. There are therefore complex interactions leading to a better nutrition of young BF, and path analyses highlighted the importance of both stand dominance and EMF community.

Between stands, communities of EMF on BF roots were not distinct in species richness but rather in composition, and for example Clavulinaceae were only detected under TA stands. Based on soil sequencing, our previous study also revealed

TABLE 3 | Statistics of each structural equation models.

Model	*P*-value (Chisq)	CFI	TLI
Mod1	0.401	0.997	0.991
Mod2	0.103	0.962	0.941
Mod3	0.019	0.930	0.901

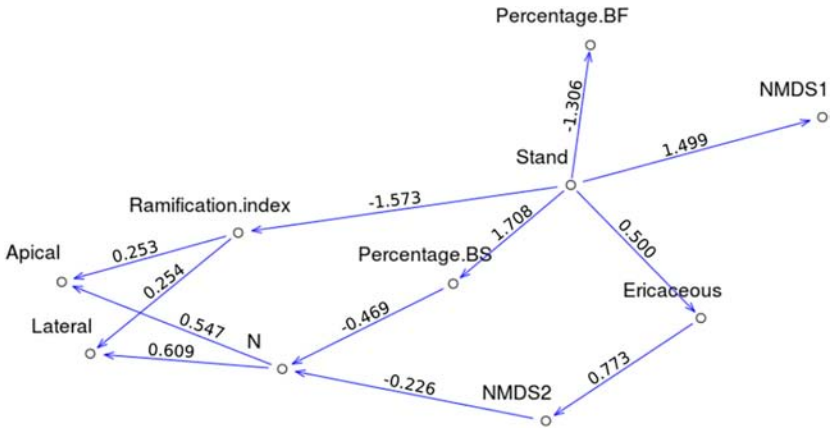

FIGURE 6 | Direct acyclic graphs corresponding to Mod1, only significant links between variables are shown, path coefficients are indicated above each arrow.

a difference of composition but not species richness between stands (Nagati et al., 2018). More generally, changes in plant dominance rather shape EMF community structure than the species richness (Tedersoo et al., 2012). Such a change in EMF community can have strong functional consequences. Based on our results, changes in community composition were correlated with changes in N concentration. We detected a higher abundance of Inocybaceae and Thelephoraceae in BF roots tips in TA than in BSE and BS stands, and Helotiaceae were more abundant in BSE than TA stand. These differences of EMF abundance between stands could partly explain differences in N uptake by BF saplings. Depending on site conditions, different EMF species or assemblage could have different abilities to uptake nutrients in soil and to transfer these nutrients to plants (Jonsson et al., 2001; Buée et al., 2007). This result could suggest that some fungi are more efficient provider of N to young BF. Nara (2006) experiments illustrated how variable can be the result of EM interactions with distinct EMF fungi. By artificially connecting two different tree species through a common mycorrhizal network from different EMF species, Nara (2006) showed that N nutrition could be 6 times higher when trees were connected by *Hebeloma mesophaeum* as compared to trees connected by *Laccaria amethystina*. As BF needles were generally richer in N under TA, the question remain if this benefit under TA could be due to N transfer through a common mycorrhizal network (Simard et al., 2012) involving BF and TA, or only to better soil conditions under TA. We did not sequence TA roots, to detect possible shared fungi and experimental manipulations may be necessary to test whether TA could bring a direct benefit to young BF saplings. As suggested by the models of Bever et al. (2010), the facilitation of BF by TA may not only be explained by shared fungi, but simply by changes in EMF abundance, which we detected between the two stands. The higher abundance of Helotiaceae associated with BF roots near ericaceous shrubs is also interesting. Several studies have demonstrated that some fungi in this family could have a dual-mode of root colonization and forms ectomycorrhiza as well as ericoid mycorrhiza (Vrålstad et al., 2000; Villarreal-Ruiz et al., 2004; Grelet et al., 2010). These species could be more efficient to provide nutrients to ericaceous shrubs than to BF saplings and could explain the lower N nutrition of BF near ericaceous shrubs.

The lower nutrient concentrations found in fir needles (N and K) under BSE stands compared to TA stands (**Figure 2**), suggest a negative effect of black spruce and ericaceous shrubs association on BF seedlings. These results are consistent with previous studies where ericaceous shrubs that are associated with non-EMF fungi may compete with EMF-associated trees (Yamasaki et al., 1998; Walker et al., 1999; Mallik, 2003). Ericoid mycorrhizal fungi are particularly competitive for recalcitrant organic matter (ROM) decomposition and uptake of N and P (Read, 1996) and probably have the ability to take up nutrient from ROM found around ericaceous shrubs (Joanisse et al., 2018) contrarily to BF-associated EMF communities. In hardwood forests of the southern Appalachians, the presence of *Rhododendron maximum* L. reduced the ramification index of eastern hemlock (*Tsuga canadensis* [L.] Carrière) saplings four-fold (Walker et al., 1999). In our study, the presence of ericaceous shrubs (associated with ericoid fungi) close to fir saplings rather affected their root EMF communities than reduced the ramification index. Numerous studies have already shown how ericaceous shrubs affect EMF communities associated with trees, such as red oak (*Quercus rubra* L.), hemlock (Walker et al., 1999), pine (*Pinus strobus* L., *P. sylvestris* L.) (Kohout et al., 2011), and black spruce (Yamasaki et al., 1998; Kennedy et al., 2018). In the boreal forest, ericaceous shrubs not only compete with fir growth and nutrition, but also modify forest dynamics and lead to thick accumulation of soil organic matter and soil acidification. This phenomenon, is a recurrent problem within boreal forests that are situated in the Ontario-Quebec Clay Belt and is often associated with the presence of ericaceous shrubs and Sphagnum mosses (Fenton et al., 2005) and a loss of forest productivity (Simard et al., 2007). The thickness of the soil organic layer is correlated with a decrease in TA establishment and growth within

the black spruce-feather moss domain (Lafleur et al., 2015), together with a decrease in black spruce establishment in sites that are dominated by *K. angustifolia* L. (Mallik and Kravchenko, 2018). Our results suggest that forest regeneration failure in areas with high ericaceous shrub abundance could be explained by their effect on EMF communities, and reciprocally, invite to consider below-ground interactions to avoid or limit regeneration failure.

Whilst our study focused on fir growth, we revealed stronger differences in foliar N concentrations and ramification indices between stands. Indeed difference in annual growth between stands was detected only in 2015. Annual growth of trees is relatively slow in the boreal forest and is correlated with the length of the growing season, which can differ from 1 year to the next (Jarvis and Linder, 2000). Differences in early growth could thus be difficult to detect over a short period of time and would be probably more pronounced when studying several years of growth (see Arbour and Bergeron, 2011). Measuring fitness is always difficult for young trees over a short period of study and measures of foliar nutrient concentrations were more useful to detect differences between stands, and reflected the benefits of EMF symbiosis. Foliar nutrient concentrations were generally greater under TA compared to BS and correlated with growth, which confirmed our hypothesis. This result could be linked to the greater availability of nutrients in TA stands than in BS stands (Cavard et al., 2011; Nagati et al., 2018).

A major goal of forest ecology today is to determine ecosystem trajectories in a context of climate change. In the case of the balsam fir-black spruce forest ecotone, it appears that trembling aspen stands would provide a favorable niche for fir establishment and growth. As demonstrated by Arbour and Bergeron (2011), the higher abundance of balsam fir in TA than BS stands is more pronounced for saplings than seedlings. This result translates a lower mortality and better growth of balsam fir in TA stands which leads to a greater abundance of mature and reproductive trees in these stands. This in turn may result in an increase of mixed forests and deep changes in ecosystem functioning. The distributional ranges of numerous tree species are likely to change within the context of climate change (Bellard et al., 2012; Iverson and McKenzie, 2013; IPCC Climate Change, 2014). Migration has already begun for many tree species in North America (Brandt, 2009; Woodall et al., 2009). Their geographic ranges have been extending northward rapidly (up to 100 km/century; Woodall et al., 2009). Our results suggest that the climatic niche could not alone explain species abilities to establish and that the mutualistic niche (sensus Peay, 2016) have to be explored to ensure a better comprehension of tree migration processes.

DATA AVAILABILITY

All datasets for this study are included in the manuscript and/or the **Supplementary Files**.

AUTHOR CONTRIBUTIONS

MG, YB, MN, MR, and AD designed the study and interpreted the results. MN and MR carried out the field and laboratory work. MN and SM carried out the molecular biology and bioinformatics. MN carried out the statistical analyses. MN, MG, and MR wrote the manuscript. All authors edited and approved the final version of the manuscript.

FUNDING

This work was supported by a MITACS Fellowship to MN in collaboration with the Norbord Inc. and the Ouranos Consortium on Climate Change (IT066831). Travel funds were provided by the Paul Sabatier University and sequencing costs were supported by the "Laboratoires d'Excellence (LABEX)" TULIP (ANR 10-LABX-0041) and CEBA (ANR 10-LABX-0025).

ACKNOWLEDGMENTS

We thank Danielle Charron, Raynald Julien, and Elias Ganivet for their assistance in fieldwork, Francine Tremblay for laboratory access, Philippe Marchand and Benjamin Andrieux for statistical advice, and Genopole Toulouse for the computing and storage resources. We are grateful to W. F. J. Parsons for revising the manuscript.

SUPPLEMENTARY MATERIAL

The Supplementary Material for this article can be found online at: https://www.frontiersin.org/articles/10.3389/fpls.2019.00932/full#supplementary-material

REFERENCES

Arbour, M. -L., and Bergeron, Y. (2011). Effect of increased *Populus* cover on *Abies* regeneration in the *Picea*-feathermoss boreal forest. *J. Veg. Sci.* 22, 1132–1142. doi: 10.1111/j.1654-1103.2011.01314.x

Barbeta, A., and Peñuelas, J. (2017). Increasing carbon discrimination rates and depth of water uptake favor the growth of mediterranean evergreen trees in the ecotone with temperate deciduous forests. *Glob. Change Biol.* 23, 5054–5068. doi: 10.1111/gcb.13770

Bellard, C., Bertelsmeier, C., Leadley, P., Thuiller, W., and Courchamp, F. (2012). Impacts of climate change on the future of biodiversity. *Ecol. Lett.* 15, 365–377. doi: 10.1111/j.1461-0248.2011.01736.x

Belleau, A., Leduc, A., Lecomte, N., and Bergeron, Y. (2011). Forest succession rate and pathways on different surface deposit types in the boreal forest of northwestern Quebec. *Écoscience* 18, 329–340. doi: 10.2980/18-4-3393

Bever, J. D., Dickie, I. A., Facelli, E., Facelli, J. M., Klironomos, J., Moora, M., et al. (2010). Rooting theories of plant community ecology in microbial interactions. *Trends Ecol. Evol.* 25, 468–478. doi: 10.1016/j.tree.2010.05.004

Boyer, F., Mercier, C., Bonin, A., Le Bras, Y., Taberlet, P., and Coissac, E. (2016). obitools: a unix -inspired software package for DNA metabarcoding. *Mol. Ecol. Res.* 16, 176–182. doi: 10.1111/1755-0998.12428

Brandt, J. P. (2009). The extent of the north american boreal zone. *Environ. Rev.* 17, 101–161. doi: 10.1139/A09-004

Brooker, R. W., Maestre, F. T., Callaway, R. M., Lortie, C. L., Cavieres, L. A., Kunstler, G., et al. (2008). Facilitation in plant communities: the past, the present, and the future. *J. Ecol.* 96, 18–34. doi: 10.1111/j.1365-2745.2007.01295.x

Buée, M., Courty, P. E., Mignot, D., and Garbaye, J. (2007). Soil niche effect on species diversity and catabolic activities in an ectomycorrhizal fungal community. *Soil Biol. Biochem.* 39, 1947–1955. doi: 10.1016/j.soilbio.2007.02.016

Callaway, R. M., and Walker, L. R. (1997). Competition and facilitation: a synthetic approach to interactions in plant communities. *Ecology* 78, 1958–1965. doi: 10.1890/0012-9658(1997)078%5B1958:cafasa%5D2.0.co;2

Cavard, X., Bergeron, Y., Chen, H. Y. H., and Paré, D. (2011). Effect of forest canopy composition on soil nutrients and dynamics of the understorey: mixed canopies serve neither vascular nor bryophyte strata. *J. Veg. Sci.* 22, 1105–1119. doi: 10.1111/j.1654-1103.2011.01311.x

Collier, F. A., and Bidartondo, M. I. (2009). Waiting for fungi: the ectomycorrhizal invasion of lowland heathlands. *J. Ecol.* 97, 950–963. doi: 10.1111/j.1365-2745.2009.01544.x

Dickie, I. A., Oleksyn, J., Reich, P. B., Karolewski, P., Zytkowiak, R., Jagodzinski, A. M., et al. (2006). Soil modification by different tree species influences the extent of seedling ectomycorrhizal infection. *Mycorrhiza* 16, 73–79. doi: 10.1007/s00572-005-0013-x

Epp, L. S., Boessenkool, S., Bellemain, E. P., Haile, J., Esposito, A., Riaz, T., et al. (2012). New environmental metabarcodes for analysing soil DNA: potential for studying past and present ecosystems. *Mol. Ecol.* 21, 1821–1833. doi: 10.1111/j.1365-294X.2012.05537.x

Fenton, N., Lecomte, N., Légaré, S., and Bergeron, Y. (2005). Paludification in black spruce (*Picea mariana*) forests of eastern Canada: potential factors and management implications. *For. Ecol. Manag.* 213, 151–159. doi: 10.1016/j.foreco.2005.03.017

Franklin, O., Näsholm, T., Högberg, P., and Högberg, M. N. (2014). Forests trapped in nitrogen limitation - an ecological market perspective on ectomycorrhizal symbiosis. *New Phytol.* 203, 657–666. doi: 10.1111/nph.12840

Gallet, C. (1994). Allelopathic potential in bilberry-spruce forests: influence of phenolic compounds on spruce seedlings. *J. Chem. Ecol.* 20, 1009–1024. doi: 10.1007/BF02059738

Grelet, G. -A., Johnson, D., Vrålstad, T., Alexander, I. J., and Anderson, I. C. (2010). New insights into the mycorrhizal rhizoscyphus ericae aggregate: spatial structure and co-colonization of ectomycorrhizal and ericoid roots. *New Phytol.* 188, 210–222. doi: 10.1111/j.1469-8137.2010.03353.x

Harsch, M. A., Hulme, P. E., McGlone, M. S., and Duncan, R. P. (2009). Are treelines advancing? a global meta-analysis of treeline response to climate warming. *Ecol. Lett.* 12, 1040–1049. doi: 10.1111/j.1461-0248.2009.01355.x

Hu, L., and Bentler, P. M. (1999). Cutoff criteria for fit indexes in covariance structure analysis: conventional criteria versus new alternatives. *Struct. Equ. Modeling* 6, 1–55. doi: 10.1080/10705519909540118.

Inselsbacher, E., and Näsholm, T. (2012). The below-ground perspective of forest plants: soil provides mainly organic nitrogen for plants and mycorrhizal fungi. *New Phytol.* 195, 329–334. doi: 10.1111/j.1469-8137.2012.04169.x

IPCC Climate Change (2014). *Impacts, Adaptation, & Vulnerability - Summary for Policymakers GlobalChange.gov*. Available at: http://www.globalchange.gov/browse/reports/ipcc-climate-change-2014-impacts-adaptation-vulnerability-summary-policymakers (accessed February 24, 2016).

Iverson, L. R., and McKenzie, D. (2013). Tree-species range shifts in a changing climate: detecting, modeling, assisting. *Lands. Ecol.* 28, 879–889. doi: 10.1007/s10980-013-9885-x

Jarvis, P., and Linder, S. (2000). Botany: constraints to growth of boreal forests. *Nature* 405, 904–905. doi: 10.1038/35016154.

Joanisse, G. D., Bradley, R. L., and Preston, C. M. (2018). The spread of *almia angustifolia* on black spruce forest cutovers contributes to the spatial heterogeneity of soil resources. *PLoS One* 13:e0198860. doi: 10.1371/journal.pone.0198860

Jonsson, L. M., Nilsson, M. -C., Wardle, D. A., and Zackrisson, O. (2001). Context dependent effects of ectomycorrhizal species richness on tree seedling productivity. *Oikos* 93, 353–364. doi: 10.1034/j.1600-0706.2001.930301.x

Kalra, Y. P. (1998). "Soil and plant analysis council,"in *Handbook of Reference Methods for Plant Analysis*, ed. Y. Kalra, (Boca Raton: CRC Press).

Kennedy, P. G., Mielke, L. A., and Nguyen, N. H. (2018). Ecological responses to forest age, habitat, and host vary by mycorrhizal type in boreal peatlands. *Mycorrhiza* 28, 315–328. doi: 10.1007/s00572-018-0821-4

Kohout, P., Sı korová, Z., Bahram, M., Hadincová, V., Albrechtová, J., Tedersoo, L., et al. (2011). Ericaceous dwarf shrubs affect ectomycorrhizal fungal community of the invasive *Pinus strobus* and native *Pinus sylvestris* in a pot experiment. *Mycorrhiza* 21, 403–412. doi: 10.1007/s00572-010-0350-2

Lafleur, B., Cazal, A., Leduc, A., and Bergeron, Y. (2015). Soil organic layer thickness influences the establishment and growth of trembling aspen (*Populus tremuloides*) in boreal forests. *For. Ecol. Manag.* 347, 209–216. doi: 10.1016/j.foreco.2015.03.031

Lecomte, N., and Bergeron, Y. (2005). Successional pathways on different surficial deposits in the coniferous boreal forest of the Quebec Clay Belt. *Can. J. For. Res.* 35, 1984–1995. doi: 10.1139/x05-114

Légaré, S., Paré, D., and Bergeron, Y. (2005). Influence of aspen on forest floor properties in black spruce-dominated stands. *Plant Soil* 275, 207–220. doi: 10.1007/s11104-005-1482-6

Lindahl, B. D., Nilsson, R. H., Tedersoo, L., Abarenkov, K., Carlsen, T., Kjøller, R., et al. (2013). Fungal community analysis by high-throughput sequencing of amplified markers – a user's guide. *New Phytol.* 199, 288–299. doi: 10.1111/nph.12243

Mallik, A., and Kravchenko, D. (2018). Recruitment and ontogenic patterns of stunting and growth release of black spruce (*Picea mariana*) in post-fire *Kalmia* heaths. *For. Ecol. Manag.* 407, 135–144. doi: 10.1016/j.foreco.2017.09.068

Mallik, A. U. (2003). Conifer regeneration problems in boreal and temperate forests with ericaceous understory: role of disturbance, seedbed limitation, and keytsone species change. *Crit. Rev. Plant Sci.* 22, 341–366. doi: 10.1080/713610860

Marchetti, G. M., Drton, M., and Sadeghi, K. (2015). *Ggm: Functions for Graphical Markov Models*. Available at: https://cran.r-project.org/web/packages/ggm/index.html (accessed December 13, 2018).

Messaoud, Y., Bergeron, Y., and Leduc, A. (2007). Ecological factors explaining the location of the boundary between the mixedwood and coniferous bioclimatic zones in the boreal biome of eastern North America. *Glob. Ecol. Biogeogr.* 16, 90–102. doi: 10.1111/j.1466-8238.2006.00277.x

Nagati, M., Roy, M., Manzi, S., Richard, F., Desrochers, A., Gardes, M., et al. (2018). Impact of local forest composition on soil fungal communities in a mixed boreal forest. *Plant Soil* 432, 345–357. doi: 10.1007/s11104-018-3806-3

Nara, K. (2006). Ectomycorrhizal networks and seedling establishment during early primary succession. *New Phytol.* 169, 169–178. doi: 10.1111/j.1469-8137.2005.01545.x

Nara, K., and Hogetsu, T. (2004). Ectomycorrhizal fungi on established shrubs facilitate subsequent seedling establishment of successional plant species. *Ecology* 85, 1700–1707. doi: 10.1890/03-0373

Nguyen, N. H., Song, Z., Bates, S. T., Branco, S., Tedersoo, L., Menke, J., et al. (2016). FUNGuild: an open annotation tool for parsing fungal community datasets by ecological guild. *Fungal Ecol.* 20, 241–248. doi: 10.1016/j.funeco.2015.06.006

Nilsson, R. H., Kristiansson, E., Ryberg, M., Hallenberg, N., and Larsson, K. -H. (2008). Intraspecific ITS variability in the kingdom fungi as expressed in the international sequence databases and its implications for molecular species identification. *Evol. Bioinform. Online* 4, 193–201.

Oksanen, J., Blanchet, F. G., Friendly, M., Kindt, R., Legendre, P., McGlinn, D., et al. (2017). *Vegan: Community Ecology Package*. Available at: https://cran.r-project.org/web/packages/vegan/index.html (accessed January 18, 2018).

Pallardy, S. G., and Kozlowski, T. T. (2008). *Physiology of Woody Plants.* 3rd ed. Amsterdam?, NE: Elsevier.

Peay, K. G. (2016). The mutualistic niche: mycorrhizal symbiosis and community dynamics. *Annu. Rev. Ecol., Evol. System.* 47, 143–164. doi: 10.1146/annurev-ecolsys-121415-032100

Peterson, E. B. (1965). Inhibition of black spruce primary roots by a water-soluble substance in *Kalmia angustifolia*. *Forest Sci.* 11, 473–479.

Pickles, B. J., and Simard, S. W. (2017). "Mycorrhizal networks and forest resilience to drought," in *Mycorrhizal Mediation of Soil* (Amsterdam?, NE: Elsevier), 319–339. doi: 10.1016/b978-0-12-804312-7.00018-8

R Core Team (2018). *R: A Language and Environment for Statistical Computing*. Vienna: R Foundation for Statistical Computing

Ratcliffe, J. L., Creevy, A., Andersen, R., Zarov, E., Gaffney, P. P. J., Taggart, M. A., et al. (2017). Ecological and environmental transition across the forested-to-open bog ecotone in a west Siberian peatland. *Sci. Total Environ.* 607–608, 816–828. doi: 10.1016/j.scitotenv.2017.06.276

Read, D. J. (1996). The structure and function of the ericoid mycorrhizal root. *Ann. Bot.* 77, 365–374. doi: 10.1006/anbo.1996.0044

Richard, F., Selosse, M. -A., and Gardes, M. (2009). Facilitated establishment of *Quercus ilex* in shrub- dominated communities within a mediterranean ecosystem: do mycorrhizal partners matter? *FEMS Microbiol. Ecol.* 68, 14–24. doi: 10.1111/j.1574-6941.2009.00646.x

Robitaille, A., and Saucier, J. -P. (1996). "Land district, ecophysiographic units and areas: the landscape mapping of the ministère des ressources naturelles du Québec," in *Global to Local: Ecological Land Classification*, eds R. A. Sims, I. G. W. Corns, K. Klinka, (Springer: Dordrecht), 127–148 doi: 10.1007/bf00396141

Rosseel, Y., Oberski, D., Byrnes, J., Vanbrabant, L., Savalei, V., Merkle, E., et al. (2018). *Lavaan: Latent Variable Analysi*. Available at: https://cran.r-project.org/package=lavaan (accessed November 21, 2018).

Shipley, B. (2000). A new inferential test for path models based on directed acyclic graphs. *Struct. Equ. Modeling* 7, 206–218. doi: 10.1207/S15328007SEM0702_4

Simard, M., Lecomte, N., Bergeron, Y., Bernier, P. Y., and Paré, D. (2007). Forest productivity decline caused by successional paludification of boreal soils. *Ecol. Appl.* 17, 1619–1637. doi: 10.1890/06-1795.1

Simard, S., Asay, A., Beiler, K., Bingham, M., Deslippe, J., He, X., et al. (2015). "Resource transfer between plants through ectomycorrhizal fungal networks," in *Mycorrhizal Networks*, ed. T. R. Horton (Dordrecht: Springer), 133–176. doi: 10.1007/978-94-017-7395-9_5

Simard, S. W., Beiler, K. J., Bingham, M. A., Deslippe, J. R., Philip, L. J., and Teste, F. P. (2012). Mycorrhizal networks: mechanisms, ecology and modelling. *Fungal Biol. Rev.* 26, 39–60. doi: 10.1016/j.fbr.2012.01.001

Smith, S. E., and Read, D. J. (2008). *Mycorrhizal Symbiosis*. Cambridge, MA: Academic Press.

Stachowicz, J. J. (2001). Mutualism, facilitation, and the structure of ecological communities. *BioScience* 51:235. doi: 10.1641/0006-3568(2001)051%5B0235:mfatso%5D2.0.co;2

Taylor, D. L., Hollingsworth, T. N., McFarland, J. W., Lennon, N. J., Nusbaum, C., and Ruess, R. W. (2013). A first comprehensive census of fungi in soil reveals both hyperdiversity and fine-scale niche partitioning. *Ecol. Monogr.* 84, 3–20. doi: 10.1890/12-1693.1

Tedersoo, L., Bahram, M., Toots, M., DiéDhiou, A. G., Henkel, T. W., KjøLler, R., et al. (2012). Towards global patterns in the diversity and community structure of ectomycorrhizal fungi: global metastudy of ectomycorrhizal fungi. *Mol. Ecol.* 21, 4160–4170. doi: 10.1111/j.1365-294X.2012.05602.x

Tedersoo, L., Mett, M., Ishida, T. A., and Bahram, M. (2013). Phylogenetic relationships among host plants explain differences in fungal species richness and community composition in ectomycorrhizal symbiosis. *New Phytol* 199, 822–831. doi: 10.1111/nph.12328

Teste, F. P., Simard, S. W., Durall, D. M., Guy, R. D., Jones, M. D., and Schoonmaker, A. L. (2009). Access to mycorrhizal networks and roots of trees: importance for seedling survival and resource transfer. *Ecology* 90, 2808–2822. doi: 10.1890/08-1884.1

Unterseher, M., Jumpponen, A., Öpik, M., Tedersoo, L., Moora, M., Dormann, C. F., et al. (2011). Species abundance distributions and richness estimations in fungal metagenomics – lessons learned from community ecology. *Mol. Ecol.* 20, 275–285. doi: 10.1111/j.1365-294X.2010.04948.x

van der Heijden, M. G. A., and Horton, T. R. (2009). Socialism in soil? The importance of mycorrhizal fungal networks for facilitation in natural ecosystems. *J. Ecol.* 97, 1139–1150. doi: 10.1111/j.1365-2745.2009.01570.x

Villarreal-Ruiz, L., Anderson, I. C., Alexander, I. J. (2004). Interaction between an isolate from the hymenoscyphus ericae aggregate and roots of pinus and vaccinium. *New Phytol.* 164, 183–192. doi: 10.1111/j.1469-8137.2004.01167.x

Vrålstad, T., Fossheim, T. Schumacher, T. (2000). Piceirhiza bicolorata- the ectomycorrhizal expression of the hymenoscyphus ericae aggregate? *New Phytol.* 145, 549–563. doi: 10.1046/j.1469-8137.2000.00605.x

Walker, J. F. Jr., Miller, O. K., Lei, T., Semones, S., Nilsen, E., and Clinton, B. D. (1999). Suppression of ectomycorrhizae on canopy tree seedlings in *Rhododendron maximum* L. *(Ericaceae*) thickets in the southern Appalachians. *Mycorrhiza* 9, 49–56. doi: 10.1007/s005720050262

White, T., Bruns, T., Lee, S., Taylor, J., Innis, M., Gelfand, D., et al. (1990). Amplification and direct sequencing of fungal ribosomal RNA genes for phylogenetics. in: *PCR Protocols: a Guide to Methods and Applications* ed. MA. Innis, (Cambridge: Academic Press), 315–322 doi: 10.1016/b978-0-12-372180-8.50042-1

Woodall, C. W., Oswalt, C. M., Westfall, J. A., Perry, C. H., Nelson, M. D., and Finley, A. O. (2009). An indicator of tree migration in forests of the eastern United States. *For. Ecol. Manag.* 257, 1434–1444. doi: 10.1016/j.foreco.2008.12.013

Yamasaki, S. H., Fyles, J. W., Egger, K. N., and Titus, B. D. (1998). The effect of *Kalmia angustifolia* on the growth, nutrition, and ectomycorrhizal symbiont community of black spruce. *For. Ecol. Manag.* 105, 197–207. doi: 10.1016/S0378-1127(97)00285

Zackrisson, O., Nilsson, M. -C., Dahlberg, A., and Jäderlund, A. (1997). Interference mechanisms in conifer-Ericaceae-feathermoss communities. *Oikos* 78, 209–220. doi: 10.2307/3546287

Conflict of Interest Statement: The authors declare that the research was conducted in the absence of any commercial or financial relationships that could be construed as a potential conflict of interest.

frontiers in Microbiology

ORIGINAL RESEARCH
published: 10 October 2019
doi: 10.3389/fmicb.2019.02251

SlZRT2 Encodes a ZIP Family Zn Transporter With Dual Localization in the Ectomycorrhizal Fungus *Suillus luteus*

Laura Coninx[1], Nick Smisdom[2], Annegret Kohler[3], Natascha Arnauts[1], Marcel Ameloot[2], François Rineau[1], Jan V. Colpaert[1] and Joske Ruytinx[1]†*

[1] Centre for Environmental Sciences, Environmental Biology, Hasselt University, Diepenbeek, Belgium, [2] Biomedical Research Institute, Hasselt University, Diepenbeek, Belgium, [3] Laboratoire d'Excellence ARBRE, Institut National de la Recherche Agronomique, UMR 1136 INRA/Université de Lorraine Interactions Arbres/Microorganismes, Champenoux, France

OPEN ACCESS

Edited by:
Heike Bücking,
South Dakota State University,
United States

Reviewed by:
Françoise Gosti,
Centre National de la Recherche Scientifique (CNRS), France
Oswaldo Valdes-Lopez,
National Autonomous University of Mexico, Mexico

***Correspondence:**
Joske Ruytinx
joske.ruytinx@vub.be;
joske.ruytinx@uhasselt.be

†Present address:
Joske Ruytinx,
Department of Bioengineering Sciences, Research Group of Microbiology, Vrije Universiteit Brussel, Brussels, Belgium

Specialty section:
This article was submitted to Plant Microbe Interactions, a section of the journal Frontiers in Microbiology

Received: 01 April 2019
Accepted: 17 September 2019
Published: 10 October 2019

Citation:
Coninx L, Smisdom N, Kohler A, Arnauts N, Ameloot M, Rineau F, Colpaert JV and Ruytinx J (2019) SlZRT2 Encodes a ZIP Family Zn Transporter With Dual Localization in the Ectomycorrhizal Fungus Suillus luteus. Front. Microbiol. 10:2251. doi: 10.3389/fmicb.2019.02251

Ectomycorrhizal (ECM) fungi are important root symbionts of trees, as they can have significant effects on the nutrient status of plants. In polluted environments, particular ECM fungi can protect their host tree from Zn toxicity by restricting the transfer of Zn while securing supply of essential nutrients. However, mechanisms and regulation of cellular Zn homeostasis in ECM fungi are largely unknown, and it remains unclear how ECM fungi affect the Zn status of their host plants. This study focuses on the characterization of a ZIP (Zrt/IrtT-like protein) transporter, *SlZRT2*, in the ECM fungus *Suillus luteus*, a common root symbiont of young pine trees. *SlZRT2* is predicted to encode a plasma membrane-located Zn importer. Heterologous expression of *SlZRT2* in yeast mutants with impaired Zn uptake resulted in a minor impact on cellular Zn accumulation and growth. The *SlZRT2* gene product showed a dual localization and was detected at the plasma membrane and perinuclear region. *S. luteus* ZIP-family Zn uptake transporters did not show the potential to induce trehalase activity in yeast and to function as Zn sensors. In response to excess environmental Zn, gene expression analysis demonstrated a rapid but minor and transient decrease in *SlZRT2* transcript level. In ECM root tips, the gene is upregulated. Whether this regulation is due to limited Zn availability at the fungal–plant interface or to developmental processes is unclear. Altogether, our results suggest a function for *SlZRT2* in cellular Zn redistribution from the ER next to a putative role in Zn uptake in *S. luteus.*

Keywords: Mycorrhiza, *Suillus luteus*, zinc transporter, zinc homeostasis, ZIP

INTRODUCTION

Mycorrhizae are omnipresent mutualistic associations between fungi and plant roots. Mycorrhizal fungi provide their host plants with nutrients in exchange for sugar and/or lipids (Martin et al., 2016; Keymer et al., 2017). In addition to the supply of nutrients, host plants may benefit from an improved resistance for organic and inorganic pollutants (Adriaensen et al., 2004; Cabral et al., 2015; Ferrol et al., 2016). Therefore, the use of mycorrhizal plants is considered in phytoremediation applications (Coninx et al., 2017a) and in strategies to improve the nutritional

quality of crops (Sharma et al., 2017). As Zn deficiency and Zn toxicity are frequently observed in plants, mycorrhizal fungi with the ability to enhance or reduce Zn transfer to the plant can be crucial for the success of phytoremediation or biofortification applications (Adriaensen et al., 2004; Cavagnaro, 2008; Yang et al., 2015; Miransari, 2017). Zn deficiency is the most widespread and recurrent micronutrient deficiency in pasture and crop plants worldwide (Alloway, 2004), whereas the less prevalent Zn toxicity is generally reported for plants growing in the vicinity of mining or metallurgic plants (Ernst, 1990; Alloway, 2004; Nagajyoti et al., 2010).

Zn deficiency can have severe physiological consequences in plants and mycorrhizal fungi, as Zn is an essential micronutrient that ensures the structural stability and catalytic activity of many proteins. Organisms must maintain adequate intracellular concentrations of Zn (usually between 0.1 and 0.5 mM total cellular Zn), even when extracellular Zn levels are low (Eide, 2006). In order to meet this high demand for Zn, cells primarily rely on integral membrane transport proteins (Gaither and Eide, 2001). Yet, unbound cytoplasmic Zn levels are kept to a minimum in the cell, since free Zn ions can cause harmful effects. Proteins can be damaged or inactivated by the uncontrolled binding of Zn ions to functional groups in these proteins (Gaither and Eide, 2001). In order to avoid Zn toxicity, cells rely on a wide range of Zn homeostasis mechanisms that are strictly regulated. Upon entry into the cell via specialized transporter systems, Zn is either chelated intracellularly by various ligands (e.g., metallothioneins) or sequestered into subcellular compartments by transporter proteins (Becquer et al., 2019). Excess Zn can be removed from the cell via an enhanced efflux (Becquer et al., 2019). Given their crucial role in Zn efflux, uptake, and sequestration, transporter proteins are considered indispensable for the cellular Zn metabolism.

Fungal Zn transporters have mainly been identified in two protein families: the ZIP (Zrt/Irt-like protein) and CDF (Cation Diffusion Facilitator) transporter families (Eide, 2006). These two protein families also include iron (Fe) and manganese (Mn) transporters. Several CDF and ZIP proteins have been demonstrated to transport, to a lesser extent, other divalent metal ions, such as cadmium (Cd), cobalt (Co), and nickel (Ni) (Guerinot, 2000; Montanini et al., 2007). While ZIP transporters are known to transport extracellular or stored Zn into the cytoplasm (Kambe et al., 2006), CDFs decrease cytoplasmic Zn levels by transporting Zn into organelles or out of the cell (Montanini et al., 2007). Several CDFs have been described in ectomycorrhizal (ECM) fungi. In *Hebeloma cylindrosporum*, Zn storage in endoplasmic reticulum (ER)-derived vesicles is mediated by HcZnT1 (Blaudez and Chalot, 2011). Vacuolar Zn storage in *Suillus luteus* (Ruytinx et al., 2017) and in *Russula atropurpurea* (Sacky et al., 2016) is governed by the CDF transporters SlZnT1 and RaCDF1, respectively. Zn export in *R. atropurpurea* is accomplished by the RaCDF2 transporter (Sacky et al., 2016). Two ZIP transporters, RaZIP1 and SlZRT1, which are involved in high-affinity Zn uptake, were described in *R. atropurpurea* (Leonhardt et al., 2018) and *S. luteus* (Coninx et al., 2017b).

Recently, it has been reported that the ZIP transporter ScZRT1, which is one of the two principal plasma membrane-located Zn uptake systems of yeast, has a role in Zn sensing (Schothorst et al., 2017). ScZRT1 governs rapid activation of the PKA (protein kinase A) pathway upon Zn repletion of Zn-deprived yeast cells. This results in a quick exit from the stationary growth phase and a rapid surge in the activity of trehalase, which is a well-established PKA target (Thevelein and de Winde, 1999). ScZRT1 is likely crucial for a swift response to abrupt changes in environmental Zn availability, illustrating the significance of ZIP transporters not only in maintaining the cellular Zn homeostasis but also in regulating the adaptive growth response. In the present study, we aim at characterizing a putative plasma membrane-located ZIP transporter, SlZRT2, in the ECM fungus *S. luteus* and investigate whether *S. luteus* ZIP transporters have the potential to function as Zn sensors. *S. luteus* is an ECM model system and a cosmopolitan pioneer fungus that associates with the roots of young pine trees. The species supports pine seedling establishment (Hayward et al., 2015) and Zn-tolerant suilloid isolates have been demonstrated to protect their host plants from Zn toxicity in Zn-polluted soils (Adriaensen et al., 2004). These features make *S. luteus* an interesting candidate for use in phytostabilization applications (Coninx et al., 2017b). However, a comprehensive understanding of Zn metabolism in *S. luteus* and how the fungus affects the host's Zn status is crucial for the development of such a strategy. While the ability of ECM fungi to decrease or increase the transfer of Zn to the host plant is well-recognized (Colpaert et al., 2011; Langer et al., 2012; Becquer et al., 2019), little is known of the molecular mechanisms involved.

MATERIALS AND METHODS

S. luteus Strains and Culture Conditions

The dikaryotic *S. luteus isolate* UH-Slu-P4 (Colpaert et al., 2004) was used in this study. The fungal isolate was maintained in culture on modified solid Fries medium (Colpaert et al., 2004). Liquid cultures of UH-Slu-P4 were initiated for use in the gene expression assay as described by Nguyen et al. (2017). Cultures were treated to induce Zn deficiency, Zn sufficiency, and mild Zn toxicity (0, 20, 500, or 1000 mM $ZnSO_4.7H_2O$) according to Coninx et al. (2017b). Zn-exposed mycelia (400 mg) were sampled at 1, 2, 4, 8, and 24 h after initiation of Zn treatment, flash frozen with liquid N_2, and stored at −70°C.

SlZnT2 Sequence Analysis

The ZIP transporter *SlZRT2* was previously identified in the genome of *S. luteus* UH-Slu-Lm8-n1 v2.0 (Coninx et al., 2017b). The corresponding amino acid sequence was further investigated *in silico*. Transmembrane domains (TMDs) were predicted by the topology prediction program TMHMM2.0 (Krogh et al., 2001). Amino acid sequence similarities were calculated with Sequence Manipulation Suite version 2 (Stothard, 2000). A subcellular localization prediction was performed with "ProtComp v.9.0. Identifying sub-cellular location (Animals and Fungi)" from

Softberry[1]. SlZRT2 and ScZRT2 (Eide, 1996) were aligned with Multiple Alignment using Fast Fourier Transform version 7 (MAFFT) (Katoh and Standley, 2013).

SlZRT2 Cloning and Heterologous Expression in Yeast

A cDNA library of the sequenced isolate UH-Slu-Lm8-n1 (Kohler et al., 2015) was constructed according to Coninx et al. (2017b). A gene-specific primer pair was developed to amplify the full-length coding sequence of *SlZRT2* (forward primer: 5′ TCAGCACTTCACCACAGGCTTACTATC 3′; reverse primer: 5′ CATCCCCACGAGCGCCAT 3′). A 30-μl PCR reaction was performed according to Coninx et al. (2017b). Reaction specificity and amplicon length were verified by visualization of 5-μl PCR product on a 1.5% agarose gel with GelRed® Nucleic Acid Gel Stain (Biotium, Fremont, CA, United States). The remaining PCR product (25 μl) was processed with the GeneJet PCR purification kit (Thermo Scientific, Waltham, MA, United States). Subsequently, the purified amplicon was cloned into the gateway entry vector pCR8/GW/TOPO (Invitrogen, Carlsbad, CA, United States) and transferred to the destination vectors pAG426GAL-ccdB-EGFP (Alberti et al., 2007) and pYES-DEST52 (Invitrogen, Carlsbad, CA, United States) with the Gateway LR-clonase II Enzyme Mix (Invitrogen, Carlsbad, CA, United States) according to the manufacturer's instructions.

Yeast Mutant Phenotype Complementation

The following yeast strains were used for the heterologous expression of *SlZRT2*: CM30 (MATa, ade6, can1-100, his3-11, 15leu2-3, trp1-1, ura3-52), CM34 or Δzrt1Δzrt2 (CM30, zrt1:LEU2, zrt2:HIS3) (MacDiarmid et al., 2000), BY4741 (MAT a; his3Δ1; leu2Δ; met15Δ0; ura3Δ0), Δsmf1 (BY4741; MATa; ura3Δ0; leu2Δ0; his3Δ1; met15Δ0; YOL122c:kanMX4), and Δftr1 (BY4741; MATa; ura3Δ0; leu2Δ0; his3Δ1; met15Δ0; YER145c:kanMX4) (EUROSCARF, Frankfurt, Germany). High-efficiency yeast transformation was performed with the LiAc/PEG method as described by Gietz and Woods (2002). Selection of the transformed yeast cells and phenotypic screening (drop assays) of the yeasts were performed as described by Coninx et al. (2017b). To induce protein production using the GAL1 promoter, induction SD-URA medium (synthetic defined medium with 20 g l^{-1} galactose instead of glucose and without uracil) was used. Yeast assays with Δzrt1Δzrt2 strains were performed in petri dishes with solid SD-URA induction medium supplemented with 1 mM $ZnSO_4.7H_2O$ (control) or 0.5 and 2 mM trisodium citrate to restrict Zn availability in the growth medium. SD-URA induction medium supplemented with 100 μM $MnSO_4.H_2O$ (control) or 8 and 15 mM egtazic acid (EGTA) was used in the complementation assays with Δsmf1 strains. Assays with Δftr1 strains were performed on SD-URA induction medium supplemented with 100 μM $FeCl.6H_2O$ (control) or 10 and 25 μM ethylenediaminetetraacetic acid (EDTA). EGTA and EDTA were supplemented to the SD-URA induction medium to limit the availability of Mn and Fe, respectively. All assays were performed in triplicate using independent yeast clones.

Subcellular Localization of the SlZRT2:EGFP Fusion Protein

Yeast Δzrt1Δzrt2 cells expressing SlZRT2:EGFP (enhanced green fluorescence protein) translational fusion proteins were grown to mid-log phase OD_{600} = 1 on SD-URA induction medium with 100 μM $ZnSO_4.7H_2O$. Staining of the plasma membrane and vacuolar membrane was performed with FM4-64 (Molecular Probes, Invitrogen, Carlsbad, CA, United States) at 0 and 30°C, respectively, as described by Vida and Emr (1995). When applied at 30°C, this lipophilic dye ends up in the vacuolar membrane of living yeast cells through an endocytic pathway. Application of the same dye in yeast cultures kept on ice (0°C) results in plasma membrane staining due to the inhibition of endocytosis by low temperatures (Vida and Emr, 1995). Nuclei were visualized with the cell-permeant nuclear counterstain Hoechst 33342 (Invitrogen, Carlsbad, CA, United States). Hoechst 33342 was added at a final concentration of 10 μg ml^{-1} to an aliquot of yeast culture in liquid SD-URA induction medium with 100 μM $ZnSO_4.7H_2O$. Yeast cells were incubated in the dark at 30°C for 40 min.

Imaging of the FM4-64 vacuolar and plasma membrane staining in EGFP-expressing yeast cells was performed with a Zeiss LSM 880 laser scanning confocal microscope (Carl Zeiss, Jena, Germany) mounted on an inverted microscope Axio observer (Carl Zeiss, Jena, Germany) using a Zeiss 63 × NA1.2 water immersion C-Apochromat objective. EGFP and FM4-64 were simultaneously excited using, respectively, the 488-nm laser line of an argon-ion laser and the 633-nm laser line of a helium–neon laser. An MBS 488/543/633 beam splitter was used to separate fluorescence emission light from this excitation light. The resulting emission light of EGFP and FM4-64 was detected using, respectively, the wavelength range of 490 to 570 nm of the spectral GaAsP detector and the wavelength range of 637 to 758 nm detected by a PMT. An image resolution of 512 by 512 pixels was used, with a pixel dwell time of 8.19 μs and a pixel size of 70 nm.

Hoechst 33342-stained EGFP-expressing yeast cells were analyzed with an Elyra PS.1 (Carl Zeiss, Jena, Germany), using a Zeiss 100 × NA1.46 oil immersion alpha Plan-Apochromat objective. A sequential recoding of two channels was performed. Hoechst 33342 was excited using a 405-nm laser line and emission was collected through a BP 420–490 nm band-pass filter. EGFP was excited using a 488-nm laser line and emission was collected through a BP 495–575 nm band-pass filter. The image was recorded using an EM-CCD camera (Andor) with a resolution of 512 by 512 pixels, a pixel size of 100 nm, and an exposure time of 300 ms. Image processing was carried out with ZEN 2.3 (blue edition) Service Pack 1 Software (Carl Zeiss, Jena).

Zn Content Analysis of Transformed Yeasts

Transformed yeast cells were grown in liquid induction medium with 100 μM $ZnSO_4.7H_2O$ at 30°C to mid log phase

[1]www.softberry.com

(OD_{600} ± 1.5). After dilution to OD_{600} = 1, 1 ml of yeast suspension was added to 20 ml of liquid induction medium with 100 μM $ZnSO_4.7H_2O$. Five independent yeast clones of each transformed yeast strain were tested. Cultures were grown for 24 h at 30°C. Yeast cells were collected by centrifugation and washed three times with 20 mM $PbNO_3$ and milli-Q water. Collected cells were resuspended, lyophilized, and acid digested according to Coninx et al. (2017b). Zn content was analyzed with inductively coupled plasma optical emission spectrometry (ICP-OES).

Trehalase Activity in Transformed Yeasts

Transformed yeast cells were grown in liquid induction medium supplemented with 500 μM trisodium citrate at 30°C until culture saturation. Saturated yeast suspension (0.5 ml) was re-inoculated in fresh induction medium with 500 μM trisodium citrate. Zn-deprived cells were grown for 2 h in Zn limitation medium containing 10 mM trisodium citrate and 1 mM EDTA and treated with 5 mM $ZnCl_2$. Culture aliquots containing 75 mg (wet weight) cells were taken at −5, 0, 1, and 4 min after treatment with Zn. Yeast cells were resuspended in 45 ml of ice-cold water and harvested by centrifugation. Crude protein extracts were prepared according to Pernambuco et al. (1996).

Crude extracts were dialyzed as described by Van Houtte and Van Dijck (2013) with the Pierce™ 96-well Microdialysis Plate (10K MWCO) (Thermo Fisher, Waltham, MA, United States). Trehalase activity assay and data analysis were performed according to Van Houtte and Van Dijck (2013).

Gene Expression Analysis in *S. luteus*

The effect of the extracellular Zn concentration on the expression of *SlZRT2* was analyzed in the isolate UH-Slu-P4 via reverse transcription quantitative polymerase chain reaction (RT-qPCR). The experimental setup and data analysis were performed as described by Coninx et al. (2017b). For the amplification of *SlZRT2*, a gene-specific primer pair was designed using Primer3web version 4.1.0 (Rozen and Skaletsky, 2000) (forward primer: 5′ TTCTACGCTCTCACTCGAAG 3′; reverse primer: 5′ CGGTGAACTGTATGACTGGA 3′, primer efficiency = 96.9%). Expression data were normalized with the reference genes TUB1, ACT1, AM085296, AM085296, and GR97562 (Ruytinx et al., 2016). Reference gene expression stability was confirmed within the current experimental setup using GeNorm (Vandesompele et al., 2002). The geometric mean of the relative expression levels of the reference genes was calculated and applied as a normalization factor. Gene expression data were expressed relative to the sample with the highest expression level via the formula $2^{-\Delta Ct}$.

Mean values of the biological replicates ($n = 4$) were calculated, rescaled to the 20 μM Zn (control) condition within each time point, and log2 transformed. To assess differences in *SlZRT2* expression levels, a two-way analysis of variance (ANOVA) followed by a Tukey's HSD test was performed in "R" version 3.2.2 (R Core Team, 2012).

The transcript profiles of *SlZRT1* and *SlZRT2* were analyzed in free living mycelium (FML) UH-Slu-Lm8-n1 (Kohler et al., 2015) and in symbiotic *S. luteus–Pinus sylvestris* ECM root tips. Expression data were obtained from the GSE63947 expression data set, which is published (Kohler et al., 2015) and can be accessed via the Gene Expression Omnibus at the NCBI website (National Center for Biotechnology Information[2]). Significant differences in *SlZRT1* and *SlZRT2* expression were assessed with the Welch Two Sample *t* test using "R" version 3.2.2 (R Core Team, 2012).

Zn Accumulation in *S. luteus*

The Zn content of the *S. luteus* isolate UH-Slu-P4 was analyzed at multiple time points following Zn exposure. The experimental setup was identical to the one used in the RT-qPCR assay. At each exposure time point, four aliquots of mycelium (± 50 mg wet weight) were collected in 2-ml Eppendorf tubes and washed three times with 20 mM $PbNO_3$ and milli-Q water. Mycelial samples were lyophilized and acid digested, and Zn content was determined by ICP-OES.

RESULTS

SlZRT2 Sequence Analysis

SlZRT1 and SlZRT2, two homologs of the yeast ZIP transporters ScZRT1 and ScZRT2, were recently identified in the genome of *S. luteus*. SlZRT1 functions as a high-affinity plasma membrane-located Zn transporter (Coninx et al., 2017b).

SlZRT2 is predicted to have a 1678-bp open reading frame consisting of eight exons. These eight exons encode a 425-amino-acid polypeptide (jgi prot ID 720881), which demonstrates several typical ZIP transporter features (**Figure 1**). SlZRT2 is predicted to localize to the plasma membrane and to have eight TMDs and a long variable cytoplasmic loop between TMD3 and TMD4. The variable cytoplasmic loop contains several histidine-rich motifs (HHXH, CXHXXHH, HXHXHX) that could function as binding site(s) for Zn and/or other metals, so-called metal binding domains (MBDs). ZIP signature sequence (Eng et al., 1998) and typically conserved histidines were identified (**Figure 1**). First two histidine-rich motifs are separated by only five amino acids and might be considered as one. As the previously characterized SlZRT1, SlZRT2 shows a high degree of sequence similarity with the yeast ZIP transporters ScZRT1 and ScZRT2. Though considerable sequence variation is observed within the cytoplasmic loop between TMD3 and TMD4. In SlZRT2, the first histidine-rich motif is preceded by a long amino acid stretch and is somehow shifted toward the second histidine-rich motif when compared with ScZRT2.

Heterologous Expression of SlZRT2 in Yeast

Heterologous expression with the empty vector (EV) did not result in complementation of any metal uptake-deficient

[2]http://www.ncbi.nlm.nih.gov/geo/

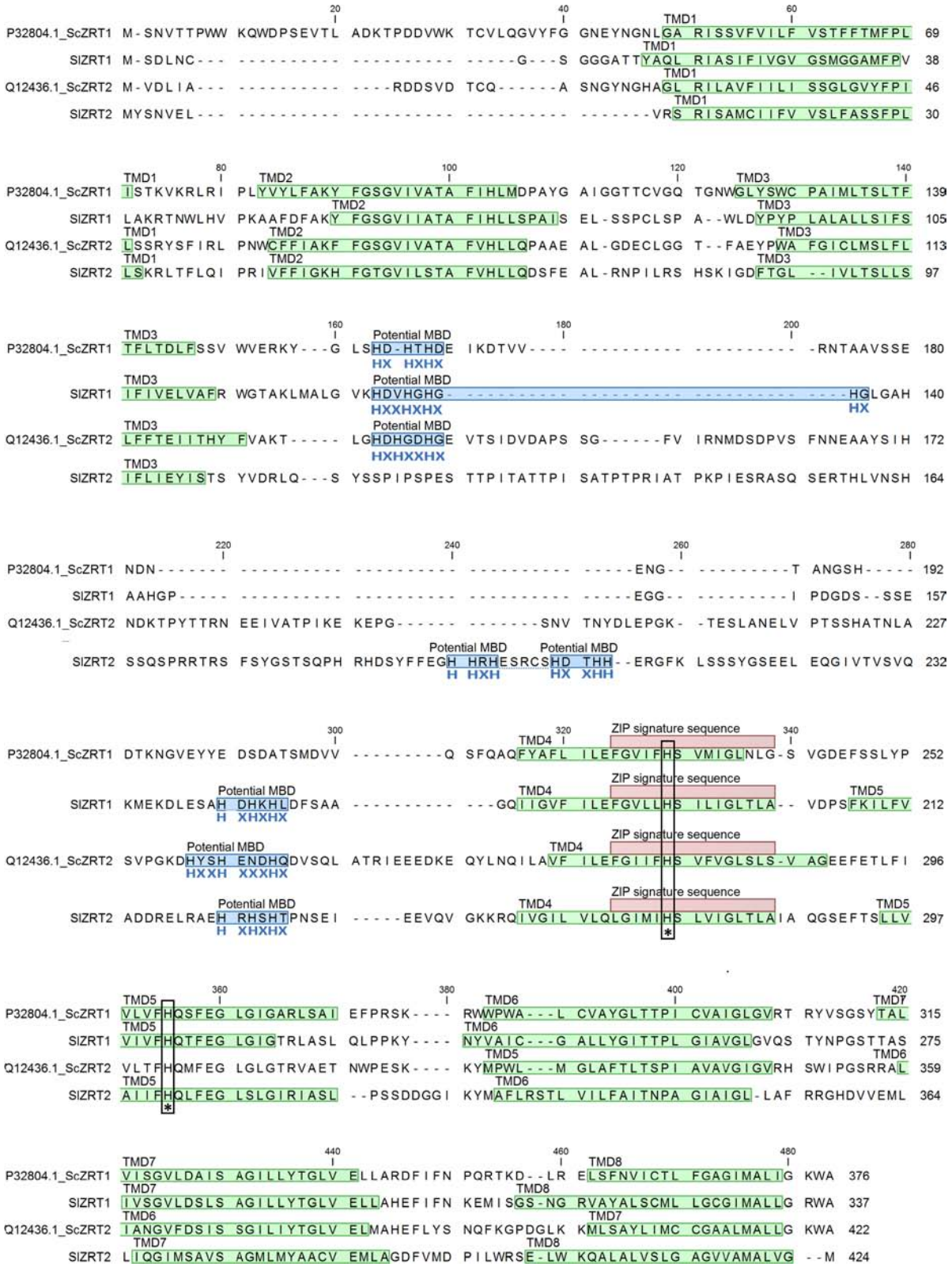

FIGURE 1 | SlZRT1, SlZRT2, ScZRT1, and ScZRT2 protein sequence. Transmembrane domains (TMDs) as predicted by TMHMM2.0, are indicated in green, putative histidine-rich metal binding domains (MBDs) in blue, and the ZIP signature sequence (Eng et al., 1998) in red. Two among ZIP proteins conserved histidines (located in TMD4 and TMD5) are indicated with an asterisk.

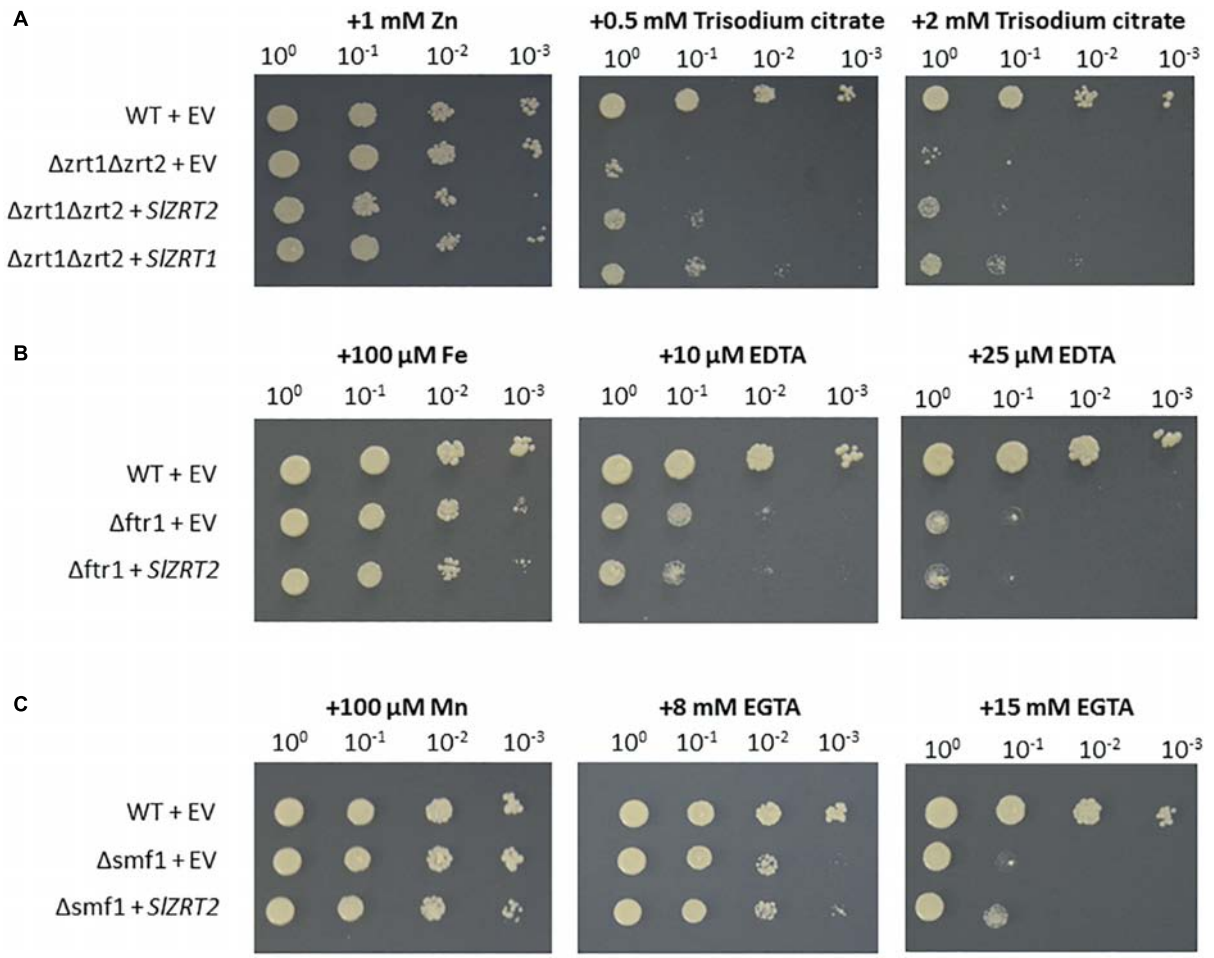

FIGURE 2 | Functional complementation assays of Zn, Fe, and Mn uptake-deficient yeast strains Δzrt1Δzrt2 **(A)**, Δftr1 **(B)**, and Δsmf1 **(C)**. Cultures of wild-type (WT) and mutant yeast cells (OD_{600} = 1) were 10-fold serial diluted (10^0, 10^{-1}, 10^{-2}, and 10^{-3}) and spotted on control (first column) or selection SD medium (second and third column). Control medium was supplemented with Zn, Fe, or Mn and selection medium with different concentrations of citrate, EDTA, or EGTA. WT cells were transformed with the empty vector (EV, pYES-DEST52; Invitrogen). Yeast mutants were transformed with the EV or the vector containing *SlZRT2* or previously characterized *SlZRT1*. Pictures were taken after 3 days of growth and experiments were carried out for three independent clones.

phenotype (**Figures 2A–C** and **Supplementary Figures S1A,B**), whereas growth of the Zn uptake-deficient yeast mutant Δzrt1Δzrt2 was partially restored by heterologous expression of *SlZRT2* (**Figure 2A** and **Supplementary Figures S1A,B**). When compared to *SlZRT1*, *SlZRT2* is less able to complement the Zn-deficient phenotype of Δzrt1Δzrt2. *SlZRT2* is not able to complement the Fe uptake-deficient phenotype of Δftr1 (**Figure 2B**). However, growth of the Mn uptake-deficient yeast mutant Δsmf1 is marginally restored (**Figure 2C**).

Yeast cells expressing the SlZRT2:EGFP fusion protein (**Figures 3A,B** and **Supplementary Figure S2A**) displayed GFP fluorescence at two distinct subcellular locations. An outer green fluorescent ring co-localizes with FM4-64 plasma membrane staining at 30°C (**Figure 3A**) and GFP fluorescence in the perinuclear region surrounding the Hoechst33342 nucleic acid stain (**Figure 3B**). No co-localization of EGFP fluorescence with FM4-64 vacuolar staining (0°C) was observed (**Supplementary Figure S2A**). EGFP fluorescence of EV transformed yeast cells was solely detected in the cytoplasm (**Supplementary Figures S2B,C**).

Zn Content Analysis of SlZRT2 Transformed Yeast Cells

Yeast cultures were grown in standard growth medium supplemented with 100 µM Zn to ensure adequate growth of all yeast mutants. Wild-type (WT) cells transformed with an empty vector (EV) contain significantly more Zn than Δzrt1Δzrt2 mutant cells transformed with the same EV (**Figure 4**). Δzrt1Δzrt2 mutants transformed with *SlZRT2* have a significantly higher Zn content than the Δzrt1Δzrt2 transformations with the EV. Yet, the Zn content of SlZRT2 transformed mutant cells is still significantly lower than the WT transformations. Similar differences in Zn content were observed in yeast strains transformed with the SlZRT2:EGFP fusion

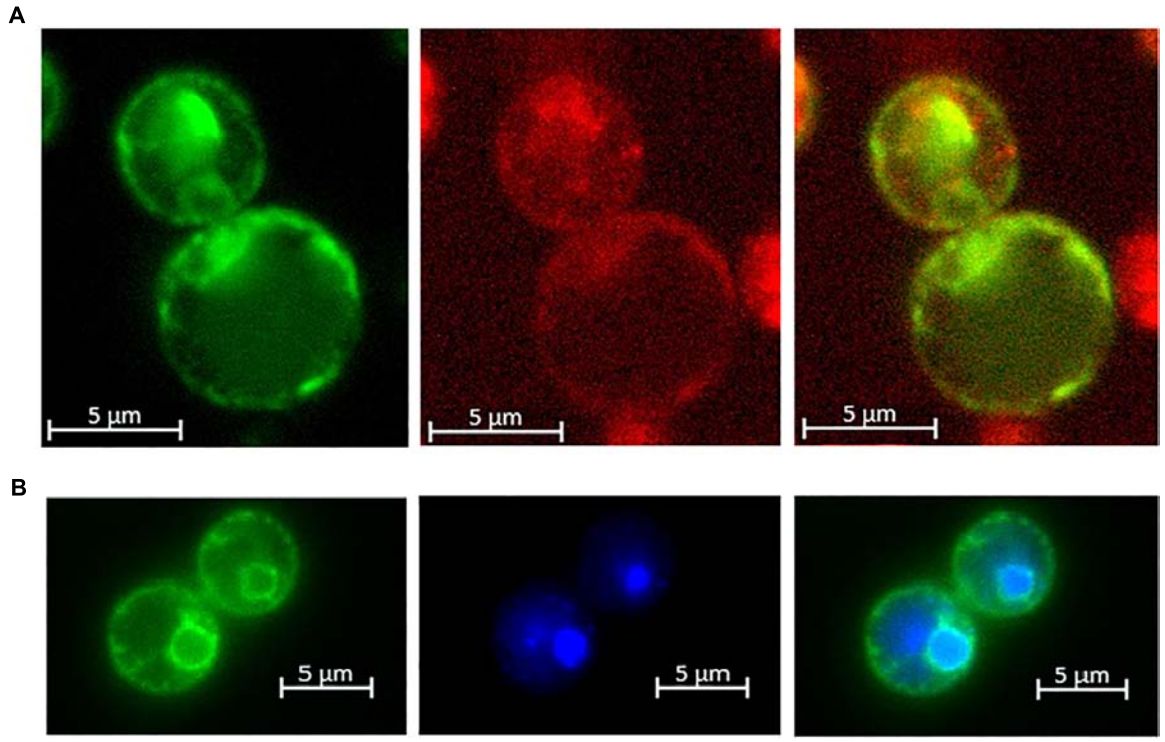

FIGURE 3 | Localization of the SlZRT2:EGFP fusion protein in yeast. **(A)** FM4-64 plasma membrane staining on ice to avoid endocytosis of the dye and **(B)** Hoechst 33324 nuclear staining. From left to right, pictures visualize the EGFP (green) fusion protein (left), FM4-64 (red) or Hoechst (blue) staining (middle), and the merged image (right).

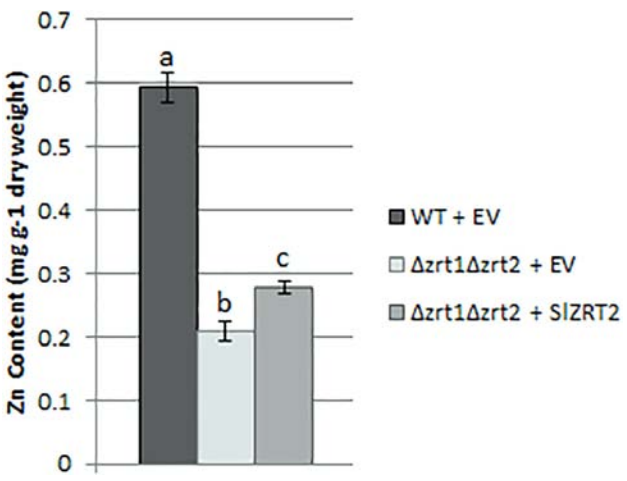

FIGURE 4 | Zn content of WT and Δzrt1Δzrt2 transformed yeast cells transformed with the EV (pYES-DEST52; Invitrogen) or the vector containing *SlZRT2*. Data are the average ± standard error (SE) of five replicates; significant differences ($p < 0.05$) are indicated by different letters.

protein (**Supplementary Figure S3**). No differences in Mn or Fe content were observed in yeast strains with either *SlZRT2* or *SlZRT2:EGFP* heterologous expression (**Supplementary Figures S4A,B**).

Trehalase Activity in Zn-Depleted Yeast Cells Re-supplemented With Zn

Trehalase activity was assessed in Zn-depleted WT and Δzrt1Δzrt2 cells upon Zn repletion. WT cells were transformed with the EV (**Figure 5A**) and Δzrt1Δzrt2 yeast cells with the EV (**Figure 5B** and **Supplementary Figures S5A,B**), *SlZRT1* (**Figure 5C** and **Supplementary Figures S5A,B**), or *SlZRT2* (**Figure 5D** and **Supplementary Figures S5A,B**).

Rapid Zn-induced signaling to the PKA pathway via an increase in trehalase activity was only observed in WT yeast cells. Re-addition of Zn to the Zn-deprived WT cells resulted in a significant 1.5-fold increase in trehalase activity after 1 min ($p = 0.0414$, unpaired t test) (**Figure 5A**). No changes in trehalase activity were observed for Δzrt1Δzrt2 cells transformed with the EV, SlZRT1, or SlZRT2.

Effect of Extracellular Zn on SlZRT2 Expression in *S. luteus*

SlZRT2 gene expression was analyzed after short exposure times (1, 2, 4, 8, and 24 h) to different Zn concentrations [0, 20 (control), 500, and 1000 µM]. **Figure 6A** illustrates that *SlZRT2* mRNA levels are rapidly affected by changes in external Zn concentration. A significant downregulation is observed after 2-h exposure to mildly toxic Zn concentrations (500 and 1000 µM). Despite the difference in Zn concentration, exposure to 500 and 1000 µm Zn resulted in a similar *SlZRT2* expression pattern.

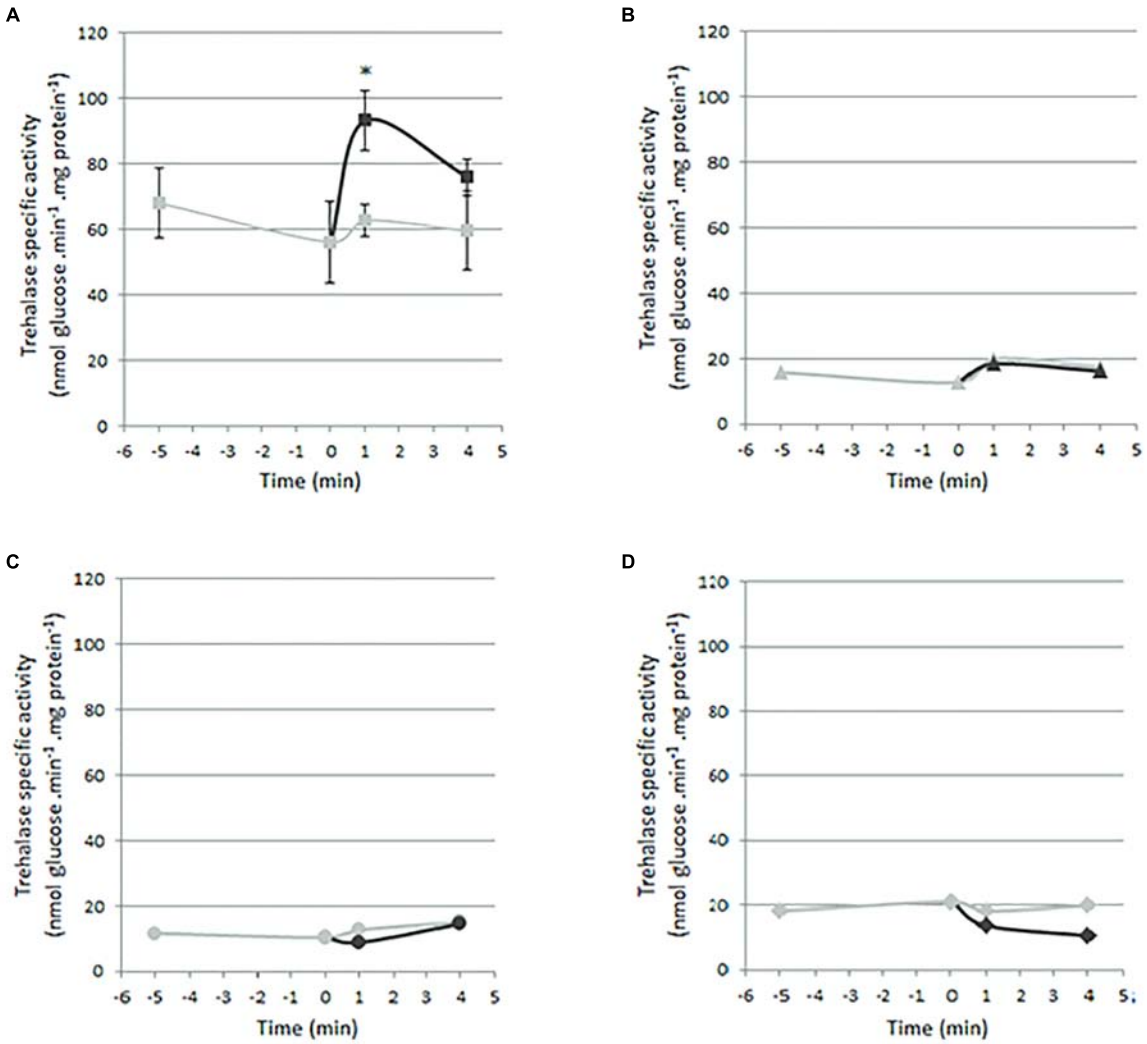

FIGURE 5 | Trehalase activity in Zn-depleted yeast cells after the re-supplementation of Zn. Trehalase activity was assessed in yeast cells maintained on Zn starvation medium (in gray; negative control) and after the addition of 5 mM $ZnCl_2$ (in black). **(A)** WT cells transformed with the EV (pYES-DEST52; Invitrogen). Data are the mean ± SE of three biological replicates. Cells were cultured for 2 days in SD medium supplemented with 10 mM citrate and 1 mM EDTA to trigger Zn starvation. **(B,C)** Trehalase activity of Δzrt1Δzrt2 yeast mutant cells. The trehalase assay with Δzrt1Δzrt2 cells was performed three times, each time under a different Zn starvation regime. Representative results from one starvation regime are shown. Cells were cultured for 2 h in SD medium supplemented with 10 mM citrate and 1 mM EDTA to trigger Zn starvation. Δzrt1Δzrt2 cells were transformed with the EV (**B**; pYES-DEST52; Invitrogen), SlZRT1 **(C)**, or SlZRT2 **(D)**. (Results from the two other Zn starvation regimes are shown in **Supplementary Figure S5**.)

Moreover, when external Zn is absent, the *SlZRT2* expression level is also observed to fluctuate in the initial time points (1, 2, and 4 h). At the later time points (8 and 24 h), *SlZRT2* mRNA levels of all the Zn treatments converge and no differences in gene expression are observed.

Zn Accumulation in *S. luteus* Exposed to Different Concentrations of Zn

Internal mycelial Zn concentrations were measured 1, 2, 4, 8, and 24 h following Zn treatment [0, 20 (control), 500, and 1000 μM] to observe the Zn accumulation pattern in *S. luteus*. While no difference in the Zn accumulation pattern of the 20 μM (control) and 0 μM Zn treatment was observed, treatment with 500 and 1000 μM Zn resulted in a significantly higher Zn uptake (**Figure 6B**). Although more Zn is accumulated in the 1000 μM treatment, compared to the 500 μM treatment, both Zn exposures have a similar accumulation pattern, with a drop in Zn content at 4 h. This drop occurs shortly after the downregulation in *SlZRT2* expression.

SlZRT1 and SlZRT2 Transcript Levels in Free-Living *S. luteus* Mycelium and Mycorrhizal Root Tips

To assess whether *SlZRT1* and *SlZRT2* are differentially expressed in *S. luteus* FLM and ECM root tips, RNA-Seq data of these morphological structures were analyzed. Indeed, transcript levels

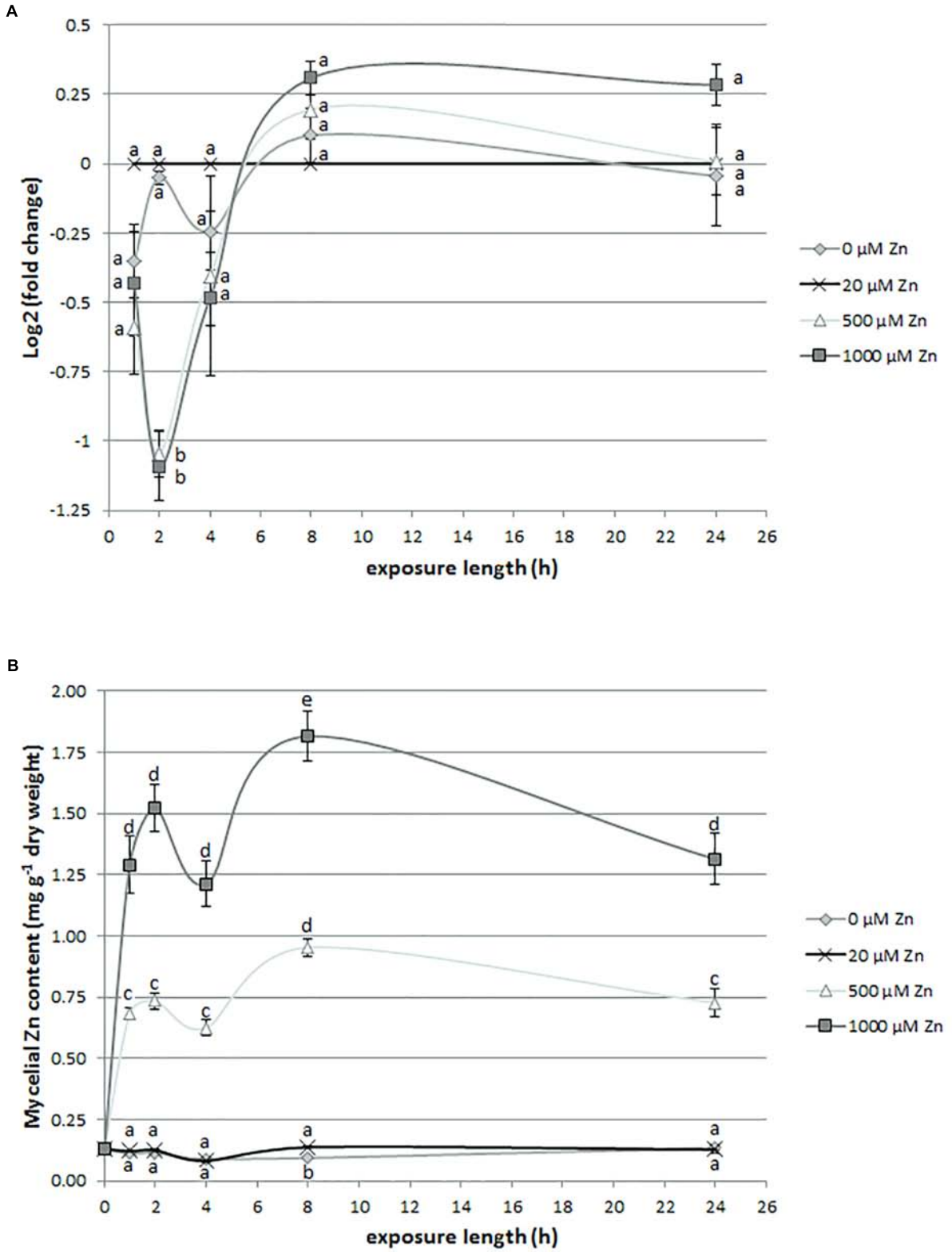

FIGURE 6 | *SlZRT2* expression **(A)** and Zn content **(B)** in *S. luteus* mycelium after 0-, 1-, 2-, 4-, 8-, and 24-h exposure to different concentrations of Zn. Significant differences within each time point are indicated by different letters ($p < 0.05$). **(A)** *SlZRT2* expression data are the average ± SE of three biological replicates and expressed relative in log2(fold change) to the control condition (20 µM Zn) within each time point. **(B)** Mycelial Zn content data are the average ± standard error (SE) of four biological replicates.

TABLE 1 | *SlZRT1* and *SlZRT2* transcript levels in *S. luteus–P. sylvestris* mycorrhizal root tips (ECM) and *S. luteus* free-living mycelium (FLM).

	ECM (rpkm)	FLM (rpkm)	Ratio ECM/FLM
SlZRT1	403.7 ± 10.4	57.0 ± 1.4	7.1
SlZRT2	31.4 ± 0.2	13.5 ± 0.8	2.3

RNA-Seq data are the average ± standard error (SE) of two biological replicates and expressed in reads per kilobase million (rpkm).

of both ZIP genes are significantly higher in the ECM root tips of the *S. luteus–P. sylvestris* association, when compared to the *in vitro* FLM (**Table 1**; p values <0.05). A sevenfold increase in the expression of *SlZRT1* was observed in ECM root tips. This change in gene activity was less pronounced for *SlZRT2*, for which the transcript levels were 2.3 times higher in the ECM root tips.

DISCUSSION

Zn is estimated to interact with ∼9% of the eukaryotic proteome to support their structure or catalytic function (Andreini et al., 2006). A tightly controlled cytoplasmic Zn concentration is essential to supply these proteins and overcome malfunction through deficiency or excess. Main gateways for Zn to the cytoplasm are ZIP transporters (Guerinot, 2000). Here, we report on the characterization of a second ZIP transporter, SlZRT2, in the ECM fungus *S. luteus*. SlZRT2 has a high sequence similarity with the previously characterized plasma membrane localized Zn importer, SlZRT1, of the same species (Coninx et al., 2017b) and both high- and low-affinity Zn importers ScZRT1 and ScZRT2 of budding yeast. Nevertheless, considerable sequence variation was observed between TMD3 and TMD4, including two histidine-rich domains. First, the SlZRT2 histidine-rich domain differs in size and position when compared to its homologs. Histidine-rich domains are potential metal binding domains and are assumed to determine substrate specificity and affinity of transporters (Guerinot, 2000). Site-directed mutations of the histidines in the histidine-rich domains of several yeast and human ZIP transporters resulted in a reduced or disrupted Zn uptake capacity (Gitan et al., 2003; Milon et al., 2006; Mao et al., 2007). The variations between the histidine-rich domains of SlZRT2 and ScZRT2 could therefore reflect an altered affinity for Zn or a modified metal specificity.

Heterologous expression of *SlZRT2* in yeast identified Zn as primary substrate and indicated a minor role for SlZRT2 in Zn uptake. SlZRT2 restored the Zn uptake-deficient phenotype of the Δzrt1Δzrt2 yeast mutant only partly and performed significantly less than the previously characterized SlZRT1 considering Zn uptake. Cellular Zn concentrations in SlZRT2 overexpressing Δzrt1Δzrt2 yeast clones were only slightly higher than those in EV transformed Δzrt1Δzrt2 clones (**Figure 4**). Under the same conditions, SlZRT1 was shown to restore cellular Zn concentrations to the WT level (Coninx et al., 2017b). As mentioned previously, in budding yeast, Zn uptake is governed by two ZIP family transporters, ScZRT1 and ScZRT2. ScZRT1 functions as a high-affinity uptake system in severe Zn limiting conditions (Zhao and Eide, 1996a). Under mild Zn deficiency, ScZRT2 mediates Zn uptake (Zhao and Eide, 1996b). This low-affinity transporter is repressed in low zinc and induced upon re-supplementation (Bird et al., 2004). A similar regulation of Zn uptake might operate in *S. luteus*, using SlZRT1 and SlZRT2 as high- and low-affinity Zn importers, respectively. Next to Zn import, SlZRT2 might contribute at Mn uptake as shown by a reduced sensitivity toward Mn deficiency of SlZRT2 overexpressing Δsmf1 yeast mutants (**Figure 2A** and **Supplementary Figures S1A,B**). Different secondary substrates, including Mn, Fe, Cu, and Cd, were suggested for many ZIP proteins (Guerinot, 2000).

The SlZRT2:EGFP fusion protein was observed at two subcellular locations in yeast: the perinuclear region and the plasma membrane (**Figures 3A,B** and **Supplementary Figure S2A**). The EGFP signal observed at the perinuclear region likely corresponds to the ER membrane and also the putative plasma membrane localized signal might be mainly due to ER localization. In yeast, the ER is composed of perinuclear ER, which surrounds the nucleus, and of peripheral ER, which is juxtaposed to the plasma membrane (Preuss et al., 1991; Prinz et al., 2000). An ER localization of fungal ZIP family Zn importers was observed previously as an artifact of GFP labeling for ScZRT1 of *Saccharomyces cerevisiae* in particular conditions (Schothorst et al., 2017) or of overexpression for RaZIP1 of *R. atropurpurea* (Leonhardt et al., 2018). We do not expect ER localization of SlZRT2:EGFP to be due to artifacts. In contrast to ScZRT1 and RaZIP1, which are both able to restore the Zn-deficient phenotype of Δzrt1Δzrt2 yeast mutants to a large extent (Zhao and Eide, 1996a; Leonhardt et al., 2018), SlZRT2 makes only a minor contribution to Zn uptake when overexpressed in the Δzrt1Δzrt2 mutant (**Figures 2**, **4**). These results for SlZRT2 were independent of the presence/absence of the EGFP tag (**Supplementary Figures S1A**, **S3**). A primary function of SlZRT2 in Zn redistribution from the ER and secondary function as low-affinity Zn uptake mechanism is likely.

Next to their transport function, some plasma membrane-localized transporters function as nutrient sensors (Steyfkens et al., 2018). ScZRT1 of budding yeast is such a protein with dual Zn transport and receptor function. This high-affinity Zn importer activates the PKA pathway and induces downstream trehalase activity upon Zn repletion after a prolonged period of starvation (Schothorst et al., 2017). As the previously characterized SlZRT1, SlZRT2 was not able to induce trehalase activity in yeast (**Figures 5B–D** and **Supplementary Figures S5A,B**) and thus translate environmental Zn availability to an adaptive growth response. A currently unknown mechanism, independent from Zn membrane importers, might connect Zn availability to an adaptive growth response in *S. luteus*.

Zn uptake in yeast and many other organisms is controlled at the transcriptional level by Zn availability (Jung, 2015; Wilson and Bird, 2016). In *S. luteus*, transcripts of the high-affinity Zn uptake transporter SlZRT1 swiftly accumulate upon Zn starvation, normalize after a few hours, and are more abundant again after 24 h. In conditions of Zn excess, transcription is significantly downregulated within 2 h and remains low over time (Coninx et al., 2017b). Cellular Zn accumulation pattern in *S. luteus* (**Figure 6B**) follows the *SlZRT1* transcription level.

Zn was also observed to regulate *SlZRT2* transcript levels (**Figure 6A**). However, the impact of external Zn concentration on transcription level was low and only significant at the early time points upon growth in excess Zn. These gene expression results in *S. luteus* suggest a major function for SlZRT2 in cellular Zn redistribution rather than Zn uptake from the environment, as was also indicated by the heterologous expression experiments in yeast.

In ECM root tips, *SlZRT2* transcript levels are 2.4-fold higher when compared to those in free-living mycelium. This might indicate a need for redistribution of ER-stored Zn pool and a low cytosolic Zn state. Indeed, also high-affinity Zn importer SlZRT1 is highly regulated in ECM root tips with a sevenfold increase in transcript levels. It is unclear (1) whether this high demand for Zn is induced by a low availability of Zn at the plant–fungal interface and (2) if both symbiotic partners are competing for this important micronutrient. Similar increases in transcript level (8×) were noted for the putative ZIP-family Zn importer of the arbuscular mycorrhizal fungus *Rhizophagus irregularis* when comparing intraradical (i.e., symbiotic) and extraradical mycelium (Tamayo et al., 2014). However, increases in transcript level of nutrient uptake transporters in ECM root tips are not restricted to Zn-transporting ZIP-family proteins but were previously observed for the nitrate/nitrite transporter TbNrt2 of *Tuber borchii* (Montanini et al., 2006) and the phosphate transporter HcPT2 of *H. cylindrosporum* (Becquer et al., 2019). Interestingly, the phosphate uptake transporter HcPT2 of *H. cylindrosporum* is indispensable for phosphate release toward the host plant (Becquer et al., 2019). This induces the question whether gene expression of nutrient uptake transporters at the symbiotic interface is regulated by substrate availability or other developmentally related cues and whether they might alter function due to unknown (post-translational) regulatory mechanisms. Rapid mobilization of ER-stored Zn was observed in the fungus *Candida albicans* in response to glucose availability (Kjellerup et al., 2018). A response of ER-localized SlZRT2 to glucose or other plant-derived cues and subsequent Zn release might be part of developmental signaling pathways in *S. luteus*. Zn released from the ER is known to function as a secondary messenger, transducing external signals to result in an adaptive response in animal cells (Yamasaki et al., 2007).

CONCLUSION

In conclusion, we characterized a second ZIP transporter, SlZRT2, in *S. luteus*. SlZRT2 localizes to the ER and plasma membrane and likely mediates Zn redistribution in response to Zn availability and developmental stage. A small contribution of SlZRT2 to Zn uptake as a low-affinity plasma membrane-localized transporter is expected. It is unclear whether a putative cytoplasmic Zn release by SlZRT2 in ECM root tips is a response to low Zn availability at the plant–fungal interface or functions as a secondary signal coordinating developmental growth responses. Further investigations of Zn mobilization and involved transporters, including their regulation mechanisms, are necessary to understand how mycorrhizal fungi contribute at an improved Zn status of plants.

DATA AVAILABILITY STATEMENT

Publicly available datasets were analyzed in this study. This data can be found here: http://www.ncbi.nlm.nih.gov/geo/.

AUTHOR CONTRIBUTIONS

LC and JR conceived and designed the experiments. LC, NS, NA, and FR performed the experiments. LC, AK, JC, and JR analyzed and interpreted the data. LC drafted the manuscript. JR edited preliminary versions. All authors reviewed the manuscript and approved the final version.

FUNDING

Funding was provided by the Research Foundation Flanders (FWO project G079213N). LC holds a Flanders Innovation & Entrepreneurships Ph.D. fellowship (IWT project 141461). Her research visit at INRA Grand Est Nancy was funded by the Laboratory of Excellence Advanced Research on the Biology of Tree and Forest Ecosystems (ARBRE; grant No. ANR-11-LABX-0002-01).

ACKNOWLEDGMENTS

We thank Carine Put, Ann Wijgaerts, and Brigitte Vanacken for their technical assistance. We are grateful to Prof. Dr. David Eide for kindly providing the Δzrt1Δzrt2 yeast mutant.

SUPPLEMENTARY MATERIAL

The Supplementary Material for this article can be found online at: https://www.frontiersin.org/articles/10.3389/fmicb.2019.02251/full#supplementary-material

FIGURE S1 | Functional complementation assays of the Zn uptake-deficient yeast strain Δzrt1Δzrt2. Cultures of WT and mutant yeast cells (OD_{600} = 1) were 10-fold serial diluted (10^0, 10^{-1}, 10^{-2}, and 10^{-3}) and spotted on control (first column) or selection SD medium (second and third columns). Control medium was supplemented with Zn and selection medium with EDTA or citrate, since both substances are known to limit Zn availability in the medium. The supplement concentrations are indicated above the pictures. Pictures were taken after 3 days of growth and experiments were carried out for three independent clones. **(A)** WT cells were transformed with the EV (pAG306GAL-ccdB-EGFP; Alberti et al., 2007). Yeast mutants were transformed with the EV or the vector containing *SlZRT2:EGFP* or *SlZRT1:EGFP*. **(B)** Δzrt1Δzrt2 complementation assay according to Coninx et al. (2017b) with EDTA supplementation in the growth medium. Culture conditions were identical to the ones used in the complementation assay of *SlZRT1* (Coninx et al., 2017b). WT cells were transformed with the EV (pYES-DEST52; Invitrogen). Yeast mutants were transformed with the EV or the vector containing *SlZRT2*.

FIGURE S2 | Fluorescence of Δzrt1Δzrt2 yeast cells expressing SlZRT2:EGFP **(A)** or an EV control (**B,C**; pAG306GAL-ccdB-EGFP; Alberti et al., 2007). Cells were visualized for EGFP (left), the counterstaining (middle), or merged images

(right). **(A)** FM4-64 vacuolar staining at 30°C to allow endocytosis of the dye by Δzrt1Δzrt2 cells expressing SlZRT2:EGFP. **(B)** FM4-64 vacuolar staining (30°C) and **(C)** Hoechst 33324 nuclear staining of EV transformed Δzrt1Δzrt2 cells.

FIGURE S3 | Zn content of WT and Δzrt1Δzrt2 transformed yeast cells transformed with the EV (pAG306GAL-ccdB-EGFP; Alberti et al., 2007) or the vector containing *SlZRT2*. Data are the average ± standard error (SE) of five biological replicates; significant differences are indicated by different letters ($p < 0.05$). For a borderline significant difference, the letter is placed within brackets ($p \leq 0.07$).

FIGURE S4 | Mn **(A)** and Fe **(B)** content of WT and Δzrt1Δzrt2 transformed yeast cells transformed with the EV or the vector containing *SlZRT2*. Yeast cells were transformed with the vector pYES-DEST52 (Invitrogen, left) or with pAG306GAL-ccdB-EGFP (Alberti et al., 2007; right). Data are the average ± standard error (SE) of five replicates; significant differences ($p < 0.05$) are indicated by different letters.

FIGURE S5 | Trehalase activity in Zn-depleted Δzrt1Δzrt2 cells after the re-addition of Zn. Δzrt1Δzrt2 cells were transformed with the EV (triangles, pYES-DEST52; Invitrogen), *SlZRT1* (circles), or *SlZRT2* (diamonds). All yeast cultures were grown for 2 days on SD medium with 0.5 mM citrate to induce Zn starvation. Trehalase activity was assessed in yeast cells maintained on Zn starvation medium (in gray; negative control) and after the addition of 1 mM $ZnCl_2$ (in black) **(A)** 4.5 h prior to the experiment, yeast cultures were transferred to fresh SD medium with 0.5 mM citrate and 200 μM EDTA. **(B)** 4 h prior to the experiment, yeast cultures were transferred to fresh SD medium with 10 mM citrate and 1 mM EDTA.

REFERENCES

Adriaensen, K., van der Lelie, D., Van Laere, A., Vangronsveld, J., and Colpaert, J. V. (2004). A zinc-adapted fungus protects pinefs from zinc stress. *New Phytol.* 161, 549–555. doi: 10.1046/j.1469-8137.2003.00941.x

Alberti, S., Gitler, A. D., and Lindquist, S. (2007). A suite of gateway cloning vectors for high-throughput genetic analysis in *Saccharomyces cerevisiae*. *Yeast* 24, 913–919. doi: 10.1002/yea.1502

Alloway, B. J. (2004). *Zinc in Soils and Crop Nutrition*. Paris: International Fertilizer Industry Association and Brussels.

Andreini, C., Banci, L., Bertini, I., and Rosato, A. (2006). Zinc through the three domains of life. *J. Proteome Res.* 5, 3173–3178. doi: 10.1021/pr0603699

Becquer, A., Guerrero-Galán, C., Eibensteiner, J. L., Houdinet, G., Bücking, H., Zimmermann, S. D., et al. (2019). The ectomycorrhizal contribution to tree nutrition. *Adv. Bot. Res.* 89, 77–126. doi: 10.1016/bs.abr.2018.11.003

Bird, A. J., Blankman, E., Stillman, D. J., Eide, D. J., and Winge, D. R. (2004). The Zap1 transcriptional activator also acts as a repressor by binding downstream of the TATA box in ZRT2. *EMBO J.* 23, 1123–1132. doi: 10.1038/sj.emboj.7600122

Blaudez, D., and Chalot, M. (2011). Characterization of the ER-located zinc transporter ZnT1 and identification of a vesicular zinc storage compartment in *Hebeloma cylindrosporum*. *Fungal Genet Biol.* 48, 496–503. doi: 10.1016/j.fgb.2010.11.007

Cabral, L., Soares, C. F. R. S., Giachini, A. J., and Siqueira, J. O. (2015). Arbuscular mycorrhizal fungi in phytoremediation of contaminated areas by trace elements: mechanisms and major benefits of their applications. *World J. Microbiol. Biotechnol.* 31, 1655–1664. doi: 10.1007/s11274-015-1918-y

Cavagnaro, T. R. (2008). The role of arbuscular mycorrhizas in improving plant zinc nutrition under low soil zinc concentrations: a review. *Plant and Soil.* 304, 315–325. doi: 10.1007/s11104-008-9559-7

Colpaert, J. V., Muller, L. A. H., Lambaerts, M., Adriaensen, K., and Vangronsveld, J. (2004). Evolutionary adaptation to Zn toxicity in populations of suilloid fungi. *New Phytol.* 162, 549–559. doi: 10.1111/j.1469-8137.2004.01037.x

Colpaert, J. V., Wevers, J. H. L., Krznaric, E., and Adriaensen, K. (2011). How metal-tolerant ecotypes of ectomycorrhizal fungi protect plants from heavy metal pollution. *Ann Forest Sci* 68, 17–24. doi: 10.1007/s13595-010-0003-9

Coninx, L., Martinova, V., and Rineau, F. (2017a). "Mycorrhiza-assisted phytoremediation," in *Phytoremediation*, eds A. Cuypers, and J. Vangronsveld (Massachusetts, US: Academic Press).

Coninx, L., Thoonen, A., Slenders, E., Morin, E., Arnauts, N., Op De Beeck, M., et al. (2017b). The SlZRT1 gene encodes a plasma membrane-located ZIP (Zrt-, Irt-Like Protein) transporter in the ectomycorrhizal fungus *Suillus luteus*. *Front. Microbiol.* 8:2320. doi: 10.3389/fmicb.2017.02320

R Core Team, (2012). *R: A Language and Environment for Statistical Computing*. Vienna: R Foundation for Statistical Computing.

Eide, D. (1996). The ZRT2 gene encodes the low affinity zinc transporter in *Saccharomyces cerevisiae*. *J. Biol. Chem.* 271, 23203–23210. doi: 10.1074/jbc.271.38.23203

Eide, D. (2006). Zinc transporters and the cellular trafficking of zinc. *Biochim. Biophys. Acta* 1763, 711–722. doi: 10.1016/j.bbamcr.2006.03.005

Eng, B. H., Guerinot, M. L., Eide, D., and Saier, M. H. (1998). Sequence analyses and phylogenetic characterization of the ZIP family of metal ion transport proteins. *J. Membr. Biol.* 166, 1–7. doi: 10.1007/s002329900442

Ernst, W. H. O. (1990). "Mine vegetations in Europe," in *Heavy Metal Tolerance in Plants: Evolutionary Aspects*, ed. E. J. Shaw (Boca Raton, FL: CRC Press), 21–37.

Ferrol, N., Tamayo, E., and Vargas, P. (2016). The heavy metal paradox in arbuscular mycorrhizas: from mechanisms to biotechnological applications. *J. Exp. Bot.* 67, 6253–6265. doi: 10.1093/jxb/erw403

Gaither, L. A., and Eide, D. J. (2001). Eukaryotic zinc transporters and their regulation. *Biometals* 14, 251–270. doi: 10.1023/A:1012988914300

Gietz, D. R., and Woods, R. A. (2002). Transformation of yeast by lithium acetate/single-stranded carrier DNA/polyethylene glycol method. *Method. Enzymol.* 350, 87–96. doi: 10.1016/S0076-6879(02)50957-5

Gitan, R. S., Shababi, M., Kramer, M., and Eide, D. J. (2003). A cytosolic domain of the yeast zrt1 zinc transporter is required for its post-translational inactivation in response to zinc and cadmium. *J. Biol. Chem.* 278, 39558–39564. doi: 10.1074/jbc.M302760200

Guerinot, M. L. (2000). The ZIP family of metal transporters. *Biochim. Biophys. Acta* 1465, 190–198. doi: 10.1016/S0005-2736(00)00138-3

Hayward, J., Horton, T. R., Pauchard, A., and Nunez, M. A. (2015). A single ectomycorrhizal fungal species can enable a Pinus invasion. *Ecology* 96, 1438–1444. doi: 10.1890/14-1100.1

Jung, W. H. (2015). The zinc transport systems and their regulation in pathogenic fungi. *Mycobiology* 43, 179–183. doi: 10.5941/MYCO.2015.43.3.179

Kambe, T., Suzuki, T., Nagao, M., and Yamaguchi-Iwai, Y. (2006). Sequence similarity and functional relationship among eukaryotic ZIP and CDF transporters. *Genom. Proteom. Bioinf.* 4, 1–9. doi: 10.1016/S1672-0229(06)60010-7

Katoh, K., and Standley, D. M. (2013). MAFFT multiple sequence alignment software version 7: improvements in performance and usability. *Mol. Biol. Evol.* 30, 772–780. doi: 10.1093/molbev/mst010

Keymer, A., Pimprikar, P., Wewer, V., Huber, C., Brands, M., Bucerius, S. L., et al. (2017). Lipid transfer from plants to arbuscular mycorrhiza fungi. *eLife* 6:e29107. doi: 10.7554/eLife.29107

Kjellerup, L., Winther, A. L., Wilson, D., and Fuglsang, A. T. (2018). Cyclic AMP pathway activation and extracellular zinc induce rapid intracellular zinc mobilization in *Candida albicans*. *Front. Microbiol.* 9:502. doi: 10.3389/fmicb.2018.00502

Kohler, A., Kuo, A., Nagy, L. G., Morin, E., Barry, K. W., Buscot, F., et al. (2015). Convergent losses of decay mechanisms and rapid turnover of symbiosis genes in mycorrhizal mutualists. *Nat. Genet.* 47, 410–415. doi: 10.1038/ng.3223

Krogh, A., Larsson, B., von Heijne, G., and Sonnhammer, E. L. L. (2001). Predicting transmembrane protein topology with a hidden Markov model: application to complete genomes. *J. Mol. Biol.* 305, 567–580. doi: 10.1006/jmbi.2000.4315

Langer, I., Santner, J., Krpata, D., Fitz, W. J., Wenzel, W. W., and Schweiger, P. F. (2012). Ectomycorrhizal impact on Zn accumulation of *Populus tremula* L. grown in metalliferous soil with increasing levels of Zn contamination. *Plant Soil.* 355, 283–297. doi: 10.1007/s11104-011-1098-y

Leonhardt, T., Sácký, J., and Kotrba, P. (2018). Functional analysis RaZIP1 transporter of the ZIP family from the ectomycorrhizal Zn-accumulating *Russula atropurpurea*. *Biometals* 31, 255–266. doi: 10.1007/s10534-018-0085-7

MacDiarmid, C. W., Gaither, L. A., and Eide, D. (2000). Zinc transporters that regulate vacuolar zinc storage in *Saccharomyces cerevisiae*. *EMBO J.* 19, 2845–2855. doi: 10.1093/emboj/19.12.2845

Mao, X., Kim, B., Wang, F., Eide, D. J., and Petris, M. J. (2007). A histidine rich cluster mediates the ubiquitination and degradation of the human zinc transporter, hZIP4, and protects against zinc cytotoxicity. *J. Biol. Chem.* 282, 6992–7000. doi: 10.1074/jbc.M610552200

Martin, F., Kohler, A., Murat, C., Veneault-Fourrey, C., and Hibbett, D. S. (2016). Unearthing the roots of ectomycorrhizal symbioses. *Nat. Rev. Microbiol.* 14, 760–773. doi: 10.1038/nrmicro.2016.149

Milon, B., Wu, Q., Zou, J., Costello, L. C., and Franklin, R. B. (2006). Histidine residues in the region between transmembrane domains III and IV of hZip1 are required for zinc transport across the plasma membrane in PC- 3 cells. *Biochim. Biophys. Acta* 1758, 1696–1701. doi: 10.1016/j.bbamem.2006.06.005

Miransari, M. (2017). "Arbuscular mycorrhizal fungi and heavy metal tolerance in plants," in *Arbuscular Mycorrhizas and Stress Tolerance of Plants*, ed. Q. S. Wu (Singapore: Springer), 147–161. doi: 10.1007/978-981-10-4115-0_7

Montanini, B., Blaudez, D., Jeandroz, S., Sanders, D., and Chalot, M. (2007). Phylogenetic and functional analysis of the cation diffusion facilitator (CDF) family: improved signature and prediction of substrate specificity. *BMC Genomics* 8:107. doi: 10.1186/1471-2164-8-107

Montanini, B., Gabella, S., Abbà, S., Peter, M., Kohler, A., Bonfante, P., et al. (2006). Gene expression profiling of the nitrogen starvation stress response in the mycorrhizal ascomycete *Tuber borchii*. *Fungal Genet. Biol.* 43, 634–641. doi: 10.1016/j.fgb.2006.04.001

Nagajyoti, P. C., Lee, K. D., and Sreekanth, T. V. M. (2010). Heavy metals, occurrence and toxicity for plants: a review. *Environ Chem Lett.* 8, 199–216. doi: 10.1007/s10311-010-0297-8

Nguyen, H., Rineau, F., Vangronsveld, J., Cuypers, A., Colpaert, J. V., and Ruytinx, J. (2017). A novel, highly conserved metallothionein family in basidiomycete fungi and characterization of two representative SlMTa and SlMTb genes in the ectomycorrhizal fungus *Suillus luteus*. *Environ. Microbiol.* 19, 2577–2587. doi: 10.1111/1462-2920.13729

Pernambuco, M. B., Winderickx, J., Crauwels, M., Griffioen, G., Mager, W. H., and Thevelein, J. M. (1996). Glucose-triggered signalling in *Saccharomyces cerevisiae*: different requirements for sugar phosphorylation between cells grown on glucose and those grown on non-fermentable carbon sources. *Microbiology* 142, 1775–1782. doi: 10.1099/13500872-142-7-1775

Preuss, D., Mulholland, J., Kaiser, C. A., Orlean, P., Albright, C., Rose, M. D., et al. (1991). Structure of the yeast endoplasmic reticulum: localization of ER proteins using immunofluorescence and immunoelectron microscopy. *Yeast* 7, 891–911. doi: 10.1002/yea.320070902

Prinz, W. A., Grzyb, L., Veenhuis, M., Kahana, J. A., Silver, P. A., and Rapoport, T. A. (2000). Mutants affecting the structure of the cortical endoplasmic reticulum in *Saccharomyces cerevisiae*. *JCB* 150, 461–474. doi: 10.1083/jcb.150.3.461

Rozen, S., and Skaletsky, H. (2000). Primer3 on the WWW for general users and for biologist programmers. *Methods Mol. Biol.* 132, 365–386. doi: 10.1385/1-59259-192-2:365

Ruytinx, J., Coninx, L., Nguyen, H., Smisdom, N., Morin, E., Kohler, A., et al. (2017). Identification, evolution and functional characterization of two Zn CDF-family transporters of the ectomycorrhizal fungus *Suillus luteus*. *Environ. Microbiol. Rep.* 9, 419–427. doi: 10.1111/1758-2229.12551

Ruytinx, J., Remans, T., and Colpaert, J. V. (2016). Gene expression studies in different genotypes of an ectomycorrhizal fungus require a high number of reliable reference genes. *Peer J Prep* 4:e2125v1.

Sacky, J., Leonhardt, T., and Kotrba, P. (2016). Functional analysis of two genes coding for distinct cation diffusion facilitators of the ectomycorrhizal Zn-accumulating fungus *Russula atropurpurea*. *Biometals* 29, 349–363. doi: 10.1007/s10534-016-9920-x

Schothorst, J., Van Zeebroeck, G., and Thevelein, J. M. (2017). Identification of Ftr1 and Zrt1 as iron and zinc micronutrient transceptors for activation of the PKA pathway in *Saccharomyces cerevisiae*. *Microb. Cell* 4, 74–89. doi: 10.15698/mic2017.03.561

Sharma, S., Sharma, A. K., Prasad, R., and Varma, A. (2017). "Arbuscular mycorrhiza: a tool for enhancing crop production," in *Mycorrhiza—Nutrient Uptake, Biocontrol, Ecorestoration*, eds A. Varma, R. Prasad, and N. Tuteja (Cham: Springer), 235–250. doi: 10.1007/978-3-319-68867-1_12

Steyfkens, F., Zhang, Z., Van Zeebroeck, G., and Thevelein, J. M. (2018). Multiple transceptors for macro- and micro-nutrients control diverse cellular properties through the PKA pathway in yeast: a paradigm for the rapidly expanding world of eukaryotic nutrient transceptors up to those in human cells. *Front. Pharmacol.* 13:191. doi: 10.3389/fphar.2018.00191

Stothard, P. (2000). The sequence manipulation suite: javascript programs for analyzing and formatting protein and DNA sequences. *Biotechniques* 28, 1102–1104. doi: 10.2144/00286ir01

Tamayo, E., Gómez-Gallego, T., Azcón-Aguilar, C., and Ferrol, N. (2014). Genome-wide analysis of copper, iron and zinc transporters in the arbuscular mycorrhizal fungus *Rhizophagus irregularis*. *Front. Plant Sci.* 5:547. doi: 10.3389/fpls.2014.00547

Thevelein, J. M., and de Winde, J. H. (1999). Novel sensing mechanisms and targets for the cAMP-protein kinase A pathway in the yeast *Saccharomyces cerevisiae*. *Mol Microbiol* 33, 904–918. doi: 10.1046/j.1365-2958.1999.01538.x

Van Houtte, H., and Van Dijck, P. (2013). Trehalase activity in *Arabidopsis thaliana* optimized for 96-well plates. *Bio Protoc.* 3:e946. doi: 10.21769/BioProtoc.946

Vandesompele, J., De Preter, K., Pattyn, F., Poppe, B., Van Roy, N., De Paepe, A., et al. (2002). Accurate normalization of real-time quantitative RT-PCR data by geometric averaging of multiple internal control genes. *Genome Biol.* 3:RESEARCH0034. doi: 10.1186/gb-2002-3-7-research0034

Vida, T. A., and Emr, S. D. (1995). A new vital stain for visualizing vacuolar membrane dynamics and endocytosis in yeast. *J. Cell Biol.* 128, 779–792. doi: 10.1083/jcb.128.5.779

Wilson, S., and Bird, A. J. (2016). Zinc sensing and regulation in yeast model systems. *Arch. Biochem. Biophys.* 611, 30–36. doi: 10.1016/j.abb.2016.02.031

Yamasaki, S., Sakata-Sogawa, K., Hasegawa, A., Suzuki, T., Kabu, E., Sato, E., et al. (2007). Zinc is a novel intracellular second messenger. *JCB* 177, 637–645. doi: 10.1083/jcb.200702081

Yang, Y., Liang, Y., Ghosh, A., Song, Y., Chen, H., and Tang, M. (2015). Assessment of arbuscular mycorrhizal fungi status and heavy metal accumulation characteristics of tree species in a lead–zinc mine area: potential applications for phytoremediation. *Environ. Sci. Pollut. Res.* 22, 13179–13193. doi: 10.1007/s11356-015-4521-8

Zhao, H., and Eide, D. (1996a). The yeast ZRT1 gene encodes the zinc transporter protein of a high-affinity uptake system induced by zinc limitation. *Proc. Natl. Acad. Sci. U.S.A.* 93, 2454–2458. doi: 10.1073/pnas.93.6.2454

Zhao, H., and Eide, D. (1996b). The ZRT2 gene encodes the low affinity zinc transporter in *Saccharomyces cerevisiae*. *J. Biol. Chem.* 271, 23203–23210. doi: 10.1074/jbc.271.38.23203

Conflict of Interest: The authors declare that the research was conducted in the absence of any commercial or financial relationships that could be construed as a potential conflict of interest.

frontiers in Microbiology

REVIEW
published: 14 August 2019
doi: 10.3389/fmicb.2019.01888

Perspectives on Endosymbiosis in Coralloid Roots: Association of Cycads and Cyanobacteria

Aimee Caye G. Chang[1,2,3], Tao Chen[2], Nan Li[2] and Jun Duan[3]**

[1] University of Chinese Academy of Sciences, Beijing, China, [2] Fairy Lake Botanical Garden, Chinese Academy of Sciences, Shenzhen, China, [3] South China Botanical Garden, Chinese Academy of Sciences, Guangzhou, China

Past endosymbiotic events allowed photosynthetic organisms to flourish and evolve in terrestrial areas. The precursor of chloroplasts was an ancient photosynthetic cyanobacterium. Presently, cyanobacteria are still capable of establishing successful symbioses in a wide range of hosts. One particular host plant among the gymnosperms is cycads (Order Cycadales) in which a special type of root system, referred to as coralloid roots, develops to house symbiotic cyanobacteria. A number of studies have explained coralloid root formation and cyanobiont invasion but the questions on mechanisms of this host-microbe association remains vague. Most researches focus on diversity of symbionts in coralloid roots but equally important is to explore the underlying mechanisms of cycads-*Nostoc* symbiosis as well. Besides providing an overview of relevant areas presently known about this association and citing putative genes involved in cycad-cyanobacteria symbioses, this paper aims to identify the limitations that hamper attempts to get to the root of the matter and suggests future research directions that may prove useful.

Keywords: cyanobacteria, cycads, coralloid roots, symbiosis, cyanobionts, endosymbiosis, heterocyst, hormogonia

OPEN ACCESS

Edited by:
Kevin Garcia,
North Carolina State University, United States

Reviewed by:
Jan de Vries,
Technische Universität Braunschweig, Germany
Katharina Pawlowski,
Stockholm University, Sweden

****Correspondence:***
Nan Li
andreali1997@126.com
Jun Duan
duanj@scib.ac.cn

Specialty section:
This article was submitted to Microbial Symbioses, a section of the journal Frontiers in Microbiology

Received: *24 March 2019*
Accepted: *30 July 2019*
Published: *14 August 2019*

Citation:
Chang ACG, Chen T, Li N and Duan J (2019) Perspectives on Endosymbiosis in Coralloid Roots: Association of Cycads and Cyanobacteria. Front. Microbiol. 10:1888. doi: 10.3389/fmicb.2019.01888

INTRODUCTION

Cyanobacteria are the ancestors of chloroplasts. Gaining a deeper understanding on how communication between a symbiont and a host occurs at the molecular level may provide insights on the evolution of green plants. Studies addressing the function and symbiotic mechanisms between cycads and cyanobacteria in coralloid roots are scant when compared to studies of associations of cyanobionts with other host plants such as the angiosperm *Gunnera*, the water fern *Azolla* and the bryophytes *Blasia* and *Anthoceros*, to cite a few (Adams et al., 2013; Warshan, 2017). Most of the literature on cyanobacterial associations with cycads are old. Recent publications (Bergman et al., 1992; Kluge et al., 1992; Adams and Duggan, 2008; Rikkinen, 2015; Pereira, 2017) based their analyses on other host-symbiont models in an attempt to explain this ancient partnership. Therefore, this review aims to summarize current knowledge about endosymbiosis and highlighting past and present work on cycads-cyanobacterial associations. A section is also dedicated to briefly citing symbiosis-associated genes already identified from other symbiotic models that are relevant in trying to determine the core functions and mechanisms of maintaining stable symbiotic relationships. This review targets readers whose knowledge about coralloid roots of cycads are limited with the aim to spark interest in this infrequently-studied root symbiosis. This

paper also aims to tackle the hindrances in this field of research and to suggest where future research may prove productive.

Early Symbiosis

The capacity of various microbes to interact with other life forms existed even before plants flourished – an evolutionary event triggered by symbiotic microbes (Suárez-Moo et al., 2019). Plastids originated from cyanobacteria (Douglas, 1998), also known as blue green algae, through the process of endosymbiosis which gave rise to the photosynthetic eukaryotes we now refer to as plants and algae (de Vries and Gould, 2017). Chloroplasts became an important component of plant cells because during the past endosymbiotic event by which a heterotrophic unicellular protist engulfed a free-living photosynthetic organism, the former did not allow digestion of the latter – a cyanobacterium. This is the brief story of how plastids originate (Chan and Bhattacharya, 2010). The endosymbiotic cyanobacterium became a plant organelle that harnesses solar energy and converts it to sugar and starch for food and in the process generated the oxygen in the atmosphere that is vital to most life forms (Sarma et al., 2016). In contrast to how free-living cyanobacteria evolved to become chloroplasts (de Vries and Gould, 2017), the event of symbiotic cyanobacteria that entered the roots of cycads had a different outcome. Instead of co-evolving and the symbiont being inherited intracellularly by the host from generation to generation, or giving rise to another organism, symbiotic cyanobacteria just enter and reside in cycad roots in a later part of its host's development (Norstog and Nicholls, 1997) in an engorged and dichotomously-branched root modification called coralloid roots (Ahern and Staff, 1994). Similar to this is the evolution of modified plant roots observed in pines (Faye et al., 1981) and legumes (Long, 1989) to house their respective microsymbionts for a specialized function (Suárez-Moo et al., 2019). Still, regardless of how symbionts invade and evolve in their hosts, life as we know it would not have flourished if not for endosymbiosis (Govindjee and Shevela, 2011; Shestakov and Karbysheva, 2017). Research focusing on endosymbiosis is interesting, since intimate associations between two unrelated species may trigger another critical event that might cause changes in the Earth's atmospheric composition which would impact many life forms (Raven and Allen, 2003; Green, 2011; Martin et al., 2015).

Based on evidence obtained from fossils, cyanobacteria are known to be among the earliest groups of microorganisms that dominated the Earth since the late Archean to early Paleoproterozoic eon around 3500 to 2700 MYA (Krings et al., 2009; Falcon et al., 2010; Schopf, 2011; Shestakov and Karbysheva, 2017). Free-living and symbiotic cyanobacteria vary from spherical and cylindrical unicellular to filamentous multicellular forms (Narainsamy et al., 2013). Known symbiotic cyanobacteria are mostly filamentous members of the genus *Nostoc* (Adams and Duggan, 2008).

Cycads are the only members of gymnosperms currently capable of forming new associations with cyanobacteria. Initially reported by Reinke in 1872 (cited in Adams et al., 2013), all known species of cycads form symbiotic associations with cyanobacteria in specialized structures called coralloid roots. Similar to cyanobionts (endosymbiotic cyanobacteria), cycads belong to the earliest members of the five major groups of seed plants – the gymnosperms Cycadales, Coniferales, Ginkgoales, Gnetales, and angiosperms. Cycads are sisters with *Ginkgo* (Wu et al., 2013) and both share a common ancestor with gnetophytes and conifers (Wu et al., 2007; Roodt et al., 2017). Cycads are assumed to have coexisted with dinosaurs during the Mesozoic era around 300 MYA and thus are often referred to as "living fossils" (Wu et al., 2007; Wu and Chaw, 2015; Jiang et al., 2016). Since cycads and cyanobacteria date back to ancient times, the symbiotic partnership and coevolution formed between the two may have developed millions of years ago (Usher et al., 2007). The origin of this association is still debated and questions regarding the purpose of this symbiosis and why it still prevails remains to be answered.

Implications of Symbiosis Between Cycads and Cyanobacteria

Since ancient soils 300 million years ago (Brenner et al., 2003) were not as fertile as they are today, it was thought that cycads developed a mechanism to harbor cyanobacteria to withstand poor-nutrient soils (Halliday and Pate, 1976). Specialized root structures to house endosymbiotic cyanobacteria were formed and a mutualistic association was maintained by both partners (Gutiérrez-García et al., 2019). Whether coralloid roots were formed by cycads only for the purpose of hosting cyanobionts is an open question. As opposed to cycads, terrestrial cyanobacteria can live in diverse and harsh environments (Sand-Jensen, 2014) and are considered to be the most successful group of microorganisms on Earth (Stewart and Falconer, 2011). Free-living cyanobacteria also form associations with other life forms such as plants and fungi and in some cases with tripartite-structured cyanolichens made up of fungi, green algae and cyanobacteria (Henskens et al., 2012). As to why they need a host to spend a part of their life cycle, some scientists believe that terrestrial cyanobacteria also prefer a stable environment to survive and prevent predation and desiccation from intense heat (Adams et al., 2013). Thus, mutualistic relationships between hosts and endosymbionts are formed wherein the host provides shelter while the symbiont performs specialized functions, such as supplying the host with various needs (Walsh et al., 2011; Haselkorn, 2016). Additionally, it was suggested that cyanobacteria produce arabinogalactan-proteins (AGPs) that contribute to helping plants grow and develop (Pennell, 1992) by assisting in plant cell proliferation, expansion and differentiation (Steele-King et al., 2000). Moreover, AGPs are known to have a role in cell signaling in plant-microbe interactions (Seifert and Roberts, 2007; Jackson et al., 2012).

In a symbiotic relationship, cyanobacteria fixes nitrogen for their hosts. Naturally-occurring dinitrogen in the atmosphere is unreactive with other chemicals, thereby preventing formation of essential and useful compounds. This is where endosymbiotic cyanobacteria enter the Earth's nitrogen cycle and play a major role. Cyanobionts are able to break down the triple bonds from atmospheric dinitrogen (N_2) using the enzyme nitrogenase to convert the inert compound into useful forms of nitrogen. The

N_2 atoms can then be converted to ammonia (NH_3) (Hoffman et al., 2014), which facilitates plant growth and soil fertilization (Halliday and Pate, 1976). Other nitrifying microbes such as *Nitrospira* sp. assist in oxidation of ammonia to nitrite and nitrate followed by the action of denitrifying microbes that completes the nitrogen cycle (Kuypers, 2015). Nitrogen fixation in *Nostoc*, the dominant species symbiotic to cycads coralloid roots (Gehringer et al., 2010), occurs in structures called heterocysts, which occur as chain of cells forming a filament. Sufficient evidence shows that nitrogenase activity of cyanobacteria in symbiosis is significantly higher than in their free-living counterparts, as shown by a 25–35% increase in heterocyst formation in cyanobionts (Lindblad et al., 1985a).

Studies show that cyanobionts in symbiosis with cycads maintain complete photosynthetic apparatus – thylakoids, phycobilisomes, phycobiliproteins, and carboxysomes, associated pigments and enzyme levels comparable with free-living cyanobacteria (Lindblad et al., 1985b; Adams et al., 2013). However, as coralloid roots grow beneath the soil surface where light is insufficient or lacking, the photosystems of cyanobionts may be inactive as shown in an *in vivo* study conducted by Lindblad et al. (1987) where coralloid roots of *Cycas revoluta* showed no evidence of carbon fixation activities when compared under light and dark conditions. It was suggested that enzymes specific for efficient function of the Calvin cycle may be missing in the cyanobacteria in coralloid roots (Lindblad et al., 1987). Since cyanobionts have no sufficient light source, they are capable of heterotrophic metabolism relying on carbon solely supplied by their hosts (Lindblad, 2009). However, it is noteworthy that coralloid roots grow apogeotropically as if phototropism is occurring, and based on personal observations (**Figure 1A**), they oftentimes reach the soil surface exposed and thus, may become capable of receiving substantial amount of light probably through dermal breaks.

The association of cyanobacteria and cycads was also found prevalent in an incident in Guam that led to the detection of neurotoxins contained in cycad seeds. The neurotoxins cause an amyotrophic lateral sclerosis/parkinsonism-dementia complex (ALS-PDC) (Brownson et al., 2002; Meneely et al., 2016). ALS-PDC is a progressive neurodegenerative disease that infected high number of Chamorro people in Guam (Metcalf et al., 2017; Zurita et al., 2019). The disease was believed to be transmitted by flying foxes that consumed cycad seeds. Flying foxes are eaten by the inhabitants of the island (Cox and Sacks, 2002; Banack and Cox, 2003). A case of "biomagnification" was said to have occurred wherein the toxin becomes more potent after being transferred from one organism to the other (Banack and Cox, 2003; Cox et al., 2003; Banack et al., 2006). But this premise remains highly debated (Snyder and Marler, 2011). In contrast, Marler et al. (2010) suggested that coralloid roots do not synthesize or biomagnify these toxins but rather, may act as toxin sinks explaining the high amounts of toxins found in the coralloid root tissues obtained from previous studies. Cyanobacteria-free cycad seedlings were in fact, found to increase in these toxins compared to symbiont-infected coralloid roots therefore refuting the role of endophytic cyanobacteria causing increase of these toxic substances in the host plant (Marler et al., 2010; Snyder and Marler, 2011). Free-living cyanobacteria are known to produce various toxins and thus it is not surprising that symbiotic cyanobacteria synthesize toxins as well (Cox et al., 2005). This neurotoxin was claimed to be β-methylamino-L-alanine (BMAA), a non-proteinogenic amino acid produced by cyanobacteria. Even though some studies have showed that cycad host plants contain BMAA (Vega and Bell, 1967; Polsky et al., 1972; Brownson et al., 2002; Banack and Cox, 2003; Cox et al., 2003), an accurate detection method of BMAA is still being perfected until the present (Metcalf et al., 2017; Zurita et al., 2019) due to various structural isomers (Rosén and Hellenäs, 2008; Banack et al., 2010; Jiang et al., 2012) making it difficult to correctly identify the compound as BMAA. And thus, all previous claims that BMAA was detected still needed further validation.

Cyanobacterial Diversity and Development in Cycads

Cyanobionts found in cycads are predominantly species of *Nostoc*, but in some studies, species of *Calothrix*, *Scytonema* and *Richelia* were also identified (Grobbelaar et al., 1987; Costa and Lindblad, 2002; Gehringer et al., 2010). Most symbiotic cyanobacteria belong to the orders Nostocales and Stigonematales (Castenholz et al., 2001). Multiple strains of cyanobacteria can be housed in a single cycad host (Zheng et al., 2002; Thajuddin et al., 2010) and a single species of cyanobacterium can be isolated in multiple cycad hosts as well (Gehringer et al., 2010). However, in a study by Gehringer et al. (2010), only a single symbiotic *Nostoc* strain was found harboring the coralloid roots of the genus *Macrozamia* (Yamada et al., 2012). Reports indicate that other heterotrophic bacteria reside with cyanobacteria in coralloid roots (Chang et al., 1988), but only in limited populations. According to Grilli Caiola (1980), this is due to the ability of cycads to produce secondary metabolites that inhibit the growth of microorganisms, but not cyanobacteria. A concerted communication between the host and a bacterium, probably through production of certain substances, may also play a role in preventing other bacteria to overpopulate the cyanobacterial layer inside the coralloid roots (Obukowicz et al., 1981; Adams et al., 2013).

Cycads form three types of roots: (1) a primary tap root similar to the root system of most terrestrial plants, (2) lateral roots and (3) coralloid roots (**Figure 1B**). The latter are distinct types of roots that grow laterally and are solely in cycads that house cyanobacteria (Norstog and Nicholls, 1997; Lindblad, 2009). Prior to coralloid root formation, young, apogeotropic papillose roots called precoralloid roots are formed (Ahern and Staff, 1994). During this phase, cyanobacteria are absent and their presence is not required in initiating the development of precoralloids. At this early stage, invasion by cyanobionts happen but note that cases of uninfected precoralloids also occur (Milindasuta, 1975). This raises the question whether precoralloid roots are formed by cycads to specifically host cyanobacteria or also to serve another purpose. Nevertheless, the affinity of cyanobacteria to enter into a symbiotic relationship with

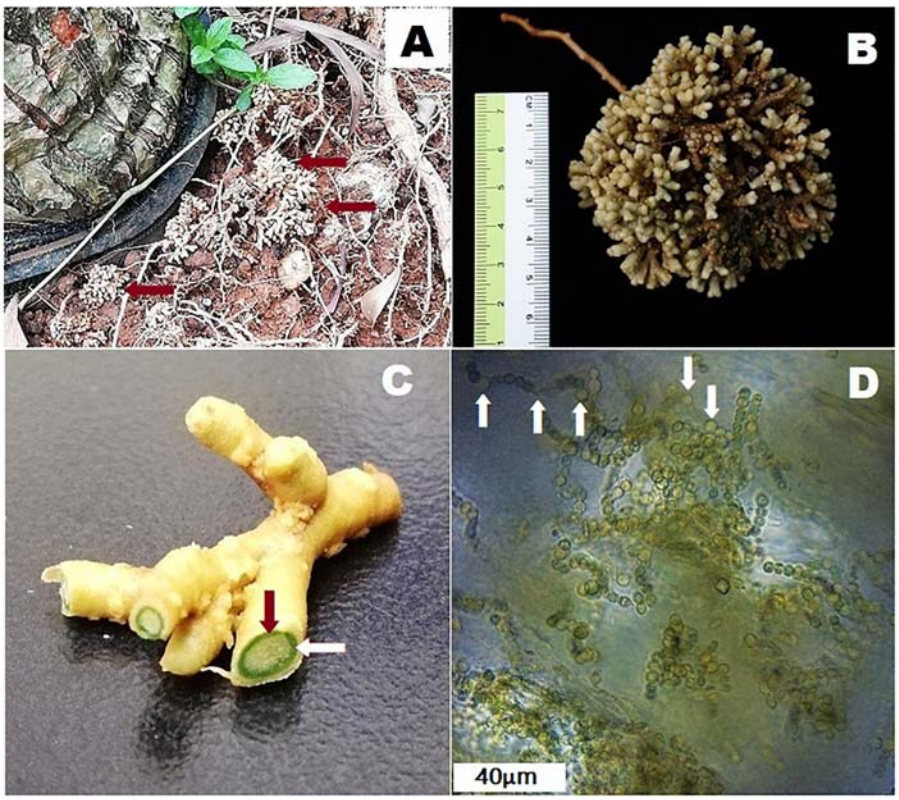

FIGURE 1 | Coralloid roots of *Cycas fairylakea* **(A)** growing apogeotropically at Shenzhen Fairy Lake Botanical Garden, **(B)** showing dichotomous branching of coralloid roots, **(C)** cross-section of coralloid root showing a distinct green layer – the cyanobacterial zone (the green ring pointed by the red and while arrows) and **(D)** microscopic image of filamentous cyanobacteria residing in the cyanobacterial zone. Heterocysts are marked with white arrows.

coralloid roots instead of with the primary and lateral roots promotes the idea that precoralloid and coralloid roots are organs developed by cycads to facilitate symbiosis. The tips of cyanobacteria-free precoralloid roots produce papillose tissue continuously (Ahern and Staff, 1994). Upon maturity, the sheath covering the papillose tissues will be replaced by a thin, external layer that generates scattered lenticels (Milindasuta, 1975; Ahern and Staff, 1994). These morphological changes, or other environmental factors, may cause disruptions in the dermal tissues of mature precoralloid roots. When cyanobacteria in the surrounding soil come in contact with the surface of coralloid roots, they gain access through the dermal breaks (Milindasuta, 1975) to eventually colonize the internal layers of the roots (Grilli Caiola and Canini, 1993; Ahern and Staff, 1994; Lindblad, 2009). At this point, the morphologically distinguishable, engorged and dichotomously-branching coralloid roots start to form. Following initial entry, cyanobacteria migrate toward the cortex and form a distinct, circular, blue-green layer dividing the cortical layer into two (Ahern and Staff, 1994). This is called the cyanobacterial zone (**Figure 1C**) containing filamentous cyanobionts (**Figure 1D**). When coralloid roots reached this stage, the process is irreversible and a permanent symbiotic relationship between cycads and cyanobacteria has been successfully established (Grilli Caiola and Canini, 1993; Ahern and Staff, 1994; Lindblad, 2009).

Associated Structures Required for Establishment of Symbiosis

Cyanobacteria that can form associations with cycads as well as with other compatible host plants are capable of cell differentiation exhibiting various morphologies (Flores, 2012). All symbiotic cyanobacterial strains from the genus *Nostoc* fix nitrogen in cells called heterocysts (Adams and Duggan, 2008). At low levels of nitrogen, cyanobionts form heterocysts to facilitate nitrogen metabolism (Bergman et al., 1996). Forming heterocysts was how nitrogen fixers evolved to protect the enzyme nitrogenase from inactivation due to exposure to oxygen (Bernhard, 2010). These cells are thick-walled allowing them to block available oxygen in diffusing inside the cells making a suitable, low-oxygen microenvironment for efficient synthesis of nitrogenase for nitrogen metabolism (Tikhonovich and Provorov, 2007). Heterocysts are specialized elliptical-shaped cells produced at regularly-spaced intervals along the cyanobacterial linear cell clusters and are distinguishable due to their larger size compared to neighboring vegetative cells (Kumar et al., 2010). Cyanobionts in coralloid roots form heterocysts at higher frequency compared to free-living

cyanobacteria but morphological changes are minimal (Adams et al., 2013). For cyanobacteria living within coralloid roots, a significant increase (up to 80%) in heterocyst frequency was observed (Norstog and Nicholls, 1997; Adams and Duggan, 1999; Zhang et al., 2006). The increase in formation of heterocysts is said to be triggered by nitrogen starvation (Zhang et al., 2006). Therefore, an effective partnership with a plant host relies on the ability of the cyanobacteria to differentiate into heterocysts for a stable symbiosis (Meeks and Elhai, 2002).

Cyanobacteria can also form filaments called hormogonia. Hormogonium lacks heterocysts and can be morphologically distinguished from the latter as the former is capable of locomotion appearing as short motile filaments (Hernández-Muñiz and Stevens, 1987). Hormogonia play a role in self-dispersal and in forming symbiotic association during the early stages of infection by responding to chemical signals produced by prospective host plants (Khayatan et al., 2017). Chemoattractants are said to be involved in stimulating hormogonia formation and directing the cyanobacteria toward the targeted plant tissue that will house the cyanobionts (Meeks et al., 2001; Meeks and Elhai, 2002; Bergman et al., 2007).

Filamentous, heterocyst-forming cyanobacteria are also capable of differentiating into spores called akinetes (Kaplan-Levy et al., 2010; Adams et al., 2013). When environmental conditions become unfavorable (e.g., low salinity, temperature fluctuations, lack of phosphates, low light, insufficient nutrients), active cells transform into a resting state that may last for up to 60 years in which they can be restored to their vegetative cell state when favorable conditions arise (Kaplan-Levy et al., 2010). Although not resistant to intense heat, akinetes can survive cold and desiccation (Adams and Duggan, 1999). Akinetes are rare but were reported to occur in strains of *Nostoc* isolated from coralloid roots (Grilli Caiola, 1980; Grobbelaar et al., 1987) and more are common in *Azolla-Anabaena* symbioses (Peters and Perkins, 1993). Additionally, Sukenik et al. (2007) state that resting cells can still perform minimal metabolic activities such as photosynthesis, carbon fixation and protein synthesis. Aside from akinetes, lysing or dying cells called necridia, which allow excision of cells along the filament, also occur in cyanobacteria. Characterized by thickened walls and non-granulated cells, these are commonly referred to as deteriorating cells that were unable to differentiate into heterocysts (Grilli Caiola and Pellegrini, 1979).

General Mechanism of Symbiosis

All known plant-cyanobacterial symbioses are acquired from the environment. The only exception is seen in the fern *Azolla*, where the cyanobiont is an integral part of the host throughout its developmental stages and gets inherited to the next generation (Bergman et al., 1996). Thus, for most symbioses, efficient communication between the host and cyanobacterium must be carried out to ensure successful entry of the symbiont (**Figure 2**). This requires signal molecules induced by the host and/or the symbiont during the initial stages of invasion. The general mechanism based on other host plant-cyanobacterial symbioses, as controlled by a set of regulatory genes, is that the host elicits hormogonium-inducing factors causing the surrounding cyanobacteria to transform into motile hormogonia (Adams and Duggan, 2012; Warshan, 2017). Chemotactic signals permit entry into the partner plant, subsequently demanding the host to produce hormogonium-repressing factors to allow the cyanobacteria to develop heterocysts for nitrogen fixation to occur (Warshan, 2017).

Formation of motile hormogonia is essential for successful migration of a cyanobiont to the internal tissues of its potential plant partner. Certain compounds which may be produced by the host, trigger this phenomenon and initiate cell differentiation (Khayatan et al., 2017). In plants known to accommodate symbiotic cyanobacteria, modified structures can be formed regardless of whether a cyanobiont will be present in its life cycle (Meeks and Elhai, 2002) such as the case in coralloid roots. Unlike *Rhizobia*, which requires specialized symbiosomes to be formed by its host, cyanobionts of coralloid roots do not need similar structures to survive within its host. However, particular spaces are dedicated to symbionts. Cyanobacteria resides in the cyanobacterial zone in the roots of cycads, in the red stem glands of *Gunnera*, in dorsal leaf cavities of *Azolla* water fern, in slime cavities within the thallus of hornworts, in auricles underneath the thallus of liverworts, and in the bladders of the fungi *Geosiphon pyriformis* (Adams et al., 2013). Among these plant-cyanobacterial symbioses, it is only in *Gunnera* where the cyanobiont invasion occurs intracellularly (Meeks and Elhai, 2002; Adams et al., 2013). In the coralloid roots, an acidic viscous mucilage in the cortex (Grilli Caiola, 1980), also observed by the authors, is present in the cortex layer probably involved in attracting motile hormogonia filaments as this was the case observed in *Gunnera* (Nilsson et al., 2006). Mucilage-filled cavities were also observed in hornworts and liverworts and this heat-labile putative signal inducer is yet to be characterized, but was estimated to be a low molecular mass protein around 12 kDa (Adams et al., 2013). In line with this, root extracts from cycad coralloid roots were found to significantly initiate hormogonia formation in strains of *Nostoc* (Campbell and Meeks, 1989; Bergman et al., 1996; Meeks, 1998) suggesting hosts produce hormogonia-inducing factors (Nilsson et al., 2006). In an *in vitro* study, hormogonia-inducing factor (HIF) was not released in a culture medium with excess nitrogen. Thus, HIF production is assumed to be stimulated when nitrogen levels are depleted (Campbell and Meeks, 1989; Adams et al., 2013). Aside from the HIF signal, plant hosts are believed to release various chemoattractants to entice potential symbionts. These were hypothesized to be sugar-based molecules, since simple sugars were proven to be attractants for hormogonia initiation (Nilsson et al., 2006; Adams et al., 2013). Recently, a bioassay was conducted using crude methanolic extracts of *Cycas revoluta* coralloid roots that transformed symbiotic *Nostoc* filaments into motile hormogonia. This led to the successful isolation of a hormogonium-inducing factor from cycads characterized as diacylglycerol 1-palmitoyl-2-linoleoyl-*sn*-glycerol (Hashidoko et al., 2019).

Once a cyanobiont successfully enters its host, the plant partner must stop releasing hormogonia-inducing factors to halt hormogonia formation. The reason is to direct the cyanobiont to the next stage of symbiosis and to start forming heterocysts

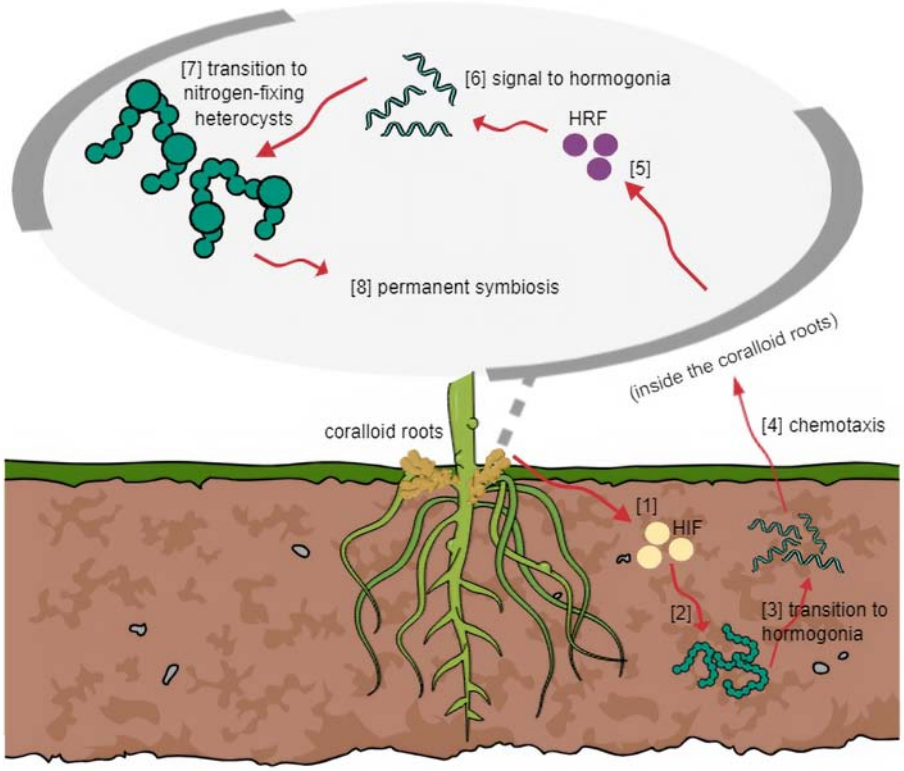

FIGURE 2 | General mechanism of symbiosis based on other host plant-cyanobiont models. (1) HIF is released by host and (2) triggers cyanobacteria in surrounding soil to (3) transition into motile filaments. (4) Through chemotaxis, host attracts hormogonia following cyanobacterial entry. (5) Host releases HRF and (6) signals hormogonia that entered the host successfully to (7) transition into heterocysts-forming cells. (8) Symbiosis at this stage becomes irreversible.

for nitrogen fixation to occur – a task that cannot be performed by hormogonia filaments. Therefore, the release of hormogonia-repressing factors (HRF) hinders HIF activities. Cohen and Meeks (1997) observed this phenomenon using aqueous tissue extracts of *Anthoceros* wherein activation of two genes blocks hormogonium formation and the expressions are only induced by HRF but not HIF.

Besides inducing and repressing factors, high amounts of phenolic substances are also present in the mucilaginous material embedded in the cyanobacterial zone of coralloid roots and surrounding cortical layers (Lobakova et al., 2004). Phenolic substances are rich sources of antimicrobial compounds and secondary metabolites (Obukowicz et al., 1981). Interestingly, phenolics are also known to participate in cell signaling and might play a role in establishing and maintaining stable cycad-cyanobacterial symbioses (Grilli Caiola, 1980; Obukowicz et al., 1981).

An Overview of Genes Involved in Cycads-Cyanobacteria Symbiosis

Though still limited, sequencing of representative complete genomes of hosts and cyanobionts led to the identification of genes involved in plant host-cyanobacterial symbiosis (Ran et al., 2010; Li et al., 2018). This section aims to list some studied genes and their functions significant in the establishment of symbiosis as well as other genes they interact with (**Table 1**). Although most of the genes cited here were not studied using cycad coralloid roots, a similar, if not exact, genetic mechanism in cycad-cyanobacterial symbiosis seems to be occurring as the genes discussed in this section were commonly found among plant-cyanobacterial symbioses.

As mentioned previously, HRF are involved in halting hormogonium formation after initial migration of the symbiont into its target organ in the host that varies among plant hosts as mentioned in the previous section. Using *Anthoceros* tissue extracts, *hrmU* and *hrmA* genes were discovered that suppresses hormogonia formation and allow differentiation of cells into heterocysts (Cohen and Meeks, 1997). The expression of these two genes appears to be controlled by the host, which hinders further activities attempted by HIF (Cohen and Meeks, 1997; Meeks et al., 1999). Other open reading frames (ORFs) – *hrmI, hrmR, hrmK* and *hrmE* – were identified that were similar to a family coding for transcriptional inhibitor proteins (Campbell et al., 2003). It was proposed that external repressing signals can possibly be detected by *Nostoc* incapacitating Hrm proteins in successfully binding to hrm operons and this affects transcription of genes that induce hormogonium formation (Meeks et al., 1999; Campbell et al., 2003; Adams et al., 2013).

The ability to form heterocysts is a vital feature for a cyanobiont to establish symbiosis with a host. Without

TABLE 1 | Symbiosis-related genes from host-symbiont models cited in this manuscript.

GENES	ORGANISMS/s	GENERAL FUNCTION/S
hrm	*Nostoc-Anthoceros*	Suppresses hormogonia formation allowing cell differentiation into heterocysts
het	*Nostoc-Anthoceros*	Responsible for heterocyst formation
ntc	*Nostoc-Anthoceros*	Regulates nitrogen and has a role in activation of other symbiotic genes
hep	*Anabaena-Azolla*	Induces formation of thickened cell envelope in heterocyst cells
nif	*Nostoc-Anthoceros, Anabaena-Azolla*	Involves in formation of nitrogenase complexes
sig	*Nostoc-Anthoceros*	Plays a role in signaling to promote symbiont entry to host tissue
ctp	*Nostoc-Anthoceros, Synechocystis-Anthoceros*	Involves in photosynthetic activities
tpr	*Nostoc-Anthoceros*	Regulates cell cycle and functions in protein transport mechanisms

heterocysts, a cyanobiont cannot fix nitrogen for its host. Mutations in *hetR* and *hetF* did not allow one strain of *Nostoc* to differentiate into heterocysts and thus, those genes were determined to be directly responsible for heterocyst formation (Wong and Meeks, 2001). The main activator for the development of heterocysts is the *hetR* gene, which works simultaneously with *hetF* gene coding, which gives rise to a protein that enhances subsequent transcription of *hetR* (Wolk, 2000; Wong and Meeks, 2002; Zhang et al., 2006). The expression of *ntcA* gene is necessary for the production of proteins that cyanobacteria use to regulate nitrogen and in addition, is involved in activating the transcription of various genes, including the *hetR* gene (Herrero et al., 2001). Studies showed that a mutant species of *Nostoc* with a defective *ntcA* gene failed to infect its host despite retention of hormogonia-forming capacity and therefore might be linked with the activation of other genes required for a successful symbiotic relationship to be established (Vega-Palas et al., 1992; Herrero et al., 2001; Adams et al., 2013). A study by Leganes et al. (1994) in *Anabaena* showed that an altered *hepA* gene disrupts proper formation of the cell envelope in both heterocysts and akinetes. The thickened walls, made up of a polysaccharide layer, are essential for nitrogen fixation activities to be concentrated in the heterocyst cells and prevent oxygen diffusion (Tikhonovich and Provorov, 2007). As a consequence of a non-functional *hepA* gene, normal development of the cell envelope is impossible and affects the ability of the cyanobiont to fix nitrogen in its host (Leganes et al., 1994). Both free-living and symbiotic bacteria have *nif* genes not restricted to cyanobacteria (Corbin et al., 1982; Fay, 1992). Those genes are responsible for forming nitrogenase complexes that convert unusable atmospheric dinitrogen to useful forms like ammonia and in this process, the *nifD* and *nifK* genes encode a dinitrogenase heterotetramer that contains an active site to reduce dinitrogen atoms (Dos Santos et al., 2012). The *nifDK* genes work together with it redox partner, an iron protein encoded by *nifH* gene, to complete the structure and function of nitrogenase complex (Jasniewski et al., 2018). Therefore, these genes are important for maintaining mutual associations with a host because defects in the genes may affect the nitrogen-fixing capacity of the symbiont (Spaink, 1998).

Several genes have been identified, but their significance in symbioses is still poorly understood. A sigma factor gene, *sigH*, which appears to be directed by HIF, might play a role in the ability of symbionts to increase invasion success in a targeted host (Campbell et al., 1998). Likewise, the *ctpH* gene, which is in close proximity with the *sigH* gene, is also controlled by HIF in *Nostoc* (Adams et al., 2013) and has a function in the photosystem II mechanisms in *Synechocystis* (Anbudurai et al., 1994). This gene is interesting as it may have varying physiological roles in different symbiotic strains. Another gene, *tprN,* codes for proteins known to be necessary in various functions, such as regulating the cell cycle, suppressing transcription mechanisms and transporting proteins (Lamb et al., 1995). This gene is also essential for heterocyst maturation process (Campbell et al., 1996). In line with this, Meeks et al. (1999) observed that a silenced *tprN* gene in *N. punctiforme* caused no phenotypic change but the infection rate doubled compared to the wild-type strain, and its transcription elevated when exposed to both HIF and HRF exudates of *A. punctatus*. However, the implications and its involvement in the infection process are still unknown.

LIMITATIONS IN CYCAD-CYANOBACTERIA RESEARCH

A substantial number of studies have focused on the growth and development of coralloid roots and the diversity of the endosymbiont community within the cyanobacterial zone using cultures and 16S identification methods (Costa et al., 1999; Thajuddin et al., 2010; Yamada et al., 2012). The underlying mechanisms, however, have been left unexplored. Probable reasons challenging the study of symbiosis compared to other hosts with a cyanobacterial partner are discussed in this section.

One of the difficulties in this field of research is studying the *in vivo* development of cycad – cyanobacterial symbiosis. To determine the mutualistic interactions exhibited by both partners, a significant length of time, which may take years of research, might be needed to confirm and validate hypotheses as development in cycads takes much time. Tissue culture methods are also lacking for most cycads to facilitate *in vitro* experimental assays that could be used to compare wild-type and symbiont-free conditions. Another reason is the availability of coralloid roots of good quantity and quality. According to McLuckie (1922) cited in Milindasuta (1975) and also based on personal observations, even when coralloid roots are present, a green layer in the cortex may be absent (Nilsson et al., 2006). Moreover, the availability of both root tissue samples and cyanobionts per plant host are often insufficient for experiments, especially when replicates are

needed. Thus, samples are usually pooled using a number of representative hosts. Also, most studies obtain their samples from botanic gardens and not from the wild. Although promising results can still be achieved, gathering samples from natural habitats could add more interesting findings.

Another frustration in this field of research is trying to separate root tissues from the endosymbiont as well as the endosymbiont from the sticky mucilaginous material. Various methods have been proposed (Ferris and Hirsch, 1991; Lindblad et al., 1991; Gehringer et al., 2010), but completely separating them from each requires improvement as most requires manually scraping off the green symbiont from the roots. In determining the functions of cycads and their cyanobionts during symbiosis, the gene expression must be analyzed capturing the symbiotic condition while both partners are together. This eliminates the need to separate them because it would cause changes in gene expression, but poses the more difficult task of how to monitor their association *in vivo*.

CONCLUSION AND FUTURE PERSPECTIVES

Research on coralloid roots is not new, but progress has been quite slow compared to research on *Rhizobia* and other host-cyanobiont associations. Due to the limitations mentioned above, the research field has been confined to studying the diversity of symbionts obtained from various cycad hosts and revalidating previous hypotheses on how both partners benefit from each other. Cruz-Morales et al. (2017) identified novel biosynthetic gene clusters unique to cycad coralloid roots-cyanobacteria symbiosis through genome mining, a research area worth undertaking to understand coevolution and to discover pathways responsible for the synthesis of natural products. With the advancements in genomic research that are becoming more affordable, even for small-scale laboratories, studying cycad host-cyanobiont symbiosis may now move forward at a quicker pace. First, whole genome and transcriptomic sequencing proved to be a valuable source of information regarding genetic functions and evolution (Ran et al., 2010; Li et al., 2018; Eily et al., 2019). In line with this, DNA microarray technology can now be used for analysis of expressed genes of microbes from multiple genomes simultaneously using probes to determine up or downregulated genes. Alternatively, RNA sequencing (RNA-Seq) of cyanobiont genomes approximately 5.4–9.0 Mbp – in obligate cyanobiont *Nostoc azollae* and facultative cyanobiont *Nostoc punctiforme* PCC 73102 of *Azolla filiculoides*, respectively (Ran et al., 2010) and 6.7 Mbp in *Nostoc cycadae* of *Cycas revoluta* (Kanesaki et al., 2018) – can be utilized that could detect new genes and splicing events. Aside from ruling out the need for manual separation of microbe from host tissues, Next generation sequencing (NGS) technology provides high resolution data. Likewise, tissue-specific whole transcriptome profiling might be applied to coralloid root tissues with genome size of about 20–30 Gbp (Wang et al., 2018) for determining expressed genes during symbiosis. Furthermore, gaining bioinformatics skills is necessary to maximize the analysis of the outputs obtained from huge amounts of genomic data.

Cyanobacteria are also valuable sources of metabolites (Haque et al., 2017). Thus, venturing into cycad and/or cyanobiont metabolomics research might help to identify useful products, such biofertilizers, antimicrobials and other natural products of economic importance. It may also facilitate studies on cyanotoxins and biomagnification theories. Likewise, metabolites are also believed to play major roles in cell signaling and communication and could also assist in providing insights on symbiotic pathways and identification of enzymes involved in symbiosis. Many areas of cycad-cyanobacteria symbiosis are still waiting to be explored. With technology rapidly advancing simultaneously with the skills of researchers, restrictions previously deemed overwhelming currently appear to be promising.

AUTHOR CONTRIBUTIONS

TC and AC designed the study. AC gathered the materials and wrote the manuscript. TC, NL, and JD reviewed the manuscript. All authors read and approved the final manuscript.

FUNDING

This work was supported by the special financial project from the National Forestry and Grassland Administration for Rescues and Breeding of Wild Rare and Endangered Species (NL 2017, 2018, and 2019), the Shenzhen Urban Management Bureau (NL 201411), the Shenzhen Key Laboratory of Southern Subtropical Plant Diversity, Fairy Lake Botanical Garden (TC 2017–2019), and South China Botanical Garden (JD 2017–2019), Chinese Academy of Sciences.

ACKNOWLEDGMENTS

We would like to thank Dr. David E. Boufford at Harvard University Herbaria for the help while preparing the manuscript.

REFERENCES

Adams, D. G., Bergman, B., Nierzwicki-Bauer, S. A., Duggan, P. S., Rai, A. N., and Schubler, A. (2013). "Cyanobacterial-plant symbioses," in *The Prokaryotes – Prokaryotic Biology and Symbiotic Associations*, eds E. Rosenberg, E. F. DeLong, S. Lory, E. Stackebrandt, and F. Thompson (Berlin: Springer-Verlag), 359–400. doi: 10.1007/978-3-642-30194-0_17

Adams, D. G., and Duggan, P. (1999). Heterocyst and akinete differentiation in cyanobacteria: Tansley Review No. 107. *New Phytol.* 144, 3–33. doi: 10.1046/j.1469-8137.1999.00505.x

Adams, D. G., and Duggan, P. (2008). Cyanobacteria-bryophyte symbioses. *J. Exp. Bot.* 59, 1047–1058. doi: 10.1093/jxb/ern005

Adams, D. G., and Duggan, P. S. (2012). "Signalling in cyanobacteria–plant symbioses," in *Signaling and Communication in Plant Symbiosis*, eds S. Perotto

and F. Baluška (Berlin: Springer Berlin Heidelberg), 93–121. doi: 10.1007/978-3-642-20966-6_5

Ahern, C. P., and Staff, I. A. (1994). Symbiosis in cycads: the origin and development of coralloid roots in *Macrozamia communis* (Cycadeceae). *Am. J. Bot.* 81, 1559–1570. doi: 10.1002/j.1537-2197.1994.tb11467.x

Anbudurai, P. R., Mor, T. S., Ohad, I., Shestakov, S. V., and Pakrasi, H. B. (1994). The *ctpA* gene encodes for the C-terminal processing protease for the D1 protein of the photosystem II reaction center complex. *Proc. Natl. Acad. Sci. U.S.A.* 91, 8082–8086. doi: 10.1073/pnas.91.17.8082

Banack, S. A., and Cox, P. A. (2003). Biomagnification of cycad neurotoxins in flying foxes: implications for ALS-PDC in Guam. *Neurology* 61, 387–389. doi: 10.1212/01.wnl.0000078320.18564.9f

Banack, S. A., Downing, T. G., Spacil, Z., Purdie, E. L., Metcalf, J. S., Downing, S., et al. (2010). Distinguishing the cyanobacterial neurotoxin β-N-methylamino-L-alanine (BMAA) from its structural isomer 2,4-diaminobutyric acid (2,4-DAB). *Toxicon* 56, 868–879. doi: 10.1016/j.toxicon.2010.06.006

Banack, S. A., Murch, S. J., and Cox, P. A. (2006). Neurotoxic flying foxes as dietary items for the Chamorro people, Marianas Islands. *J. Ethnopharmacol.* 106, 97–104. doi: 10.1016/j.jep.2005.12.032

Bergman, B., Johansson, C., and Soderback, E. (1992). The *Nostoc-Gunnera* symbiosis. *New Phytol.* 122, 379–400. doi: 10.1111/j.1469-8137.1992.tb00067.x

Bergman, B., Matveyev, A., and Rasmussen, U. (1996). Chemical signaling in cyanobacterial-plant symbioses. *Trends Plant Sci.* 1, 191–197. doi: 10.1016/1360-1385(96)10021-2

Bergman, B., Rai, A. N., and Rasmussen, U. (2007). "Cyanobacterial assocations," in *Associative and Endophytic Nitrogen-Fixing Bacteria and Cyanobacterial Associations*, eds C. Elmerich and W. E. Newton (Dordrecht: Springer), 257–301.

Bernhard, A. (2010). The nitrogen cycle: processes, players, and human impact. *Nat. Educ. Knowl.* 3:25.

Brenner, E. D., Stevenson, D. W., and Twigg, R. W. (2003). Cycads: evolutionary innovations and the role of plant-derived neurotoxins. *Trends Plant Sci.* 8, 446–452. doi: 10.1016/s1360-1385(03)00190-0

Brownson, D. M., Mabry, T. J., and Leslie, S. W. (2002). The cycad neurotoxic amino acid, beta-N-methylamino-L-alanine (BMAA), elevates intracellular calcium levels in dissociated rat brain cells. *J. Ethnopharmacol.* 82, 159–167. doi: 10.1016/s0378-8741(02)00170-8

Campbell, E. L., Brahamsha, B., and Meeks, J. C. (1998). Mutation of an alternative sigma factor in the cyanobacterium *Nostoc punctiforme* results in increased infection of its symbiotic plant partner, *Anthoceros punctatus*. *J. Bacteriol.* 180, 4938–4941.

Campbell, E. L., Hagen, K. D., Cohen, M. F., Summers, M. L., and Meeks, J. C. (1996). The *devR* gene product is characteristic of receivers of two-component regulatory systems and is essential for heterocyst development in the filamentous cyanobacterium *Nostoc* sp. strain ATCC 29133. *J. Bacteriol.* 178, 2037–2043. doi: 10.1128/jb.178.7.2037-2043.1996

Campbell, E. L., and Meeks, J. C. (1989). Characteristics of hormogonia formation by symbiotic *Nostoc* spp. in response to the presence of *Anthoceros punctatus* or its extracellular products. *Appl. Environ. Microbiol.* 55, 125–131.

Campbell, E. L., Wong, F. C. Y., and Meeks, J. C. (2003). DNA binding properties of the HrmR protein of *Nostoc punctiforme* responsible for transcriptional regulation of genes involved in the differentiation of hormogonia. *Mol. Microbiol.* 47, 573–582. doi: 10.1046/j.1365-2958.2003.03320.x

Castenholz, R. W., Wilmotte, A., Herdman, M., Rippka, R., Waterbury, J. B., Iteman, I., et al. (2001). "Phylum BX. Cyanobacteria," in *Bergey's Manual of Systematic Bacteriology*, eds D. R. Boone, R. W. Castenholz, and G. M. Garrity (New York, NY: Springer), 473–599. doi: 10.1007/978-0-387-21609-6_27

Chan, C. X., and Bhattacharya, D. (2010). The origin of plastids. *Nat. Educ.* 3:84.

Chang, D. C. N., Grobelaar, N., and Coetzee, J. (1988). SEM observations on cyanobacteria-infected cycad coralloid roots. *S. Afr. J. Bot.* 54, 491–495. doi: 10.1016/s0254-6299(16)31284-4

Cohen, M. F., and Meeks, J. C. (1997). A hormogonium regulating locus, *hrmUA*, of the cyanobacterium *Nostoc punctiforme* strain ATCC 29133 and its response to an extract of a symbiotic plant partner *Anthoceros punctatus*. *Mol. Plant Microbe Interact.* 10, 280–289. doi: 10.1094/mpmi.1997.10.2.280

Corbin, D., Ditta, G., and Helinski, D. R. (1982). Clustering of nitrogen fixation (*nif* genes) in *Rhizobium meliloti*. *J. Bacteriol.* 149, 221–228.

Costa, J. L., and Lindblad, P. (2002). "Cyanobacteria in symbiosis with cycads," in *Cyanobacteria in Symbiosis*, eds A. N. Rai, B. Bergman, and U. Rasmussen (Dordrecht: Kluwer), 195–205. doi: 10.1007/0-306-48005-0_11

Costa, J. L., Paulsrud, P., and Lindblad, P. (1999). Cyanobiont diversity within coralloid roots of selected cycad species. *FEMS Microbiol. Ecol.* 28, 85–91. doi: 10.1016/s0168-6496(98)00095-6

Cox, P. A., Banack, S. A., and Murch, S. J. (2003). Biomagnification of cyanibacterial neurotoxins and neurodegenerative disease among the Chamorro people of Guam. *Proc. Natl. Acad. Sci. U.S.A.* 100, 13380–13383. doi: 10.1073/pnas.2235808100

Cox, P. A., Banack, S. A., Murch, S. J., Rasmussen, U., Tien, G., Bidigare, R. R., et al. (2005). Diverse taxa of cyanobacteria produce β-N-methylamino-L-alanine, a neurotoxic amino acid. *Proc. Natl. Acad. Sci. U.S.A.* 102, 5074–5078. doi: 10.1073/pnas.0501526102

Cox, P. A., and Sacks, O. W. (2002). Cycad neurotoxins, consumption of flying foxes, and ALS-PDC disease in Guam. *Neurology* 58, 956–959. doi: 10.1212/wnl.58.6.956

Cruz-Morales, P., Corona-Gomez, A., Selem-Mojica, N., Perez-Farrera, M. A., Barona-Gomez, F., and Cibrian-Jaramillo, A. (2017). The cycad coralloid root contains a diverse endophytic bacterial community with novel biosynthetic gene clusters unique to its microbiome. *bioRxiv* 1–53.

de Vries, J., and Gould, S. B. (2017). The monoplastidic bottleneck in algae and plant evolution. *J. Cell Sci.* 0, 1–13. doi: 10.1242/jcs.203414

Dos Santos, P. C., Fang, Z., Mason, S. W., Setubal, J. C., and Dixon, R. (2012). Distribution of nitrogen fixation and nitrogenase-like sequences amongst microbial genomes. *BMC Genomics* 13:162. doi: 10.1186/1471-2164-13-162

Douglas, S. E. (1998). Plastid evolution: origins, diversity and trends. *Curr. Opin. Genet. Dev.* 8, 655–661. doi: 10.1016/s0959-437x(98)80033-6

Eily, A. N., Pryer, K. M., and Li, F.-W. (2019). A first glimpse at genes important to the azolla–nostoc symbiosis. *Symbiosis* 78, 149–162. doi: 10.1007/s13199-019-00599-2

Falcon, L. I., Magallon, S., and Castillo, A. (2010). Dating the cyanobacterial ancestor of the chloroplast. *Int. Soc. Microb. Ecol.* 4, 777–783. doi: 10.1038/ismej.2010.2

Fay, P. (1992). Oxygen relations in nitrogen fixation in cyanobacteria. *Microbiol. Rev.* 56, 340–373.

Faye, M., Rancillac, M., and David, A. (1981). Determinism of the mycorrhizogenic root formation in *Pinus pinaster* Sol. *New Phytol.* 87, 557–565. doi: 10.1111/j.1469-8137.1981.tb03226.x

Ferris, M. J., and Hirsch, C. F. (1991). Method for isolation and purification of cyanobacteria. *Appl. Environ. Microbiol.* 57, 1448–1452.

Flores, E. (2012). Restricted cellular differentiation in cyanobacterial filaments. *Proc. Natl. Acad. Sci. U.S.A.* 109, 15080–15081. doi: 10.1073/pnas.1213507109

Gehringer, M. M., Pengelly, J. J. L., Cuddy, W. S., Fieker, C., Forster, P. I, and Neilan, B. A. (2010). Host selection of symbiotic cyanobacteria in 31 species of the Australian cycad genus: *Macrozamia* (Zamiaceae). *Mol. Plant Microbe Interact.* 23, 811–822. doi: 10.1094/MPMI-23-6-0811

Govindjee, and Shevela, D. (2011). Adventures with cyanobacteria: a personal perspective. *Front. Plant Sci.* 2:28. doi: 10.3389/fpls.2011.00028

Green, B. R. (2011). Chloroplast genomes of photosynthetic eukaryotes. *Plant J.* 66, 34–44. doi: 10.1111/j.1365-313x.2011.04541.x

Grilli Caiola, M. (1980). On the phycobionts of the cycad coralloid roots. *New Phytol.* 85, 537–544. doi: 10.1111/j.1469-8137.1980.tb00769.x

Grilli Caiola, M., and Canini, A. (1993). Structure and physiology of Cycad coralloid roots. *G. Bot. Ital.* 127, 428–445. doi: 10.1111/j.1574-6941.2012.01403.x

Grilli Caiola, M., and Pellegrini, S. (1979). Effects of various nitrogen sources on *Nostoc punctiforme* (Kützing). *Caryologia* 32, 485–498. doi: 10.1080/00087114.1979.10796812

Grobbelaar, N., Scott, W. E., Hattingh, W., and Marshall, J. (1987). The identification of the coralloid root endophytes of the southern African cycads and the ability of the isolates to fix dinitrogen. *S. Afr. J. Bot.* 53, 111–118. doi: 10.1016/s0254-6299(16)31444-2

Gutiérrez-García, K., Bustos-Díaz, E. D., Corona-Gómez, J. A., Ramos-Aboites, H. E., Sélem-Mojica, N., Cruz-Morales, P., et al. (2019). Cycad coralloid roots contain bacterial communities including cyanobacteria and *Caulobacter* spp. that encode niche-specific biosynthetic gene clusters. *Genome Biol. Evol.* 11, 319–334. doi: 10.1093/gbe/evy266

Halliday, J., and Pate, J. (1976). Symbiotic nitrogen fixation by coralloid roots of the Cycad *Macrozamia riedlei*: physiological characteristics and ecological significance. *Aust. J. Plant Physiol.* 3, 349–358.

Haque, F., Banayan, S., Yee, J., and Chiang, Y. W. (2017). Extraction and applications of cyanotoxins and other cyanobacterial secondary metabolites. *Chemosphere* 183, 164–175. doi: 10.1016/j.chemosphere.2017.05.106

Haselkorn, R. (2016). Cyanobacteria. *Curr. Biol.* 19, 277–278.

Hashidoko, Y., Nishizuka, H., Tanaka, M., Murata, K., Murai, Y., and Hashimoto, M. (2019). Isolation and characterization of 1-palmitoyl-2-linoleoyl-sn-glycerol as a hormogonium-inducing factor (HIF) from the coralloid roots of *Cycas revoluta* (Cycadaceae). *Sci. Rep.* 9:4751. doi: 10.1038/s41598-019-39647-8

Henskens, F. L., Green, T. G., and Wilkins, A. (2012). Cyanolichens can have both cyanobacteria and green algae in a common layer as a major contributors to photosynthesis. *Ann. Bot.* 110, 555–563. doi: 10.1093/aob/mcs108

Hernández-Muñiz, W., and Stevens, S. E. (1987). Characterization of the motile hormogonia of *Mastigocladus laminosus*. *J. Bacteriol.* 169, 218–223. doi: 10.1128/jb.169.1.218-223.1987

Herrero, A., Muro-Pastor, A. M., and Flores, E. (2001). Nitrogen control in cyanobacteria. *J. Bacteriol.* 183, 411–425. doi: 10.1128/jb.183.2.411-425.2001

Hoffman, B. M., Lukoyanov, D., Yang, Z. Y., Dean, D. R., and Seefeldt, L. C. (2014). Mechanism of nitrogen fixation by nitrogenase: the next stage. *Chem. Rev.* 114, 4041–4062. doi: 10.1021/cr400641x

Jackson, O., Taylor, O., Adams, D. G., and Knox, J. P. (2012). Arabinogalactan proteins occur in the free-living cyanobacterium genus *Nostoc* and in plant–*Nostoc* symbioses. *MPMI* 25, 1338–1349. doi: 10.1094/MPMI-04-12-0095-R

Jasniewski, A. J., Sickerman, N. S., Hu, Y., and Ribbe, M. W. (2018). The fe protein: an unsung hero of nitrogenase. *Inorganics* 6:25. doi: 10.3390/inorganics6010025

Jiang, G. F., Hinsinger, D. D., and Strijk, J. S. (2016). Comparison of intraspecific, interspecific and intergeneric chloroplast diversity in Cycads. *Sci. Rep.* 6:31473. doi: 10.1038/srep31473

Jiang, L., Aigret, B., De Borggraeve, W. M., Spacil, Z., and Ilag, L. L. (2012). Selective LC-MS/MS method for the identification of BMAA from its isomers in biological samples. *Anal. Bioanal. Chem.* 403, 1719–1730. doi: 10.1007/s00216-012-5966-y

Kanesaki, Y., Hirose, M., Hirose, Y., Fujisawa, T., Nakamura, Y., Watanabe, S., et al. (2018). Draft genome sequence of the nitrogen-fixing and hormogonia-inducing cyanobacterium *Nostoc cycadae* strain WK-1, isolated from the coralloid roots of *Cycas revoluta*. *Genome Announc.* 6:e00021-18. doi: 10.1128/genomeA.00021-18

Kaplan-Levy, R. N., Hadas, O., Summers, M. L., Rücker, J., and Sukenik, A. (2010). "Akinetes: dormant cells of Cyanobacteria," in *Dormancy and Resistance in Harsh Environments. Topics in Current Genetics*, eds E. Lubzens, J. Cerda, and M. Clark (Berlin: Springer), 5–27. doi: 10.1007/978-3-642-12422-8_2

Khayatan, B., Bains, D. K., Cheng, M. H., Cho, Y. W., Hyunh, J., Kim, R., et al. (2017). A putative O-linked β-N-acetylglucosamine transferase is essential for hormogonium development and motility in the filamentous cyanobacterium *Nostoc punctiforme*. *J. Bacteriol.* 199:e00075-17.

Kluge, M., Mollenhauer, D., Mollenhauer, R., and Kape, R. (1992). *Geosiphon pyriforme*, an endosymbiotic consortium of a fungus and a cyanobacterium (*Nostoc*), fixes nitrogen. *Bot. Acta* 105, 343–344. doi: 10.1111/j.1438-8677.1992.tb00309.x

Krings, M., Hass, H., Kerp, H., Taylor, T. N., Agerer, R., and Dotzler, N. (2009). Endophytic cyanobacteria in a 400-million-yr-old land plant: a scenario for the origin of a symbiosis? *Rev. Palaeobot. Palynol.* 153, 62–69. doi: 10.1016/j.revpalbo.2008.06.006

Kumar, K., Mella-Herrera, R. A., and Golden, J. W. (2010). Cyanobacterial heterocysts. *Cold Spring Harb. Perspect. Biol.* 2:a000315. doi: 10.1101/cshperspect.a000315

Kuypers, M. M. (2015). Microbiology: a division of labour combined. *Nature* 528, 487–488. doi: 10.1038/528487a

Lamb, J. R., Tugendreich, S., and Hieter, P. (1995). Tetratrico peptide repeat interaction: to TPR or not to TPR? *Trends Biochem. Sci.* 20, 257–259. doi: 10.1016/s0968-0004(00)89037-4

Leganes, F., Fernandez-Piñas, F., and Wolk, C. P. (1994). Two mutations that block heterocyst differentiation have different effects on akinete differentiation in *Nostoc ellipsosporum*. *Mol. Microbiol.* 12, 679–684. doi: 10.1111/j.1365-2958.1994.tb01055.x

Li, F. W., Brouwer, P., Carretero-Paulet, L., Cheng, S., de Vries, J., Delaux, P. M., et al. (2018). Fern genomes elucidate land plant evolution and cyanobacterial symbioses. *Nat. Plants* 4, 460–472. doi: 10.1038/s41477-018-0188-8

Lindblad, P. (2009). Cyanobacteria in symbiosis with cycads. *Microbiol. Monogr.* 8, 225–233. doi: 10.1007/7171_2008_118

Lindblad, P., Atkins, C. A., and Pate, J. S. (1991). N2-Fixation by freshly isolated *Nostoc* from coralloid roots of the cycad *Macrozamia riedlei* (Fisch. ex Gaud.) Gardn. *Plant Physiol.* 95, 753–759. doi: 10.1104/pp.95.3.753

Lindblad, P., Hallblom, L., and Bergman, B. (1985b). The cyanobacterium-*Zamia* symbiosis: C2H2 reduction and heterocyst frequency. *Symbiosis* 1, 19–28.

Lindblad, P., Bergman, B., Hofsten, A. V., Hallblom, L., and Nylund, J. E. (1985a). The cyanobacterium-*Zamia* symbiosis: an ultrastructural study. *New Phytol.* 101, 707–716. doi: 10.1111/j.1469-8137.1985.tb02876.x

Lindblad, P., Rai, A. N., and Bergman, B. (1987). The *Cycas revoluta–Nostoc* symbiosis: enzyme activities of nitrogen and carbon metabolism in the cyanobiont. *J. Gen. Microbiol.* 133, 1695–1699. doi: 10.1099/00221287-133-7-1695

Lobakova, E. S., Dubravina, G. A., and Zagoskina, N. V. (2004). Formation of phenolic compounds in apogeotrophic roots of cycad plants. *Russ. J. Plant Physiol.* 51, 486–493. doi: 10.1023/b:rupp.0000035741.31754.e6

Long, S. R. (1989). Rhizobium-legume nodulation: life together in the underground. *Cell* 56, 203–214. doi: 10.1016/0092-8674(89)90893-3

Marler, T. E., Snyder, L. R., and Shaw, C. A. (2010). *Cycas micronesia* (Cycadales) plants devoid of endophytic cyanobacteria increase in beta-methylamino-L-alanine. *Toxicon* 56, 563–568. doi: 10.1016/j.toxicon.2010.05.015

Martin, W. F., Garg, S., and Zimorski, V. (2015). Endosymbiotic theories for eukaryote origin. *Philos. Trans. R. Soc. B* 370:20140330. doi: 10.1098/rstb.2014.0330

McLuckie, J. (1922). Studies in symbiosis II The apogeotropic roots of macrozamia spiralis and their physiological significance. *Proc. Linn. Soc. N.S.W.* 47, 319–328.

Meeks, J. C. (1998). Symbiosis between nitrogen-fixing cyanobacteria and plants. *Bioscience* 48, 266–276. doi: 10.2307/1313353

Meeks, J. C., Campbell, E., Hagen, K., Hanson, T., Hitzeman, N., and Wong, F. (1999). "Developmental alternatives of symbiotic *Nostoc punctiforme* in response to its symbiotic partner *Anthoceros punctatus*," in *The Phototrophic Prokaryotes*, eds G. A. Peschek, W. Loffelhardt, and G. Schmetterer (New York, NY: Kluwer/Plenum), 665–678. doi: 10.1007/978-1-4615-4827-0_77

Meeks, J. C., and Elhai, J. (2002). Regulation of cellular differentiation in filamentous cyanobacteria in free-living and plant-associated symbiotic growth states. *Microbiol. Mol. Biol. Rev.* 66, 94–121. doi: 10.1128/mmbr.66.1.94-121.2002

Meeks, J. C., Elhai, J., Thiel, T., Potts, M., Larimer, F., Lamerdin, J., et al. (2001). An overview of the genome of *Nostoc punctiforme*, a multicellular, symbiotic cyanobacterium. *Photosynth. Res.* 70, 85–106.

Meneely, J. P., Chevallier, O. P., Graham, S., Greer, B., Green, B. D., and Elliott, C. T. (2016). β-methylamino-L-alanine (BMAA) is not found in the brains of patients with confirmed Alzheimer's disease. *Sci. Rep.* 6:36363. doi: 10.1038/srep36363

Metcalf, J. S., Lobner, D., Banack, S. A., Cox, G. A., Nunn, P. B., Wyatt, P. B., et al. (2017). Analysis of BMAA enantiomers in cycads, cyanobacteria, and mammals: in vivo formation and toxicity of d-BMAA. *Amino Acids* 49, 1427–1439. doi: 10.1007/s00726-017-2445-y

Milindasuta, B. E. (1975). Developmental anatomy of coralloid roots in cycads. *Am. J. Bot.* 62, 468–472. doi: 10.1002/j.1537-2197.1975.tb14071.x

Narainsamy, K., Marteyn, B., Sakr, S., Cassier-Chauvat, C., and Chauvat, F. (2013). Genomics of the pleiotropic glutathione system in cyanobacteria (Chapter 5). *Adv. Bot. Res.* 65, 157–188. doi: 10.1016/b978-0-12-394313-2.00005-6

Nilsson, M., Rasmussen, U., and Bergman, B. (2006). Cyanobacterial chemotaxis to extracts of host and nonhost plants. *FEMS Microbiol. Ecol.* 55, 382–390. doi: 10.1111/j.1574-6941.2005.00043.x

Norstog, K. J., and Nicholls, T. J. (1997). *The Biology of the Cycads*. Ithaca, NY: Cornell University Press.

Obukowicz, M., Schallerm, M., and Kennedy, G. S. (1981). Ultrastructure and phenolic histochemistry of the *Cycas revoluta-Anabaena* symbiosis. *New Phytol.* 87, 751–759. doi: 10.1111/j.1469-8137.1981.tb01711.x

Pennell, R. I. (1992). "Cell surface arabinogalactan proteins, arabinogalactans and plant development," in *Perspectives in Plant Cell Recognition*, eds J. A. Collow and J. R. Green (Cambridge: Cambridge University Press), 105–121.

Pereira, A. L. (2017). *The Unique Symbiotic System Between a Fern and a Cyanobacterium, Azolla-Anabaena azollae: Their potential as biofertilizer, feed, and remediation*. London: IntechOpen.

Peters, G. A., and Perkins, S. K. (1993). The *Azolla-Anabaena* symbiosis: endophyte continuity in the *Azolla* life cycle is facilitated by epidermal trichomes I: partitioning of endophytic Anabaena into developing sporocarps. *New Phytol.* 123, 53–64. doi: 10.1111/j.1469-8137.1993.tb04531.x

Polsky, F. I., Nunn, P. B., and Bell, E. A. (1972). Distribution and toxicity of α-amino-β-methylaminopropionic acid. *Fed. Proc.* 31, 1473–1475.

Ran, L., Larsson, J., Vigil-Stenman, T., Nylander, J. A. A., Ininbergs, K., Zheng, W. W., et al. (2010). Genome erosion in a nitrogen-fixing vertically transmitted endosymbiotic multicellular cyanobacterium. *PLoS One* 5:e11486. doi: 10.1371/journal.pone.0011486

Raven, J. A., and Allen, J. F. (2003). Genomics and chloroplast evolution: what did cyanobacteria do for plants? *Genome Biol.* 4:209.

Rikkinen, J. (2015). Cyanolichens. *Biodivers. Conserv.* 24, 973–993. doi: 10.1007/s10531-015-0906-8

Roodt, D., Lohaus, R., Sterck, L., Swanepoel, R. L., Van de Peer, Y., and Mizrachi, E. (2017). Evidence for an ancient whole genome duplication in the cycad lineage. *PLoS One* 12:e0184454. doi: 10.1371/journal.pone.0184454

Rosén, J., and Hellenäs, K. E. (2008). Determination of the neurotoxin BMAA (beta-N-methylamino-L-alanine) in cycad seed and cyanobacteria by LC-MS/MS (liquid chromatography tandem mass spectrometry). *Analyst* 133, 1785–1789. doi: 10.1039/b809231a

Sand-Jensen, K. (2014). Ecophysiology of gelatinous *Nostoc* colonies: unprecedented slow growth and survival in resource-poor and harsh environments. *Ann. Bot.* 114, 17–33. doi: 10.1093/aob/mcu085

Sarma, M. K., Kaushik, S., and Goswami, P. (2016). Cyanobacteria: a metabolic power house for harvesting solar energy to produce bio-electricity and biofuels. *Biomass Bioenergy* 90, 187–201. doi: 10.1016/j.biombioe.2016.03.043

Schopf, J. W. (2011). "The fossil record: tracing the roots of the cyanobacterial lineage," in *The Ecology of Cyanobacteria*, eds B. A. Whitton and M. Potts (Dordrecht: Kluwer Academic Publishers), 13–35. doi: 10.1007/0-306-46855-7_2

Seifert, G. J., and Roberts, K. (2007). The biology of arabinogalactan proteins. *Annu. Rev. Plant Biol.* 58, 137–161.

Shestakov, S. V., and Karbysheva, E. A. (2017). The origin and evolution of cyanobacteria. *Biol. Bull. Rev.* 7, 259–272. doi: 10.1134/s2079086417040090

Snyder, L. R., and Marler, T. E. (2011). Rethinking cycad metabolite research. *Commun. Integr. Biol.* 4, 86–88. doi: 10.4161/cib.4.1.14084

Spaink, H. P. (1998). *The Rhizobiaceae: Molecular Biology of Model Plant-Associated Bacteria*. Berlin: Springer.

Steele-King, C. G., Willats, W. G. T., and Paul Knox, J. (2000). "Arabinogalactan-proteins and cell development in roots and somatic embryos," in *Cell and Developmental Biology of Arabinogalactan-Proteins*, eds E. A. Nothnagel, A. Bacic, and A. E. Clarkecpesnm (Boston, MA: Springer).

Stewart, I., and Falconer, I. R. (2011). "Cyanobacteria and cyanobacterial toxins," in *Oceans and Human Health: Risks and Remedies from the Seas*, eds P. J. Walsh, S. Smith, L. Fleming, H. Solo-Gabriele, and W. H. Gerwick (Cambridge, MA: Academic Press), 271–296.

Suárez-Moo, P. D. J., Vovides, A. P., Griffith, M. P., Barona-Gómez, F., and Cibrián-Jaramillo, A. (2019). Unlocking a high bacterial diversity in the coralloid root microbiome from the cycad genus Dioon. *PLoS One* 14:e0211271. doi: 10.1371/journal.pone.0211271

Sukenik, A., Beardall, J., and Hadas, O. (2007). Photosynthetic characterization of developing and mature akinetes of *Aphanizomenon ovalisporum* (Cyanoprokaryota). *J. Phycol.* 43, 780–788. doi: 10.1111/j.1529-8817.2007.00374.x

Thajuddin, N., Muralitharan, G., Sundaramoorthy, M., Ramamoorthy, R., Ramachandran, S., Akbarsha, M. A., et al. (2010). Morphological and genetic diversity of symbiotic cyanobacteria from cycads. *J. Basic Microbiol.* 50, 254–265. doi: 10.1002/jobm.200900343

Tikhonovich, I. A., and Provorov, N. A. (2007). "Beneficial plant-microbe interactions," in *Studies in Plant Science: Comprehensive and Molecular Phytopathology*, eds Y. T. Dyakov, T. Korpela, and V. G. Dzhavakhiya (Amsterdam: Elsevier), 365–420. doi: 10.1016/b978-044452132-3/50018-3

Usher, K. M., Bergman, B., and Raven, J. A. (2007). Exploring cyanobacterial mutualisms. *Annu. Rev. Ecol. Evol. Syst.* 38, 255–273. doi: 10.1146/annurev.ecolsys.38.091206.095641

Vega, A., and Bell, E. A. (1967). α-amino-β-methylaminopropionic acid, a new amino acid from seeds of *Cycas circinalis*. *Phytochemistry* 6, 759–762. doi: 10.1016/s0031-9422(00)86018-5

Vega-Palas, M. A., Flores, E., and Herrero, A. (1992). NtcA, a global nitrogen regulator from the cyanobacterium *Synechococcus* that belongs to the Crp family of bacterial regulators. *Mol. Microbiol.* 6, 1853–1859. doi: 10.1111/j.1365-2958.1992.tb01357.x

Walsh, P. J., Smith, S., Fleming, L., Solo-Gabriele, H., and Gerwick, W. H. (2011). *Cyanobacteria and Cyanobacterial Toxins. Oceans and Human Health: Risks and Remedies from the Seas*. Cambridge, MA: Academic Press, 271–296.

Wang, Y., Li, N., Chen, T., and Gong, Y. (2018). Generation and characterization of expressed sequence tags (ESTs) from coralloid root cDNA library of *Cycas debaoensis*. *Plant Divers.* 40, 245–252. doi: 10.1016/j.pld.2018.09.002

Warshan, D. (2017). *Cyanobacteria in Symbiosis with Boreal Forest Feathermosses: From Genome Evolution and Gene Regulation to Impact on the Ecosystem*. PhD Dissertation, Stockholm University: Stockholm.

Wolk, C. P. (2000). "Heterocyst formation in *Anabaena*," in *Prokaryotic Development*, eds Y. V. Brun and L. J. Shimkets (Washington, DC: ASM Press), 83–104. doi: 10.1128/9781555818166.ch4

Wong, F. C. Y., and Meeks, J. C. (2002). Establishment of functional symbiosis between the cyanobacterium *Nostoc punctiforme* and the bryophyte *Anthoceros punctatus* requires genes involved in nitrogen control and initiation of heterocyst differentiation. *Microbiology* 148, 315–323. doi: 10.1099/00221287-148-1-315

Wong, F. C. Y., and Meeks, J. C. (2001). The *hetF* gene product is essential to heterocyst differentiation and affects HetR function in the cyanobacterium *Nostoc punctiforme*. *J. Bacteriol.* 183, 2654–2661. doi: 10.1128/JB.183.8.2654-2661.2001

Wu, C. S., and Chaw, S. M. (2015). Evolutionary stasis in cycad plastomes and the first case of plastome GC-biased gene conversion. *Genome Biol. Evol.* 7, 2000–2009. doi: 10.1093/gbe/evv125

Wu, C. S., Chaw, S. M., and Huang, Y. Y. (2013). Chloroplast phylogenomics indicates that *Ginkgo biloba* is sister to cycads. *Genome Biol. Evol.* 5, 243–254. doi: 10.1093/gbe/evt001

Wu, C. S., Wang, Y. N., Liu, S. M., and Chaw, S. M. (2007). Chloroplast genome (cpDNA) of *Cycas taitungensis* and 56 cp protein-coding genes of *Gnetum parvifolium*: insights into cpDNA evolution and phylogeny of extant seed plants. *Mol. Biol. Evol.* 24, 1366–1379. doi: 10.1093/molbev/msm059

Yamada, S., Ohkubo, S., Miyashita, H., and Setoguchi, H. (2012). Genetic diversity of symbiotic cyanobacteria in *Cycas revoluta* (Cycadaceae). *FEMS Microbiol. Ecol.* 81, 696–706. doi: 10.1111/j.1574-6941.2012.01403.x

Zhang, C. C., Laurent, S., Sakr, S., Peng, L., and Bedu, S. (2006). Heterocyst differentiation and pattern formation in cyanobacteria: a chorus of signals. *Mol. Microbiol.* 59, 367–375. doi: 10.1111/j.1365-2958.2005.04979.x

Zheng, W., Song, T., Bao, X., Bergman, B., and Rasmussen, U. (2002). High cyanobacterial diversity in coralloid roots of cycads revealed by PCR fingerprinting. *FEMS Microbiol. Ecol.* 40, 215–222. doi: 10.1111/j.1574-6941.2002.tb00954.x

Zurita, J., Zguna, N., Andrys, R., Strzelczak, A., Jiang, L., Thorsen, G., et al. (2019). Chiral analysis of b-methylamino alanine (BMAA) enantiomers after (+)-1-(9-fluorenyl)-ethyl chloroformate (FLEC) derivatization and LC-MS/MS. *Anal. Methods* 11, 432–442. doi: 10.1039/c8ay02287a

Conflict of Interest Statement: The authors declare that the research was conducted in the absence of any commercial or financial relationships that could be construed as a potential conflict of interest.

frontiers in Plant Science

ORIGINAL RESEARCH
published: 07 February 2020
doi: 10.3389/fpls.2019.01779

The Non-Legume *Parasponia andersonii* Mediates the Fitness of Nitrogen-Fixing Rhizobial Symbionts Under High Nitrogen Conditions

Simon E. Dupin[1,2*], *René Geurts*[2†] *and E. Toby Kiers*[1†]

[1] Department of Ecological Science, Vrije Universiteit Amsterdam, Amsterdam, Netherlands, [2] Department of Plant Sciences, Wageningen University, Wageningen, Netherlands

OPEN ACCESS

Edited by:
Kevin Garcia,
North Carolina State University,
United States

Reviewed by:
Sergio Svistoonoff,
Institut de Recherche pour le Développement (IRD), France
Oswaldo Valdes-Lopez,
National Autonomous University of Mexico, Mexico

***Correspondence:**
Simon E. Dupin
sd.dupin@gmail.com

[†]These authors have contributed equally to this work

Specialty section:
This article was submitted to Plant Microbe Interactions, a section of the journal Frontiers in Plant Science

Received: 18 March 2019
Accepted: 20 December 2019
Published: 07 February 2020

Citation:
Dupin SE, Geurts R and Kiers ET (2020) The Non-Legume Parasponia andersonii Mediates the Fitness of Nitrogen-Fixing Rhizobial Symbionts Under High Nitrogen Conditions. Front. Plant Sci. 10:1779. doi: 10.3389/fpls.2019.01779

Organisms rely on symbiotic associations for metabolism, protection, and energy. However, these intimate partnerships can be vulnerable to exploitation. What prevents microbial mutualists from parasitizing their hosts? In legumes, there is evidence that hosts have evolved sophisticated mechanisms to manage their symbiotic rhizobia, but the generality and evolutionary origins of these control mechanisms are under debate. Here, we focused on the symbiosis between *Parasponia* hosts and N_2-fixing rhizobium bacteria. *Parasponia* is the only non-legume lineage to have evolved a rhizobial symbiosis and thus provides an evolutionary replicate to test how rhizobial exploitation is controlled. A key question is whether *Parasponia* hosts can prevent colonization of rhizobia under high nitrogen conditions, when the contribution of the symbiont becomes nonessential. We grew *Parasponia andersonii* inoculated with *Bradyrhizobium elkanii* under four ammonium nitrate concentrations in a controlled growth chamber. We measured shoot and root dry weight, nodule number, nodule fresh weight, nodule volume. To quantify viable rhizobial populations *in planta*, we crushed nodules and determined colony forming units (CFU), as a rhizobia fitness proxy. We show that, like legumes and actinorhizal plants, *P. andersonii* is able to control nodule symbiosis in response to exogenous nitrogen. While the relative host growth benefits of inoculation decreased with nitrogen fertilization, our highest ammonium nitrate concentration (3.75 mM) was sufficient to prevent nodule formation on inoculated roots. Rhizobial populations were highest in nitrogen free medium. While we do not yet know the mechanism, our results suggest that control mechanisms over rhizobia are not exclusive to the legume clade.

Keywords: *Parasponia*, nitrogen fixing bacteria, plant nutrition, host control, rhizobium fitness, nitrogen fertilizer, non-legume, nodulation

INTRODUCTION

Symbiotic partnerships have transformed the Earth's nutrient cycles and facilitated rapid adaptation of species to divergent new niches (Joy, 2013; McFall-Ngai et al., 2013; Oldroyd, 2013). Because almost all organisms rely on symbiotic associations for some form of metabolism, protection, or energy (Bronstein, 2015), this immense symbiotic microbial world has been called "the biggest frontier that biology has presented us in a long time" (Carey, 2015).

Despite their importance, understanding the origins and evolutionary trajectories of symbiotic partnerships remains a major challenge. The problem is that mutual benefit does not guarantee evolutionary stability, and partnerships can be vulnerable to exploitation (Sachs and Simms, 2006; Kiers and Denison, 2008; Sachs et al., 2011; Sachs and Hollowell, 2012). What prevents microbial mutualists from defecting from symbiotic cooperation and parasitizing their hosts? This is a question being asked across a diversity of host organisms, from plants and insects to humans (Werner et al., 2014; Hallam and McCutcheon, 2015; Keeling et al., 2015; Werner et al., 2015). While it is appreciated that symbiosis is a key underlying mechanism behind the complexity of life, we do not have a general understanding of how symbiotic associations are controlled and harnessed (Keeling et al., 2015).

The legume-rhizobia N_2 fixing symbiosis has become an emerging model system in evolutionary biology to study host control (Kiers et al., 2006; Kiers et al., 2007; Oono et al., 2009; Porter and Simms, 2014; Regus et al., 2015; Westhoek et al., 2017; Porter et al., 2019). Host plants employ a range of (non-exclusive) strategies to maximize rhizobial benefits, including: 1) pre-nodule control in which the plant evolved high levels of specificity to achieve species, or even strain-specific selection on rhizobial partners, and 2) control based on rhizobial performance, such that higher performing nodules receive proportionally more resources than poor performing nodules (Kiers and Denison, 2008; Westhoek et al., 2017). Because signaling (i.e., pre-nodule control) can be vulnerable to partners that cheat by evolving the correct signal while providing few resources (Edwards and Yu, 2007), it is thought that some form of basal nodule-level control is necessary to prevent rhizobial exploitation (Denison and Kiers, 2011; Regus et al., 2017a; Kiers et al., 2003; Kiers et al., 2006; Oono et al., 2011).

Control of exploitation is particularly important when plant hosts have direct access to high levels of nitrogen in the soil. Under these conditions, the nitrogen benefits provided by the rhizobial symbiont become redundant with nitrogen provided by the environment. Hosts are therefore expected to evolve mechanisms which prevent nodule formation when grown in high nitrogen soils (Regus et al., 2017b). While such regulatory pathways have been documented in legume species (Streeter and Wong, 1988; Cabeza et al., 2014; Soyano et al., 2014; Nishida et al., 2016; Nishida and Suzaki, 2018), the generality of these control mechanisms are unknown (Heath et al., 2010; Regus et al., 2014; Regus et al., 2015).

Our aim was to study host control mechanisms outside the legumes. We focused on the non-legume *Parasponia andersonii* (Cannabaceae). The genus *Parasponia* is composed of pioneer plant species typically found on nitrogen poor slopes of volcanic hills in the Malay Archipelago. *Parasponia* is the only lineage outside the legume family to be able to form a nodule symbiosis with rhizobium (Trinick, 1973; Trinick and Galbraith, 1980; Trinick and Hadobas, 1988). Recent phylogenomic studies suggest that nodule symbioses with diazotrophic bacteria share a single evolutionary origin (Griesmann et al., 2018; van Velzen et al., 2019). As the *Parasponia* and legumes diverged >100 million years ago, microbial partner selection strategies were shaped independently in both lineages (van Velzen et al., 2019). Therefore, *Parasponia* is a unique evolutionary replicate of rhizobium symbiosis that allows us to better understand the evolutionary origins of control mechanisms.

In legumes, such *Glycine max*, past work has shown that the severity of symbiont control is mediated by the addition of external nitrate—as nitrogen availability increases, the host reduces resources allocated to the symbiont. Because soil nitrate is generally less costly for legumes compared to biologically fixed nitrogen, this leads to an inhibition or severe reduction of legume nodule formation (Streeter and Wong, 1988; Voisin et al., 2002; Wendlandt et al., 2018; Regus et al., 2017b). This process, however, is not well understood in non-legumes. In *Parasponia*, early work has shown nodules can continue to form in high nitrogen environments (Becking, 1983b), but whether rhizobia remain viable in nodules under high nitrogen conditions is unknown. This is important because in *Parasponia* nodules, rhizobium are not terminally differentiated (Alunni and Gourion, 2016). This means that the endosymbiont population within nodules can replicate, and will be added to the soil population upon nodule senescence. Can non-legumes control symbionts under conditions when the symbionts become a cost rather than a benefit? Studying the existence of control patterns has been particularly challenging in *Parasponia* nodules due to the difficulty of growing these tropical trees in greenhouses, and the small size of their nodules compared to most model legumes. Typical metrics, such as growth parameters of individual nodules, poly-3-hydroxybutyrate (PHB) content, and rhizobial fitness measures, have been historically difficult to obtain.

Here we study the effects of increasing nitrogen fertilization on the symbiosis between *P. andersonii* and the rhizobial symbiont *Bradyrhizobium elkanii*. Our aim was to ask if fertilization: 1) reduced or eliminate the growth benefits of rhizobial nodulation for *P. andersonii*, and 2) reduced the fitness benefits for the rhizobial symbiont. If *Parasponia* has evolved effective mechanisms to control nodulation under high nitrogen, then we expect increasing fertilization to be correlated with negative fitness consequences for rhizobia. If these mechanisms are costly for the host to enact, then we expect to see a host growth depression in the presence—but not absence—of a rhizobial symbiont under the high nitrogen treatments.

We grew plants under 0, 0.0375, 0.375, 3.75 mM ammonium nitrate concentrations, either with or without rhizobial inoculation. Our four levels were chosen to represent specific ecological challenges for the host-symbiont, namely: i) when *Parasponia* depends entirely on its symbiont for nitrogen input (0 and

0.0375 mM), ii) when benefits from inoculation are minimal (0.375 mM), iii) when benefits from inoculation are absent/negative (3.75 mM). After 4 weeks, we quantified shoot and root dry weight, nodule number, and nodule fresh weight. We developed an imaging protocol to measure the projected surface of individual nodule areas and then converted it to volume as a second metric for rhizobia benefit. We crushed nodules for measures of colony forming units (CFU) to determine rhizobial populations per nodule. Together, these metrics (nodule number, biomass, volume, and CFUs) provided us with a proxy for *in planta* rhizobial fitness that allowed us to better understand host control in non-legumes.

MATERIALS AND METHODS

Seed Germination

We harvested fresh berries from *in-vitro* propagated *Parasponia andersonii* trees genotype W1-14 (Van Velzen et al., 2018) maintained in a tropical greenhouse. We extracted the seeds from the berries by soaking them in water and gentle rubbing against a fine sieve. We surface sterilized all seeds in 4% sodium hypochlorite for 15 min and washed seven times with sterile MQ water. We induced germination by temperature cycle (4 h 28°C, 4 h 7°C) for 12 days. We incubated seed on Schenk and Hildebrandt medium agar plates for 10 days until cotyledons were fully emerged.

Experimental Design and Plant Growth

We prepared the growing medium of sterile perlite and sterile river sand. We added 210 g of each perlite mixture to 10 sterile polypropylene containers (OS140box, Duchefa Biochemie) allowing for better gas exchange. Per pot, we placed 4 cm^3 of the river sand mixture to transfer the seedling and avoid root desiccation. We used a factorial design experiment consisting of two rhizobia conditions, four nitrogen levels, and 10 replicates per treatment (2 x 4 x 10 = 80 pots).

Inoculation and Nitrogen Treatments

To inoculate *P. andersonii*, we chose the highly efficient nodulating strain *B. elkanii* WUR3 (Op den Camp et al., 2012). To prepare the inoculum, we grew a WUR3 pre-culture from a single colony in liquid peptone-salts-yeast (PSY) medium at 28°C, 60 rpm (Regensburger and Hennecke, 1983). One milliliter of the pre-culture OD_{600} = 0.8 was used to inoculate a 200 ml Erlenmeyer culture. We harvested the culture by centrifugation [10 min at 3,500 x relative centrifugal force (rcf)] at OD_{600} = 0.8. We suspended the cells in the different EKM (Becking, 1983a) solutions to an OD_{600} = 0.05. The nitrogen treatments were based on an EKM-medium with four levels (0, 0.0375, 0.375, and 3.75 mM) ammonium nitrate. Nitrogen and rhizobia inoculum were added by saturating the perlite and river sand with the four EKM-medium prior to transferring the seedlings to pots. Non-inoculated controls received EKM solutions (see below) but without the rhizobia culture. We then randomly placed the pots on a growth chamber table under a 16/8 h light cycle, temperature 26/24°C, light intensity 185 µmol/m2/s, and a relative humidity of 90%.

Harvest

We harvested plants after 30 days. We carefully washed off the perlite and sand from the root systems. We counted nodules and harvested each one individually. We then used binoculars equipped with a Nikon camera (DS–Fi2) to image each nodule. To obtain nodule volume, we extracted and measured the area and perimeter of the nodules photographed using FIJI (Schindelin et al., 2012). We calculated the corresponding prolate spheroid volume using the best fitted ellipse of each nodule based on a previously developed formula (Nedomová et al., 2014). We weighed nodules and kept them at 4°C in 0.9% NaCl solution until they could be crushed for fitness assays. We separated shoots and roots, dried them 72 h at 60°C, and weighed them.

Metrics for Rhizobial Fitness Proxies

To determine a fitness proxy for rhizobia per plant, we surface sterilized all nodules with 96% ethanol for 20 s, 4% sodium hypochlorite for 1 min, and washed seven times with sterile water. We crushed nodules in 150 µl 0.9% sterile saline solution. Fifty microliters of the crushed nodules was diluted in series and both 10,000 and 100,000 dilutions were streaked on PSY plates with sterile glass beads and incubated at 28°C for 7 days. We then counted colonies to determine total rhizobia per plant.

Statistical Analysis

We used R version 3.6.0 (2019-04-26) to conduct all statistical tests. In case of heteroscedasticity or non-normality, a decimal logarithm transformation of the data was performed to meet ANOVA assumptions. If ANOVA assumption could not be met with a transformation of the response variables, a non-parametric Kruskal test was conducted. To compare plant biomass among treatments, we tested the decimal logarithm mean plant dry biomass for significant differences with two-way ANOVA and a *post-hoc* Tukey tests for pairwise comparison with a 95% confidence interval. To test for differences in allocation to above and belowground parts, we compared mean root to shoot ratio with a pair-wise Wilcoxon test. To compare plant biomass as a function of rhizobial inoculation, we compared decimal logarithm relative plant biomass among nitrogen treatments with a one way ANOVA and a Tukey test for multiple group comparison with a 95% confidence interval. To test for differences in nodule formation, we compared mean nodule number and nodule fresh per plant with one-way ANOVA and a Tukey test for multiple group comparison with a 95% confidence interval. For nodule volume we used the Kruskal test and Dunn's *post-hoc*. Rhizobial fitness components, defined as viable rhizobia per milligram of plant, nodule mass, or volume, were compared among the four nitrogen treatments of inoculated plants with Kruskal test and Dunn's *post-hoc*. Dunn's test is appropriate for groups with unequal numbers of observations (Zar, 2010), and was corrected for multiple comparisons following Benjamini and Hochberg method (1995) with a 95% confidence interval.

RESULTS

Plant Biomass

We first asked how increasing soil nitrogen affected plant growth patterns in the presence and absence of rhizobial symbionts. We found that nitrogen treatment and rhizobial treatment both had a significant effect on total plant biomass (ANOVA; $F_{3,72} = 330.6$, $p < 0.001$ and $F_{1,72} = 112.5$, $p < 0.001$ respectively), with a significant interaction term between the two variables (ANOVA; $F_{3,72} = 40.2$, $p < 0.001$, **Figure 1A**). Specifically, we found the presence of rhizobia increased total plant biomass at 0, 0.0375, and 0.375 mM ammonium nitrate levels. At the highest nitrate level (3.75 mM), we found that the presence of rhizobia became a cost (**Figure 1A**). By quantifying the root to shoot ratio across these nitrogen levels, we found that at the highest nitrate level, the rhizobial cost was related to a decrease in root biomass (**Figure 1B**).

To assess plant biomass relative to rhizobia inoculation under different nitrogen regime, we calculated the relative growth benefit of inoculation for the plant (**Figure 1C**). Here, we took the difference of the total dry weight of the size-matched inoculated and non-inoculated control, divided by the total dry weight of non-inoculated control. We found that the relative growth benefits of rhizobial inoculation decreased with nitrogen fertilization (ANOVA; $F_{3,36} = 2,685$, $p < 0.001$).

Formation of Symbiotic Organs

We then asked how nitrogen fertilization affected the formation of symbiotic organs, namely nodule number, total nodule fresh weight, and nodule volume. We found a significant effect of fertilization on all three parameters: nodule number (one-way ANOVA; $F_{3,35} = 16.5$, $p < 0.001$) nodule weight (one-way ANOVA; $F_{3,36} = 41.08$, $p < 0.001$), and nodule volume (Kruskal-Wallis test; chi-squared = 23.07, df = 3, p-value < 0.001) (**Figure 2**). This effect was driven largely by the highest nitrogen concentration. In the three lowest nitrogen concentrations, we found no difference in nodule number (~4–5 per plant, **Figure 2A**), fresh weight (~6 mg, **Figure 2B**), or volume (~70 mm^3, **Figure 2C**). However, when fertilization was increased to 3.75 mM NH_4NO_3, all nodule parameters were reduced to nearly zero, across all replicates. This demonstrates

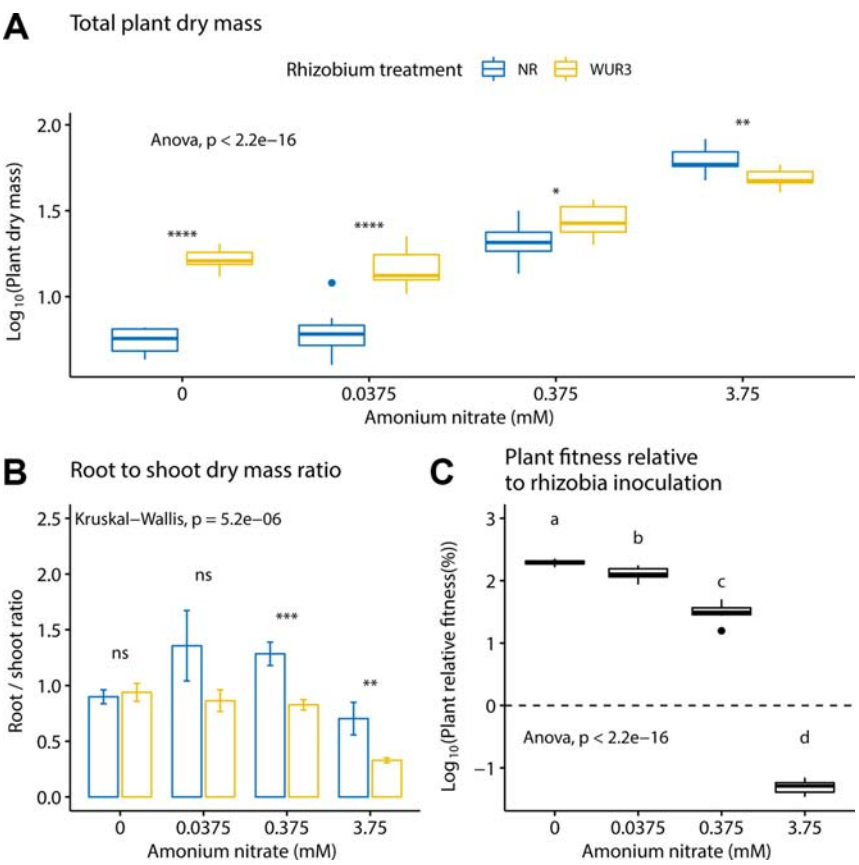

FIGURE 1 | Inoculated and non-inoculated *Parasponia andersonii* plant mass under four nitrogen levels. **(A)** Mean total (shoot + root) plant dry weight. Asterisks show pair-wise comparison significance for each nitrogen level [ANOVA, Tukey honest significant difference (HSD) test]. **(B)** Mean root to shoot dry weight ratio. Asterisks show pair-wise comparison significance for each nitrogen level (Wilcoxon rank sum test) NR = non-rhizobial (blue), WUR3 = Rhizobial strain B. elkanii WUR3 (yellow). **(C)** Mean relative host growth response to rhizobia inoculation as the difference of the total dry weight of inoculated and non-inoculated control, divided by the total dry weight of non-inoculated control. Letters represent groups significantly different from each other (ANOVA, Tukey HSD test). Error bars show standard error.

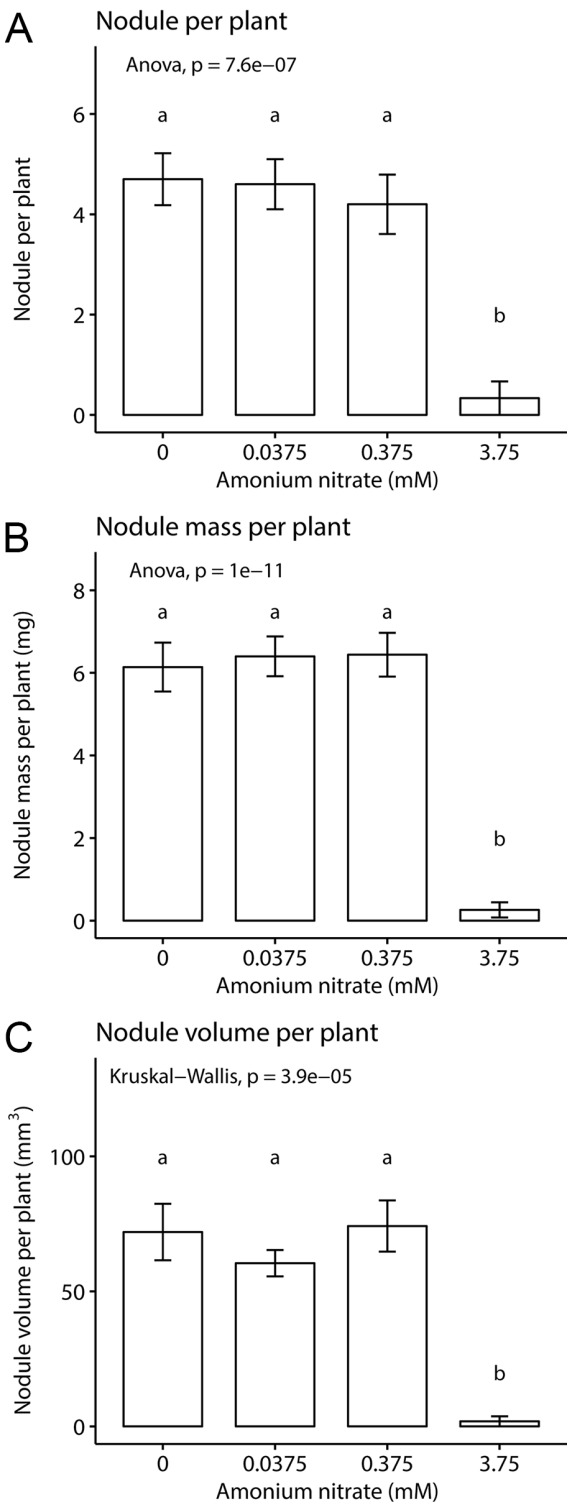

FIGURE 2 | Inoculated *Parasponia andersonii* nodulation under four nitrogen levels. **(A)** Mean nodule number per plant. **(B)** Mean nodule fresh weight per plant. **(C)** Mean nodule volume per plant. Letters represent groups significantly different from each other (ANOVA, Tukey HSD test and Kruskal test, Dunn's test). Error bars show standard error.

that with enough exogenous nitrogen available, *P. andersonii* is able to prevent nodule organogenesis, similar as reported for legumes and actinorhizal plants.

In legumes, it has been demonstrated that the rhizobia—as well as exogenous fixed-nitrogen—can trigger expression of CLE peptide encoding genes, which can trigger systemic signalling and inhibit nodulation (Okamoto et al., 2009; Reid et al., 2011a). Studies in *Lotus japonicus* revealed that whereas *LjCLE-RS1* and *LjCLE-RS2* are induced upon rhizobium inoculation, only *LjCLE-RS2* is induced by application of exogenous nitrogen (Okamoto et al., 2009). The latter gene is a close homolog of the soybean (*G. max*) CLE peptide encoding gene *GmNIC1a* that is induced by exogenous nitrate (Reid et al., 2011b; Hastwell et al., 2017). For *P. andersonii*, *CLE* genes have been annotated (**Table S1**). Of these, *PanCLE5* and *PanCLE9* showed to be close homologs of *LjCLE-RS1* and *LjCLE-RS2*, and their counterparts *MtCLE12* and *MtCLE13* in *Medicago truncatula* (Van Velzen et al., 2018). To obtain insight whether any of the *P. andersonii CLE* genes is induced by exogenous nitrate, we exploited available RNA sequencing (RNA-seq) data (Van Velzen et al., 2018). This revealed that three *CLE* genes, namely *PanCLE2*, *PanCLE8*, and *PanCLE9,* have an increased expression in inoculated roots grown at relatively high exogenous nitrate levels (5 mM KNO_3) (**Figure S1**). These three genes showed a similar induction in young, non-infected, nodule primordia (**Figure S1**). This suggests that in *P. andersonii* rhizobium and exogenous nitrate trigger an overlapping *CLE* gene repertoire to regulate nodulation.

Rhizobial Fitness Proxies

While nodule number and weight can give some rough estimates of rhizobial benefit, a key parameter is to directly quantify rhizobial densities in nodules. We therefore next measured CFUs per mg of plant and nodule biomass or volume (n = 2 for 3.75 mM as only two plants formed nodules). We found that as exogenous nitrogen levels increased, there was a concurrent decrease in CFUs per plant biomass (Kruskal-Wallis test; chi-squared = 9.1, df = 3, p-value = 0.028), and CFUs per mg of nodule (Kruskal-Wallis test; chi-squared = 8.2, df = 3, p-value = 0.041). But surprisingly, no significance difference was found for CFUs per nodule volume (Kruskal-Wallis test; chi-squared = 4.9, df = 3, p-value = 0.18). Despite the fact that nodule number and fresh weight remained the same across the lowest three nitrogen levels, we documented a decrease in viable rhizobial density in nodules as nitrogen levels increased (**Figure 3**).

DISCUSSION

Plant species found in the nitrogen fixing clade rely on diazotrophic symbionts to acquire nitrogen in poor soils (McKey, 1994; Crews, 1999; Vitousek et al., 2002). The ability to control resource allocation to these symbionts is likely a key requirement for evolutionary maintenance of the symbiosis (Werner et al., 2015). We found evidence that the non-legume *P. andersonii* has likewise evolved mechanisms to control rhizobial fitness, despite an independent evolutionary trajectory from the legume lineage of >100 million years ago. Specifically, we found that increasing

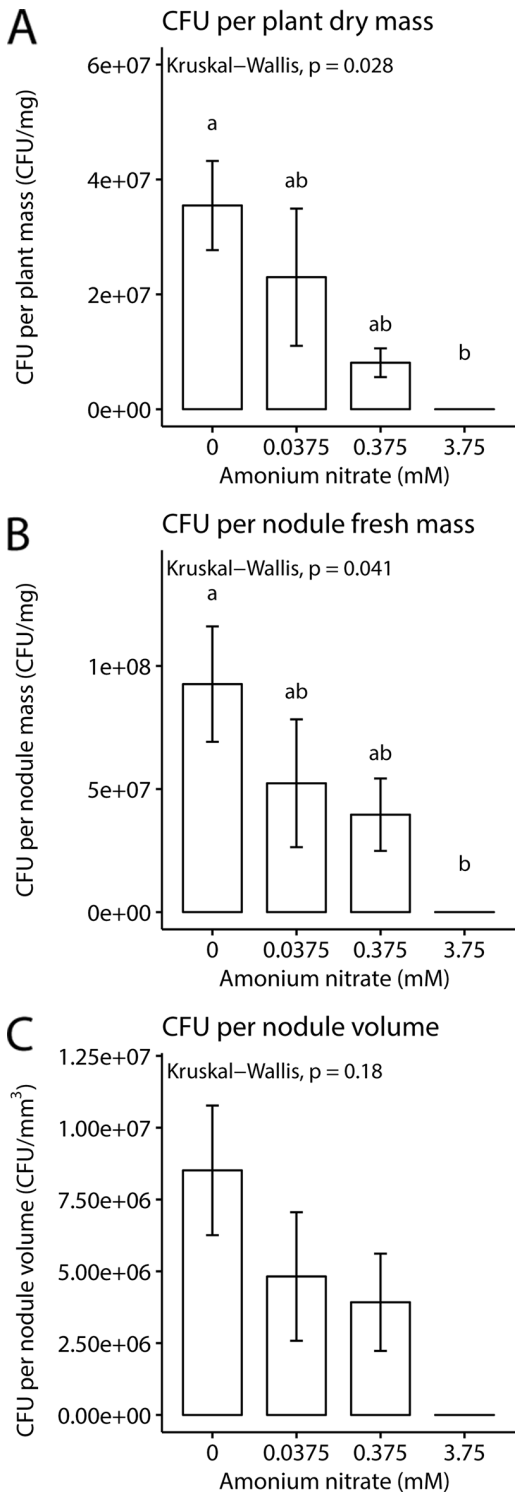

FIGURE 3 | Rhizobia fitness under four nitrogen levels. **(A)** Mean colony forming units per mg plant dry weight. **(B)** Mean colony forming units per milligram nodule fresh weight. **(C)** Mean colony forming units per volume of nodule. Letters represent groups significantly different from each other (Kruskal test, Dunn's test). Error bars show standard error.

nitrogen levels lead to a decrease in rhizobial populations within nodules. In contrast, evidence for control of nodule formation (i.e., organogenesis) was only evident from the highest nitrogen level, in which nodule formation was almost completely suppressed. In the lower nitrogen treatments, we found no evidence for differences in nodule size, number, or volume. Together, these data suggest that despite the continued growth and formation of nodules at lower nitrogen levels, the host still can control the success of the rhizobial populations within those nodules.

An open question is whether *Parasponia* nodulation is somehow less advanced than in legumes (Behm et al., 2014): our results point to similar levels of nodulation control as found in some legume species. Specifically, it has been shown that at high nitrogen levels, legumes can control nodule formation and mass—a process known as autoregulation of nodulation (Cho and Harper, 1991; Sueyoshi et al., 2003; Jeudy et al., 2010). This has also been demonstrated in nodulated actinorhizal plants, which likewise show a reduced investment in nodulation with application of exogenous nitrogen (Kohls and Baker, 1989; Thomas and Berry, 1989; Arnone et al., 1994; Markham and Zekveld, 2007; Wall and Berry, 2007). Our findings are therefore in line with the idea that a shared mechanism to control nodulation investment across the nitrogen fixing clade was in place before the evolutionary diversion of the nodulating lineages.

How does such control operate? New work has shown that legumes employ a nitrate response to inhibit rhizobial symbiosis by upregulating specific transcription factors (Nishida et al., 2018). Autoregulation of nodulation works as a negative feedback from the key transcription factor NIN targeting CLE peptides, which induces a shoot response, production of cytokinin and inhibition of nodulation (Nishida and Suzaki, 2018). The nitrate-induced inhibition induces the NIN-like transcription factor NRSYM1 targeting the same CLE peptides. Furthermore, in the actinorhizal plant *Casuarina glauca*, RNA interference (RNAi) NIN knockdown also showed the essential role of NIN in controlling nodule formation (Clavijo et al., 2015). While it is unknown if *Parasponia* employs these same mechanisms, CLE peptides are expressed in *P. andersonii* nodules (**Figure S1**), suggesting it could be the case (Van Velzen et al., 2018).

However, the ability to control resource allocation to nodules may be less important to *Parasponia* hosts, given the extremely nutrient poor soils in which they are typically found (Achmad and Hadi, 2016). In this ecological niche, we would not expect hosts to be exposed to high nitrogen conditions, nor the concurrent selection pressures against nodulation. There is also evidence that host responses to nitrate may evolve differently across different plant lineages. Studies of the legume *Acmispon strigosus* found increases in nodule number and size at low nitrate levels, as expected, but also revealed that nodulation suppression was linked with high plant mortality suggesting a high, direct sensitivity to nitrate (Regus et al., 2017b). In *L. japonicus*, fertilization reduced nodule size and nodule number, but with no apparent cost on plant fitness (Nishida et al., 2018). In actinorhizal plant lineages closely related to *P. andersonii*, added nitrate reduces and blocks nodule formation of the *Frankia* symbiosis. In a split root experiment, *Casuarina*

cunninghamiana showed localized control depending on exogenous nitrate concentration (Kohls and Baker, 1989; Arnone et al., 1994). In *Parasponia*, nodule size and number did not vary with nitrogen concentration. Instead, nodulation was nearly eliminated for the highest level of fertilization.

Our data show that *P. andersonii* can block nodulation, but that this might entail a cost. We found that at the highest nitrogen level, plant root biomass was reduced in the presence of rhizobia compared to non-inoculated controls. But this growth depression was not observed at lower nitrogen concentrations. Moreover, we observed a linear decrease in the benefit to plant growth conferred by rhizobia as nitrogen increased. Specifically, our data show that resource allocation to root growth was negatively impacted under high N when rhizobia were present (**Figure 1B**). This cost in high nitrogen context was not linked with allocation to resources to nodules organogenesis because nodule formation was suppressed. Instead, this may be linked to the presence of intercellular bacteria, nutrient uptake, or plant defense mechanisms (Bakker et al., 2018). A similar result was also found in *A. strigosus,* whereby the authors noted a cost to the presence of rhizobia under high nitrogen, even though the cost was also not linked to nodule formation (Regus et al., 2017b). They point to past work showing the cost of chemically induced plants defense response to pathogens (Heil et al., 2000). Whether our reduction in root growth (**Figure 1B**) is linked to the costs of upregulating plant defense response is unknown.

Although our data suggest that *Parasponia* employs a mechanism to control nodulation upon presence of exogenous nitrogen—and that this is likely linked to CLE signaling—we also find that rhizobial density may be likewise regulated within nodules. Specifically, we found that *P. andersonii* controlled rhizobial colonization levels at a per nodule milligram and per plant milligram basis. While plants had similar numbers of nodules and equivalent nodule weights across three nitrogen levels, we found that the amount of viable rhizobia hosted in host cells varied. Control of rhizobial fitness within nodules has been shown in legumes, most recently in *L. japonicus,* in which there is evidence that plants can differentially control fitness of effective and ineffective rhizobia within a single nodule (Quides et al., 2017). Similarly, sanction strength—meaning the ability to control rhizobial fitness in individual nodules—was also predicted (West et al., 2002) and shown (Kiers et al., 2006) to increase with addition of external nitrate in soybeans.

While our data suggest that within nodule regulation of rhizobial fitness depends on nitrogen levels, a broader question is whether *Parasponia* has evolved a similar response to ineffective rhizobia that fail to provide nitrogen. Increasingly, work has shown that allocation to nodules will depend on the quality of the rhizobial partners, such that nodules containing low-quality partners will be sanctioned, and experience a reduction in resources (Regus et al., 2017a; Kiers et al., 2003; Oono et al., 2009; Oono et al., 2011). For example work in *Lupinus arboreus* has shown that the size of the nodule is linked with the quality of its occupant (Simms et al., 2006). While we used a well-characterized effective strain, future work should aim to understand how rhizobial partner quality and nitrogen levels interact in the *Parasponia*-rhizobia symbiosis, studied in some legumes (Grillo et al., 2016; Regus et al., 2017a; Regus et al., 2014; Wendlandt et al., 2018).

A second open question is how the physiology of *Parasponia* nodules affects the potential for hosts to control rhizobial fitness. *P. andersonii* has indeterminate nodule with a central vasculature, meaning a meristem sustains a continuous growth of the nodule such that cells become colonized with infection threads containing rhizobia (Behm et al., 2014). When the cells are fully colonized, the rhizobia cells are kept in fixation threads and do not differentiate to bacteroids (i.e., swollen bacteria unable of cell division) (Trinick and Galbraith, 1976). Because of this mode of growth, we had expected *P. andersonii* to reduce nodule growth (meristematic cell division) upon fertilization, yet we observed similar nodule size with an overall lower cell colonization by rhizobia. While the mechanisms is still unknown, this result suggests that *P. andersonii* can directly reduce rhizobia cell division within its nodules or reduce rhizobia nodule occupancy by inducing cell senescence.

More generally, future work is needed to better characterize the costs and benefits of the symbiosis physiologically. For example, from the host side, measurements of %Ndfa (nitrogen derived from the atmosphere) can help us more accurately understand the contribution of nitrogen fixation under different fertilizer regimes. Likewise, detailed microscopy of *P. andersonii* nodules could be conducted. Here, electron microscopy would be useful to study the integrity of the fixation threads and endosymbiotic bacteria, whereas light microscopy on replicate nodules could help develop reliable quantifying techniques based on visual inspection [as in (Regus et al., 2017a)]. From the symbiont side, quantification of metrics such as (PHB), could be helpful in understanding rhizobial fitness, specifically how PHB is linked to reproduction and survival during starvation [e.g., (Ratcliff et al., 2008)].

Overall our work suggests that rhizobial control mechanisms are not exclusive to legumes. While there was evidence that the relative host growth benefits of inoculation decreased with nitrogen fertilization, we found that *Parasponia* controls rhizobial fitness, likely by mediating rhizobial density, depending on ammonium nitrate availability. A key open question is how these processes operate in the field, where *Parasponia* evolved on nutrient poor volcanic soils. Given increasing global nutrient inputs, even to pristine ecosystems, more data are needed to understand fitness alignment in the *Parasponia*—rhizobium symbiosis under changing nutrient conditions.

DATA AVAILABILITY STATEMENT

The datasets generated for this study are available on request to the corresponding author.

AUTHOR CONTRIBUTIONS

All authors contributed to frame the research question and design of the experiments. SD performed the experimental work. All authors contributed to write the manuscript and participated in the discussion.

FUNDING

This work was supported by NWO open competition grant to ETK (819.01.007).

ACKNOWLEDGMENTS

We thank Victor Caldas for the help with developing the nodule image analysis, and the three referees for their useful feedback and suggestions.

SUPPLEMENTARY MATERIAL

The Supplementary Material for this article can be found online at: https://www.frontiersin.org/articles/10.3389/fpls.2019.01779/full#supplementary-material

FIGURE S1 | Expression profile of *P. andersonii* CLE peptide encoding gene. Expression profile of *P. andersonii* CLE genes in non inoculated roots, nodule promordia and inoculated roots under low (0.5 mM KNO_3) and high nitrate (5.0 mM KNO_3) conditions. Expression is given in DESeq2-normalized read counts; error bars represent SE of three biological replicates. Dots represent individual expression levels.

REFERENCES

Achmad, S. R., and Hadi, H. (2016). Identifikasi Sifat Kimia Abu Vulkanik Dan Upaya Pemulihan Tanaman Karet Terdampak Letusan Gunung Kelud (Studi Kasus: Kebun Ngrangkah Pawon, Jawa Timur). *War. Perkaretan* 34, 19. doi: 10.22302/ppk.wp.v34i1.60

Alunni, B., and Gourion, B. (2016). Terminal bacteroid differentiation in the legume–rhizobium symbiosis: nodule-specific cysteine-rich peptides and beyond. *New Phytol.* 211, 411–417. doi: 10.1111/nph.14025

Arnone, J. A., Kohls, S. J., and Baker, D. D. (1994). Nitrate effects on nodulation and nitrogenase activity of actinorhizal Casuarina studied in split-root systems. *Soil Biol. Biochem.* 26, 599–606. doi: 10.1016/0038-0717(94)90248-8

Bakker, P. A. H. M., Pieterse, C. M. J., de Jonge, R., and Berendsen, R. L. (2018). The soil-borne legacy. *Cell* 172, 1178–1180. doi: 10.1016/j.cell.2018.02.024

Becking, J. H. (1983a). The Parasponia parviflora-Rhizobium symbiosis. Host specificity, growth and nitrogen fixation under various conditions. *Plant Soil* 75, 309–342. doi: 10.1007/BF02369969

Becking, J. H. (1983b). The Parasponia parviflora - Rhizobium symbiosis. Isotopic nitrogen fixation, hydrogen evolution and nitrogen-fixation efficiency, and oxygen relations. *Plant Soil* 75, 343–360. doi: 10.1007/BF02369970

Behm, J. E., Geurts, R., and Kiers, E. T. (2014). Parasponia: a novel system for studying mutualism stability. *Trends Plant Sci.* 19, 757–763. doi: 10.1016/j.tplants.2014.08.007

Bronstein, J. L. (2015). *Mutualism* (Oxford, UK: Oxford University Press).

Cabeza, R., Koester, B., Liese, R., Lingner, A., Baumgarten, V., Dirks, J., et al. (2014). RNA sequencing transcriptome analysis reveals novel insights into molecular aspects of the Nitrate impact on the nodule activity of Medicago truncatula. *Plant Physiol.* 164, 400–411. doi: 10.1104/pp.113.228312

Carey, J. (2015). News feature: intimate partnerships. *Proc. Natl. Acad. Sci.* 112, 10071–10073. doi: 10.1073/pnas.1514276112

Cho, M.-J., and Harper, J. E. (1991). Effect of localized Nitrate application on Isoflavonoid concentration and nodulation in split-root systems of wild-type and nodulation-mutant soybean plants. *Plant Physiol.* 95, 1106–1112. doi: 10.1104/pp.95.4.1106

Clavijo, F., Diedhiou, I., Vaissayre, V., Brottier, L., Acolatse, J., Moukouanga, D., et al. (2015). The Casuarina NIN gene is transcriptionally activated throughout Frankia root infection as well as in response to bacterial diffusible signals. *New Phytol.* 208, 887–903. doi: 10.1111/nph.13506

Crews, T. E. (1999). The presence of nitrogen fixing legumes in terrestrial communities: evolutionary vs ecological considerations. *Biogeochemistry* 46, 233–246. doi: 10.1007/BF01007581

Denison, R. F., and Kiers, E. T. (2011). Life histories of symbiotic rhizobia and mycorrhizal fungi. doi: 10.1016/j.cub.2011.06.018

Edwards, D. P., and Yu, D. W. (2007). The roles of sensory traps in the origin, maintenance, and breakdown of mutualism. *Behav. Ecol. Sociobiol.* 61, 1321–1327. doi: 10.1007/s00265-007-0369-3

Griesmann, M., Chang, Y., Liu, X., Song, Y., Haberer, G., Crook, M. B., et al. (2018). Phylogenomics reveals multiple losses of nitrogen-fixing root nodule symbiosis. *Science* (80), eaat1743. doi: 10.1126/science.aat1743

Grillo, M. A., Stinchcombe, J. R., and Heath, K. D. (2016). Nitrogen addition does not influence pre-infection partner choice in the legume-rhizobium symbiosis. *Am. J. Bot.* 103, 1763–1770. doi: 10.3732/ajb.1600090

Hallam, S. J., and McCutcheon, J. P. (2015). Microbes don't play solitaire: how cooperation trumps isolation in the microbial world. *Environ. Microbiol. Rep.* 7, 26–28. doi: 10.1111/1758-2229.12248

Hastwell, A. H., De Bang, T. C., Gresshoff, P. M., and Ferguson, B. J. (2017). CLE peptide-encoding gene families in Medicago truncatula and Lotus japonicus, compared with those of soybean, common bean and Arabidopsis. *Sci. Rep.* 7, 1–13. doi: 10.1038/s41598-017-09296-w

Heath, K. D., Stock, A. J., and Stinchcombe, J. R. (2010). Mutualism variation in the nodulation response to nitrate *J. Evol. Biol.* 23, 2494–2500. doi: 10.1111/j.1420-9101.2010.02092.x

Heil, M., Hilpert, A., Kaiser, W., and Linsenmair, K. E. (2000). Reduced growth and seed set following chemical induction of pathogen defence: does systemic acquired resistance (SAR) incur allocation costs? *J. Ecol.* 88, 645–654. doi: 10.1046/j.1365-2745.2000.00479.x

Jeudy, C., Ruffel, S., Freixes, S., Tillard, P., Santoni, A. L., Morel, S., et al. (2010). Adaptation of Medicago truncatula to nitrogen limitation is modulated via local and systemic nodule developmental responses. *New Phytol.* 185, 817–828. doi: 10.1111/j.1469-8137.2009.03103.x

Joy, J. B. (2013). Symbiosis catalyses niche expansion and diversification. *Proc.R. Soc. B Biol. Sci.* 280, 20122820–20122820. doi: 10.1098/rspb.2012.2820

Keeling, P. J., McCutcheon, J. P., and Doolittle, W. F. (2015). Symbiosis becoming permanent: survival of the luckiest. *Proc.Natl.Acad.Sci.* 112, 10101–10103. doi: 10.1073/pnas.1513346112

Kiers, E. T., and Denison, R. F. (2008). Sanctions, cooperation, and the stability of plant-rhizosphere mutualisms. *Annu.Rev.Ecol.Evol.Syst.* 39, 215–236. doi: 10.1146/annurev.ecolsys.39.110707.173423

Kiers, E. T., Rousseau, R. A., West, S. A., and Denison, R. F. (2003). Host sanctions and the legume-rhizobium mutualism. *Nature* 425, 78–81. doi: 10.1038/nature01931

Kiers, E. T., Rousseau, R. A., and Denison, R. F. (2006). Measured sanctions: legume hosts detect quantitative variation in rhizobium cooperation and punish accordingly. *Evol.Ecol.Res.* 8, 1077–1086.

Kiers, E. T., Hutton, M. G., and Denison, R. F. (2007). Human selection and the relaxation of legume defences against ineffective rhizobia. *Proc. R. Soc. B Biol.Sci.* 274, 3119–3126. doi: 10.1098/rspb.2007.1187

Kohls, S. J., and Baker, D. D. (1989). Effects of substrate nitrate concentration on symbiotic nodule formation in actinorhizal plants. *Plant Soil* 118, 171–179. doi: 10.1007/BF02232804

Markham, J. H., and Zekveld, C. (2007). Nitrogen fixation makes biomass allocation to roots independent of soil nitrogen supply. *Can. J. Bot.* 85, 787–793. doi: 10.1139/b07-075

McFall-Ngai, M., Hadfield, M. G., Bosch, T. C. G., Carey, H. V., Domazet-Lošo, T., Douglas, A. E., et al. (2013). Animals in a bacterial world, a new imperative for the life sciences. *Proc. Natl. Acad. Sci.* 110, 3229–3236. doi: 10.1073/pnas.1218525110

McKey, D. (1994). Legumes and nitrogen: the evolutionary ecology of a nitrogen-demanding lifestyle. *Adv. Legum. Syst. Five Nitrogen Factor* 5, 211–228. doi: 10.1007/s13398-014-0173-7.2

Nedomová, Š., Jůzl, M., Kumbár, V., Bubeníčková, A., and Simeonovová, J. (2014). Mathematical descriptive characteristics of potato tubers' shape. *Acta Univ. Agric. Silvic. Mendelianae Brun.* 59, 63–68. doi: 10.11118/actaun201159060063

Nishida, H., and Suzaki, T. (2018). Nitrate-mediated control of root nodule symbiosis. *Curr. Opin. Plant Biol.* 44, 129–136. doi: 10.1016/j.pbi.2018.04.006

Nishida, H., Handa, Y., Tanaka, S., Suzaki, T., and Kawaguchi, M. (2016). Expression of the CLE-RS3 gene suppresses root nodulation in Lotus japonicus. *J. Plant Res.* 129, 909–919. doi: 10.1007/s10265-016-0842-z

Nishida, H., Tanaka, S., Handa, Y., Ito, M., Sakamoto, Y., Matsunaga, S., et al. (2018). A NIN-LIKE PROTEIN mediates nitrate-induced control of root nodule symbiosis in Lotus japonicus. *Nat. Commun.* 9, 499. doi: 10.1038/s41467-018-02831-x

Okamoto, S., Ohnishi, E., Sato, S., Takahashi, H., Nakazono, M., Tabata, S., et al. (2009). Nod factor/nitrate-induced CLE genes that drive HAR1-mediated systemic regulation of nodulation. *Plant Cell Physiol.* 50, 67–77. doi: 10.1093/pcp/pcn194

Oldroyd, G. E. D. (2013). Speak, friend, and enter: signalling systems that promote beneficial symbiotic associations in plants. *Nat. Rev. Microbiol.* 11, 252–263. doi: 10.1038/nrmicro2990

Oono, R., Denison, R. F., and Kiers, E. T. (2009). Controlling the reproductive fate of rhizobia: how universal are legume sanctions? *New Phytol.* 183, 967–979. doi: 10.1111/j.1469-8137.2009.02941.x

Oono, R., Anderson, C. G., and Denison, R. F. (2011). Failure to fix nitrogen by non-reproductive symbiotic rhizobia triggers host sanctions that reduce fitness of their reproductive clonemates. *Proc. Biol. Sci.* 278, 2698–2703. doi: 10.1098/rspb.2010.2193

Op den Camp, R. H. M., Polone, E., Fedorova, E., Roelofsen, W., Squartini, A., Op den Camp, H. J. M., et al. (2012). Nonlegume parasponia andersonii deploys a broad rhizobium host range strategy resulting in largely variable symbiotic effectiveness. *Mol. Plant-Microbe Interact.* 25, 954–963. doi: 10.1094/MPMI-11-11-0304

Porter, S. S., and Simms, E. L. (2014). Selection for cheating across disparate environments in the legume-rhizobium mutualism. *Ecol. Lett.* 17, 1121–1129. doi: 10.1111/ele.12318

Porter, S. S., Faber-Hammond, J., Montoya, A. P., Friesen, M. L., and Sackos, C. (2019). Dynamic genomic architecture of mutualistic cooperation in a wild population of Mesorhizobium. *ISME J.* 13, 301–315. doi: 10.1038/s41396-018-0266-y

Quides, K. W., Stomackin, G. M., Lee, H.-H., Chang, J. H., and Sachs, J. L. (2017). Lotus japonicus alters in planta fitness of Mesorhizobium loti dependent on symbiotic nitrogen fixation. *PLoS One* 12, e0185568. doi: 10.1371/journal.pone.0185568

Ratcliff, W. C., Kadam, S. V., and Denison, R. F. (2008). Poly-3-hydroxybutyrate (PHB) supports survival and reproduction in starving rhizobia. *FEMS Microbiol. Ecol.* 65, 391–399. doi: 10.1111/j.1574-6941.2008.00544.x

Regensburger, B., and Hennecke, H. (1983). RNA polymerase from Rhizobium japonicum. *Arch. Microbiol.* 135, 103–109. doi: 10.1007/BF00408017

Regus, J. U., Gano, K. A., Hollowell, A. C., and Sachs, J. L. (2014). Efficiency of partner choice and sanctions in Lotus is not altered by nitrogen fertilization. *Proc. Biol. Sci.* 281, 20132587. doi: 10.1098/rspb.2013.2587

Regus, J. U., Gano, K. A., Hollowell, A. C., Sofish, V., and Sachs, J. L. (2015). Lotus hosts delimit the mutualism-parasitism continuum of Bradyrhizobium. *J. Evol. Biol.* 28, 447–456. doi: 10.1111/jeb.12579

Regus, J. U., Quides, K. W., O'Neill, M. R., Suzuki, R., Savory, E. A., Chang, J. H., et al. (2017a). Cell autonomous sanctions in legumes target ineffective rhizobia in nodules with mixed infections. *Am. J. Bot.* 104, 1299–1312. doi: 10.3732/ajb.1700165

Regus, J. U., Wendlandt, C. E., Bantay, R. M., Gano-Cohen, K. A., Gleason, N. J., Hollowell, A. C., et al. (2017b). Nitrogen deposition decreases the benefits of symbiosis in a native legume. *Plant Soil* 414, 159–170. doi: 10.1007/s11104-016-3114-8

Reid, D. E., Ferguson, B. J., and Gresshoff, P. M. (2011a). Inoculation- and nitrate-induced CLE peptides of soybean control NARK-dependent nodule formation. *Mol. Plant-Microbe Interact.* 24, 606–618. doi: 10.1094/MPMI-09-10-0207

Reid, D. E., Ferguson, B. J., and Gresshoff, P. M. (2011b). Inoculation- and Nitrate-induced CLE peptides of soybean control NARK-dependent nodule formation. *Mol. Plant-Microbe Interact.* 24, 606–618. doi: 10.1094/MPMI-09-10-0207

Sachs, J. L., and Hollowell, A. C. (2012). The origins of cooperative bacterial communities. *MBio* 3. doi: 10.1128/mBio.00099-12

Sachs, J. L., and Simms, E. L. (2006). Pathways to mutualism breakdown. *Trends Ecol. Evol.* 21, 585–592. doi: 10.1016/j.tree.2006.06.018

Sachs, J. L., Russell, J. E., and Hollowell, A. C. (2011). Evolutionary instability of symbiotic function in Bradyrhizobium japonicum. *PLoS One* 6, e26370. doi: 10.1371/journal.pone.0026370

Schindelin, J., Arganda-Carreras, I., Frise, E., Kaynig, V., Longair, M., Pietzsch, T., et al. (2012). Fiji: an open-source platform for biological-image analysis. *Nat. Methods* 9, 676–682. doi: 10.1038/nmeth.2019

Simms, E. L., Taylor, D. L., Povich, J., Shefferson, R. P., Sachs, J., Urbina, M., et al. (2006). An empirical test of partner choice mechanisms in a wild legume–rhizobium interaction. *Proc. R. Soc. B Biol. Sci.* 273, 77–81. doi: 10.1098/rspb.2005.3292

Soyano, T., Hayashi, M., Sato, S., Hirakawa, H., and Kawaguchi, M. (2014). NODULE INCEPTION creates a long-distance negative feedback loop involved in homeostatic regulation of nodule organ production *Proc. Natl. Acad. Sci.* 111, 14607–14612. doi: 10.1073/pnas.1412716111

Streeter, J., and Wong, P. P. (1988). Inhibition of legume nodule formation and N 2 fixation by nitrate. *CRC. Crit. Rev. Plant Sci.* 7, 1–23. doi: 10.1080/07352688809382257

Sueyoshi, K., Fujikake, H., Ohyama, T., Yashima, H., Ohtake, N., Sato, T., et al. (2003). Systemic and local effects of long-term application of nitrate on nodule growth and N2 fixation in soybean (Glycine max [L.] Merr.). *Soil Sci. Plant Nutr.* 49, 825–834. doi: 10.1080/00380768.2003.10410344

Thomas, K. A., and Berry, A. M. (1989). Effects of continuous nitrogen application and nitrogen preconditioning on nodulation and growth of Ceanothus griseus var horizontalis. *Plant Soil* 118, 181–187. doi: 10.1007/BF02232805

Trinick, M. J., and Galbraith, J. (1976). Structure of root nodules formed by Rhizobium on the non-legume Trema cannabina var. scabra. *Arch. Microbiol.* 108, 159–166. doi: 10.1007/BF00428946

Trinick, M. J., and Galbraith, J. (1980). The rhizobium requirements of the non-legume Parasponia in relationship to the cross-inoculation group concept of legumes. *New Phytol.* 86, 17–26. doi: 10.1111/j.1469-8137.1980.tb00775.x

Trinick, M. J., and Hadobas, P. A. (1988). Biology of the Parasponia-Bradyrhizobium symbiosis. *Plant Soil* 110, 177–185. doi: 10.1007/BF02226797

Trinick, M. J. (1973). Symbiosis between Rhizobium and the non-legume, Trema aspera. *Nature* 244, 459–460. doi: 10.1038/244459a0

Van Velzen, R., Holmer, R., Bu, F., Rutten, L., Van Zeijl, A., Liu, W., et al. (2018). Comparative genomics of the nonlegume Parasponia reveals insights into evolution of nitrogen-fixing rhizobium symbioses. doi: 10.1073/pnas.1721395115

van Velzen, R., Doyle, J. J., and Geurts, R. (2019). A resurrected scenario: single gain and massive loss of nitrogen-fixing nodulation. *Trends Plant Sci.* 24, 49–57. doi: 10.1016/j.tplants.2018.10.005

Vitousek, P. M., Cassman, K., Cleveland, C., Crews, T., Field, C. B., Grimm, N. B., et al. (2002). "Towards an ecological understanding of biological nitrogen fixation," in *The nitrogen cycle at regional to global scales*. Eds. E. W. Boyer and R. W. Howarth (Dordrecht: Springer Netherlands), 1–45. doi: 10.1007/978-94-017-3405-9_1

Voisin, A.-S., Salon, C., Munier-Jolain, N. G., and Ney, B. (2002). Effect of mineral nitrogen on nitrogen nutrition and biomass partitioning between the shoot and roots of pea (Pisum sativum L.). *Plant Soil* 242, 251–262. doi: 10.1023/A:1016214223900

Wall, L. G., and Berry, A. M. (2007). "Early Interactions, Infection And Nodulation In Actinorhizal Symbiosis," in *Nitrogen-fixing Actinorhizal Symbioses* (Dordrecht: Springer Netherlands), 147–166. doi: 10.1007/978-1-4020-3547-0_6

Wendlandt, C. E., Regus, J. U., Gano-Cohen, K. A., Hollowell, A. C., Quides, K. W., Lyu, J. Y., et al (2018). Host investment into symbiosis varies among genotypes of the legume Acmispon strigosus, but host sanctions are uniform *New Phytol.* 221, 446–458. doi: 10.1111/nph.15378

Werner, G. D. A., Strassmann, J. E., Ivens, A. B. F., Engelmoer, D. J. P., Verbruggen, E., Queller, D. C., et al. (2014). Evolution of microbial markets. *Proc. Natl. Acad. Sci.* 111, 1237–1244. doi: 10.1073/pnas.1315980111

Werner, G. D. A., Cornwell, W. K., Cornelissen, J. H. C., and Kiers, E. T. (2015). Evolutionary signals of symbiotic persistence in the legume–rhizobia mutualism. *Proc. Natl. Acad. Sci.* 112, 10262–10269. doi: 10.1073/pnas.1424030112

West, S. A., Kiers, E. T., Simms, E. L., and Denison, R. F. (2002). Sanctions and mutualism stability: why do rhizobia fix nitrogen? *Proc. Biol. Sci.* 269, 685–694. doi: 10.1098/rspb.2001.1878

Westhoek, A., Field, E., Rehling, F., Mulley, G., Webb, I., Poole, P. S., et al. (2017). Policing the legume-Rhizobium symbiosis: a critical test of partner choice. *Sci. Rep.* 7, 1419. doi: 10.1038/s41598-017-01634-2

Zar, J. H. (2010). *Biostatistical analysis fifth edition* Vol. 11. Eds. D. Santos-Fita, E. J. Naranjo, E. Estrad., R. Mariaca and E. Bello (Saddie River, New Jersey, USA: Pearson Educ. Up), 71. Symb. Ritual Pract. Relat. to Hunt. maya communities from Cent. Quintana Roo, Mex. J. Ethnobiol. Eth.

Conflict of Interest: The authors declare that the research was conducted in the absence of any commercial or financial relationships that could be construed as a potential conflict of interest.

frontiers in Plant Science

ORIGINAL RESEARCH
published: 12 July 2019
doi: 10.3389/fpls.2019.00895

Aphids Influence Soil Fungal Communities in Conventional Agricultural Systems

Thomas D. J. Wilkinson[1†], Jean-Pascal Miranda[1], Julia Ferrari[1], Sue E. Hartley[1,2] and Angela Hodge[1]*

[1] Department of Biology, University of York, York, United Kingdom, [2] York Environmental Sustainability Institute, University of York, York, United Kingdom

Arbuscular mycorrhizal fungi (AMF) form symbioses with the roots of most plant species, including cereals. AMF can increase the uptake of nutrients including nitrogen (N) and phosphorus (P), and of silicon (Si) as well as increase host resistance to various stresses. Plants can simultaneously interact with above-ground insect herbivores such as aphids, which can alter the proportion of plant roots colonized by AMF. However, it is unknown if aphids impact the structure of AMF communities colonizing plants or the extent of the extraradical mycelium produced in the soil, both of which can influence the defensive and nutritional benefit a plant derives from the symbiosis. This study investigated the effect of aphids on the plant-AMF interaction in a conventionally managed agricultural system. As plants also interact with other soil fungi, the non-AMF fungal community was also investigated. We hypothesized that aphids would depress plant growth, and reduce intraradical AMF colonization, soil fungal hyphal density and the diversity of AM and non-AM fungal communities. To test the effects of aphids, field plots of barley enclosed with insect proof cages were inoculated with *Sitobion avenae* or remained uninoculated. AMF specific and total fungal amplicon sequencing assessed root fungal communities 46 days after aphid addition. Aphids did not impact above-ground plant biomass, but did increase the grain N:P ratio. Whilst aphid presence had no impact on AMF intraradical colonization, soil fungal hyphal length density, or AMF community characteristics, there was a trend for the aphid treatment to increase vesicle numbers and the relative abundance of the AMF family Gigasporaceae. Contrary to expectations, the aphid treatment also increased the evenness of the total fungal community. This suggests that aphids can influence soil communities in conventional arable systems, a result that could have implications for multitrophic feedback loops between crop pests and soil organisms across the above-below-ground interface.

Keywords: arbuscular mycorrhizal fungi, community diversity, amplicon sequencing, *Hordeum vulgare*, *Sitobion avenae*, rhizosphere, multitrophic interactions

OPEN ACCESS

Edited by:
Heike Bücking, South Dakota State University, United States

Reviewed by:
Jan Jansa, Institute of Microbiology (ASCR), Czechia
Sergio Saia, Council for Agricultural Research and Economics, Italy

***Correspondence:**
Julia Ferrari
julia.ferrari@york.ac.uk
orcid.org/0000-0001-6519-4254

†Present address:
Thomas D. J. Wilkinson, ADAS Gleadthorpe, Mansfield, United Kingdom

Specialty section:
This article was submitted to Plant Microbe Interactions, a section of the journal Frontiers in Plant Science

Received: *05 March 2019*
Accepted: *24 June 2019*
Published: *12 July 2019*

Citation:
Wilkinson TDJ, Miranda J-P, Ferrari J, Hartley SE and Hodge A (2019) Aphids Influence Soil Fungal Communities in Conventional Agricultural Systems. Front. Plant Sci. 10:895. doi: 10.3389/fpls.2019.00895

INTRODUCTION

Arbuscular mycorrhizal fungi (AMF) form obligate symbioses with the roots of c. two-thirds of land plant species, including agriculturally important cereals (Smith and Read, 2008; Fitter et al., 2011). Enhancing this symbiosis has been proposed as an important tool for increasing food security and agricultural sustainability (Gosling et al., 2006;

Fitter et al., 2011; Jacott et al., 2017; Thirkell et al., 2017). Whilst the host plant provides a fixed carbon (C) source for AMF, AMF transfer nutrients such as nitrogen (N) and phosphorus (P) to the plant (Hodge et al., 2001; Smith et al., 2009; Hodge and Fitter, 2010; Karasawa et al., 2012). AMF colonization affects multitrophic interactions between above- and below-ground herbivores (Yang et al., 2014) and may also enhance the uptake of silicon (Si), which can alleviate the impact of both biotic and abiotic stress (Dias et al., 2014; Garg and Bhandari, 2016; Frew et al., 2017).

The bottom-up effect of below-ground AMF on the performance of above-ground herbivores such as aphids can range from positive to negative (Gange and West, 1994; Wurst et al., 2004; Ueda et al., 2013; Simon et al., 2017; Wilkinson et al., 2019). These impacts on aphid performance likely occur because of alterations to plant defense and nutrition due to the AMF symbiosis (Wurst et al., 2004; Meir and Hunter, 2018b) and can depend on the level of AMF colonization of the host plant (Tomczak and Müller, 2017; Maurya et al., 2018; Meir and Hunter, 2018a). In turn, aphids may impose top-down effects on AMF colonization via the host plant (Babikova et al., 2014; Meir and Hunter, 2018a). Top-down and bottom-up effects can therefore modulate the outcome of each other, potentially resulting in above-below-ground multitrophic feedback loops (Meir and Hunter, 2018a). Thus, if aphids influence AMF colonization this could impact how AMF affect plant nutrient uptake and tolerance to abiotic stress in multitrophic systems. The AMF extraradical mycelium (ERM) phase is of also of key importance for interactions between plants and other rhizosphere organisms (Perotto and Bonfante, 1997; Jones et al., 2004; Hodge and Fitter, 2013) and can be directly related to AMF derived plant nutrient acquisition (Hodge et al., 2001; Barrett et al., 2011). Additionally, the ERM can be involved in plant defense, carrying signals of aphid attack to neighboring plants connected via ERM underground networks (Babikova et al., 2013). Elucidating how intra- and extraradical structures of AMF respond to top down effects is therefore important in understanding their potential for use in complex agro-ecosystems. However, current knowledge of how AMF respond to aphids sharing the same host plant is limited to the impact on AMF colonization (Babikova et al., 2014; Vannette and Hunter, 2014; Maurya et al., 2018; Meir and Hunter, 2018a).

The identity of the taxa within the AMF community colonizing the host plant can be important in determining the nutrient uptake or defense benefit gained from the symbiosis. In small, artificially selected AMF communities, AMF species identity determines the level of protection the AMF provides for the host plant against biotic stressors (Pozo et al., 2002; Sikes et al., 2009; Malik et al., 2016), and certain AMF species may deliver more or less nutrients to their host plant (Jansa et al., 2008; Leigh et al., 2009; Thirkell et al., 2016). Similarly, soil community transfer experiments suggests the AMF community structure can also be important in determining nutrient acquisition and plant growth responses (Hodge and Fitter, 2013; Williams et al., 2014; Manoharan et al., 2017; Jiang et al., 2018). Large vertebrate grazing can affect AMF communities (Ba et al., 2012; Guo et al., 2016), and insect herbivory can alter below-ground ectomycorrhizal (Gehring and Bennett, 2009), non-mycorrhizal fungi (Kostenko et al., 2012) and rhizosphere bacterial community characteristics (Kong et al., 2016), but the impact of arthropod herbivory on AMF communities is currently unknown.

The impact of herbivory on AMF structures is variable (Barto and Rillig, 2010), and phloem feeding aphids can increase or decrease the intraradical AMF colonization of their host plant (Babikova et al., 2014; Meir and Hunter, 2018a). The C limitation hypothesis proposes that above-ground removal of fixed C by herbivory will result in less C available below-ground (Wallace, 1987), although the subsequent allocation of this limited amount of C between roots and AMF contained within roots is unknown. The reduced C availability might result in changes to the AMF community because only a limited number of AMF species can be supported and thus the number and relative abundance of less competitive species might be reduced (Gange, 2007; Ba et al., 2012). Alternatively, low levels of herbivory could lead to more C allocated below-ground in an attempt for the plant to take up more nutrients for regrowth (Wamberg et al., 2003), which could increase fungal diversity (Ba et al., 2012). There are also examples of herbivory affecting the composition of ectomycorrhizal communities rather than species richness, and thus altering the beta diversity of communities, making communities more distinct (Gehring and Bennett, 2009).

Arbuscular mycorrhizal fungi communities in conventionally managed agricultural systems are often distinct from AMF communities in other settings and often have low diversity due to tillage, chemical fertilizer, pesticide and fungicide regimes (Jansa et al., 2002; Gosling et al., 2006; Wetzel et al., 2014; Hartmann et al., 2015; Manoharan et al., 2017). We selected a conventionally managed system to investigate agriculturally relevant AMF communities that are tolerant to such practices. Apart from AMF, other fungi also associate with plant roots, including other endophytic mutualists (Murphy et al., 2015; Lugtenberg et al., 2016). As some of these other fungi and their community composition can influence aphid performance (Hartley and Gange, 2009; Battaglia et al., 2013; Kos et al., 2015), the AMF community must be placed in the context of any changes in the wider fungal community.

Here, we investigate the impact of aphids on the below-ground fungal community with a focus on AMF given their key role as ecosystem engineers. Specifically, we tested the following hypotheses: (1) As aphids will depress plant growth and nutrient status, the AMF will benefit less from the association with the plant, and consequently AMF structures, both internal and external to the root, will be reduced. (2) Aphids will cause a reduction in both the alpha diversity and evenness of the soil communities, which results in a distinct soil fungal community composition (increased beta diversity).

MATERIALS AND METHODS

Site Selection

Spring barley (*Hordeum vulgare* L., cultivar: Planet) was drilled into silty clay loam over chalk (Towthorpe, North Yorkshire, SE 91086 62387, GPS: 54.049412, −0.610267, elevation above sea level: 100 m) on March 15th, 2017. Average soil characteristics of the whole field were sampled on May 12th, 2017 and analyzed by NRM Laboratories (Berkshire, United Kingdom; **Table 1**). The field had been conventionally cropped with wheat and oats for the previous 5 years and was treated with conventional agrochemical inputs throughout the duration of this study (**Table 1**).

Aphid Treatments

On the April 21st, 2017, lidless and bottomless PVC boxes (40 cm × 40 cm × 25 cm) were inserted 2–3 cm below the surface of the soil around sections of developing three leaf stage seedlings, averaging 26 ± 1.7 SE plants per box. This shallow insertion, so as not to disturb plant roots, allowed an aphid impermeable seal to form between the soil and a cage structure. The interior of each box thus formed an experimental "plot." Experimental plots were assigned to "+Aphid" or "-Aphid" treatments and arranged in a randomized block design. As the site lay on a North Western slope, plots were set out in two rows perpendicular to the slope, in a North East direction. The location of the plots in the North East and North West direction were coded as the NE and NW coordinate (respectively) of each plot within the field site. This attempted to account for any locational environmental gradients within the site, and are referred to as the NE and NW plot location hereafter (**Figure 1**).

One week later (April 28th, 2017) cages were constructed to cover all plots. The frames of the cage consisted of wooden posts inserted 20 cm into the soil and were attached to the interior of the PVC box. The cage extended 90 cm above the soil and was covered with polypropylene horticultural fleece (**Figure 2**), which intercepted c. 14% of the photosynthetically active radiation. English grain aphids (*Sitobion avenae*) (a single genotype, originally supplied by Koppert, Holland) were cultured on barley plants (cultivar Quench) at 20°C. From these cultures, ten 4th instar adults were taken at random and added to each +Aphid plot. All experimental plots (including −Aphid) were sealed with cages. *S. avenae* populations usually peak in the late summer months (Blackman and Eastop, 2000), however, aphids and cages were added to the crop in the current study earlier than this to stop the natural ingress of aphids into the plots. Initially, eight replicates of each treatment were set up, although one +Aphid replicate was discarded during the study due to damage to the cage caused by high wind speeds and so $N = 8$ for −Aphid treatments and $N = 7$ for +Aphid treatments. Cages remained over all treatments for the duration of the experiment, and may have reduced direct contact of some of the agrochemical inputs (see **Table 1**) with the plots after this date.

Harvest

Plots were harvested on the June 13th, 2017, 46 days post-aphid addition. The number of aphids on five tillers chosen at random within each plot were recorded, and plots were dug out to 20 cm soil depth before storage at 4°C overnight. Three soil cores at each plot location were taken with a 2 cm diameter cheese corer between 20 and 30 cm soil depth. These technical replicates were processed separately to assess for the fungal hyphal length density (HLD) from each core (Hodge, 2001) but then the resulting data was pooled to create a biological replicate. After storage, the aphids were washed from any above-ground material and plant roots were separated from the soil and washed whilst still attached to the above-ground biomass. Only those roots visibly attached to a plant were stored at −20°C for DNA extraction or in 40% ethanol for the staining of fungal structures. The above-ground plant material was oven dried at 70°C for at least 96 h and the total number of plants, tillers and fertile tillers were recorded. The above-ground plant material for each plot was separated into a combined stem and leaf fraction (henceforth referred to as stem material) as well as a separate grain fraction. It should be noted that due to the size of the stem and leaf material, the stem and leaf fraction was weighed to the nearest gram. These fractions were homogenized in a kitchen blender (Igenix ig 8330, Ipswich, United Kingdom) before ball milling to a fine powder (Retsch MM400, Retsch GmbH, Haan, Germany). The resulting material was then analyzed for C and N ratios via a Elementar Vario El Cube (Elementar UK, Ltd., Stockport, United Kingdom) and pelleted for X-ray fluorescence (XRF) analysis (Thermo Fisher Scientific^{TM} portable X-ray fluorescence analyzer) to determine P and Si concentrations as described by Reidinger et al. (2012).

The roots stored in 40% ethanol were stained for fungal structures via the acetic acid–ink staining method (Vierheilig et al., 1998), modified as in Wilkinson et al. (2019). Structures were assessed under a Nikon 50i eclipse microscope (Nikon UK Ltd., Surrey, United Kingdom) under 200 X magnification. As fungi other than AMF colonize plant roots in natural systems, a method that calculates both the most conservative estimation of AMF root length colonization (RLC) (RLC min) and least conservative (RLC max) was employed (Brundrett et al., 1994).

DNA Extraction, PCRs, and Sequencing

Frozen root material was lyophilized for 36 h and ball milled to a fine powder. The DNA was extracted from this material using a DNeasy PowerPlant Pro Kit (QIAGEN N.V, Venlo, Netherlands) according to the manufacturer's instructions with the exception that, in order to increase the DNA yield, the DNA solution was eluted twice through the membrane in the final step. DNA concentrations were assessed (NanoDrop^{TM} 8000 Spectrophotometer Thermo Fisher Scientific) and diluted to 20 ng μl^{-1} before the PCR analysis.

Two regions (amplicons) of fungal ribosomal DNA were amplified via PCR (**Table 2**); an amplicon that captures the diversity of the entire fungal community (total fungi), and an amplicon that captures AMF specific diversity at a higher resolution and species coverage (AMF specific). After initial amplification via primary PCRs, secondary PCRs attached illumina sequencing barcodes. For all PCRs the reaction consisted of 0.5 μl DNA, 0.1 μl of forward and reverse primers (20 mM) and 12.5 μl BioMix Red (Bioline, London, United Kingdom) made up to 25 μl reaction volume with molecular grade dH_2O.

TABLE 1 | Fieldsite soil chemical analyses and agrochemical inputs used throughout the study.

Soil analyses (sampled May 12, 2017)			
P (Olsen's)		182 mg l^{-1}	
K (Ammonium nitrate extracted)		274 mg l^{-1}	
Mg (Ammonium nitrate extracted)		47 mg l^{-1}	
pH		7.4	
Organic matter % (Loss on ignition)		6.8	
Agrochemical inputs		**Active ingredient concentration in concentrated product**	**Date of input**
Herbicides			
	Crystal 1.9 l^{-ha}	60 g l^{-1} flufenacet, 300 g l^{-1} gl pendimethalin	March 15, 2017
	Duplosan 1.74 l^{-ha} + Harmony 0.1 l^{-ha}	310 g l^{-1} Dichlorprop-P acid, 160 g l^{-1} MCPA acid, 130 g l^{-1} Mecoprop-P acid 40 g kg^{-1} metsulfuron-methyl, 400 g kg^{-1} thifensulfuron-methyl	May 25, 2017
	Gal-Gone 0.5 l^{-ha}	200 g l^{-1} fluroxypy	June 03, 2017
	Axial 0.3 l^{-ha} + Agidor (Adjuvant) 0.1 l^{-ha}	100 g l^{-1} pinoxaden 47% w/w methylated rapeseed oil	June 04, 2017
Fungicides			
	Siltra Xpro 0.4 l^{-ha}	60 g l^{-1} bixafen, 200 g l^{-1} prothioconazole and N,N-Dimethyldecanamide	May 25, 2017
	Chlorothalonil 1.0 l^{-ha} + Siltra Xpro 0.4 l^{-ha}		June 12, 2017
Plant Growth Regulators			
	Terpal 0.58 l^{-ha}	395 g l^{-1} mepiquat chloride, 155 g l^{-1} 2-chloroethylphosphonic acid	June 03, 2017
Fertilizer			
	YARA N35 + 7SO3 231 kg^{-ha}		March 16, 2017
	OMEX 0:10:15 623 kg^{-ha}		March 31, 2017
	YARA N35 + 7 SO3 280 kg^{-ha}		April 20, 2017

PCRs were carried out using a T100™ Thermal Cycler (BioRAD, Hercules, CA, United States). The PCR products of the secondary PCRs were purified using a QIAquick PCR Purification Kit (Qiagen) and the purified concentrations were measured using a Qubit®3.0 fluorometer (Thermo Fisher Scientific™, Waltham, MA, United States). To mix the products of the two amplicons at equimolar concentrations to reduce sequencing depth bias during simultaneous DNA sequencing, these products were lyophilized overnight and re-suspended in molecular grade H_2O to achieve desired concentrations. Quality control and library preparation was carried out by the University of York Bioscience Technology Facility, and the resulting samples were sequenced using an illumina MiSeq system (illumina, San Diego, CA, United States) at 2 ∼ 300 bp: Briefly, unique barcode sequences (Nextera XT index primers, illumina) were added onto amplicons tagged with illumina adapter sequences via

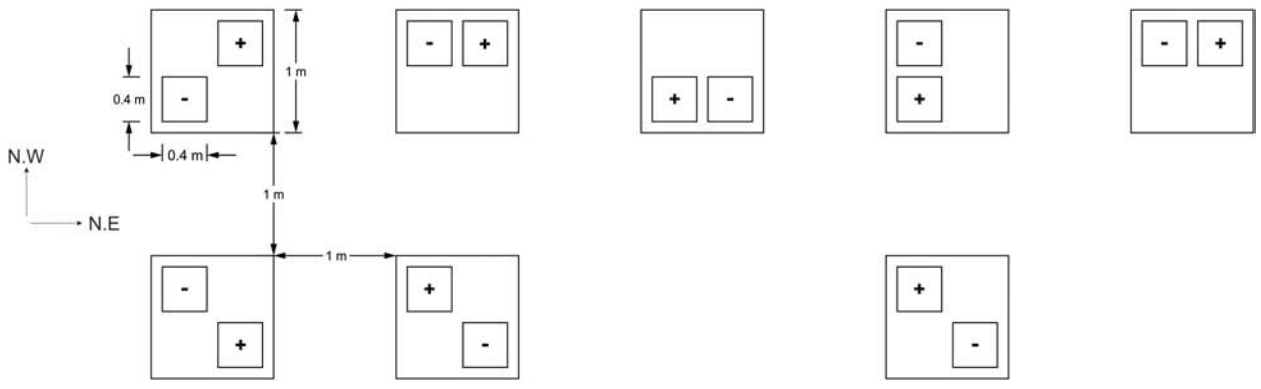

FIGURE 1 | Field plot layout (3 m ×9 m). Plots of barley with (+) or without (–) aphids, *Sitobion avenae*, were arranged randomly in space within one of eight blocks (large squares) which were situated 1 m from each other. Plots were assigned a quarter of each block at random in order to reduce any positional bias within each block. The field site stood on a North West slope (NW direction of the site), and two rows were arranged perpendicular to this slope (in the North East direction; NE direction of the site).

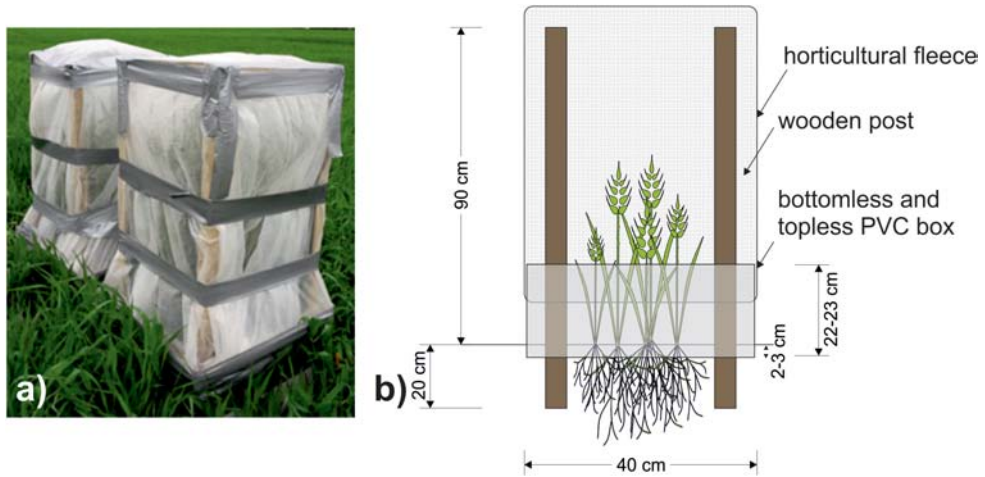

FIGURE 2 | (a) Photograph of a pair of completed aphid cages covering plots taken on 17th May 2017. **(b)** Schematic of cage design used to prevent aphid movement between the plots. Wooden posts reaching 90 cm high were inserted 20 cm into the ground to support a cage of polypropylene horticultural fleece sealed to a 40 cm × 40 cm PVC box reaching 22–23 cm above ground.

PCR. Amplicons were then purified and pooled at equimolar ratios and then diluted and denatured. Samples were spiked with PhiX library spikes (illumina) for added sequence variety to enhance the distinguishing of fluorescent signals of clusters during sequencing. Samples were run using the MiSeq 600 cycle kit (illumina).

Bioinformatic Analysis

The raw forward and reverse reads were merged together resulting in a total of *c.* 1.5 million reads which were processed using QIIME2[1] (Caporaso et al., 2010). Reads were stripped of their primer and barcoding sequences and untrimmed reads were discarded (0.9%). Read quality of the merged reads were estimated using eestats2 and reads from AMF specific amplicons were truncated to 270 bp from the front end due to estimated sequence quality drop off at this point, whilst total fungal amplicons were not truncated. Reads were then dereplicated and clustered into operational taxonomic units (OTUs) using Usearch10 (Edgar, 2010) with 97% similarity. The resulting 517 total fungi amplicon OTUs were BLASTed against the UNITE ITS (Kõljalg et al., 2013) database and eight non-fungal OTUs were removed, resulting in 509 total fungi OTUs, with the total read number per sample ranging from 53,333 to 129,338. Samples were normalized to 70,000 reads per sample using Usearch10's "norm" function. Identical virtual taxon accessions according to the UNITE database were merged together yielding the 155 total fungi amplicon OTUs used in subsequent analysis.

A total of 27 OTUs were identified for the AMF specific amplicon. These were BLASTed against the maarjAM database (Öpik et al., 2010) accessed on 13th June 2018 and five OTUs with less than 96% coverage or similarity to taxa in the database were discarded. This resulted in a total read number from 12,035 to 21,706 per sample. Reads per sample were normalized to 16,500. AMF virtual taxonomic (VT) identities were assigned to the OTUs according to the greatest BLAST coverage and similarity; where OTUs could not be assigned to a single VT, VTs were labeled as unassigned. A phylogenetic tree of the sequences was built to identify identical VT accessions. Identical VTs were merged together resulting in 15 OTUs used in subsequent analysis.

[1]https://qiime2.org

TABLE 2 | Primer sets and PCR conditions used in nested PCRs for "total fungi" and "AMF specific" amplicon sequencing.

Amplicon		Primer pairs	Cycling conditions	DNA used in reaction
Total fungi				
	Primary PCR	ITS1F (Gardes and Bruns, 1993) to ITS4 (White et al., 1990)	5 min @ 95°C; 35 cycles (30 s @ 94°C, 45 s @ 55°C, 90 s @ 72°C); 10 min @ 72°C.	10 ng extracted DNA
	Secondary PCR (illumina tagged primers)	GITS7 (Ihrmark et al., 2012) to ITS4 (White et al., 1990)	5 min @ 95°C; 30 cycles (30 s @ 94°C, 45 s @ 55°C, 90 s @ 72°C); 5 min @ 72°C.	Total fungi primary PCR product (diluted 1:1000)
AMF specific				
	Primary PCR	AML1 to AML2 (Lee et al., 2008)	2 min @ 95°C; 30 cycles (30 s @ 94°C, 30 s @ 59°C, 90 s @ 72°C), 10 min @ 72°C.	10 ng extracted DNA
	Secondary PCR (illumina tagged primers)	WANDA (Dumbrell et al., 2011) to AML2 (Lee et al., 2008)	5 min @ 95°C; 30 cycles (30 s @94°C, 40 s @ 59°C, 90 s @ 72°C), 10 min @ 72°C.	AMF specific primary PCR product (undiluted)

Statistical Analysis

Alpha diversity metrics [OTU/VT richness, Shannon's Index (e), Peilou's Evenness and Simpson's Diversity] were calculated using Usearch10's (Edgar, 2010) alpha diversity command and all subsequent analyses were carried out in R version 3.3.2 (October 31, 2016) (R Core Team, 2016). To test the effect of the aphid treatment on AMF and total fungi alpha diversity metrics, AMF family relative abundance, and plant and AMF structures, aphid presence was used as an explanatory variable in a linear model, using the R packages "lme4," "lmerTest," "lsmeans," and "car." Plot location, measured as the NE and NW distance of each plot from the NW corner of the field site, was used as a covariate (see **Table 3**). To identify fungal OTUs/VTs whose presence predicts aphid treatment we employed indicator species analysis using the "indicspecies" package. The identification and estimation of abundances of AMF is more accurate using the AMF specific amplicon (Berruti et al., 2017), thus total fungi OTUs corresponding to AMF taxa were excluded from the indicator species analysis of the total fungi amplicon. The effect of aphid presence on community composition between samples as measured via Bray-Curtis dissimilarity (Beta diversity) was analyzed using a PERMANOVA via the "Adonis" function in the "Vegan" R package. This was visualized via non-metric multidimensional scaling (NMDS). Relationships between community composition and plant biomass and nutrition, and AMF structures as well as plot location were tested by applying the "envfit" function to the NMDS.

RESULTS

Effect of Aphid Presence on Plant Nutrition and Biomass, and AMF Structures

The mean number of aphids *per tiller* ± SE in "+Aphid" plots was 24.9 ± 8.2, and ranged from between 1.8 and 75, whilst no aphids were present on any tillers investigated for "-Aphid" plots. Whilst the majority of plant biomass and nutrition, and AMF physiological traits were not influenced by aphid treatment (**Table 3**), aphid treatment significantly increased the stem N:P ratio by 5.4% (**Table 3**), and there was a near significant increase of 8.9% (P = 0.052) of the grain N:P ratio. Grain P concentration and N:P ratio was associated with the position of the plot in the NE direction of the site (**Table 3**). While aphid treatment did not significantly impact any AMF structures, there was a trend that the vesicle frequency almost doubled in the roots of plants hosting aphids (P = 0.097). The frequency of vesicles was associated with the position of the plot in the NW direction (**Table 3**).

Effect of Aphid Presence on Total Fungal and AMF Communities in the Root

Within the entire fungal community in plant roots across both aphid treatments, 153 "total fungi" OTUs were identified from nine fungal phyla and 2 OTUs that could not be assigned at the phylum level. The highest abundance of sequences were assigned to Ascomycota (90.2%), followed by Basidiomycota (5.3%), unclassified fungi (3.5%), Glomeromycota (0.83%), and Chytridiomycota (0.08%). In contrast, sequences from Rozellomycota, Mortierellomycota, Entomophthoromycota, Mucoromycota, and Zoopagomycota contributed less than a combined 0.1% of sequence abundance. Within the AMF specific amplicon, 12 OTUs were assigned to VTs whilst three OTUs could not be assigned to a singular VT (see **Supplementary Table S1**). These VTs belonged to seven AMF families: Glomeraceae (6), Paraglomeraceae (1), Diversisporaceae (2), Ambisporaceae (1), Gigasporaceae (1), Archaeosporaceae (3), and Acaulosporaceae (1).

Aphid presence did not affect the species richness within the entire fungal community, but did increase its evenness (**Table 4**). Aphid presence also did not affect any AMF specific alpha diversity metrics. The Simpson's diversity of the AMF specific community was linked to plot location in the NE direction of the field site (**Table 4**).

Aphid presence had no effect on the relative abundance of AMF reads within the entire fungal community. Within the AMF specific amplicon the relative abundance of the Gigasporaceae family tended to increase when aphids were present (**Table 5**). The relative abundance of AMF reads within the entire fungal community, and the relative abundance of the Gigasporaceae and Ambisporaceae families present in the AMF specific community were associated with the location of the plot in the NE direction of the site (**Table 6**).

All but two AMF specific amplicon VTs were found in both aphid and no aphid treatments, however, the exceptions were not strong indicators of aphid presence or absence (**Table 6**). Several Ascomycota taxa were strong predictors of the absence of aphids for the total fungi amplicon, whilst a member of the family Cystobasidiaceae indicated aphid presence.

The total fungi amplicon community composition between plots, measured as Bray-Curtis dissimilarity (beta diversity) was not significantly affected by aphid presence (PERMANOVA: $F_{1,13}$ = 1.75, P = 0.131). However, community composition correlated with plot location in the NE direction of the site (R^2 = 0.46, P = 0.031) and grain P concentration (R^2 = 0.46, P = 0.021; **Figure 3**).

The community composition of AMF specific VTs in the roots of barley plants between plots was not affected by the presence of aphids ($F_{1,13}$ = 0.46, P = 0.604). However, the environmental factors of stem Si concentration and location of the plots in the NE direction of the field site were significantly correlated with the community composition (R^2 = 0.39, P = 0.049 and R^2 = 0.40, P = 0.049, respectively; **Figure 4**).

DISCUSSION

This study aimed to investigate the impact of aphids on soil fungi in a conventionally managed agricultural system. It was hypothesized that by supressing plant nutrition and growth, aphid feeding would lead to negative impacts on AMF structures and species richness, as well as the evenness

TABLE 3 | Mean (±SE) above-ground plant biomass and nutrient concentrations, and AMF structures of experimental barley plots treated with or without aphids, using the location of the plot in the NE and NW direction of the site as a model covariate.

					Plot location covariate			
			Aphid presence		NE		NW	
	−Aphid	+Aphid	$F_{1,11}$	*P*	$F_{1,11}$	*P*	$F_{1,11}$	*P*
Plant No m^{-2} [1.]	172.5 ± 20	156.9 ± 11.3	0.439	0.521	0.085	0.777	0.764	0.401
Fertile tiller No m^{-2}	301.9 ± 29.4	319.4 ± 36.3	0.164	0.693	0.353	0.565	0.647	0.438
Total tiller No m^{-2}	446.3 ± 28.1	418.8 ± 31.3	0.440	0.521	1.99	0.186	0.460	0.512
Stem DW m^{-2} [2.]	356 ± 29.4	356 ± 21.9	0.002	0.963	0.097	0.761	1.731	0.215
Plot grain DW m^{-2}	68.1 ± 8.6	67.9 ± 2.9	<0.001	0.982	0.244	0.631	0.024	0.880
Mean tiller DW	0.95 ± 0.06	1.02 ± 0.05	0.985	0.342	1.706	0.218	0.767	0.399
Mean grain DW	0.22 ± 0.01	0.23 ± 0.03	0.007	0.934	0.182	0.678	0.967	0.347
Stem [P] [3.]	2.46 ± 0.10	2.46 ± 0.14	<0.001	0.996	0.030	0.865	0.040	0.845
Stem [N]	18.16 ± 0.71	19.08 ± 0.89	0.664	0.432	0.139	0.716	0.035	0.855
Stem [Si]	9.69 ± 0.70	8.57 ± 0.48	1.599	0.232	0.005	0.943	0.077	0.786
Stem [C]	420.9 ± 2.13	420.1 ± 2.16	0.055	0.819	0.370	0.556	<0.001	0.979
Stem C:N	23.38 ± 1.06	22.28 ± 0.97	0.574	0.465	0.343	0.570	0.009	0.926
Stem N:P	7.40 ± 0.11	7.80 ± 0.18	5.143	**0.045**	2.806	0.122	1.200	0.297
Grain [P]	3.63 ± 0.14	3.49 ± 0.10	0.899	0.363	5.122	**0.045**	0.059	0.813
Grain [N]	17.50 ± 0.52	18.38 ± 0.43	1.734	0.215	0.719	0.415	0.154	0.702
Grain [Si]	10.30 ± 0.55	9.43 ± 0.58	1.239	0.289	0.443	0.519	0.031	0.864
Grain [C]	418.7 ± 1.89	421.7 ± 1.74	1.324	0.274	0.194	0.668	0.025	0.876
Grain C:N	24.05 ± 0.72	23.00 ± 0.62	1.194	0.298	0.442	0.520	0.102	0.756
Grain N:P	4.85 ± 0.21	5.28 ± 0.16	4.736	0.052·	10.591	**0.008**	0.376	0.552
RLC Min [4.]	32.67 ± 3.14	33.48 ± 3.06	0.034	0.857	0.021	0.888	0.409	0.536
RLC Max [4.]	47.45 ± 3.71	49.91 ± 3.91	0.284	0.605	0.149	0.707	0.715	0.416
HLD [5.]	0.32 ± 0.03	0.34 ± 0.04	0.315	0.586	0.026	0.875	0.001	0.973
Arbuscule [4.]	29.20 ± 2.57	29.77 ± 3.56	0.019	0.893	0.139	0.716	1.078	0.322
Vesicle [4.]	2.75 ± 1.03	5.29 ± 1.78	3.296	0.097·	0.021	0.888	11.606	**0.006**

P-values highlighted in bold are significant at a value of <0.05, P-values highlighted with · are >0.05 and <0.1. [1]No., Number; [2]DW, dry weight (g); [3][], concentration (mg g^{-1}); [4]RLC, AMF root length colonization where Min, most conservative estimate; Max, least conservative estimate; RLC, arbuscule and vesicle values are % of root length; [5]HLD, hyphal length density (m hyphae g^{-1} soil).

TABLE 4 | Mean (±SE) Alpha diversity metrics for "total fungi" amplicon OTUs, and "AMF specific" amplicon VTs from barley plots without or without the presence of aphids, using the location of the plot in the NE and NW direction of the site as a model covariate.

					Plot location covariate			
			Aphid presence		NE		NW	
	−Aphid	+Aphid	$F_{1,11}$	*P*	$F_{1,11}$	*P*	$F_{1,11}$	*P*
Total fungi								
OTU richness	92.6 ± 2.5	89.4 ± 2.3	0.889	0.366	0.281	0.607	0.087	0.774
Shannon's index	2.54 ± 0.09	2.75 ± 0.06	3.725	0.080·	0.008	0.932	0.170	0.688
Peilou's evenness	0.56 ± 0.02	0.61 ± 0.01	5.090	**0.045**	<0.001	0.977	0.260	0.620
Simpson's diversity	0.15 ± 0.02	0.11 ± 0.01	3.059	0.108	0.527	0.483	0.377	0.551
AMF								
VT richness	11.3 ± 0.3	11.1 ± 0.5	0.033	0.859	0.004	0.953	0.105	0.752
Shannon's index	1.17 ± 0.11	1.20 ± 0.09	0.047	0.833	2.646	0.132	0.264	0.618
Peilou's evenness	0.49 ± 0.04	0.51 ± 0.04	0.075	0.790	3.018	0.110	0.429	0.526
Simpson's diversity	0.47 ± 0.05	0.44 ± 0.05	0.226	0.644	6.207	**0.030**	0.176	0.683

Richness: number of OTUs/VTs. P-values highlighted in bold are significant at a value of <0.05, P-values highlighted with · are >0.05 and <0.1.

TABLE 5 | Mean (±SE) relative abundances of the AMF sequences within the "total fungi" amplicon, and of AMF family sequences from the "AMF specific amplicon," from experimental barley plots infested with or without aphids, using the location of the plot in the NE and NW direction of the site as a model covariate.

					Plot location covariate			
			Aphid presence		NE		NW	
Relative abundance	**−Aphid**	**+Aphid**	$F_{1,11}$	***P***	$F_{1,11}$	***P***	$F_{1,11}$	***P***
AMF	0.53 ± 0.29	1.18 ± 0.63	1.450	0.254	5.447	**0.040**	0.145	0.710
Acaulosporaceae	0.02 ± 0.02	0	–	–	–	–	–	–
Ambisporaceae	3.21 ± 0.79	2.92 ± 0.71	0.123	0.732	8.111	**0.016**	0.036	0.854
Archaeosporaceae	1.23 ± 0.41	0.63 ± 0.19	1.828	0.204	0.056	0.817	1.848	0.201
Diversisporaceae	3.72 ± 0.68	5.68 ± 2.52	0.767	0.400	2.241	0.163	0.198	0.665
Gigasporaceae	0.77 ± 0.20	1.48 ± 0.52	4.106	0.067·	13.560	**0.004**	0.553	0.473
Glomeraceae	85.44 ± 2.18	83.43 ± 2.30	0.420	0.530	0.778	0.397	<0.001	0.990
Paraglomeraceae	5.62 ± 1.32	5.86 ± 1.54	0.016	0.900	0.658	0.434	1.119	0.313

P-values highlighted in bold are significant at a value of <0.05, P-values highlighted with · are >0.05 and <0.1.

of the AMF and other fungi communities, measured here through analysis of an AMF specific amplicon and another less precise, but wider encompassing amplicon (total fungi). It was also proposed that the effects of aphids would impact the compositions of these communities (Gehring and Bennett, 2009), and the relative abundance of AMF taxa within them. In fact, aphid presence had less of an impact on AMF community structure than the location of the host plant in the field, although there was a trend of the abundance of AMF vesicles, and the abundance of the Gigasporaceae family to increase when aphids fed on the host plant. Within the total fungi community, the relative abundance of AMF was also affected by location rather than aphid presence. However, aphid presence increased evenness across the total fungi community.

TABLE 6 | Indicator species analysis of AMF specific amplicon VTs and total fungi amplicon OTUs as indicators of untreated or aphid treated barley plots.

OTU/VT	VT/OTU present within treatment		IndVal	*P*
	−Aphid	**+Aphid**		
AMF specific				
Acaulospora VTX00030	✓	×	0.35	1.000
Glomus VTX00199	×	✓	0.49	0.349
Total fungi				
Ascomycota; Pseudeurotiaceae	✓	×	0.92	**0.006**
Ascomycota; Helotiales	✓	×	0.88	**0.046**
Ascomycota; Halosphaeriaceae	✓	×	0.87	**0.032**
Basidiomycota; Cystobasidiaceae	×	✓	0.81	**0.029**

Only total fungi amplicon OTUs which significantly indicate (bold) the aphid treatments are shown. ✓ indicates the presence of the taxon, while × indicates its absence.

Effects of Aphids on the Plant Biomass and Nutrition, and AMF Structures

Contrary to our hypothesis, *S. avenae* had little effect on the above-ground nutrition of barley in the field, although aphid presence tended to increase the above-ground plant N:P ratio (**Table 3**), possibly due to nutrient re-allocation caused by aphid feeding (Sandstrom et al., 2000; Thompson and Goggin, 2006; Nowak and Komor, 2010), or differences between the requirement for N and P by aphids (Tao and Hunter, 2012). Moreover, aphid presence did not reduce above-ground biomass in the present study. Since the aphids used in this experiment were cultured under controlled conditions it is likely that as the aphids did not vector any plant viruses that are a major contributor to aphid related yield loss in cereals (McKirdy et al., 2002). While it is possible that the agro-chemical inputs of fungicides, herbicides and plant growth regulators in this conventionally managed system may have influenced aphid development, the total number of aphids per tiller, and thus, estimated in each "+ Aphid" plot, remained high. However, the aphid population in the current experiment was launched at an earlier date than in non-controlled systems (Blackman and Eastop, 2000) which may have also influenced the results. AMF colonization of barley roots was high compared to that measured in field studies previously (Boyetchko and Tewari, 1995), and in certain glasshouse studies (Grace et al., 2009). Thus, while we originally hypothesized that aphids would have a negative impact on above-ground plant biomass and nutrition which in turn, would reduce both the internal and external phases of the AMF, no negative impact occurred. This may explain why both AMF RLC and hyphal length density were not affected by the presence of aphids in this study. However, there was a trend for aphids to increase the proportion of vesicles in plant roots. Mechanical defoliation has also been shown to influence the proportion of vesicles in plant roots when grown with a native AMF soil community (Garcia and Mendoza, 2012). As vesicles are lipid storage organs in AMF, and AMF derive lipids from the host plant (Keymer and Gutjahr, 2018), this might suggest that more fixed C is available to the AMF via the plant under aphid herbivory.

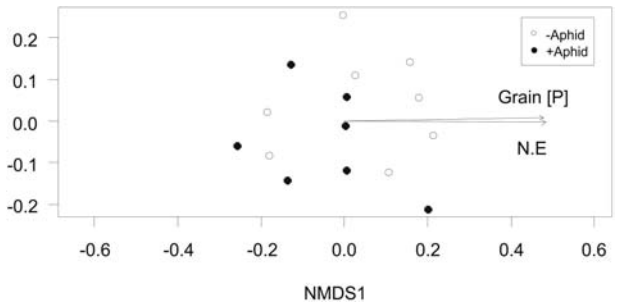

FIGURE 3 | Total fungi community composition: Non-Metric Multidimensional Scaling (NMDS) of total fungi community distribution based on Bray-Curtis dissimilarity (stress = 0.158) obtained from the abundance of "total fungi amplicon" OTUs under "+Aphid," or "–Aphid" treatments. Total fungi community composition was significantly associated with the grain P concentration (mg g^{-1}) in the plots (Grain [P]) and the location of the plot in the NE direction of the site (NE).

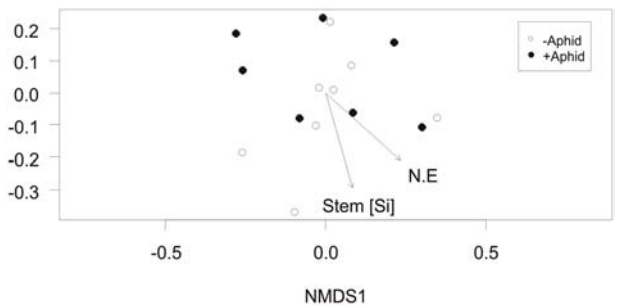

FIGURE 4 | Arbuscular mycorrhizal fungi specific community composition: Non-Metric Multidimensional Scaling (NMDS) of the AMF community distribution based on Bray-Curtis dissimilarity (stress = 0.154) obtained from the abundance of "AMF specific amplicon" VTs under "+Aphid" or "–Aphid" treatments. AMF specific community composition was significantly associated with the barley stem silicon Si (mg g^{-1}) concentration in the plots (Stem [Si]), and the location of the plot in the NE direction of the site (NE coordinate).

Alternatively, AMF vesicle numbers may have increased in a response to less C flow from the plant in order to aid survival under stressed conditions, similar to the AMF response observed in cool conditions (Hawkes et al., 2008), It is also possible that the frequency of AMF with a propensity to form more vesicles occurred *within* the Glomeracea community. However, the tendency for aphid presence to increase the relative abundance of the AMF family Gigasporaceae, which do not develop vesicles (Smith and Read, 2008), suggests that this explanation is less likely.

Effects of Aphids on AMF and Total Fungal Communities

The second hypothesis proposed that the effects of aphid feeding on the host plant would reduce AMF and total fungal species richness and evenness. The low richness of AMF species identified in the current study is similar to that documented in other conventionally managed barley monoculture systems (Manoharan et al., 2017), and as the read depth achieved for the AMF specific amplicon is sufficient to capture AMF diversity (Vasar et al., 2017), it can be assumed that this is an accurate representation. The number of species of AMF were not impacted by aphid presence perhaps as there was no effect of aphid presence on above-ground plant biomass; however, this is similar to the lack of an effect of arthropod feeding on pinyon pine associated ectomycorrhizal communities (Gehring and Bennett, 2009). This was also reflected in the number of species in the entire fungal community in the current study. Moreover, and counter to expectations, aphid presence increased the evenness of the entire fungal community in the present study. Nutrient flows below-ground were not measured in the current study, but aphids can affect below-ground respiration depending on plant growth stage, potentially due to alterations in C availability to soil microbes (Vestergård et al., 2004). Aphids can also alter the profiles of compounds, released from plant roots (Hoysted et al., 2018) and can also change the profiles of sugars found in AMF hyphae sharing the same host plant (Cabral et al., 2018). Moreover, aphids excrete honeydew as a result of their C rich diet of phloem sap which can be utilized as a C source by soil microbiota, thus shaping community structure and biomass (Katayama et al., 2014; Milcu et al., 2015). As more C sources become available in the root, it is possible that niches may enlarge allowing less competitive fungi to compete, reducing the dominance of abundant taxa. However, it should be noted that aphid induced alterations to soil organisms can occur independently of honeydew C inputs (Sinka et al., 2009), and that soil microbes can be influenced by aphid induced changes to plant root exudates in systems where honeydew does not reach the microbe (Kim et al., 2016). Above-ground herbivory generally stimulates the cycling of nutrients by decomposers in the soil (A'Bear et al., 2014), which could partly explain increases in the N:P ratios of plant tissues infested by aphids in the current study.

It was hypothesized that the abundance of AMF taxa within the AMF community would be impacted by aphid presence, and there was a marginal increase in the abundance of Gigasporaceae under aphid infestation of the host plant. A recent meta-analysis revealed that members of this family are tolerant to fertilizer input disturbances, suggesting a role aside from nutrient acquisition, perhaps in plant defense (van der Heyde et al., 2017b). Species indicator analysis may also identify taxa affected by treatments, however, as low abundance taxa typically score as poor indicators, the results of this method may differ from those investigating relative abundances (Longa et al., 2017). None of the AMF VTs were indicators of either treatment, but several total fungi amplicon OTUs were significant indicators of aphid presence or absence. Currently, it is unclear whether these fungi are responding to changes in nutrient availability, whether the plant recruits them in response to aphid feeding to aid with defense (Kong et al., 2016; Pineda et al., 2017), or whether the recruitment of specific soil microbes ultimately benefits the aphid (Kim et al., 2016).

No clear effects of aphid presence were found on community composition, perhaps as a longer period of top down pressure is required to impact this metric. For example, the effects of grazing by large vertebrates on AMF community structure are

strongly linked to the length of the grazing (van der Heyde et al., 2017a). However, as plant communities are removed regularly in cereal systems, and aphid feeding is seasonal (Blackman and Eastop, 2000), only a relatively short window is available for these interactions to occur. Plot location, grain P concentration and AMF abundance as well as community composition were tightly linked in the current study. AMF communities may be associated with environmental and nutritional gradients in soil systems (Bainard et al., 2014; Horn et al., 2014; Guo et al., 2016; Yao et al., 2018) which also likely reflects the spatial differences measured in above-ground plant nutrition and AMF physiology here. Although care was taken to reduce the spread of plots across the slope of the site, these spatial differences highlight the importance of environmental heterogeneity within relatively small distances (less than 10 m) in field sites, and this could have contributed to masking top down effects of aphids on community composition in the current study. Whether the associations between AMF community composition and plant Si are due to AMF uptake of Si (Garg and Bhandari, 2016; Frew et al., 2017), or an artifact of AMF responses to soil pH gradients or water availability (Bainard et al., 2014) requires further study.

CONCLUSION

Aphids increased the evenness of the entire fungal community within plant roots, and also tended to increase the level of vesicles and abundance of the AMF family Gigasporaceae. Whether these increases are due to increased C allocation below-ground by plants attempting to increase nutrient uptake, or the active selection of fungal taxa in response to herbivory requires elucidation. Whether these changes in the below-ground soil community feed back into altered aphid performance is currently unclear, but the response of agriculturally relevant fungal communities to top-down effects of herbivory suggests that above-below-ground community feedback could occur in agricultural systems.

DATA AVAILABILITY

The raw sequence datasets for this study are available in the European Nucleotide Archive accession number PRJEB31469. The datasets for this study are available in the Dryad digital depository (doi: 10.5061/dryad.864pt1f/1).

AUTHOR CONTRIBUTIONS

TW, AH, SH, and JF contributed to the experimental design of the study. TW conducted the experiments and analyzed the data with consultation of the bioinformatics analysis from J-PM. All authors contributed to the writing of the manuscript.

FUNDING

This work was funded by the Biotechnology and Biological Sciences Research Council (BBSRC) United Kingdom, Doctoral Training Partnership grant (BB/J014443/1).

ACKNOWLEDGMENTS

We thank the RSK A.D.A.S Ltd. (High Mowthorpe, North Yorkshire, United Kingdom), in particular Dr. Kate Storer for advice and facilitation of the field study reported. We also thank members of the Dr. Thorunn Helgason group, particularly Dr. Susannah Bird and Phillip Brailey for advice and facilitation regarding sequencing and bioinformatics analysis. This work was derived from the work presented in a Ph.D. thesis of Wilkinson (2018).

SUPPLEMENTARY MATERIAL

The Supplementary Material for this article can be found online at: https://www.frontiersin.org/articles/10.3389/fpls.2019.00895/full#supplementary-material

REFERENCES

A'Bear, A. D., Johnson, S. N., and Jones, T. H. (2014). Putting the 'upstairs-downstairs' into ecosystem service: what can aboveground-belowground ecology tell us? *Biol. Control* 75, 97–107. doi: 10.1016/j.biocontrol.2013.10.004

Ba, L., Ning, J. X., Wang, D. L., Facelli, E., Facelli, J. M., Yang, Y. N., et al. (2012). The relationship between the diversity of arbuscular mycorrhizal fungi and grazing in a meadow steppe. *Plant Soil* 352, 143–156. doi: 10.1007/s11104-011-0985-6

Babikova, Z., Gilbert, L., Bruce, T., Dewhirst, S. Y., Pickett, J. A., and Johnson, D. (2014). Arbuscular mycorrhizal fungi and aphids interact by changing host plant quality and volatile emission. *Funct. Ecol.* 28, 375–385. doi: 10.1111/1365-2435.12181

Babikova, Z., Gilbert, L., Bruce, T. J. A., Birkett, M., Caulfield, J. C., Woodcock, C., et al. (2013). Underground signals carried through common mycelial networks warn neighbouring plants of aphid attack. *Ecol. Lett.* 16, 835–843. doi: 10.1111/ele.12115

Bainard, L. D., Bainard, J. D., Hamel, C., and Gan, Y. (2014). Spatial and temporal structuring of arbuscular mycorrhizal communities is differentially influenced by abiotic factors and host crop in a semi-arid prairie agroecosystem. *FEMS Microbiol. Ecol.* 88, 333–344. doi: 10.1111/1574-6941.12300

Barrett, G., Campbell, C. D., Fitter, A. H., and Hodge, A. (2011). The arbuscular mycorrhizal fungus *Glomus hoi* can capture and transfer nitrogen from organic patches to its associated host plant at low temperature. *Appl. Soil Ecol.* 48, 102–105. doi: 10.1016/j.apsoil.2011.02.002

Barto, E. K., and Rillig, M. C. (2010). Does herbivory really suppress mycorrhiza? a meta-analysis. *J. Ecol.* 98, 745–753. doi: 10.1111/j.1365-2745.2010.01658.x

Battaglia, D., Bossi, S., Cascone, P., Digilio, M. C., Prieto, J. D., Fanti, P., et al. (2013). Tomato below ground-above ground interactions: *Trichoderma longibrachiatum* affects the performance of *Macrosiphum euphorbiae* and its natural antagonists. *Mol. Plant Microbe Interact.* 26, 1249–1256. doi: 10.1094/mpmi-02-13-0059-r

Berruti, A., Desirò, A., Visentin, S., Zecca, O., and Bonfante, P. (2017). ITS fungal barcoding primers versus 18S AMF-specific primers reveal similar AMF-based diversity patterns in roots and soils of three mountain vineyards. *Environ. Microbiol. Rep.* 9, 658–667. doi: 10.1111/1758-2229.12574

Blackman, R., and Eastop, V. (2000). *Aphids on the World's Crops an Identification and Information Guide*, (2nd Edn). Hoboken, NJ: John Wiley & Sons Ltd.

Boyetchko, S. M., and Tewari, J. P. (1995). Susceptibility of barley cultivars to vesicular arbuscular mycorrhizal fungi. *Can. J. Plant Sci.* 75:269. doi: 10.4141/cjps95-048

Brundrett, M., Melville, L., and Peterson, L. (1994). Practical methods in mycorrhiza research. in *Proceedings of the Practical Methods in Mycorrhiza Research: Based on a Workshop Organized in Conjuction With the Ninth North American Conference on Mycorrhizae* Waterloo, ON: Mycologue Publications.

Cabral, C., Wollenweber, B., António, C., Rodrigues, A. M., and Ravnskov, S. (2018). Aphid infestation in the phyllosphere affects primary metabolic profiles in the arbuscular mycorrhizal hyphosphere. *Sci. Rep*. 8:14442. doi: 10.1038/s41598-018-32670-1

Caporaso, J. G., Kuczynski, J., Stombaugh, J., Bittinger, K., Bushman, F. D., Costello, E. K., et al. (2010). QIIME allows analysis of high-throughput community sequencing data. *Nat. Methods* 7, 335–336. doi: 10.1038/nmeth.f.303

Core Team, R. (2016). *R: A Language and Environment for Statistical Computing*. Vienna: R Foundation for Statistical Computing.

Dias, P. A. S., Sampaio, M. V., Rodrigues, M. P., Korndörfer, A. P., Oliveira, R. S., Ferreira, S. E., et al. (2014). Induction of resistance by silicon in wheat plants to alate and apterous morphs of *Sitobion avenae* (Hemiptera: Aphididae). *Environ. Entomol.* 43, 949–956. doi: 10.1603/en13234

Dumbrell, A. J., Ashton, P. D., Aziz, N., Feng, G., Nelson, M., Dytham, C., et al. (2011). Distinct seasonal assemblages of arbuscular mycorrhizal fungi revealed by massively parallel pyrosequencing. *New Phytol.* 190, 794–804. doi: 10.1111/j.1469-8137.2010.03636.x

Edgar, R. C. (2010). Search and clustering orders of magnitude faster than BLAST. *Bioinformatics* 26, 2460–2461. doi: 10.1093/bioinformatics/btq461

Fitter, A. H., Helgason, T., and Hodge, A. (2011). Nutritional exchange in the arbuscular mycorrhizal symbiosis: implications for sustainable agriculture. *Fungal Biol. Rev.* 25, 68–72. doi: 10.1016/j.fbr.2011.01.002

Frew, A., Powell, J. R., Allsopp, P. G., Sallam, N., and Johnson, S. N. (2017). Arbuscular mycorrhizal fungi promote silicon accumulation in plant roots, reducing the impacts of root herbivory. *Plant Soil* 419, 423–433. doi: 10.1007/s11104-017-3357-z

Gange, A. (2007). "Insect-mycorrhizal interactions: patterns, processes, and consequences," in *Ecological Communities: Plant Mediation in Indirect Interaction Webs*, eds T. Ohgushi, T. Craig, and P. Price (Cambridge: Cambridge University Press).

Gange, A. C., and West, H. M. (1994). Interactions between arbuscular mycorrhizal fungi and foliar feeding insects in *Plantago lanceolata* L. *New Phytol.* 128, 79–87. doi: 10.1111/j.1469-8137.1994.tb03989.x

Garcia, I., and Mendoza, R. (2012). Impact of defoliation intensities on plant biomass, nutrient uptake and arbuscular mycorrhizal symbiosis in *Lotus tenuis* growing in a saline-sodic soil. *Plant Biol.* 14, 964–971. doi: 10.1111/j.1438-8677.2012.00581.x

Gardes, M., and Bruns, T. D. (1993). ITS primers with enhanced specificity for Basidiomycetes - application to the identification of mycorrhizae and rusts. *Mol. Ecol.* 2, 113–118. doi: 10.1111/j.1365-294X.1993.tb00005.x

Garg, N., and Bhandari, P. (2016). Silicon nutrition and mycorrhizal inoculations improve growth, nutrient status, K+/Na+ ratio and yield of *Cicer arietinum* L. genotypes under salinity stress. *Plant Growth Regul.* 78, 371–387. doi: 10.1007/s10725-015-0099-x

Gehring, C., and Bennett, A. (2009). Mycorrhizal fungal-plant-insect interactions: the importance of a community approach. *Environ. Entomol.* 38, 93–102. doi: 10.1603/022.038.0111

Gosling, P., Hodge, A., Goodlass, G., and Bending, G. D. (2006). Arbuscular mycorrhizal fungi and organic farming. *Agric. Ecosyst. Environ.* 113, 17–35. doi: 10.1016/j.agee.2005.09.009

Grace, E. J., Cotsaftis, O., Tester, M., Smith, F. A., and Smith, S. E. (2009). Arbuscular mycorrhizal inhibition of growth in barley cannot be attributed to extent of colonization, fungal phosphorus uptake or effects on expression of plant phosphate transporter genes. *New Phytol.* 181:938–949. doi: 10.1111/j.1469-8137.2008.02720.x

Guo, Y. J., Du, Q. F., Li, G. D., Ni, Y., Zhang, Z., Ren, W. B., et al. (2016). Soil phosphorus fractions and arbuscular mycorrhizal fungi diversity following long-term grazing exclusion on semi-arid steppes in inner Mongolia. *Geoderma* 269, 79–90. doi: 10.1016/j.geoderma.2016.01.039

Hartley, S. E., and Gange, A. C. (2009). Impacts of plant symbiotic fungi on insect herbivores: mutualism in a multitrophic context. *Annu. Rev. Entomol.* 54, 323–342. doi: 10.1146/annurev.ento.54.110807.090614

Hartmann, M., Frey, B., Mayer, J., Mäder, P., and Widmer, F. (2015). Distinct soil microbial diversity under long-term organic and conventional farming. *ISME J.* 9, 1177–1194. doi: 10.1038/ismej.2014.210

Hawkes, C. V., Hartley, I. P., Ineson, P., and Fitter, A. H. (2008). Soil temperature affects carbon allocation within arbuscular mycorrhizal networks and carbon transport from plant to fungus. *Glob. Change Biol.* 14, 1181–1190. doi: 10.1111/j.1365-2486.2007.01535.x

Hodge, A. (2001). Arbuscular mycorrhizal fungi influence decomposition of, but not plant nutrient capture from, glycine patches in soil. *New Phytol.* 151, 725–734. doi: 10.1046/j.0028-646x.2001.00200.x

Hodge, A., Campbell, C. D., and Fitter, A. H. (2001). An arbuscular mycorrhizal fungus accelerates decomposition and acquires nitrogen directly from organic material. *Nature* 413, 297–299. doi: 10.1038/35095041

Hodge, A., and Fitter, A. H. (2010). Substantial nitrogen acquisition by arbuscular mycorrhizal fungi from organic material has implications for N cycling. *Proc. Nat. Acad. Sci. U.S.A.* 107, 13754–13759. doi: 10.1073/pnas.1005874107

Hodge, A., and Fitter, A. H. (2013). Microbial mediation of plant competition and community structure. *Funct. Ecol.* 27, 865–875. doi: 10.1111/1365-2435.12002

Horn, S., Caruso, T., Verbruggen, E., Rillig, M. C., and Hempel, S. (2014). Arbuscular mycorrhizal fungal communities are phylogenetically clustered at small scales. *ISME J.* 8, 2231–2242. doi: 10.1038/ismej.2014.72

Hoysted, G., Bell, C., Lilley, C., and Urwin, P. (2018). Aphid colonization affects potato root exudate composition and the hatching of a soil borne pathogen. *Front. Plant Sci.* 9:1278. doi: 10.3389/fpls.2018.01278

Ihrmark, K., Bödeker, I. T. M., Cruz-Martinez, K., Friberg, H., Kubartova, A., Schenck, J., et al. (2012). New primers to amplify the fungal ITS2 region - evaluation by 454-sequencing of artificial and natural communities. *FEMS Microbiol. Ecol.* 82, 666–677. doi: 10.1111/j.1574-6941.2012.01437.x

Jacott, C. N., Murray, J. D., and Ridout, C. J. (2017). Trade-offs in arbuscular mycorrhizal symbiosis: disease resistance, growth responses and perspectives for crop breeding. *Agronomy* 7:75. doi: 10.3390/agronomy7040075

Jansa, J., Mozafar, A., Anken, T., Ruh, R., Sanders, I. R., and Frossard, E. (2002). Diversity and structure of AMF communities as affected by tillage in a temperate soil. *Mycorrhiza* 12, 225–234. doi: 10.1007/s00572-002-0163-z

Jansa, J., Smith, F. A., and Smith, S. E. (2008). Are there benefits of simultaneous root colonization by different arbuscular mycorrhizal fungi? *New Phytol.* 177, 779–789. doi: 10.1111/j.1469-8137.2007.02294.x

Jiang, S., Liu, Y., Luo, J., Qin, M., Johnson, N. C., Öpik, M., et al. (2018). Dynamics of arbuscular mycorrhizal fungal community structure and functioning along a nitrogen enrichment gradient in an alpine meadow ecosystem. *New Phytol.* 220, 1222–1235. doi: 10.1111/nph.15112

Jones, D. L., Hodge, A., and Kuzyakov, Y. (2004). Plant and mycorrhizal regulation of rhizodeposition. *New Phytol.* 163, 459–480. doi: 10.1111/j.1469-8137.2004.01130.x

Karasawa, T., Hodge, A., and Fitter, A. H. (2012). Growth, respiration and nutrient acquisition by the arbuscular mycorrhizal fungus *Glomus mosseae* and its host plant *Plantago lanceolata* in cooled soil. *Plant Cell Environ.* 35, 819–828. doi: 10.1111/j.1365-3040.2011.02455.x

Katayama, N., Silva, A. O., Kishida, O., Ushio, M., Kita, S., and Ohgushi, T. (2014). Herbivorous insect decreases plant nutrient uptake: the role of soil nutrient availability and association of below-ground symbionts. *Ecol. Entomol.* 39, 511–518. doi: 10.1111/een.12125

Keymer, A., and Gutjahr, C. (2018). Cross-kingdom lipid transfer in arbuscular mycorrhiza symbiosis and beyond. *Curr. Opin. Plant Biol.* 44, 137–144. doi: 10.1016/j.pbi.2018.04.005

Kim, B., Song, G. C., and Ryu, C. M. (2016). Root exudation by aphid leaf infestation recruits root-associated *Paenibacillus* spp. to lead plant insect susceptibility. *J. Microbiol. Biotechnol.* 26, 549–557. doi: 10.4014/jmb.1511.11058

Kõljalg, U., Nilsson, R. H., Abarenkov, K., Tedersoo, L., Taylor, A. F. S., Bahram, M., et al. (2013). Towards a unified paradigm for sequence-based identification of fungi. *Mol. Ecol.* 22, 5271–5277. doi: 10.1111/mec.12481

Kong, H. G., Kim, B. K., Song, G. C., Lee, S., and Ryu, C.-M. (2016). Aboveground whitefly infestation-mediated reshaping of the root microbiota. *Front. Microbiol.* 7:1314. doi: 10.3389/fmicb.2016.01314

Kos, M., Tuijl, M. A. B., De Roo, J., Mulder, P. P. J., and Bezemer, T. M. (2015). Species-specific plant-soil feedback effects on above-ground plant-insect interactions. *J. Ecol.* 103, 904–914. doi: 10.1111/1365-2745.12402

Kostenko, O., van de Voorde, T. F. J., Mulder, P. P. J., van der Putten, W. H., and Bezemer, T. M. (2012). Legacy effects of aboveground-belowground interactions. *Ecol. Lett.* 15, 813–821. doi: 10.1111/j.1461-0248.2012.01801.x

Lee, J., Lee, S., and Young, J. P. W. (2008). Improved PCR primers for the detection and identification of arbuscular mycorrhizal fungi. *FEMS Microbiol. Ecol.* 65, 339–349. doi: 10.1111/j.1574-6941.2008.00531.x

Leigh, J., Hodge, A., and Fitter, A. H. (2009). Arbuscular mycorrhizal fungi can transfer substantial amounts of nitrogen to their host plant from organic material. *New Phytol.* 181, 199–207. doi: 10.1111/j.1469-8137.2008.02630.x

Longa, C. M. O., Nicola, L., Antonielli, L., Mescalchin, E., Zanzotti, R., Turco, E., et al. (2017). Soil microbiota respond to green manure in organic vineyards. *J. Appl. Microbiol.* 123, 1547–1560. doi: 10.1111/jam.13606

Lugtenberg, B. J. J., Caradus, J. R., and Johnson, L. J. (2016). Fungal endophytes for sustainable crop production. *FEMS Microbiol. Ecol.* 92:fiw194. doi: 10.1093/femsec/fiw194

Malik, R. J., Dixon, M. H., and Bever, J. D. (2016). Mycorrhizal composition can predict foliar pathogen colonization in soybean. *Biol. Control* 103, 46–53. doi: 10.1016/j.biocontrol.2016.08.004

Manoharan, L., Rosenstock, N. P., Williams, A., and Hedlund, K. (2017). Agricultural management practices influence AMF diversity and community composition with cascading effects on plant productivity. *Appl. Soil Ecol.* 115, 53–59. doi: 10.1016/j.apsoil.2017.03.012

Maurya, A. K., Kelly, M. P., Mahaney, S. M., and Gomez, S. K. (2018). Arbuscular mycorrhizal symbiosis alters plant gene expression and aphid weight in a tripartite interaction. *J. Plant Interact.* 13, 294–305. doi: 10.1080/17429145.2018.1475020

McKirdy, S. J., Jones, R. A. C., and Nutter, F. W. (2002). Quantification of yield losses caused by barley yellow dwarf virus in wheat and oats. *Plant Dis.* 86, 769–773. doi: 10.1094/pdis.2002.86.7.769

Meir, A., and Hunter, D. (2018a). Arbuscular mycorrhizal fungi mediate herbivore-induction of plant defenses differently above and belowground. *Oikos* 127, 1759–1775. doi: 10.1111/oik.05402

Meir, A., and Hunter, M. (2018b). Mycorrhizae alter toxin sequestration and performance of two specialist herbivores. *Front. Ecol. Evol.* 6:33. doi: 10.3389/fevo.2018.00033

Milcu, A., Bonkowski, M., Collins, C. M., and Crawley, M. J. (2015). Aphid honeydew-induced changes in soil biota can cascade up to tree crown architecture. *Pedobiologia* 58, 119–127. doi: 10.1016/j.pedobi.2015.07.002

Murphy, B. R., Doohan, F. M., and Hodkinson, T. R. (2015). Fungal root endophytes of a wild barley species increase yield in a nutrient-stressed barley cultivar. *Symbiosis* 65, 1–7. doi: 10.1007/s13199-015-0314-6

Nowak, H., and Komor, E. (2010). How aphids decide what is good for them: experiments to test aphid feeding behaviour on *Tanacetum vulgare* (L.) using different nitrogen regimes. *Oecologia* 163, 973–984. doi: 10.1007/s00442-010-1652-y

Öpik, M., Vanatoa, A., Vanatoa, E., Moora, M., Davison, J., Kalwij, J. M., et al. (2010). The online database Maarj*AM* reveals global and ecosystemic distribution patterns in arbuscular mycorrhizal fungi (*Glomeromycota*). *New Phytol.* 188, 223–241. doi: 10.1111/j.1469-8137.2010.03334.x

Perotto, S., and Bonfante, P. (1997). Bacterial associations with mycorrhizal fungi: close and distant friends in the rhizosphere. *Trends Microbiol.* 5, 496–501. doi: 10.1016/S0966-842X(97)01154-2

Pineda, A., Kaplan, I., and Bezemer, T. M. (2017). Steering soil microbiomes to suppress aboveground insect pests. *Trends Plant Sci.* 22, 770–778. doi: 10.1016/j.tplants.2017.07.002

Pozo, M. J., Cordier, C., Dumas-Gaudot, E., Gianinazzi, S., Barea, J. M., and Azcón-Aguilar, C. (2002). Localized versus systemic effect of arbuscular mycorrhizal fungi on defence responses to *Phytophthora* infection in tomato plants. *J. Exp. Bot.* 53, 525–534. doi: 10.1093/jexbot/53.368.525

Reidinger, S., Ramsey, M. H., and Hartley, S. E. (2012). Rapid and accurate analyses of silicon and phosphorus in plants using a portable X-ray fluorescence spectrometer. *New Phytol.* 195, 699–706. doi: 10.1111/j.1469-8137.2012.04179.x

Sandstrom, J., Telang, A., and Moran, N. A. (2000). Nutritional enhancement of host plants by aphids - a comparison of three aphid species on grasses. *J. Insect Physiol.* 46, 33–40. doi: 10.1016/s0022-1910(99)00098-0

Sikes, B. A., Cottenie, K., and Klironomos, J. N. (2009). Plant and fungal identity determines pathogen protection of plant roots by arbuscular mycorrhizas. *J. Ecol.* 97, 1274–1280. doi: 10.1111/j.1365-2745.2009.01557.x

Simon, A. L., Wellham, P. A. D., Aradottir, G. I., and Gange, A. C. (2017). Unravelling mycorrhiza-induced wheat susceptibility to the English grain aphid *Sitobion avenae*. *Sci. Rep.* 7:46497. doi: 10.1038/srep46497

Sinka, M., Jones, T. H., and Hartley, S. E. (2009). Collembola respond to aphid herbivory but not to honeydew addition. *Ecol. Entomol.* 34, 588–594. doi: 10.1111/j.1365-2311.2009.01106.x

Smith, F. A., Grace, E. J., and Smith, S. E. (2009). More than a carbon economy: nutrient trade and ecological sustainability in facultative arbuscular mycorrhizal symbioses. *New Phytol.* 182, 347–358. doi: 10.1111/j.1469-8137.2008.02753.x

Smith, S., and Read, D. (2008). *Mycorrhizal Symbiosis*. Cambridge, MA: Academic Press.

Tao, L. L., and Hunter, M. D. (2012). Does anthropogenic nitrogen deposition induce phosphorus limitation in herbivorous insects? *Glob. Change Biol.* 18:1843. doi: 10.1111/j.1365-2486.2012.02645.x

Thirkell, T. J., Cameron, D. D., and Hodge, A. (2016). Resolving the 'nitrogen paradox' of arbuscular mycorrhizas: fertilization with organic matter brings considerable benefits for plant nutrition and growth. *Plant Cell Environ.* 39, 1683–1690. doi: 10.1111/pce.12667

Thirkell, T. J., Charters, M. D., Elliott, A. J., Sait, S. M., and Field, K. J. (2017). Are mycorrhizal fungi our sustainable saviours? considerations for achieving food security. *J. Ecol.* 105, 921–929. doi: 10.1111/1365-2745.12788

Thompson, G. A., and Goggin, F. L. (2006). Transcriptomics and functional genomics of plant defence induction by phloem-feeding insects. *J. Exp. Bot.* 57, 755–766. doi: 10.1093/jxb/erj135

Tomczak, V. V., and Müller, C. (2017). Influence of arbuscular mycorrhizal stage and plant age on the performance of a generalist aphid. *J. Insect Physiol.* 98, 258–266. doi: 10.1016/j.jinsphys.2017.01.016

Ueda, K., Tawaraya, K., Murayama, H., Sato, S., Nishizawa, T., Toyomasu, T., et al. (2013). Effects of arbuscular mycorrhizal fungi on the abundance of foliar-feeding insects and their natural enemy. *Appl. Entomol. Zool.* 48, 79–85. doi: 10.1007/s13355-012-0155-1

van der Heyde, M., Bennett, J. A., Pither, J., and Hart, M. (2017a). Longterm effects of grazing on arbuscular mycorrhizal fungi. *Agric. Ecosyst. Environ.* 243, 27–33. doi: 10.1016/j.agee.2017.04.003

van der Heyde, M., Ohsowski, B., Abbott, L. K., and Hart, M. (2017b). Arbuscular mycorrhizal fungus responses to disturbance are context-dependent. *Mycorrhiza* 27, 431–440. doi: 10.1007/s00572-016-0759-3

Vannette, R. L., and Hunter, M. D. (2014). Genetic variation in plant below-ground response to elevated CO_2 and two herbivore species. *Plant Soil* 384, 303–314. doi: 10.1007/s11104-014-2203-9

Vasar, M., Andreson, R., Davison, J., Jairus, T., Moora, M., Remm, M., et al. (2017). Increased sequencing depth does not increase captured diversity of arbuscular mycorrhizal fungi. *Mycorrhiza* 27, 761–773. doi: 10.1007/s00572-017-0791-y

Vestergård, M., Bjørnlund, L., and Christensen, S. (2004). Aphid effects on rhizosphere microorganisms and microfauna depend more on barley growth phase than on soil fertilization. *Oecologia* 141, 84–93. doi: 10.1007/s00442-004-1651-y

Vierheilig, H., Coughlan, A. P., Wyss, U., and Piché, Y. (1998). Ink and vinegar, a simple staining technique for arbuscular-mycorrhizal fungi. *Appl. Environ. Microbiol.* 64, 5004–5007.

Wallace, L. L. (1987). Mycorrhizas in grasslands - interactions of ungulates, fungi and drought. *New Phytol.* 105, 619–632. doi: 10.1111/j.1469-8137.1987.tb00900.x

Wamberg, C., Christensen, S., and Jakobsen, I. (2003). Interaction between foliar-feeding insects, mycorrhizal fungi, and rhizosphere protozoa on pea plants. *Pedobiologia* 47, 281–287. doi: 10.1078/0031-4056-00191

Wetzel, K., Silva, G., Matczinski, U., Oehl, F., and Fester, T. (2014). Superior differentiation of arbuscular mycorrhizal fungal communities from till and no-till plots by morphological spore identification when compared to T-RFLP. *Soil Biol. Biochem.* 72, 88–96. doi: 10.1016/j.soilbio.2014.01.033

White, T. J., Bruns, T. D., Lee, S., and Taylor, J. (1990). "Amplification and direct sequencing of fungal ribosomal RNA genes for phylogenetics," in *PCR Protocols: A Guide to Methods and Applications*, eds M. A. Innis, D. H. Gelfland, J. J. Sninsky, and T. J. White (Cambridge, MA: Academic Press), 315–322. doi: 10.1016/b978-0-12-372180-8.50042-1

Wilkinson„ T. D. J. (2018). *Interactions between above and below ground symbionts: Implications for food security*. York: University of York. Ph.D. thesis.

Wilkinson, T. D. J., Ferrari, J., Hartley, S. E., and Hodge, A. (2019). Aphids can acquire the nitrogen delivered to plants by arbuscular mycorrhizal fungi. *Funct. Ecol.* 33, 576–586. doi: 10.1111/1365-2435.13283

Williams, A., Birkhofer, K., and Hedlund, K. (2014). Above- and below-ground interactions with agricultural management: effects of soil microbial communities on barley and aphids. *Pedobiologia* 57, 67–74. doi: 10.1016/j.pedobi.2014.01.004

Wurst, S., Dugassa-Gobena, D., Langel, R., Bonkowski, M., and Scheu, S. (2004). Combined effects of earthworms and vesicular-arbuscular mycorrhizas on plant and aphid performance. *New Phytol.* 163, 169–176. doi: 10.1111/j.1469-8137.2004.01106.x

Yang, H., Dai, Y., Wang, X., Zhang, Q., Zhu, L., and Bian, X. (2014). Meta-analysis of interactions between arbuscular mycorrhizal fungi and biotic stressors of plants. *Sci. World J.* 2014:746506. doi: 10.1155/2014/746506

Yao, L. H., Wang, D. J., Kang, L., Wang, D. K., Zhang, Y., Hou, X. Y., et al. (2018). Effects of fertilizations on soil bacteria and fungi communities in a degraded arid steppe revealed by high through-put sequencing. *PeerJ* 6:e4623. doi: 10.7717/peerj.4623

Conflict of Interest Statement: The authors declare that the research was conducted in the absence of any commercial or financial relationships that could be construed as a potential conflict of interest.

frontiers in Microbiology

ORIGINAL RESEARCH
published: 31 October 2019
doi: 10.3389/fmicb.2019.02423

Soil Amendment With Different Maize Biochars Improves Chickpea Growth Under Different Moisture Levels by Improving Symbiotic Performance With *Mesorhizobium ciceri* and Soil Biochemical Properties to Varying Degrees

Dilfuza Egamberdieva[1,2,3†], Li Li[3†], Hua Ma[1], Stephan Wirth[1] and Sonoko Dorothea Bellingrath-Kimura[1]*

[1] Leibniz Centre for Agricultural Landscape Research, Müncheberg, Germany, [2] Department of Microbiology, Faculty of Biology, National University of Uzbekistan, Tashkent, Uzbekistan, [3] CAS Key Laboratory of Biogeography and Bioresource in Arid Land, Xinjiang Institute of Ecology and Geography, Ürümqi, China

OPEN ACCESS

Edited by:
Sabine Dagmar Zimmermann, Centre National de la Recherche Scientifique (CNRS), France

Reviewed by:
Monica Calvo Polanco, Montpellier SupAgro, France
Marta Laranjo, University of Evora, Portugal

***Correspondence:**
Dilfuza Egamberdieva
egamberdieva@zalf.de;
Dilfuza.egamberdieva@zalf.de

† These authors have contributed equally to this work

Specialty section:
This article was submitted to Plant Microbe Interactions, a section of the journal Frontiers in Microbiology

Received: *05 March 2019*
Accepted: *07 October 2019*
Published: *31 October 2019*

Citation:
Egamberdieva D, Li L, Ma H, Wirth S and Bellingrath-Kimura SD (2019) Soil Amendment With Different Maize Biochars Improves Chickpea Growth Under Different Moisture Levels by Improving Symbiotic Performance With Mesorhizobium ciceri and Soil Biochemical Properties to Varying Degrees. Front. Microbiol. 10:2423. doi: 10.3389/fmicb.2019.02423

Chickpea (*Cicer arietinum* L.) is an important legume originating in the Mediterranean and the Middle East and is now cultivated in several varieties throughout the world due to its high protein and fiber content as well as its potential health benefits. However, production is drastically affected by prevalent water stress in most soybean-growing regions. This study investigates the potential of biochar to affect chickpea-*Rhizobium* symbiotic performance and soil biological activity in a pot experiment. Two different biochar types were produced from maize using different pyrolysis techniques, i.e., by heating at 600°C (MBC) and by batch-wise hydrothermal carbonization at 210°C (HTC), and used as soil amendments. The plant biomass, plant nutrient concentration, nodule numbers, leghemoglobin (Lb) content, soil enzyme activities, and nutrient contents of the grown chickpeas were examined. Our results indicated that plant root and shoot biomass, the acquisition of N, P, K, and Mg, soil nutrient contents, soil alkaline and acid phosphomonoesterases, and proteases were significantly increased by HTC char application in comparison to MBC char under both well-watered and drought conditions. Furthermore, the application of both biochar types caused an increase in nodule number by 52% in well-watered and drought conditions by improving the symbiotic performance of chickpea with *Mesorhizobium ciceri*. Rhizobial inoculation combined with HTC char showed a positive effect on soil FDA activity, proteases and alkaline phosphomonoesterases under well-watered and drought conditions compared to the control or MBC char-amended soils. This concept, whereby the type of producing biochar plays a central role in the effect of the biochar, conforms to the fact that there is a link between biochar chemical and physical properties and enhanced plant nutrient acquisition, symbiotic performance and stress tolerance.

Keywords: maize biochar, loamy sand, chickpea, rhizobia, nutrient acquisition, soil enzymes

INTRODUCTION

The long-term use of inorganic nitrogen fertilizers, or the application of such fertilizers at rates higher than the optimum, increases residual inorganic N with adverse effects such as soil degradation or the decline of soil biological health (Gong et al., 2013; Reckling et al., 2016). An alternative N resource to mitigate such drawbacks is biological nitrogen fixation by legumes, which plays a major role in sustaining or improving soil productivity (Santi et al., 2013; Egamberdieva et al., 2018). Legumes are grown in many countries of the world and are considered an important food source for human and animal nutrition (Lüscher et al., 2014; Egamberdieva et al., 2015). However, abiotic stresses such as drought and salinity threaten the growth and yield of legumes and other crops (Bodner et al., 2015; Egamberdieva et al., 2016a, 2017b; Abd Allah et al., 2017). Grain legumes are sensitive to drought stress, and the symbiotic performance of plants with rhizobia is known to be especially hindered by drought, resulting in decreased nodulation and nitrogen fixation (Bouhmouch et al., 2005; Farooq et al., 2017). Inhibition of root nodule formation in legumes can be attributed to the failure of rhizobial colonization in the rhizosphere, which indicates the susceptibility of bacterial proliferation to stress factors (Rehman and Nautiyal, 2002).

Chickpea (*Cicer arietinum* L.) is an important legume crop in many countries and is considered a functional food source, mostly due to its high protein content (17–31% protein) (Merga and Haji, 2019). Water deficit reduces chickpea growth and yield and leads to low N fixation due to the limitation of *rhizobium* survival and growth in the soil (Rahbarian et al., 2011). Furthermore, a reduction in photosynthetic pigments, CO_2 assimilation rate, leaf water contents and disturbance in nutrient acquisition by plants were found under drought stress (Vadez et al., 2012; Siddiqui et al., 2015).

Different strategies have been developed to improve the tolerance of crops to drought, e.g., breeding for stress tolerant varieties (Witcombe et al., 2008), genetic engineering (Roy et al., 2011), and application of microbial inoculants (Hashem et al., 2016; Parray et al., 2016). Biochar amendment has also been repeatedly discussed as a technique to increase plant tolerance to various biotic and abiotic stresses (Akhtar et al., 2015). Biochar has been widely used as a soil amendment to improve soil fertility through improved water holding capacity (Yu et al., 2013; Lim et al., 2016), soil cation exchange capacity (Novak et al., 2009), nutrient retention, especially in soils deficient in organic matter content (Chan et al., 2007; Ibrahim et al., 2013), or soil microbial activities (Kolton et al., 2011; Egamberdieva et al., 2016b, 2017a; Soudek et al., 2016). Several reports have demonstrated improved plant growth of soybean (*Glycine max* L.) (Egamberdieva et al., 2016b), pepper (*Capsicum annuum* L.), tomato (*Lycopersicum esculentum* Mill.) (Graber et al., 2010), maize (Islami et al., 2011), and wheat (Alburquerque et al., 2014) after biochar amendment. Moreover, nodule number in the cases of soybean (Mete et al., 2015) and faba bean (Mohamed et al., 2017) significantly increased due to the addition of biochar to the soil, indicating improved symbiotic performance of the plant with rhizobia. Concerning soil biochemical properties, enzyme activities were studied to rate or monitor soil fertility and productivity (Dempster et al., 2012; Song et al., 2018). Several studies reported an increase in soil enzyme activity after biochar application; however, others reported a decrease in activity (Ameloot et al., 2013; Paz-Ferreiro et al., 2014). There is evidence accumulating that the response of plant growth, nutrient acquisition, soil biogeochemical processes and microbial communities to biochar depends on the type of feedstock and the thermal conditions during production (e.g., heating period and the final set point temperature) (Gul and Whalen, 2016).

According to Deenik et al. (2011), the chemical composition of biochar, especially pyrolysis conditions, plays a vital role in soil biological responses to biochar soil amendments. For example, Butnan et al. (2015) observed that plant growth was reduced in a sandy Ultisol amended with eucalyptus wood-derived biochar produced by high (800°C) temperatures, whereas biochar produced at 350°C enhanced plant growth. Moreover, the effect of biochar characteristics such as pyrolysis temperature and duration and the application rate of biochar on soil biological activities is highly variable (Paz-Ferreiro et al., 2014; Song et al., 2018).

In another study, straw gasification biochar increased the shoot and root growth of barley (*Hordeum vulgare* L.) in sandy soil compared to the addition of wood gasification biochar (Hansen et al., 2016). In addition, the interaction of biochar with environmental conditions is essential for determining any contrasting effects, which also depend on the physicochemical properties of biochar (Joseph et al., 2010). Therefore, elucidation of the effect of biochar type on plant growth, development and soil biochemical properties provides important guidance on the selection of feedstock type and production technology, which could be applied under specific environmental conditions. Only limited information is available in the literature regarding the effect of biochar types on the symbiotic performance of legume plants with rhizobia and plant growth under drought stress conditions.

We hypothesized that amending soil with biochar might alleviate drought stress in chickpea by improving its symbiotic interactions with rhizobia in a loamy, sandy soil. Moreover, considering that sandy loam has a pH value below 7, it was unknown whether using different biochar types would promote soil biological activity. We selected biochars produced from maize by two different pyrolysis techniques, i.e., heating at 600°C (MBC) and batch-wise hydrothermal carbonization at 210°C (HTC), and amended loamy, sandy soil under drought and well-watered conditions. The aim of the present study was (1) to evaluate the effect of two contrasting biochar types on chickpea growth, nutrient uptake (N, P, and K) and symbiotic performance with *Mesorhizobium ciceri* and (2) to determine the impact on soil nutrients and soil enzymes linked to carbon, nitrogen and phosphorus cycling.

MATERIALS AND METHODS

Soil, Biochars and Plant Material

The soil used in the study was sandy loam collected from the upper horizon (0–15 cm depth) of an experimental arable field under irrigation operated by the Experimental Field Station of Leibniz Centre for Agricultural Landscape Research (ZALF), Müncheberg, Germany. The soil consists of clay and fine silt (7%), coarse and medium silt (19%), and sand (74%) and is characterized by the following properties: pH, 6.2; organic C content (0.55%), total N content (0.07%), P content (0.03%), K content (1.25%), and Mg content (0.18%).

Two biochar materials were used in this study, supplied from the Leibniz-Institut for Agrartechnik Potsdam-Bornim e.V. (ATB), Germany (Reibe et al., 2015). Both biochar materials were produced from maize using two different pyrolysis techniques: (i) heating at 600°C for 30 min (MBC) and (ii) batch-wise hydrothermal carbonization at 210°C and 23 bar for 8 h (HTC). The biochar properties are presented in **Table 1**. Chickpea (*Cicer arietinum* L.) seeds (var. Xalima) were obtained from the International Centre for Agricultural Research in the Dry Areas (ICARDA), Tashkent, Uzbekistan.

Plant Growth Experiment

The experiment was conducted in a plant growth chamber at the Leibniz Centre for Agricultural Landscape Research (ZALF), Germany. The following six treatments were set up under well-watered and drought conditions, for a total of 12 treatments:

(i) un-inoculated plants grown in soil without MBC or HTC biochar
(ii) un-inoculated plants grown in soil amended with MBC
(iii) un-inoculated plants grown in soil amended with HTC
(iv) inoculated plants with *M. ciceri* and grown in soil without MBC or HTC biochar
(v) inoculated plants with *M. ciceri* and grown in soil amended with MBC
(vi) inoculated plants with *M. ciceri* and grown in soil amended with HTC

Two different biochar types derived from maize, namely, MBC and HTC, were used as soil amendments. Pots (d = 0.16 m, v = 3016 cm^3) were filled with 1000 g of air-dried soil mixed with crushed char (particle size < 3 mm) at a 2% (w/v) concentration. The chickpea seeds were surface-sterilized using 10% v/v NaOCl for 5 min and 70% ethanol for 5 min. Afterward, the seeds were rinsed five times with sterile distilled water and transferred to paper tissue for germination in a dark room at 25°C for 3–4 days. The bacterial strain *Mesorhizobium ciceri* HAMBI1750 was obtained from the Culture Collection of Helsinki University. The strain was grown in yeast mannitol broth (Sigma Aldrich, United States) for 4 days, 2 ml of the bacterial culture was pelleted by centrifugation (10,000 × g for 10 min), and the supernatant was discarded. The cell pellets were washed with 2 ml of PBS (20 mM sodium phosphate and 150 mM NaCl, pH of 7.0) and re-suspended in PBS to obtain a final bacterial density of 10^8 CFU ml^{-1}. Germinated seeds were dipped in bacterial suspension for 5 min and transferred to pots. Three seeds were sown in each pot, and after 1 week, the seedlings were thinned to one plant per pot.

Each treatment was replicated for three times and was arranged in a randomized complete block design. Only one plant was cultured in each pot for nodule and plant analysis. The soil moisture levels, i.e., drought (40% soil moisture) and well-watered (80% soil moisture) conditions, were monitored using the commercially available UMP-1 BT soil moisture sensor (Umwelt-Geräte-Technik GmbH, Müncheberg, Germany). Plants were grown for 40 days at a temperature of 24°C/16°C (day/night) and humidity of 50–60%. Well-watered and drought conditions were controlled at 80 and 40% soil moisture, respectively. At harvest, the chickpea root system was carefully removed, and soil adhering to the roots was collected and considered root-associated soil. The number of nodules (nodule size > 1 mm) was counted for each plant visually. The roots and shoots were oven-dried at 70°C for 48 h. After determination of the dry weight, the materials were ground using a mill fitted with a 1 mm screen and then sub-sampled for analysis.

Plant and Leghemoglobin Content Analyses

After 40 days, the root and shoot dry biomass and nodule numbers were determined. The LB content of nodules was determined by the following method of Wilson and Reisenauer (1963). First, 0.5 mg of crushed and ground nodule tissue was mixed into 3 ml of Drabkin's solution. The supernatant was transferred to a 10 ml tube after centrifugation at 500 g for 15 min. The nodule tissue was extracted twice more with 3 ml of Drabkin's solution and combined with the supernatants. The volume was adjusted to 10 ml with Drabkin's solution, mixed and centrifuged at 20,000*g for 30 min. The assay was standardized with a freshly prepared solution of bovine hemoglobin.

Soil Nutrients and Soil Enzyme Measurements

The carbon (C), nitrogen (N), phosphorus (P), and potassium (K) concentrations in plant tissues were analyzed with an inductively coupled plasma optical emission spectrometer (ICP-OES; iCAP

TABLE 1 | Chemical characterization of chars (Reibe et al., 2015).

Material	DM (%FM)	Ash (%DM)	C (%DM)	N (%DM)	P (g/kg FM)	K (g/kg FM)	pH	EC
HTC	47.39	3.19	64.55	2.09	1.02	3.58	5.25	0.30
MBC	92.85	18.42	75.16	1.65	5.26	31.12	9.89	3.08

FM, fresh matter; DM, dry matter; MBC, maize biochar; HTC, hydrochar; EC, electrical conductivity.

6300 Duo). The total carbon (Ct) and nitrogen (Nt) of the soil samples were determined by the dry combustion method (Nelson and Sommers, 1996) using an elemental determinator (TruSpec CNS). P, K, and magnesium (Mg) were analyzed with an ICP-OES (iCAP 6300 Duo). Acid and alkaline phosphomonoesterase activities were assayed according to Tabatabai and Bremner (1969). Briefly, 0.5 g of moist soil was placed in a 15 ml vial, and 2 ml of MUB buffer (pH of 6.5 for the assay of acid phosphatase or pH of 11 for the assay of alkaline phosphatase) and 0.5 ml of *p*-nitrophenyl phosphate substrate solution (0.05 M) were added. The soil suspension was incubated in a water bath at 37°C with 300 rpm shaking after the vial was capped. After 1 h of incubation, the vial was removed from the water bath, and 2 ml of NaOH (0.5 M), 0.5 ml of $CaCl_2$ (0.5 M) and 5 ml of distilled water were added to stop the reaction. One milliliter of soil suspension was centrifuged at 6500 rpm for 5 min. The concentration of *p*-nitrophenol (*p*-NP) produced in the assays of acid and alkaline phosphomonoesterase and phosphodiesterase activities was calculated from a *p*-NP calibration curve after subtracting the absorbance of the control at 400 nm wavelength using a Lambda 2 UV-VIS spectrophotometer (Perkin Elmer) (Acosta-Martínez and Tabatabai, 2011).

Protease activity was assayed using the method described by Ladd and Butler (1972). Briefly, 0.5 g of soil was weighed into a glass vial, and 2.5 ml of phosphate buffer (0.2 M, pH of 7.0) and 0.5 ml of *N*-benzoyl-L-arginine amide (BAA) substrate solution (0.03 M) were added. The vials were capped and shaken in a water bath at 37°C with a rotary speed of 300 rpm for 1 h. After the incubation, 2 ml of KCl (2 M) was added to the vials to stop the reaction. One milliliter of the solution was pipetted into a microcentrifuge tube and centrifuged at 6000*g for 10 min. A total of 0.5 ml of the clear supernatant was mixed with 4.5 ml of distilled water, 2.5 ml of sodium salicylate-NaOH and 1 ml of sodium dichloroisocyanide solution. The reaction mixture was incubated at room temperature for 30 min. The absorbance of the colored mixture was measured at 690 nm against a blank reagent solution in a spectrophotometer. Controls were used to follow the procedure described for the assay, with the exception that the BAA substrate was added after the incubation. The ammonium released was calculated by relating the measured absorbance at 690 nm to that of a calibration graph containing 0, 1.0, 1.5, 2.0, and 2.5 μg of NH_4^+–N mL^{-1}.

The FDA hydrolytic activity assay was performed according to Green et al. (2006). A total of 0.5 mg of soil was added to a 50 ml vial, with the subsequent addition of 25 ml of sodium phosphate (0.06 M; pH of 7.6). Then, 0.25 ml of 4.9 mM FDA substrate solution was added to all vials. The tightly capped vials were mixed and incubated in a water bath at 37°C for 1 h. A 1 ml soil suspension was transferred to a 1.5 ml tube and centrifuged at 8000 rpm for 5 min. The clear supernatant was measured at 490 nm against a blank reagent solution in a spectrophotometer. Controls were used according to the procedure described for the assay, but 0.25 ml of acetone was added instead of the FDA substrate solution. The concentration of fluorescein released was calculated by reference to a standard curve with 0, 0.001, 0.005, 0.05 and 0.15 mg of fluorescein.

Statistical Analysis

The data were subjected to univariate analysis using a general linear model in the statistical software package SPSS 22 (SPSS Inc., Chicago, IL, United States). Multiple comparisons between treatments were tested at the $p < 0.05$ level using Tukey's honestly significant difference (HSD) test.

RESULTS

Plant Shoot and Root Growth

Well-Watered Conditions

The responses of chickpea to the two biochar types were different under well-watered conditions. The growth of chickpea was significantly ($p < 0.05$) higher in soil amended with HTC than in soil without HTC addition (**Figure 1**). The shoot and root biomass of un-inoculated chickpea increased by 36%, whereas the shoot and root growth of inoculated plants increased by 16 and 22%, respectively. However, there were no significant effects of MBC on the growth of un-inoculated or inoculated chickpea. MBC char improved the shoot biomass of un-inoculated and inoculated chickpea by 18 and 13%, respectively, but the effect was not significant. The root biomass of neither un-inoculated nor inoculated chickpea was changed in MBC-amended soil (**Figures 1**, **2**).

Drought Conditions

Overall, there were positive and significant effects of HTC on the root and shoot growth of both un-inoculated and inoculated chickpea grown under drought conditions. The soil amendment with MBC char produced more benefits to chickpea growth under drought stress than under the well-watered condition. The shoot growth was increased by 9% and root growth by 24% in both un-inoculated and inoculated plants (**Figure 3**). However, the stimulation was not significant when compared to control plants grown without biochar addition.

The interrelation of biochar × moisture level and biochar × inoculation showed no effects but moisture level × inoculation revealed significant interaction effects on shoot biomass (**Table 2**). Biochar × moisture level showed a significant interaction effect but biochar × inoculation and moisture level × inoculation showed no interaction effect on root biomass. Biochar × moisture level × inoculation showed a significant interaction effect on root biomass but not on shoot biomass.

Nodulation and Leghemoglobin Content

Well-Watered Conditions

It is notable that both biochars improved the symbiotic performance of chickpea with *M. ciceri* under well-watered conditions. The nodule numbers of inoculated chickpea were 17 ± 4.01, while HTC addition to soil increased nodule numbers to 52 ± 8.1 per plant, and MBC, by 23 ± 7.2 per plant (**Figure 4A**). The LB content was significantly higher (9.0 mg gFW^{-1}) in the nodules of plants grown in HTC-amended soil than in plants grown in control and MBC-amended soil (**Figure 4B**). There was no significant difference in the

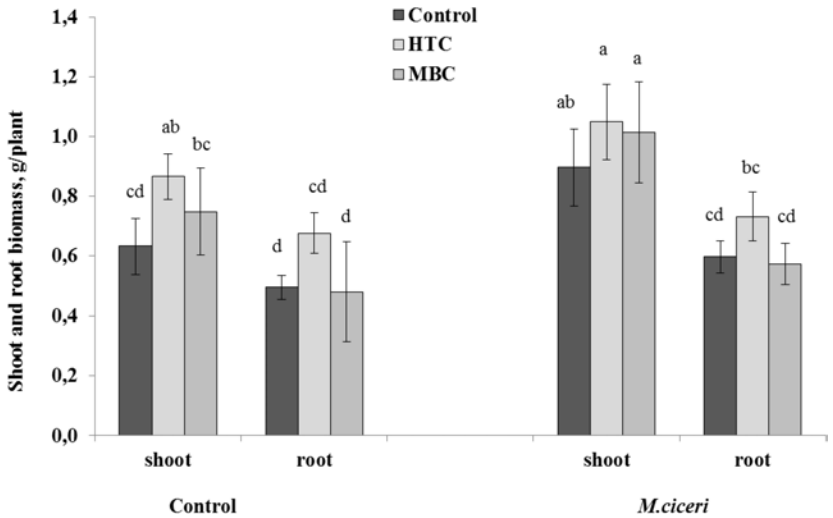

FIGURE 1 | The shoot and root growth of chickpea grown in soil amended with HTC (produced from maize by batch-wise hydrothermal carbonization at 210°C) and MBC (produced from maize through pyrolysis by heating at 600°C) under well-watered conditions. The plants were un-inoculated (control) or inoculated with *M. ciceri*. Column means with different letters are significantly different based on Tukey's HSD test at $P < 0.05$.

FIGURE 2 | The growth of chickpea inoculated with *M. ciceri* in soil amended with 2% of HTC, MBC and without biochar (control) under the well-watered condition. Plants were grown for 40 days after the start of the experiment.

nodule LB content between plants grown in MBC-amended soil and control plants.

Drought Conditions

The nodule numbers decreased in chickpea grown under drought conditions for all variants (**Figures 4A,B**). The symbiotic performance of chickpea with *M. ciceri* was inhibited by drought stress, reducing nodule numbers from 17.6 to 3.4 per plant. The biochar addition increased nodule numbers to 25 ± 4.2 in HTC char-amended soil and 14.6 ± 3.1 in MBC char-amended soil, which were higher than the nodule numbers in control plants (3.4 ± 2.51) (**Figure 4A**).

The LB content per g of fresh weight of nodule tissue was considerably lower in the nodules of plants grown

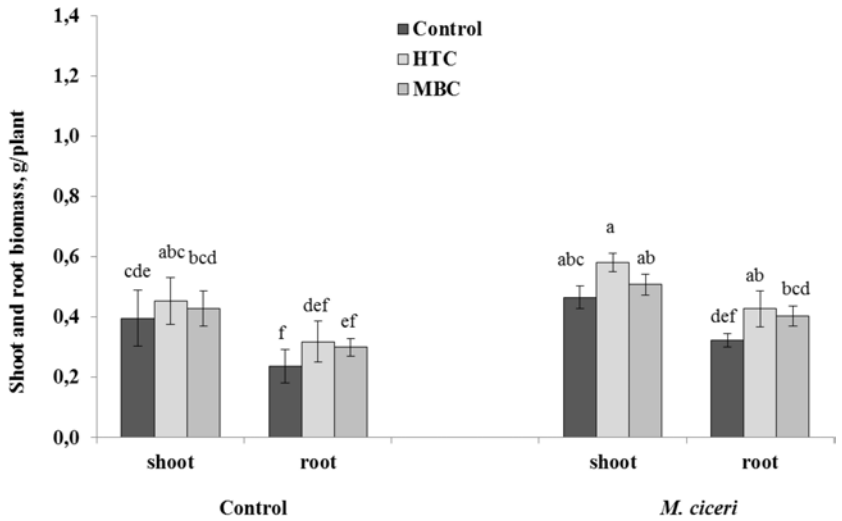

FIGURE 3 | The shoot and root growth of chickpea grown in soil amended with HTC and MBC under drought conditions. The plants were un-inoculated (control) or inoculated with *M. ciceri*. Column means with different letters are significantly different based on Tukey's HSD test at $P < 0.05$.

TABLE 2 | Interaction effects of biochar, moisture level, and inoculation on plant biomass, LB content, and plant nutrients.

Interaction effects	Shoot biomass	Root biomass	LB content	Shoot C	Shoot N	Shoot P	Shoot K	Shoot Mg	Root C	Root N	Root P	Root K	Root Mg
Biochar × Moisture level	ns	**	ns	ns	ns	ns	**	**	***	**	ns	***	ns
Biochar × Inoculation	ns	ns		ns	**	**	**	***	ns	***	ns	ns	***
Moisture level × Inoculation	**	ns		ns	ns	ns	ns	***	*	*	ns	ns	ns
Biochar × Moisture level × Inoculation	ns	*		***	ns	ns	ns	**	**	***	ns	ns	*

*Significance denoted by *$p < 0.05$, **$p < 0.01$, ***$p < 0.001$.*

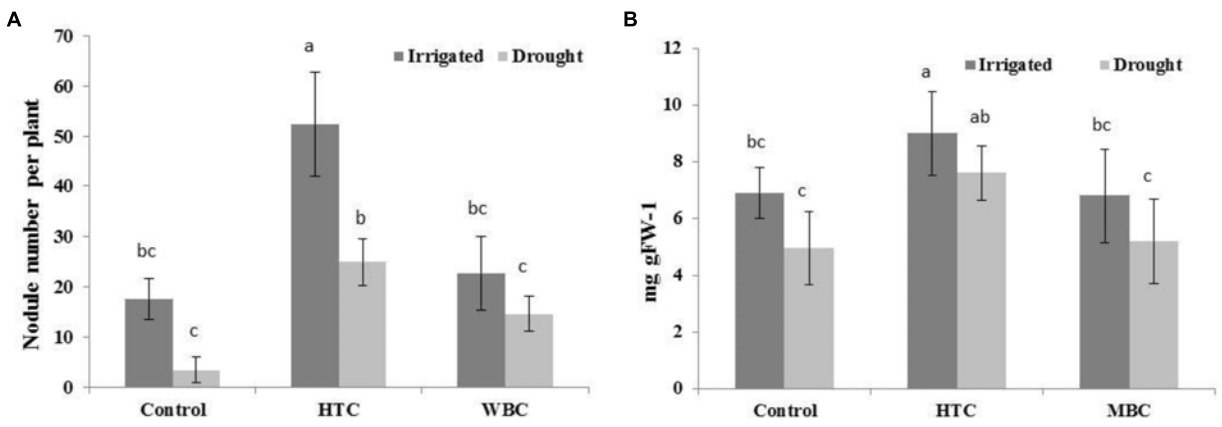

FIGURE 4 | The nodule number **(A)** and LB content **(B)** of chickpea grown in soil amended with HTC and MBC under well-watered and drought conditions. The plants were inoculated with *M. ciceri*. Column means with different letters are significantly different based on Tukey's HSD test at $P < 0.05$.

under drought conditions. The LB content in chickpea nodules was not changed in MBC-amended soil compared to control soil. However, there was a significant positive effect on the LB content in nodules of plants grown in soil with HTC addition.

The Interaction of biochar × moisture level showed no significant effect on LB content (**Table 2**).

Plant Nutrient Content

Well-Watered Conditions

In general, the concentrations of N, P, K, and Mg in plant tissues were affected by the type of biochar and by plant growth conditions. In HTC char-amended soil, the nutrient concentration of un-inoculated and inoculated plants with *M. ciceri* was higher than that of plants grown in soil without

biochar addition. Significant ($p < 0.05$) increases in N, P, K, and Mg concentrations over those in the controls were observed after HTC amendment under the well-watered conditions, with increases of 15, 35, 17, and 51%, respectively. Only K and Mg concentrations increased significantly (20–26%) in shoot tissue. The soil amendment with HTC char positively affected inoculated chickpea as well, increasing mainly N, P, and K uptake (**Table 3**). In MBC-amended soil, only K concentrations in the roots and shoots of un-inoculated and inoculated plants were increased compared to those in control plants grown in soil without biochar addition. The K concentration in the root tissue of un-inoculated and inoculated plants was increased by 123 and 119%, respectively, whereas that in the shoot tissue was increased by 84 and 58%. Among the nutrients, only the N and Mg concentrations in the shoots of un-inoculated plants were significantly ($p < 0.05$) increased by MBC char (**Table 3**).

Drought Conditions

Furthermore, a positive effect of MBC char on the nutrient uptake of plants was observed under drought conditions. The soil amended with MBC showed an increased concentration of N, P, and K contents in plant roots inoculated with *M. ciceri* by 20, 16, and 79%, compared to control plants, respectively (**Table 3**). The highest concentration of K in roots and shoots was also observed under drought conditions, increasing by 86% for un-inoculated plants and 78% for plants inoculated with *M. ciceri*. A notable result was observed where the MBC char amendment reduced the Mg concentration in plant tissue under drought conditions. The acquisition of N, P, K, and Mg by roots and shoots was improved under drought conditions by HTC char amendment, and significant stimulation was observed in inoculated plants (**Table 3**). For example, the concentrations of C, N, P, K, and Mg in root tissue increased by up to 27, 33, 28, 23, and 26%, respectively.

The interaction of biochar × moisture level showed significant effects on shoot K, shoot Mg, root C, root N, and root K contents but no interaction effect on shoot C, shoot N, shoot P, root P, and root Mg content (**Table 2**). Biochar × inoculation showed significant interaction effects on shoot N, shoot P, shoot K, shoot Mg, root N, and root Mg content but no effect on shoot C, root C, root P, and root K content. Moisture level × inoculation showed significant interaction effects on shoot Mg, root C, and root N content but no impacts on shoot C, shoot N, shoot P, shoot K, root P, root K, and root Mg content. Furthermore, the interaction of biochar × moisture level × inoculation showed significant impacts on shoot C, shoot Mg, root C, root N, and root Mg content but no interaction effect on shoot N, shoot P, shoot K, root P, and root K contents.

Soil Carbon and Nutrient Contents

Well-Watered Conditions

Table 4 shows the soil nutrient concentrations under well-watered and drought conditions with biochar treatment. The highest values of soil organic C, N, and Mg were observed in soil amended with HTC and MBC under both inoculation with *M. ciceri* and no inoculation. The lowest value was found in soil without biochar treatments. The soil organic C, N, P, K, and Mg concentrations in soil amended with HTC (inoculated with *M. ciceri* or without inoculation) were increased by up to 66, 29, 14, 44, and 44%, respectively, under well-watered conditions compared to uninoculated soil without biochar. The C, P, and Mg concentrations in the MBC-amended soil were twofold higher and the K concentration was threefold higher than those in the soil without MBC addition and inoculation with *M. ciceri* (**Table 4**). Our results reveal that the uptake of available P and K was significantly affected by MBC biochar amendment compared to soil without biochar and regardless of inoculation with *M. ciceri*. There were no significant differences in soil nutrients between treatments with inoculated and non-inoculated plants.

Drought Conditions

The nutrient concentrations in soil without biochar amendment were similar between drought and well-watered soils, except for the K concentration, which was higher under drought conditions. Under drought conditions, both biochar amendments increased soil organic C as well as N content by up to 84 and 46% compared to soil without biochar, respectively. The P, K, and Mg concentrations in soil were not significantly affected by HTC amendment of soil; only the soil with MBC biochar showed higher contents, regardless of *M. ciceri* inoculation. Furthermore, the P concentration increased by 75%, that of K, by 186%, and that of Mg, by 22% in soil with inoculated plants and amended with MBC. The nutrient content did not differ significantly between the soil of plants inoculated with *M. ciceri* and that of uninoculated plants.

The interaction of biochar × moisture level showed significant effects on soil P, K, and Mg contents but no impacts on soil N content (**Table 5**). Biochar × inoculation showed significant interaction effects only on soil K content but no impacts on soil N, P, and Mg content. Moisture level × inoculation showed significant interaction effects on soil Mg content but no effects on either soil N, P, or K contents. There were no interaction effects of biochar × moisture level × inoculation on soil nutrients.

Soil Enzymes

Well-Watered Conditions

Among the biochar treatments, adding HTC char to soil increased FDA activity in well-watered soil with inoculated and uninoculated plants by 37% (**Figure 5A**). The soil FDA activities did not differ between soil amended with MBC biochar and control soil without biochar (**Figure 5A**). The soil acid and alkaline phosphomonoesterase activities under chickpea were also affected by biochar amendment. A significant increase of 70 and 40% in acid phosphomonoesterase activity was observed under HTC and MBC amendments compared to soil without biochar, respectively. Alkaline phosphomonoesterase activity was increased by up to 30% in HTC-amended soil. Both enzyme activities were slightly but not significantly higher for chickpea inoculated with *M. ciceri* than for uninoculated controls.

Protease activity was slightly higher in HTC-amended soil than in the control and MBC-amended soil; however, the effect was not significant (**Figure 6**). There was no difference in protease activity between MBC-amended soil and soil without biochar.

TABLE 3 | Carbon and nutrient concentrations (%) in chickpea shoot and root tissue grown in soils after application of HTC and MBC chars under well-watered and drought conditions.

	Root					Shoot				
	C	N	P	K	Mg	C	N	P	K	Mg
Well-watered										
Control	32,56^{b}	1,42^{c}	0,25^{bc}	2,15^{c}	0,94^{b}	40,53^{b}	1,99^{b}	0,31^{b}	2,13^{d}	0,28^{c}
M. ciceri	33.65^{ab}	1.93^{ab}	0.26^{abc}	2.27^{c}	1.21^{ab}	44.35^{a}	2.96^{a}	0.30^{b}	2.32^{cd}	0.45^{a}
HTC	35,62^{a}	1,64^{bc}	0,33^{ab}	2,52^{bc}	1,43^{a}	43,35^{a}	2,17^{b}	0,32^{b}	2,56^{bc}	0,35^{bc}
HTC + *M. ciceri*	35.04^{ab}	2.15^{a}	0.35^{a}	3.34^{b}	1.23^{ab}	44.10^{a}	3.12^{a}	0.36^{a}	2.69^{b}	0.45^{a}
MBC	32,31^{b}	1,46^{c}	0,25^{c}	4,82^{a}	0,94^{b}	43,31^{a}	2,08^{b}	0,31^{b}	3,92^{a}	0,38^{ab}
MBC + *M. ciceri*	34.14^{ab}	1.72^{ab}	0.30^{abc}	4.99^{a}	1.09^{b}	43.55^{a}	3.06^{a}	0.31^{b}	3.66^{a}	0.42^{ab}
Drought										
Control	27,85^{c}	1,66^{cd}	0,25^{b}	1,99^{c}	0,91^{bc}	43,35^{ab}	2,67^{ab}	0,31^{ab}	2,44^{c}	0,44^{c}
M. ciceri	25.36^{c}	1.56^{cd}	0.25^{b}	2.00^{c}	1.01^{ab}	40.80^{b}	3.42^{a}	0.29^{b}	2.62^{bc}	0.49^{bc}
HTC	33,86^{ab}	1,53^{d}	0,29^{ab}	2,03^{c}	1,16^{a}	41,70^{ab}	2,14^{b}	0,31^{ab}	2,81^{b}	0,62^{a}
HTC + *M. ciceri*	35.51^{a}	2.21^{a}	0.32^{a}	2.45^{b}	1.15^{a}	44.25^{a}	3.50^{a}	0.35^{a}	2.53^{bc}	0.51^{b}
MBC	33,51^{ab}	1,70^{c}	0,29^{ab}	3,72^{a}	0,72^{d}	41,40^{b}	3,14^{a}	0,30^{b}	3,74^{a}	0,43^{c}
MBC + *M. ciceri*	31.78^{b}	1.88^{b}	0.29^{ab}	3.59^{a}	0.78^{cd}	42.54^{ab}	3.18^{a}	0.31^{ab}	3.48^{a}	0.50^{b}

Plants were grown for 40 days after the start of the experiment. The different letters indicate significant differences based on Tukey's HSD test at $P < 0.05$.

TABLE 4 | Soil carbon and nutrient concentrations after application of HTC and MBC chars under well-watered and drought conditions.

	Well-watered					Drought				
	C (%)	N (%)	P	K	Mg	C (%)	N (%)	P	K	Mg
			mg 100 g^{-1} soil					mg 100 g^{-1} soil		
Control	0.89^{c}	0,095^{b}	7,49^{c}	6,9^{c}	4,67^{c}	0.95^{c}	0,094^{c}	7,47^{d}	13,52^{b}	7,18^{c}
M. ciceri	0.95^{c}	0,099^{b}	7,97^{bc}	7,4^{c}	5,38^{c}	0.91^{c}	0,100^{c}	7,89^{cd}	12,61^{b}	6,54^{c}
HTC	1.39^{b}	0,132^{a}	8,25^{bc}	10,6^{c}	6,68^{b}	1.51^{ab}	0,138^{a}	8,75^{b}	14,09^{b}	7,48^{bc}
HTC + *M. ciceri*	1.48^{ab}	0,123^{a}	8,55^{b}	10,0^{c}	6,75^{b}	1.42^{b}	0,138^{a}	8,38^{bc}	13,80^{b}	7,07^{c}
MBC	1.69^{a}	0,129^{a}	13,30^{a}	27,3^{b}	8,09^{a}	1.75^{a}	0,124^{b}	12,52^{a}	36,23^{a}	8,48^{ab}
MBC + *M. ciceri*	1.75^{a}	0,128^{a}	13,53^{a}	32,7^{a}	8,56^{a}	1.71^{a}	0,136^{ab}	13,13^{a}	38,79^{a}	8,78^{a}

Plants were grown for 40 days after the start of the experiment. The different letters indicate significant differences based on Tukey's HSD test at $P < 0.05$.

TABLE 5 | Interaction effects of biochar, moisture level, and inoculation on soil nutrients and soil enzyme activities.

Interaction effects	Soil N	Soil P	Soil K	Soil Mg	FDA	Protease activity	Alkaline phosphomonoesterase activity	Acid phosphomonoesterase activity
Biochar × Moisture level	ns	*	*	***	ns	ns	ns	***
Biochar × Inoculation	ns	ns	*	ns	ns	ns	ns	*
Moisture level × Inoculation	ns	ns	ns	**	ns	ns	ns	*
Biochar × Moisture level × Inoculation	ns	ns	ns	ns	ns	ns	ns	ns

*Significance denoted by *$p < 0.05$, **$p < 0.01$, ***$p < 0.001$.*

Drought Conditions

Under drought conditions, soil FDA activity was higher under both biochar types, regardless of bacterial inoculation, than that of soil without biochar (**Figure 5B**). The HTC char amendment increased soil FDA activity by 44% and MBC by 24%, and soil FDA activity was higher with bacterial inoculation than without inoculation. Drought stress inhibited the acid and alkaline phosphomonoesterase activities of soil without biochar, regardless of inoculation with *M ciceri* (**Figures 7**, **8**). Only HTC showed a positive effect on acid and alkaline phosphomonoesterase activities, with an increase of 17 and 49% compared to the control, but the effects were not significant for uninoculated soil (**Figure 8**).

There were no changes in soil protease activity under drought stress after the biochar amendments. However, an increase of 30% was observed in soil with rhizobial inoculation after HTC char amendment compared to soil without biochar (**Figure 6**).

The interactions of biochar × moisture level, biochar × inoculation, and biochar × inoculation showed

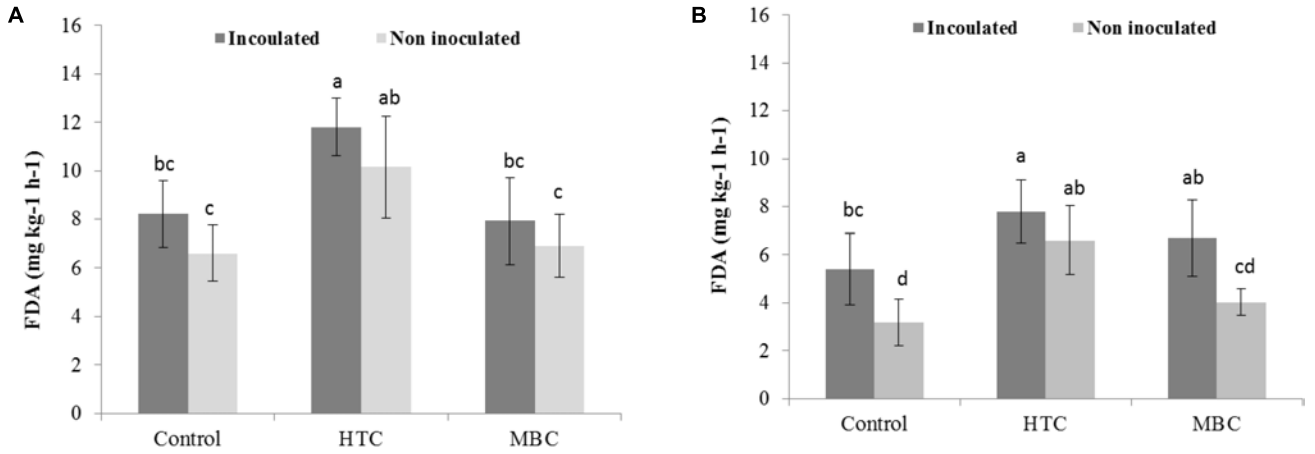

FIGURE 5 | Effect of HTC and MBC on soil FDA activity under well-watered **(A)** and drought **(B)** conditions. Error bars (standard error) followed by a different letter within each column are significantly different at $P < 0.05$ based on Tukey's HSD test.

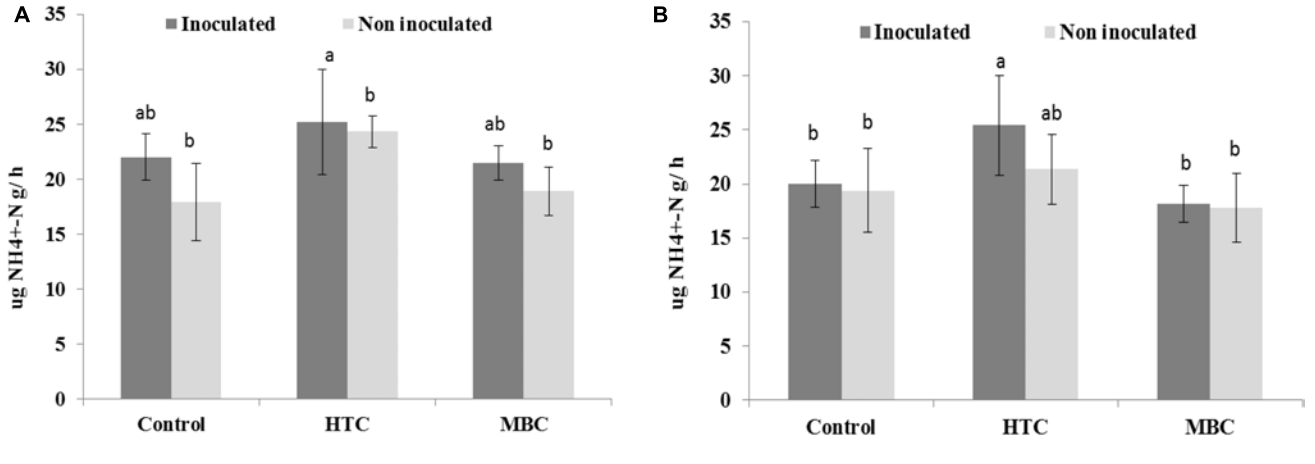

FIGURE 6 | Effect of HTC and MBC on soil protease activity under well-watered **(A)** and drought **(B)** conditions. Error bars (standard error) followed by a different letter within each column are significantly different at $P < 0.05$ based on Tukey's HSD test.

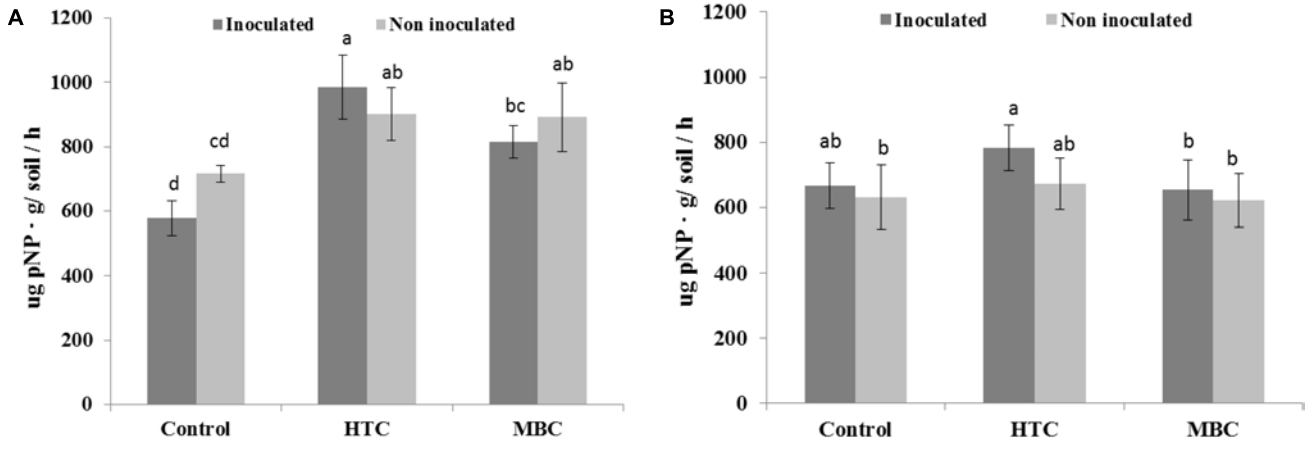

FIGURE 7 | Effect of HTC and MBC on soil acid phosphomonoesterase activity under well-watered **(A)** and drought **(B)** conditions. Error bars (standard error) followed by a different letter within each column are significantly different at $P < 0.05$ based on Tukey's HSD test.

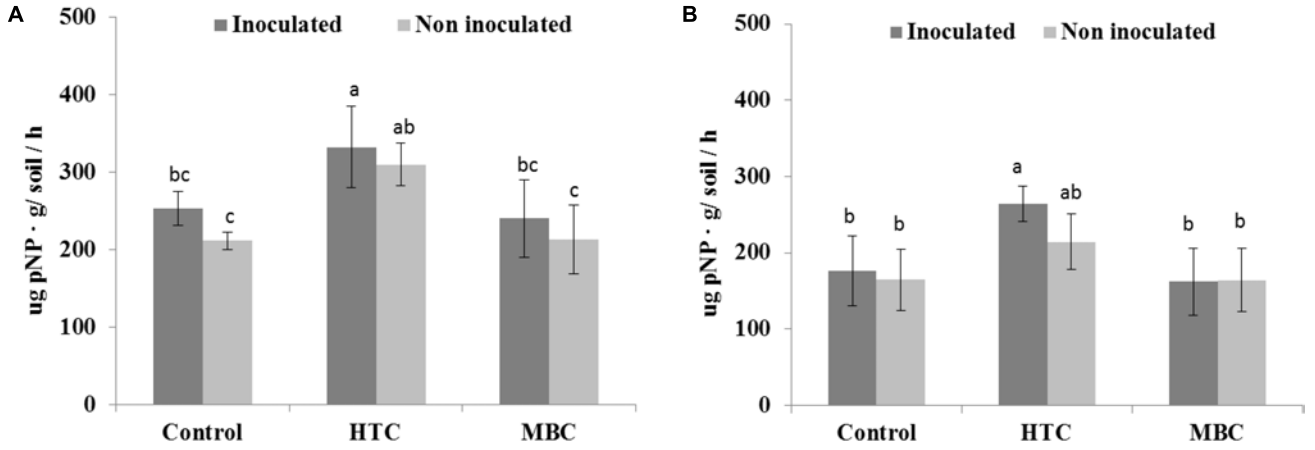

FIGURE 8 | Effect of HTC and MBC on soil alkaline phosphomonoesterase activity under well-watered **(A)** and drought **(B)** conditions. Error bars (standard error) followed by a different letter within each column are significantly different at $P < 0.05$ based on Tukey's HSD test.

significant impacts on soil acid phosphomonoesterase activity while biochar × moisture level × inoculation showed no interaction effect on soil acid phosphomonoesterase activity (**Table 5**). No interactions were found for FDA, protease, and alkaline phosphomonoesterase activities.

DISCUSSION

Overall, our experiment showed that the shoot and root growth, nutrient acquisition and symbiotic performance of chickpea with *M. ciceri* under well-watered and drought conditions were improved by HTC char amendment of soil. However, MBC char produced more benefits to chickpea growth under drought stress than under well-watered conditions. However, biochar and moisture level showed no significant interaction on soybean shoot biomass. It has been reported that biochar amendment increases the water holding capacity of soil (Abel et al., 2013; Bruun et al., 2014), which affects the availability of K (Rogovska et al., 2014). Joseph et al. (2010) report that the interaction of biochar with environmental conditions is an important requirement for revealing contrasting effects, which might depend on the physicochemical properties of biochar. For example, Butnan et al. (2015) observed reduced plant growth on a sandy Ultisol amended with eucalyptus wood-derived biochar produced by pyrolysis (800°C), whereas biochar produced at a lower temperature (350°C) provided higher benefits. Biochar amendment has also been shown to increase plant root and shoot growth and drought tolerance without increasing soil water availability, thus improving plant eco-physiological responses related to water status such as leaf osmotic potential, stomata resistance and water use efficiency (Kammann et al., 2011; Haider et al., 2015). Shen et al. (2016) studied the effect of two types of biochar on the plant growth and P uptake of *Lotus pedunculatus* cv barsille. The authors found that the addition of biochar from willow woodchips increased plant growth, whereas pine-based biochar did not show any positive effect on plant growth and P uptake when added to a nutrient-poor soil.

In our study, the nodule numbers and LB content were decreased in chickpea grown under drought conditions. It is notable that both biochars improved the symbiotic performance of chickpea with *M. ciceri* under both well-watered and drought conditions. Additionally, providing biochar and moisture level showed no significant interaction on LB content. According to Iijima et al. (2015), the biochar amendment of soil provides more air to nodule bacteria that adhere to the surface of biochar pores. In another study, Pietikainen et al. (2000) reported that the survival of bacteria, which were sorbed to biochar surfaces was due to the capability of biochar protecting bacteria in soil. Kolton et al. (2011) proved that soil amendment with carbon-rich biochar from citrus wood provided favorable conditions for bacterial proliferation, which increased microbial community composition in soil growing sweet peppers (*Capsicum annuum* L.). In another study, the rhizobial cell counts and nodulation of soybean were increased by the addition of biochar mixed with compost (Lehmann et al., 2011). According to Vanek and Thies (2016), the survival of *Rhizobium tropici* in biochar pores was observed over 6 months. Zahran et al. (1994) illustrated that osmotic stress might lead to an alteration in the *Rhizobium*-host plant recognition process. The severe inhibition by water deficit of root hair infection by *Rhizobium* and the formation of infection threads have also been observed (Graham, 1992; Serraj et al., 1999). In both well-watered and drought conditions, our results showed significant stimulation of root nodulation of chickpea. There are other reports on the importance of signaling factors for nodule formation impacted by biochar, e.g., Mia et al. (2014) observed stimulation of signaling for nodulation with the absorption of flavonoids and Nod factors by biochar. Wang et al. (2018) observed similar results to our findings, where soil amended with bamboo biochar that had been pyrolyzed at a temperature below 500°C stimulated root nodulation as well as soybean growth. The LB content of

chickpea nodules was higher under soil amended with HTC char, but we found no distinction between MBC char and untreated control soil.

Biochar addition can induce changes in nutrient availability and may provide additional N and P (Prendergast-Miller et al., 2011) or bioavailable C sources for microbial proliferation in the rhizosphere (Zimmerman, 2010), depending on the type of biochar. For example, Shen et al. (2016) observed an increase in P uptake and plant growth by the application of biochar produced from willow woodchips compared to the non-amended soil. Soil amendment with pine-based biochar did not show any stimulatory effect on plant growth. In our study, we observed that HTC biochar increased the C content in plants, while MBC char significantly increased the K content in the roots and shoots of plants under both well-watered and drought conditions. The first indication of this positive effect was that MBC char contains higher K content than HTC char, contributing to the availability of K in soil. Wang et al. (2018) observed similar results with bamboo biochar that had been pyrolyzed at a temperature below 500°C, increasing plant growth and K uptake in soybean. In our study, biochar addition did not affect the N uptake of chickpea roots. However, the combined application of biochar with *M. ciceri* significantly increased N uptake. Corresponding results were found in a pot experiment by Rondon et al. (2007), who showed that biochar addition increased N concentrations in beans from 50% in non-biochar treatments to 72% in a biochar treatment. Furthermore, both biochar types increased the Mg uptake of chickpea roots or shoots under well-watered and drought conditions.

In our study, the addition of both types of biochar alone or combined with *M. ciceri* resulted in higher total soil N content under well-watered and drought conditions than in untreated soil, while the difference was not significant under drought conditions when amended with MBC char. In addition, no significant interaction effects among biochar, moisture level, and inoculation was found. Similar observations were reported by Han et al. (2016), where soil amendment with biochar produced from Chinese pine resulted in significant increases in soil total nitrogen. As previously reported, biochar has the capability of reducing nitrogen loss and improving nitrogen cycling in the soil (Huang et al., 2014). The mechanisms directly involved are the large surface area, highly porous structure and strong ion exchange capacity of biochars (Glaser et al., 2001), which contribute to improving the physical and chemical properties of soil and which impact soil biological activities (Anderson et al., 2014; Lentz et al., 2014). In our study, HTC char alone or combined with *M. ciceri* did not show any significant influence on soil P, K, and Mg content while the soil P, K, and Mg contents increased in the soil amended with MBC char. Nevertheless, there were significant interaction effects between biochar and moisture level on soil P, K, and Mg contents.

FDA hydrolytic activity, a measure of overall microbial activity which particularly includes esterases and protease, showed no significant distinction between MBC char and the control under well-watered conditions. However, under drought stress, soil FDA activity was higher under both biochar types than in soil without biochar. Inoculation of chickpea with *M. ciceri* increased activity under well-watered and drought conditions compared to untreated soil. In addition, no interaction effects were found among biochar, moisture level and inoculation factors on soil FDA activity. The enhancement of soil FDA hydrolytic activity by rhizobial inoculation was also observed in a 2-year field trial by Fall et al. (2016). Furthermore, increased activity of soil acid phosphomonoesterase activity was observed in HTC and MBC char treatments under well-watered conditions, whereas drought suppressed enzyme activity. However, the interaction between biochar and moisture level was pronounced for soil acid phosphomonoesterase activity. On the other hand, alkaline phosphomonoesterase activity did not change after MBC char application under either condition, whereas HTC char amendment showed a significant increase. Previous reports found increased alkaline phosphomonoesterase activities and suppression of acid phosphomonoesterase activities by application of manure-derived biochar in loamy sand soil (Jin et al., 2016). Uncertainties in the biochar effect on soil enzyme activities have also been reported (Paz-Ferreiro et al., 2014; Song et al., 2018). Wang et al. (2015) stated that the addition of maize biochar increased the activities of soil enzymes involved in C and N cycles. In our study, soil protease activity slightly increased in HTC char-amended soil and decreased in soil with MBC char amendment under drought conditions.

Rhizobial inoculation showed a positive effect on soil FDA activity, protease and alkaline phosphomonoesterases under well-watered conditions while no interaction effects were found among biochar, moisture level and inoculation. Moreover, *Rhizobia* inoculation combined with HTC char amendment improved soil enzyme activity under drought conditions compared to the control or MBC char-amended soils. These results agree with several studies reporting that *Rhizobia* might increase enzyme activity in the soil-root zone, e.g., Siczek and Lipiec (2016) found that *Rhizobium* inoculation consistently increased the activity of several enzymes in the rhizosphere.

CONCLUSION

The results of our study demonstrated positive synergistic effects of biochar amendments on plant growth, plant nutrient uptake, soil nutrient contents and soil biological properties in sandy loam soil. In general, HTC char produced by batch-wise hydrothermal carbonization at 210°C had a more significant effect on the measured biological indicators than MBC char produced by pyrolysis at 600°C. This finding, that different methods of producing biochar from the same source (maize) play a critical role in the expression of soil ecological effects, underpins the assumption of a link between chemical and physical properties

of biochar and enhanced plant nutrient acquisition, symbiotic performance and plant stress tolerance.

DATA AVAILABILITY STATEMENT

The raw data supporting the conclusions of this manuscript will be made available by the authors, without undue reservation, to any qualified researcher.

AUTHOR CONTRIBUTIONS

DE, SW, and SB-K designed the experiment. DE and HM conducted the experiment. LL, HM, and DE analyzed the data. DE, SW, and SB-K wrote the manuscript. All authors read and approved the manuscript.

FUNDING

This research was supported by a Georg Forster Research Fellowship (HERMES), Alexander von Humboldt Foundation, by the Chinese Academy of Sciences President's International Fellowship Initiative (Grant No. 2018VBA002S) to DE, and by the Xinjiang Uygur Autonomous Region regional coordinated innovation project (Shanghai cooperation organization science and technology partnership program) (No. 2017E01031) to LL.

REFERENCES

Abd Allah, E. F., Alqarawi, A. A., Hashem, A., Radhakrishnan, R., Al-Huqail, A. A., Al-Otibi, F. A., et al. (2017). Endophytic bacterium *Bacillus subtilis* (BERA 71) improves salt tolerance in chickpea plants by regulating the plant defence mechanisms. *J. Plant Interact.* 3, 37–44. doi: 10.1080/17429145.2017.1414321

Abel, S., Peters, A., Trinks, S., Schonsky, H., Facklam, M., and Wessolek, G. (2013). Impact of biochar and hydrochar addition on water retention and water repellency of sandy soil geoderma. 202–203, 183–191. doi: 10.1016/j.geoderma.2013.03.003

Acosta-Martínez, V., and Tabatabai, M. A. (2011). "Phosphorus cycle enzymes," in *Methods of Soil Enzymology, SSSA Book Ser*, ed. R. P. Dick (Madison, WI: SSSA).

Akhtar, S. S., Andersen, M. N., and Liu, F. (2015). Residual effects of biochar on improving growth, physiology and yield of wheat under salt stress. *Agric. Water Manag.* 158, 61–68. doi: 10.1016/j.agwat.2015.04.010

Alburquerque, J. A., Calero, J. M., Barrón, V., Torrent, J., del Campillo, M. C., Gallardo, A., et al. (2014). Effects of biochars produced from different feedstocks on soil properties and sunflower growth. *J. Plant Nutr. Soil Sci.* 177, 16–25. doi: 10.1002/jpln.201200652

Ameloot, N., De Neve, S., Jegajeevagan, K., Yildiz, G., Buchan, D., Funkuin, Y. N., et al. (2013). Short-term CO2 and N2O emissions and microbial properties of biochar amended sandy loam soils. *Soil Biol. Biochem.* 57, 401–410. doi: 10.1016/j.soilbio.2012.10.025

Anderson, C. R., Hamonts, K., Clough, T. J., and Condron, L. M. (2014). Biochar does not affect soil N-transformations or microbial community structure under ruminant urine patches but does alter relative proportions of nitrogen cycling bacteria. *Agric. Ecosyst. Environ.* 191, 63–72. doi: 10.1016/j.agee.2014.02.021

Bodner, G., Nakhforoosh, A., and Kaul, H. P. (2015). Management of crop water under drought: a review. *Agron. Sustain. Develop.* 35, 401–442. doi: 10.1007/s13593-015-0283-4

Bouhmouch, I., Souad-Mouhsine, B., Brhada, F., and Aurag, J. (2005). Influence of host cultivars and Rhizobium species on the growth and symbiotic performance of *Phaseolus vulgaris* under salt stress. *J. Plant Physiol.* 162, 1103–1113. doi: 10.1016/j.jplph.2004.12.003

Bruun, E. W., Petersen, C. T., Hansen, E., Holm, J. K., and Hauggaard-Nielsen, H. (2014). Biochar amendment to coarse sandy subsoil improves root growth and increases water retention. *Soil Use Manag.* 30, 109–118. doi: 10.1111/sum.12102

Butnan, S., Deenik, J. L., Toomsan, B., Antal, M. J., and Vityakona, P. (2015). Biochar characteristics and application rates affecting corn growth and properties of soils contrasting in texture and mineralogy. *Geoderma* 23, 105–116. doi: 10.1016/j.geoderma.2014.08.010

Chan, K. Y., Van Zwieten, L., Meszaros, I., Downie, A., and Joseph, S. (2007). Agronomic values of greenwaste biochar as a soil amendment. *Aust. J. Soil Res.* 45, 629–634.

Deenik, J. L., Diarra, A., Uehara, G., Campbell, S., Sumiyoshi, Y., and Antal, M. J. (2011). Charcoal ash and volatile matter effects on soil properties and plant growth in an acid Ultisol. *Soil Sci.* 176, 336–345. doi: 10.1097/ss.0b013e31821fbfea

Dempster, D. N., Jones, D. L., and Murphy, D. V. (2012). Organic nitrogen mineralisation in two contrasting agro-ecosystems is unchanged by biochar addition. *Soil Biol. Biochem.* 48, 47–50. doi: 10.1016/j.soilbio.2012.01.013

Egamberdieva, D., Jabborova, D., Wirth, S., Alam, P., Alyemeni, M. N., and Ahmad, P. (2018). Interactive effects of nutrients and *bradyrhizobium japonicum* on the growth and root architecture of soybean (*Glycine max* L.). *Front. Microbiol.* 9:1000. doi: 10.3389/fmicb.2018.01000

Egamberdieva, D., Li, L., Wirth, S., Lindström, K., and Räsänen, L. A. (2016a). Microbial cooperation in the rhizosphere improves liquorice growth under salt stress. *Bioengineered* 26, 1–6. doi: 10.1080/21655979.2016.1250983

Egamberdieva, D., Wirth, S., Behrendt, U., Abd-Allah, E. F., and Berg, G. (2016b). Biochar treatment resulted in a combined effect on soybean growth promotion and a shift in plant growth promoting rhizobacteria. *Front. Microbiol.* 7:209. doi: 10.3389/fmicb.2016.00209

Egamberdieva, D., Shurigin, V., Gopalakrishnan, S., and Sharma, R. (2015). "Microbial strategy for the improvement of legume production under hostile environment," in *Legumes Under Environmental Stress: Yield, Improvement and Adaptations*, eds M. M. Azooz, and P. Ahmad, (Hoboken, NJ: Whiley and Sons), 133–142.

Egamberdieva, D., Wirth, S., Shurigin, V., Hashem, A., and Abd Allah, E. F. (2017b). Endophytic bacteria improve plant growth, symbiotic performance of chickpea (*Cicer arietinum* L.) and induce suppression of root rot caused by *Fusarium solani* under salt stress. *Front. Microbiol.* 28:8. doi: 10.3389/fmicb.2017.01887

Egamberdieva, D., Reckling, M., and Wirth, S. (2017a). Biochar-based inoculum of Bradyrhizobium sp. improves plant growth and yield of lupin (*Lupinus albus* L.) under drought stress. *Eur. J. Soil Biol.* 78, 38–42. doi: 10.1016/j.ejsobi.2016.11.007

Fall, D., Bakhoum, N., Nourou Sall, S., Zoubeirou, A. M., Sylla, S. N., and Diouf, D. (2016). Rhizobial inoculation increases soil microbial functioning and gum arabic production of 13-year-old senegalia senegal (L.) britton, trees in the north part of senegal. *Front. Plant Sci.* 7:1–9. doi: 10.3389/fpls.2016.01355

Farooq, M., Gogoi, N., Barthakur, S., Baroowa, B., Bharadwaj, N., Alghamdi, S. S., et al. (2017). Drought Stress in grain legumes during reproduction and grain filling. *J. Agron. Crop Sci.* 203, 81–102. doi: 10.1093/jxb/err139

Glaser, B., Haumaier, L., Guggenberger, G., and Zech, W. (2001). The terra preta phenomenon: a model for sustainable agriculture in the humid tropics. *Naturwissenschaften* 88, 37–41. doi: 10.1007/s001140000193

Gong, H., Meng, D., Li, X., and Zhu, F. (2013). Soil degradation and food security coupled with global climate change in northeastern China. *Chin. Geograph. Sci.* 23, 562–573. doi: 10.1007/s11769-013-0626-5

Graber, E. R., Meller Harel, Y., Kolton, M., Cytryn, E., Silber, A., David, D. R., et al. (2010). Biochar impact on development and productivity of pepper and tomato grown in fertigated soilless media. *Plant Soil* 337, 481–496. doi: 10.1007/s11104-010-0544-6

Graham, P. H. (1992). Stress tolerance in *Rhizobium* and *Bradyrhizobium*, and nodulation under adverse soil conditions. *Can. J. Microb.* 38, 475–484. doi: 10.1139/m92-079

Green, V. S., Stott, D. E., and Diack, M. (2006). Assay for fluorescein diacetate hydrolytic activity: Optimization for soil samples. *Soil Biol. Biochem.* 38, 693–701. doi: 10.1016/j.soilbio.2005.06.020

Gul, S., and Whalen, J. K. (2016). Biochemical cycling of nitrogen and phosphorus in biochar-amended soils. *Soil Biol. Biochem.* 103, 1–15. doi: 10.1016/j.soilbio.2016.08.001

Haider, G., Koyro, H. W., Azam, F., Steffens, D., Müller, C., and Kam-mann, C. (2015). Biochar but not humic acid product amend-ment affected maize yields via improving plant-soil moisture relations. *Plant Soil* 395, 141–157. doi: 10.1007/s11104-014-2294-3

Han, L., Ro, K. S., Sun, K., Sun, H., Wang, Z., Libra, J. A., et al. (2016). New evidence for high sorption capacity of hydrochar for hydrophobic organic pollutants. *Environ. Sci. Technol.* 50, 13274–13282. doi: 10.1021/acs.est.6b02401

Hansen, V., Hauggaard-Nielsen, H., Petersen, C. T., Mikkelsen, T. N., and Müller-Stöver, D. (2016). Effects of gasification biochar on plant-available water capacity and plant growth in two contrasting soil types. *Soil Tillage Res.* 161, 1–9. doi: 10.1016/j.still.2016.03.002

Hashem, A., Abd Allah, E. F., Alqarawi, A., Al-Huqail, A. A., Wirth, S., and Egamberdieva, D. (2016). The interaction between arbuscular mycorrhizal fungi and endophytic bacteria enhances plant growth of *Acacia gerrardii* under salt stress. *Front. Plant Sci.* 7:1089. doi: 10.3389/fmicb.2016.01089

Huang, M., Yang, L., Qin, H., Jiang, L., and Zou, Y. (2014). Fertilizer nitrogen uptake by rice increased by biochar application. *Biol. Fert. Soils* 50, 997–1000. doi: 10.1007/s00374-014-0908-9

Ibrahim, H. M., Al-Wabel, M. I., Usman, A. R. A., and Al-Omran, A. (2013). Effect of conocarpus biochar application on the hydraulic properties of a sandy loam soil. *Soil Sci.* 178, 165–173. doi: 10.1097/ss.0b013e3182979eac

Iijima, M., Yamane, K., Izumi, Y., Daimon, H., and Motonaga, T. (2015). Continuous application of biochar inoculated with root nodule bacteria to subsoil enhances yield of soybean by the nodulation control using crack fertilization technique. *Plant Product. Sci.* 18, 197–208. doi: 10.1626/pps.18.197

Islami, T., Curitno, B., Basuki, N., and Suryanto, A. (2011). Maize yield and associated soil quality changes in cassava and maize intercropping system after three years of biochar application. *J. Agric. Food Technol.* 1, 112–115.

Jin, Y., Liang, X., He, M., Liu, Y., Tian, G., and Shi, J. (2016). Manure biochar influence upon soil properties, phosphorus distribution and phosphatase activities: a microcosm incubation study. *Chemosphere* 142, 128–135. doi: 10.1016/j.chemosphere.2015.07.015

Joseph, S. D., Camps-Arbestain, M., Lin, Y., Munroe, P., Chia, C. H., Hook, J., et al. (2010). An investigation into the reactions of biochar in soil. *Aust. J. Soil Res.* 48, 501–515. doi: 10.1016/j.scitotenv.2017.09.200

Kammann, C. I., Linsel, S., Gößling, J. W., and Koyro, H. W. (2011). Influence of biochar on drought tolerance of *Chenopodium quinoa* willd and on soil-plant relations. *Plant Soil* 345, 195–210. doi: 10.1007/s11104-011-0771-5

Kolton, M., Harel, Y. M., Pasternak, Z., Graber, E. R., Elad, Y., and Cytryn, E. (2011). Impact of biochar application to soil on the root-associated bacterial community structure of fully developed greenhouse pepper plants. *Appl. Environ. Microb.* 77, 4924–4930. doi: 10.1128/AEM.00148-11

Ladd, J. N., and Butler, J. H. A. (1972). Short∼term assays of soil proteolytic enzyme activities using proteins and dipeptide derivatives as substrates. *Soil Biol. Biochern.* 4, 19–30. doi: 10.1016/0038-0717(72)90038-7

Lehmann, J., Rillig, M. C., Thies, J., Masiello, C. A., Hockaday, W. C., and Crowley, D. (2011). Biochar effects on soil biota - a review. *Soil Biol. Biochem.* 43, 1812–1836. doi: 10.1016/j.soilbio.2011.04.022

Lentz, R. D., Ippolito, J. A., and Spokas, K. A. (2014). . *Soil Sci. Soc. Am. J.* 78, 1641–1655.

Lim, T. J., Spokas, K. A., Feyereisen, G., and Novak, J. M. (2016). Predicting the impact of biochar additions on soil hydraulic properties. *Chemosphere* 142, 136–144. doi: 10.1016/j.chemosphere.2015.06.069

Lüscher, A., Mueller-Harvey, I., Soussana, J. F., Rees, R. M., and Peyraud, J. L. (2014). Potential of legume-based grassland-livestock systems in europe: a review. *Grass Forage Sci.* 69, 206–228. doi: 10.1111/gfs.12124

Merga, B., and Haji, J. (2019). Economic importance of chickpea: Production,value, and world trade. *Cogent Food Agric.* 5. doi: 10.1080/23311932.2019.1615718

Mete, F. Z., Mia, S., Dijkstra, F. A., Abuyusuf, M., and Iqbal Hossain, A. S. M. (2015). Synergistic effects of biochar and NPK Fertilizer on soybean yield in an alkaline soil. *Pedosphere* 25, 713–719. doi: 10.1016/s1002-0160(15)30052-7

Mia, S., van Groenigen, J. W., van de Voorde, T. F. J., Oram, N. J., Bezemer, T. M., Mommer, L., et al. (2014). Biochar application rate affects biological nitrogen fixation in red clover conditional on potassium availability. *Agric. Ecosyst. Environ.* 191, 83–91. doi: 10.1016/j.agee.2014.03.011

Mohamed, I., El-Meihy, R., Ali, M., Chen, F., and Raleve, D. (2017). Interactive effects of biochar and micronutrients on faba bean growth, symbiotic performance, and soil properties. *J. Plant Nutr. Soil Sci.* 180, 729–738. doi: 10.1002/jpln.201700293

Nelson, D. W., and Sommers, L. E. (1996). "Total carbon, organic carbon, and organic matter," in *Methods of Soil Analysis, Part 3. Chemical Methods*, ed. D. L. Sparks, (Madison, WI: Soil Science Society of America Inc), 961–1010.

Novak, J., Lima, I., and Xing, B. (2009). Characterization of designer biochar produced at different temperatures and their effects on a loamy sand. *Ann. Environ. Sci.* 3, 195–206.

Parray, A. P., Jan, S., Kamili, A. N., Qadri, R. A., Egamberdieva, D., and Ahmad, P. (2016). Current perspectives on plant growth promoting rhizobacteria. *Plant Growth Regul.* 35, 877–902.

Paz-Ferreiro, J., Fu, S. L., Méndez, A., and Gascó, G. (2014). Interactive effects of biochar and the earthworm Pontoscolex corethrurus on plant productivity and soil enzyme activities. *J. Soils Sediments* 14, 483–494. doi: 10.1007/s11368-013-0806-z

Pietikainen, J., Kiikkila, O., and Fritze, H. (2000). Charcoal as a habitat for microbes and its effects on the microbial community of the underlying humus. *Oikos* 89, 231–242. doi: 10.1034/j.1600-0706.2000.890203.x

Prendergast-Miller, M. T., Duvall, M., and Sohi, S. P. (2011). Localisation of nitrate in the rhizosphere of biochar-amended soils. *Soil Biol. Biochem.* 43, 2243–2246. doi: 10.1016/j.soilbio.2011.07.019

Rahbarian, R., Nejad, R. K., Ganjeali, A., Bagheri, A., and Najafi, F. (2011). Drought stress effects on photosynthesis, chlorophyll fluorescence and water relations in tolerant and susceptible chickpea (*Cicer arietinum* L.) *genotypes. Acta Biol. Cracov. Bot.* 53, 47–56.

Reckling, M., Bergkvist, G., Watson, C. A., Stoddard, F. L., Zander, P. M., Walker, R., et al. (2016). Trade-offs between economic and environmental impacts of introducing legumes into cropping systems. *Front. Plant Sci.* 7:669. doi: 10.3389/fpls.2016.00669

Rehman, A., and Nautiyal, C. S. (2002). Effect of drought on the growth and survival of the stress-tolerant bacterium *Rhizobium* sp. *NBRI*2505 sesbania and its drought-sensitive transposon Tn 5 mutant. *Curr. Microb.* 45, 368–377. doi: 10.1007/s00284-002-3770-1

Reibe, K., Roß, C. L., and Ellmer, F. (2015). Hydro-/Biochar application to sandy soils: impact on yield components and nutrients of spring wheat in pots. *Arch. Agron. Soil Sci.* 61, 1055–1060. doi: 10.1080/03650340.2014.977786

Rogovska, N., Laird, D. A., Rathke, S. J., and Karlen, D. L. (2014). Biochar impact on midwestern mollisols and maize nutrient availability. *Geoderma* 23, 340–347. doi: 10.1016/j.geoderma.2014.04.009

Rondon, M. A., Lehmann, J., Ramírez, J., and Hurtado, M. (2007). Biological nitrogen fixation by common beans (*Phaseolus vulgaris* L.) increases with bio-char additions. *Biol. Fertil. Soils* 43, 699–708. doi: 10.1007/s00374-006-0152-z

Roy, S. J., Tucker, E. J., and Tester, M. (2011). Genetic analysis of abiotic stress tolerance in crops Cur. *Opin. Plant Biol.* 14, 232–239. doi: 10.1016/j.pbi.2011.03.002

Santi, C., Bogusz, D., and Franche, C. (2013). Biological nitrogen fixation in non-legume plants. *Ann. Bot.* 111, 743–767. doi: 10.1093/aob/mct048

Serraj, R., Vadez, V., Denison, R. F., and Sinclair, T. R. (1999). Involvement of ureides in nitrogen fixation inhibition in soybean. *Plant Physiol.* 119, 289–296. doi: 10.1104/pp.119.1.289

Shen, Q., Hedley, M., Camps Arbestain, M., and Kirschbaum, M. U. F. (2016). Can biochar increase the bioavailability of phosphorus? *J. Soil Sci. Plant Nutr.* 16, 268–286.

Siczek, A., and Lipiec, J. (2016). Impact of faba bean-seed rhizobial inoculation on microbial activity in the rhizosphere soil during growing season. *Intern. J. Mol. Sci.* 17:E784.

Siddiqui, M. H., Al-Khaishany, M. Y., Al-Qutami, M. A., Al-Whaibi, M. H., Grover, A., Ali, H. M., et al. (2015). Response of different genotypes of faba bean plant to drought stress. *Int. J. Mol. Sci.* 16, 10214–10227. doi: 10.3390/ijms160510214

Song, D., Tang, J., Xi, X., Zhang, S., Liang, G., Zhou, W., et al. (2018). Responses of soil nutrients and microbial activities to additions of maize straw biochar

and chemical fertilization in a calcareous soil. *Eur. J. Soil Biol.* 84, 1–10. doi: 10.1016/j.ejsobi.2017.11.003

Soudek, P., Rodriguez Valseca, I. M., Petrova, S., Song, J., and Vanek, T. (2016). Characteristics of different types of biochar and effects on the toxicity of heavy metals to germinating sorghum seeds. *J. Geochem. Explor.* 182, 157–165. doi: 10.1016/j.gexplo.2016.12.013

Tabatabai, M. A., and Bremner, J. M. (1969). Use of p-nitrophenol phosphate for the assay of soil phosphatase activity. *Soil Biol. Biochem.* 1, 301–307. doi: 10.1186/1756-0500-7-221

Vadez, V., Rao, J. S., Bhatnagar-Mathur, P., and Sharma, K. K. (2012). DREB1A promotes root development in deep soil layers and increases water extraction under water stress in groundnut. *Plant Biol.* 15, 45–52. doi: 10.1111/j.1438-8677.2012.00588.x

Vanek, S. J., and Thies, J. (2016). Pore-size and water activity effects on survival of *Rhizobium tropici* in biochar inoculant carriers. *J. Microb. Biochem. Technol.* 8, 296–306.

Wang, C., Alidousta, D., Yng, X., and Isoda, A. (2018). Effects of bamboo biochar on soybean root nodulation in multi-elements contaminated soils. *Ecotox. Environ. Safe.* 150, 62–69. doi: 10.1016/j.ecoenv.2017.12.036

Wang, X. B., Song, D. L., Liang, G. Q., Zhang, Q., Ai, C., and Zhou, W. (2015). Maize biochar addition rate influences soil enzyme activity and microbial community composition in a fluvo-aquic soil. *Appl. Soil Ecol.* 96, 265–272. doi: 10.1016/j.apsoil.2015.08.018

Wilson, D. O., and Reisenauer, H. M. (1963). Determination of leghemoglobin in legume nodules. *Anal. Biochem.* 6, 27–30. doi: 10.1016/0003-2697(63)90004-6

Witcombe, J. R., Hollington, P. A., Howarth, C. J., Reader, S., and Steele, K. A. (2008). Breeding for abiotic stresses for sustainable agriculture. *Phil. Trans. R. Soc. B.* 363, 703–716.

Yu, O. Y., Raichle, B., and Sink, S. (2013). Impact of biochar on the water holding capacity of loamy sand soil. *Intern. J. Energ. Environ. Eng.* 4, 1–9.

Zahran, H. H., Räsänen, L. A., Karsisto, M., and Lindström, K. (1994). Alteration of lipopolysaccharide and protein profiles in SDS-PAGE of rhizobia by osmotic and heat stress. *World J. Microbiol. Biotech.* 10, 100–105. doi: 10.1007/BF00357572

Zimmerman, A. R. (2010). Abiotic and microbial oxidation of laboratory-produced black carbon (biochar). *Environ. Sci. Technol.* 44, 1295–1301. doi: 10.1021/es903140c

Conflict of Interest: The authors declare that the research was conducted in the absence of any commercial or financial relationships that could be construed as a potential conflict of interest.

frontiers in Plant Science

ORIGINAL RESEARCH
published: 22 October 2019
doi: 10.3389/fpls.2019.01308

Organic or Inorganic Nitrogen and Rhizobia Inoculation Provide Synergistic Growth Response of a Leguminous Forb and Tree

Peng Zhang[1], R. Kasten Dumroese[2] and Jeremiah R. Pinto[2]*

[1] Key Laboratory of Sustainable Forest Ecosystem Management-Ministry of Education, School of Forestry, Northeast Forestry University, Harbin, China, [2] Rocky Mountain Research Station, Forest Service, U.S. Department of Agriculture, Moscow, ID, United States

Our objective was to better understand how organic and inorganic nitrogen (N) forms supplied to a tree, *Robinia pseudoacacia*, and a perennial forb, *Lupinus latifolius*, affected plant growth and performance of their symbiotic, N-fixing rhizobia. In one experiment, we tested five sources of N [none; three inorganic forms (ammonium, nitrate, ammonium-nitrate); and an organic form (arginine)] in combination with or without rhizobia inoculation. We measured seedling morphology, allometry, nodule biomass, and N status. A second experiment explored combinations of supplied ^{15}N and inoculation to examine if inorganic or organic N was deleterious to nodule N-fixation. Plant growth was similar among N forms. A positive response of nodule biomass to N was greater in *Robinia* than *Lupinus.* For *Robinia*, inorganic ammonium promoted more nodule biomass than organic arginine. N-fixation was concurrent with robust supply of either inorganic or organic N, and N supply and inoculation significantly interacted to enhance growth of *Robinia.* For *Lupinus*, the main effects of inoculation and N supply increased growth but no interaction was observed. Our results indicate that these important restoration species for forest ecosystems respond well to organic or inorganic N forms (or various forms of inorganic N), suggest that the nodulation response may depend on plant species, and show that, in terms of plant growth, N supply and nodulation can be synergistic.

Keywords: amino acid, arginine, inorganic nitrogen, isotopic nitrogen, *Lupinus latifolius*, nitrogen fixation, organic nitrogen, *Robinia pseudoacacia*

OPEN ACCESS

Edited by:
Heike Bücking,
South Dakota State University, United States

Reviewed by:
Corina Carranca,
National Institute of Agricultural and Veterinary Research (INIAV), Portugal
Marco Betti,
University of Seville, Spain

****Correspondence:***
R. Kasten Dumroese
kas.dumroese@usda.gov

Specialty section:
This article was submitted to Plant Nutrition, a section of the journal Frontiers in Plant Science

Received: *23 January 2019*
Accepted: *19 September 2019*
Published: *22 October 2019*

Citation:
Zhang P, Dumroese RK and Pinto JR (2019) Organic or Inorganic Nitrogen and Rhizobia Inoculation Provide Synergistic Growth Response of a Leguminous Forb and Tree. Front. Plant Sci. 10:1308. doi: 10.3389/fpls.2019.01308

INTRODUCTION

Nitrogen (N) has long been demonstrated as the most critical element for enhanced productivity of plant growth. Soil N is present in inorganic forms, such as ammonium and nitrate, and organic forms, such as amino acids (Christou et al., 2006). Ammonium and nitrate are the predominant inorganic N forms usually taken up by plants (Hawkins and Robbins, 2010). Studies confirmed, however, that amino acids sometimes serve as a primary N source for vegetation (Kielland, 1994; Persson and Näsholm, 2001; Inselsbacher and Näsholm, 2012; Whiteside et al., 2012; Wei et al., 2015) and plants have a reduced carbon cost when assimilating organic N into proteins (Franklin et al., 2017). Organic N can be an efficient and environmentally favorable N source (Öhlund and Näsholm, 2002).

Plants may show different growth responses to the form of N they are provided. For trees, Bigg and Daniel (1978) and Yao et al. (2011) collectively examined six conifer species and found that three species grow better with ammonium than nitrate (*Picea engelmannii*, *Pinus contorta*, *Pinus yunnanensis*), two grow better with nitrate than ammonium (*Pseudotsuga menziesii*, *Pinus densata*), and one had no preference (*Pinus tabuliformis*). *Picea abies* and *Pinus sylvestris* seedlings, with an ability to uptake intact amino acids, grow as well as, or better, when they are supplied with amino acids compared to seedlings with access to inorganic N sources (Öhlund and Näsholm, 2001; Gruffman et al., 2012). Conversely, a field study with *Abies fraseri*, *Pinus resinosa*, and *Populus nigra* × *Populus maximowiczii* found that seedling growth and foliar N response resulting after an amino acid supply was similar to inorganic N applications only when the organic form was applied at rates two or three times higher than that of the inorganic form (Wilson et al., 2013). The N form provided in the growth substrate affects not only plant growth but also plant biomass allocation. Amino acids were suggested to have a direct positive effect on root growth of the small herb *Arabidopsis thaliana* cultivated in a sterile agar growth system (Cambui et al., 2011). *Picea abies* and *P. sylvestris* seedlings given organic N (arginine) in a container nursery had larger root systems and a greater root-to-shoot ratio than did seedlings with access to inorganic N (Gruffman et al., 2012).

Inoculation of seeds with rhizobia is known to increase nodulation, leading to enhanced N content, growth, and yield of legume crops (Adgo and Schulze, 2002; Gan et al., 2010; Namvar et al., 2011) and woody species (Dan et al., 1993; Diabate et al., 2005; Jayakumar and Tan, 2006; Dumroese et al., 2009). The effectiveness of inoculation on nodulation and subsequent plant growth response can be affected by N fertilization, but the conclusions are mixed. While broadly concluded that mineral soil N [nitrate (NO_3^-) and ammonium (NH_4^+)] inhibits nodulation, nodule growth, and activity in legumes (Imsande, 1986; Streeter and Wong, 1988; Guo et al., 1992; Bollman and Vessey, 2006; Camargos and Sodek, 2010), studies have shown that low (Rohm and Werner, 1991; Vessey and Waterer, 1992; Gulden and Vessey, 1997; Goicoechea et al., 2005; Yashima et al., 2005) and moderate (Peoples et al., 1995; Bado et al., 2006) supplies of N can stimulate nodulation and N fixation. Nodulation with apparent N-fixing ability has also been noted when N was supplied in high amounts (Dumroese et al., 2009). These differences may be a function of either the symbiosis or the N source.

The response of legumes to N level is species specific and depends upon the particular rhizobia-legume symbiosis (Manhart and Wong, 1980; Harper and Gibson, 1983). Nodules of *Lupinus angustifolius* infected with *Rhizobium* sp. 127E15 were unaffected by addition of 15 mM NO_3^-, whereas all other combinations of rhizobia–*L. angustifolius* and rhizobia–*Vigna unguiculata* averaged a 30% reduction in nodule biomass (Manhart and Wong, 1980). Nitrate was found to induce an inhibitory effect on nodulation and N fixation in pea plants at levels as low as 0.1 mM, while the level at which NH_4^+ became inhibitory was 1.0 mM and higher (Rys and Phung, 1984; Silsbury et al., 1986; Waterer and Vessey, 1993a, Waterer and Vessey, 1993b; Svenning et al., 1996). While sensitivity to NO_3^- has been found to occur in all legume species studied so far (Streeter and Wong, 1988; Lucinski et al., 2002; Fei and Vessey, 2003), the impact of NH_4^+ on symbiosis is weaker than that observed for NO_3^- (Bollman and Vessey, 2006). Streeter and Wong (1988) noted that nitrate may affect the symbiotic process by reducing nodule formation, reducing nitrogenase activity, or by affecting the ratio of nodule dry mass to whole plant mass. These lines of research continue (Lucinski et al., 2002) but with increasing attention to molecular changes that influence N-fixation brought about by NO_3^- (e.g., Valkov et al., 2017). Despite this intensive effort, the combined effects of N and rhizobia inoculation on nonagronomic legumes have received little attention. To our knowledge, no studies have examined the effects of organic N on nodule formation and subsequent plant growth.

In this study, we assessed the plant response of two Fabaceae (legume) species supplied with different sources of N and rhizobia inoculation in a controlled greenhouse system. *Lupinus latifolius*, hereafter lupine, is a native perennial forb occurring in forests of western North America from British Columbia to Baja California to New Mexico. It has a bushy, densely branched growth habit originating from a woody caudex (Antos and Halpern, 1997). It is commonly used for rehabilitation of disturbed forest sites and for erosion control because it grows well on droughty and/or low-fertility sites, has a deep root system for stabilizing soil, and forms associations with N-fixing microorganisms (Halverson et al., 1986; Doede, 2005). *Robinia pseudoacacia*, hereafter black locust, is a medium-sized tree native to the southeastern United States that has been widely planted and naturalized elsewhere in temperate North America, Europe, southern Africa, and Asia (Olson and Karrfalt, 2008). In the United States, it has been used for afforestation of abandoned farmlands, timber, erosion control, and soil stabilization on disturbed sites (Keresztesi, 1980; Roberts et al., 1983). Both species are commonly grown as container seedlings in some nurseries in North America, and so determining proper N supply and inoculation regimes will undoubtedly have a significant impact on the availability of these two species for restoration activities.

Therefore, our goal was to investigate the growth and allometry, physiological responses, and nodulation status of lupine and black locust provided N in organic and inorganic forms, with or without rhizobia inoculation. To the best of our knowledge, this is the first study to examine the effects of supplying organic N to seedlings and subsequent rhizobia nodule development and function. Arginine was chosen as our model amino acid partly because it had been used in other studies (Öhlund and Näsholm, 2001; Öhlund and Näsholm, 2002; Persson et al., 2003; Öhlund and Näsholm, 2004; Gruffman et al., 2013; Wilson et al., 2013) and partly because of its chemical properties. Arginine is an N-rich molecule containing four N atoms, which collectively contribute 32% of its molecular weight. It is positively charged and thus acts as a basic cation in soils with acidic pH, binding to negatively charged soil particles, which restricts its mobility. Our objectives were to see whether (1) seedlings supplied with organic and inorganic N forms have similar growth; (2) inoculated and noninoculated seedlings supplied with organic and inorganic N forms have similar rhizobia nodule biomass; and (3) high rates of organic and inorganic N supply discourage N fixation.

METHODS AND MATERIALS

Species Selection and Seed Treatment

To meet our objectives, we grew lupine (collected in 2010 at 919 m elevation on the Newport Ranger District, Colville National Forest, Washington, USA) and black locust (collected in 2012 in Kentucky, USA; Lawyer Nursery, Inc., Plains, Montana, USA). Seeds were treated with hot water scarification before sowing. Lupine seeds were submerged 1 min in 100°C water (seeds:water = 10 g:800 ml), immediately soaked in running tap water for 48 h, and stratified 15 days at 3°C. Black locust seeds were submerged in 70°C water (seeds:water = 15 g:500 ml), the heat source was immediately removed, and the seeds and water were allowed to cool for 24 h. Expanded seeds of each species were sown.

Experiment One—Seedling and Nodule Growth

Design and Seed Sowing

Our first experiment was a completely randomized design with two independent factors: rhizobia inoculation and N source. We employed two levels of rhizobia inoculation (control or inoculated) and five sources of N: none; three inorganic forms [ammonium (NH_4^+), nitrate (NO_3^-), ammonium-nitrate (NH_4NO_3)]; and an organic form (L-arginine; Sigma-Aldrich Co., St. Louis, Missouri, USA). At the time of planting, one half of the seeds was inoculated with either lupine- or black locust-appropriate rhizobia. The lupine inoculant included three proprietary isolates, whereas black locust was a combination of a proprietary isolate and USDA 3436 (Plant Probiotics Company, Indianapolis, Indiana, USA). For each inocula replication, we slightly moistened the scarified seeds, applied each peat-based inocula at a rate of 1 g (~3×10^8 CFUs) per 100 g of seeds, thoroughly mixed the seeds and inocula, and immediately hand-planted 3 seeds into Ray Leach™ Super Cells (164 cm^3, 3.8-cm diameter, 21-cm depth; Stuewe & Sons, Inc., Tangent, Oregon, USA) filled with a 1:1 (v:v) mix of Sphagnum peatmoss:vermiculite (Forestry #1, SunGro Horticulture Canada Ltd., Canada). Sown seeds were covered with 1 cm of coarse grit to reduce evaporation and cryptogam growth. We planted eight cells for each species, inoculation, and N source combination (each seedling served as a replicate). Sown cells were randomly placed onto a table inside a fully controlled greenhouse at the U.S. Department of Agriculture, Forest Service, Rocky Mountain Research Station in Moscow, Idaho (46.7232°, –117.0029°; 798 m elevation), thinned to a single seedling after germination, and rearranged during each irrigation to minimize edge effects.

Seedling Culture

Seedling irrigation needs were determined gravimetrically for each species, inoculation, and N source combination. When mass of the water reached 75% of the total water mass at container capacity, seedlings were irrigated with just enough water to return the cells to container capacity (Dumroese et al., 2015); this occurred one or more times each week. Fourteen days after planting (DAP), we began supplying N. Each lupine seedling received a total of 6 mg N during a 6-week period (1 mg per week; 14 to 56 DAP), whereas black locust seedlings each received a total of 24 mg N during a 12-week period (2 mg per week; 14 to 98 DAP). We used three different nutrient stock solutions, differing only with respect to the chemical form of N (**Table 1**). Each stock solution also included micronutrients [sulfur (S), 13%; manganese (Mn), 8%; iron (Fe), 7.5%; copper (Cu), 2.3%; boron (B), 1.35%; molybdenum (Mo), 0.04%; Peters Professional® S.T.E.M.™, the Scotts Company, Marysville, Ohio, USA] at 15 mg L^{-1} and Sprint 330 [10% Fe (chelated); Becker Underwood, Inc., Ames, Iowa, USA] at 20 mg L^{-1}. Once each week, when gravimetric weights indicated irrigation was needed, we calculated the amount of water required to replenish the medium for each seedling to container capacity. This value was always >15 ml $seedling^{-1}$. Starting with 15 ml of stock solution, we added the appropriate N source at either 1 (lupine) or 2 (black locust) mg N and applied the subsequent solution to an individual seedling *via* syringe. As required, we then added plain water to reach the total irrigation amount calculated for each seedling based on the gravimetric measurements. The resulting solutions had 67 (lupine) and 134 (black locust) mg N L^{-1} with concentrations of phosphorus (P), potassium (K), S, calcium (Ca), and magnesium (Mg) provided at ratios of 1.0, 0.7, 1.1, 0.9, and 1.2 to 1.0 N (**Table 1**). We reinoculated seedlings 28 DAP to ensure inoculation; 0.5 g of inoculant was diluted in 1.25 L water and then 5 ml of inoculant solution (2 mg inoculant) was applied to each seedling.

Seedling Measurements

For lupine, the longest petiole length and the widest leaf width were measured weekly from 28 DAP until harvest 56 DAP. For black locust, seedling height and root-collar diameter (RCD) were measured every 14 days from 42 DAP until harvest 112 DAP. At harvest, we gently washed root systems of both species free of medium and counted and harvested nodules. Shoots (leaf and stems for block locust), roots, and nodules were separated and oven-dried 72 h at 65°C for biomass determination. The oven dried shoots and roots for each treatment were subsequently ground to pass a 0.44-mm mesh and analyzed for N concentration by dry combustion in a LECO CN600 (LECO Corp., St. Joseph, Michigan, USA).

Experiment Two—Nodule Activity

Based on our results from the first experiment, we sowed a second crop of each species as described above (except for N source, total N applied, and growing time) to measure differential dilution of absorbed ^{15}N-labeled fertilizer by N inputs through N-fixation by rhizobia (Hardarson and Danso, 1993). Because preliminary data analyses revealed no significant differences among inorganic N forms for seedling growth, we supplied inorganic N only as NH_4NO_3 amended with NH_4NO_3 enriched to 98 atom % ^{15}N (Sigma Aldrich, St. Louis, Missouri, USA). Organic N was supplied as arginine hydrochloride amended with L-arginine-α-hydrochloride enriched to 98 atom % ^{15}N (Cambridge Isotope Laboratory, Inc., Tewksbury, Massachusetts, USA). The ^{15}N:^{14}N was about 0.0037:1. Irrigation and N were supplied as described above, but this time, the black locust seedlings were only treated for 8 weeks (16 mg N total).

TABLE 1 | Nutrient stock solutions for application of different nitrogen sources.

Stock nutrient solution components	Nitrogen sources				
	$(NH_4)_2SO_4$	$Ca(NO_3)_2$	NH_4NO_3	Arginine	None
Solution number =	**1**	**2**	**3**	**3**	**3**
	Chemicals (10^{-3} mol L^{-1})				
Lupine					
$(NH_4)_2SO_4$	2.42	–	–	–	–
$Ca(NO_3)_2$	–	2.40	–	–	–
NH_4NO_3	–	–	2.46	–	–
$C_6H_{14}N_4O_2$	–	–	–	1.19	–
75% H_3PO_4	1.95	1.95	1.95	1.95	1.95
KH_2PO_4	0.34	0.34	0.34	0.34	0.34
KCl	0.90	0.90	0.90	0.90	0.90
$CaCl_2$	2.41	–	2.41	2.41	2.41
$MgSO_4$	–	2.42	2.42	2.42	2.42
$MgCl_2$	2.46	–	–	–	–
Black locust					
$(NH_4)_2SO_4$	4.80	–	–	–	–
$Ca(NO_3)_2$	–	4.77	–	–	–
NH_4NO_3	–	–	4.89	–	–
$C_6H_{14}N_4O_2$	–	–	–	2.38	–
75% H_3PO_4	1.95	1.95	1.95	1.95	1.95
KH_2PO_4	2.33	2.33	2.33	2.33	2.33
$CaCl_2$	4.76	–	4.76	4.76	4.76
$MgSO_4$	–	4.75	4.75	4.75	4.75
$MgCl_2$	4.88	–	–	–	–
	N[z]	**P**	**K**	**S**	**Ca**	**Mg**
	Applied element concentration (mg L^{-1})					
Lupine	67	70	46	79	96	59
Black locust	133	140	91	154	190	114

[z]*Control seedlings received no nitrogen but the other nutrients at these rates.*

Individual seedlings were harvested 56 DAP (lupine) and 70 DAP (black locust). Seedlings were washed free of growing media and rinsed in deionized water, partitioned into leaves, stems, and roots, then oven dried 48 h at 60°C, weighed, and ground as previously described to determine biomass. At least five seedlings from each species × N combination were analyzed for isotopic N. The concentrations of ^{15}N and ^{14}N in each tissue were determined with a continuous flow isotope ratio mass spectrometer (Finnigan Delta PlusXP, Thermo Fisher Scientific, Breman, Germany) at the Washington State University Stable Isotope Core Laboratory (Pullman, Washington, USA). Nitrogen isotope ratio was expressed as follows:

$$\delta^{15}\mathrm{N} = \left(\left[{}^{15}\mathrm{N}\,\mathrm{sample}/{}^{14}\mathrm{N}\,\mathrm{sample}\right]/\left[{}^{15}\mathrm{N}\,\mathrm{air}/{}^{14}\mathrm{N}\,\mathrm{air}\right]-1\right)\times 1{,}000$$

Statistical Analysis

Both experiments were analyzed as factorial designs. Analysis of variance (two-way ANOVA) was used to examine the effects of the independent variables (N, rhizobia inoculation) and their interaction on final seedling petiole length (cm); leaf width (mm); height (cm); RCD (mm); dry biomass (g) of leaves, stems, shoots, roots, and nodules; ratio of shoot dry biomass to root dry biomass (S:R); N concentration (g kg^{-1}) and content (mg kg^{-1}) of leaves, stems, shoots, and roots; and $\delta^{15}N$. Residual plots were used to assure data met model assumptions for homoscedasticity and normality. We used Tukey's HSD for *post hoc* tests of differences between model means. Results were considered significant at $\alpha = 0.05$. Box-plot visualizations were created using SigmaPlot (version 13.0; Systat Software, San Jose, California, USA).

RESULTS

Lupine

In the first experiment, none of the final measured response variables were affected by an N × inoculation interaction. While N overall was a significant factor, only the presence of N (as opposed to no N) significantly affected every measured response variable except shoot-to-root ratio (S:R) and nodule biomass (**Table 2**). Seedlings supplied with N had significantly longer petioles and greater leaf width, and a trend toward greater shoot and root biomass, than those not supplied N. Inoculation significantly affected every final measured response variable (**Table 2**; **Figure 1**). Inoculated seedlings had significantly longer petioles and wider leaves, as well as significantly more shoot, root, and nodule biomass than the

TABLE 2 | Mean morphological parameters of lupine seedlings inoculated (I) with (+) or without (–) rhizobia and supplied with different nitrogen (N) sources [none, ammonium (NH_4), nitrate (NO_3), ammonium nitrate (NH_4NO_3), or arginine (A)] for 6 weeks (n = 8). Main effect (ME) means are presented in italics. Different letters within a dependent variable indicate significant differences (α = 0.05) using Tukey's HSD.

Dependent variable	I	ME	Nitrogen sources					ME	Sources of variation		
									P values		
			None	NH_4	NO_3	NH_4NO_3	A	*I*	N	I	N × I
Petiole length	+		12.5	15.9	15.1	15.6	15.6	*14.9 a*		**<0.0001**	
(cm)	–		8.1	10.6	12.2	12.1	11.4	*10.9 b*			0.8686
		N	*10.3 b*	*13.3 ab*	*13.6 a*	*13.9 a*	*13.5 a*		**<0.0096**		
Leaf width	+		8.2	9.6	9.6	10.8	10.7	*9.8 a*		**<0.0001**	
(mm)	–		4.2	6.2	6.2	6.3	5.4	*5.7 b*			0.3253
		N	*6.2 b*	*7.9 a*	*7.9 a*	*8.5 a*	*8.1 a*		**0.0005**		
Shoot biomass	+		0.39	0.51	0.52	0.74	0.67	*0.57 a*		**<0.0001**	
(g)	–		0.06	0.17	0.20	0.19	0.16	*0.16 b*			0.0544
		N	*0.23 b*	*0.34 ab*	*0.36 ab*	*0.47 a*	*0.42 a*		**0.0002**		
Root biomass	+		0.17	0.23	0.22	0.30	0.27	*0.24 a*		**<0.0001**	
(g)	–		0.02	0.05	0.07	0.06	0.05	*0.05 b*			0.2813
		N	*0.09 b*	*0.14 ab*	*0.15 ab*	*0.18 a*	*0.16 ab*		**0.0082**		
Nodule biomass	+		0.049	0.055	0.063	0.080	0.070	*0.063 a*		**<0.0001**	
(g)	–		0.002	0.002	0.009	0.005	0.000	*0.004 b*			0.1575
		N	*0.025*	*0.028*	*0.036*	*0.042*	*0.035*		0.0796		
Shoot:root	+		2.9	2.4	2.3	2.6	2.6	*2.5 a*		**0.0001**	
	–		4.5	3.9	3.0	4.0	4.0	*3.9 b*			0.9342
		N	*3.7*	*3.2*	*2.6*	*3.3*	*3.3*		0.3985		

noninoculated seedlings, but noninoculated seedlings had a significantly higher S:R.

Nitrogen significantly affected shoot and root N concentration and content (**Table 3**). The shoot N concentration was largest for seedlings supplied with inorganic N forms, with arginine and the no-N treatment having the lowest concentrations. Inorganic NH_4^+ and NH_4NO_3 had significantly greater root N concentration than seedlings not supplied N, whereas NO_3^- and arginine were intermediate, yielding results similar to the no-N treatment and the other inorganic sources. Seedlings supplied inorganic and organic N had significantly more shoot N content than no-N seedlings. The largest root N content was provided by NH_4NO_3 and was significantly more than the no-N treatment, while NH_4^+, NO_3^-, and arginine were intermediate, yielding results similar to the no-N treatment and NH_4NO_3. Inoculation significantly affected shoot and root N concentration and N content (**Table 3**). Inoculated seedlings had 2×, 1.5×, 10×, and 7× the shoot N concentration, root N concentration, shoot N content, and root N content of the noninoculated seedlings.

In the nodule activity experiment, no interaction of N form (arginine and NH_4NO_3) and inoculation was observed for shoot, root, or total seedling biomass. Although N form was not significant for any biomass parameter, inoculation was (all $p \leq 0.0088$). For arginine and NH_4NO_3, including inoculation increased total biomass (**Figure 1**). N form and inoculation significantly interacted (all $p \leq 0.0051$) to affect shoot, root, and total seedling N isotope ratio ($\delta^{15}N$); $\delta^{15}N$ values were lower when seedlings were inoculated but the magnitude of difference was greater in seedlings supplied arginine than for those supplied NH_4NO_3 (**Figure 2**). No significant N form × inoculation interaction was observed for shoot or root N content and the main effect of N form was not significant. Inoculation was, however, significant for N content of shoot and root ($p < 0.0001$), with inoculated seedlings having significantly more N (**Figure 2**).

Black Locust

In the first experiment, N and inoculation significantly interacted to affect final measurements of seedling height, leaf biomass, stem biomass, shoot biomass, and root biomass (**Table 4**). The pattern of the interaction was orderly and similar: without inoculation, seedlings supplied N were taller and had greater biomass than those not supplied N; adding inoculation resulted in additional growth to seedlings either supplied N or not supplied N, but the increase in growth was much greater for those supplied N (**Table 4**; **Figure 1**).

Nitrogen significantly affected every final measured response variable except S:R (**Table 4**). In general, N-supplied seedlings had significantly more height, RCD, leaf biomass, and stem, shoot, nodule, and root biomass than seedlings not supplied N, but values among N forms were similar. For N-supplied seedlings, N form did not affect seedling size but it did significantly affect nodule biomass, with NH_4^+ producing the most, followed by NO_3^-, NH_4NO_3, and arginine; the no-N treatment yielded the least amount of nodule biomass. Similar to N, inoculation significantly

FIGURE 1 | Growth responses of black locust and lupine seedlings (98 and 56 days after planting, respectively) supplied inorganic or organic nitrogen with or without rhizobia inoculation and grown in a greenhouse. Noninoculated **(A)** and inoculated **(B)** black locust seedlings. Lupine seedlings fertilized with arginine (left plants noninoculated, right plants inoculated) **(C)** or ammonium-nitrate (left plants noninoculated, right plants inoculated) **(D)**.

TABLE 3 | Mean nitrogen (N) concentrations and contents of lupine seedlings inoculated (I) with (+) or without (–) rhizobia and supplied with different N sources [none, ammonium (NH_4), nitrate (NO_3), ammonium nitrate (NH_4NO_3), or arginine (A)] for 6 weeks (n = 8). Main effect (ME) means are presented in italics. Different letters within a dependent variable indicate significant differences (α = 0.05) using Tukey's HSD.

Dependent variable	I	ME	Nitrogen sources					ME	Sources of variation		
									P values		
			None	NH_4	NO_3	NH_4NO_3	A	*I*	N	I	N × I
N concentration (mg g^{-1})											
Shoot	+		27.5	38.9	38.8	33.3	28.2	33.3 a		**<0.0001**	
	–		11.7	15.8	14.8	16.9	11.9	*14.2 b*			0.0642
		N	*19.6 b*	*27.3 a*	*26.8 a*	*25.1 a*	*20.0 b*		**0.0001**		
Root	+		24.1	32.3	31.0	31.3	27.2	*29.2 a*		**<0.0001**	
	–		15.7	21.4	20.3	21.9	19.9	*19.8 b*			0.7584
		N	*22.4 b*	*26.8 a*	*25.7 ab*	*26.6 a*	*23.5 ab*		**0.0095**		
N content (mg $seedling^{-1}$)											
Shoot	+		11.1	20.1	19.9	24.7	19.0	*18.9 a*		**<0.0001**	
	–		0.7	2.7	3.1	3.3	1.9	*2.3 b*			0.1121
		N	*5.9 b*	*11.4 a*	*11.5 a*	*14.0 a*	*10.4 a*		**0.0050**		
Root	+		4.2	7.6	6.9	9.4	7.4	*7.1 a*		**<0.0001**	
	–		0.2	1.0	1.5	1.4	0.9	*1.0 b*			0.1620
		N	*3.4 b*	*4.3 ab*	*4.2 ab*	*5.4 a*	*4.2 ab*		**0.0146**		

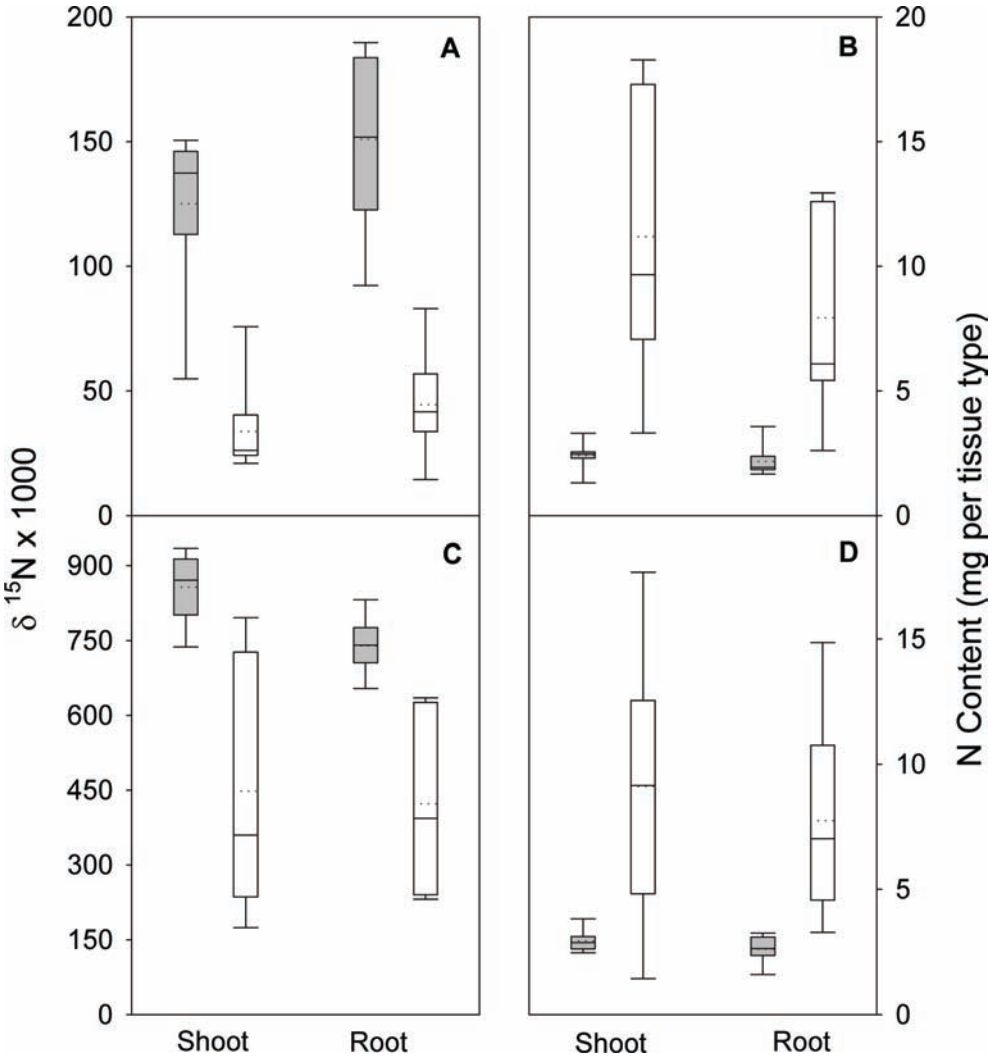

FIGURE 2 | Nitrogen isotope ratio ($\delta^{15}N$) and N content in shoots and roots of lupine seedlings 56 days after planting in the greenhouse. Seedlings were supplied with either arginine **(A** and **B)** or ammonium-nitrate **(C** and **D)** after either being inoculated (white boxes) or not inoculated (gray boxes) with rhizobia. Vertical boxes represent approximately 50% of the observations and lines extending from each box are the upper and lower 25% of the distribution. The solid horizontal line in the center of each box is the median value and the dotted line is the mean.

affected every final measured response variable except S:R (**Table 4**), with inoculated seedlings having greater values than their noninoculated cohorts.

The N × inoculation interaction was significant for leaf N concentration (**Table 5**). Noninoculated and inoculated seedlings grown without N had similar leaf N concentration, but for seedlings supplied with N, noninoculated seedlings had significantly greater N concentration than inoculated ones. N significantly affected N concentration in leaves and stems but not roots: leaf N concentration was greatest for seedlings not supplied N followed by those supplied with NH_4^+ or NH_4NO_3, with those supplied with arginine or NO_3^- producing the lowest leaf N concentration. In general, no-N seedlings had significantly larger stem N concentration than N-supplied seedlings, but seedling stem N concentrations for seedlings supplied with N were similar regardless of N form. Inoculation had no effect on N concentration of leaves, stems, or roots (**Table 5**).

Nitrogen and inoculation interacted to affect root N content (**Table 5**). The pattern followed the interaction observed for seedling growth: without N, noninoculated and inoculated seedlings had the same root N content, whereas with N, inoculated seedlings had more N than their noninoculated cohorts. Nitrogen significantly affected leaf, stem, and root N content. In general, N-supplied seedlings had significantly higher N content in leaves, stems, and roots than those not receiving N, but seedling N content was similar regardless of N form. Inoculation significantly increased N content of leaves, stems, and roots (**Table 5**).

In the nodule activity experiment, no interaction of N form (arginine and NH_4NO_3) and inoculation was observed for shoot, root, or total seedling biomass, but N form and inoculation were

TABLE 4 | Mean morphological parameters of black locust seedlings inoculated (I) with (+) or without (–) rhizobia and supplied with different nitrogen (N) sources [none, ammonium (NH_4), nitrate (NO_3), ammonium nitrate (NH_4NO_3), or arginine (A)] for 12 weeks (n = 8). Main effect (ME) means are presented in italics. Different letters within a dependent variable indicate significant differences (α = 0.05) using Tukey's HSD.

Dependent variable	I	ME	Nitrogen sources					ME	Sources of variation		
									P values		
			None	NH_4	NO_3	NH_4NO_3	A	*I*	N	I	N × I
Height	+		11.4 d	47.6 a	45.0 ab	39.4 b	40.8 ab	*36.8*		**<0.0001**	
(cm)	–		6.6 d	22.7 c	24.1 c	20.3 c	20.7 c	*18.9*			**0.0006**
		N	*9.0*	*35.2*	*34.5*	*29.8*	*30.8*		**<0.0001**		
Root-collar	+		3.04	6.83	6.64	6.64	6.61	*5.95 a*		**<0.0001**	
diameter	–		1.54	4.51	4.39	4.19	3.90	*3.70 b*			0.3226
(mm)		*N*	*2.29 b*	*5.67 a*	*5.52 a*	*5.41 a*	*5.25 a*		**<0.0001**		
Leaf biomass	+		0.73 bc	4.42 a	4.60 a	4.16 a	4.20 a	*3.62*		**<0.0001**	
(g)	–		0.12 c	1.70 b	1.41 b	1.17 bc	1.26 b	*1.13*			**0.0029**
		N	*0.43*	*3.06*	*3.01*	*2.67*	*2.73*		**<0.0001**		
Stem biomass	+		0.28 cd	3.49 a	3.14 ab	2.78 b	2.69 b	*2.47*		**<0.0001**	
(g)	–		0.05 d	0.84 c	0.97 c	0.79 c	0.72 c	*0.67*			**<0.0001**
		N	*0.16*	*2.17*	*2.05*	*1.78*	*1.70*		**<0.0001**		
Shoot biomass	+		1.01 bc	7.91 a	7.74 a	6.94 a	6.89 a	*6.10*		**<0.0001**	
(g)	–		0.17 c	2.54 b	2.38 b	1.96 b	1.97 b	*1.80*			**0.0003**
		N	*0.59*	*5.22*	*5.06*	*4.45*	*4.43*		**<0.0001**		
Root biomass	+		0.75 cd	4.94 a	3.91 b	4.10 ab	3.66 b	*3.47*		**<0.0001**	
(g)	–		0.09 d	1.47 c	1.76 c	1.40 c	1.25 c	*1.19*			**0.0027**
		N	*0.42*	*3.20*	*2.84*	*2.75*	*2.45*		**<0.0001**		
Nodule biomass	+		0.09 ef	0.46 a	0.36 ab	0.26 bcd	0.30 bc	*0.30*		**<0.0001**	
(g)	–		0.02 f	0.20 cde	0.14 def	0.17 cde	0.11 ef	*0.13*			0.1588
		N	*0.05*	*0.33*	*0.25*	*0.22*	*0.20*		**<0.0001**		
Shoot:root	+		1.9	1.6	2.0	1.7	2.1	*1.9*		0.1846	
	–		2.3	1.7	1.5	1.5	1.6	*1.7*			0.1499
		N	*2.1*	*1.6*	*1.8*	*1.6*	*1.9*		0.1165		

both significant ($p \leq 0.0151$), except for stem biomass. Regardless of N form, inoculation increased total biomass about 35%. The interaction of N form and inoculation was significant for all tissue types and total seedling $\delta^{15}N$ (all $p \leq 0.0212$); $\delta^{15}N$ decreased with inoculation (**Figure 3**). For N content, the interaction was not significant for any tissue type or total seedling, N form had no effect on total seedling N content, and inoculation significantly ($p < 0.0013$) increased N content (**Figure 3**).

DISCUSSION

In this study, noninoculated lupine and black locust seedlings supplied organic or inorganic N had similar growth; moreover, these seedlings grew significantly larger than their cohorts not supplied N (**Tables 2** and **4**). Inoculation with rhizobia, with or without N supply, improved seedling growth and increased N content compared to noninoculated seedlings (**Tables 2**–**5**), similar to the response noted for other legume plants (Dan et al., 1993; Adgo and Schulze, 2002; Diabate et al., 2005; Jayakumar and Tan, 2006; Dumroese et al., 2009; Gan et al., 2010; Namvar et al., 2011). Inoculated black locust seedlings supplied N had 157% more biomass than those not supplied N (Uselman et al., 2000). We noted, however, that inoculation decreased the S:R for lupine seedlings (**Table 2**) but not for black locust seedlings (**Table 4**), suggesting that the subsequent allocation response of the plant to improved N status may be either species or plant form dependent. Although we observed minor and sporadic nodulation on noninoculated plants, we did not evaluate their N-fixing availability; other research suggests that these types of nodules may not actively fix atmospheric N (Tirichine et al., 2006).

It has long been proposed that mineral N inhibits nodulation, nodule growth, and activity in legumes (Imsande, 1986; Streeter and Wong, 1988; Guo et al., 1992; Bollman and Vessey, 2006; Camargos and Sodek, 2010). While low N rates improved nodule formation in black locust (Rohm and Werner, 1991), N rates exceeding 0.84 mg N $week^{-1}$ reduced nodule number and nodule biomass (Roberts et al., 1983; Rohm and Werner, 1991). Our results, however, show that, although N form did not affect seedling size, N supplied at 2 mg N $week^{-1}$ significantly enhanced nodule formation on black locust compared to seedlings not supplied N (**Table 4**); NH_4^+ seemed to favor nodulation the most, confirming that the impact of NH_4^+ on symbiosis is weaker than that observed for NO_3^- (Bollman and Vessey, 2006). Our data suggests that more robust N supply may not preclude nodule formation, similar to results observed in some species (Peoples et al., 1995; Bado et al., 2006; Dumroese et al., 2009). A similar result was, however, not apparent on lupine seedlings (**Table 2**).

TABLE 5 | Mean nitrogen (N) concentrations and contents of black locust seedlings inoculated (I) with (+) or without (–) rhizobia and supplied with different nitrogen (N) sources [none, ammonium (NH_4), nitrate (NO_3), ammonium nitrate (NH_4NO_3), or arginine (A)] for 12 weeks (n = 8). Main effect (ME) means are presented in italics. Different letters within a dependent variable indicate significant differences (α = 0.05) using Tukey's HSD.

Dependent variable	I	ME	Nitrogen sources					ME	Sources of variation		
									P values		
			None	NH_4	NO_3	NH_4NO_3	A	*I*	N	I	N × I
N concentration (mg g^{-1})											
Leaf	+		32.4 a	27.9 a	28.6 a	29.5 a	28.2 a	*29.8*		0.3936	
	–		34.4 a	32.0 a	20.9 b	30.9 a	28.2 a	*28.6*			**0.0365**
		N	*33.1*	*30.0*	*24.7*	*30.2*	*28.2*		**0.0098**		
Stem	+		28.0	20.1	22.0	23.2	24.3	*23.6*		0.1709	
	–		26.9	21.9	16.4	24.8	20.3	*21.7*			0.2169
		N	*26.7 a*	*21.0 b*	*19.2 b*	*24.0 b*	*22.3 b*		**0.0362**		
Root	+		27.4	26.8	31.6	31.2	30.3	*29.3*		0.1444	
	–		27.6	29.6	24.0	26.7	23.7	*26.2*			0.5865
		N	*27.3*	*28.9*	*27.0*	*28.2*	*27.3*		0.9633		
N content (mg $seedling^{-1}$)											
Leaf	+		24.4	123.6	131.3	122.6	118.3	*104.1 a*		**<0.0001**	
	–		4.3	55.4	32.6	36.7	38.2	*33.4 b*			0.0526
		N	*14.4 b*	*89.5 a*	*82.0 a*	*79.7 a*	*78.2 a*		**<0.0001**		
Stem	+		9.3	70.4	69.4	64.9	64.1	*55.4 a*		**<0.0001**	
	–		2.6	19.8	17.3	20.0	15.9	*14.8 b*			0.0564
		N	*4.6 b*	*45.1 a*	*43.4 a*	*42.5 a*	*40.0 a*		**0.0002**		
Root	+		21.8 ab	101.9 a	89.7 ab	101.9 a	88.3 ab	*80.7*		**<0.0001**	
	–		7.6 b	76.3 ab	64.4 ab	57.3 ab	37.4 ab	*28.6*			**0.0061**
		N	*10.7*	*94.3*	*75.5*	*76.2*	*68.4*		**<0.0001**		

Nodulation on lupine was unaffected by N form, but for black locust, N supplied as NH_4^+ was superior to arginine, suggesting that the nodulation response may be plant species dependent (Manhart and Wong, 1980; Harper and Gibson, 1983).

Although increasing N rates have been associated with decreasing nodule number on black locust (Roberts et al., 1983; Rohm and Werner, 1991), the nitrogenase activity of the nodules was either unaffected (Roberts et al., 1983) or increased (Rohm and Werner, 1991). Our results of the N isotope ratio in different parts of lupine and black locust seedlings supplied with organic or inorganic N showed that $\delta^{15}N$ was decreased in different tissue types in inoculated seedlings relative to noninoculated seedlings, indicating dilution within the seedling caused by additions of atmospheric N-fixation within the nodules (Hardarson and Danso, 1993). Indeed, our seedlings had 3× (black locust; **Table 5**) to 9× (lupine; **Table 3**) more N content when inoculation was combined with additions of N.

Thus, it is not surprising that N supply and inoculation significantly interacted to affect morphology and root N content of black locust (**Tables 4** and **5**). The combination of inoculation and access to N promoted more growth (i.e., height, biomass, nodules) than did inoculation alone. Despite higher N contents in inoculated black locust seedlings supplied N, their leaf N concentration was lower than noninoculated seedlings supplied N. This lower N concentration is due to dilution (Salifu and Jacobs, 2006) that likely occurred in these rapidly growing plants during the three weeks between the final application and harvest. Thus, for black locust, the combination of inoculation and access to N improved growth more than either factor alone. Uselman et al. (2000) also found that the combination of inoculation and N supply produced larger seedlings than inoculation alone. For lupine, we were unable to detect a significant N supply by inoculation interaction (**Tables 2** and **3**) but N content data (**Table 3**) followed a pattern similar to that for black locust. For noninoculated black locust seedlings, we noted N contents that exceeded those expected by supply of N alone. The additional N may originate from the substrate we used. Peat initially contains appreciable N that may have subsequently been mineralized and available for plant uptake. In their review, Cheng and Kuzyakov, (2005) report that rapid soil wetting-drying cycles tend to increase mineral soil organic matter mineralization; this condition is common in small-volume seedling containers such as the ones we used, especially as the seedlings became larger (Landis et al., 1989). Moreover, the presence of roots can lead to a threefold increase in mineralization (Cheng and Kuzyakov, 2005).

Many plant species (e.g., Persson and Näsholm, 2001; Metcalfe et al., 2011), including trees (e.g., Wei et al., 2015; Uscola et al., 2017) show the capacity for intact uptake of amino acids, especially through their mycorrhizal networks (McFarland et al., 2010; Whiteside et al., 2012). Microbes utilize more amino acid N in the short term (e.g., Warren,

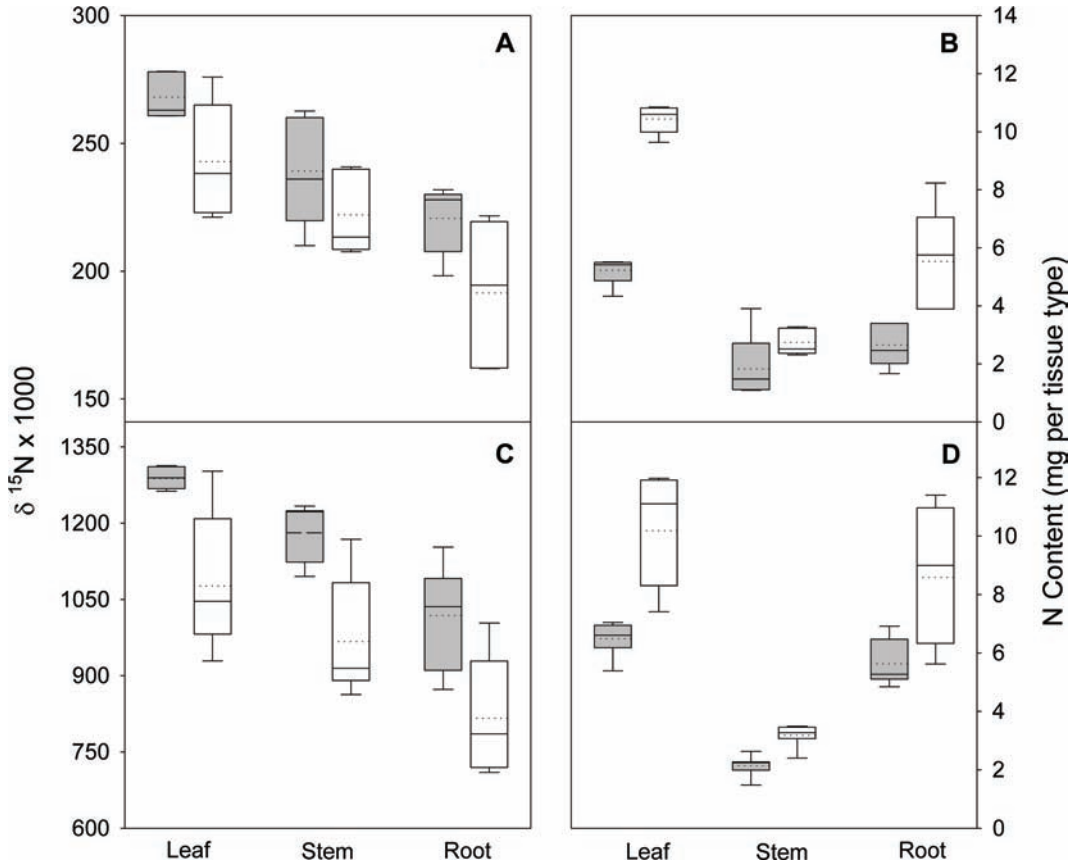

FIGURE 3 | Nitrogen isotope ratio ($\delta^{15}N$) and N content in leaves, stems, and roots of black locust seedlings 70 days after planting in the greenhouse. Seedlings were supplied with either arginine **(A** and **B)** or ammonium-nitrate **(C** and **D)** after either being inoculated (white boxes) or not inoculated (gray boxes) with rhizobia. Vertical boxes represent approximately 50% of the observations and lines extending from each box are the upper and lower 25% of the distribution. The solid horizontal line in the center of each box is the median value and the dotted line is the mean.

2009; Farrell et al., 2014). In the longer term (more than 2 days), seedlings may capitalize on the rapid cycling of amino acid N through the microbial biomass (Harrison et al., 2008; Warren, 2009), which may explain the results of studies in greenhouses showing that plants grown on amino acid N performed as well as those given inorganic N (Öhlund and Näsholm, 2001; Gruffman et al., 2012). Amino acid application in field settings, however, could alter the plant-microorganism balance due to an enhanced carbon environmnet (Schobert et al., 1988), leading to unexpected varations in N taken up by plants, which may explain the reduced growth with amino acids observed by Wilson et al. (2013). Our results showed that seedlings of both broadleaved plant species supplied with arginine grew as well as seedlings given inorganic N, although we did not measure if the organic N was taken up intact by either species.

Although amino acids are suggested to have a direct positive effect on root growth (Cambui et al., 2011), in our study, neither root growth or S:R of lupine or black locust seedlings were affected (**Tables 2** and **4**). The stimulatory effect on root growth is thought to be associated with development of mycorrhizal symbioses (Cambui et al., 2011), an aspect that we did not examine in our study.

Successful use of seedlings in forest restoration activities requires that they meet specific target criteria needed to overcome environmental limitations on their intended outplanting site (Dumroese et al., 2016). Fertilization in the nursery can provide a more rapid method for obtaining target plant size than the sole use of an N-fixing symbiont on a leguminous tree and can be done within current operational standards (Dumroese et al., 2009). This is important because nursery efficiency (e.g., plant growth per unit time) is one of many factors supporting successful nursery operation (Dumroese et al., 2011). In addition, Villar-Salvador et al. (2008) report that seedlings supplied high rates of fertilizer during nursery production grew larger and had improved morphological and physiological traits (i.e., greater biomass, root growth capacity, photosynthetic rates, and N concentrations) than their cohorts supplied low rates of fertilizer regardless of rhizobial inoculation; this translated into more survival and growth after outplanting. Our results demonstrate that robust fertilization need not sacrifice development of nodules capable of N-fixation.

In summary, we grew a forb and tree species using inorganic and organic N forms with and without genus-specific (lupine) or species-specific (black locust) rhizobia inoculation. We found that seedlings grew equally well with either N form; nodule biomass in lupine was unaffected by N form, whereas in black locust, nodule biomass in NH_4^+-supplied seedlings was greater than that in arginine-supplied seedlings, an apparent species-specific response; and that N-fixation readily occurred in the presence of high levels of N supply, leading to enhance seedling N content. Our results suggest that these potentially important species for forest restoration activities can be produced in nurseries to acceptable morphological targets using robust levels of either organic or inorganic forms of N and have functioning symbionts as well.

AUTHOR CONTRIBUTIONS

PZ, KD, and JP shared equally in conceiving the research, designing the experiment, interpreting results, and drafting the manuscript. RD and JP provided research funding and technical expertise in seedling production. PZ tended and sampled seedlings. KZ and JP performed the data analyses.

FUNDING

This study was funded by the Fundamental Research Funds for the Central Universities (China; 2572019CP16), U.S. Department of Agriculture, Forest Service (USFS) Rocky Mountain Research Station (RMRS), and the USFS National Center for Reforestation, Nurseries, and Genetic Resources.

ACKNOWLEDGMENTS

We thank Jasmine Drapeau and Nathan Robertson at the USFS Coeur d'Alene Nursery for providing lupine seeds, Thomas Wacek at Plant Probiotics Company for providing rhizobia inoculants, and USFS RMRS employees Katherine McBurney and Charles Eckman for assistance with sample processing. We also thank the associate editor and reviewers for their comments.

REFERENCES

Adgo, E., and Schulze, J. (2002). Nitrogen fixation and assimilation efficiency in Ethiopian and German pea varieties. *Plant Soil* 239, 291–299. doi: 10.1023/A:1015048331366

Antos, J. A., and Halpern, C. B. (1997). Root system differences among species: implications for early successional changes in forest of western Oregon. *Am. Midl. Nat.* 138, 97–108. doi: 10.2307/2426658

Bado, B. V., Bationo, A., and Cescas, M. P. (2006). Assessment of cowpea and groundnut contributions to soil fertility and succeeding sorghum yields in the Guinean savannah zone of Burkina Faso (West Africa). *Biol. Fertil. Soils* 43, 171–176. doi: 10.1007/s00374-006-0076-7

Bigg, W. L., and Daniel, T. W. (1978). Effects of nitrate, ammonium and pH on the growth of conifer seedlings and their production of nitrate reductase. *Plant Soil* 50, 371–385. doi: 10.1007/BF02107186

Bollman, M. I., and Vessey, J. K. (2006). Differential effects of nitrate and ammonium supply on nodule initiation, development, and distribution on roots of pea (*Pisum sativum*). *Can. J. Bot.* 84, 893–903. doi: 10.1139/b06-027

Camargos, L. S., and Sodek, L. (2010). Nodule growth and nitrogen fixation of *Calopogonium mucunoides* L. show low sensitivity to nitrate. *Symbiosis* 51, 167–174. doi: 10.1007/s13199-010-0063-5

Cambui, C. A., Svennerstam, H., Gruffman, L., Nordin, A., Ganeteg, U., and Näsholm, T. (2011). Patterns of plant biomass partitioning depend on nitrogen source. *PloS One* 6, e19211. doi: 10.1371/journal.pone.0019211

Cheng, W., and Kuzyakov, Y. (2005). "Root effects on soil organic matter decomposition," in *Roots and Soil Management: Interactions between Roots and the Soil, Agronomy Monograph 48.* Eds. S. Wright and R. Zobel (Madison, WI: American Society of Agronomy), 119–143.

Christou, M., Avramides, E. J., and Jones, D. L. (2006). Dissolved organic nitrogen dynamics in a Mediterranean vineyard soil. *Soil Biol. Biochem.* 38, 2265–2277. doi: 10.1016/j.soilbio.2006.01.025

Dan, T., Keyser, H. H., and Singleton, P. W. (1993). Response of tree legumes to rhizobial inoculation in relation to the population density of indigenous rhizobia. *Soil Biol. Biochem.* 25, 75–81. doi: 10.1016/0038-0717(93)90244-6

Diabate, M., Munive, A., de Faria, S. M., Ba, A., Dreyfus, B., and Galiana, A. (2005). Occurrence of nodulation in unexplored leguminous trees native to the West African tropical rainforest and inoculation response of native species useful in reforestation. *New Phytol.* 166, 231–239. doi: 10.1111/j.1469-8137.2005.01318.x

Doede, D. L. (2005). Genetic variation in broadleaf lupine *Lupinus latifolius* on the Mt Hood National Forest and implications for seed collection and deployment. *Native Plants J.* 6, 36–48. doi: 10.1353/npj.2005.0018

Dumroese, R. K., Jacobs, D. F., and Davis, A. S. (2009). Inoculating *Acacia koa* with *Bradyrhizobium* and applying fertilizer in the nursery: effects on nodule formation and seedling growth. *HortScience* 44, 443–446. doi: 10.21273/HORTSCI.44.2.443

Dumroese, R. K., Davis, A. S., and Jacobs, D. F. (2011). Nursery response of *Acacia koa* seedlings to container size, irrigation method, and fertilization rate. *J. Plant Nutr.* 34, 877–887. doi: 10.1080/01904167.2011.544356

Dumroese, R. K., Montville, M. E., and Pinto, J. R. (2015). Using container weights to determine irrigation needs: a simple method. *Native Plants J.* 16, 67–71. doi: 10.3368/npj.16.1.67

Dumroese, R. K., Landis, T. D., Pinto, J. R., Haase, D. L., Wilkinson, K. M., and Davis, A. S. (2016). Meeting forest restoration challenges: using the Target Plant Concept. *Reforesta* 1, 37–52. doi: 10.21750/REFOR.1.03.3

Fei, H., and Vessey, J. K. (2003). Involvement of cytokinin in the stimulation of nodulation by low concentrations of ammonium in *Pisum sativum* L. *Physiol. Plant.* 118, 447–455. doi: 10.1034/j.1399-3054.2003.00123.x

Farrell, M., Prendergast-Miller, M., Jones, D. L., Hill, P. W., and Condron, L. M. (2014). Soil microbial organic nitrogen uptake is regulated by carbon availability. *Soil Biol. Biochem.* 77, 261–267. doi: 10.1016/j.soilbio.2014.07.003

Franklin, O., Cambui, C. A., Gruffman, L., Palmroth, S., Oren, R., and Näsholm, T. (2017). The carbon bonus of organic nitrogen enhances nitrogen use efficiency of plants. *Plant Cell Environ.* 40, 25–35. doi: 10.1111/pce.12772

Gan, Y. T., Johnston, A. M., Knight, J. D., McDonald, C., and Stevenson, C. (2010). Nitrogen dynamics of chickpea: effects of cultivar choice, N fertilization, *Rhizobium* inoculation, and cropping systems. *Can. J. Plant Sci.* 90, 655–666. doi: 10.4141/CJPS10019

Goicoechea, N., Merino, S., and Sanchez-Diaz, M. (2005). Management of phosphorus and nitrogen fertilization to optimize *Anthyllis-Glomus-Rhizobium* symbiosis for revegetation of desertification semiarid areas. *J. Plant Nutr.* 27, 1395–1413. doi: 10.1081/PLN-200025850

Gruffman, L., Ishida, T., Nordin, A., and Näsholm, T. (2012). Cultivation of Norway spruce and Scots pine on organic nitrogen improves seedling morphology and field performance. *Forest Ecol. Manag.* 276, 118–124. doi: 10.1016/j.foreco.2012.03.030

Gruffman, L., Palmroth, S., and Näsholm, T. (2013). Organic nitrogen uptake of Scots pine seedlings is independent of current carbohydrate supply. *Tree Physiol.* 33, 590–600. doi: 10.1093/treephys/tpt041

Gulden, R. H., and Vessey, J. K. (1997). The stimulating effect of ammonium on nodulation in *Pisum sativum* L. is not long lived once ammonium supply is discontinued. *Plant Soil* 195, 195–205. doi: 10.1023/A:1004249017255

Guo, R., Silsbury, J. H., and Graham, R. D. (1992). Effect of four nitrogen compounds on nodulation and nitrogen fixation in faba bean, white lupin and medic plants. *Aust. J. Plant Physiol.* 19, 501–508. doi: 10.1071/PP9920501

Halverson, N. M., Lesher, R., McClure, R. H., Riley, J., and Topik, C. (1986). Major indicator shrubs and herbs on national forests of western Oregon and southwestern Washington. Portland, OR: U.S. Department of Agriculture, Forest Service, Pacific Northwest Region, R6-TM-229, 180.

Hardarson, G., and Danso, S. K. A. (1993). Methods for measuring biological nitrogen-fixation in grain legumes. *Plant Soil* 152, 19–23. doi: 10.1007/BF00016330

Harper, J. E., and Gibson, A. H. (1983). Differential nodulation tolerance to nitrate among legume species. *Crop Sci.* 24, 797–801. doi: 10.2135/cropsci1984.00111 83X002400040040x

Harrison, K. A., Bol, R., and Bardgett, R. D. (2008). Do plant species with different growth strategies vary in their ability to compete with soil microbes for chemical forms of nitrogen? *Soil Biol. Biochem.* 40, 228–237. doi: 10.1016/j.soilbio.2007.08.004

Hawkins, B. J., and Robbins, S. (2010). pH affects ammonium, nitrate and proton fluxes in the apical region of conifer and soybean roots. *Physiol. Plant.* 138, 238–247. doi: 10.1111/j.1399-3054.2009.01317.x

Imsande, J. (1986). Inhibition of nodule development in soybean by nitrate or reduced nitrogen. *J. Exp. Bot.* 37, 348–355. doi: 10.1093/jxb/37.3.348

Inselsbacher, E., and Näsholm, T. (2012). The below-ground perspective of forest plants: soil provides mainly organic nitrogen for plants and mycorrhizal fungi. *New Phytol.* 195, 329–334. doi: 10.1111/j.1469-8137.2012.04169.x

Jayakumar, P., and Tan, T. K. (2006). Variations in the responses of *Acacia mangium* to inoculation with different strains of *Bradyrhizobium* sp. under nursery conditions. *Symbiosis* 41, 31–37.

Keresztesi, B. (1980). The black locust. *Unasylva* 32, 23–33.

Kielland, K. (1994). Amino-acid-absorption by Arctic plants: implications for plant nutrition and nitrogen cycling. *Ecology* 75, 2373–2383. doi: 10.2307/1940891

Landis, T. D., Tinus, R. W., McDonald, S. E., and Barnett, J. P. (1989). Seedling nutrition and irrigation, volume 4. in *The Container Tree Nursery Manual. Agriculture Handbook 674*, (Washington, DC: U.S. Department of Agriculture, Forest Service), 119 p.

Lucinski, R., Polcyn, W., and Ratajczac, L. (2002). Nitrate reduction and nitrogen fixation in symbiotic association *Rhizobium*-legumes. *Acta Biochim. Pol.* 49, 537–546.

Manhart, J. R., and Wong, P. P. (1980). Nitrate effect on nitrogen-fixation (acetylene reduction)—activities of legume root-nodules induced by rhizobia with varied nitrate reductase activities. *Plant Physiol.* 65, 502–505. doi: 10.1104/pp.65.3.502

McFarland, J. W., Ruess, R. W., Kielland, K., Pregitzer, K., Hendrick, R., and Allen, M. (2010). Cross-ecosystem comparisons of *in situ* plant uptake of amino acid-N and NH_4^+. *Ecosystems* 13, 177–193. doi: 10.1007/s10021-009-9309-6

Metcalfe, R. J., Nault, J., and Hawkins, B. J. (2011). Adaptations to nitrogen form: comparing inorganic nitrogen and amino acid availability and uptake by four temperate forest plants. *Can. J. Forest Res.* 41, 1626–1637. doi: 10.1139/x11-090

Namvar, A., Sharifi, R. S., Sedghi, M., Zakaria, R. A., Khandan, T., and Eskandarpour, B. (2011). Study on the effects of organic and inorganic nitrogen fertilizer on yield, yield components, and nodulation state of chickpea (*Cicer arietinum* L.). *Commun. Soil Sci. Plan.* 42, 1097–1109. doi: 10.1080/00103624.2011.562587

Öhlund, J., and Näsholm, T. (2001). Growth of conifer seedlings on organic and inorganic nitrogen sources. *Tree Physiol.* 21, 1319–1326. doi: 10.1093/treephys/21.18.1319

Öhlund, J., and Näsholm, T. (2002). Low nitrogen losses with a new source of nitrogen for cultivation of conifer seedlings. *Environ. Sci. Technol.* 36, 4854–4859. doi: 10.1021/es025629b

Öhlund, J., and Näsholm, T. (2004). Regulation of organic and inorganic nitrogen uptake in Scots pine (*Pinus sylvestris*) seedlings. *Tree Physiol.* 24, 1397–1402. doi: 10.1093/treephys/24.12.1397

Olson, D. F. Jr., and Karrfalt, R. P. (2008). "*Robinia L.*" in *The Woody Plant Seed Manual. Agriculture Handbook 727*, Eds. F. T. Bonner and R. P. Karrfalt (Washington, DC: U.S. Department of Agriculture, Forest Service), 969–973.

Peoples, M. B., Ladha, J. K., and Herridge, D. F. (1995). Enhancing legume N_2 fixation through plant and soil management. *Plant Soil* 174, 83–101. doi: 10.1007/978-94-011-0055-7_4

Persson, J., Hogberg, P., Ekblad, A., Hogberg, M. N., Nordgren, A., and Näsholm, T. (2003). Nitrogen acquisition from inorganic and organic sources by boreal forest plants in the field. *Oecologia* 137, 252–257. doi: 10.1007/s00442-003-1334-0

Persson, J., and Näsholm, T. (2001). Amino acid uptake: a widespread ability among boreal forest plants. *Ecol. Lett.* 4, 434–438. doi: 10.1046/j.1461-0248.2001.00260.x

Roberts, D. R., Zimmerman, R. W., Stringer, J. W., and Carpenter, S. B. (1983). The effects of combined nitrogen on growth, nodulation, and nitrogen fixation of black locust seedlings. *Can. J. Forest Res.* 13, 1251–1254. doi: 10.1139/x83-165

Rohm, M., and Werner, D. (1991). Nitrate levels affect the development of the black locust-*Rhizobium* symbiosis. *Trees-Struct. Funct.* 5, 227–231. doi: 10.1007/BF00227529

Rys, G. J., and Phung, T. (1984). Effect of nitrogen form and counterion on establishment of the *Rhizobium trifolii–Trifolium repens* symbiosis. *J. Exp. Bot.* 35, 1811–1819. doi: 10.1093/jxb/35.12.1811

Salifu, K. F., and Jacobs, D. F. (2006). Characterizing fertility targets and multi-element interactions in nursery culture of *Quercus rubra* seedlings. *Ann. For. Sci.* 63, 231–237. doi: 10.1051/forest:2006001

Schobert, C., Köckenberger, W., and Komor, E. (1988). Uptake of amino acids by plants from the soil: a comparative study with castor bean seedlings grown under natural and axenic soil conditions. *Plant Soil* 109, 181–188. doi: 10.1007/BF02202082

Silsbury, J. H., Catchpoole, D. W., and Wallace, W. (1986). Effects of nitrate and ammonium on nitrogenase (C_2H_2 reduction) activity of swards of subterranean clover, *Trifolium subterraneum* L. *Aust. J. Plant Physiol.* 13, 257–273. doi: 10.1071/PP9860257

Streeter, J. G., and Wong, P. P. (1988). Inhibition of legume nodule formation and N_2 fixation by nitrate. *CRC Crit. Rev. Plant Sci.* 7, 1–23. doi: 10.1080/07352688809382257

Svenning, M. M., Junttila, O., and Macduff, J. H. (1996). Differential rates of inhibition of N_2 fixation by sustained low concentrations of NH_4 and NO_3 in northern ecotypes of white clover (*Trifolium repens* L.). *J. Exp. Bot.* 47, 729–738. doi: 10.1093/jxb/47.6.729

Tirichine, L., Imaizumi-Anraku, H., Yoshida, S., Murakami, Y., Madsen, L. H., Miwa, H., et al. (2006). Deregulation of a Ca_2^+/calmodulin-dependent kinase leads to spontaneous nodule development. *Nature* 441, 1153–1156. doi: 10.1038/nature04862

Uscola, M., Villar-Salvador, P., Oliet, J., and Warren, C. R. (2017). Root uptake of inorganic and organic N chemical forms in two coexisting Mediterranean forest trees. *Plant Soil* 415, 387–392. doi: 10.1007/s11104-017-3172-6

Uselman, S. M., Qualls, R. G., and Thomas, R. B. (2000). Effects of increased atmospheric CO_2, temperature, and soil N availability on root exudation of dissolved organic carbon by a N-fixing tree (*Robinia pseudoacacia* L.). *Plant Soil* 222, 191–202. doi: 10.1023/A:1004705416108

Valkov, V. T., Rogato, A., Alves, L. M., Sol, S., Noguero, M., Léran, S., et al. (2017). The nitrate transporter family protein LjNPF8.6 controls the N-fixing nodule activity. *Plant Physiol.* 175, 1269–1282. doi: 10.1104/pp.17.01187

Vessey, J. K., and Waterer, J. (1992). In search of the mechanism of nitrate inhibition of nitrogenase activity in legume nodules: recent developments. *Physiol. Plant.* 84, 171–176. doi: 10.1111/j.1399-3054.1992.tb08780.x

Villar-Salvador, P., Valladares, F., Domínguez-Lerena, S., Ruiz-Díez, B., Fernäández-Pascual, M., Delgado, A., et al. (2008). Functional traits related to seedling performance in the Mediterranean leguminous shrub *Retama sphaerocarpa*: insights from a provenance, fertilization, and rhizobial noculation study. *Environ. Exp. Bot.* 64, 145–154. doi: 10.1016/j.envexpbot.2008.04.005

Warren, C. R. (2009). Uptake of inorganic and amino acid nitrogen from soil by *Eucalyptus regnans* and *Eucalyptus pauciflora* seedlings. *Tree Physiol.* 29, 401–409. doi: 10.1093/treephys/tpn037

Waterer, J. G., and Vessey, J. K. (1993a). Effect of low static nitrate concentrations on mineral nitrogen uptake, nodulation, and nitrogen fixation in field pea. *J. Plant Nutr.* 16, 1775–1789. doi: 10.1080/01904169309364649

Waterer, J. G., and Vessey, J. K. (1993b). Nodulation response of autoregulated or NH_4^+-inhibited pea (*Pisum sativum*) after transfer to stimulatory (low) concentrations of NH_4^+. *Physiol. Plant.* 88, 460–466. doi: 10.1111/j.1399-3054.1993.tb01360.x

Wei, L., Chen, C., and Yu, S. (2015). Uptake of organic nitrogen and preference for inorganic nitrogen by two Australian native Araucariaceae species. *Plant Ecol. Divers.* 8, 259–264. doi: 10.1080/17550874.2013.871656

Whiteside, M. D., Garcia, M. O., and Treseder, K. K. (2012). Amino acid uptake in arbuscular mycorrhizal plants. *PLoS One* 7, e47643. doi: 10.1371/journal.pone.0047643

Wilson, A. R., Nzokou, P., Guney, D., and Kulac, S. (2013). Growth response and nitrogen use physiology of Fraser fir (*Abies fraseri*), red pine (*Pinus resinosa*), and hybrid poplar under amino acid nutrition. *New For.* 44, 281–295. doi: 10.1007/s11056-012-9317-9

Yao, B., Cao, J., Zhao, C., and Rengel, Z. (2011). Influence of ammonium and nitrate supply on growth, nitrate reductase activity and N-use efficiency in a natural hybrid pine and its parents. *J. Plant Ecol.* 4, 275–282. doi: 10.1093/jpe/rtq033

Yashima, H., Fujikake, H., Yamazaki, A., Ito, S., Sato, T., Tewari, K., et al. (2005). Long-term effect of nitrate application from lower part roots on nodulation and N_2 fixation in upper part roots of soybean (*Glycine max* (L.) Merr.) in two-layered pot experiment. *Soil Sci. Plant Nutr.* 7, 981–990. doi: 10.1111/j.1747-0765.2005.tb00137.x

Conflict of Interest: The authors declare that the research was conducted in the absence of any commercial or financial relationships that could be construed as a potential conflict of interest.

frontiers in Microbiology

ORIGINAL RESEARCH
published: 09 July 2019
doi: 10.3389/fmicb.2019.01506

ACC Deaminase Producing Bacteria With Multifarious Plant Growth Promoting Traits Alleviates Salinity Stress in French Bean (*Phaseolus vulgaris*) Plants

*Shikha Gupta and Sangeeta Pandey**

Amity Institute of Organic Agriculture, Amity University, Noida, India

Plant growth promoting rhizobacteria (PGPR) with 1-aminocyclopropane-1-carboxylic acid (ACC) deaminase activity has the potential to promote plant growth and development under adverse environmental conditions. In the present study, rhizobacterial strains were isolated from Garlic (*Allium sativum*) rhizosphere and were screened *in vitro* ACC deaminase activity in DF salt minimal media supplemented with 3 mM ACC. Out of six isolates, two could degrade ACC into α-ketobutyrate, exhibiting ACC deaminase activity producing more than ∼1500 nmol of α-ketobutyrate mg protein^{-1} h^{-1}, and assessed for other plant growth promoting (PGP) functions including indole acetic acid production (greater than ∼30 μg/ml), siderophore, Ammonia, Hydrogen cyanide production and inorganic $Ca_3(PO_4)_2$ (∼85 mg/L) and $ZnSO_4$ solubilization. Besides facilitating multifarious PGP activities, these two isolates augmented *in vitro* stress tolerance in response to 6% w/v NaCl salt stress and drought stress (−0.73 Mpa). The strains ACC02 and ACC06 were identified *Aneurinibacillus aneurinilyticus* and *Paenibacillus* sp., respectively on the basis of 16S rDNA gene sequence analysis and were evaluated for growth promoting potential in French bean seedlings under non-saline and salinity stress conditions through pot experiments. The seed bacterization by ACC02 and ACC06 revealed that treatment of plants with bacterial isolates in the form of consortia significantly declined (∼60%) stress stimulated ethylene levels and its associated growth inhibition by virtue of their ACC deaminase activity. The consortia treatment alleviated the negative effects of salinity stress and increased root length (110%), root fresh weight (∼45%), shoot length (60%), shoot fresh weight (255%), root biomass (220%), shoot biomass (425%), and total chlorophyll content (∼57%) of French bean seedlings subjected to salinity stress.

Keywords: ACC deaminase, PGPR, salinity stress, siderophore, indole acetic acid

OPEN ACCESS

Edited by:
Heike Bücking,
South Dakota State University, United States

Reviewed by:
Birinchi Kumar Sarma,
Banaras Hindu University, India
Maqshoof Ahmad,
Islamia University of Bahawalpur, Pakistan

***Correspondence:**
Sangeeta Pandey
sangeetamicro@gmail.com;
spandey5@amity.edu

Specialty section:
This article was submitted to Plant Microbe Interactions, a section of the journal Frontiers in Microbiology

Received: *11 December 2018*
Accepted: *17 June 2019*
Published: *09 July 2019*

Citation:
Gupta S and Pandey S (2019) ACC Deaminase Producing Bacteria With Multifarious Plant Growth Promoting Traits Alleviates Salinity Stress in French Bean (Phaseolus vulgaris) Plants. Front. Microbiol. 10:1506. doi: 10.3389/fmicb.2019.01506

INTRODUCTION

In most of the developing countries, the crop production is majorly hampered by the negative impact of abiotic (environmental stressors) and biotic stress. Plants being immobile means that they are confronted to various kind of stresses such as drought, flooding, salinity, heat, cold, exposure to heavy metals and nutrient deficiency, as well as phytopathogen and pests attack.

The increment in synthesis of ethylene from its immediate precursor, ACC, secreted by plants as root exudates, has been found in almost all plants growing under stress conditions (Wang et al., 2013; Liu et al., 2015; Abiri et al., 2017). Ethylene is a plant hormone involved in regulation of various physiological processes of plants, but the climate change induced ethylene production in plants inflicts a significant reduction in plant growth and development and if not monitored properly could result in plant death (Iqbal et al., 2017; Dubois et al., 2018). Therefore, enhancement in ethylene production is an indicator of susceptibility toward various stresses (Glick, 2014; Müller and Munné-Bosch, 2015).

Among various environmental stressors, excessive presence of salts in soil (soil salinity) is one of the major problematic factors responsible for a reduction of plant growth and crop productivity across the globe. It is reported that more than 1000 million hectares of land is affected by salinity throughout the world as per FAO salt affected soil portal. High concentration of salt (NaCl) not only enhanced the stress ethylene production but also induced ion toxicity, oxidative stress, and disturbed the osmotic potential in plants. All physiological processes like respiration, photosynthesis, nitrogen fixation, etc. are affected by the soil salinity resulting in a decrease in farm productivity and yield (Shabala and Munns, 2012; Paul and Lade, 2014; Acosta-Motos et al., 2017). The problem of soil salinity is frequent in arid and semiarid regions, aggravating due to irrational use of chemical fertilizers and improper use of irrigation water (Bharti et al., 2013).

Plant growth promoting rhizobacteria (PGPR) consisting of a group of beneficial bacteria found in the rhizosphere and rhizoplane of the plants, were proven to be the most environmentally friendly and a better alternative to synthetic agrochemicals and other conventional agricultural practices in augmenting growth and stress tolerance in plants, as well as in attaining sustainable agriculture (Shrivastava and Kumar, 2015; Turan et al., 2017; Gouda et al., 2018; Grobelak et al., 2018; Nagargade et al., 2018). They influence the plant growth both directly and indirectly via various mechanisms like nitrogen fixation, production of plant growth hormone (auxins, cytokinin, and gibberellins), solubilization of phosphates and sequestration of iron by production of siderophores (Bhattacharyya and Jha, 2012; Egamberdieva and Lugtenberg, 2014; Shameer and Prasad, 2018).

The major mechanisms utilized by PGP bacteria to reduce the stress includes lowering the level of ethylene via hydrolysing 1-aminocyclopropane-1-carboxylic acid (ACC) by the enzyme ACC deaminase. ACC is the immediate precursor of the hormone ethylene in plants. It is widely reported that certain PGPR possess ACC deaminase enzyme that can degrade ACC to ammonia and α-ketobutyrate, thus reducing the level of ethylene inside the plants (Gamalero and Glick, 2015; Singh et al., 2015; Raghuwanshi and Prasad, 2018). Therefore, the PGPR containing ACC deaminase has the potential to curb the abiotic stress induced ethylene production and its associated adverse effect on plants. There are several published literatures suggesting that plants inoculated with PGPR containing ACC deaminase make the plant more resistant to various stresses like salinity, drought, flood, and against various pathogens (Pourbabaee et al., 2016; Ravanbakhsh et al., 2017; Ghosh et al., 2018; Saikia et al., 2018).

Therefore, the present study was designed to isolate ACC deaminase producing microbes from rhizospheric soil of garlic (*A. sativum*). Other PGP traits like phosphate solubilization, indole acetic acid (IAA) production, HCN production, and zinc solubilization were also estimated for these isolates. Further, evaluation of plant growth promotion was done in French bean (*Phaseolus vulgaris* L.) variety (*Akra Komal*) plants by bio-priming seeds with individual isolates and consortia of isolates under normal conditions as well as in salinity stress conditions.

MATERIALS AND METHODS

Collection of Rhizospheric Soil Sample

The rhizospheric soil samples of *A. sativum* (garlic), member of *Liliaceae* family was collected during the months of February–March 2018 from the four sites of agricultural farm of *A. sativum* situated at Amity University Uttar Pradesh, India (28.3239°N 77.1959°E), employing organic cultivation practices. Five crop plants were uprooted along with the soil from each site and brought to the laboratory in the zip lock bags for further analysis. The non-rhizospheric soil, as well as large soil aggregates, were removed and soil adhered to the roots were separated from each plant, and mixed together to form one composite pool of rhizospheric soil sample.

Isolation of Rhizobacteria and Qualitative Estimation of ACC Deaminase Activity

The rhizobacteria were isolated from the soil sample by serial dilution technique in Luria-Bertani (LB) medium (g/L: peptone 10 g; yeast extract 5 g; NaCl 10 g) supplemented with 1.5% agar. 0.1 mL of appropriate dilutions of the sample was plated on LB agar plates and incubated for 24 h at 28°C. The morphologically distinct colonies were screened for ACC deaminase activity on the sterile minimal DF (Dworkin and Foster) salts media (DF salts per liter: 4.0 g KH_2PO_4, 6.0 g Na_2HPO_4, 0.2 g $MgSO_4.7H_2O$, 2.0 g glucose, 2.0 g gluconic acid and 2.0 g citric acid with trace elements: 1 mg $FeSO_4.7H_2O$, 10 mg H_3BO_3, 11.19 mg $MnSO_4.H_2O$, 124.6 mg $ZnSO_4.7H_2O$, 78.22 mg $CuSO_4.5H_2O$, 10 mg MoO_3, pH 7.2) amended with 3 mM ACC instead of $(NH_4)_2SO_4$ as sole nitrogen source (Dworkin and Foster, 1958; Penrose and Glick, 2003). The inoculated plates were incubated at 28°C for 3 days and growth was monitored on a daily basis. Colonies growing on the plates were taken as ACC deaminase producers and were purified by sub culturing the isolates.

Quantification of ACC Deaminase Activity and Confirmation by Fourier Transform Infrared Spectra Analysis

The quantitative assessment of ACC deaminase activity was done spectrophotometrically in terms of α-ketobutyrate production at 540 nm by comparing with the standard curve of α-ketobutyrate, which ranged from 0.1 to 1.0 μmol (Honma and Shimomura, 1978). The protein estimation was done as per Bradford

methodology (Bradford, 1976). One unit of ACC deaminase activity was expressed as the amount of α-ketobutyrate liberated in nmol per milligram of cellular protein per hour.

Further, the verification of α-ketobutyrate liberation from a deamination reaction of sole nitrogen source ACC, in DF salt minimal media by isolates with maximum ACC deaminase activity was done as potassium bromide (KBr) cell pellet with the help of Fourier-transform infrared spectroscopy (FTIR) in a FTIR-6700 spectrometer (Nicolet, United States).

Indole Acetic Acid Production by Rhizobacterial Isolates

The rhizobacterial strains were inoculated in LB medium amended with 5 mM tryptophan and incubated in orbital shaker for 7 days at 28°C at 200 rpm. The IAA production was assessed by the colorimetric method using Salkowski reagent (0.5M FeCl3 + 70% perchloric acid). Development of red color (which indicates the formation of indolic compounds) with addition of Salkowski reagent and cell free culture supernatant (4:1) was measured by UV–vis spectrophotometer at 530 nm (Gordon and Weber, 1951). The concentration of IAA can be determined with a standard curve of pure indole-3-acetic acid (IAA, Hi-media) ranging between 0 and 100 $\mu g\ mL^{-1}$.

Optimization of Indole Acetic Acid Production by Selected ACC Deaminase Producing Isolates

The optimization of IAA production was done based on two parameters, i.e., incubation time and Tryptophan concentration. The overnight grown bacterial culture was inoculated in LB medium supplemented with 5 mM tryptophan. The aliquots of 5 ml bacterial culture were each withdrawn at 24-h intervals for up to 168-h and evaluated for IAA production. Further, to assess the effect of substrate concentration on IAA production, the LB medium was amended with a different concentration of L-tryptophan, which ranged from 0 to 15 mg/ml, and analyzed for IAA production using Salkowski method.

Phosphate Solubilization by Rhizobacterial Isolates

The ACC utilizing isolates were spot inoculated onto Pikovaskya's agar medium (Hi-media) amended with 2% (w/v) tricalcium phosphate (TCP) and incubated at 28°C for 4 days. The development of clear zones around the colonies were considered as positive phosphate solublizers. The phosphate solubilizing index (PSI) was calculated by using following formula,

$$\text{PSI} = \frac{\text{Colony diameter} + \text{Halozone diameter}}{\text{Colony diameter}}$$

Further, the quantitative estimation of soluble phosphate was carried out by using National Botanical Research Institute's Phosphate Growth (NBRIP) medium (Nautiyal, 1999). The amount of soluble phosphate in culture free supernatant was determined by Fiske and Subbarow method (Fiske and Subbarow, 1925) and expressed as Soluble P (mg/L). Quantification of soluble phosphate was done through standard plot of KH_2PO_4.

Optimization for Phosphate Solubilization by Selected ACC Deaminase Producing Isolates

The optimization study of phosphate solubilization was based on two attributes viz. incubation time and pH of the spent medium. The NBRIP medium was inoculated with overnight cultivated bacterial culture and incubated at 28°C in shaking incubator at 200 rpm. 5 ml bacterial culture was withdrawn at 24-h intervals to monitor the final pH of the medium and to evaluate efficiency of phosphate solubilization by ACC02 and ACC06 by Fiske and Subbarow method.

Zinc Solubilization Assay of Selected Isolates

The zinc solubilizing potential of isolates was determined by spot inoculating the isolates in the Tris-minimal medium (per liter: Tris–HCl 6.06 g; NaCl 4.68 g; KCl 1.49 g; NH_4Cl 1.07 g; Na_2SO_4 0.43 g; $MgCl_2.2H_2O$ 0.2 g; $CaCl_2.2H_2O$, 30 mg, pH 7.0; Fasim et al., 2002), supplemented with 1.5% agar and 0.1% (w/v) insoluble zinc in the form of zinc sulfate ($ZnSO_4$) (Sharma et al., 2012). The plates were incubated for 14 days at 30°C and examined for the formation of halo zones around colonies for zinc solubilization.

HCN, Ammonia, and Siderophore Production of Selected Isolates

For HCN production, the selected bacterial isolates were streaked on King's B medium supplemented with 0.4% (w/v) glycine. A Whatman filter paper saturated with alkaline picric acid solution (2% Na_2CO_3 in 0.5% picric acid) was placed on the upper lids of Petri plates and monitored for 4 days for the development of red-brown from yellow color of filter paper, which served as the indicator for the HCN production (Miller and Higgins, 1970).

Estimation of ammonia was carried out by addition of Nessler's reagent to bacterial culture in peptone water broth (peptone – 10 g/L; NaCl – 5 g/L) and development of slight yellow to brownish color (Kavamura et al., 2013).

The siderophore production was determined by the Chrome Azurol S (CAS) assay according to Schwyn and Neilands (1987). The bacterial colonies were spot inoculated on CAS agar plates and incubated at 28°C for 4 days. Development of orange-yellow halo around the growth was an indicator of siderophore producing bacterial isolates.

In vitro Assay for Stress Tolerance in Response to Drought and Salinity

Salinity Stress Tolerance

For salt tolerance characterization, the growth of isolates was observed at 28°C for 72 h in the LB agar medium, supplemented with 2–8% NaCl concentration (Barra et al., 2016).

Drought Stress Tolerance

The drought tolerance of isolates was evaluated in polyethylene glycol (PEG 6000) supplemented LB agar medium. The growth

of isolates was observed at 28°C for 24 h in LB agar media, with different osmotic potentials ranging from -0.05 to -0.73 MPa, and 25% polyethylene glycol (PEG 6000) was added to the medium for inducing drought stress (−0.73 MPa) (Ali et al., 2014).

Effects of ACC Deaminase Producing Strains on French Bean Growth Under Salt Stress

The plant root elongation assay under normal watered and saline (25 mM NaCl) solution irrigated conditions was performed in accordance with Penrose et al. (2001) in an environmentally controlled growth chamber. Two putative ACC deaminase producing isolates, ACC02 and ACC06, were tested for their efficiency in augmenting growth and in alleviating the negative effects of salinity stress manifested on morphological parameters and chlorophyll content of French bean plants.

Preparation of Bacterial Inoculum Suspension

The selected bacterial inoculum was prepared in the DF salt minimal medium, supplemented with 3 mM ACC and incubated at 28°C in an orbital shaking incubator at 180 rpm for 3 days, in order to induce ACC deaminase activity of isolates. The cells were harvested at 12000 × g for 15 min and resultant cell pellet was suspended in 0.03M $MgSO_4$ to achieve requisite concentration of cells (10^8–10^9 cfu/ml) at OD_{600}. For preparation of microbial consortia, two bacterial strains must be compatible with each other in order to synergistically augment plant growth under non-stressed and salinity stressed conditions. The compatibility of two ACC deaminating rhizobacterial isolates, ACC02 and ACC06, was tested on nutrient agar medium by dual culture antagonism assay (Molina-Romero et al., 2017). The bacterial consortia were prepared by inoculating overnight grown bacterial suspensions of ACC02 and ACC06 strains in nutrient medium in the ratio of 1:1 (Saikia et al., 2018).

Sterilization and Bacterization of Seed

The seeds of French beans (*P. vulgaris* L.) variety (*A. Komal*) procured from Indian Agricultural Research Institute, New Delhi, India, were used for growth promoting experiments. They were surface sterilized in 70% (v/v) ethanol for 1 min followed by 10 min immersion in 1% (v/v) sodium hypochlorite solution (NaClO) and finally rinsed with sterile deionized water (6–7 times). For bacterial inoculation, the French bean seeds were inoculated for 1 h in the appropriate suspension of bacterial cultures and air dried aseptically in the laminar air flow. The control group comprised surface sterilized, unprimed French bean seeds, immersed in 0.03M $MgSO_4$ solution.

Experimental Design and Salinity Treatment

The pot experimental trials were carried out in randomized block design (RBD) including four treatments in each normal and saline (25 mM NaCl) conditions for growth of French bean plants. The details of treatment under normal conditions in which plants were irrigated with distilled water without adding any external source of salt are shown in **Table 1**. The experimental design is similar in case of saline stress conditions but NaCl salt solution of EC 2.5 ds m^{-1} (25 mM NaCl), instead of distilled water, was used to irrigate French bean plants in order to artificially impose salinity stress (**Table 1**).

TABLE 1 | Details of treatment for growth promotion assay of French bean plant by ACC02 and ACC06 in normal and saline conditions.

Growth conditions	Treatment no.	Seed treatment
Normal	T1; Treatment 1	Uninoculated seeds
	T2; Treatment 2	ACC02 bacterized seeds
	T3; Treatment 3	ACC06 bacterized seeds
	T4; Treatment 4	Consortium (ACC02 + ACC06) bacterized seeds
Saline (25 mM NaCl)	T1; Treatment 1	Uninoculated seeds
	T2; Treatment 2	ACC02 bacterized seeds
	T3; Treatment 3	ACC06 bacterized seeds
	T4; Treatment 4	Consortium (ACC02 + ACC06) bacterized seeds

Pot Experiment Assay

Three inoculated and uninoculated French bean seeds of respective treatment were then sown per plastic pots (30 cm in height and 30 cm in diameter), filled with autoclave-sterilized potting mixture of garden soil and coco peat in 1:1 ratio (3 kg soil pot^{-1}). The experimental soil was characterized as sandy loam with pH 4.5, EC 0.0354 dS m^{-1}, 66% sand, 9% slit, and 26% clay (**Table 2**). The pots were placed in a growth chamber and maintained under optimum light and temperature condition, i.e., 80% relative humidity, 16:8 light: dark photoperiod and at 25°C for 30 days. After 10 days of seedling emergence, French bean seedlings were irrigated daily, twice a day, with either sterile distilled water or solution of EC 2.5 ds m^{-1} (25 mM NaCl; to artificially induce salinity stress) as per the treatment condition. The unbacterized plants subjected to salinity stress were presented as a negative control group while non-saline, unbacterized plants served as positive control group.

Morphological and Physiological Analysis of Plants

French bean plants, after being grown for 20 days under saline and non-saline condition, were harvested (three plants per treatment) and analyzed for growth related parameters including root/shoot length, root/shoot fresh and dry weight. The roots and shoots were oven dried separately at 60°C for 3 days and weighed to determine dry biomass of French bean plants. The leaf chlorophyll content was measured by UV/Vis spectrophotometer at 645 and 663 nm in accordance with (Lorenzen, 1967; Hiscox and Israelstam, 1979). In response to salinity stress, electrical conductivity of soil suspension (1:4) of respective treatment was recorded at the stage of harvesting.

Ethylene Measurement

The ethylene emission from French bean seedlings of each treatment was determined by following the protocol of Sarkar et al. (2018), in order to evaluate the potential of ACC deaminase producing strains ACC02 and ACC06 in lowering stress generated ethylene production. The French bean seedlings

TABLE 2 | Physio-chemical characteristics of experimental soil.

Texture	pH	EC (ds m^{-1})	Organic C (g kg^{-1})	Total N (g kg^{-1})	Total P (g kg^{-1})	Total K (g kg^{-1})
Sandy loam	4.5	0.0354	0.58	0.19	0.02	0.23

(three seedlings per treatment) were placed inside the 60-mL glass tubes, sealed with rubber septum and incubated at 28°C for 4 h. One milliliter of headspace gas was withdrawn and injected into the Gas Chromatograph (Bruker 450-GC, Bruker Corporation, United States) equipped with flame ionization detector (FID). The amount of ethylene evolved was expressed as micromole of ethylene per gram of fresh weight by comparing with the standard curve of pure ethylene.

Molecular Identification of Rhizobacterial Isolates

DNA Isolation and 16S rRNA Gene Sequencing

The genomic DNA of two potent ACC deaminase producing PGPR was extracted in accordance with Pandey et al. (2013). The isolated genomic DNA from strains was analyzed on 0.8% agarose gel and amplification of 16S rRNA (∼1500 bp) was carried out in a polymerase chain reaction (PCR) using universal primers forward (5′AGAGTTTGATCCTGGCTCAG3′) and reverse (5′AAGGAGGTGATCCAGCCGCA3′).

The 25 μL reaction mixture for PCR amplification was composed of PCR Buffer 2.5 μL; MgCl2 2 μL; 2 mM dNTPs 1 μL; Primers 0.5 μL each; Taq DNA polymerase 0.5 μL; Template DNA 2 μL; Sterile deionized water 16 μL. The PCR amplified product was purified with Qiaquick PCR purification kit (Qiagen, Valencia, CA).

Phylogenetic Characterization

The 16S rRNA gene was sequenced by Eurofins Genomics India Pvt. Ltd. (Bengaluru, India) by Sanger's di-deoxy nucleotide sequencing method. A similarity search for the sequence so generated was performed using National Centre of Biotechnology Information (NCBI) BLAST program[1]. The phylogenetic tree was constructed by Neighbour-joining (NJ) method using software MEGA X with the bootstrap of 1000 replicates and evolutionary distances were computed.

Nucleotide Accession Number

The 16S rRNA gene sequences so obtained in the present study were submitted to NCBI GenBank database and assigned the accession numbers MH645748 and MH645749 for isolates ACC2 and ACC6, respectively.

Statistical Analysis

All the data regarding quantitative estimation of PGP traits were subjected to one-way ANOVA followed by Tukey's test. All the statistical analyses were carried out with help of SPSS software. The experiments were performed in three replicates and the mean, as well as standard deviation, were calculated using Microsoft Excel 2016.

[1]https://blast.ncbi.nlm.nih.gov/Blast.cgi

RESULTS

Bacterial Isolation and Preliminary Assessment of ACC Deaminase Activity

A total of twenty rhizobacteria were isolated from rhizospheric soil of *A. sativum* on enrichment media, of which, six strains were able to grow on DF minimal salt medium supplemented with 3 mM ACC as a nitrogen source, implying ACC deaminase activity.

The ACC deaminase activity of these six isolates, labeled as ACC02, ACC04, ACC06, ACC07, ACC011, and ACC012, was further quantified in terms of α-ketobutyrate production.

Quantitative Estimation of ACC Deaminase Activity

The ACC deaminase activity of isolates was quantified by α-ketobutyrate production by catalyzing the deamination reaction of sole nitrogen source, ACC in DF minimal salt broth media at 540 nm. All the test isolates showed variation in ACC deaminase activity in the range of 900–1800 nmol α-ketobutyrate per mg of cellular protein per hour. The highest ACC deaminase activity was exhibited by bacterial strain ACC02 (1677 nmol α-ketobutyrate mg $protein^{-1}$ h^{-1}) followed by ACC06 (1589 nmol α-ketobutyrate mg $protein^{-1}$ h^{-1}), ACC11 (936 nmol α-ketobutyrate mg $protein^{-1}$ h^{-1}), ACC04 (916 nmol α-ketobutyrate mg $protein^{-1}$ h^{-1}), ACC12 (891 nmol α-ketobutyrate mg $protein^{-1}$ h^{-1}) and ACC07 (824 nmol α-ketobutyrate mg $protein^{-1}$ h^{-1}) (**Figure 1A**).The highest enzymatic activity of ACC deaminase produced by ACC02 and ACC06, i.e., conversion of nitrogen source ACC into α-ketobutyrate, was further verified by FTIR spectra analysis results (**Figure 2**), which showed peaks at 1689 and 3343 cm^{-1}, confirming the presence of a ketonic group and amino functional group, respectively recognized as α-ketobutyrate as per Sarkar et al. (2018).

Quantitative Determination of Indole Acetic Acid Production

The production of IAA by six putative ACC deaminase producing isolates was quantified at 530 nm by supplementing the growth media with L-tryptophan. The IAA production of all isolates ranged between 10.96 and 37.78 μg/mL with ACC02 (37.38 μg/mL) isolate being displayed as the highest IAA producer followed by isolate ACC06 (34.48 μg/mL) (**Figure 1B**).

The isolates showing positive results with respect to others, ACC02 and ACC06, were further selected for optimization studies to study the effects of incubation period (**Figures 3A,B**) and substrate, L-tryptophan concentration (ranging from 1 to 15 mg/mL) on IAA production (**Figure 3C**). In the time course of IAA production, the maximum production of IAA by both

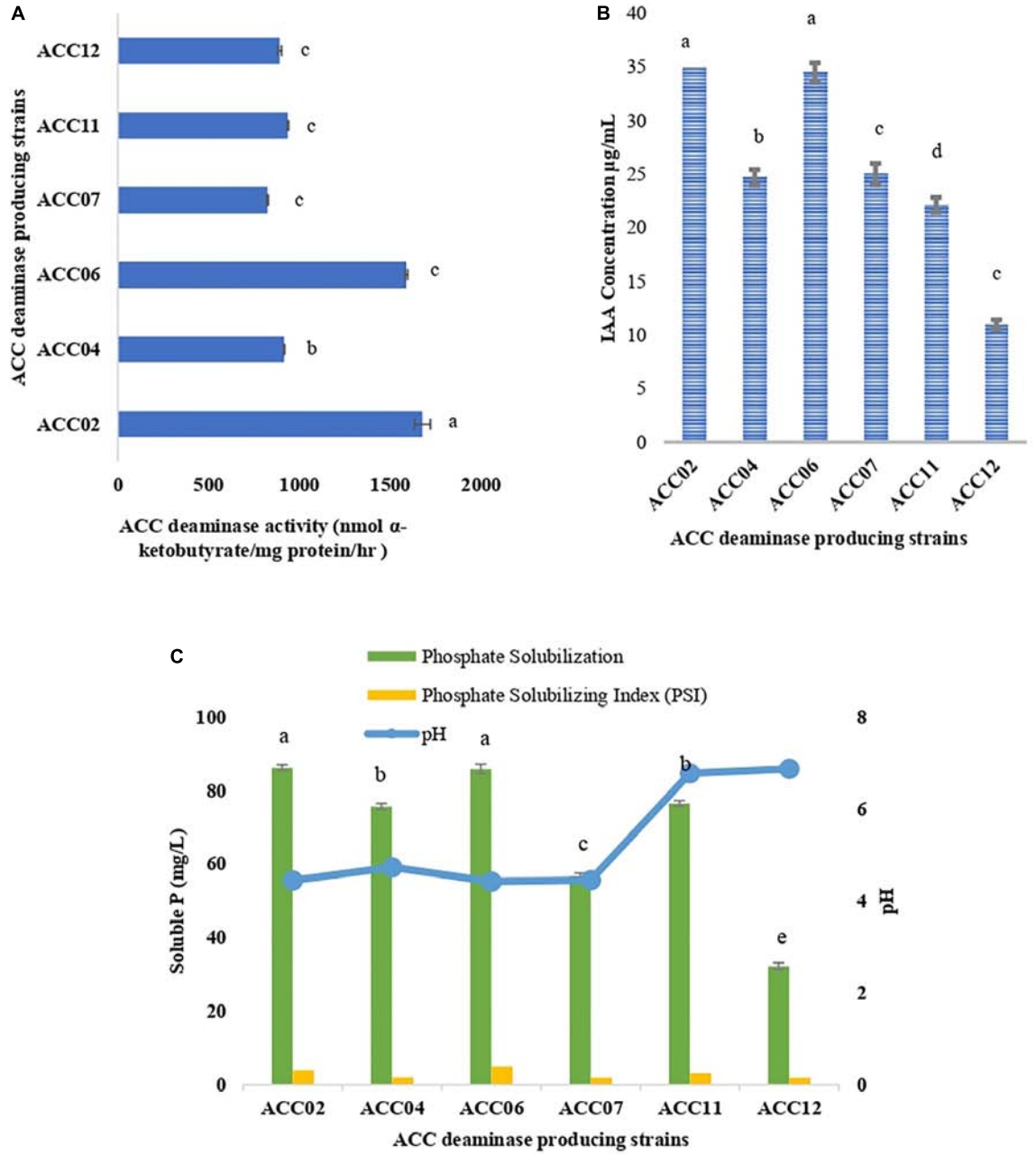

FIGURE 1 | Quantitative estimation of **(A)** ACC deaminase activity, **(B)** IAA production, and **(C)** phosphate solubilization of six isolates from *Allium sativum* rhizospheric soil in respective DF minimal salt, LB-trp, and NBRIP medium. Columns represent mean values while bars represent standard deviation ($n = 3$). Different letters show statistically significant different values ($P < 0.05$) from each other as evaluated from Turkey's test.

the putative ACC deaminase producers, ACC02 and ACC06, was found on the 7th day of the incubation period. According to our results, the maximum IAA production was found when the media was supplemented with L-tryptophan concentration (15 mg/mL) in comparison to unamended media (without L-trp).

Phosphate Solubilization

The potential of six ACC deaminase producing isolates to convert inorganic forms of phosphorous TCP into the solubilized form was assessed when the yellow color zone of phosphate solubilization was displayed around the colonies on Pikovaskya's agar supplemented with 2% TCP (**Figure 4**). The maximum solubilization index was exhibited by isolates ACC02 and ACC06 (>3).

These calcium phosphate solublizers were further analyzed quantitatively in NBRIP medium as shown in **Figure 7**, where the amount of soluble phosphate was within the range of 30–88 mg/L P. The highest phosphate solubilization of 86.25 mg/L

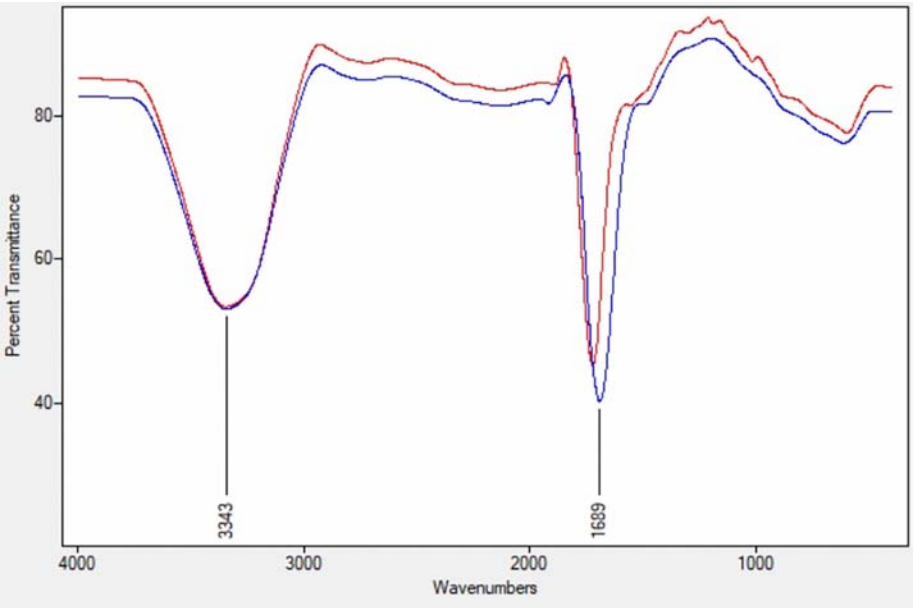

FIGURE 2 | FTIR spectra of α-ketobutyrate in the strain ACC02 (red; upper line) and ACC06 (blue; lower line).

was shown by ACC02 followed by ACC06 and ACC11. The result observed indicates that isolates showing maximum zone of solubilization on solid medium, are also showing maximum phosphate solubilization in liquid medium. The pH of NBRIP medium was found to be acidic after 7 days of incubation as compared to uninoculated control (pH 6.5), except in the case of two isolates, ACC11 and ACC12 (6.7 and 6.8, respectively) (**Figure 1C**).

The two strains ACC02 and ACC06 with highest phosphate solubilizing ability were further selected for determining the profile of phosphate solubilization with respect to incubation period and pH of the NBRIP medium. The highest solubilization was recorded on the 6th day of incubation for both the isolates, ACC02 and ACC06. Further, the optimization studies also represented that both the isolates lowered the pH of broth medium as the incubation period increases with respect to uninoculated control medium (**Figure 5**). The lowering of pH of medium, attributed by the production of organic acids, was in correlation with P solubilizing activity, with lowest pH recorded during maximum calcium phosphate solubilization.

Production of Ammonia, HCN, Siderophore, and Solubilization of Zinc

The HCN (hydrogen cyanide) production was observed for isolate ACC02 (*A. aneurinilyticus* AIOA1), while the yellow picrate filter paper did not turn red brown for other isolate ACC06 (*Paenibacillus* sp. strain SG_AIOA2) as shown in **Figure 6A**. Another indirect PGP mechanism, Ammonia (NH_3) production, was checked for both the potent ACC deaminase producers. Both the isolates ACC02 (*A. aneurinilyticus* AIOA1) and ACC06 (*Paenibacillus* sp. strain SG_AIOA2) were positive for ammonia production. In addition to this, both isolates exhibited a color change of greenish blue CAS agar media to yellow indicating significant production of siderophore (**Figure 6B**). The Zinc solubilization ability of the ACC deaminase producing bacterial isolates were evaluated by determining zone of solubilization on $ZnSO_4$ supplemented Tris-minimal medium. The isolate ACC06 did not solubilize zinc while another isolate ACC02 produced halo zone (**Figure 6C**).

In vitro Stress Tolerance in Response to Salinity and Drought

In addition to this, both the isolates were screened *in vitro* for their potential to tolerate high salt concentration (2–8%) and osmotic stress conditions. In the case of salinity, the isolate ACC02 could be able to tolerate salinity levels up to 6% NaCl while the isolate ACC06 exhibited growth on LB media supplemented with 4% NaCl only. No isolates could not tolerate high concentration of NaCl (8%) added in growth media.

The ACC02 isolate was able to tolerate the osmotic stress of 0.05 MPa only and not higher drought conditions, while ACC06 could survive in drought conditions of 0.05 MPa, 0.30 MPa as well as 0.73 MPa osmotic stress.

Molecular Identification and Phylogenetic Analysis

The 16S rRNA gene sequencing and phylogenetic analysis revealed that two ACC deaminase producing PGPR isolates indicated 95–100% similarity with the known sequences in GenBank and belonged to different genera of *Aneurinibacillus* and *Paenibacillus*. The Phylogenetic analysis of two ACC deaminase producing strains using MEGA X software revealed their relatedness with other strains of respective species (**Figure 7**).

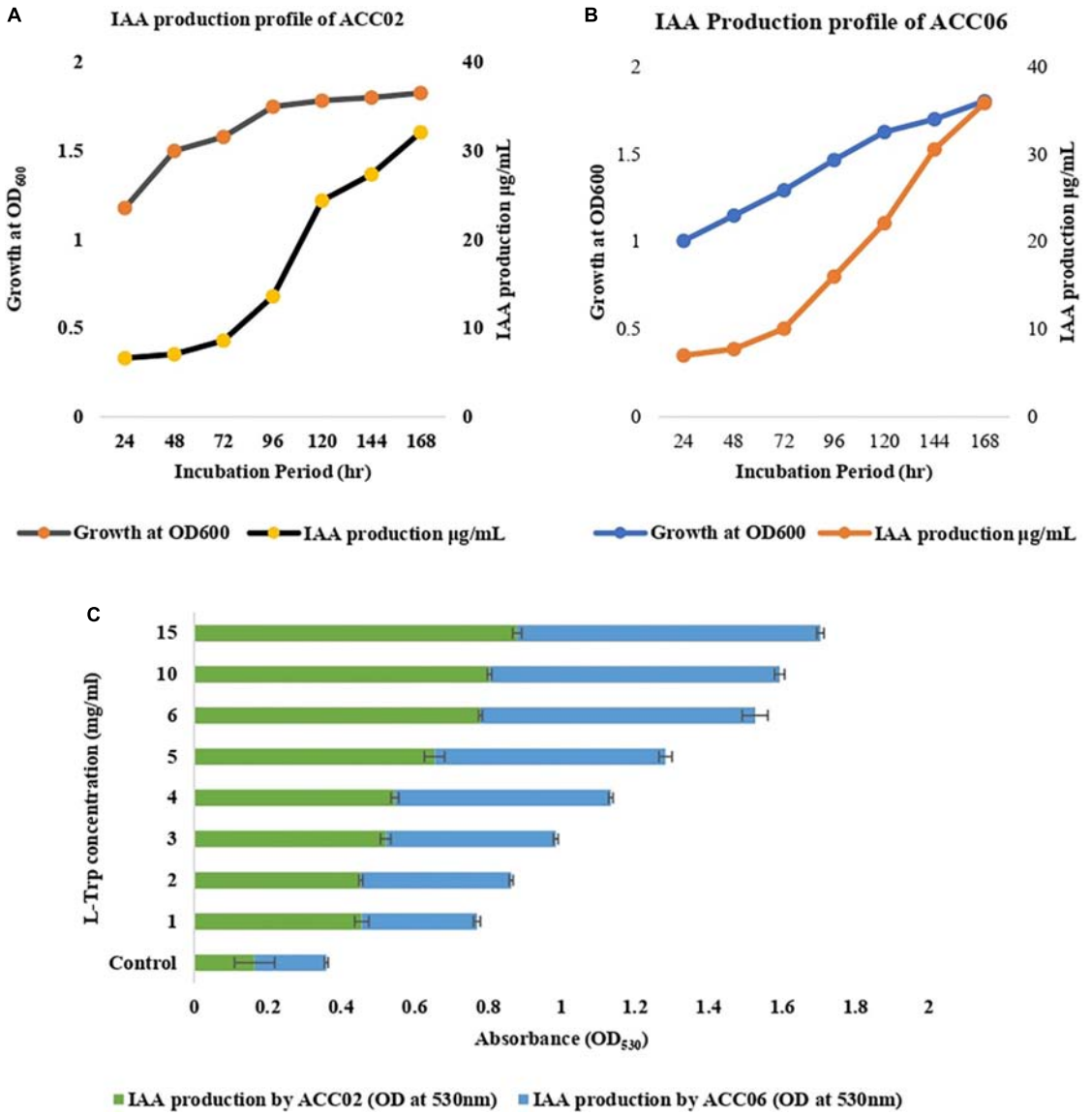

FIGURE 3 | IAA production profile of ACC02 **(A)** and ACC06 **(B)** isolates as a function of incubation period and of L-tryptophan concentration **(C)**.

Effects of ACC Deaminase Producing Strains on French Bean Growth Under Salt Stress

The influence of the two highest ACC deaminase, IAA producing and Phosphate solubilizing PGPR strains, ACC02 and ACC06, on growth promotion of French bean under no stress and salinity stress conditions, was evaluated through pot trials (**Figure 8**). The dual culture antagonism assay between these two selected strains did not show any antagonistic effects against each other (**Supplementary Figure 1**).

The negative effects of salinity stress resulted in a reduction in growth parameters such as root length, shoot length, fresh and dry biomass of root and shoot of French bean plants in relation to corresponding non-stressed, uninoculated French bean plants. The EC of the experimental soil of all salt treated pots was recorded in the range of 4–4.8 ds m^{-1}.

However, the plant growth in terms of growth parameters, including length, fresh and dry weight of root/shoot biomass, was significantly ($P < 0.05$) increased in bacterial inoculated plants under salinity stressed and non-saline conditions.

The consortium application of ACC02 and ACC06 enhanced the growth of root and shoot of French bean plant exposed to salt stressed conditions. The shoot length was significantly ($P < 0.05$) improved by 60% in T4 treatment in comparison with corresponding uninoculated control plants. However, no significant difference was found in the case of shoot length between individual strain application, i.e., T2 and T3 treated French plants (**Figure 9B**). Similarly, the combined treatment of ACC deaminase producing strains, ACC02 and ACC06, has

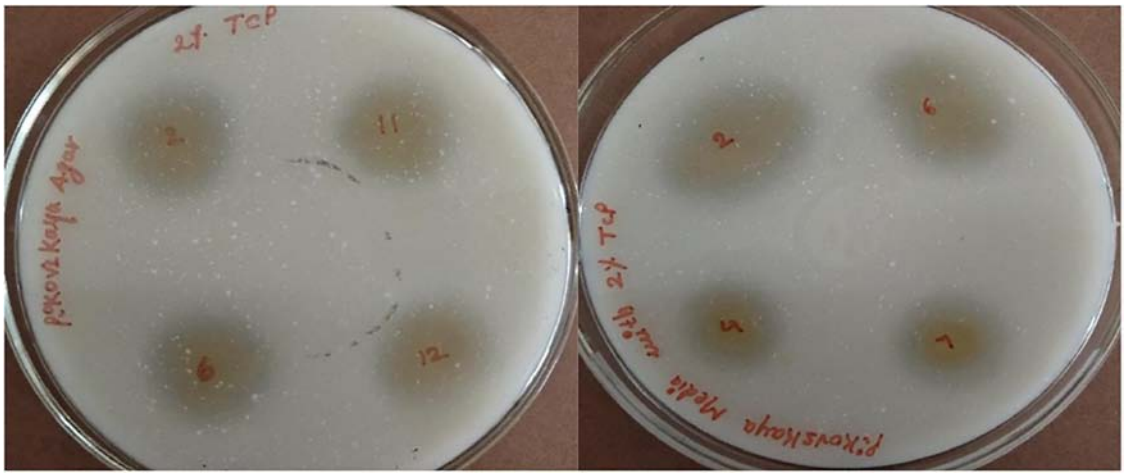

FIGURE 4 | Phosphate solubilization by different isolates from *Allium sativum* rhizospheric soil on Pikovaskya's agar supplemented with 2% TCP.

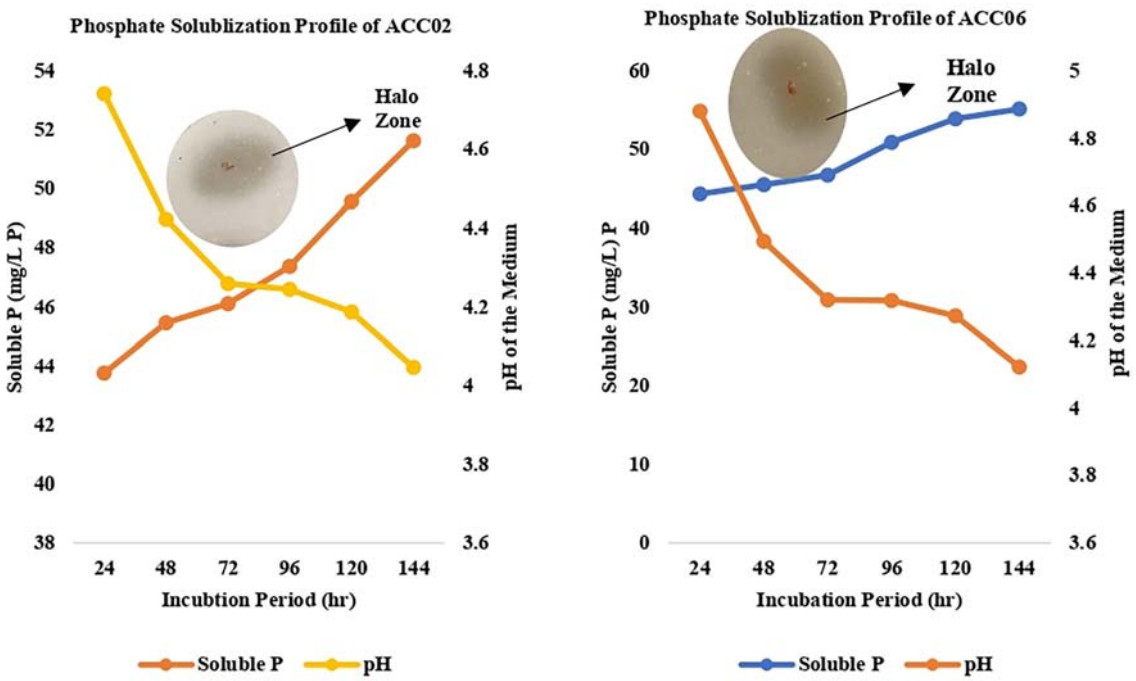

FIGURE 5 | Calcium phosphate solubilization profile of ACC02 and ACC06 isolates as a function of incubation period and pH of spent medium.

a tremendous influence on root length of French bean plants on exposure to salt stressed conditions. The root length was increased by ∼79, 58, and 110% in T2, T3, and T4 treatments as compared to control stressed group of plants (**Figure 9A**).

The consortium treatment improved the fresh and dry biomass of root/shoot of French bean plants under saline stress conditions. The shoot fresh weight and dry weight of French bean plants increased by ∼255 and ∼425% under saline stress conditions in relation to corresponding control. No considerable difference was found in the case of shoot biomass of French plants treated with individual strains ACC02 and ACC06. Similar improvements were achieved in terms of root fresh weight and dry weight of French bean plants under salt stress. Root fresh weight significantly ($P < 0.05$) increased by ∼46, 36, and 81%, while Root dry weight improved by 180, 142, and 220% at T2, T3, and T4 treatments with respect to T1 treated control plants (**Figures 9C–F**).

The consortium treatment was found to be effective in improving the leaf chlorophyll content of stressed French bean plants by ∼57%, followed by ∼35% at Treatment T3 and ∼28% at treatment T2, in comparison with the uninoculated stressed plants (**Figure 9G**). The higher levels

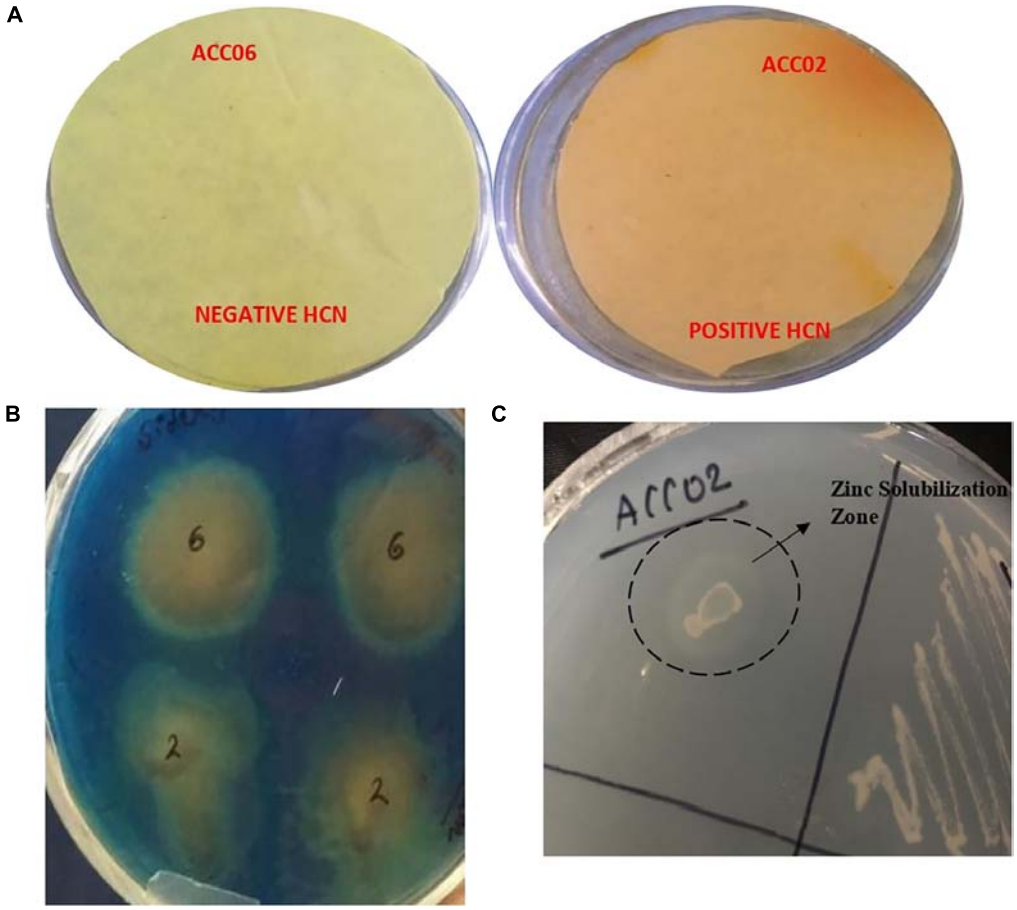

FIGURE 6 | Estimation of HCN production **(A)**, Siderophore production on solid blue CAS agar media **(B)**, and zinc solubilization on Tris minimal salts agar medium supplemented with $ZnSO_4$ **(C)** by ACC deaminase producing isolates ACC02 and ACC06.

of ethylene production ∼133% was observed in salt stressed uninoculated French bean plants, in comparison to plants grown in normal (0 mM NaCl) conditions. However, inoculation of French bean plants with ACC deaminase producers, *A. aneurinilyticus* and *Paenibacillus* sp., reduced the ethylene emission by 38 and 42%, respectively, compared with uninoculated French bean plants. The consortium application of *A. aneurinilyticus* and *Paenibacillus* sp. has more potential in decreasing salinity stress induced ethylene by ∼61% followed by treatment 2 and treatment 3 in inoculated plants (**Figure 9H**).

These results suggested that consortia of isolates *A. aneurinilyticus* (ACC02) and *Paenibacillus* sp. (ACC06) have the potential to mitigate the negative effects of salt stress on the growth of French bean plants.

DISCUSSION

The possession of enzymatic activity of ACC deaminase by PGPR is one of the key growth stimulating traits that facilitate growth and stress tolerance in plants under normal as well as stressed conditions (Glick, 2012; Chandra et al., 2018). This microbial enzyme, ACC deaminase, is responsible for dissociation of stress induced ACC (secreted as root exudates) into Ammonia and α-ketobutyrate, which otherwise forwarded to produce ethylene that has a drastic impact on physiology, growth and development of plants (Barnawal et al., 2014; Heydarian et al., 2016; Ali and Kim, 2018; Saleem et al., 2018; Zhang et al., 2018). Therefore, the role of microbial ACC deaminase producers is immensely significant in today's agricultural system, which is more prone to climate change.

In the present work, two bacterial isolates ACC02 and ACC06 with a high amount of ACC deaminase activity were selected from the rhizosphere of *A. sativum* crop plant for further assessment for growth promoting abilities such as IAA production, insoluble phosphate and zinc solubilization, siderophore secretion, HCN and ammonia production.

The PGPR altered the indigenous pool of growth regulating hormones, such as IAA, which resulted in root elongation as well as formation of lateral roots and root hairs. This enhancement of root system of plants improves water and nutrient uptake efficiency of plants. The endogenous IAA along with bacterial

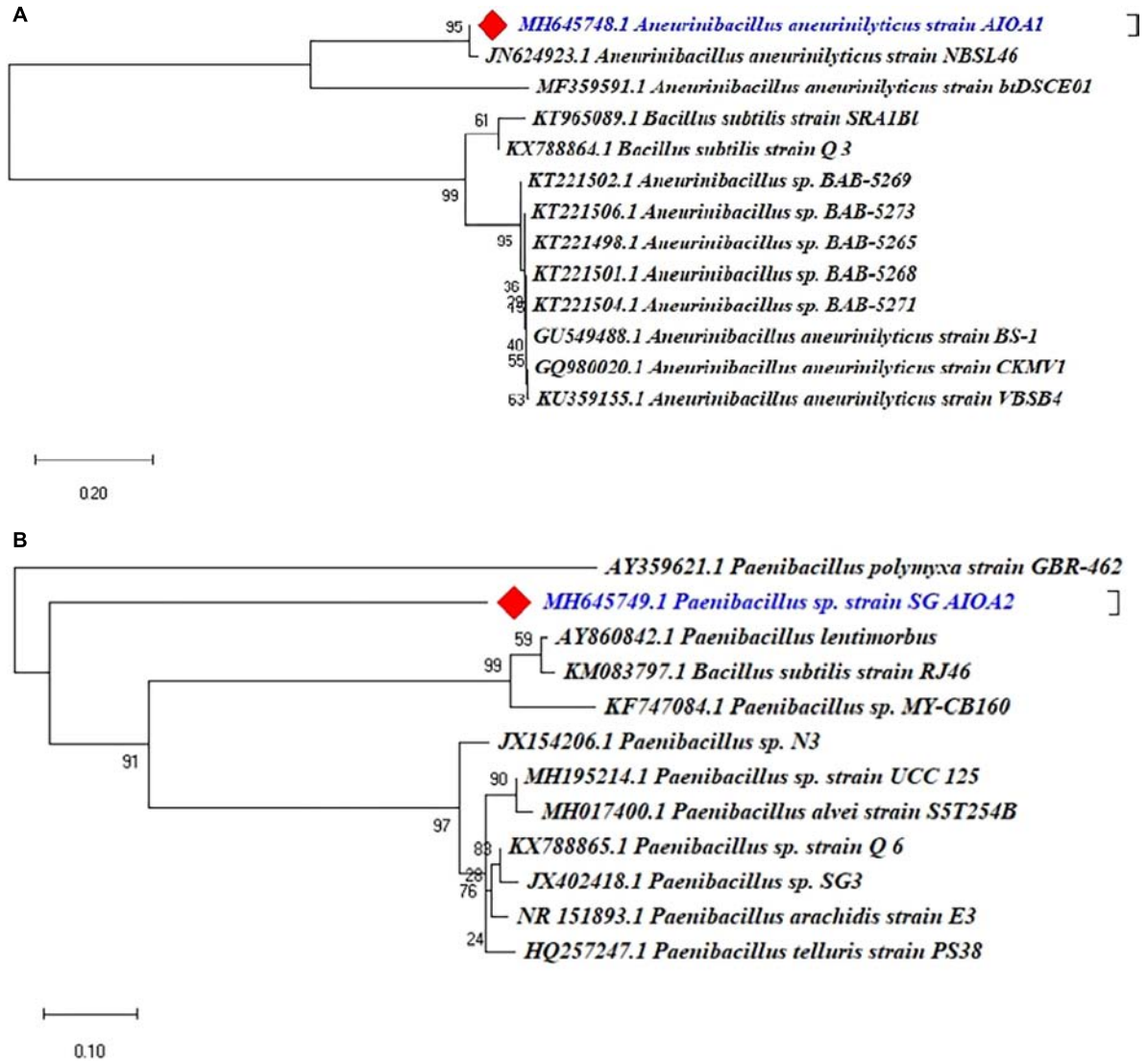

FIGURE 7 | Phylogenetic dendrograms, based on partial 16S rRNA nucleotide sequences, showing the relationship between the selected ACC deaminase producing strains ACC02 and ACC06 with closely related taxa of **(A)** *Aneurinibacillus* and **(B)** *Paenibacillus*, respectively. The 16S rRNA gene sequences of closely related species were retrieved from NCBI GenBank databases. The Neighbour joining phylogenetic tree was inferred using MEGA-X software; evolutionary distance was computed using Maximum Composite Likelihood method at bootstrap value of 1000.

synthesized IAA increased the secretion of plant root exudates that directly serve as an energy source for root associated growth promoting bacteria, improving their growth and colonization efficiency (Etesami et al., 2015). Several strains of genus *Bacillus*, *Azotobacter*, *Pseudomonas* were reported to produce IAA (Cassán et al., 2014; Verma et al., 2018). The evaluation of bacterial isolates, ACC02 and ACC06 for production of IAA, revealed that both are significant producers of IAA suggesting that they could be used as PGPR.

The optimization process is very important as it helps in optimizing the attributes, such as the minimum number of days as well as optimum precursor, L-tryptophan concentration responsible for maximum IAA production by PGPR. The optimization of IAA production by these two isolates indicated highest production after 7th day of inoculation. A similar result was reported by Chaiharn and Lumyong (2011), indicating maximum IAA production on the 9th day of inoculation. The L-tryptophan is observed as the direct precursor for IAA synthesis by root colonizing bacteria through the indole-3-acetamide pathway (Patten and Glick, 1996), therefore, the amount of precursor concentration has a direct influence on IAA production. As per our study, growth media amended with different concentrations of L-tryptophan was used to investigate the effect of substrate concentration on IAA production. On the basis of spectrophotometric data (OD_{530}), it was evaluated that IAA production was increased with an increasing concentration of externally supplied L-tryptophan with maximum production in medium supplemented with

FIGURE 8 | Effect of ACC deaminase producers, ACC02 and ACC06, as individual strains and consortium on plant growth promotion of French bean under salinity stress **(A)** and normal condition **(B)**, as compared to positive (uninoculated plants growing in normal conditions) and negative control (uninoculated plants growing saline stress conditions).

15 mg/mL of tryptophan. Similar results were observed by Bharucha et al. (2013) who demonstrated the influence of L-tryptophan concentration on indole production and found a positive correlation between IAA production and L-tryptophan concentration.

Phosphate solubilization is another important trait of PGPR and the isolates of the current study revealed a significant release of PO_4^{3-} from insoluble complex TCP. The findings of the current study are in agreement with numerous published literatures reporting solubilization of phosphate by *Bacillus*, *Pseudomonas*, and *Azotobacter* (Ahmad et al., 2008; Bhattacharyya and Jha, 2012; Panwar et al., 2014; Maitra et al., 2015). Besides providing phosphorous to the plants, the PSBs also enhance the plant's growth by stimulating nitrogen fixation, enhancing availability of trace metals and by formation of plant growth hormones (Kumar et al., 2013). It has been reported that quantitative measurement of P-solubilization in NBRIP broth medium provides a more accurate result than regular plate assay (Baig et al., 2010). Therefore, evaluation of isolates to solubilize phosphorous in NBRIP broth was also completed, which revealed direct co-relation between P-solubilization on plates and broth medium. The P solubilization by these two isolates was accompanied by a decrease in pH of the medium, indicating the mechanism behind P-solubilization is secretion of organic acids, such as gluconic acid and citric acid, by the isolates (Serrano et al., 2013; Khan et al., 2014; Chen et al., 2016; Paul and Sinha, 2017; Wei et al., 2018). Furthermore, the optimization analysis revealed that phosphate solubilizing efficiency of isolates, ACC02 and ACC06, progressively increased with the number of incubation days. The maximum phosphate solubilization in NBRIP medium was observed at the 6th day of incubation for both isolates, followed by a decline in the pH of the medium. The results of optimization of phosphate solubilizing potential of our isolates are in agreement with the similar work of Manzoor et al. (2017).

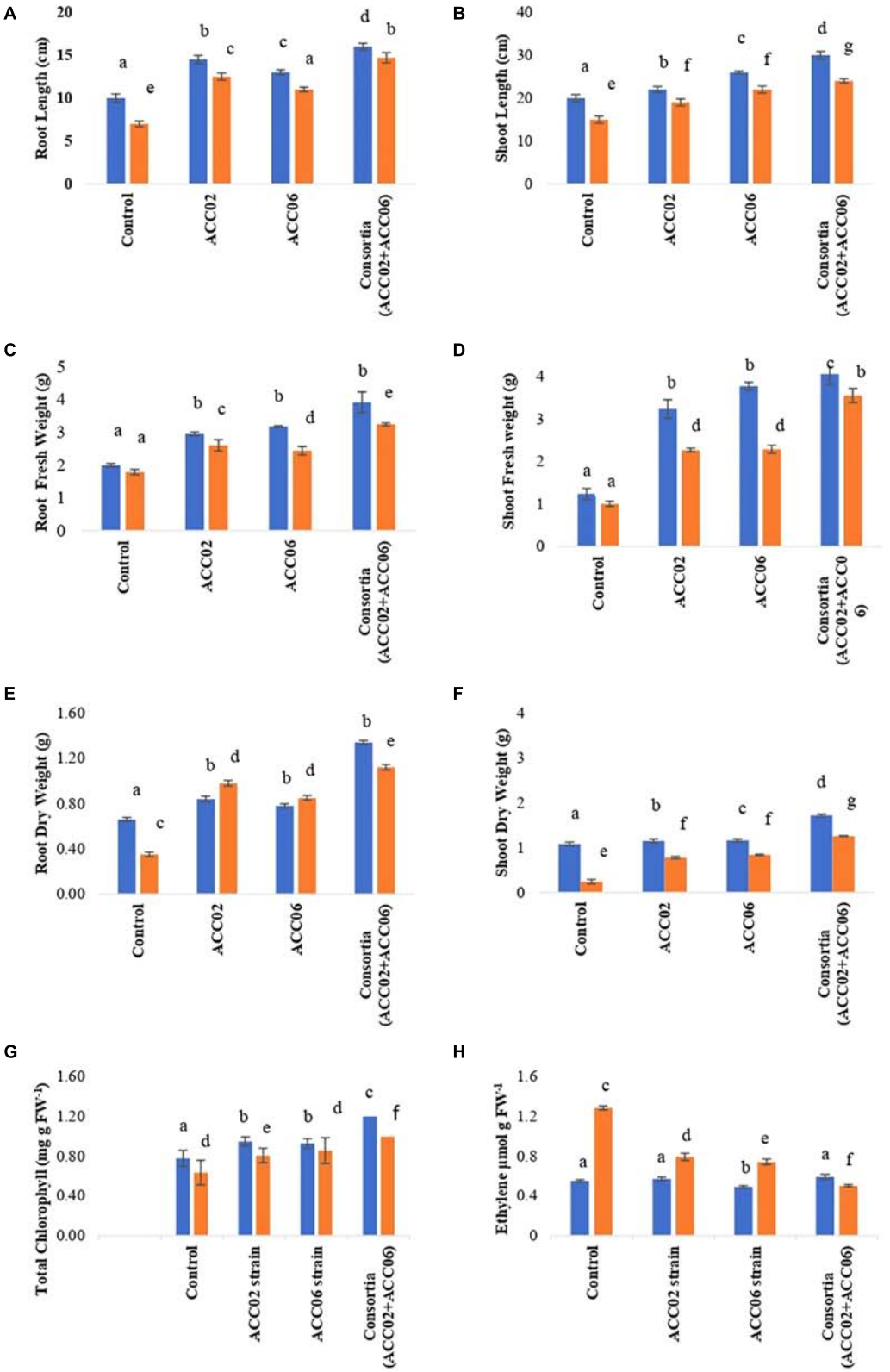

FIGURE 9 | Effect of potent ACC deaminase isolates on physio-morphology parameters: **(A)** Root Length; **(B)** Shoot Length; **(C)** Root Fresh weight; **(D)** Shoot Fresh weight; **(E)** Root Dry weight; **(F)** Shoot Dry Weight; **(G)** Total Chlorophyll content and **(H)** Ethylene content of French beans plants under stress (saline; orange bar) and non-stressed (normal; blue bar) conditions. Control, plants from unbacterized seeds; ACC02, seeds inoculated with *A. aneurinilyticus* strain AlOA1; ACC06, seeds inoculated with *Paenibacillus* sp. strain SG_AlOA2. Columns represent Mean values while bars represent Standard deviation ($n = 3$). Different letters show statistically significant different values ($P < 0.05$) between treatments as evaluated from Duncan's test.

The production of siderophore, ammonia and HCN are some of the indirect PGP traits found among the isolates of the present study. Siderophores, low molecular weight iron chelators, produced by various soil microorganisms, bind Fe^{3+} and make it available for their own growth and also for plants. There are several reports describing the production of siderophores by the rhizospheric micro flora enhancing the iron uptake of plants (Kotasthane et al., 2017; Priyanka et al., 2017).

The production of ammonia by the microbes helps the plants both directly and indirectly. The ammonia excreted by diazotrophic bacteria is one of the most important characters of the PGPR's which benefits the crop (Pérez-Montaño et al., 2014; Richard et al., 2018). This accumulation of ammonia in soil may increase in pH creating alkaline condition of soil at pH 9–9.5. It suppresses the growth of certain fungi and nitrobacteria as it has potent inhibition effect. It also disturbs the equilibrium of the microbial community and inhibits germination of spores of many fungi (Swamy et al., 2016).

Zinc is a crucial micronutrient for growth and development of plants governing several their physiological processes. Use of zinc solubilizers in place of chemical fertilizers is an eco-friendly and sustainable method to meet the requirements of zinc by the plants (Kamran et al., 2017). The zinc solubilizing ability of ACC deaminase containing PGPR was evaluated on the Tris-minimal plates supplemented with insoluble zinc complex, $ZnSO_4$, and only ACC02 was found to be categorized as zinc solubilizing bacteria.

The tolerance of bacteria toward high salinity and drought was also screened under *in vitro* conditions. Both isolates indicated moderate tolerance toward salt and drought stress. Therefore, isolates ACC02 and ACC06 have could be used as stress tolerating PGPR in soils facing challenges of salinity and drought.

The BLAST similarity searches and phylogenetic analysis revealed that isolates of our study, ACC02 and ACC06, belonged to *A. aneurinilyticus* strain AIOA1 and *Paenibacillus* sp. strain SG_AIOA2, respectively. There are few reports available in the literature documenting the ACC deaminase producing ability and PGPR potential of *Aneurinibacillus* and *Paenibacillus* (Goswami et al., 2015; Chauhan et al., 2017).

The present study reports that inoculation of seeds with ACC deaminase producing bacteria reduces the stress of salinity in plants. The results of *in vivo* experiments also reveal that there is a significant improvement in plant growth of the test plant under both no salt and salt stressed conditions when both strains were applied as consortium compared to application of individual strains. The finding dual culture antagonism assay as well as pot study reveals that both strains were compatible to each other and exhibited their cumulative growth promotion effect when applied together. The interaction between different microbial strains result into enhanced PGP potential of PGPR. It has been reported that the syntrophic relationship among microbes is a common phenomenon in microbial ecosystem (Morris et al., 2013). Thus, use of consortia of microbes having synergistic relation is more beneficial and exerts improved results (Shaharoona et al., 2006; Verma et al., 2013). The presence of a higher number of bacterial cells in a consortium could be the reason behind greater PGP effects under stressed conditions (Barra et al., 2016; Grobelak et al., 2018; Saikia et al., 2018).

The ethylene is a significant plant hormone required for every aspect of plant development and growth cycle but it stimulates, growth repressive effects, such as retardation of root development, inhibition of seed germination, promotion of aging, senescence and abscission process in plants under stressed conditions (Gupta and Pandey, 2019). Several reports suggested that application of ACC deaminase producers mitigate the adverse effect of salt stress manifested on plants by minimizing the ethylene emission to its optimum level and thus confers growth promotion and stress tolerance in stressed plants (Orhan, 2016; Maxton et al., 2018; Safari et al., 2018). The growth of French bean plants when subjected to salinity stress might be attributed to the ACC deaminase activity ($>$20 nmol α-ketobutyrate mg protein^{-1} h^{-1}) of two selected strains, which declines the production of stress generated ethylene by deaminating its precursors, ACC into ammonia and α-ketobutyrate (Penrose and Glick, 2003). Based on our results and previous findings, ACC utilizing bacterial strains promote plant growth, increase root/shoot length and improve plant biomass under salinity stress conditions by lowering ethylene accumulation in plants. However, the presence of multifarious PGP traits could be the added advantage of these isolates, which could be harnessed to develop these strains as bio-fertilizers in a wide range of plants under normal conditions. Our study suggests that the application of a consortia of microbes enhances plant growth in both normal and saline conditions. It is very much possible that IAA and ACC deaminase promote root growth in a co-ordinated manner (Glick et al., 2007). Similarly, siderophore production and phosphate solubilization has also been reported by various researchers as an important attribute significantly responsible for plant growth and development (Rajkumar et al., 2010; Taurian et al., 2010; Sadeghi et al., 2012; Zhang et al., 2017; Kumar et al., 2018; Patel et al., 2018). Therefore, use of microbial consortia having the potential to induce salt tolerance and also enhance plant growth and development under normal condition will be a very useful strategy in sustainable agriculture. However, further research is needed to evaluate the efficiency of these strains as their consortium under field condition to provide tolerance in the case of abiotic stress like salinity and exertion of their PGP potential under normal field condition.

CONCLUSION

The present study describes the isolation of ACC deaminase producing bacteria from rhizospheric soil of Garlic. Two potential strains, ACC02 and ACC06, were found to possess other growth promoting potential like IAA production, phosphate solubilization, siderophore and ammonia production. The result of *in vivo* study of these isolates revealed that they promote plant growth both under normal and saline conditions.

The production of ACC deaminase and other PGP traits by these isolates project the potential that they could be used as a bio-fertilizer under both normal and saline soils. However, further research is needed to evaluate the efficiency of these strains under actual field conditions to reduce the stress of salinity and as an effective plant growth promoter.

AUTHOR CONTRIBUTIONS

SG has conducted all the experiments under the guidance of SP. SP conceived and designed the research. Both the authors analyzed the data and wrote manuscript.

ACKNOWLEDGMENTS

The authors thank DST-SERB for providing financial support with research grant ECR/2017/000080 to carry out this research work. The authors are also thankful to the Amity University, Noida for providing infrastructural support.

SUPPLEMENTARY MATERIAL

The Supplementary Material for this article can be found online at: https://www.frontiersin.org/articles/10.3389/fmicb.2019.01506/full#supplementary-material

REFERENCES

Abiri, R., Shaharuddin, N. A., Maziah, M., Yusof, Z. N. B., Atabaki, N., Sahebi, M., et al. (2017). Role of ethylene and the APETALA 2/ethylene response factor superfamily in rice under various abiotic and biotic stress conditions. *Environ. Exp. Bot.* 134, 33–44. doi: 10.1016/j.envexpbot.2016.10.015

Acosta-Motos, J., Ortuño, M., Bernal-Vicente, A., Diaz-Vivancos, P., Sanchez-Blanco, M., and Hernandez, J. (2017). Plant responses to salt stress: adaptive mechanisms. *Agronomy* 7:18. doi: 10.3390/agronomy7010018

Ahmad, F., Ahmad, I., and Khan, M. (2008). Screening of free-living rhizospheric bacteria for their multiple plant growth promoting activities. *Microbiol. Res.* 163, 173–181. doi: 10.1016/j.micres.2006.04.001

Ali, S., and Kim, W.-C. (2018). Plant growth promotion under water: decrease of waterlogging-induced ACC and ethylene levels by ACC deaminase-producing bacteria. *Front. Microbiol.* 9:1096. doi: 10.3389/fmicb.2018.01096

Ali, S. Z., Sandhya, V., and Rao, L. V. (2014). Isolation and characterization of drought-tolerant ACC deaminase and exopolysaccharide-producing fluorescent *Pseudomonas* sp. *Ann. Microbiol.* 64, 493–502. doi: 10.1007/s13213-013-0680-3

Baig, K., Arshad, M., Zahir, Z., and Cheema, M. (2010). Comparative efficacy of qualitative and quantitative methods for rock phosphate solubilization with phosphate solubilizing rhizobacteria. *Soil Environ.* 29, 82–86.

Barnawal, D., Bharti, N., Maji, D., Chanotiya, C. S., and Kalra, A. (2014). ACC deaminase-containing *Arthrobacter protophormiae* induces NaCl stress tolerance through reduced ACC oxidase activity and ethylene production resulting in improved nodulation and mycorrhization in Pisum sativum. *J. Plant Physiol.* 171, 884–894. doi: 10.1016/j.jplph.2014.03.007

Barra, P. J., Inostroza, N. G., Acuña, J. J., Mora, M. L., Crowley, D. E., and Jorquera, M. A. (2016). Formulation of bacterial consortia from avocado (*Persea americana* Mill.) and their effect on growth, biomass and superoxide dismutase activity of wheat seedlings under salt stress. *Appl. Soil Ecol.* 102, 80–91. doi: 10.1016/j.apsoil.2016.02.014

Bharti, N., Yadav, D., Barnawal, D., Maji, D., and Kalra, A. (2013). Exiguobacterium oxidotolerans, a halotolerant plant growth promoting rhizobacteria, improves yield and content of secondary metabolites in *Bacopa monnieri* (L.) Pennell under primary and secondary salt stress. *World J. Microbiol. Biotechnol.* 29, 379–387. doi: 10.1007/s11274-012-1192-1

Bharucha, U., Patel, K., and Trivedi, U. B. (2013). Optimization of indole acetic acid production by *Pseudomonas putida* UB1 and its effect as plant growth-promoting rhizobacteria on mustard (*Brassica nigra*). *Agric. Res.* 2, 215–221. doi: 10.1007/s40003-013-0065-7

Bhattacharyya, P. N., and Jha, D. K. (2012). Plant growth-promoting rhizobacteria (PGPR): emergence in agriculture. *World J. Microbiol. Biotechnol.* 28, 1327–1350. doi: 10.1007/s11274-011-0979-9

Bradford, M. M. (1976). A rapid and sensitive method for the quantitation of microgram quantities of protein utilizing the principle of protein-dye binding. *Anal. Biochem.* 72, 248–254. doi: 10.1016/0003-2697(76)90527-3

Cassán, F., Vanderleyden, J., and Spaepen, S. (2014). Physiological and agronomical aspects of phytohormone production by model plant-growth-promoting rhizobacteria (PGPR) belonging to the genus *Azospirillum*. *J. Plant Growth Regul.* 33, 440–459. doi: 10.1007/s00344-013-9362-4

Chaiharn, M., and Lumyong, S. (2011). Screening and optimization of indole-3-acetic acid production and phosphate solubilization from rhizobacteria aimed at improving plant growth. *Curr. Microbiol.* 62, 173–181. doi: 10.1007/s00284-010-9674-6

Chandra, D., Srivastava, R., Glick, B. R., and Sharma, A. K. (2018). Drought-tolerant *Pseudomonas* spp. Improve the growth performance of finger millet *(Eleusine coracana (L.) Gaertn.)* under non-stressed and drought-stressed conditions. *Pedosphere* 28, 227–240. doi: 10.1016/s1002-0160(18)60013-x

Chauhan, A., Guleria, S., Balgir, P. P., Walia, A., Mahajan, R., Mehta, P., et al. (2017). Tricalcium phosphate solubilization and nitrogen fixation by newly isolated *Aneurinibacillus aneurinilyticus* CKMV1 from rhizosphere of *Valeriana jatamansi* and its growth promotional effect. *Braz. J. Microbiol.* 48, 294–304. doi: 10.1016/j.bjm.2016.12.001

Chen, W., Yang, F., Zhang, L., and Wang, J. (2016). Organic acid secretion and phosphate solubilizing efficiency of *Pseudomonas* sp. *PSB*12: effects of phosphorus forms and carbon sources. *Geomicrobiol. J.* 33, 870–877. doi: 10.1080/01490451.2015.1123329

Dubois, M., Van Den Broeck, L., and Inzé, D. (2018). The pivotal role of ethylene in plant growth. *Trends Plant Sci.* 23, 311–323. doi: 10.1016/j.tplants.2018.01.003

Dworkin, M., and Foster, J. (1958). Experiments with some microorganisms which utilize ethane and hydrogen. *J. Bacteriol.* 75, 592–603.

Egamberdieva, D., and Lugtenberg, B. (2014). "Use of plant growth-promoting rhizobacteria to alleviate salinity stress in plants," in *Use of Microbes for the Alleviation of Soil Stresses*, ed. M. Miransari (New York, NY: Springer), 73–96. doi: 10.1007/978-1-4614-9466-9_4

Etesami, H., Alikhani, H. A., and Hosseini, H. M. (2015). Indole-3-acetic acid (IAA) production trait, a useful screening to select endophytic and rhizosphere competent bacteria for rice growth promoting agents. *Methods X* 2, 72–78. doi: 10.1016/j.mex.2015.02.008

Fasim, F., Ahmed, N., Parsons, R., and Gadd, G. M. (2002). Solubilization of zinc salts by a bacterium isolated from the air environment of a tannery. *FEMS Microbiol. Lett.* 213, 1–6. doi: 10.1111/j.1574-6968.2002.tb11277.x

Fiske, C. H., and Subbarow, Y. (1925). The colorimetric determination of phosphorus. *J. Biol. Chem.* 66, 375–400.

Gamalero, E., and Glick, B. R. (2015). Bacterial modulation of plant ethylene levels. *Plant Physiol.* 169, 13–22. doi: 10.1104/pp.15.00284

Ghosh, P. K., De, T. K., and Maiti, T. K. (2018). "Role of ACC Deaminase as a Stress Ameliorating Enzyme of Plant Growth-Promoting Rhizobacteria Useful in Stress Agriculture: A Review," in *Role of Rhizospheric Microbes in Soil: Volume 1: Stress Management and Agricultural Sustainability*, ed. V. S. Meena (Singapore: Springer Singapore), 57–106. doi: 10.1007/978-981-10-8402-7_3

Glick, B. R. (2012). Plant growth-promoting bacteria: mechanisms and applications. *Scientifica* 2012:963401.

Glick, B. R. (2014). Bacteria with ACC deaminase can promote plant growth and help to feed the world. *Microbiol. Res.* 169, 30–39. doi: 10.1016/j.micres.2013.09.009

Glick, B. R., Cheng, Z., Czarny, J., and Duan, J. (2007). "Promotion of plant growth by ACC deaminase-producing soil bacteria," in *New Perspectives and Approaches in Plant Growth-Promoting Rhizobacteria research* (Dordrecht: Springer), 329–339.

Gordon, S. A., and Weber, R. P. (1951). Colorimetric estimation of indoleacetic acid. *Plant Physiol.* 26, 192–195. doi: 10.1104/pp.26.1.192

Goswami, D., Parmar, S., Vaghela, H., Dhandhukia, P., and Thakker, J. N. (2015). Describing *Paenibacillus mucilaginosus* strain N3 as an efficient plant growth promoting rhizobacteria (PGPR). *Cogent Food Agric.* 1:1000714.

Gouda, S., Kerry, R. G., Das, G., Paramithiotis, S., Shin, H.-S., and Patra, J. K. (2018). Revitalization of plant growth promoting rhizobacteria for sustainable development in agriculture. *Microbiol. Res.* 206, 131–140. doi: 10.1016/j.micres.2017.08.016

Grobelak, A., Kokot, P., Hutchison, D., Grosser, A., and Kacprzak, M. (2018). Plant growth-promoting rhizobacteria as an alternative to mineral fertilizers in assisted bioremediation-sustainable land and waste management. *J. Environ. Manag.* 227, 1–9. doi: 10.1016/j.jenvman.2018.08.075

Gupta, S., and Pandey, S. (2019). Unravelling the biochemistry and genetics of ACC deaminase-An enzyme alleviating the biotic and abiotic stress in plants. *Plant Gene* 18:100175. doi: 10.1016/j.plgene.2019.100175

Heydarian, Z., Yu, M., Gruber, M., Glick, B. R., Zhou, R., and Hegedus, D. D. (2016). Inoculation of soil with plant growth promoting bacteria producing 1-aminocyclopropane-1-carboxylate deaminase or expression of the corresponding *acdS* gene in transgenic plants increases salinity tolerance in *Camelina sativa*. *Front. Microbiol.* 7:1966. doi: 10.3389/fmicb.2016.01966

Hiscox, J., and Israelstam, G. (1979). A method for the extraction of chlorophyll from leaf tissue without maceration. *Can. J. Bot.* 57, 1332–1334. doi: 10.1139/b79-163

Honma, M., and Shimomura, T. (1978). Metabolism of 1-aminocyclopropane-1-carboxylic acid. *Agric. Biol. Chem.* 42, 1825–1831. doi: 10.1080/00021369.1978.10863261

Iqbal, N., Khan, N. A., Ferrante, A., Trivellini, A., Francini, A., and Khan, M. (2017). Ethylene role in plant growth, development and senescence: interaction with other phytohormones. *Front. Plant Sci.* 8:475. doi: 10.3389/fpls.2017.00475

Kamran, S., Shahid, I., Baig, D. N., Rizwan, M., Malik, K. A., and Mehnaz, S. (2017). Contribution of zinc solubilizing bacteria in growth promotion and zinc content of wheat. *Front. Microbiol.* 8:2593. doi: 10.3389/fmicb.2017.02593

Kavamura, V. N., Santos, S. N., Da Silva, J. L., Parma, M. M., Ávila, L. A., Visconti, A., et al. (2013). Screening of brazilian cacti rhizobacteria for plant growth promotion under drought. *Microbiol. Res.* 168, 183–191. doi: 10.1016/j.micres.2012.12.002

Khan, M. S., Zaidi, A., and Ahmad, E. (2014). "Mechanism of Phosphate Solubilization and Physiological Functions of Phosphate-Solubilizing Microorganisms," in *Phosphate Solubilizing Microorganisms: Principles and Application of Microphos Technology*, eds M. S. Khan, A. Zaidi, and J. Musarrat (Cham: Springer International Publishing), 31–62. doi: 10.1007/978-3-319-08216-5_2

Kotasthane, A. S., Agrawal, T., Zaidi, N. W., and Singh, U. (2017). Identification of siderophore producing and cynogenic fluorescent *Pseudomonas* and a simple confrontation assay to identify potential bio-control agent for collar rot of chickpea. *3 Biotech* 7:137. doi: 10.1007/s13205-017-0761-2

Kumar, P., Thakur, S., Dhingra, G., Singh, A., Pal, M. K., Harshvardhan, K., et al. (2018). Inoculation of siderophore producing rhizobacteria and their consortium for growth enhancement of wheat plant. *Biocatal. Agric. Biotechnol.* 15, 264–269. doi: 10.1016/j.bcab.2018.06.019

Kumar, V., Singh, P., Jorquera, M. A., Sangwan, P., Kumar, P., Verma, A., et al. (2013). Isolation of phytase-producing bacteria from Himalayan soils and their effect on growth and phosphorus uptake of Indian mustard (*Brassica juncea*). *World J. Microbiol. Biotechnol.* 29, 1361–1369. doi: 10.1007/s11274-013-1299-z

Liu, J., Xie, B., Shi, X., Ma, J., and Guo, C. (2015). Effects of two plant growth-promoting rhizobacteria containing 1-aminocyclopropane-1-carboxylate deaminase on oat growth in petroleum-contaminated soil. *Int. J. Environ. Sci. Technol.* 12, 3887–3894. doi: 10.1007/s13762-015-0798-x

Lorenzen, C. J. (1967). Determination of chlorophyll and pheo-pigments: spectrophotometric equations1. *Limnol. Oceanogr.* 12, 343–346. doi: 10.4319/lo.1967.12.2.0343

Maitra, N., Manna, S. K., Samanta, S., Sarkar, K., Debnath, D., Bandopadhyay, C., et al. (2015). Ecological significance and phosphorus release potential of phosphate solubilizing bacteria in freshwater ecosystems. *Hydrobiologia* 745, 69–83. doi: 10.1007/s10750-014-2094-z

Manzoor, M., Abbasi, M. K., and Sultan, T. (2017). Isolation of phosphate solubilizing bacteria from maize rhizosphere and their potential for rock phosphate solubilization–mineralization and plant growth promotion. *Geomicrobiol. J.* 34, 81–95. doi: 10.1080/01490451.2016.1146373

Maxton, A., Singh, P., and Masih, S. A. (2018). ACC deaminase-producing bacteria mediated drought and salt tolerance in *Capsicum annuum*. *J. Plant Nutr.* 41, 574–583. doi: 10.1080/01904167.2017.1392574

Miller, R., and Higgins, V. J. (1970). Association of cyanide with infection of birdsfoot trefoil by *Stemphylium loti*. *Phytopathology* 60, 104–110.

Molina-Romero, D., Baez, A., Quintero-Hernández, V., Castañeda-Lucio, M., Fuentes-Ramírez, L. E., Del Rocío Bustillos-Cristales, M., et al. (2017). Compatible bacterial mixture, tolerant to desiccation, improves maize plant growth. *PLoS One* 12:e0187913. doi: 10.1371/journal.pone.0187913

Morris, B. E., Henneberger, R., Huber, H., and Moissl-Eichinger, C. (2013). Microbial syntrophy: interaction for the common good. *FEMS Microbiol. Rev.* 37, 384–406. doi: 10.1111/1574-6976.12019

Müller, M., and Munné-Bosch, S. (2015). Ethylene response factors: a key regulatory hub in hormone and stress signalling. *Plant Physiol.* 169, 32–41. doi: 10.1104/pp.15.00677

Nagargade, M., Tyagi, V., and Singh, M. K. (2018). "Plant Growth-Promoting Rhizobacteria: A Biological Approach Toward the Production of Sustainable Agriculture," in *Role of Rhizospheric Microbes in Soil: Volume 1: Stress Management and Agricultural Sustainability*, ed. V. S. Meena (Singapore: Springer Singapore), 205–223. doi: 10.1007/978-981-10-8402-7_8

Nautiyal, C. S. (1999). An efficient microbiological growth medium for screening phosphate solubilizing microorganisms. *FEMS Microbiol. Lett.* 170, 265–270. doi: 10.1016/s0378-1097(98)00555-2

Orhan, F. (2016). Alleviation of salt stress by halotolerant and halophilic plant growth-promoting bacteria in wheat (*Triticum aestivum*). *Braz. J. Microbiol.* 47, 621–627. doi: 10.1016/j.bjm.2016.04.001

Pandey, S., Singh, S., Yadav, A. N., Nain, L., and Saxena, A. K. (2013). Phylogenetic diversity and characterization of novel and efficient cellulase producing bacterial isolates from various extreme environments. *Biosci. Biotechnol. Biochem.* 77, 1474–1480. doi: 10.1271/bbb.130121

Panwar, M., Tewari, R., and Nayyar, H. (2014). "Microbial Consortium of Plant Growth-Promoting Rhizobacteria Improves the Performance of Plants Growing in Stressed Soils: An Overview," in *Phosphate Solubilizing Microorganisms: Principles and Application of Microphos Technology*, eds M. S. Khan, A. Zaidi, and J. Musarrat (Cham: Springer International Publishing), 257–285. doi: 10.1007/978-3-319-08216-5_11

Patel, P., Trivedi, G., and Saraf, M. (2018). Iron biofortification in mungbean using siderophore producing plant growth promoting bacteria. *Environ. Sustain.* 1, 357–365. doi: 10.1007/s42398-018-00031-3

Patten, C. L., and Glick, B. R. (1996). Bacterial biosynthesis of indole-3-acetic acid. *Can. J. Microbiol.* 42, 207–220. doi: 10.1139/m96-032

Paul, D., and Lade, H. (2014). Plant-growth-promoting rhizobacteria to improve crop growth in saline soils: a review. *Agron. Sustain. Dev.* 34, 737–752. doi: 10.1007/s13593-014-0233-6

Paul, D., and Sinha, S. N. (2017). Isolation and characterization of phosphate solubilizing bacterium *Pseudomonas aeruginosa* KUPSB12 with antibacterial potential from river Ganga, India. *Ann. Agrarian Sci.* 15, 130–136. doi: 10.1016/j.aasci.2016.10.001

Penrose, D. M., and Glick, B. R. (2003). Methods for isolating and characterizing ACC deaminase-containing plant growth-promoting rhizobacteria. *Physiol. Plant.* 118, 10–15. doi: 10.1034/j.1399-3054.2003.00086.x

Penrose, D. M., Moffatt, B. A., and Glick, B. R. (2001). Determination of 1-aminocycopropane-1-carboxylic acid (ACC) to assess the effects of ACC deaminase-containing bacteria on roots of canola seedlings. *Can. J. Microbiol.* 47, 77–80. doi: 10.1139/w00-128

Pérez-Montaño, F., Alías-Villegas, C., Bellogín, R., Del Cerro, P., Espuny, M., Jiménez-Guerrero, I., et al. (2014). Plant growth promotion in cereal and leguminous agricultural important plants: from microorganism capacities to crop production. *Microbiol. Res.* 169, 325–336. doi: 10.1016/j.micres.2013.09.011

Pourbabaee, A., Bahmani, E., Alikhani, H., and Emami, S. (2016). Promotion of wheat growth under salt stress by halotolerant bacteria containing ACC deaminase. *JAST* 18, 855–864.

Priyanka, A. T., Kotasthane, A. S., Kosharia, A., Kushwah, R., Zaidi, N. W., and Singh, U. S. (2017). Crop specific plant growth promoting effects of *ACCd* enzyme and siderophore producing and cynogenic fluorescent *Pseudomonas*. *3 Biotech* 7:27. doi: 10.1007/s13205-017-0602-3

Raghuwanshi, R., and Prasad, J. K. (2018). "Perspectives of Rhizobacteria with ACC Deaminase Activity in Plant Growth Under Abiotic Stress," in *Root Biology*, eds B. Giri, R. Prasad, and A. Varma (Cham: Springer International Publishing), 303–321. doi: 10.1007/978-3-319-75910-4_12

Rajkumar, M., Ae, N., Prasad, M. N. V., and Freitas, H. (2010). Potential of siderophore-producing bacteria for improving heavy metal phytoextraction. *Trends Biotechnol.* 28, 142–149. doi: 10.1016/j.tibtech.2009.12.002

Ravanbakhsh, M., Sasidharan, R., Voesenek, L. A., Kowalchuk, G. A., and Jousset, A. (2017). ACC deaminase-producing rhizosphere bacteria modulate plant responses to flooding. *J. Ecol.* 105, 979–986. doi: 10.1111/1365-2745.12721

Richard, P. O., Adekanmbi, A. O., and Ogunjobi, A. A. (2018). Screening of bacteria isolated from the rhizosphere of maize plant (*Zea mays* L.) for ammonia production and nitrogen fixation. *Afr. J. Microbiol. Res.* 12, 829–834. doi: 10.5897/ajmr2018.8957

Sadeghi, A., Karimi, E., Dahaji, P. A., Javid, M. G., Dalvand, Y., and Askari, H. (2012). Plant growth promoting activity of an auxin and siderophore producing isolate of *Streptomyces* under saline soil conditions. *World J. Microbiol. Biotechnol.* 28, 1503–1509. doi: 10.1007/s11274-011-0952-7

Safari, D., Jamali, F., Nooryazdan, H.-R., and Bayat, F. (2018). Evaluation of ACC deaminase producing '*Pseudomonas fluorescens*' strains for their effects on seed germination and early growth of wheat under salt stress. *Aust. J. Crop Sci.* 12, 413–421. doi: 10.21475/ajcs.18.12.03.pne801

Saikia, J., Sarma, R. K., Dhandia, R., Yadav, A., Bharali, R., Gupta, V. K., et al. (2018). Alleviation of drought stress in pulse crops with ACC deaminase producing rhizobacteria isolated from acidic soil of Northeast India. *Sci. Rep.* 8:3560. doi: 10.1038/s41598-018-21921-w

Saleem, A. R., Brunetti, C., Khalid, A., Della Rocca, G., Raio, A., Emiliani, G., et al. (2018). Drought response of *Mucuna pruriens* (L.) DC. Inoculated with ACC deaminase and IAA producing rhizobacteria. *PLoS One* 13:e0191218. doi: 10.1371/journal.pone.0191218

Sarkar, A., Ghosh, P. K., Pramanik, K., Mitra, S., Soren, T., Pandey, S., et al. (2018). A halotolerant *Enterobacter* sp. displaying ACC deaminase activity promotes rice seedling growth under salt stress. *Res. Microbiol.* 169, 20–32. doi: 10.1016/j.resmic.2017.08.005

Schwyn, B., and Neilands, J. (1987). Universal chemical assay for the detection and determination of siderophores. *Anal. Biochem.* 160, 47–56. doi: 10.1016/0003-2697(87)90612-9

Serrano, A., Mardad, I., and Soukri, A. (2013). Solubilization of inorganic phosphate and production of organic acids by bacteria isolated from a Moroccan mineral phosphate deposit. *Afr. J. Microbiol. Res.* 7, 626–635.

Shabala, S., and Munns, R. (2012). Salinity stress: physiological constraints and adaptive mechanisms. *Plant Stress Physiol.* 1, 59–93. doi: 10.1079/9781845939953.0059

Shaharoona, B., Arshad, M., and Zahir, Z. (2006). Effect of plant growth promoting rhizobacteria containing ACC-deaminase on maize (*Zea mays* L.) growth under axenic conditions and on nodulation in mung bean *(Vigna radiata L.)*. *Lett. Appl. Microbiol.* 42, 155–159. doi: 10.1111/j.1472-765x.2005.01827.x

Shameer, S., and Prasad, T. (2018). Plant growth promoting rhizobacteria for sustainable agricultural practices with special reference to biotic and abiotic stresses. *Plant Growth Regul.* 84, 603–615. doi: 10.1007/s10725-017-0365-1

Sharma, S. K., Sharma, M. P., Ramesh, A., and Joshi, O. P. (2012). Characterization of zinc-solubilizing *Bacillus* isolates and their potential to influence zinc assimilation in soybean seeds. *J. Microbiol. Biotechnol.* 22, 352–359. doi: 10.4014/jmb.1106.05063

Shrivastava, P., and Kumar, R. (2015). Soil salinity: a serious environmental issue and plant growth promoting bacteria as one of the tools for its alleviation. *Saudi J. Biol. Sci.* 22, 123–131. doi: 10.1016/j.sjbs.2014.12.001

Singh, R. P., Shelke, G. M., Kumar, A., and Jha, P. N. (2015). Biochemistry and genetics of ACC deaminase: a weapon to "stress ethylene" produced in plants. *Front. Microbiol.* 6:937. doi: 10.3389/fmicb.2015.00937

Swamy, M. K., Akhtar, M. S., and Sinniah, U. R. (2016). "Response of PGPR and AM fungi toward growth and secondary metabolite production in medicinal and aromatic plants," in *Plant, Soil and Microbes*, eds K. Hakeem and M. Akhtar (Cham: Springer), 145–168. doi: 10.1007/978-3-319-29573-2_7

Taurian, T., Anzuay, M. S., Angelini, J. G., Tonelli, M. L., Ludueña, L., Pena, D., et al. (2010). Phosphate-solubilizing peanut associated bacteria: screening for plant growth-promoting activities. *Plant Soil* 329, 421–431. doi: 10.1007/s11104-009-0168-x

Turan, M., Yildirim, E., Kitir, N., Unek, C., Nikerel, E., Ozdemir, B. S., et al. (2017). "Beneficial Role of Plant Growth-Promoting Bacteria in Vegetable Production Under Abiotic Stress," in *Microbial Strategies for Vegetable Production*, eds A. Zaidi and M. S. Khan (Cham: Springer International Publishing), 151–166. doi: 10.1007/978-3-319-54401-4_7

Verma, J. P., Jaiswal, D. K., Krishna, R., Prakash, S., Yadav, J., and Singh, V. (2018). Characterization and screening of thermophilic *Bacillus* strains for developing plant growth promoting consortium from hot spring of Leh and Ladakh region of India. *Front. Microbiol.* 9:1293. doi: 10.3389/fmicb.2018.01293

Verma, J. P., Yadav, J., Tiwari, K. N., and Kumar, A. (2013). Effect of indigenous *Mesorhizobium* spp. and plant growth promoting rhizobacteria on yields and nutrients uptake of chickpea *(Cicer arietinum L.)* under sustainable agriculture. *Ecol. Eng.* 51, 282–286. doi: 10.1016/j.ecoleng.2012.12.022

Wang, F., Cui, X., Sun, Y., and Dong, C.-H. (2013). Ethylene signalling and regulation in plant growth and stress responses. *Plant Cell Rep.* 32, 1099–1109. doi: 10.1007/s00299-013-1421-6

Wei, Y., Zhao, Y., Shi, M., Cao, Z., Lu, Q., Yang, T., et al. (2018). Effect of organic acids production and bacterial community on the possible mechanism of phosphorus solubilization during composting with enriched phosphate-solubilizing bacteria inoculation. *Bioresour. Technol.* 247, 190–199. doi: 10.1016/j.biortech.2017.09.092

Zhang, G., Sun, Y., Sheng, H., Li, H., and Liu, X. (2018). Effects of the inoculations using bacteria producing ACC deaminase on ethylene metabolism and growth of wheat grown under different soil water contents. *Plant Physiol. Biochem.* 125, 178–184. doi: 10.1016/j.plaphy.2018.02.005

Zhang, J., Wang, P., Fang, L., Zhang, Q.-A., Yan, C., and Chen, J. (2017). Isolation and characterization of phosphate-solubilizing bacteria from mushroom residues and their effect on tomato plant growth promotion. *Pol. J. Microbiol.* 66, 57–65. doi: 10.5604/17331331.1234993

Conflict of Interest Statement: The authors declare that the research was conducted in the absence of any commercial or financial relationships that could be construed as a potential conflict of interest.

frontiers in Microbiology

ORIGINAL RESEARCH
published: 29 May 2019
doi: 10.3389/fmicb.2019.01207

Halomonas Rhizobacteria of *Avicennia marina* of Indian Sundarbans Promote Rice Growth Under Saline and Heavy Metal Stresses Through Exopolysaccharide Production

Pritam Mukherjee[1], *Abhijit Mitra*[2] *and Madhumita Roy*[3]*

[1] Department of Biotechnology, Techno India University, Kolkata, India, [2] Department of Marine Science, University of Calcutta, Kolkata, India, [3] Department of Microbiology, Bose Institute, Kolkata, India

OPEN ACCESS

Edited by:
Heike Bücking,
South Dakota State University,
United States

Reviewed by:
Doan Trung Luu,
Centre National de la Recherche Scientifique (CNRS), France
Maqshoof Ahmad,
Islamia University of Bahawalpur, Pakistan
Puneet Singh Chauhan,
National Botanical Research Institute (CSIR), India

***Correspondence:**
Madhumita Roy
roymadhumita@rediffmail.com

Specialty section:
This article was submitted to Plant Microbe Interactions, a section of the journal Frontiers in Microbiology

Received: 21 October 2018
Accepted: 13 May 2019
Published: 29 May 2019

Citation:
Mukherjee P, Mitra A and Roy M (2019) Halomonas Rhizobacteria of Avicennia marina of Indian Sundarbans Promote Rice Growth Under Saline and Heavy Metal Stresses Through Exopolysaccharide Production. Front. Microbiol. 10:1207. doi: 10.3389/fmicb.2019.01207

The *Halomonas* species isolated from the rhizosphere of the true mangrove *Avicennia marina* of Indian Sundarbans showed enhanced rice growth promotion under combined stress of salt and arsenic in pot assay. Interestingly, under abiotic stress conditions, *Halomonas* sp. Exo1 was observed as an efficient producer of exopolysaccharide. The study revealed that salt triggered exopolysaccharide production, which in turn, increased osmotic tolerance of the strain. Again, like salt, presence of arsenic also caused increased exopolysaccharide production that in turn sequestered arsenic showing a positive feedback mechanism. To understand the role of exopolysaccharide in salt and arsenic biosorption, purified exopolysaccharide mediated salt and arsenic sequestration were studied both under *in vivo* and *in vitro* conditions and the substrate binding properties were characterized through FT-IR and SEM-EDX analyses. Finally, observation of enhanced plant growth in pot assay in the presence of the strain and pure exopolysaccharide separately, confirmed direct role of exopolysaccharide in plant growth promotion.

Keywords: abiotic stress, arsenic bioremediation, exopolysaccharide, *Halomonas*, rhizobacteria, rice growth promotion, salt sequestration, true mangrove *Avicennia marina*

INTRODUCTION

Soil salinity is one of the major abiotic stresses that limit plant productivity throughout the globe. Increased salinity due to climate change and sea level rise is causing daily extinction of many flora and fauna in the coastal world including Indian Sundarbans, inscribed as a World Heritage site by UNESCO (Mitra and Zaman, 2016). In Indian Sundarbans, rice cultivation (80–90% of total crop production in India) is the primary agricultural activity and is the main source of income generation but is restricted mainly to the monsoon season due to high salinity of soil in other seasons (Yadav et al., 1979). In addition to the existing problem of soil salinity, toxic heavy metal (HM) contamination in Indian Sundarbans is another major abiotic stress (Pal et al., 2002). Heavy metal pollution has attained a serious threat here due to discharge of HM rich semi-treated or untreated effluents from industries (tanneries, jute mills, pulp and paper mills, pesticide

manufacturing plants, thermal power plants, brick kilns, rubber, fertilizer and soap factories, antibiotic plants, and oil refineries), located on the banks of the river Hooghly. Slow continuous release of HM from the antifouling paints used to coat the bottom of the numerous fishing trawlers and recreational vessels is another reason of HM pollution in this region (Bighiu et al., 2017). Upon entering the estuarine system, these HMs get dissolubilized or precipitated on the soil and sediment based on the localized environmental conditions especially pH. Nevertheless, over the years, the region has turned out as a natural sink by virtue of its rich and unique indigenous flora, fauna and a diverse group of largely unexplored mangrove microbiota (Mitra, 2013). Previous research on Indian saline ecosystem identified the potential of eco-friendly halo-tolerant plant growth-promoting rhizomicrobes (PGPR) for application in sustenance of agronomy under diverse saline ecologies (Shrivastava and Kumar, 2015). Application of these native PGPR to alleviate salt stress can be regarded as a better alternative toward sustainable agriculture than developing salt and other stress tolerant transgenic varieties due to high production cost and other environmental hazards (Shrivastava and Kumar, 2015). These osmotolerant microbes possess special mechanisms such as optimization of Na^+/K^+ flow, accumulation of essential osmolytes, transcriptional, and/or translational regulation of salt-tolerant enzymes (osmozymes) for sustaining environmental osmotic shock (Yang et al., 2009). In comparison to the mesophilic (halo-sensitive) counterparts, halo-tolerant microbes are more dynamic owing to their ability to function under both stress and stress-free conditions (Nadeem et al., 2014). Yang et al. (2009) pointed out that the halo-tolerant PGPR causes "induced systemic tolerance" (IST) to salt-sensitive plants and enhances nutrient uptake from soils, thus decreasing the need of the fertilizers. In general, salt-sensitive plants cannot grow or show poor growth in saline media due to ion toxicity (replacement of K^+ by Na^+ in biochemical reactions, and Na^+ and Cl^- induced conformational changes in proteins), osmotic stress (excessive accumulation of sodium in cell walls causing osmotic stress and cell death), nutrient (N, Ca, K, P, Fe, Zn) deficiency due to salt related imbalance and oxidative stress on plants apart from reduced water uptake from the soil. On the other hand, in salt-tolerant plants, salt stress activates specialized genes that are involved in the sustenance of salt-induced and other abiotic stresses (Yang et al., 2009). As salt-sensitive plants do not possess these special genes, their salt stress is ameliorated by the PGPR mediated IST. Although bacterial determinants of IST and their activation pathways in plants have been significantly evaluated during the past decade but the response of the PGPR toward the abiotic stresses has been revealed very recently (Timmusk and Wagner, 1999; Zhang et al., 2008). Use of these PGPR for minimizing agricultural chemical load, HM load (Nadeem et al., 2014; Yu et al., 2014) and soil salinity (Siddikee et al., 2010) is earning considerable appreciation in boosting environmental quality. Although salt stress alleviation by PGPR inoculants had already been reported in rice, wheat and many other crops (Goswami et al., 2014), but the exact mechanism of salt stress alleviation is not fully explored. In addition, exopolysaccharide (EPS) production was noticed in a number of halophilic bacteria, halophilic PGPR, and metal mobilizing bacteria (Llamas et al., 2006). With a growing interest in extremophiles, a large number of halophiles, particularly species belonging to the *Halomonas* genera have been found to be the possessors of EPS (Béjar et al., 1998; Arias et al., 2003; Martínez-Cánovas et al., 2004; Llamas et al., 2006; Poli et al., 2013).

The purpose of this paper is to understand the role of EPS produced by halophilic PGPR belonging to the genus *Halomonas*, isolated from the rhizosphere of the *Avicennia marina* of Indian Sundarbans, in abiotic stress alleviation during rice growth promotion under combined stress of salt and arsenic (As).

MATERIALS AND METHODS

Sampling and Physico-Chemical Assessment of *Avicennia marina* Rhizosphere Soil

The root associated soil of *Avicennia marina* seedling growing in the intertidal mud flat of Bonnie Camp (21°49′45.3″ N; 88°37′13.6″ E) situated in the central region of Indian Sundarbans was collected during monsoon season in the month of September, 2014. The sample was sieved (pore size of 2 mm), grounded to powder using a mortar and pestle, and stored in a clean polyethylene bag at 4°C until use. The soil salinity, electrical conductivity, and pH were recorded with refractometer (Atago, Tokyo, Japan), digital electrical conductivity/TDS meter (Global, India) and digital pH meter (Global, India), respectively, on spot. Moisture content was measured in lab by subtracting dry weight (in oven at 105°C) from the wet weight of the sample. Soil chemical features like Soil Organic Carbon (SOC), % organic matter, N, P, K (U.S. Environmental Protection Agency, 1994) and biologically available HMs were determined (Malo, 1977).

Isolation and Identification of Exopolysaccharide Producing Arsenic and Salt Resistant Halo-Rhizobacteria

Enrichment and isolation of halo-rhizobacteria from *A. marina* rhizosphere soil was done in 8% total salt modified growth media (8% TSMGM) [a specific medium for cultivation of halophiles and haloarchaea that contain 266.7 ml of concentrated salt water (30% stock) {NaCl (240 g l^{-1}), $MgCl_2.6H_2O$ (30 g l^{-1}), $MgSO_4.7H_2O$ (35 g l^{-1}), KCl (7 g l^{-1}), 5 ml 1M Tris-Cl (pH-7.5), 5 ml 1M $CaCl_2.2H_2O$ (0.5 g l^{-1}), adjusted to pH-7.5 with 1M Tris base}, peptone (5 g l^{-1}), yeast extract (1 g l^{-1}), adjusted pH to 7.5 with 1M Tris base] (Dyall-Smith, 2009). Isolates that showed moderate growth in 4 mM [As(III)] were selected for further purification. For screening of the EPS secreting isolates, pure colonies were transferred to nutrient agar (NA) media supplemented with 5% dextrose. Isolates showing mucoid phenotypes were finally selected and purified. After morphological study, the isolates were finally identified by 16S rRNA gene analysis using universal PCR primers 27F and 1492R as mentioned by Mukherjee et al. (2017). The amplified products were sequenced according to the manufacturer's specifications for Taq DNA polymerase-initiated cycle sequencing reactions using fluorescently labeled dideoxynucleotide terminators with

an ABI PRISM 377 automated sequencer (Perkin-Elmer Applied Biosystems). 16S rRNA gene sequence similarity was determined using BLAST version 2.2.12 of the National Center for Biotechnology Information (Altschul et al., 1990). The partial 16S rRNA gene sequences were submitted to GenBank and accession numbers were obtained. Phylogenetic analyses were performed by neighbor-joining method (Saitou and Nei, 1987) with bootstrapping using 1000 replications using MEGA version 7 (Kumar et al., 2016) with Kimura two-parameter model. The bootstrap consensus tree inferred from 1,000 replicates was taken to represent the evolutionary history of the taxa analyzed. The evolutionary distances were computed using the Maximum Composite Likelihood method (Tamura et al., 2004).

Selected bacterial surface morphology was determined by Field Emission Scanning Electron Microscope (FESEM) (Model JEOLJSM 6700F) after growing the isolate for 5 days in salt media (8% TSMGM) amended with [As(III)]. The bacterial sample was mounted on aluminum stubs with conductive carbon cement, dried for 3 h, and coated with 15 nm platinum film with an agar automatic sputter coater. After processing, the sample was visualized in the high-vacuum mode at 15 kV and the images were processed using Photoshop software (Adobe Systems Inc., Calif.).

Characterization of the Isolate Toward Abiotic Stress Tolerance: Salt and Heavy Metals

For all growth-related experiments, cultures were set up in triplicates, incubations were performed at 30 ± 2°C for 3–5 days and the growths were determined both visually and spectrophotometrically at OD_{600nm}. For determination of the minimal inhibitory concentration (MIC) of the *Halomonas* sp. Exo1 toward total salt and NaCl, agar plates with increasing concentrations of mixed sea salt and NaCl in presence and absence of 2 mM [As(III)] were streaked with pure isolates and incubated. Detailed growth kinetics of the strain was studied in LB with increasing concentrations of NaCl, 8% TSMGM broth, and 8% TSMGM broth with increasing concentrations of total salt and/or [As(III)]. For determination of *in vivo* bioaccumulation of osmolytes including both monovalent (Na^+, K^+) and divalent (Mg^{2+}, Ca^{2+}) cations, 5-day old culture broth was prepared in LB and liquid 8% TSMGM. Centrifugation was done and cell-pellet was washed thrice with deionized H_2O and oven-dried at 50°C, digested with pure concentrated HNO_3 (5 ml, Merck) at 65–75°C and filtered through Whatman filter paper. The amounts of osmolytes (Na^+, K^+, Mg^{2+}, and Ca^{2+}) accumulated within cell-biomass were assessed via flame-photometry (Aimil Ltd., India) and the concentrations were calculated from the standard curves of the respective ions. *In vivo* as bioaccumulation study was carried out by live cells and dead cells both. For determination of As accumulation by live cells, time-dependent study was undertaken. The isolate was cultured in 250 ml liquid 8% TSMGM containing 2 mM [As(III)]. 50 ml of culture media was withdrawn at regular intervals of 0, 3, 6, 9, and 12 days. Samples were centrifuged at 7,000 rpm for 10 min to collect both cell-free media and bacterial cell-biomass. Media supernatant was filtered through a 0.22-micron membrane filter (Nuclepore Corp., CA, USA). 10 ml cell-free media filtrate and 0.1 g of dried cell-biomass were digested separately with concentrated HNO_3 (5 ml, Merck) at 65–75°C on a hot plate equipped with a fume hood and filtered through Whatman filter paper No. 1 (125 mm). Acid-digested media supernatant from As-free salt media (0-day time-point) and acid-digested cell-biomass from As-free salt media (3-day time-point) were used as negative controls. For determination of [As(III)] biosorption by dead halo-rhizobacterial biomass, pellet was obtained from 200 ml 5-day old culture grown in 8% TSMGM in the absence of $NaAsO_2$. The cell pellet was washed twice to remove residual media, re-suspended in sterile deionized water, and autoclaved at 121°C at 15 lb/in^2 for 45 min. After this step, the absence of live bacteria was checked by plating onto 8% TSMGM agar plates. 10 ml dead cell suspension (∼7.14 mg bacterial biomass per ml) was incubated at room temperature for 24 h under shaking in the presence of 4 mM [As(III)] and was then centrifuged at 10,000 rpm for 15 min. The cell pellet was again washed thrice with sterile deionized water and dried at 50°C, while the cell-free supernatant was filtered through 0.2–0.45 micron hydrophilic membrane (HiMedia Laboratories Pvt. Ltd.,). Sample preparation and AAS were carried out as mentioned earlier.

Determination of the MIC of the strain for other HMs were done in LB and 8% TSMGM agar plates and broths containing test HMs with increasing concentrations.

In vivo as biotransformation assay was done using a qualitative $AgNO_3$ screening method as described by Simeonova et al. (2004) with modifications. Briefly, plate-based assay was performed where 8% TSMGM agar plates containing 2 mM [As(III)] were spot inoculated with the test bacterial culture, incubated for 3 days at 30 ± 2°C and flooded with 0.1 M $AgNO_3$ solution containing 1 M Tris-HCl (pH 8.0). The reaction between $AgNO_3$ and the arsenic species i.e., [As(III)] or [As(V)] in Tris-HCl environment produces colored precipitates containing arsenic. Presence of [As(III)] species by arsenate reducing bacteria produces light yellow color (due to Ag_3AsO_3 or silver orthoarsenite) and presence of [As(V)] species by arsenite oxidizing bacteria produces light brownish-red color (due to Ag_3AsO_4 or silver orthoarsenate).

Extraction, Purification, and Estimation of Exopolysaccharide Production Under Salt and Arsenic Stresses

For estimation of EPS production under As stress, 100 μl of 24-h old culture of *Halomonas* sp. Exo1 was inoculated (0.1% v/v) into 250 ml Erlenmeyer flasks containing 100 ml of As-free and As-supplemented (2, 4, 6, 8 mM) liquid 8% TSMGM, mixed thoroughly and placed on a rotary shaker (125 rpm) at 30 ± 2°C for 5 days. For determination of the effect of salt stress on EPS yield of *Halomonas* sp. Exo1, 100 ml Erlenmeyer flasks each containing 50 ml of LB broth with varying concentrations of NaCl (0.5, 1, 2.5, 5, 7.5, 10, 12.5, 15, 20, 22.5 %) were inoculated with the bacterial strain. For extraction of EPS in all the treatments, 5-day old cultures were centrifuged at 7,000 rpm for 20 min. The supernatants were vacuum-filtered through cellulose nitrate filter. The EPS was precipitated from the cell-free

supernatant by the addition of ice-cold ethanol (100%, Merck) in 1:3 ratios. The cell-free extract-ethanol mixture was shaken vigorously and incubated overnight at 4°C. For removal of salt and impurities, EPS was dialyzed for 24–48 h using 12–14 kDa MW cut-off dialysis bags against deionized H_2O at 4°C. A fraction of the partially purified EPS solution was dried at 60°C and weighed to determine crude EPS yield (Corzo et al., 1994). For further purification of EPS, methods described by Bales et al. (2013) were followed. In brief, the EPS solution was mixed with ice-cold 20% (w/v) trichloroacetic acid (TCA) solution to precipitate proteins and nucleic acids. After 30 min of incubation, the solution was centrifuged at 15,000 rpm for 1 h at 4°C. To the supernatant, 1.5 volume of 95% ethanol was added and the mixture was kept at −20°C for 24 h to facilitate precipitation of EPS from lipids. To collect the precipitated EPS, the solution was centrifuged at 15,000 rpm for 1 h at 4°C and the EPS pellet was re-suspended in Milli-Q H_2O and dialyzed against the same for 24 h at 4°C using a 12–14 kDa MW cut-off dialysis membrane to remove low molecular weight impurities. The remaining retentate containing purified EPS was lyophilized overnight and stored in sterile containers at −20°C until further analyses. The lyophilized powder of purified EPS was weighed again to determine pure EPS yield. In order to extract cell-bound EPS, the bacterial cell-pellet was re-suspended in 300 µl EDTA solution (10 mM EDTA + 1.5 mM NaCl) and heated at 50°C in water bath for 3 min. The bacterial cell suspension was again centrifuged and cell-free supernatant was decanted and EPS was purified as above. Finally, to understand the exact time-point of getting highest EPS yield, total EPS yield was calculated from cultures grown for 0, 3, 6, 9, and 12 days.

Biophysical Characterization of the Exopolysaccharide

The purified EPS was tested for solubility in various polar and non-polar organic solvents and water. Salinity and electrical conductivity of the pure desalted Exo1 grown in 8% TSMGM were compared with the crude EPS.

Carbohydrate, protein, lipid and sulfate contents of the pure Exo1 were analyzed by spectrophotometer. Total neutral-carbohydrate contents were determined by phenol-sulfuric acid method using D-glucose as a standard (Dubois et al., 1956). The protein contents were measured by Folin-Ciocalteau method using bovine serum albumin (BSA) as a standard (Lowry et al., 1951). Lipid contents were measured by the method described by Novak (Novák, 1965) using olive oil as the standard. Sulfate contents were estimated by barium chloride ($BaCl_2$) method using a H_2SO_4 standard curve established in the range of 2–20 µg ml^{-1} (Dodgson and Price, 1962). The visual appearance of the purified EPS was evaluated via scanning electron microscopy (SEM). The surface morphology of EPSs was visualized by using SEM (JEOL make JSM6360, UK) with an accelerating voltage of 20 kV (Kavita et al., 2013). Functional groups of crude and purified EPS were determined via Fourier Transformed-Infrared (FT-IR) spectroscopy. The pellets were prepared by grinding 2 mg of EPS with 200 mg of dry potassium bromide (KBr) and the mixture was pressed into a mold of 16 mm diameter. The FT-IR spectra were acquired in the 4,000–400 cm^{-1} region with a resolution of 4 cm^{-1} using an IR- Prestige-21 system (Shimatzu, Japan) (Sardari et al., 2017). Elemental analyses of purified and crude EPS were done using Energy-Dispersive X-ray (EDX) spectroscopy. 5 mg of EPS was attached on a stub and analyzed by SEM-EDX (JEOL make JSM6360, UK). The X-rays emitted by the EPS revealed the weight and atomic percentage of the different elements, which were present in the sample. X-ray diffraction (XRD) analysis was carried out to determine the biophysical properties of the EPS using X-ray diffractometer (RIGAKU make ULTIMA-III, Tokyo, Japan) with Cu target slit (10 mm). The dried EPS sample was examined in powdered form under different operating ranges of 2θ angles between 2 and 80° at a scanning speed of 2° min^{-1} using Cu Kα radiation (λ = 1.54056 Å). The intensity peaks of diffracted X-rays were recorded continuously and the d-spacings corresponding to diffracted X-rays at that value of "θ" were calculated using Bragg's law($D = \lambda \div 2\ Sin\theta$ where "θ" is half of the scattering angle measured from the incident beam) (Ricou et al., 2005).

Functional Characterization of the Exopolysaccharide

Purified Exo1 was examined for *in vivo* and *in vitro* As and salt sequestration/biosorption. Determination of *in vivo* bioadsorption of As by Exo1 was done using both concentration-dependent and time-dependent assays. *Halomonas* sp. Exo1 was cultured in 250 ml liquid 8% TSMGM containing either 0, 2, 4, 6 mM As for 3 days (concentration-dependent) or 2 mM As for 3, 6, 9, and 12 days (time-dependent) at 30 ± 2°C under constant agitation. At each time-point, cell-secreted EPS was extracted from each 100 ml cell-free extract (0, 2, 4, 6 mM As) as described earlier. 0.5 g of oven-dried bacterial EPS was transferred to a 100 ml beaker containing 10 ml of deionized H_2O and 5 ml of concentrated HNO_3 (Merck), and digested overnight at 65–75°C followed by filtration using a Whatman filter paper (125 mm) in a volumetric flask. Acid digested EPS from 3-day (As-minus) time-point was used as a negative control for both concentration-dependent and time-dependent assays. Detection of EPS-bound As was carried out using AAS (novAA 350, Analytik Jena) as per standard protocol stated in APHA (2012). On the other hand, *in vitro* bioadsorption of [As(III)] and [As(V)] or metal binding by purified Exo1 was determined by methods of Bhaskar and Bhosle (2006) with modifications. Briefly, bacterial EPS was extracted from liquid 8% TSMGM in the absence of As and 1 g dried EPS was dissolved in 10 ml Milli-Q H_2O and 2 ml of this EPS solution was taken in a dialysis bag (12–14 kDa MW cut-off, HiMedia Laboratories Pvt. Ltd., India). The dialysis bag containing 0.1 g ml^{-1} bacterial EPS was suspended in an acid-washed polyvinyl chloride (PVC) beaker containing either 4 mM [As(III)] or 10 mM [As(V)] solution with a stir bar. The PVC beaker containing the desired metal solution and the EPS-filled dialysis bag was then placed on a magnetic stirrer overnight at 28 ± 2°C. The dialysis was repeated thrice with Milli-Q H_2O to remove any traces of weakly bound As metal ions from EPS. The metal complexed EPS solution from the dialysis bag was then transferred to clean microfuge tubes and stored at −20°C prior to AAS analysis. For blank preparation, the bacterial EPS was substituted with equal volume of Milli-Q H_2O and incubated

under similar conditions. Similarly, bacterial EPS without As treatment was used as control. For determination of *in vitro* salt sequestration by purified Exo1, flame-photometry was used. In brief, bacterial EPS was extracted from liquid 8% TSMGM and 1 g dried EPS was dissolved in 4 ml Milli-Q H_2O. The EPS solution was then transferred to a dialysis bag of 12–14 kDa MW cut-off. The dialysis bag containing 0.25 g ml^{-1} bacterial EPS was suspended in an acid-cleaned PVC beaker containing 80 ml of 5, 15, or 20% (w/v) NaCl solution with a stir bar. The PVC beakers containing the desired salt solution and the EPS-filled dialysis bag were then placed on a magnetic stirrer overnight at 28 ± 2°C. The dialysis was repeated thrice with equal proportion of Milli-Q H_2O to remove any traces of weakly bound Na^+ ions from the EPS and the electrical conductivity of the H_2O was routinely monitored after completion of every dialysis. The solution containing Na^+-EPS complex was then dried at 60°C prior to analysis. The amount of EPS-bound Na^+ ions were analyzed via flame-photometry (Aimil Ltd., India) as mentioned earlier. For blank preparation, the bacterial EPS was replaced with equal proportion of Milli-Q H_2O and incubated under similar conditions whereas bacterial EPS without salt treatment was incubated in Milli-Q H_2O and used as control. Finally, the concentration of Na^+ ion was calculated from the standard curve generated using known concentrations of Na^+ solution. For detection and measurement of antioxidant activity, ascorbic acid of various concentrations (1–10 mg ml^{-1}) was prepared from a standard stock solution of 100 mg ml^{-1} in deionized water. Solutions of purified EPS (10 mg ml^{-1}) were also prepared in deionized water. 0.05 mM of DPPH (M.W. = 394.32 g) was prepared in absolute ethanol. For preparation of standard curve, 1 ml of each ascorbic acid solution (1, 2, 4, 6, 8, 10 mg ml^{-1}) was mixed with 2 ml of ethanolic DPPH (0.05 mM) and kept in dark for 30 min. Similarly, 1 ml of each EPS solution was mixed with 2 ml of ethanolic DPPH (0.05 mM) and kept in dark for 30 min. The absorbance was measured at 517 nm using deionized water as blank and DPPH. Absolute ethanol was used as reference. The % scavenging of DPPH was calculated using the following equation:

$$\% \text{ Scavenging} = (A_{\text{blank}} - A_{\text{sample}}/A_{\text{blank}}) \times 100 \quad (1)$$

Qualitative and Quantitative Estimation of Plant Growth-Promoting Metabolites Under Salt and Arsenic Stresses

Plant growth-promoting properties like phosphate solubilization, production of IAA, siderophore, ammonia, HCN, biocontrol, and nitrogen fixing abilities of the strain were investigated under normal condition and salt and As stress conditions.

Estimation of Inorganic Phosphate Solubilization and Organic Acid Production

The phosphate solubilization activity was determined by the protocol of Mehta and Nautiyal (2001) with modifications. Briefly, the isolate was grown in NBRIP medium (in absence and presence of NaCl and/or As) containing a pH indicator (Bromophenol Blue) for 10 days at 30 ± 2°C with continuous agitation. At 10th day, the final OD_{600} value was subtracted from the initial A_{600} value (0th day). Phosphate solubilization efficiency was determined by spot inoculating 3 μl of each isolate on Pikovskaya's (PVK) agar plate. Phosphate solubilization index (PSI) was calculated (diameter of phosphate solubilization (PS) zone on PVK agar/ growth diameter of spot inoculant) after 12 days of incubation at 30 ± 2°C. Finally, the kinetics of $Ca_3(PO_4)_2$ solubilization mediated by each of the isolates were monitored in liquid NBRIP medium at five time-points (0, 4, 8, 12, and 16 days). Soluble Pi concentration in the medium was estimated spectrophotometrically by using the molybdenum blue method (Mukherjee et al., 2017) and the decrease in pH values over time (because of organic acid production) was also recorded.

Estimation of Indole-3-Acetic Acid (IAA) Production

Spectrophotometric estimation of IAA was conducted as per the method of Goswami et al. (2015). An aliquot (2 ml) of 3 to 8-day old culture supernatant grown in LB broth and 8% TSMGM supplemented with 500 mg l^{-1} of L-tryptophan (in absence or presence of As i.e., 0, 2, 4, 6 mM As) at 30 ± 2°C was transferred to a clean test tube to which 100 μl of ortho-phosphoric acid and 4 ml of Salkowski reagent (50 ml, 35% of perchloric acid ($HClO_4$), 1 ml of 0.5 M $FeCl_3$ solution) were added. The mixture was incubated at room temperature (dark) for 25 min and the intensity of pink color developed was recorded at 530 nm. A standard curve of IAA (10–100 μg ml^{-1}) was used for estimation of IAA produced.

Estimation of Siderophore Production

For the six isolates, production of siderophore was initially assessed using Chromazurol S (CAS, Loba Chemie) agar medium as described by Schwyn and Neilands (1987). Test cultures were spot inoculated (3 μl) on CAS agar plates (with or without 5% NaCl) and incubated at 30 ± 2°C. An orange halo zone around the growth confirms positive siderophore production, the diameter of which was measured after 24, 48, and 72 h. Amount of siderophore produced was further quantified using CAS-shuttle assay (Payne, 1994). Bacterial cultures were grown in King's B media in presence and absence of NaCl and [As(III)]. Samples were withdrawn and centrifuged at 10,000 rpm for 5 min. CAS assay solution was added to culture supernatant in equal proportion, mixed and allowed to stand for 20 min. Siderophore, if present, removes the iron from the dye complex, causing reduction in the intensity of blue color, which was recorded at 630 nm. For the measurements, minimal medium was used as blank and % siderophore units were calculated by the following equation:

$$[(Ar - As)/Ar] \times 100 = \% \text{ siderophore units} \quad (2)$$

where Ar = absorbance of reference (minimal media + CAS assay solution), As = absorbance of sample.

Estimation of Ammonia (NH_3) Production

Production of ammonia was determined as described in Cappuccino and Sherman (1992) with modifications. 24-h old bacterial cultures were inoculated in 10 ml peptone broth (1% NaCl) and liquid 8% TSMGM (without yeast extract)

supplemented with peptone and As (2, 4, 6 mM), and incubated at 30 ± 2°C for 4–12 days with constant shaking. After incubation, 2 ml of bacterial culture was taken in an eppendorf tube and centrifuged at 10,000 rpm for 5 min. Then, 40 μl of Rochelle salt (K-Na-tartrate) and 40 μl of Nessler's reagent were added in each tube containing the supernatant. The development of yellow to dark brown color indicated the production of ammonia and absorbance was measured at 425 nm. NH_3-N standard curve (in the range of 100–1,000 $\mu g\ l^{-1}$) was prepared using Nesslerization spectrophotometric method to estimate the concentrations of NH_3 produced.

Estimation of Hydrogen Cyanide (HCN) Production

For qualitative estimation of HCN production, Picrate assay as described by Castric (1975) was followed. The isolate was streaked on LB agar and incubated overnight. A Whatman filter paper No. 1 soaked in solution of 2% Na_2CO_3 and 0.5% picric acid was placed in between base and lid of the culture plate. Plate was sealed with parafilm and incubated at 30 ± 2°C for 72 h. Production of HCN was indicated by color change of filter paper from yellow to orange-brown. For quantitative estimation of HCN production, 24-h old bacterial cultures were inoculated in 10 ml LB broth and liquid 8% TSMGM (with and without As) and incubated at 30 ± 2°C for 24–48 h with constant shaking. Then, 1 ml solution containing 2% Na_2CO_3 and 0.5% picric acid was added to the 2-days old culture and further incubated at 30 ± 2°C with constant shaking. Then, after every 24 h, 2 ml of bacterial culture was taken in a microfuge tube and centrifuged at 10,000 rpm for 5 min. The development of yellow to brownish red color indicated the production of HCN and the absorbance was measured at 490 nm. A broth without inoculum was used as a reference. The total cyanide (in $mg\ l^{-1}$) was estimated by using the following equation:

$$\text{Total cyanide content (in mg l}^{-1}) = 396 \times A_{490}\ \text{nm} \quad \text{(Kumar et al., 2015).} \quad (3)$$

Estimation of Nitrogen (N_2) Fixation

N_2-fixation ability was evaluated by growing isolate on N-free solid agar media without salt-supplementation like Norris Glucose N-free medium (10 g l^{-1} glucose, 1 g l^{-1} K_2PO_4, 0.2 g l^{-1} $MgSO_4.7H_2O$, 1 g l^{-1} $CaCO_3$, 5 g l^{-1} NaCl, 0.005 g l^{-1} $Na_2MoO_4.2H_2O$, 0.1 g l^{-1} $FeSO_4$, final pH-7.0 ± 0.2) and supplemented with 1.5% (w/v) agar and in semi-solid Burk's N-free medium (BHM) adjusted to the appropriate saline concentration of 7.5% (w/v) (0.64 g l^{-1} K_2HPO_4, 0.16 g l^{-1} KH_2PO_4, 58.5 g l^{-1} NaCl, 14.73 g l^{-1} $MgSO_4.7H_2O$, 0.4 g l^{-1} $CaSO_4.2H_2O$, 8 g l^{-1} glucose, 0.001 g l^{-1} $Na_2MoO_4.2H_2O$, 0.003 g l^{-1} $FeSO_4$), and supplemented with 0.2% (w/v) agarose (Argandoña et al., 2005).

Determination of Biocontrol Activities

Anti-microbial activity of the isolate was tested on Potato Dextrose Agar (PDA) using agar well diffusion method (Bauer et al., 1966). Briefly, overnight culture of *Fusarium oxysporium* was inoculated into PDA by pour-plating and the 24-h old bacterial culture was placed in the well. Same experiment was repeated using pure EPS in the wells of the plates. The plates were incubated for 48 hours and observed for the zone formation.

Germination and Growth of Salt-Tolerant Rice Seeds Treated With Whole Bacterial Cells or Purified Exopolysaccharide Under Salt and Arsenic Stresses

Seeds of moderately salt-tolerant rice variety-Jarava (IET- 15420) were obtained from Salt and Flood Resistant Paddy Research Station, Gosaba (Rice Research Station, Chinsurah, West Bengal, India). Soil for the pot assay was also obtained from paddy cultivation field of Gosaba. pH, electrical conductivity and salinity of the soil were found to be 7.2, 0.32 mS/cm and 3 PSU, respectively. Nitrogen (N), available phosphorous (P), potassium (K), total organic matter, organic carbon and total arsenic (As) contents of the soil were found to be 0.10%, 14.20 mg kg^{-1}, 2267.28 mg kg^{-1}, 1.12%, 0.85%, and 2.96 mg kg^{-1}, respectively. Rice seeds were surface sterilized by immersion into solution A (70% ethanol and 0.3% Tween 80) for 5 min, and then in solution B (3% sodium hypochlorite and 0.3% Tween 80) for 15 min and then washed thrice with sterile distilled water. For germination, rice seeds were soaked in sterile distilled water for 12 h, and then covered with a clean wet cloth for 12 h. *Halomonas* sp. Exo1 was cultivated (either alone or in consortia with other 5 *Halomonas* strains) in LB broth for 24–48 h and centrifuged. The collected bacterial cells were washed three times with deionized water and re-suspended in deionized water to obtain ∼10^8 CFU/ml (A_{600} nm = 0.5). Each petri plate containing one sheet of paper was moistened with 10 ml of deionized water. For bacterization, 2 ml of test bacterial suspension was initially applied to the rice seeds in each treatment plates and 2 ml of deionized water was added to the control plate. Germination was carried out for 15 days under artificial light for 12-h photoperiod with a light intensity of 2,100 Lux, a temperature of 28 ± 4°C, and humidity of 54 ± 8% and percentage of germination and growth parameters of germinated seedlings were measured. Post-germination plantlets were directly sown in watertight brown plastic pots (16 cm diameter × 9 cm height). The *in vivo* pot trials were carried out in triplicates under natural light with a 15-h photoperiod during the month of Nov to Feb when the average temperature and humidity were 28 ± 4°C and 50 ± 10%, respectively. Pots were filled with 1,000 g of saline treatment soil containing 1 g NaCl (EC at 2–4 dS m^{-1}), urea (90 kg N ha^{-1}), muriate of potash (11 kg K_2O ha^{-1}) and single superphosphate (40 kg P_2O_5 ha^{-1}). In addition, 20 mg of $NaAsO_2$ and 2 g of NaCl were added per 1,000 g of saline treatment soil in case of As and salt treatment pots, respectively. In each pot, 6 surface-sterilized 15-days old seedlings were uniformly transplanted at the depth of ∼2.5 cm below the soil surface and each seedling was inoculated with 5 ml test bacterial suspension or 0.2 g of pure Exo1. For negative control (plants germinated from non-coated seeds), soil was not treated with the test bacteria or bacterial EPS. Rice seedlings were harvested (uprooted) after 15 days of plantation/sowing, and vegetative parameters (root and shoot lengths, fresh and dry weights) were analyzed. Oven-dried soil and plant samples (roots and shoots) were grounded to powder, acid digested, and [As(III)] contents were analyzed by AAS (NovAA 350, Germany). Bioaccumulation Factor and Translocation Factor of [As(III)] and germination

index were calculated by the following equations:

$$\text{Bioaccumulation Factor (BAF)} = C_{root[As(III)]}/C_{soil[As(III)]} \quad (4)$$

$$\text{Translocation Factor (TF)} = C_{shoot[As(III)]}/C_{root[As(III)]} \quad (5)$$

$$\text{Germination Index (GI)} = \left(\text{Number of seeds germinated/total number of seeds}\right) \times 100 \quad (6)$$

Total Kjeldahl Nitrogen (TKN) and phosphate (PO_4^{3-}) contents in acid-digested roots, shoots and pot soil from each treatment conditions were analyzed using methods described in APHA (2012).

Statistical Analysis

Statistical significance was analyzed with respect to control in all the cases and performed using One-Way ANOVA. "a," "b," and "c" mean that the result is significant at $p < 0.01$, $p < 0.05$, and $p < 0.1$, respectively, and $p > 0.1$ has been considered less or insignificant and is denoted as "d" in the figures. All statistical analyses were done using SPSS 12.0 for Windows (SPSS Inc., USA). Plant growth-promoting activities were performed in a completely randomized block design. Each experiment was repeated three times. The differences among the mean values were determined using Duncan's Multiple Range Tests (DMRTs) at $P < 0.05$. The results have been graphically presented using GraphPad Prism Software 7 for Mac OS (San Diego, California, USA) while Statistic Analysis System (SAS 9.1) was used for DMRT analysis.

Nucleotide Sequence Accession Numbers

The accession numbers of the 16S gene sequences of the isolates *Halomonas* sp. Exo1, *Halomonas* sp. Exo2, *Halomonas* sp. Exo6, *Halomonas* sp. Exo7, *Halomonas* sp. Exo8, and *Halomonas* sp. Exo9 obtained from GenBank were KT238978.1, KT238979.1, KT238983.1, KT238984.1, KX026971.1, and KX026972.1 respectively.

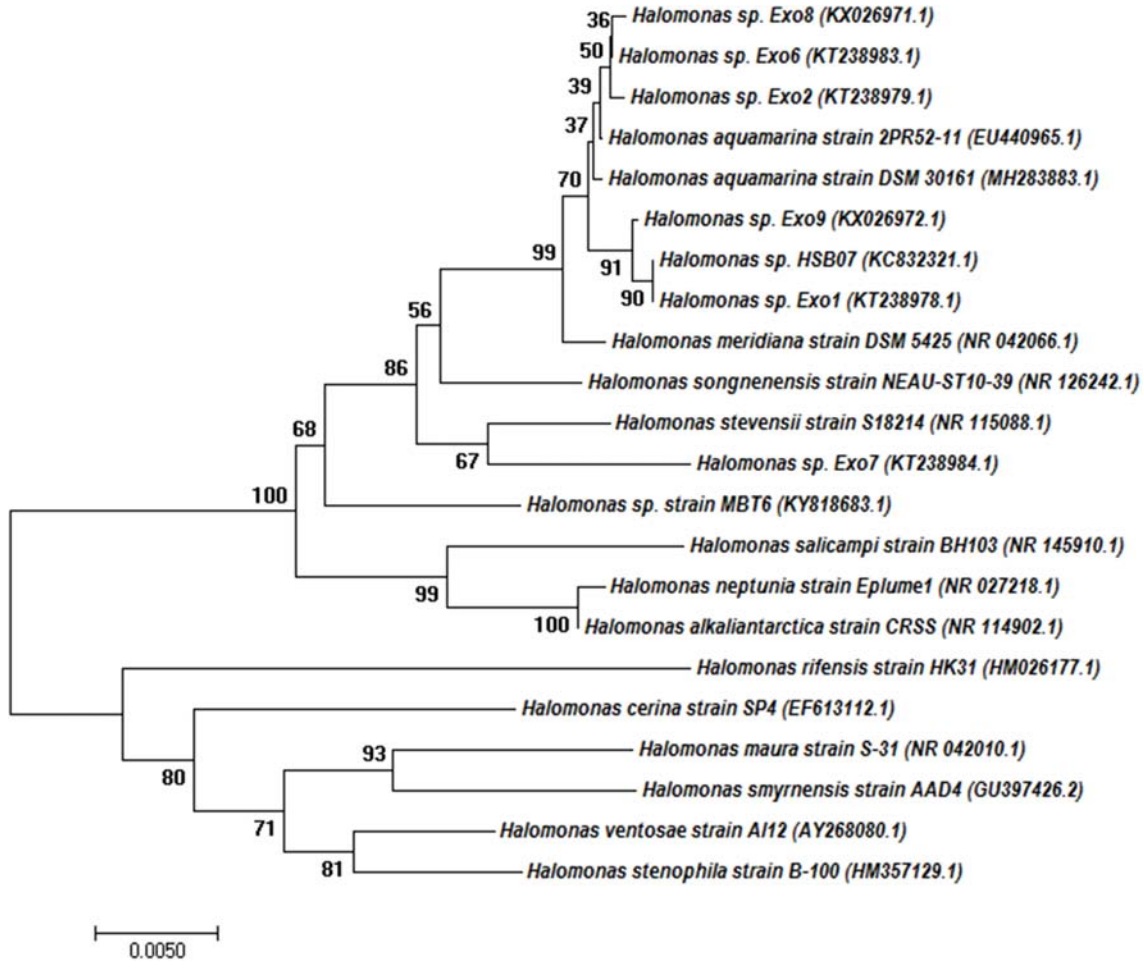

FIGURE 1 | Phylogenetic tree based on 16S rRNA gene sequences obtained by the neighbor-joining (NJ) method showing the phylogenetic relationship of the *Halomonas* sp. Exo1 with the related species. The percentage of replicate trees in which the associated taxa clustered together in the bootstrap test (1,000 replicates) is shown next to the branches. Branches corresponding to partitions reproduced in <50% bootstrap replicates are collapsed. Accession numbers are written after the species or strain names.

RESULTS

Physico-Chemical Analysis of *Avicennia marina* Rhizosphere Soil

The rhizosphere soil was found to contain 1.427% of NaCl and 1.96 ppm of As. The detailed physico-chemical properties of the soil sample (pH 7.0) are listed in the **Supplementary Table S1**.

Isolation and Identification of Exopolysaccharide Producing Halo-Rhizobacteria

Out of the 14 plant growth-promoting halo-rhizobacterial strains growing in 4 mM [As(III)] supplemented 8% TSMGM, six strains were initially selected due to their production of EPS. 16S rDNA sequence analysis showed all the six strains belong to the members of the genus *Halomonas*. **Figure 1** shows the evolutionary relationship of the *Halomonas* isolates among themselves and with other EPS producing or non-EPS producing *Halomonas* strains.

Phylogenetic analysis demonstrated that *Halomonas* sp. Exo1 is more closely related to *Halomonas* sp. Exo9 than *Halomonas* sp. Exo2, *Halomonas* sp. Exo6, *Halomonas* sp. Exo8 and *Halomonas* sp. Exo7. *Halomonas* sp. strain Exo1 showed 100% identity to non-EPS producing *Halomonas* sp. HSB07 (KC832321.1) (Liu et al., 2013) but only 94% similarity with EPS producing strain *Halomonas ventosae* Al12 (Martínez-Cánovas et al., 2004) and 93% identity to three strains: mauran (EPS) producing *Halomonas maura* strain S-31 (NR_042010.1) (Bouchotroch et al., 2001), *Halomonas rifensis* strain HK31(Amjres et al., 2011) and *Halomonas smyrnensis* strain AAD4 (Poli et al., 2013).

All the 6 *Halomonas* strains produced water-soluble EPS of varying amounts (15.8–27.9 mg ml^{-1}) in 8% TSMGM (**Figure 2**). Among them, *Halomonas* sp. strain Exo1 was selected for further study based on its highest yield of EPS production.

Figure 3 shows Field Emission Scanning Electron Microscopy (FESEM) images of the topography of EPS coated cell of *Halomonas* sp. Exo1 in which a single short rod-shaped cell with polymer-like substances forming a thin matrix over the cell surface was seen (**Figure 3A**). In addition, closer microscopic observation revealed the presence of numerous irregular crystal-like structures probably of cell-bound EPSs on the cell surface (**Figures 3B,C**). Instead of SEM, FESEM was selected as this technique provides a clearer, less electro statically distorted image with nanometer level spatial resolution that is three to six times better than SEM and allows measurements of fine structural and micromechanical properties of sample. Further it minimizes sample charge up and damage as it is operated at lower electron-accelerating voltages, and gives better images of immediate biological surfaces due to a reduction in electron penetration.

Characterization of the Plant Growth-Promoting Rhizomicrobes Toward Abiotic Stress Tolerance: Salt and Arsenic

The isolated PGPR, *Halomonas* sp. Exo1 was found to be euryhaline facultative mesohalophilic in nature and could tolerate wide range of salt concentrations (upto 20% NaCl and 24% total salt). The strain was found to accumulate fairly large amounts of osmolytes when grown in 8% TSMGM. The order of accumulation of osmolytes in 8% TSMGM grown cells of *Halomonas* sp. Exo1 were in the following order: Na^+ (42,839 mg kg^{-1} dry weight) > Mg^{2+} (29,288.1 mg kg^{-1} dry weight) > K^+ (13,601.7 mg kg^{-1} dry weight) > Ca^{2+} (1,847.46 mg kg^{-1} dry weight). On the other hand, in the LB broth grown control cells, Na^+ accumulation was 6,310 mg kg^{-1} dry weight while that of K^+, Mg^{2+}, and Ca^{2+} were found to be below detectable limits (**Supplementary Figure S1**). In the 8% TSMGM medium, amount of Na, Mg, K, and Ca cations were 6.4, 1.733, 0.187, and 0.013% respectively. Although presence of organic osmolytes or exact mechanism of osmoregulation in *Halomonas* sp. Exo1 was not investigated but higher intracellular concentration of Na^+ than K^+ ions indicates that it is following the same haloadaptation mode as most other moderate halophiles displaying "low salt in" strategy (Oren, 2008). Although the strain could tolerate up to 8 mM [As(III)], increasing concentration of As lowered growth rate and salt tolerance. **Supplementary Figure S2** shows growth profiles of *Halomonas* sp. Exo1 in presence of the abiotic stresses and MIC values toward salt and As tolerances. The As tolerance ability of *Halomonas* sp. Exo1 is believed to be partly due to detoxification ability to oxidize more toxic form of [As(III)] to less toxic form of [As(V)] as observed biochemically (**Supplementary Figure S3**) and partly due to bioaccumulative ability of [As(III)] as evidenced by AAS study of the acid digested cell biomass grown in

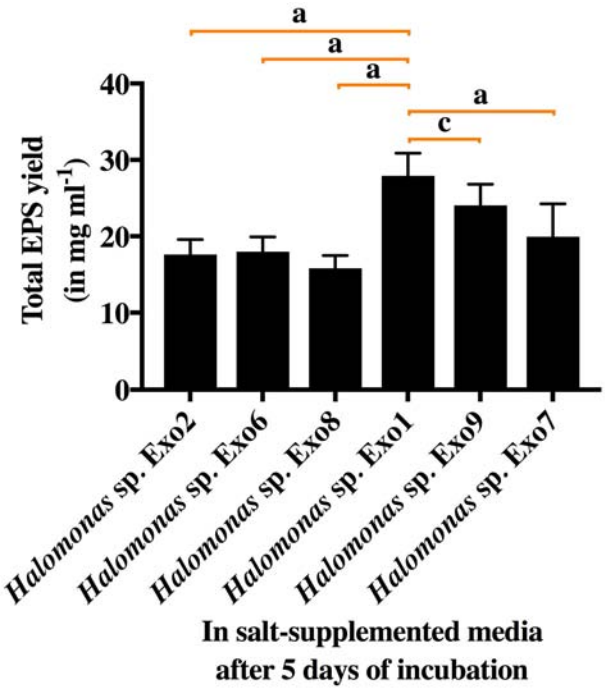

FIGURE 2 | Total EPS yield from 6 selected *Halomonas* strains in salt-supplemented medium (8% TSMGM) after 5 days of incubation. Vertical bars represent mean ± standard deviation of triplicate measurements. Statistical significance of EPS yield from *Halomonas* sp. Exo1 was measured separately with each of the 5 isolates and shown accordingly.

As supplemented medium (**Figure 4**). In *Halomonas* sp. Exo1, maximum amount of As bioaccumulation occurred during early to late log phase of growth where 252.4 mg l^{-1} As was detected in the cell-free medium on day 0 in which 2 mM [As(III)] was originally added. Highest accumulation of As (1527 mg kg^{-1} dry weight) was found in the pellet on day 3 after which it started to decline. Arsenic level in the media started to increase and reached a steady state during late stationary to death phase. Bacterial culture grown in 8% TSMGM for three generations in the absence of As showed only trace amount of As in the 3-days old cell-pellet (0.83 mg kg^{-1} dry weight) and served as negative control. The whole experiment was conducted in the presence of salt which was found to enhance HM tolerance. It has been hypothesized that the decrease in As level within cell-pellets could be owing to cell autolysis during death phase resulting in the release of As back into the growth medium.

To further proof biomass mediated physical adsorption of As, in addition to live cells, dead bacterial biomass mediated [As(III)] biosorption was quantified. The dead cell-biomass of *Halomonas* sp. Exo1 induced 20.91% depletion of the initial 4 mM sodium arsenite and the As content of the cell-free extract post incubation was 45.38% (considering the initial metal concentration of the metal solution to be 100% prior to incubation with dead bacterial cell). The loosely bound As (adhering to the dead cell surface) must have been removed during the washing steps. The mass of [As(III)] bioadsorped was 43 mg kg^{-1} (dry weight) of dead cell-biomass. The percentages of As in the supernatants and the bacterial pellets may not have reached 100%. Some As may be lost during multiple washing of the cells with deionized water. The washing may have caused release of some cell-bound EPS (with bound As) into the washed-out fraction. This washed-out fraction would not be present in the supernatant, as the supernatant was filtered prior to quantification in order to suppress the potential contribution of the secreted bacterial EPS to As adsorption. In addition to As, stress responses of *Halomonas* sp. Exo1 toward 10 other heavy metals in LB and

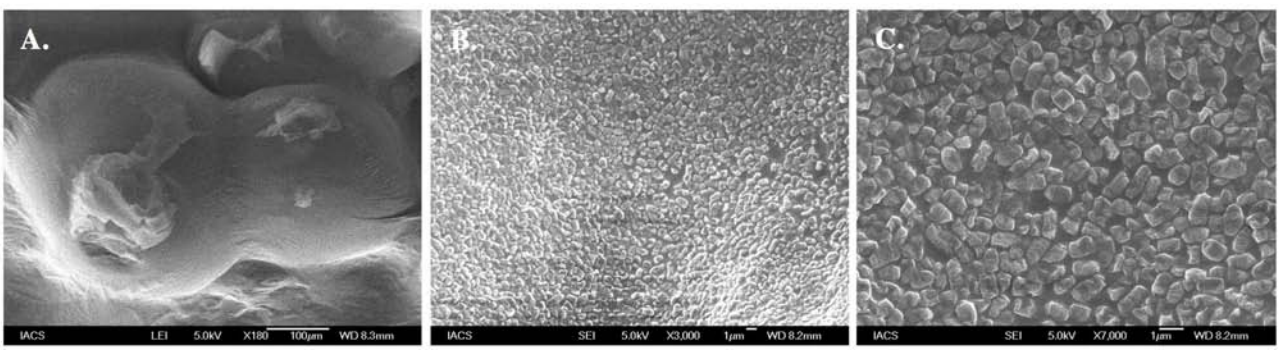

FIGURE 3 | Morphological analysis of EPS producing *Halomonas* sp. Exo1. Field Emission Scanning Electron Micrograph (FESEM) images of *Halomonas* sp. Exo1 displaying loosely attached polymeric substances on its cell surface **(A)** with zoomed in images of numerous crystal like structures of cell-bound EPS on the bacterial cell surface **(B,C)**.

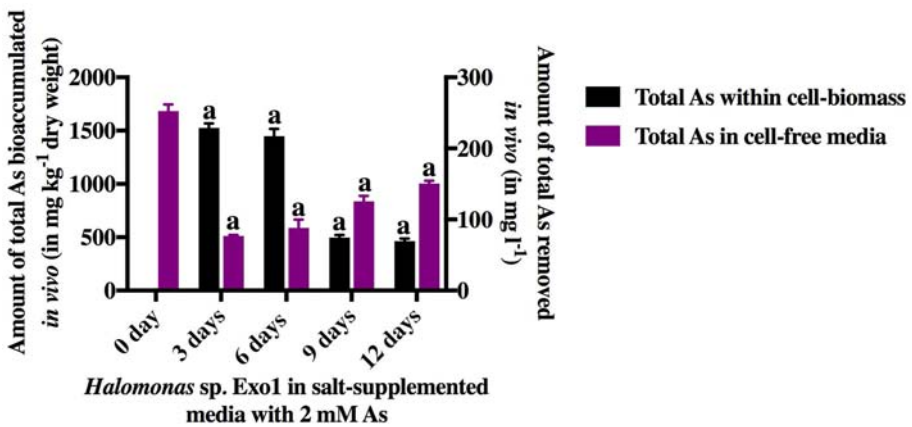

FIGURE 4 | *In vivo* time-dependent arsenic bioaccumulation by live cells. The amount of total [As(III)] in ambient media and total [As(III)] bioaccumulated within cell-biomass of *Halomonas* sp. Exo1 are represented as mg l^{-1} and mg kg^{-1} (dry weight), respectively. Vertical bars represent mean ± standard deviation of triplicate measurements values. 252.42 mg l^{-1} As was detected in 0-day cell-free 8% TSMGM containing 2 mM [As(III)] (positive control for As in ambient media). 0.83 mg kg^{-1} (dry weight) trace As was detected in 3-day cell-pellet grown in 8% TSMGM without As (negative control for As bioaccumulation).

salt media were also studied. The MIC values of the strain in 8% TSMGM were 8 mM for [As(III)], 140 mM for [As(V)], 15 mM for [Cr(III)], 2 mM for [Cr(VI)], 1 mM for [Co(II)], 0.4 mM for [Pb(II)], 1 mM for [Cu(II)], 0.4 mM for [Zn], 500 mM for [Mo], 90 mM for [Mn], 2.0 mM for [Ni(II)], and 0.5 mM for [Cd]. In the absence of salt (i.e., in LB media), the MIC values were 1 mM for [As(III)], 150 mM for [As(V)], 8 mM for [Cr(III)], 1 mM for [Cr(VI)], 1 mM for [Co(II)], 0.5 mM for [Pb(II)], 1.5 mM for [Cu(II)], 2 mM for [Zn], 550 mM for [Mo], 20 mM for [Mn], 2.5 mM for [Ni(II)], and 0.2 mM for [Cd]. So, for certain metals like [As(III)], Cr, Cd, and Mn, MIC values dropped in the absence of salt. This indicated the role of salt in increasing resistivity toward these metals in *Halomonas* sp. strain Exo1. In later studies, it was found that EPS secreted by the strain in presence of salt was responsible for their increased tolerance toward selected HMs. This result is significant as this is the first report, which shows that salt can play a role in increasing metal tolerance of selected HMs.

Exopolysaccharide Production Under Salt and Arsenic Stresses

Effects of increasing concentration of salt and As on EPS yield in *Halomonas* sp. strain Exo1 is shown in **Supplementary Figure S4**. It may be mentioned here that in the absence of salt or with 0.5% NaCl supplementation in LB broth, detectable EPS production was not noticed in *Halomonas* sp. Exo1. Interestingly, EPS production was detected when LB broth was amended with 1% NaCl. EPS production increased with increase in NaCl concentration up to 20%, where maximum EPS yield was observed. A sudden sharp fall in EPS production was noticed when NaCl concentration was increased to 22.5%. It is believed that a breakdown of osmo-tolerance caused growth inhibition and decrease in EPS production. Effect of As stress on the production of EPS (both cell-free and cell-bound) in 8% TSMGM was depicted in *Halomonas* sp. Exo1 (**Supplementary Figure S4B**). It was found that EPS yield increased with increasing [As(III)] concentration up to 6 mM. However, 8 mM [As(III)] caused significant decrease in EPS yield. Amount of cell-bound EPS was negligible in comparison to cell-free EPS both in absence and presence of different concentrations of [As(III)], suggesting that majority of the EPS produced in *Halomonas* sp. Exo1 was secreted in the surrounding medium. Time-dependent study in 8% TSMGM containing 2 mM As showed that total EPS yield increased with days elapsed and maximum yield was observed during late stationary phase of bacterial growth.

Biophysical Characterization of the Exopolysaccharide

The secreted EPS was found to be soluble in water. The salinity and electrical conductivity of the crude EPS prepared in deionized H_2O (20 mg ml^{-1}) prior to desalting was 17 PSU and 25 $\pm$ 0.2 mS/cm, respectively. With an increase in As stress (6 mM) under saline condition, the salinity and electrical conductivity of crude Exo1 became18 PSU and 26.4 $\pm$ 0.5mS/cm. After desalting, the extracted EPS showed salinity and electrical conductivity of 0.5 PSU and 0.083 mS/cm, respectively. This observation suggests that the cell-free EPS is capable of quenching mixed sea salts from the cultivating medium. Total neutral-carbohydrate in cell-free and cell-bound EPS were 0.58 and 20.87 $\mu g\ \mu l^{-1}$, respectively. Concentrations of proteins in cell-free and cell-bound EPS were 76.12 and 75.53 $\mu g\ \mu l^{-1}$, respectively. Lipid estimation showed 25 mg g^{-1} lipids content in total EPS while that of sulfate content was found to be 90.36 mg g^{-1}. Scanning electron micrograph revealed that the purified EPS was compact and globular in nature (**Figure 5**), which is a characteristic of plasticized films (Wang et al., 2010).

The XRD profile of EPS exhibited non-crystalline nature of the substance with major characteristic diffraction peaks at 32.1 and 45.6 Å containing inter planar spacing (d-spacing) of 2.786 and 1.988 Å respectively (**Supplementary Figure S5**). To understand the role of EPS in salt and As sequestration, pure untreated EPS and pure EPS incubated with NaCl and As were analyzed by FT-IR (**Figure 6**). The adsorption of heavy metals or inorganic osmolytes by EPS is energy independent, and could occur through interaction between metal cations and functional groups of the EPS. So, the effects of salt and As stresses the functional groups of the purified EPS were determined. The FT-IR analysis of untreated pure EPS showed a broad stretching peak at 3415.93 cm^{-1} (range 3,600–3,200 cm^{-1}), corresponding to hydroxyl group(s) (Kavita et al., 2013; Wang et al., 2015), which is generally the characteristic of a carbohydrate ring (Lim et al., 2005; Kumar et al., 2011) while a small peak at 2092.77 cm^{-1} corresponds to the presence of free carboxyl groups (Osman et al., 2012). Presence of an asymmetric medium stretching peak at 1,631 cm^{-1} may correspond to the ring stretching of mannose or galactose (Freitas et al., 2009) or to the stretch vibration of C = O bond (François et al., 2012; Zhang et al., 2017). The absorption

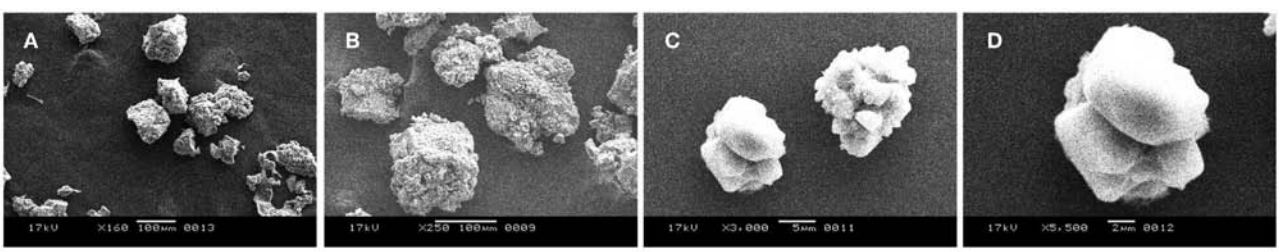

FIGURE 5 | Scanning Electron Micrograph (SEM) images of purified Exo1 showing compact globular nature **(A–D)**.

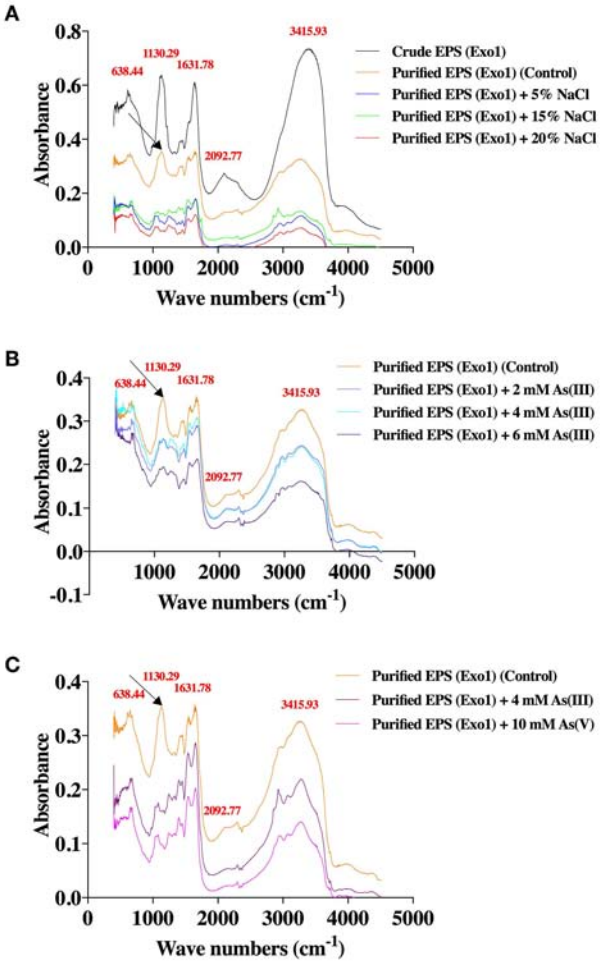

FIGURE 6 | Effects of salt and arsenic stresses on the FT-IR spectra of functional groups of purified Exo1 done in solid (KBr) phase. A. *In vitro* assay: Exo1 extracted from cells grown in 8% TSMGM media was incubated with 5, 15, and 20% NaCl. B. *In vivo* assay: Purified Exo1 was extracted from bacteria grown in 8% TSMGM containing different concentrations of [As(III)]. C. *In vitro* assay: Purified Exo1 was extracted from bacteria grown in salt-supplemented (8% TSMGM) media without As and purified EPS was incubated *in vitro* with 4 mM [As(III)] and 10 mM [As(V)]. The wave numbers of distinct peaks in cm^{-1} are shown in red with respect to crude/purified Exo1. An arrow demarcates a peak that is absent in salt-treated purified Exo1 **(A)** and in As-treated purified Exo1 in case of both *in vivo* **(B)** and *in vitro* **(C)** assays.

peaks ranging from 1,000 to 1,200cm^{-1} were designated to C-O-C and C-O (Freitas et al., 2009; Kavita et al., 2011). A peak at 1130.29 cm^{-1} (1,000–1,125 cm^{-1}) may be attributed to O-acetyl ester linkage bond of uronic acid (Bramhachari and Dubey, 2006). The absorption peak at 638 cm^{-1} (690–515 cm^{-1}) corresponds to stretching of alkyl-halides (Kavita et al., 2011). Interestingly, both salt and metal laden EPS from *in vivo* and *in vitro* studies clearly reveal the absence of the peak at 1130.29 cm^{-1} (**Figures 6A–C**). This shows significant association of acetyl group of EPS in Na^+ and As binding as has been postulated by another report where CO group was involved in divalent cation binding (Ozturk et al., 2014).

Analysis of the composition of crude EPS, purified EPS and purified EPS treated with different concentrations of salt produced by *Halomonas* sp. Exo1 by SEM-EDX revealed the presence of common elements (C, N, O) and osmolytes (Na, K, Mg, Ca), apart from chlorine, sulfur and phosphorous residues. **Supplementary Table S2** shows weight and atomic percentages of these elements. Accumulation of these osmolytes within EPS perhaps occurred during EPS production in salt-supplemented media, which contained several sea salts including NaCl, KCl, $MgCl_2$, $MgSO_4$, and $CaCl_2$. However, the weight % and atomic % of different elements between crude and purified Exo1 showed marked variations, probably owing to the removal of considerable amounts of salts and impurities like trace metals from crude EPS during desalting and purification processes. *In vitro* assays of purified EPS laden with NaCl using salt solutions with different NaCl concentrations showed an increase of Na % weight from 1.13 of control to 2.95 for 5% NaCl and to 3.19 for 15 % NaCl concentration. For atomic weight, the values were 0.67 (control), 1.78 (5% NaCl), and 1.97 (15% NaCl).

Functional Characterization of the Exopolysaccharide

Finally the role of EPS in salt and As sequestration was confirmed through *in vivo* and *in vitro* arsenic and salt bioadsorption. In the *in vivo* As bioadsorption assay, purified EPS was found to be capable of sequestering [As(III)] in a dose and time-dependent manner (**Figure 7**). Arsenic dose-dependent study showed that the amount of EPS-mediated bioadsorped [As(III)] increased ∼two-folds with every two-fold increase in [As(III)] concentration (0, 2, 4, 6 mM) and as such showed a linear correlation (**Figure 7A**). It has been observed that 5-day EPS from 8% TSMGM without As (negative control) contained only 0.86 mg kg^{-1} (dry weight) [As(III)]. Moreover, the results from time-dependent study showed a decrease in [As(III)] bioadsorption with increase in time, and after a period of 9 to 12 days it reached a level of saturation. The amount of [As(III)] bioadsorped by bacterial EPS from its ambient medium with time is shown in **Figure 7B**. A trace amount [2.46 mg kg^{-1} (dry weight)] of [As(III)] was detected in 3-day EPS from 8% TSMGM without As (negative control). In the *in vitro* EPS-mediated As bioadsorption assay, purified EPS was found to be capable of sequestering both the species of As [As(III) and As(V)]. On the other hand, only trace amounts of [As(III)] (2.86 mg kg^{-1} dry weight) and [As(V)] (1.46 mg kg^{-1}dry weight) were detected in controls. Although, sequestration of [As(III)] from 4 mM $NaAsO_2$ solution was higher (593.81 mg kg^{-1} dry weight) than [As(V)] sequestered from 10 mM Na_3AsO_4 solution (289.07 mg kg^{-1} dry weight), however, the values were not statistically significant (**Figure 7C**).

Like As, *in vitro* EPS-mediated salt (Na^+) sequestration assay showed that the purified EPS from *Halomonas* sp. Exo1 can sequester Na^+ ions from salt solutions with different NaCl concentrations (5, 15, and 20%). The amount of EPS-bound Na^+ was found to increase with increase in NaCl concentration in the solution (28,390 mg kg^{-1} dry weight for 5% NaCl and 37,500 mg kg^{-1} dry weight for 15% NaCl), and reached a saturation level

(36,000 mg kg^{-1} dry weight) at 20% NaCl. Although, the control (EPS without salt treatment) showed some amount of ionic Na^+ (1,910 mg kg^{-1} dry weight) probably owing to residual indigenous Na^+ that remained bound with the EPS molecules during EPS production in salt media, however, this amount was significantly less compared to the EPS-bound Na^+ obtained under the salt-treated conditions (**Figure 8**).

Antioxidant ability of the pure EPS was also calculated and the percentage DPPH-free radical scavenging activity for cell-free and cell-bound EPS was found to be 33.75 and 34.03%, respectively (**Supplementary Figure S6**).

Estimation of Essential Plant Growth-Promoting Properties Under Salt and Arsenic Stresses

Halomonas sp. Exo1 was positive for phosphate solubilization (phosphate solubilization index 2), IAA, siderophore, NH_3 and HCN production and showed biocontrol activity against one phytopathogenic fungus *Fusarium oxysporium*. Although the isolate showed N_2-fixing abilities as determined by growth in N-deficient media, however, the presence of *nifH* genes could not be established by PCR-based method. All plant growth-promoting properties except N_2 fixation and biocontrol activity were analyzed under two types of abiotic stresses: salt and As. **Supplementary Figure S7** shows images of the results obtained from biochemical assays on various PGP traits. **Supplementary Figure S8** shows the effect of salt and As on PGP properties of the strain. OD shift assay in salt-free and salt-supplemented NBRIP-BPB media (NBRIP with bromophenol blue) showed that salt had positive impact on phosphate solubilization but As exhibited negative impact (**Supplmentary Figure S9**). Strain Exo1 showed maximum Pi solubilization of 286.44 μg ml^{-1} and the final media pH dropped to pH 5.36 after 8 days of growth indicating organic acid production. Similar to Pi solubilization, IAA production was more in salt-supplemented media (8% TSMGM) than in salt-deficient media. However, in salt-supplemented media under [As(III)] stress (2, 4, and 6 mM), production of IAA decreased with increase in As concentration suggesting that As stress was inhibitory to IAA production. Ammonia and HCN production were decreased under both salt and As stress conditions. So, IAA, ammonia and HCN production can be ruled out to promote enhanced plant growth under combined pressure of salt and arsenic. In salt-supplemented media, although siderophore production was initially less compared to salt-deficient media but gradually increased over time and finally became comparable after 72 h of growth. Interestingly, siderophore production was enhanced in presence of [As(III)] stress (2, 4 and 6 mM) in salt-supplemented media.

Effects of Salt and Arsenic on Rice Growth Promotion by *Halomonas* Strains and Their Secreted Exopolysaccharide

Laboratory-scale plate and pot-based bioassays were conducted for germination and growth of moderately salt-tolerant rice variety (Jarava) with *Halomonas* sp. Exo1 and purified EPS. The salt-tolerant rice seeds showed good germination in distilled water (control). Seed germination stopped completely in the presence of NaCl (data not shown). As freshwater germination is must for Jarava variety, no germination was observed when seeds were incubated with bacteria grown in presence of salt. After 15 days of bacterization, the isolate either alone or in consortia showed little effect on germination percentage. In presence of Exo1 and bacterial consortia, the germination indices were calculated to be 83 and 82%, respectively whereas the control plates containing only water-germinated seedlings showed 80% germination. Similar results were observed when average lengths and average (fresh and dry) weights of roots and shoots of germinated seedlings (bacteria-treated) were measured and compared with the untreated control (**Figures 9A,B**). This is perhaps due to the fact that in presence of the microbes, the germination of few rice seeds was enhanced while others either remained unaltered or exhibited poor germination. Addition of 2 mM [As(III)] caused 0% germination in the control and 20% in the test plates. This slight increase in germination in the presence of As in the Exo1 treated test plates may be attributed to the microbes. The growth performances of the plants in pots (root and shoot lengths, fresh and dry weights of roots and shoots) were highest in the consortia treatment followed by *Halomonas* sp. Exo1 and lowest in untreated control. However, increase in NaCl stress (twice with respect to control) in bacteria-treated pots resulted in slight decrease in the overall growth performances, which were observed in normal unstressed plants (**Figures 9C,D**). Uninoculated plants showed no extra growth under this NaCl stress. Interestingly, when pot soil was amended with EPS instead of microbe, growth performance parameters of the plantlets were significantly increased as compared to the H_2O-treated control soil. Furthermore, N_2 and PO_4^{3-} contents in the roots and shoots were found to be higher in treated plants (bacteria-inoculated plants and plants grown in pots containing EPS) than in control (**Figures 9E,F**). The amounts of N_2 and PO_4^{3-} in the pot soil for all treatment conditions were also comparable. Increased PO_4^{3-} content is probably the result of the Pi solubilization ability of the PGPR isolates that may have released soluble P from the native inorganic phosphate present in the pot soil. However, the cause of increased N_2 uptake is not clear. This may be either due to direct N_2-fixation ability of the strains, which could not be fully confirmed in this study or N_2 uptake-promoting ability of the phosphate solubilizing bacteria (PSBs). **Supplementary Figure S10** shows images of rice growth promotion assay. Again, it was observed that all control plants that germinated normally died within 24 h in the pots amended with 20 mg kg^{-1} [As(III)]. But bacteria-treated and/or EPS-treated plants survived for 5 more days with poor growth performances, suggesting prominent metal toxicity (**Figures 9C,D**). Additionally, in order to confirm As toxicity the roots and shoots were separately processed for estimation of [As(III)] concentrations. Maximum accumulation of As was noticed in shoots (15 ± 0.42 mg kg^{-1}) while roots showed little accumulation (1.1 ± 0.23 mg kg^{-1}). Translocation Factor (TF) and Bioaccumulation Factor (BAF) were calculated to be 13.64 and 0.06, respectively. Finally, As bioremediation potential of *Halomonas* strains and purified Exo1 was further analyzed

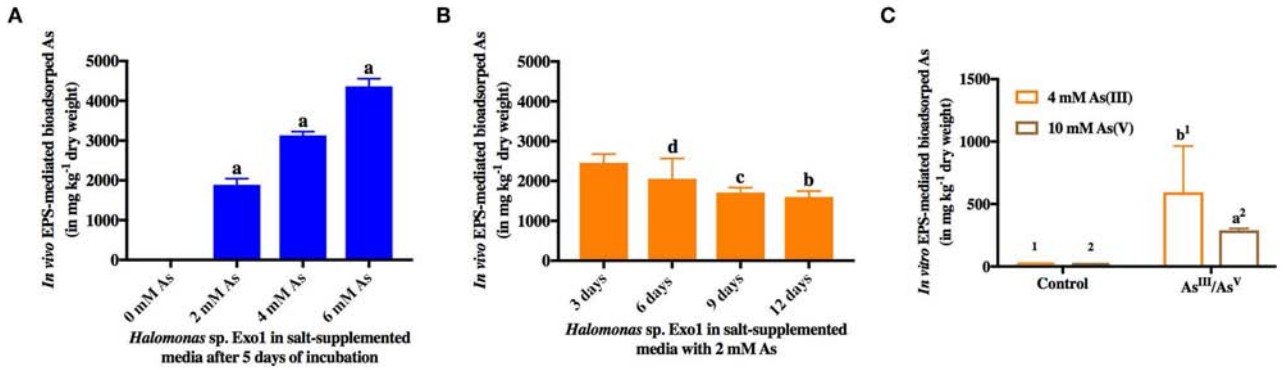

FIGURE 7 | *In vivo* and *in vitro* EPS-mediated bioadsorption of arsenic. *In vivo* dose-dependent (0, 2, 4, 6 mM) **(A)** and time-dependent (3, 6, 9, 12 days) **(B)** arsenic sequestration from ambient salt media by EPS from *Halomonas* sp. Exo1. 0.86 mg kg^{-1} (dry weight) [As(III)] was detected in 5-day EPS from 8% TSMGM without As while 2.46 mg kg^{-1} (dry weight) trace [As(III)] was detected in 3-day EPS from 8% TSMGM without As (negative control) **(C)** *In vitro* bioadsorption of arsenic by Exo1. The amounts of bioadsorped [As(III)] and [As(V)] in mg kg^{-1} dry weight of purified EPS incubated overnight at 4°C in solutions containing 4 mM [As(III)] and 10 mM [As(V)], respectively. Exo1 without [As(III)]/[As(V)] treatment was used as control. Error bars represent mean ± standard deviation of triplicate values.

directly under salt stress. [As(III)] was also estimated from roots and shoots of rice seedlings grown in normal pot soil containing indigenous As (2.96 mg kg^{-1} dry weight) derived from the environment. In control plants, roots and shoots contained 1.89 and 2 mg kg^{-1} of As, respectively and the TF and BAF were 1.06 and 0.64, respectively. 3.89 and 8.04 mg kg^{-1} of As were observed in the roots of plants treated with *Halomonas* sp. Exo1 and bacterial consortia, respectively. Shoots of plants treated with *Halomonas* sp. Exo1 and bacterial consortia contained 2.6 and 3.61 mg kg^{-1} of As, respectively. For plants treated with *Halomonas* sp. Exo1, the TF and BAF were 0.67 and 1.31, respectively. For plants treated with bacterial consortia, the TF and BAF were 0.45 and 2.72, respectively. Interestingly, for purified EPS-treated plants, the TF and BAF were 0.23 and 1.43, respectively.

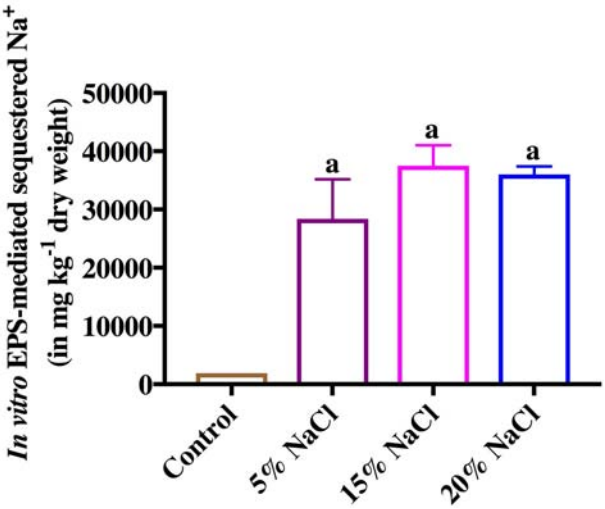

FIGURE 8 | *In vitro* Exo1 mediated Na^+ sequestration. Bars show the amounts of bioadsorped Na^+ in mg kg^{-1} dry weight of purified EPS, which was incubated overnight at 4°C in solutions containing 5, 15 and 20% NaCl (w/v). EPS without salt treatment (0% NaCl) was used as control. Error bars represent mean ± standard deviation of triplicate values.

DISCUSSION

Extracellular polymeric substances or exopolysaccharides (EPSs) are complex blend of high molecular weight microbial secretary biopolymeric by-products that are composed of organic macromolecules like polysaccharides along with smaller proportions of proteins, lipids, humic substances and uronic acids. Nevertheless, the fine structures of EPSs vary greatly among microbial genera and living habitats (Gupta and Diwan, 2017). Structural and compositional makeover of EPS favors the sequestration of metal ions that occurs through biosorption, by interaction between positively charged metal ions and negatively charged EPS. Abundant active and ionisable functional groups and non-carbohydrate substituents like acetamido, amine, sulfhydryl and carboxyl groups in proteins and phosphodiester (techoic acid), phosphate, hydroxyl groups in polysaccharides impart an overall negative charge to the biopolymer (Costa et al., 2018).

This study demonstrated the ability of *Halomonas* sp. Exo1 and its secreted EPS to sequester As confirming EPS-mediated As adsorption. However, there are reports of As-induced bacterial biofilm formation apart from As inducible EPS production, which can effectively adsorp the metalloid (Marchal et al., 2010, 2011). This study observed that salt acted as inducer of EPS production while addition of As in the salt-amended media enhanced EPS production. Role of salt in biofilm formation and/or EPS accumulation was already reported in a few halotolerant strains (Ozturk and Aslim, 2010; Qurashi and Sabri, 2012). Although production of EPSs in response to salt, starvation, dehydration, antibiotic or heavy metal stress had been reported (Gupta and Diwan, 2017), the role of EPS in osmoregulation was s least studied in general. Interestingly, the resistivity toward [As(III)] was also related to salt stress while

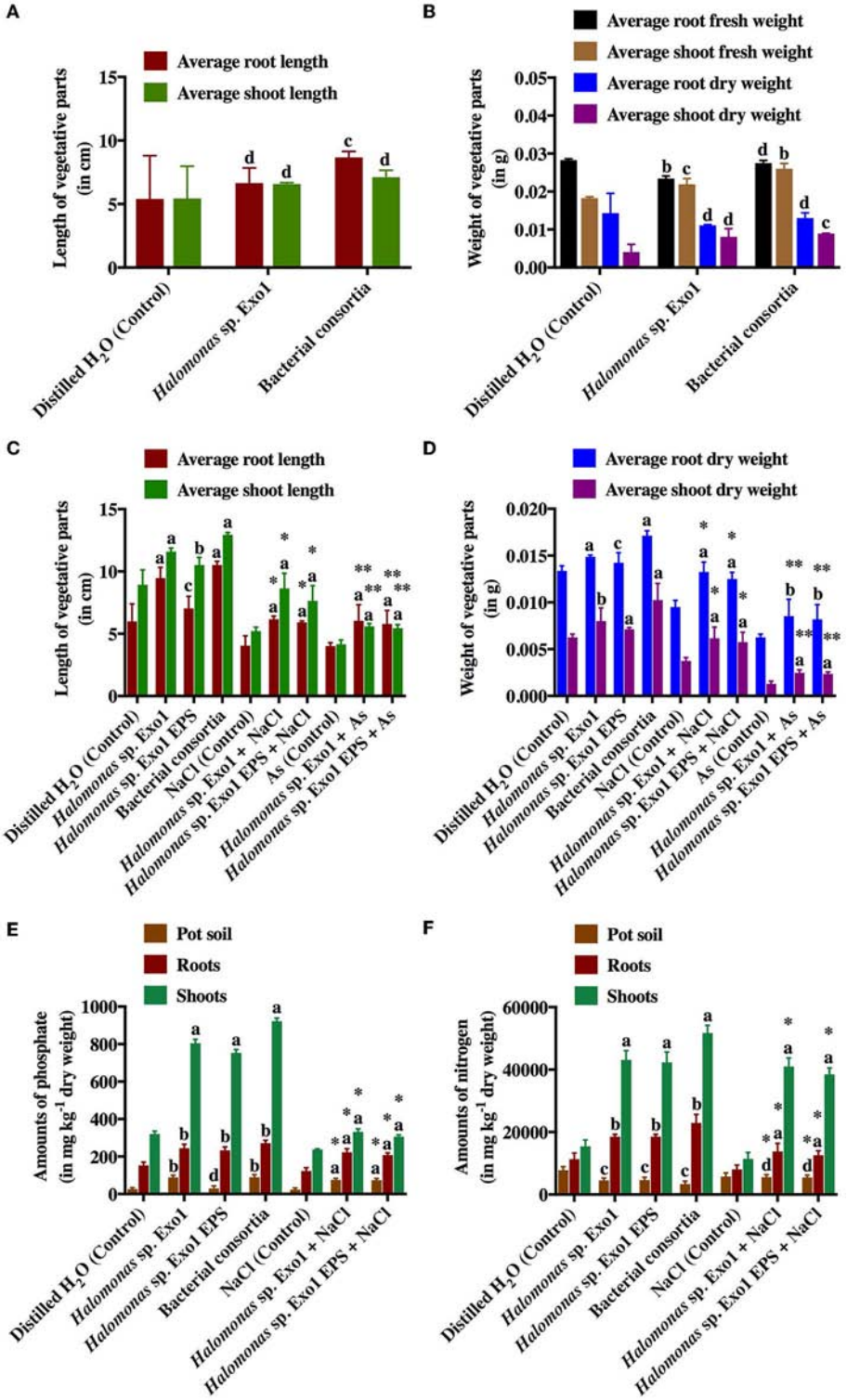

FIGURE 9 | Effects of selected halo-rhizobacteria and purified Exo1 on the germination, growth and nutrient uptake ability of salt-tolerant rice under salt and arsenic stresses. Average root and shoot lengths **(A)** and average fresh and dry weights of roots and shoots **(B)** of germinated rice seeds in plate-based germination assay. Average root and shoot lengths **(C)** and average dry weights of roots and shoots **(D)** of 15-day old germinated rice seedlings in pot-based growth assay. Amounts of phosphate (PO_4^{3-}) **(E)** and nitrogen (N_2) **(F)** uptaken by the roots and shoots of 15-day old germinated rice seedlings in pot-based growth assay. Error bars represent mean ± standard deviation of triplicate values. * denotes statistical significance with respect to NaCl (control) whereas ** denotes statistical significance with respect to As (control).

in the absence of salt, the observed MIC value of *Halomonas* sp. Exo1 toward [As(III)] was lower than that found in the presence of salt. On the other hand, for [As(V)] no change in MIC values was noticed either in the presence or absence of salt. It is believed that some kind of positive feedback is operating in *Halomonas* sp. Exo1 to keep As mediated damage low. Increased As in the medium triggers the cells to synthesize more EPS, which sequesters more As thereby reducing the toxic effect of the metal.

In addition to the EPS-mediated As adsorption, *Halomonas* sp. Exo1 can bioremediate or detoxify As by oxidation of more toxic [As(III)] to less toxic [As(V)]. Apart from the biosorption of As, increase in MIC level of selected other HMs (Cr, Cd, and Mn) in presence of EPS indicated that EPS may have role in biosorption of these HMs too. Nevertheless, As resistant microbes employ different strategies to cope with As stress like oxidation, reduction, dissimilatory arsenate reducing activity and bioaccumulation through complexion, chelation etc. (Roy et al., 2015). Purified EPS was readily soluble in water and was produced maximally under metal (As) contaminated saline ambience during late stationary phase of bacterial growth. XRD data indicated that the EPS was amorphous in nature, which was further corroborated by the SEM analysis. EDX data showed that the EPS contains elements such as Na and Ca, which might aid in adsorption of oppositely charged metals like As from the ambient media and the sulfate group present in it confered its anionic character in the saline environment (Nielsen and Jahn, 1999). The distribution of cations such as Na^+ and Ca^+ in the EPS also suggested their ability to bind to the negative charges of the sulfate groups rendering them more bioavailable to plants. The present study shows the As bioadsorption potential of EPS both *in vivo* and *in vitro* in dose-dependent and time-dependent manner. It has been observed that with a linear increase in As dose, a proportional increase of the amount of EPS-mediated As bioadsorption occurred. However, with increase in time, the amount of bioadsorped As attained a steady state probably owing to the saturation of As binding sites in the EPS. In an earlier report, Deschatre et al. (2013) showed that one marine bacterium produced EPS that bioadsorped positively charged metal ions (Ag^+ and Cu^{2+}). Although, EPS-mediated HM sequestration was studied by several research groups (Pereira et al., 2011), the current study has its own merits in the sense that *in vivo* EPS-mediated metal sequestration is more physiologically relevant compared to the *in vitro* studies conducted by earlier groups.

Role of halo-tolerant PGPR in promoting growth of agricultural crops in soil suffering from increased salinity has been studied previously while only a few studies described the role of EPS on direct plant growth promotion. Most scientists reported that EPS promotes growth by its biocontrol property (Upadhyay et al., 2017). The present study focused on all the aspects of plant growth promotion and showed that application of pure EPS to the pot soil improved rice growth under abiotic stresses. The PGP traits of the whole cells under different conditions of salt and As stresses were investigated as these factors modulated EPS production. Halo-tolerant PGPR withstand high salinity by virtue of their efficient osmoregulatory mechanism that facilitates in carrying out normal cell functions in salt stress and they help salt-sensitive plants to overcome saline stress via restoration of their improper hormonal balance with activities that includes synthesis of essential phytohormones like indole-3-acetic acid (IAA), gibberellins (GA), cytokinins (CK), abscisic acid (ABA) together with solubilization of inorganic phosphate, nitrogen fixation and synthesis and excretion of essential metabolites such as siderophores and EPSs. The halo-rhizobacterial isolate under investigation exhibited PGP traits like IAA, NH_3, HCN and siderophore production and inorganic phosphate solubilization. A preliminary investigation on N_2-fixation property in the test organism indicated that the strain may be N_2-fixer as it showed good growth in semi-solid Burk's N-free media. However, As exerted negative impact on all the PGP traits except production of siderophores, which increased with increase in As stress up to 6 mM. Siderophores are high-affinity, metal-binding plant metabolites secreted outside of the cell envelope. Present literature suggests that siderophores that are produced under conditions of iron (Fe) deficiency to quench Fe from the surroundings are also able to effectively bind other metal and metalloids including As (Rajkumar et al., 2010). Siderophores also take part in preventing infections from several phytopathogens such as *Fusarium oxysporium* by making Fe less available to certain pathogenic microbes, and therefore act as an essential biocontrol metabolite (Berthelin et al., 1991). As this strain also showed antagonism against *Fusarium oxysporium,* so in addition to the direct growth-promoting features of the PGPR in this study, *Halomonas* sp. Exo1 could be effective as biocontrol agent thereby boosting plant growth indirectly by keeping away phytopathogenic bacteria and fungi. PGP activities of *Halomonas* and other halo-tolerant bacteria that work under salt and HM stresses have already been reported from a few studies (Siddikee et al., 2010; Desale et al., 2014). Moreover, some of them are EPS producers but none of the studies revealed the role of EPS with direct plant growth promotion. This is the first report where EPS was found to directly enhance rice growth. Nevertheless, Arora et al. (2010) showed that crude cyanobacterial EPS from non-halophilic *Nostoc* species enhanced seed germination and growth vigor of rice, wheat and maize (plate-based assay) by binding the free Na^+ ions from aqueous media. They also hypothesized the possible role of EPS in increasing the growth vigor of the seedlings. Interestingly, the present study demonstrated the ability of *Halomonas* sp. Exo1 to bioaccumulate essential osmolytes including Na^+ and K^+, and showed direct *in vitro* evidence for EPS-mediated sequestration of Na^+ ions. Presence of increased level of Na^+ in NaCl-treated EPS was further corroborated by SEM-EDX analysis. Therefore, consistent with the results of Arora et al. (2010), one of the mechanisms of plant growth promotion by purified EPS (Exo1) is through salt stress alleviation by EPS-mediated Na^+ ion chelation and making them less available to plants under saline conditions. Moreover, EPS can improve soil structure by binding to soil particles to form microaggregates and macroaggregates and improves the water holding capacity of soil (Amellal et al., 1998). EPS produced by *Paenibacillus polymyxa* increases the aggregation of root adhering soil/root tissue ratio in wheat (Amellal et al., 1998). Additionally, plants that harbor EPS-producing rhizobacteria have selective advantage over others during environmental stresses like excessive salt and water logging. Yi et al. (2008)

suggested the role of EPSs in inorganic phosphate solubilization and plant growth promotion. However, the actual mechanism by which bacteria employ EPS in inorganic phosphate solubilization is yet to be elucidated. Another role of EPS is antioxidant activity (Kohler et al., 2009), which has also been reflected in the present study where EPS derived from *Halomonas* sp. Exo1 showed DPPH-free radical scavenging activity.

Most of the rice varieties including Jarava used in this study are non-tolerant varieties that do not survive at higher concentration of As. Nevertheless, As translocation was lower in the microbe-treated plants than the control plants. Hence the application of As-accumulating rhizomicrobes decreases the risk of As food chain contamination. Another advantage of the test rhizobacterium, used as bioinoculum, is that it does not exhibit antibiotic resistance properties and hence is absolutely fit for field applications (data not shown). Moreover, antifungal property and presence of siderophores would help the plants to survive in the competitive environment of the rhizosphere.

Therefore, the isolated salt- and As-tolerant PGPR and its EPS would be ideal candidates for application as biofertilizers or as bioinoculants, which would help in bioremediation of contaminated saline soil and support agronomy of salt-tolerant rice cultivation through salinity stress alleviation.

CONCLUSION AND FUTURE OUTLOOK

This research work demonstrated that the salt and As-tolerant strain *Halomonas* sp. Exo1 facilitated growth promotion of a salt-tolerant rice variety in the presence of growth inhibitory level of salt. Growth promotion of rice by the *Halomonas* strain under salt and As stresses occurred primarily through its PGP traits (production of IAA, siderophores, NH_3 and HCN, Pi solubilization, non-symbiotic N_2 fixation and anti-microbial or biocontrol activities) and most importantly through EPS secretion. The *Halomonas* sp. Exo1 was found capable of accumulating high amount of As within its cell-biomass. Although, the exact location of accumulation of As within the cell could not be exclusively ascertained in this study but *in vitro* EPS mediated and dead cell biomass-mediated [As(III)] biosorption studies supported the hypothesis that majority of As sequestration in *Halomonas* sp. Exo1 occurred through EPS-mediated bioadsorption. Among the other functional roles of the purified EPS, *in vitro* Na^+ ion sequestration and antioxidant activity were significant. Finally, direct growth-promoting effect of the purified EPS was observed based on the increased growth vigor of the salt-tolerant rice seedlings in pot-based bioassay. Therefore, this study established the role of halo-rhizobacterial EPS in promoting plant growth where EPS-mediated growth promotion of rice perhaps occurred through salt stress alleviation, inorganic phosphate solubilization and enhanced nutrient uptake. So, the overall results of the present research suggested that the isolated halo-PGPR and its purified EPS would find application as bioinoculant or biofertilizer in the cultivation of salt-tolerant crops such as rice in the low-lying contaminated coastal areas.

AUTHOR CONTRIBUTIONS

AM provided the soil and plant samples and helped in outsourcing. PM carried out all the lab based experiments with guidance from MR. MR and PM prepared the manuscript. The manuscript was checked several times by the three authors and all of them agreed on the final version.

ACKNOWLEDGMENTS

We thank Geological Survey of India (GSI, Kolkata), SGS India Pvt. Ltd., and Good Earth Enviro Care, Kolkata for AAS analysis. We are also thankful to Indian Association for the Cultivation of Science (IACS, Kolkata) for FESEM analysis and Department of Metallurgical & Material Engineering (Jadavpur University, Kolkata) for FT-IR, SEM-EDX, and XRD analyses. We gratefully acknowledge Dr. Tapan K. Dutta (Department of Microbiology, Bose Institute, Kolkata-700054, India) for providing valuable inputs and for critically reviewing the manuscript.

SUPPLEMENTARY MATERIAL

The Supplementary Material for this article can be found online at: https://www.frontiersin.org/articles/10.3389/fmicb.2019.01207/full#supplementary-material

REFERENCES

Altschul, S. F., Gish, W., Miller, W., Myers, E. W., and Lipman, D. J. (1990). Basic local alignment search tool. *J. Mol. Biol.* 215, 403–410. doi: 10.1016/S0022-2836(05)80360-2

Amellal, N., Burtin, G., Bartoli, F., and Heulin, T. (1998). Colonization of wheat roots by an exopolysaccharide-producing pantoeaagglomerans strain and its effect on rhizosphere soil aggregation. *Appl. Environ. Microbiol.* 64, 3740–3747.

Amjres, H., Béjar, V., Quesada, E., Abrini, J., and Llamas, I. (2011). Halomonas rifensis sp. nov., an exopolysaccharide producing, halophilic bacterium isolated from a solar saltern. *Int. J. Syst. Evol. Micr.* 61, 2600–2605 doi: 10.1099/ijs.0.027268-0

APHA (2012). *Standard Methods for the Examination of Water and Wastewater*. Washington, DC: American Public Health Association (APHA); American Water Works Association (AWWA); Water Environment Federation (WEF).

Argandoña, M., Fernández-Carazo, R., Llamas, I., Martínez-Checa, F., Caba, J. M., Quesada, E., et al. (2005). The moderately halophilic bacterium Halomonas maura is a free-living diazotroph. *FEMS. Microbiol. Lett.* 244, 69–74. doi: 10.1016/j.femsle.2005.01.019

Arias, S., Ferrer, M. R., Del, M. A., Quesada, E., and Be'jar, V. (2003). Mauran, an exopolysaccharide produced by the halophilic bacterium Halomonasmaura, with a novel composition and interesting properties for biotechnology. *Extremophiles.* 7, 319–326. doi: 10.1007/s00792-003-0325-8

Arora, M., Kaushik, A., Rani, N., and Kaushik, C. P. (2010). Effect of cyanobacterial exopolysaccharides on salt stress alleviation and seed germination. *J. Env. Biol.* 31, 701–704.

Bales, P. M., Renke, E. M., May, S. L., Shen, Y., and Nelson, D. C. (2013). Purification and characterization of biofilm-associated EPS EPS from ESKAPE organisms and other pathogens. *PLoS ONE* 8:e67950. doi: 10.1371/journal.pone.0067950

Bauer, A. W., Kirby, W. M., Sherris, J. C., and Turck, M. (1966). Antibiotic susceptibility testing by a standardized single disk method. *Am. J. Clin. Pathol.* 45:493. doi: 10.1093/ajcp/45.4_ts.493

Béjar, V., Llamas, I., Calvo, C., and Quesada, E. (1998). Characterization of EPS produced by 19 halophilic strains of the species *Halomonas eurihalina*. *J. Biotechnol.* 61, 135–141. doi: 10.1016/S0168-1656(98)00024-8

Berthelin, J., Leyrol, C., Laheurt, F., and Degiudici, P. (1991). "Some considerations on the relations between phosphate solubilizing rhizobacteria and their effect on seedling and plant growth related to phosphorus solubilizing," in *Growth-promoting Rhizobacteria: Progress and Prospects,* eds C. Keel, B. Koller, G. (Switzerland: IOBC), 359–364.

Bhaskar, P. V., and Bhosle, N. B. (2006). Bacterial extracellular polymeric substance (EPS): a carrier of heavy metals in the marine food-chain. *Environ. Int.* 32, 191–198. doi: 10.1016/j.envint.2005.08.010

Bighiu, M. A., Eriksson-Wiklund, A. K., and Eklund, B. (2017). Biofouling of leisure boats as a source of metal pollution. *Environ. Sci. Pollut. Res. Int.* 24, 997–1006. doi: 10.1007/s11356-016-7883-7

Bouchotroch, S., Quesada, E., Moral, A., Llamas, I., and Bejar,V. (2001). *Halomonas maura* sp. nov., a novel moderately halophilic, exopolysaccharide-producing bacterium. *Int. J. Syst. Evol. Microbiol.* 51, 1625–1632. doi: 10.1099/00207713-51-5-1625

Bramhachari, P. V., and Dubey, S. K. (2006). Isolation and characterization of exopolysaccharide produced by Vibrio harveyi strain VB23. *Lett. Appl. Microbiol.* 43, 571–577. doi: 10.1111/j.1472-765X.2006.01967.x

Cappuccino, J. G., and Sherman, N. (1992). *Microbiology: a laboratory manual.* San Francisco, CA: Benjamin-Cummings Publishing Company.

Castric, P. A. (1975). Hydrogen cyanide, a secondary metabolite of Pseudomonas aeruginosa. *Can. J. Microbiol.* 21, 613–618. doi: 10.1139/m75-088

Corzo, J., Leon-Barrios, M., Hernando-Rico, V., and Gutierrez-Navarro, A. M. (1994). Precipitation of metallic cations by the acidic exopolysaccharides from bradyrhizobium japonicum and *Bradyrhizobium* (*Chamaecytisus*) Strain BGA-1. *Appl. Environ. Microbiol.* 60, 4531–4536.

Costa, O. Y. A., Raaijmakers, J. M., and Kuramae, E. E. (2018). Microbial extracellular polymeric substances: ecological function and impact on soil aggregation. *Front. Microbiol.* 9:1636. doi: 10.3389/fmicb.2018.01636

Desale, P., Patel, B., Singh, S., Malhotra, A., and Nawani, N. (2014). Plant growth promoting properties of *Halobacillus* sp. and *Halomonas* sp. in presence of salinity and heavy metal. *J. Basic. Microbiol.* 54, 781–791. doi: 10.1002/jobm.201200778

Deschatre, M., Ghillebaert, F., Guezennec, J., and Colin, C. S. (2013). Sorption of copper (II) and silver (I) by four bacterial EPS. *Appl. Biochem. Biotechnol.* 171, 1313–1327. doi: 10.1007/s12010-013-0343-7

Dodgson, K. S., and Price, R. G. (1962). A note on the determination of the ester sulphate content of sulphated polysaccharides. *J. Biochem.* 84, 106–110. doi: 10.1042/bj0840106

Dubois, M., Gilles, K. A., Hamilton, J. K., Rebers, P. A., and Smith, F. (1956). Colorimetric method for determination of sugars and related substances. *Anal. Chem.* 28, 350–356. doi: 10.1021/ac60111a017

Dyall-Smith, M. (2009). *The Halohandbook: Protocols for Halobacterial Genetics*, Martinsried, Germany. Avaliable online at: http://www.haloarchaea.com/resources/halohandbook/Halohandbook_2009_v7.2mds.pdf

François, F., Lombard, C., Guigner, J. M., Soreau, P., and Brian-Jaisson,, F., et al (2012). Isolation and characterization of environmental bacteria capable of extracellular biosorption of mercury. *Appl. Environ. Microbiol.* 78, 1097–1106. doi: 10.1128/AEM.06522-11

Freitas, F., Alves, V. D., Pais, J., Costa, N., Oliveira, C., Mafra, L., et al. (2009). Characterization of an extracellular polysaccharide produced by a Pseudomonas strain grown on glycerol. *Bioresour. Technol.* 100, 859–865. doi: 10.1016/j.biortech.2008.07.002

Goswami, D., Dhandhukia, P., Patel, P., and Thakker, J. N. (2014). Screening of PGPR from saline desert of Kutch: growth promotion in Arachis hypogea by *Bacillus licheniformis* A2. *Microbiol. Res.* 169, 66–75. doi: 10.1016/j.micres.2013.07.004

Goswami, D., Thakker, J. N., and Dhandhukia, P.C. (2015). Simultaneous detection and quantification of indole-3-acetic acid (IAA) and indole-3-butyric acid (IBA) produced by rhizobacteria from l-tryptophan (Trp) using HPTLC. *J. Microbiol. Methods* 110, 7–14. doi: 10.1016/j.mimet.2015.01.001

Gupta, P., and Diwan, B. (2017). Bacterial Exopolysaccharide mediated heavy metal removal: a review on biosynthesis, mechanism, and remediation strategies. *Biotechnol. Rep.* 13, 58–71. doi: 10.1016/j.btre.2016.12.006

Kavita, K., Mishra, A., and Jha, B. (2011). Isolation and physico-chemical characterisation of extracellular polymeric substances produced by the marine bacterium *Vibrio parahaemolyticus*. *Biofouling.* 27, 309–317. doi: 10.1080/08927014.2011.562605

Kavita, K., Mishra, A., and Jha, B. (2013). Extracellular polymeric substances from two biofilm forming *Vibrio* species: characterization and applications. *Carbohydr. Polym.* 94, 882–888. doi: 10.1016/j.carbpol.2013.02.010

Kohler, J., Hernández, J. A., Caravaca, F., and Roldán, A. (2009). Induction of antioxidant enzymes is involved in the greater effectiveness of a PGPR versus AM fungi with respect to increasing the tolerance of lettuce to severe salt stress. *Environ. Exper. Bot.* 65, 245–252. doi: 10.1016/j.envexpbot.2008.09.008

Kumar, M. A., Anandapandian, K. T. K., and Parthiban, K. (2011). Production and characterization of exopolysaccharides (EPS) from biofilm forming marine bacterium. *Braz. Arch. Biol. Technol.* 54, 259–265. doi: 10.1590/S1516-89132011000200006

Kumar, S., Stecher, G., and Tamura, K. (2016). MEGA7: Molecular evolutionary genetics analysis version 7.0 for bigger datasets. *Mol. Biol. Evol.* 33, 1870–1874. doi: 10.1093/molbev/msw054

Kumar, V., Singh, S., Singh, J., and Upadhyay, N. (2015). Potential of plant growth promoting traits by bacteria isolated from heavy metal contaminated soils. *Bull. Environ. Contam. Toxicol.* 94, 807–814. doi: 10.1007/s00128-015-1523-7

Lim, J. M., Joo, J. H., Kim, H. O., Kim, H. M., Kim, S. W., Hwang, H. J., et al. (2005). Structural analysis and molecular characterization of exopolysaccharides produced by submerged mycelial culture of Collybia maculata TG-1. *Carbohydr. Polym.* 61, 296–303. doi: 10.1016/j.carbpol.2005.04.004

Liu, J., Li, F., Liu, L., Jiang, P., and Liu, Z. (2013). Inhibitory activity of an extract from a marine bacterium *Halomonas* sp. HSB07 against the red-tide microalga *Gymnodinium* sp. (*Pyrrophyta*). *Chinese J. Oceanol. Limnol.* 31, 1241–1247. doi: 10.1007/s00343-013-3160-5

Llamas, I., Del Moral, A., Martínez-Checa, F., Arco, Y., Arias, S., and Quesada, E. (2006). Halomonasmaura is a physiologically versatile bacterium of both ecological and biotechnological interest. *Antonie Leeuwenhoek* 89, 395–403. doi: 10.1007/s10482-005-9043-9

Lowry, O. H., Rosebrough, N. J., Farr, A. L., and Randall, R. J. (1951). Protein measurement with the Folin phenol reagent. *J. Biol. Chem.* 193, 265–275.

Malo, B. A. (1977). Partial extraction of metals from aquatic sediments. *Environ. Sci. Technol.* 11, 277–288. doi: 10.1021/es60126a007

Marchal, M., Briandet, R., Halter, D., Koechler, S., Dubow, M. S., Lett, M. C., et al. (2011). Subinhibitoryarsenite concentrations lead to population dispersal in Thiomonas sp. *PLoS ONE* 6:e23181. doi: 10.1371/journal.pone.0023181

Marchal, M., Briandet, R., Koechler, S., Kammerer, B., and Bertin, P. N. (2010). Effect of arsenite on swimming motility delays surface colonization in Herminiimonasarsenicoxydans. *Microbiology.* 156, 2336–2342. doi: 10.1099/mic.0.039313-0

Martínez-Cánovas, M. J., Quesada, E., Llamas, I., and Be'jar, V. (2004). *Halomonas ventosae* sp. nov., a moderately halophilic, denitrifying, exopolysaccharide producing bacterium. *Int. J. Syst. Evol. Microbiol.* 54, 733–737. doi: 10.1099/ijs.0.02942-0

Mehta, S., and Nautiyal, C. S. (2001). An efficient method for qualitative screening of phosphate-solubilizing bacteria. *Curr. Microbiol.* 43, 51–56. doi: 10.1007/s002840010259

Mitra, A. (2013). "Mangroves: a unique gift of nature," in *Sensitivity of Mangrove* Ecosystem *to Changing Climate* (New Delhi: Springer), 33–105. doi: 10.1007/978-81-322-1509-7_2

Mitra, A., and Zaman, S. (2016). "Threats to marine and estuarine ecosystems," in *Basics of Marine and Estuarine Ecology* (New Delhi: Springer), 365–417. doi: 10.1007/978-81-322-2707-6_10

Mukherjee, P., Roychowdhury, R., and Roy, M. (2017). Phytoremediation potential of rhizobacterial isolates from Kans grass (*Saccharumspontaneum*) of fly ash ponds. *Clean. Technol. Environ. Policy.*19, 1373–1385. doi: 10.1007/s10098-017-1336-y

Nadeem, S. M., Ahmad, M., Zahir, Z. A., Javaid, A., and Ashraf, M. (2014). The role of mycorrhizae and plant growth promoting rhizobacteria (PGPR) in improving crop productivity under stressful environments. *Biotechnol. Adv.* 32, 429–448. doi: 10.1016/j.biotechadv.2013.12.005

Nielsen, P. H., and Jahn, A. (1999). "Extraction of EPS," in *Microbial Extracellular Polymeric Substances: Characterization, Structure and Function*. eds J. Wingender, T. R. Neu, H. C. Flemming (Heidelberg: Springer), 49–72. doi: 10.1007/978-3-642-60147-7_3

Novák, M. (1965). Colorimetric ultramicro method for the determination of free fatty acids. *J. Lipid. Res.* 6, 431–433.

Oren, A. (2008). Microbial life at high salt concentrations: phylogenetic and metabolic diversity. *Saline Syst.* 4:2. doi: 10.1186/1746-1448-4-2

Osman, M. E. A., El-Shouny, W., Talat, R., and El-Zahaby, H. (2012). Polysaccharides production from some Pseudomonas syringae pathovars as affected by different types of culture media. *J. Microbiol. Biotechnol. Food. Sci.* 1:1305.

Ozturk, S., and Aslim, B. (2010). Modification of exopolysaccharide composition and production by three cyanobacterial isolates under salt stress. *Environ. Sci. Pollut. Res.* 17, 595–602. doi: 10.1007/s11356-009-0233-2

Ozturk, S., Aslim, B., Suludere, Z., and Tan, S. (2014). Metal removal of cyanobacterial EPS by uronic acid content and monosaccharide composition. *Carbohydr. Polym.* 101, 265–271. doi: 10.1016/j.carbpol.2013.09.040

Pal, T., Mukherjee, P. K., Sengupta, S., Bhattacharyya, A. K., and Shomea, S. (2002). Arsenic pollution in groundwater of West Bengal, India - an insight into the problem by subsurface sediment analysis. *Gondwana Res.* 5, 501–512. doi: 10.1016/S1342-937X(05)70738-3

Payne, S. M. (1994). Detection, isolation, and characterization of siderophores. *Methods. Enzymol.* 235, 329–344. doi: 10.1016/0076-6879(94)35151-1

Pereira, S., Micheletti, E., Zille, A., Santos, A., Moradas-Ferreira, P., Tamagnini, P., et al. (2011). Using extracellular polymeric substances (EPS)-producing cyanobacteria for the bioremediation of HM: do cations compete for the EPS functional groups and also accumulate inside the cell? *Microbiology* 157, 451–458. doi: 10.1099/mic.0.041038-0

Poli, A., Nicolaus, B., Denizci, A. A., Yavuzturk,. B., and Kazan, D. (2013). *Halomonas smyrnensis* sp. nov., a moderately halophilic, exopolysaccharide-producing bacterium. *Int. J. Syst. Evol. Microbiol.* 63, 10–18. doi: 10.1099/ijs.0.037036-0

Qurashi, A. W., and Sabri, A. N. (2012). Bacterial exopolysaccharide and biofilm formation stimulate chickpea growth and soil aggregation under salt stress. *Braz. J. Microbiol.* 43, 1183–1191. doi: 10.1590/S1517-83822012000300046

Rajkumar, M., Ae, N., Prasad, M. N., and Freitas, H. (2010). Potential of siderophore-producing bacteria for improving heavy metal phytoextraction. *Trends. Biotechnol.* 28, 142–149. doi: 10.1016/j.tibtech.2009.12.002

Ricou, P., Pinel, E., and Juhasz, N. (2005). Temperature experiments for improved accuracy in the calculation of polyamide-11 crystallinity by x-ray diffraction. *Adv. X-Ray. Anal.* 48, 170–175.

Roy, M., Giri, A. K., Dutta, S., and Mukherjee, P. (2015). Integrated phytobial remediation for sustainable management of arsenic in soil and water. *Environ. Int.* 75, 180–198. doi: 10.1016/j.envint.2014.11.010

Saitou, N., and Nei, M. (1987). The neighbor-joining method: a new method for reconstructing phylogenetic trees. *Mol. Biol. Evol.* 4, 406–425.

Sardari, R. R., Kulcinskaja, E., Ron, E. Y., Björnsdóttir, S., Frið*jónsson, Ó. H., Hreggvið*sson, G. Ó., et al. (2017). Evaluation of the production of EPS by two strains of the thermophilic bacterium *Rhodothermus marinus*. *Carbohydr. Polym.* 156, 1–8. doi: 10.1016/j.carbpol.2016.08.062

Schwyn, B., and Neilands, J. B. (1987). Universal chemical assay for the detection and determination of siderophores. *Anal. Biochem.* 160, 47–56. doi: 10.1016/0003-2697(87)90612-9

Shrivastava, P., and Kumar, R. (2015). Soil salinity: a serious environmental issue and plant growth-promoting bacteria as one of the tools for its alleviation. *Saudi. J. Biol. Sci.* 22, 123–131. doi: 10.1016/j.sjbs.2014.12.001

Siddikee, M. A., Chauhan, P. S., Anandham, R., Han, G. H., and Sa, T. (2010). Isolation, characterization, and use for plant growth promotion under salt stress, of ACC deaminase-producing halotolerant bacteria derived from coastal soil. *J. Microbiol. Biotechnol.* 20, 1577–1584. doi: 10.4014/jmb.1007.07011

Simeonova, D. D., Lièvremont, D., Lagarde, F., Muller, D. A., Groudeva, V. I., and Lett, M. C. (2004). Microplate screening assay for the detection of arsenite-oxidizing and arsenate-reducing bacteria. *FEMS. Microbiol. Lett.* 237, 249–253. doi: 10.1111/j.1574-6968.2004.tb09703.x

Tamura, K., Nei, M., and Kumar, S. (2004). Prospects for inferring very large phylogenies by using the neighbor-joining method. *Proc. Natl. Acad. Sci. U.S.A.* 101, 11030–11035. doi: 10.1073/pnas.0404206101

Timmusk, S., and Wagner, E. G. H. (1999). The plant-growth-promoting rhizobacterium *Paenibacillus polymyxa* induces changes in *Arabidopsis thaliana* gene expression: a possible connection between biotic and abiotic stress responses. *Mol. Plant. Microbe. Interact.* 12, 951–959. doi: 10.1094/MPMI.1999.12.11.951

U.S. Environmental Protection Agency (1994). *A Plain English Guide to the EPA Part 503 Biosolids Rule*. Washington, D.C: U.S. Environmental Protection Agency.

Upadhyay, A., Kochar, M., Rajam, M. V., and Srivastava, S. (2017). Players over the surface: unraveling the role of exopolysaccharides in zinc biosorption by fluorescent *Pseudomonas* strain psd. *Front. Microbiol.* 8:284. doi: 10.3389/fmicb,.2017.00284

Wang, Y., Li, C., Liu, P., Ahmed, Z., Xiao, P., and Bai, X. (2010). Physical characterization of exopolysaccharide produced by *Lactobacillus plantarum* KF5 isolated from Tibet Kefir. *Carbohydr. Polym.* 82, 895–903. doi: 10.1016/j.carbpol.2010.06.013

Wang, Y., Wei, D., Li, K., Wang, B., Shi, L., Zhang, X., et al. (2015). Response of extracellular polymeric substances to the toxicity of 2,4-dichlorophenol in aerobic granular sludge system: production and interaction mechanism. *RSC Adv* 5, 33016–33022. doi: 10.1039/C5RA03076E

Yadav, J. S. P., Bandyopadhyay, A. K., Raq, K. V. G. K., Sinha, T. S., and Biswas, C. R. (1979). *Coastal Saline Soils of India*. Bull. No. 5, Karnal: C.S.S.R.I.

Yang, J., Kloepper, J. W., and Ryu, C. M. (2009). Rhizosphere bacteria help plants tolerate abiotic stress. *Trends. Plant. Sci.* 14, 1–4. doi: 10.1016/j.tplants.2008.10.004

Yi, Y., Huang, W., and Ge, Y. (2008). Exopolysaccharide: a novel important factor in the microbial dissolution of tricalcium phosphate. *World. J. Microbiol. Biotechnol.* 24, 1059–1065. doi: 10.1007/s11274-007-9575-4

Yu, X., Li, Y., Zhang, C., Liu, H., Liu, J., et al. (2014). Culturable heavy metal-resistant and plant growth-promoting bacteria in V-Ti magnetite mine tailing soil from panzhihua, China. *PLoS ONE* 9:e106618. doi: 10.1371/journal.pone.0106618

Zhang, H., Kim, M. S., Sun, Y., Dowd, S. E., Shi, H., and Paré, P. W. (2008). Soil bacteria confer plant salt tolerance by tissue-specific regulation of the sodium transporter HKT1. *Mol. Plant. Microbe. Interact.* 21, 737–744. doi: 10.1094/MPMI-21-6-0737

Zhang, Z., Cai, R., Zhang, W., Fu, Y., and Jiao, N. (2017). A novel exopolysaccharide with metal adsorption capacity produced by a marine bacterium *Alteromonas* sp. JL2810. *Mar. Drugs.* doi: 10.3390/md15060175

Conflict of Interest Statement: The authors declare that the research was conducted in the absence of any commercial or financial relationships that could be construed as a potential conflict of interest.

Advantages of publishing in Frontiers

OPEN ACCESS
Articles are free to read for greatest visibility and readership

FAST PUBLICATION
Around 90 days from submission to decision

HIGH QUALITY PEER-REVIEW
Rigorous, collaborative, and constructive peer-review

TRANSPARENT PEER-REVIEW
Editors and reviewers acknowledged by name on published articles

Frontiers
Avenue du Tribunal-Fédéral 34
1005 Lausanne | Switzerland

Visit us: www.frontiersin.org
Contact us: info@frontiersin.org | +41 21 510 17 00

REPRODUCIBILITY OF RESEARCH
Support open data and methods to enhance research reproducibility

DIGITAL PUBLISHING
Articles designed for optimal readership across devices

FOLLOW US
@frontiersin

IMPACT METRICS
Advanced article metrics track visibility across digital media

EXTENSIVE PROMOTION
Marketing and promotion of impactful research

LOOP RESEARCH NETWORK
Our network increases your article's readership